Università degli Studi della Tuscia di Viterbo

Dipartimento di Scienze ecologiche e biologiche

Corso di Dottorato di Ricerca in

Ecologia e gestione sostenibile delle risorse ambientali -XXXV ciclo

Development of heterogeneous catalysts and green chemistry based approach in the field of prebiotic chemistry
(s.s.d. CHIM/06)

Tesi di dottorato di:

Dott.ssa Angelica Fanelli

Firma

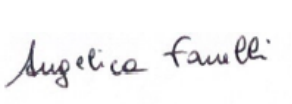

Tutore

Prof. Raffaele Saladino

Firma

Coordinatore del corso

Prof. Claudio Carere

Firma

Co-tutore

Dott. Bruno Mattia Bizzarri

Firma

A.A. 2022/2023

INDEX

Summary 5

Introduction 7
1.1 Green Chemistry 7
1.1.0 Twelve principles of green chemistry 8
1.1.0.1 Catalysis 16
1.1.0.1.1 Homogeneous catalysis 17
1.1.0.1.2 Heterogeneous catalysis 18
1.1.0.1.3 Oxidative catalysis 19
1.1.0.2 Atom Economy 19
1.1.0.2.1 Multicomponent chemistry 22

2.1 Prebiotic Chemistry 28
2.1.0 Formamide 29
2.1.0.1 Formation of purines and pyrimidines passing through HCN chemistry 31
2.1.0.2 Peptide nucleic acids (PNAs) 33
2.1.1 The role of meteorites in prebiotic chemistry 36
2.1.1.0 Thermal energy 37
2.1.1.1 Proton irradiation 39
2.1.1.2 Heavy Ion 41

Part 1: Development and application of catalytic procedure to natural substances 42

1.1 Rhenium based catalysts. 42
1.1.0 MTO as heterogeneous catalysts. 44
1.2 Synthesis and application of new MWCNTs MTO catalysts. 45
1.2.1. Preparation of MWCNTs-B15C5/MTO catalysts IV A-D. 48
1.2.2 Preparation of MWCNTs-B15C5/PAMAM/MTO catalysts V E-H. 51
1.2.3 Epoxidation of olefins with catalysts IV A-D and V E-H. 54
1.3 Conclusions 61
1.4 Materials and Methods 61
1.4.1 Preparation of oxidized MWCNTs I. 62
1.4.2 Preparation of MWCNTs-B15C5/MTO catalysts IV A-D. 62
1.4.3 Preparation of MWCNTs-B15C5/PAMAM/MTO catalysts V E-H. 63
1.4.4 FT-IR analysis 63
1.4.5 Scanning Electron Microscopy (SEM) and Transmission Electron Microscopy (TEM) 66
1.4.6 XRD analysis 67
1.4.7 Inductively Coupled Plasma Mass-Spectrometry (ICP–MS) Analysis 68
1.4.8 Oxidation of olefins 1-7 68
1.4.9 Mass spectrometry profiles of compounds 1-21 69
1.4.10 Nuclear magnetic resonance of compounds 1-21 80

2.1 Application of heterogeneous catalysis in the prebiotic trans-glycosylation process. 101
2.1.1 Synthesis of pyrimidine nucleosides 3. 103
2.1.2 Synthesis of nucleosides 9 and 10. 107
2.2 Conclusions 110
2.3 Materials and Methods. 111
2.3.1 Preparation of the powdered sample, elemental composition and cosmo-origin data of meteorite NWA 1465. 111
2.3.2 Synthesis of N^6-(D-2'-deoxyribos-1-yl)-2'-deoxyadenosine 1. 112
2.3.3 Synthesis of N^6-(D-ribos-1-yl)-adenosine 6. 115
2.3.4 Synthesis of pyrimidine nucleosides 3, 9 and 10 in dry-film condition (condition A). 118
2.3.5 Synthesis of pyrimidine nucleosides 3, 9 and 10 in formamide and NWA 1465 (conditions B and C). 121
2.3.6 Relative percentage of the α/β–pyranose and furanose isomers of compounds 1, 3, 6, 9, and 10. 121
2.3.7 Mass to charge (m/z) ratio values and relative MS peak abundances of products of 1-11. 122
2.3.8 Original m/z fragmentation spectra of compounds 2-5, 7-11. 122
2.3.9 UHPLC of compounds 9-10. 124

Part 2: Application of prebiotic multicomponent chemistry for the synthesis of bioactive compounds. 130
1.1 Synthesis of bioactive PNA's derivatives from HCN polymeric species. 130
1.1.0 Aminomalononitrile inspired prebiotic chemistry as a novel multicomponent tool for the synthesis of imidazole and purine derivatives with antiinfluenza A virus activity. 131
1.1.0.1 Synthesis of amino imidazole carbonitrile derivatives 4a-f and 5 a-f . 131
1.1.0.2 Synthesis of 8,9-disubstituted-6,9-dihydro-1H-purin-6-one derivatives 6a-f and 7 a-f. 135
1.1.0.3. Biological assay 136
1.1.1 Conclusions 139
2.1.0 Multicomponent synthesis of diaminopurine and guanine PNA's analogues active against influenza A virus from prebiotic compounds. 140
2.1.0.1 Synthesis of diaminopurine analogues (8a-f, 9a-f) and guanine analogues (10a-g, 11a-g). 140
2.1.0.2 Biological assay 146
2.1.1 Conclusions 149
3.1.0 A Three-Way Regioselective Synthesis of Amino Acid Decorated Imidazole, Purine and Pyrimidine Derivatives by Multicomponent Chemistry Starting from Prebiotic Diaminomaleonitrile 150
3.1.0.1 Synthesis of amino-acid decorated Imidazole derivatives-DAMN pathway 151
3.1.0.2 Synthesis of amino-acid decorated pyrimidine derivatives-DAFN pathway 153
3.1.0.3 Synthesis of amino-acid decorated purine derivatives-AICN Pathway 155
3.1.1 Conclusions 157
4.1.0 Materials and Methods 158
4.1.0.1 General procedure for the synthesis of 5- Amino-1,2-disubstituted-1H-imidazole-4-carbonitriles (4 a-g). 158

4.1.0.2 General procedure for the synthesis of amino-purine-analogues (6a-f). 159
4.1.0.3 General procedure for the synthesis of diaminopurine analogues 8a-f and guanine analogues 10a-g. 159
4.1.0.4 General procedure for the synthesis of amino-purine-analogues (5a-f and 7a-f), diaminopurine analogues (9a-f) and guanine analogues (11a-g) bearing free carboxylic acid moiety. 160
4.1.0.5 General procedure for the synthesis of amino-acid decorated Imidazole derivatives 14a-f DAMN pathway. 160
4.1.0.6 General procedure for the synthesis of amino-acid decorated pyrimidine derivatives 16a-f DAFN pathway. 160
4.1.0.7 General procedure for the synthesis of amino-acid decorated purine derivatives 19a-f AICN pathway. 161
4.1.0.8 UV-visible analyses of compound 13, 15, 16a, 17, 18 and 19a. 252
4.1.0.9 UV-visible analyses of reaction affording compounds 16a and 19a. 255
4.1.0.10 ATR FT-IR Analysis of compounds 13, 17 and of the reaction mixture affording compound 16a. 257
4.1.0.11 Cell Cultures 259
4.1.0.12 Cell toxicity assays 259
4.1.0.13 Virus Production and Infection 259
4.1.0.14 In Cell Western (ICW) Assay 259

References 260

List of publications 283

Summary

This project fits in the field of green chemistry, paying particular attention to catalysis and multi-component chemistry in the prebiotic field.

In the first part of the project, the oxidative catalysis for traditional reactions and prebiotic chemistry was investigated. Initially, heterogeneous catalysts based on carbon nanotubes were designed as support for an organometallic redox species, methyltrioxorhenium. The catalysts were prepared using a common structural scheme consisting of the presence of spacer chains of different length and branching, a dendritic platform and the active specie complexed into internal cavity of crown ether, and used for the selective oxidation of a panel of aliphatic and aromatics olefins to epoxides, using hydrogen peroxide as an environmentally friendly primary oxidant. Catalysis in prebiotic chemistry has been applied to trans-glycosylation processes under various reaction conditions, using high-energy proton sources and chondrite meteorites (NWA 1465) as a source of heterogeneous catalysis. The meteorite increases the conversion of the reaction, the yield of nucleoside formation through a stereo and regio selective process.

The second part of the project concerns the development of new models of prebiotic chemistry starting from formamide derivatives in a multicomponent chemistry approach. Studies show that formamide leads to a purine and pyrimidine nucleus, passing through intermediates of prebiotic interest such as amino imidazole carbonitrile (**AICN**,) aminomalononitrile (**AMN**) and diaminomaleonitrile (**DAMN**). In a first work, imidazole derivatives were synthesized through a condensation reaction between AMN, a panel of α-amino acids and trimethyl orthoacetate, in the presence of tetrahydrofuran under microwave irradiation. The imidazole derivatives were annuled into the corresponding amino-purine analogues in the presence of formic acid through a microwave-mediated, solvent-free reaction. The new compounds showed good activity against influenza A virus. The panel of derivatives has been expanded using urea and guanidine as annulation reagents. Diaminopurine and guanine derivatives, analogues of peptide nucleic acids, with selective inhibitory activity against influenza A virus in the nano-molar range, were obtained respectively. Finally, the multicomponent chemistry inspired by the prebiotic chemistry of DAMN was investigated. The regioselectivity of the multi-component reaction between diaminomaleonitrile, trimethyl orthoacetate and a selected panel of a-amino acids, was controlled by the energy source used for triggering the condensation. The energy source can control the selectivity of the in-situ isomerization and annulation of DAMN to DAFN and AICN, respectively: these intermediates may afford heterocycles characterized by rings of different size and chemical composition. Imidazole

derivatives were obtained under thermal condition, while photochemical and combined photothermal conditions afforded pyrimidine and purine derivatives, respectively.

Introduction

1.1 Green Chemistry

Chemistry occupies a special place in the development of civilization, and its role in industrial world is particularly important. It is chemistry that bears on the development of alternative energy sources (in particular, hydrogen energy) and new fuel types, synthesis of pharmaceuticals, new material design, sustainable harvests in agriculture and many others. However, there is also “the other side of the coin” of chemistry, it is not without reason that chemistry is accused of environmental pollution including air, water and soil pollutions.

One can endlessly criticize chemical industry, however it is clear to everybody that mankind already cannot do without drugs, crop protection chemicals, dyes, photo materials, polymers and fibres, and many other chemical products.

Is it possible to propose a compromise?

A way out is offered by green chemistry, albeit, naturally, it would be naive to expect solution to all the problems within the framework of one concept.

According to the EPA definition, Green or Sustainable chemistry is the design of chemical products and processes that reduce or eliminate the use and generation of hazardous substances.[1] As a new branch of chemistry with ecological approaches it involves reducing or eliminating the use of harmful substances in chemical processes as well as reducing harmful and toxic intermediates and products.

To be called "green," each reaction should have three green components: solvent, reagent / catalyst and energy consumption.

Advances in green chemistry address both obvious hazards and those associated with such global issues as climate change, energy production,

availability of a safe and adequate water supply, food production, and the presence of toxic substances in the environment. Alternative blowing agents replace millions of pounds of chlorofluorocarbons (CFCs) in insulating foams, new energy sources lessen our dependence on

fossil fuels, and pesticides are designed to be more selective and less persistent than traditional organic pesticides. The challenge of sustainability will be met with new technologies that provide society with the products we depend on in an environmentally responsible manner.

The activities in green chemistry research, education, industrial implementation, awards, and outreach are all based on the fundamental definition of green chemistry as stated above. The

concept of “design” in the definition is an essential element in requiring the conscious and deliberative use of a set of criteria, principles, and methodologies in the practice of green chemistry. Because green chemistry is intentionally designed, it is definitionally impossible to do green chemistry by accident. The phrase the “use or generation” implies the requirement of life-cycle considerations.

Green chemistry can be utilized anywhere in the life cycle, from feedstock origins to beyond end of useful life. The term “hazardous” is used in its broadest context including physical (e.g., explosion, flammability), toxicological (e.g., carcinogenic, mutagenic), and global (e.g., ozone depletion, climate change). [1]

Green chemistry is not a separate scientific discipline, but a responsible interdisciplinary approach to science, based on chemical, ecological and social responsibility, which enables creativity and the advancement of innovative research.[2] As a propulsive area of research, it tries to find and maintain a balance between the use of natural resources, economic growth and environmental conservation.

In order to achieve the main goals of green chemistry, green program comes through several dominant trends:

a. Research in the field of catalytic and biocatalytic reactions in order to obtain highly selective, pure compounds without the formation of toxic byproducts.

b. Seeking new raw materials, harmless and renewable, such as biomass.

c. Designing less toxic eco-compatible chemicals.

d. Finding and testing new alternative, non-toxic and renewable reaction media such as water, ionic liquids and supercritical fluids.

e. Finding and testing new alternative reaction conditions, such as microwave, ultrasound and light reacting.

f. Exploration of alternative routes for the purification of poisoned air and water to improve their quality, such as photocatalytic reactions.[3]

Green chemistry is a Hippocratic oath for chemists, and in order to preserve natural resources and the environment, a new generation of scientists and technologists is being developed, which economically analyse the processes and materials used in production and development.

1.1.0 Twelve principles of Green Chemistry

Green chemistry or ecologically harmless and sustainable chemistry is the manufacture and application of chemical products and processes that reduce or eliminate the use and creation of

hazardous substances. Instead of limiting the risk by controlling exposure to harmful chemicals, green chemistry seeks to reduce, and possibly eliminate, the danger, denying the need for exposure control. If no hazardous substances are used or produced, then the risk is zero and there is no need to worry about removing hazardous substances from the environment or limiting exposure to them or "Green chemistry is about reducing waste, raw materials, risks, energy, environmental impact and cost".[3]

In detail, the author of this concept, Anastas and Warner,[4] developed 12 principles of green chemistry in 1998 by relying on a motto that is spiritually close to the physician maxim “Primum non nocere -Seek prevention, not cure”.

Twelve principles can be used to create or recreate molecules, materials, reactions and processes that are safer for human health and the environment, and the processes of green chemistry developed to date include mainly all areas of chemistry, including organic, inorganic, biochemical, polymeric, toxicological, environmental, physical, technological, etc.

Basic principles of green chemistry cover a wide spectrum of synthetic organic synthesis: designing processes in organic synthesis to reduce byproduct/waste generation, reduce the use of hazardous chemicals/raw materials and enhance the use of safer or more environmentally-safe solvents and (bio) catalysts, renewable raw materials and how would improve energy efficiency. In addition, green chemistry is interested in the best form of waste disposal and designing the process of degradation of chemical products after use, all in accordance with pollution prevention and sustainable development measures.[5]

The goals of green chemistry in environmental protection and economic profit are achieved through several dominant directions such as catalysis, biocatalysis, the use of alternative renewable raw materials (biomass), alternative reaction media (water, ionic liquids, supercritical fluids), alternative reaction conditions (microwave activation, mechanochemistry and ultrasound) as well as new photocatalytic reactions.[3]

These principles are a categorization of the fundamental approaches taken to achieve the green chemistry goals of benign products and processes, and have been used as guidelines and design criteria by molecular scientists. Like all multiparameter systems, trade-offs and balances will be made in striving toward optimization based on the specific circumstances of application. The current state-of-the-art in green chemistry has been reached due to advances in research, implementation, education, and outreach over the past decade (Figure 1).

Figure 1: The 12 principles of green chemistry

Following, the 12 principles of green chemistry (Figure 1)[6]:

1. It is better to prevent waste than to treat or clean up waste after it is formed. Although the chemical industry, as well as other chemical manufacturers, have long ago avoided prevention, the interest of green chemistry and the community is precisely to prevent waste generation. However, the absolute prevention of waste generation in practice is virtually impossible since no input raw material can be fully utilized. On the other hand, one waste disposed of represents the final loss of material goods in the circular flow: production - consumption. Therefore, any return of material goods to a circular stream represents a pure economic gain and it is necessary to think first whether it is possible to prevent the generation of waste and if it is not necessary to devise the way in which the amount of waste produced in production can be utilized in the best possible way, so it becomes useful.[2] A good example is the new "green" production process of sertraline (Scheme 1) by which the introduction of ethanol as the sole solvent eliminates the need for the use, distillation and recovery of four solvents such as methylene chloride, tetrahydrofuran, toluene and hexanes, resulting in a reduction in solvent consumption of 250 to 25 litres per kg of sertraline.[7]

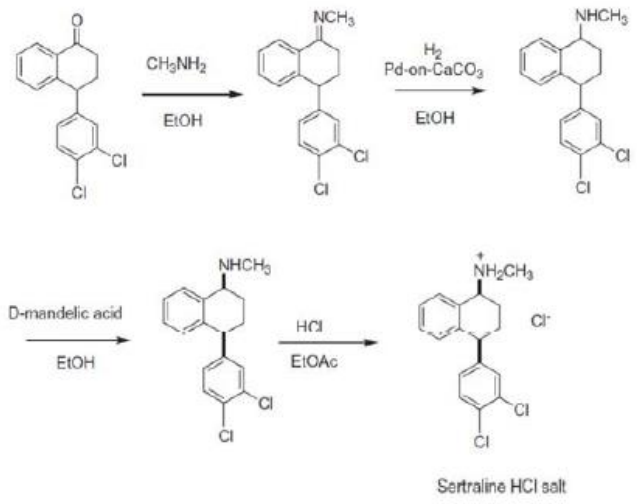

Scheme 1: Green synthesis of sertraline.[7]

2. Synthetic methods should be designed to maximize the incorporation of all materials used in the process into the final product. Atom economy (AE) seeks to maximize the incorporation of the starting materials into the final product of any given reaction. The additional corollary is that, if maximum incorporation cannot be achieved, then ideally the quantities of side products should be minute and environmentally innocuous. There is a fundamental difference in the manner in which a reaction yield and the atom economy yield is calculated. The reaction yield is only concerned with the quantity of the desired product that is isolated, relative to the theoretical quantity of the product. Atom economy takes all used reagents and unwanted side products into account along with the desired product.[8] The Atom economy is measured as the ratio of the molecular weight of the desired product over the molecular weights of all reactants used in the reaction (Figure 2). It is a theoretical value meant to quickly assess how efficient a reaction will be.[4]

$$AE = \frac{\text{MW Product}}{\text{MW of reagents}}$$

Figure 2: The Atom Economy (AE).

3. Whenever practicable, synthetic methodologies should be designed to use and generate substances that possess little or no toxicity to human health and the environment. It is

often overlooked that the manufacturing pathway to ultimately synthesize a product may in fact go through a series of chemical intermediates. This principle seeks to minimize the hazards associated with these intermediates. It is important to make the distinction that this principle is focused on materials that, in a perfect world, should not appear in the product. However, when considering worker exposure and the other associated costs related to handling, storage and disposal of hazardous materials, the avoidance of hazardous intermediates is extremely important. Reducing the hazards associated with the way a product is made can drastically reduce worker liabilities, contribute towards worker health and safety, and minimize the potential for chemical accidents.[9] As an example, a new Asahi Kasei's polycarbamate synthesis (PC) process is conceptually simple (Scheme 2), based on the substitution of toxic carbonyl dichloride (COC_2) with CO_2. This process also results in the removal of dichloromethane (CH_2Cl_2) as a solvent. The total reaction consists of ethylene oxide (CH_2), CO_2 and bisphenol-A ($C_{15}H_{16}O_2$) to give polycarbamate and ethylene glycol $C_2H_6O_2$.[10]

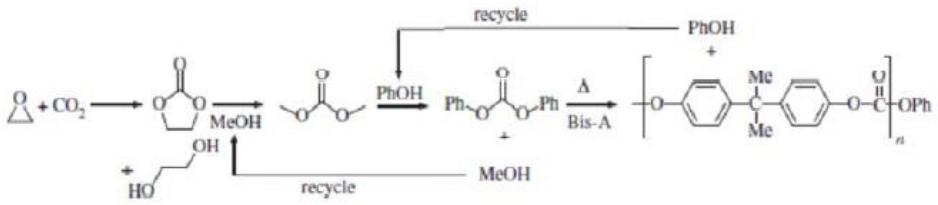

Scheme 2: Synthesis of polycarbamate.[11]

4. Chemical products should be designed to preserve efficacy of function while reducing toxicity. Minimizing toxicity, while maintaining function and efficiency, can be one of the most challenging aspects of designing safer products and processes, and achieving that goal requires understanding not only chemistry but also the principles of toxicology and environmental science. The use of toxic chemicals should be avoided and replaced inhospitable wherever possible, but should take account of their efficacy.[2] An example is the production of polymers of polyphenylene sulfone (PPSU), which is now widely used for indoor airplanes and is also introduced in underground trains where it is also important to use non-flammable materials. It is a new engineering plastic characterized by a unique combination of useful environmental, mechanical, and flame resistant properties.[12]

5. The use of auxiliary substances (e.g. solvents, separation agents, etc.) should be made unnecessary whenever possible and innocuous when used. Solvents are auxiliary materials used in chemical synthesis. They are not an integral part of the compounds undergoing reaction, yet they play an important role in chemical production and synthesis. The primary function of solvents in classical chemical syntheses is to facilitate mass transfer to modulate chemical reactions in terms of reaction rate, yields, conversions, and selectivity. They do this by dissolving the reactants in dilute homogeneous mixtures. The ironic aspect of this process is that, after the reaction, the final product has to be reseparated from the solvent through energy-intensive means. The development of Green Chemistry redefines the role of a solvent: *An ideal solvent facilitates the mass transfer but does not dissolve*! In addition, a desirable green solvent should be natural, nontoxic, cheap, and readily available. According to the suitability of use, conventional solvents are suitable, usable, and undesirable (Table 1).[8]

   Table 1: Solvent selection according to usability.[13]

Suitable	Usable	Undesirable
methanol	cyclohexane	pentane
ethanol	methylcyclohexane	hexane
propan-1-ol	heptane	diisopropyl ether
propan-2-ol	isooctane	dichloromethane
butan-1-ol	t-Butyl methyl ether	chloroform
t-butanol	acetonitrile	benzene
ethyl acetate	tetrahydrofuran	dimethyl acetate
isopropyl acetate	acetic acid	carbon tetrachloride
acetone	xylene	dimethoxyethane
methyl ethyl ketone	toluene	pyridine

6. Energy requirements should be recognized for their environmental and economic impact and should be minimized. Synthetic methods should be conducted at ambient temperature and pressure. Strategies that can result in increased energy efficiency include but are not limited to solventless reactions, catalysis, microwave-assisted synthesis, and synthetic photochemistry. Solventless reactions, even if they require activation which can be either thermal or mechanical or photochemical are relatively energy efficient because they do not require heating or agitation of a solvent.[9]

7. A raw material feedstock should be renewable rather than depleting whenever technically and economically practical. "Renewable" is defined by the Oxford English Dictionary as "not depleted by its utilization". Renewable materials may be, in many cases, green and sustainable, but we should not make the mistake of assuming that this is always the case. The seventh principle of green chemistry advocates Use of Renewable Feedstocks wherever it is technically and economically acceptable.[2] For example, it is more convenient to use renewable raw materials than a variety of plastic materials, and then to waste away the waste materials. Examples of renewable material include cellulose, lignin, suberin and other wood compounds, polyhydroxyalkanoates, lactic acid, chitin, starch, glycerol and oil. The principle also implies the use of renewable energy technologies that include solar energy, wind power, hydropower, biomass energy and biofuels.[9]
8. Unnecessary derivatization (blocking group, protection/deprotection, temporary modification of physical/chemical processes) should be avoided whenever possible. These steps require additional reagents and can generate waste. Typical example is the production of antibiotics (Scheme 3) based on penicillin or replacement of classical chemical enzymatic processes whereby the 6-aminopenicillic acid is obtained by reacting with the catalyzed immobilized enzyme penicillin amide. This resulted in several chemical steps being replaced by an enzymatic reaction, and no longer required a low temperature (-60°C), organic solvents, and completely unsuitable conditions that increased and complicated production in the case of chemical synthesis.[2]

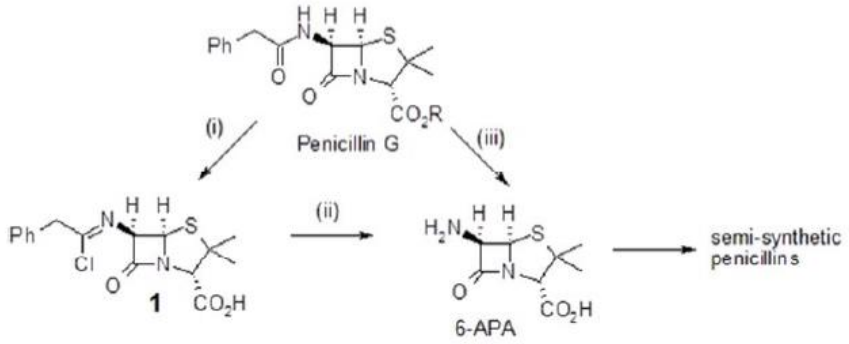

Scheme 3: Synthesis of 6-aminopenicilic acid catalyzed by immobilized penicillin G amide.

9. Catalytic reagents (as selective as possible) are superior to stoichiometric reagents. In many cases, the formation of waste is linked to the traditional use of a stoichiometric amount of reagents. Switching from stoichiometric methodologies to catalytic processes is perceived as one major way to improve the efficiency of the synthetic process.[4]
10. Chemical products should be designed so that at the end of their function they do no persist in the environment and break down into innocuous degradation products. The principle of creating degradable chemicals and products or design for degradation demands the creation of chemical products that, upon termination of their activity, must be able to convert into products that are harmless to the environment. The aim is to prevent the formation of harmful substances and to return to production as much waste as possible, which is achieved by recycling.
11. Analytical methodologies need to be further developed to allow for real-time in-process monitoring and control prior to the formation of hazardous substances. It is the goal of green analytical chemistry to measure chemicals without generating waste. Process analytical chemistry is defined as the ability to monitor a transformation and act immediately upon it to prevent unwanted outcomes. Green analytical chemistry can be defined as the use of analytical procedures that generate less waste and are safer to human health and the environment.[14]
12. Substances and the form of a substance used in a chemical process should be chosen so as to minimize the potential for chemical accidents, including releases, explosions, and fires. All types of hazards whether it is toxicity, physical hazards such as explosivity or flammability, and global hazards should be addressed in the design of chemicals and processes and should be replaced by safer alternatives in order to prevent accidents.[15]

Despite the countless efforts made by the scientific community still no industrial process can be defined as having zero impact.

However, innumerable advances have been made in green chemistry and the work done can be divided into 4 main categories depending on the specific aspect in which a green product or process differs from that conventionally used.

The 4 categories are:

1. Alternative starting materials

2. Alternative reagents or alternative transformations
3. Alternative reaction conditions
4. Final products or alternative target molecules

In many situations these research areas are closely linked.

Research programs and centres located in countries in the Americas, Europe, Asia/Pacific, and Africa are focusing efforts around the principles of green chemistry.

The breadth of this research is very wide and incorporates areas such as polymers, solvents, catalysis, bio based/renewables, analytical method development, synthetic methodology development, and the design of safer chemicals.

Excellent research is being conducted within each of these areas that strives to incorporate one or more of the 12 Principles of Green Chemistry.[1]

1.1.0.1 Catalysis

Catalysis plays a central role in chemical transformations and is one of the "fundamental pillars" of green chemistry. The design and application of new catalysts and catalytic systems are simultaneously achieving the dual goals of environmental protection and economic benefit.[11]

Designing and developing ideal catalysts is one of the very important concepts of green chemistry. According to these principles catalytic reagents (as selective as possible) are superior to stoichiometric reagents. Stoichiometric reagents are used in excess and work only once while catalytic reagents used in small amounts and can carry out a single reaction many times. To work more like nature is the base of all the twelve principles of green chemistry.[16]

Catalysis can be classified into:

-homogeneous catalysis, when reagents, products and catalyst are in the same phase;

-heterogeneous catalysis, when catalyst isn't in the same phase as the reagents.

A catalyst is defined as a chemical species that acts during a chemical reaction, lowering the activation energy, increasing the speed, remaining unchanged at the end of the process (Figure 3).

The catalysts do not appear in the global reaction equations and do not cause variations in the value of the equilibrium constant.

Catalysts can be divided into positive catalysts, that increase the reaction speed and negative catalysts, that decrease the reaction speed.

How does a catalyst work? During a chemical reaction, the bonds between the atoms in molecules are broken, rearranged, and rebuilt, recombining the atoms into new molecules. Catalysts make this

process more efficient by lowering the activation energy, which is the energy barrier that must be surmounted for a chemical reaction to occur. As a result, catalysts make it easier for atoms to break and form chemical bonds to produce new combinations and new substances.

In general, the catalysts allow the molecules to react according to a different mechanism which is more convenient (or less convenient in the case of inhibitors) from the energy point of view.

A catalyst, although participating in the reaction, is not consumed.

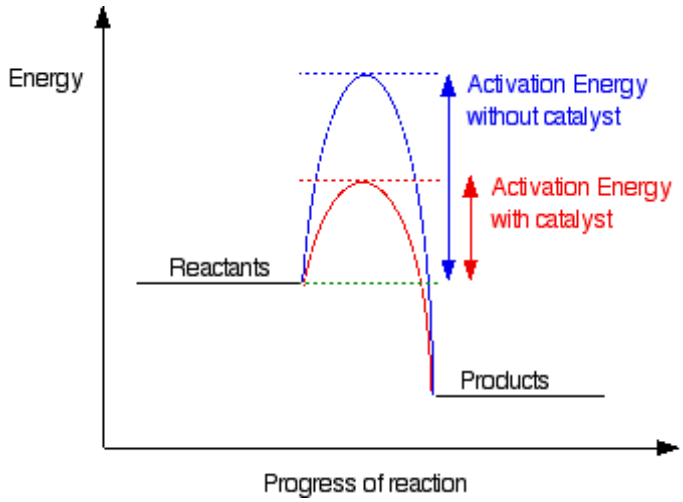

Figure 3: Catalyst's action mechanism.

1.1.0.1.1 Homogeneous catalysis.

Homogeneous catalysis, by definition, refers to a catalytic system in which the substrates for a reaction and the catalyst components are brought together in one phase, most often the liquid phase. More recently a narrower definition has become fashionable according to which homogeneous catalysis involves (organo) metallic complexes as the catalysts.

As a shorthand notation it will also be used here, but it should be borne in mind that there are many interesting and important reactions employing homogeneous catalysts that are not (organo) metallic complexes.

Examples of such systems or catalysts are:

- general acid and base catalysis (ester hydrolysis),
- Lewis acids as catalysts (Diels-Alder reactions),
- organic catalysts (thiazolium ions in Cannizzarro reactions),

- porphyrin complexes (epoxidations, hydroxylation),
- enzymatic processes,
- co-ordination complexes (polyester condensations).

Ligand effects are extremely important in homogeneous catalysis by metal complexes. One metal can give a variety of products from one single substrate simply by changing the ligands around the metal centre.[17]

Homogeneous catalysts generally are well understood at the molecular level and are highly reactive as each of the catalyst entities acts as an active site, but they often need extra steps as well as complex techniques for separation from the reaction products.

1.1.0.1.2 Heterogeneous catalysis.

Heterogeneous catalysis, in particular, addresses the goals of green chemistry by providing the ease of separation of product and catalyst, thereby eliminating the need for separation through distillation or extraction.

In addition to separation of product and catalyst, the most common advantages of heterogeneous catalysis are:

- ease of recovery of the catalyst, often very expensive or characterized by high toxicity;
- possibility of recycling the catalyst to achieve more successive transformations;
- less wastewater to be treated;
- the greater adaptability to carry out continuous processes that allow greater selectivity, better product quality and greater process safety;
- less contamination of the products by catalyst residues;
- possibility of replacing homogeneous chemical processes characterized by the use of toxic and environmentally harmful reagents.

In the specific area of application of heterogeneous catalysis to environmental problems, the most followed strategies are:

- the development of new catalysts active at low temperatures, even at room temperature, selective and stable;
- the heterogenization of homogeneous catalysts;
- the use of inert supports with the homogeneous catalytic species distributed in cavities or on the external surface; the inorganic matrices (supports) used for the development of heterogenized systems of this type are oxides (particularly SiO_2 as well as TiO_2 and Al_2O_3), zeolites and other

materials with the properties of molecular sieve (alumina-phosphates, silicates), mesoporous systems of the MCM-41 21 and SBA-15 types, carbon supports (MWCNTs) , especially with functional groups involved in interaction with ligands of the complex;[18]

- the modification of surface properties of supports;
- the use of particular solvents to facilitate product desorption, transformation of intermediates, orientation and activation of reagents.

The design of a catalyst strives to optimize factors such as stability, solubility, and ease of separation from the product. Changes in ligand design or metal selection can provide significant improvements in selectivity, energy consumption, and solvent utilization. In some cases, design of better catalysts also permits the use of more environmentally friendly feedstocks and reagents.

Four main classes of heterogeneous catalysis can be identified: hydrogenation catalysis, asymmetric catalysis, acid-base catalysis and oxidative catalysis.[19]

1.1.0.1.3 Oxidative catalysis.

The oxidative heterogeneous catalysis has been proposed as a valid alternative to numerous oxidation processes conducted with stoichiometric oxidizing reagents such as potassium permanganate, potassium dichromate (toxic, mutagenic and carcinogenic compound) etc.

To limit the environmental impact of these processes it is advisable to use eco-compatible oxidants such as hydrogen peroxide (H_2O_2), molecular oxygen (O_2).

H_2O_2 and O_2 have a redox potential that is too low for the oxidation of most natural organic substances and fine chemicals products.

Therefore, these primary oxidants must be activated by appropriate catalysts.

In general, the heterogeneous oxidation catalysts consist of transition metals (rhenium, cobalt, iron, molybdenum etc..) supported by inert organic and inorganic matrices.

Through reactions with hydrogen peroxide these metals tend to form metal-peroxy-complexes of various structure or radicals activated by oxygen which represent the active species of the oxidative process.[20]

1.1.0.2 Atom economy

In 1990 Barry Trost introduced the concept of synthetic efficiency: Atom Economy (AE) also called Atom Efficiency.[21]

The principle of Atom Economy is logically linked to the principle of waste prevention, since it requires all raw materials used in production to maximize utilization or inclusion in the final product to ultimately reduce the amount of waste. This means that the chemical synthesis should be designed in such a way that the final product maximizes the input of raw materials or design such synthetic products that will use the entire material used for synthesis in the final product. The ideal reaction would incorporate all of the atoms of the reactants.

To illustrate this concept, a few examples such as the Grignard reaction, A3 coupling and the Diels–Alder reaction are presented (Figure 7). The Grignard reaction, which received the recognition of the scientific community for its importance in organic synthesis, is unfortunately a relatively poor atom economical reaction due to the use of a stoichiometric amount of metal reactant and the necessity to prepare the Grignard reagent separately. Figure 7 presents a typical Grignard reaction[22] and an application of the Grignard reagent to build a propargylic amine type structure.[23] The values of the AE respectively are 44 and 56% which reflect a loss of half of the raw material. A solution in respect to the last example was proposed by C.-J. Li et al. in 2002 through the A3 coupling (Alkyne, Aldehyde and Amine).[24,25] This one-step multicomponent coupling reaction is more efficient and conserves atoms since 92% of the original atoms used are found in the final product. The Diels–Alder reaction is also an excellent example of an atom-economical reaction (Figure 4).[21,26] Its AE is equal to 100% since all atoms from the reactants are incorporated into the final product. Diels–Alder type reactions belong to the category of cycloaddition which is among the greenest types of reactions in traditional chemistry.

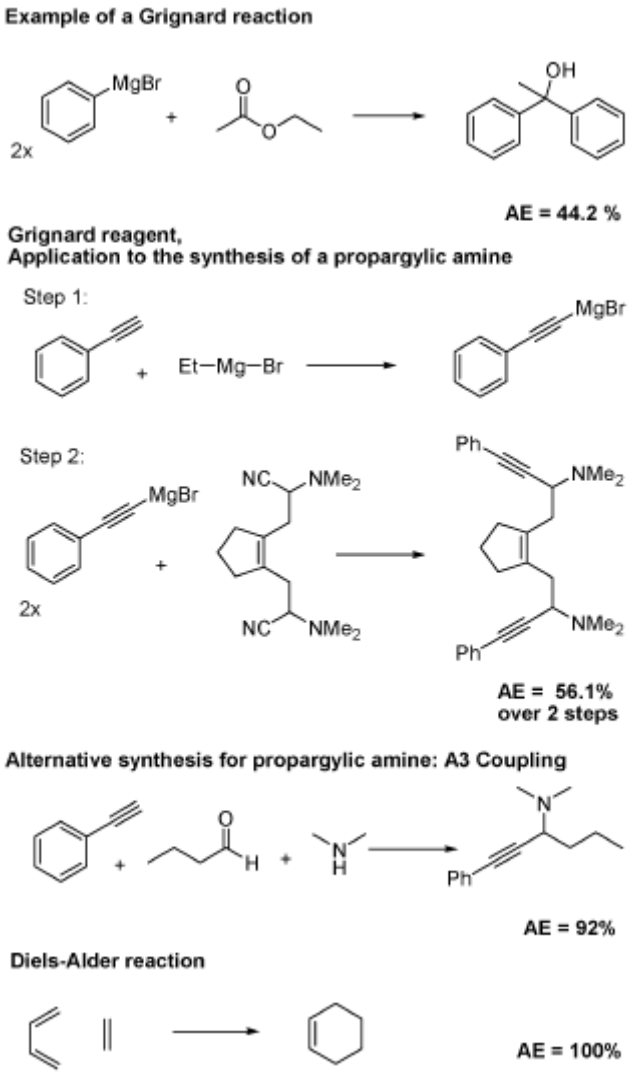

Figure 4: Several illustrations of Atom economy

Moreover, there is a known progress in the synthesis of ibuprofen.[27] The main problem of old synthesis (boots process) is low economic cost, because the utilization of input raw materials is only about 40%. In the 1990s a new "green" method of ibuprofen synthesis was developed, involving only three steps, and almost all transitional materials were converted to the product (up to 99%) or regenerated and returned in the process and almost eliminated the generation of waste materials. This process is one of the processes of "green synthesis".[28,11]

Scheme 4 shows a comparison between classic Boots and "green" Hoechst synthesis of ibuprofen. The new process has much higher atomic efficiency and almost no waste (waste materials are recycled in the process) thus contributing to pollution prevention.

The Boots synthesis consists of six synthetic steps, while the Hoechst process of obtaining ibuprofen consists of only three steps.[7]

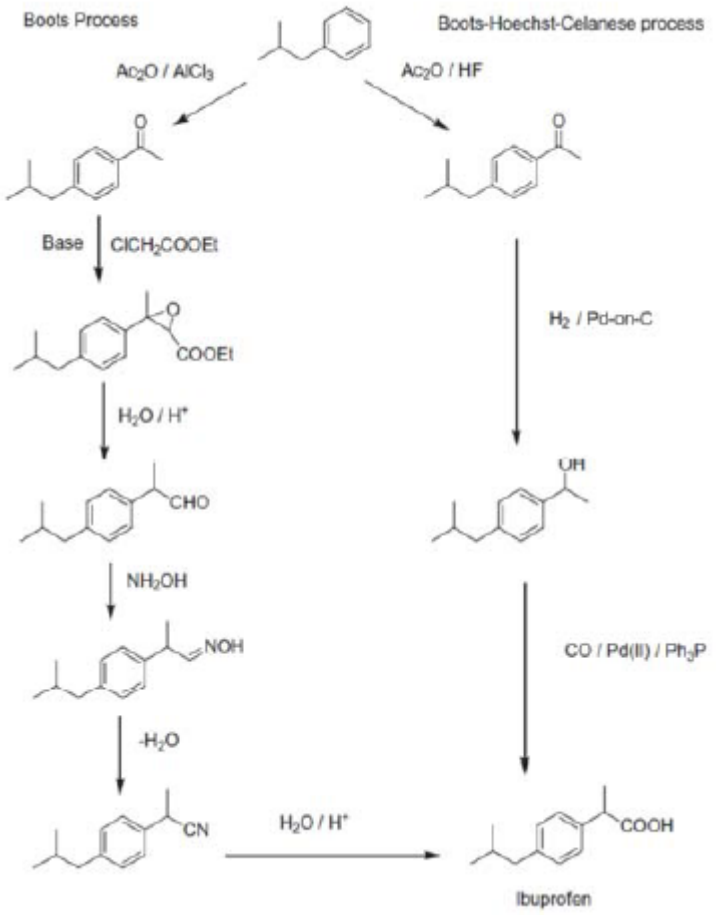

Scheme 4: Comparison of the Boots Process and the "Green" Hoechst Ibuprofen Synthesis Process[7]

1.1.0.2.1 Multicomponent chemistry

Multicomponent reactions (MCRs) are effective, flexible, and elegant one-pot procedures that usually involve three or more reagents as input material and give, as output, a final product containing almost all the atoms of the starting materials. Over time, MCRs have attracted significant attention from the medicinal chemistry point of view due to the possibility to synthesize complex heterocyclic scaffolds and heteroatoms containing derivatives with high biological activity. Although MCRs have been known for more than 150 years, they represent a modern synthetic tool in accordance with present time sustainability and green concerns. MCRs are fully connected with the twelve principles of Green Chemistry, as proposed by the pivotal study of Anastas and Warner in 1998,[29,30] especially regarding the minimum waste production and the use of alternative solvents. According to the third principle of Green Chemistry introduced by Barry Trost in 1990, MCRs are

an efficient tool for the "Atom Economy" strategy,[26] in order to convert all the starting materials in the final product in a highly conservative manner. As a result, the desired final compound is characterized by a high degree of chemical complexity. Among the benefits of MCRs, there is also the "Step Efficiency", that is, the possibility to reach a high product selectivity, maximizing the yield and minimizing the number of synthetic steps. This leads to the reduction of the overall working time, maintaining a high purity, low waste production, and a limited cost for the purification procedures.[30] In terms of sustainability, these green conditions represent an extraordinary goal.[31] MCRs are traditionally expected to occur at room temperature and environmental pressure, but nowadays, innovative technologies have been proposed with the aim to further increase the energy efficiency of the process. Above all, modernization of MCRs by the use of microwave-assisted synthesis has been reported, as well as the use of organo- and transition-metal catalysis or visible-light photochemistry. The combined use of these tools is a valid approach for lowering the activation energy of the process. Photochemical and microwave-assisted protocols allow the conversion of stable reagents into reactive intermediates, making the reaction conditions safer, selective, fast, and less expensive.[32] The first description of MCRs is dated back to 1838 when Laurent and Gerhardt reported the synthesis of cyano-imine (**b**) by mixing ammonia, hydrogen cyanide and two parts of benzaldehyde (Scheme **5** panel A). This three-component process was proceeded by the initial formation of α-aminonitrile (**a**), followed by the final conversion to (**b**) in the presence of the second aliquot of benzaldehyde. In 1850, the Strecker synthesis of α-aminocyanides, always involving α-aminonitrile (**c**) was reported in the field of the Origin of Life Study (Scheme **5** panel B).[33] The final product of the Strecker procedure is the α-amino acid (**d**) isolated after acidic hydrolysis (Strecker's amino acid synthesis). After these examples, many different MCRs were developed and classified according to the nature of the reaction intermediate into; i) isocyanide-based and ii) non-isocyanide or imine-based processes.[34] The Passerini and the Ugi reactions fall in the isocyanide-based MCRs. Passerini discovered a three-component procedure (P-3CR) for the synthesis of acyloxycarbonamides (**e**) from a mixture of carboxylic acid, carbonyl compound, and isocyanate derivatives (Scheme **5** panel C). In 1951, Ugi reported a four-component reaction (U-4CR) in which condensation occurred between aldehyde, amine, carboxylic acid, and isonitrile in a polar protic solvent (Scheme **5** panel D).[35] The U-4CR allows the preparation of α-aminoacyl amides (**f**) with peptidomimetic property in bio-medical applications. Strecker, Hantzsch and Biginelli reactions are characteristic of the non-isocyanide or imine-based MCRs. Hantzsch reported, in 1881, a three-component procedure (H-

3CR) during which β-ketoesters, aldehydes and ammonia are mixed to afford highly decorated dihydro-pyridine derivatives (**g**) (Scheme **5** panel E).[36] As an alternative, Biginelli described the threecomponent synthesis (B-3CR) of 3,4- dihydropyrimidin-2-(1H)-ones (**h**) from aldehydes, (thio)ureas and β-ketoesters (Scheme **5** panel F).[37]

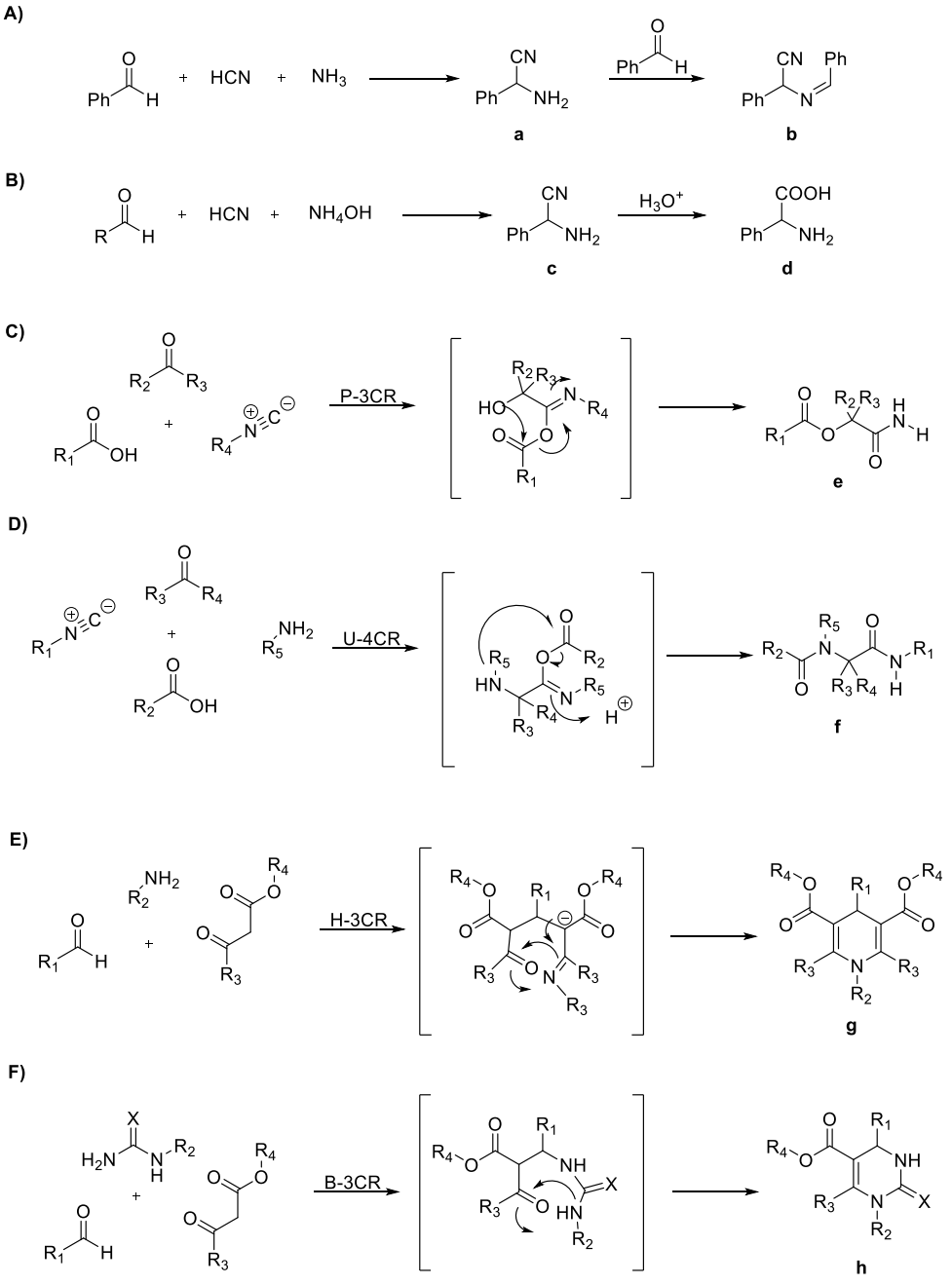

Scheme 5: Panel A) Laurent and Gerhardt synthesis of cyano-imine 2; panel B) Strecker's amino acid synthesis; Panel C) P- 3CR; Panel D) U-4CR; Panel E) H-3CR; Panel F) B-3CR.

MCRs are a very useful tool in medicinal chemistry and drug discovery, favouring the identification of lead compounds and the construction of a library of derivatives, as well as the design of large-scale drug preparations. In this context, the company Hofmann LaRoche described the synthesis of two trombine inhibitors through the U-4CR procedure,[38,39] and Merck Sharp & Dohme Corp. reported the production of a novel HIV protease inhibitor Crixivan® (Indinavir) by U-4CR.[40] MCRs were applied in the synthesis of antiviral compounds active against DNA and RNA viruses.[41] Viral pathogens, represent a serious threat for global health. MCR processes were successfully employed to obtain a variety of antiviral agents against HBV, HCMV, orthopox virus, HADV, VZV, HSV, HCV, coronaviruses, Influenza A and B, Dengue, TMV, and HIV endowed with remarkable activity and various mechanisms of action. The possibility to apply these highly versatile and useful protocols to the development of broad-spectrum antiviral agents is a possible and desirable future scenario in the areas of medicinal chemistry and drug discovery. The identification of drug candidates able to target more than one pathogen will represent a possible solution in case of infection by well-known viruses.

Influenza A virus

Influenza, commonly known as the "flu", is an acute viral infection that affects the upper respiratory tract and sometimes infects the lungs, and which is transmitted from person to person. Influenza comes from the Latin word influentia, meaning “influence of the stars”. In ancient times people didn't know that flu is caused by a viral infection but they thought that the stars influenced the spread of influenza. The name of this illness in fact, reflects that belief. In the early 1930s Richard Shope isolated influenza virus from infected pigs and from humans. This revolutionary discovery has proved that a virus, not a bacterium, as widely believed, caused influenza.[42] Influenza viruses continue to represent a severe threat worldwide that have substantial economic impact due to the costs of prevention and treatment, work absenteeism, physician visits and excess hospitalizations.[43] These annual epidemics are estimated to result about 3 to 5 million cases of severe illness and about 250000 to 500000 deaths. Influenza viruses belonging to the Orthomyxoviridae family, are enveloped viruses and are characterized by a segmented single-stranded RNA genome. There are four types of influenza viruses: A, B, C and D. Human influenza A and B viruses cause seasonal epidemics of disease almost every winter. Influenza type C infections generally cause a mild respiratory illness and are not thought to cause epidemics. Influenza D viruses primarily affect cattle and are not known to infect or cause illness in people. Influenza A viruses are divided into

subtypes based on two proteins on the surface of the virus: the hemagglutinin (HA) and the neuraminidase (N). There are 18 different hemagglutinin subtypes and 11 different neuraminidase subtypes (H1 through H18 and N1 through N11 respectively).[44] A characteristic that distinguishes the influenza A viruses from influenza B and C, is their capability of infecting a wide variety of avian species, humans, and several mammals, including swine, horses, cats and dogs. The genomes of influenza viruses are changeable due to point mutations and recombination events that contribute to the evolution of new variants and strains with epidemic or pandemic potential, as the recent global pandemic caused by the origin swine influenza A/H1N1 virus in 2009, a viral subtype that has led to 18000 deaths. Influenza viruses cause annual epidemics and occasional pandemics that have claimed the lives of millions. The emergence of new strains will continue to pose challenges to public health and the scientific communities.[45] Influenza A viruses have a complex structure and possess a lipid membrane (envelope) derived from the host cell. Inside this envelope there are eight segments of single-stranded negative sense RNA that conventionally, are defined from largest to smallest.[46] Every segment encode for 16 proteins, some of them protein are most important for the virus life-cycle.[47] This gene products are subdivided into early proteins or late proteins in function of the infection phase. Three segments encode proteins that form the virus polymerase complex: basic polymerase 2 (PB2) which controls the recognition of host-cell RNA; basic polymerase 1 (PB1), which catalyses nucleotide addition (and which also encodes a small proapoptotic mitochondrial protein that is translated in a different reading frame PB1-F2); and the acid protein (PA), which might possess a transcriptase protease activity.[46] This three polymerases associated with the nucleoprotein (NP) form helical ribonucleoprotein capsids (vRNPs). After infection, the vRNPS are transported to the host cell nucleus, where they undergo transcription and replication.[48] Haemagglutinin and neuraminidase are the two major viral envelope glycoproteins, there are late gene products. The matrix (M1), transmembrane (M2) and second non-structural (NS2) proteins are also transcribed by late genes. The life cycle of influenza A viruses is similar irrespective of strain shown in Figure 5.[45]

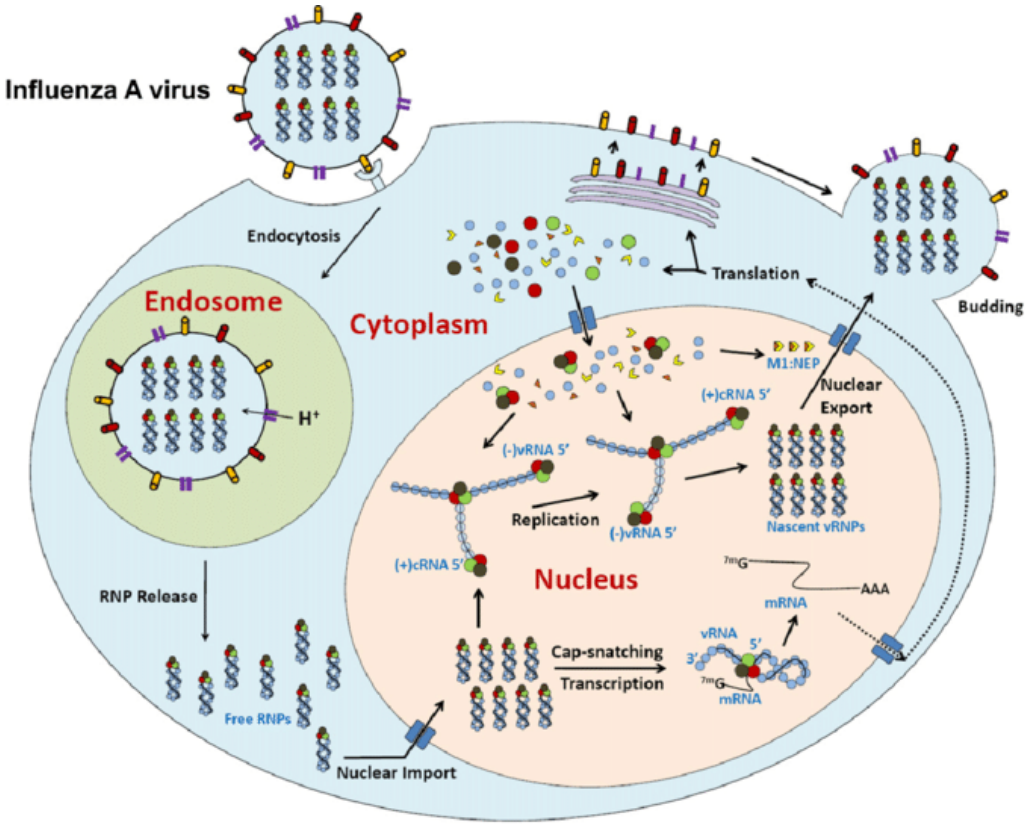

Figure 5: Influenza A Virus life cycle.

The replication of virus starts by a binding between sialic acid galactose link to a cell surface glycoprotein or glycolipid and haemagglutinin on the virus. The virion is taken up in an endocytic vesicle, where acidification activates cellular proteases that cleave haemagglutinin, leading to the release of a fusion peptide and a conformational change that bring viral and endosomal membranes together. Acidification also produces a flow of protons through the M2 ion channel into the interior of the virion, causing the RNPs to dissociate from the M1 matrix and be released into the cytoplasm. After that, they are transported to the nucleus, where a viral polymerase complex performs transcription and replication. The resulting mRNAs move to the cytoplasm and are translated, producing new RNP protein components that are transported back to the nucleus to associate with nascent genome segments. The exit of new RNPs from the nucleus is aided by the viral NS2 (nuclear export protein, NEP). Meanwhile, nascent HA, NA and M2 molecules pass through the Golgi apparatus and undergo glycosylation before moving to the cell membrane. Virion assembly occurs as RNPs and M1 proteins associate with cytoplasmic tails of HA and NA. Successful release of new virus particles requires that NA cleave sialic acid from galactose on the cell surface or on adjacent virions to prevent HA binding.[49] The therapeutic efficacy of current

vaccines and drugs is limited due to the multidrug-resistant influenza viruses' phenomenon. Actually, there are two classes of FDA-approved molecules against the influenza virus, namely M2 channel blockers and neuraminidase inhibitors. Oseltamivir phosphate (Tamiflu), a neuraminidase inhibitor for the treatment of both type A and type B human influenza, is one of the most promising drugs.[50]

2.1 Prebiotic Chemistry

One of the most asked questions by science concerns precisely the modalities and conditions that led to the origin of life. Prebiotic chemistry plays a central role in investigating the possible scenarios of early chemical environments. Its goal is to shed light on the events involved in the synthesis of the initial biomolecules and on the self-organizing processes that led to "the last universal common ancestor" LUCA, the progenitor of all forms of life known to date.[51]

The origin of life is one of the most studied topics in science.[52,53,54]

Probably, it occurred on Earth between 3.8 and 4.1billion years ago.[55]

Prebiotic chemistry focuses on the chemical processes that occurred on the erly Erth before the appearance of the life.[56]

It is generally recognized that RNA is the most relevant molecule for the origin of life (RNA world), since its specific catalytic and storage information properties.[57,58]

The classic Miller–Urey experiment demonstrated that amino acids can be synthesized from a primitive atmosphere under conditions comparable to that existing on the early Earth. Various sources of energy have been proposed for these transformations, including electric discharges, redox processes and radiation. Other approaches (such as "metabolism-first" hypotheses) highlight the role of catalysis to provide biomolecules.[59]

These processes are not confined to early Earth, since complex molecules are continuosly found in the Solar System and in the interstellar space, suggesting the generality of the phenomenum.[60,61]

Molecules can be transferred from space to planets by meteorites, asteroids or cosmic dusts, a way that in principle is available for simple micro-organisms (the "panspermia" hypothesis).[62,63,64]

The panspermia hypothesis therefore answers questions of where, not how, life came to be. It only postulates that life may have originated outside of the Earth. Nonetheless, Earth remains the only place in the Universe known to harbour life,[65] and fossils evidence from the Earth supplies most studies of abiogenesis. The age of the Earth is about 4.54 billion years;[66] the earliest undisputed

evidence of life on Earth dates from at least 3.5 billion years ago,[67] possibly as early as the Eoarchean Era, when the crust started to solidify following the earlier molten Hadean Eon.
Microbial mat fossils have been found in 3.48 billion-year-old sandstone in Western Australia.[68]
Other early physical evidence of biogenic substances includes graphite[69] and possibly stromatolites discovered in 3.7billion-year-old metasedimentary rocks in southwestern Greenland, as well as "remains of biotic life" found in 4.1billion-year-old rocks in Western Australia.[70]
According to a scientist who commented on the study, "If life arose relatively quickly on Earth … then it could be common in the universe".

2.1.0 Formamide

Formamide (chemical formula: NH_2CHO) is the simplest natural amide. This compound contains in its structure all the elements required for the synthesis of biomolecules, including hydrogen, carbon, oxygen and nitrogen with the only exception of phosphorus and sulfur. In recent years, the prebiotic chemistry of formamide has provided a unique and simple synthetic framework for the formation of components of nucleic acids (purine and pyrimidine nucleobases, nucleosides and nucleotides), amino acids, sugars, amino sugars and carboxylic acids, including important intermediates for cellular metabolism.[71] The formamide is a ubiquitous molecule in the universe, was detected in comets,[72] as in the case of the comet C / 1995 O1 (Hale-Bopp),[73] in the solid phase in granules around the young stellar object W33A and generally in the interstellar space. Furthermore, recent studies suggest the presence of formamide on some moons of the solar system, including Titan and Europa, where it has been postulated the presence of liquid formamide (pure or partially mixed with water) below the frozen surface.[74]
Several experimental and theoretical studies have been conducted to determine how the formamide can be originated in space.[75] This molecule can be synthesized from mixtures of methane and nitrogen under proton radiation (solar wind and cosmic ray radiation)[76] or from frozen hydrogen cyanide (HCN), water and ammonia (NH_3) by irradiation with ultraviolet rays.[77]
The formamide can also be synthesized in terrestrial conditions from mixtures of low molecular weight compounds such as NH_3, formic acid (HCOOH), carbon monoxide and alcohols under both catalysed and uncatalyzed experimental conditions.[70]
Among these routes of synthesis, probably the one that has most significant in terms of chemical terrestrial prebiotic, is the formation of formamide for HCN hydrolysis, a molecule presents in

significant concentration on the primitive Earth. The HCN in aqueous solution can result in two processes: the polymerization in biomolecules or hydrolysis to formamide. The hydrolysis predominates in dilute solutions, while the polymerization takes place at higher concentrations.[78] The estimated concentration of HCN in the ocean primitive was too low to give rise to polymerization reactions, thus favouring the formation of the formamide.[78,79]

An interesting property that characterizes the formamide, as a precursor prebiotic, is linked to the possibility of a partial thermal degradation to generate a group of low molecular weight compounds which turn out to be, in turn, useful intermediates for the prebiotic synthesis of biomolecules, thus increasing the number and variety of possible ways of transformation.[80] Formamide decomposes thermally into NH_3 and CO or HCN and H_2O (Figure 6). The formation of HCN is usually favoured in the presence of suitable catalysts, while in their absence predominates the formation NH_3 and CO.[81]

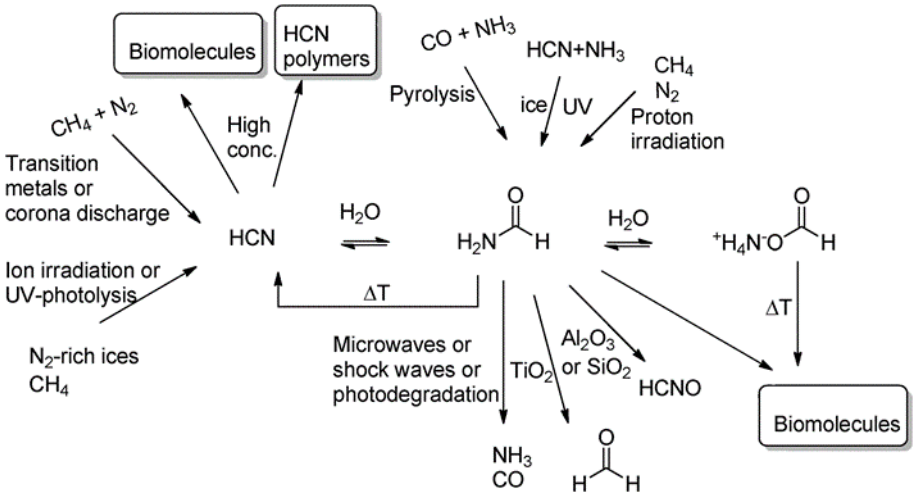

Figure 6: Formation, degradation and evolution of formamide.

Furthermore, in the moment in which the formamide is in the presence of suitable metal oxides (such as titanium dioxide) can degrade to form (HCOH) formaldehyde, the precursor prebiotic currently most studied for the origin of the sugars. The synthetic potential of formamide is also incremented by particular physical conditions, such as by the action of microwave or high pressures.[82] Due to its high dielectric constant, the formamide is also a good solvent for both the polar organic compounds and inorganic, the latter play an important role in the synthesis of prebiotics processes by acting as catalysts.[83]

The balance between formamide and HCN has made it possible to develop reactions in which these two molecules coexist to give increasingly complex products from the structural point of view up to the formation of biomolecules.

2.1.0.1 Formation of purines and pyrimidines passing through HCN chemistry.

The chemistry of a simple molecule such as HCN is generally considered as the preferential route for the synthesis of purine and pyrimidine derivatives. HCN may have been a key ingredient for the formation of the first biomolecules or of their precursors.

The first evidence of a contribution of HCN to the synthesis of pre-biological molecules came from the pioneering experiment (1952) of Urey and Miller,[84] rightfully considered as the founding of the "prebiotic chemistry" research field. This experiment aimed to verify the Oparin-Haldane theory (Oparin-Haldane, 1938) according to which simple prebiotic organic molecules were first formed under the effect of external energy sources (lightning or UV solar photons) in a primordial reduced (oxygen free) atmosphere, where CH_4, H_2 and NH_3 were the prevailing gases, and then accumulated in the warm primitive ocean to form a "primordial soup". Following random chemical processes occurring in this soup, self-replicating molecules (proteins or nucleic acids) would have formed, thus opening the road to life. Oparin and Haldane were the first to indicate HCN and formaldehyde as the primordial components of the early soup from which all complex molecules would have spontaneously formed.

HCN is an ubiquitary molecule in the universe.[85] It has been detected in large amounts (c.a. 1 %) in comets,[86] in interplanetary dust,[86,87,88] in the atmosphere of planets[89] and on the surface of moons.[90] HCN may be formed under prebiotic conditions by electric discharges[91] and shock waves.[92]

The mechanism of formation of purines from HCN has been studied in detail by several authors due to its relevance for the prebiotic accumulation of nucleic acid bases on the primitive Earth.

Ferris and Orgel first suggested that the HCN trimer, aminomalonitrile (AMN)[93] and the HCN tetramer, diaminomalonitrile (DAMN),[94] were important intermediates for these transformations. Aminomalonitrile (AMN) is obtained by the initial addition of cyanide (CN-) to HCN. Further addition of HCN to AMN yields DAMN. Starting from these data, the mechanism of Orò's synthesis was explained as follows: AMN is supposed to react with formamidine to give 4-aminoimidazole-5-carbonitrile (AICN), a compound which readily yields a variety of purines under plausible prebiotic conditions.[95,96] This synthesis is not possible in dilute solutions because of the competing hydrolysis of formamidine to formamide. On the other hand, irrespective of the

formamidine concentration, DAMN can be directly transformed into AICN by photochemical rearrangement in essentially quantitative yield.[96] AICN and a product of its hydrolysis, 4-aminoimidazole-5-carboxamide (AICA), reacts with HCN, cyanide (NCO-), formamidine, or cyanogens $(CN)_2$ to give adenine, hypoxanthine, diaminopurine, xanthine, isoguanine and guanine, respectively. According to Eschenmoser's suggestions, the current biological processes can be considered as being chemomimetic of the first prebiotic syntheses (Scheme **6**).[97,98,99]

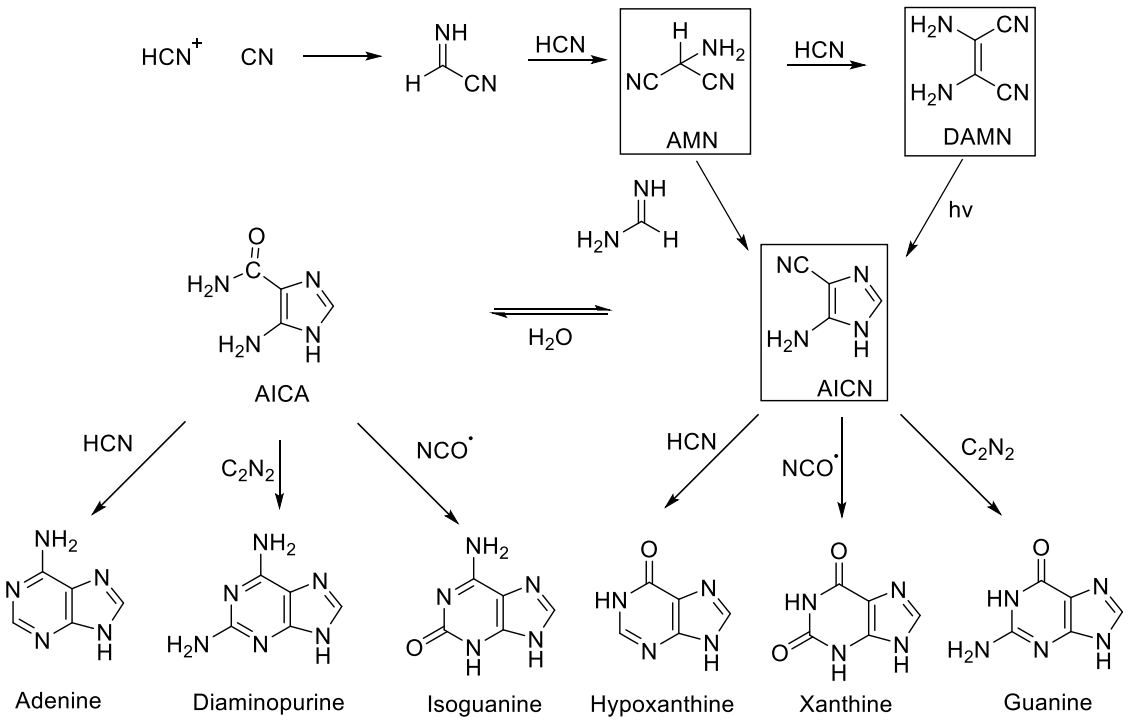

Scheme 6: Prebiotic synthesis of purine starting from HCN.

Depending on the polymerization and reactions conditions, on the analytical tools, besides purines and pyrimidines, also a great variety of other compounds of biological interests, including amino acids, carboxylic acids, aldehydes, and ketones, pteridines, hydantoins, urea etc. have been identified. The main biomolecules identified in HCN polymers are listed in Figure 7, taken from the comprehensive review published by Ruiz Bermejo et al.[100]

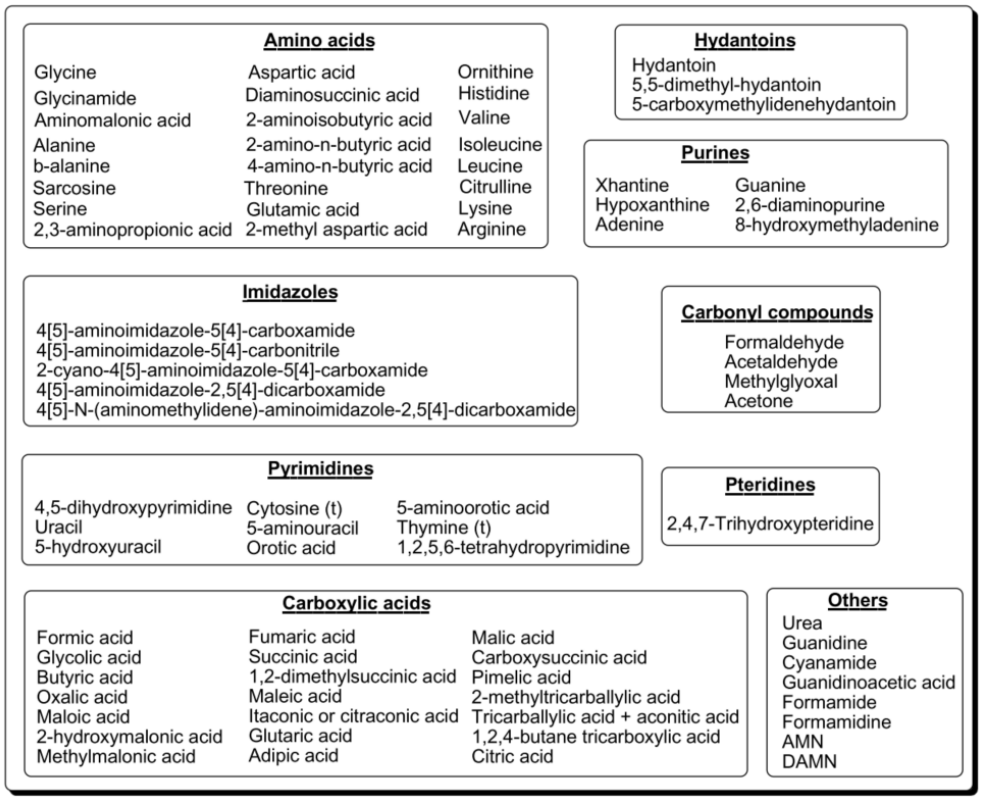

Figure 7. Summary of the simple organics and bio monomers identified in HCN polymers.[100]

Many of these organic compounds are building blocks of current proteins and nucleic acids or are active participants in metabolism. On the basis of this short resume, the central role attributed nowadays to HCN and formamide in the chemical evolution processes appears fully justified.

2.1.0.2 Peptide nuclei acids (PNAs)

Peptide nucleic acids (PNAs) played a key role in prebiotic chemistry as a chimera between RNA and proteins.[101]

Peptide nucleic acid (PNA) is a nucleobase oligomer in which the entire backbone has been replaced by a backbone composed of *N*-(2-aminoethyl)glycine units. Peptide nucleic acid was discovered during the 1990s as a result of the combined efforts of biochemist Peter Nielsen's and organic chemist Ole Buchardt's groups. Based on the observation by flow linear dichroism that aromatic chromophores form stacked complexes with α-helical poly-γ -benzylglutamate (PBG), it was proposed that PBG with alternating nucleobases and acridine moieties could bind sequences selectively to duplex DNA by combined Hoogsteen base pair formation (the type of base pairing

that occurs between adenine and thymine where adenine N7 acts as the hydrogen bonding acceptor rather than N1 of the Watson–Crick geometry) and intercalation with the helical backbone in the major groove. The proposed peptide nucleobase compound was given the name peptide nucleic acid (PNA). PNAs as we know them today have a backbone made from repeating *N*-(2-aminoethyl)glycine units linked by peptide bonds.[102,103,104,105] The different bases (purines and pyrimidines) are joined to the backbone by methylene carbonyl linkages. Unlike DNA or other DNA analogues, PNAs do not contain any pentose sugar moieties or phosphate groups. They are depicted as peptides from the N terminus to the C terminus, corresponding to the 5' to 3' direction as in DNA (Figure 8). Because all intramolecular distances and the configuration of the nucleobases are similar to those in natural DNA molecules, specific hybridisation occurs between PNA and DNA or RNA sequences by hydrogen bonding (Figure 8).

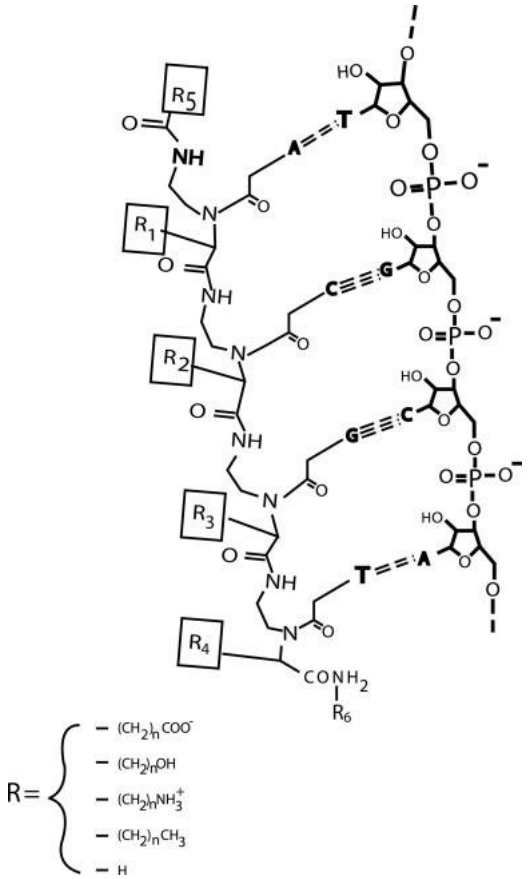

Figure 8: Comparison between PNA and DNA with hydrogen bonding shown between them.

The uncharged nature of PNA is responsible for the better thermal stability of PNA/DNA duplexes compared with their DNA/DNA equivalents. As a result, single-base mismatches have a

considerably more destabilising effect. As with DNA, the decrease in duplex stability depends on the position of the mismatch within the sequence. The neutral amide backbone also enables PNA to hybridise to DNA molecules under low-salt conditions, because no positive ions are necessary for counteracting the inter-strand repulsion that hampers duplex formation between two negatively charged nucleic acids. Consequently, the abundance and stability of intramolecular folding structures in the DNA or RNA analytes are significantly reduced, making the molecules more accessible to complementary PNA oligomers. Furthermore, PNA is stable across a wide range of temperatures and pH values,5 unlike DNA which depurinates under acidic conditions. However, under alkaline conditions a rearrangement of the PNA molecules might occur. Additionally, PNA is resistant to nucleases and proteases.[106]

PNAs and PNA analogues exhibit unique features useful for therapeutic applications: firstly, they are resistant to nucleases and proteinases, secondly, they can be modified to obtain molecules able to be selectively delivered to target cells. Delivery of PNAs is expected to be one of the major research field in the future. On the other hand, PNAs exhibit extremely interesting effects in molecular recognition, being able to generate highly stable PNA/DNA and PNA/RNA hybrid molecules and (PNA)2-DNA triplexes. Accordingly, PNAs have been proposed for antisense therapy (target molecules: mRNA, rRNA), antigéne therapy (target molecules: genes involved in human pathologies), decoy approach (target molecules: transcription factors).[107,108,109]

Finally, consistent results allow to propose PNAs as anticancer, antibacterial and antiviral agents as well as molecules against medically important parasitic organisms.

An example of applications of PNAs as antiviral agents is represented by recent papers using the HIV-1 LTR as a model system. For instance, Mayhood et al.[110] demonstrated that PNAs targeted to TAR hairpin element are able to inhibit Tat-mediated transactivation of HIV-1 LTR transcription. It is known that Tat, an essential HIV-1 protein, interacts with the TAR element and stimulates transcription from the viral LTR. Blockage of Tat-TAR interaction halts viral transcription and hence replication. These authors found that PNAs targeted to the TAR sequences of viral RNA genome is able to prevent Tat-TAR interaction by efficient sequestration of the TAR. PNA targeted to the TAR sequence of the viral genome may be a potential inhibitor of HIV-1 gene expression. On the other hand, Lee et al.[111] found that PNAs and PNA-DNA chimeras targeted to the primer binding site of the HIV-1 RNA genome blocks in vitro HIV-1 reverse transcription. These observations suggest that oligomeric PNAs targeted to various critical regions of the viral genome

are likely to have strong therapeutic potential for interrupting multiple steps involved in the replication of HIV-1.

2.1.1 The role of meteorites in prebiotic chemistry

It is assumed that meteorites played a role in the origin of life, behaving as carriers of organic compounds during the Heavy Bombardment period on Earth[112] before the earliest appearance of living organisms.[113]

Meteorites were considered to be involved in the origin of life on this Planet for several functions and at different levels: (i) as providers of impact energy during their passage through the atmosphere; (ii) as agents of geodynamics, intended both as starters of the Earth's tectonics and as activators of local hydrothermal systems upon their fall; (iii) as sources of organic materials, at varying levels of limited complexity; and (iv) as catalysts.[114]

In particular, it is necessary to get an overview of the catalytic on the catalytic activities of the various types of meteorites in reactions relevant for prebiotic chemistry.

The starting material selected for testing the catalytic properties of different types of meteorites was formamide. In prebiotic chemistry, formamide can be considered a substrate, a solvent, and a catalyst itself. Why is formamide so interesting from a prebiotic point of view?

Formamide (NH_2CHO) is a simple molecule, a logical starting point for reconstituting prebiotic syntheses because of its availability,[115, 116,117], stability,[118] and solvent properties due to is a possible prebiotic solvent alternative to water.[119,120,70] Previous studies have established that in the presence of catalysts of terrestrial origin, formamide affords the five nucleic bases biologically extant ones and others, numerous carboxylic acids, several aminoacids, condensing agents, long-chained aliphatic compounds, and a large body of miscellanea.[119,120]

The catalysts analysed were calcium carbonate, alumina, silica, zeolite, titanium dioxide, clays of the montmorillonite family, cosmic dust analogues (CDAs) of terrestrial olivines (from fayalite to forsterite), mineral phosphates, iron-sulphur and iron-copper-sulphur minerals, zirconium minerals, and borate minerals. The results showed that all the catalytic systems analysed were active, yielding different mixtures varying according to the catalyst used.

It has been considered the catalytic role of several types of meteorites in the chemistry of formamide using different sources of energy: thermal,[121,122,123] proton irradiation from accelerated Helium,[124] and high-energy radiation from accelerated Boron.[125]

In all type of experiments, meteorites were used as powered fractions of the original sample and selected as representative of the four major classes such as iron, stony-iron, chondrites, achondrites.

2.1.1.0 Thermal Energy

It has been reported experiment in which formamide was heated at low and high temperature (60°C or 140 °C) in the presence of appropriate meteorite dust: Canyon-Diablo, Campo-del-Cielo, and Sikhote-Alin as Iron meteorites, Seymchan and NWA 4482 as Stony-Iron; NWA 2828, Gold Basin, Dhofar 959, Murchison, NWA 1465 as Chondrites and NWA 5357 and Al-Haggounia as Achondrites.[123] The results showed the one-pot synthesis of an astonishingly reach and composite panel of compounds of prebiotic interest, encompassing heterocycles (nucleic bases), carboxylic acids, amino acids, and a rich miscellanea of low-molecular-weight compounds including potential condensing agents like carbodiimide and urea. Remarkably, among the recovered nucleic bases, uracil, cytosine, adenine, guanine, and the closely related species isocytosine, dihydrouracil, and hypoxanthine, were observed. Among the amino acids, glycine, alanine, valine, leucine, and phenylalanine were detected. Carboxylic acids were observed up to C-9, nonanoic acid (Scheme 7).

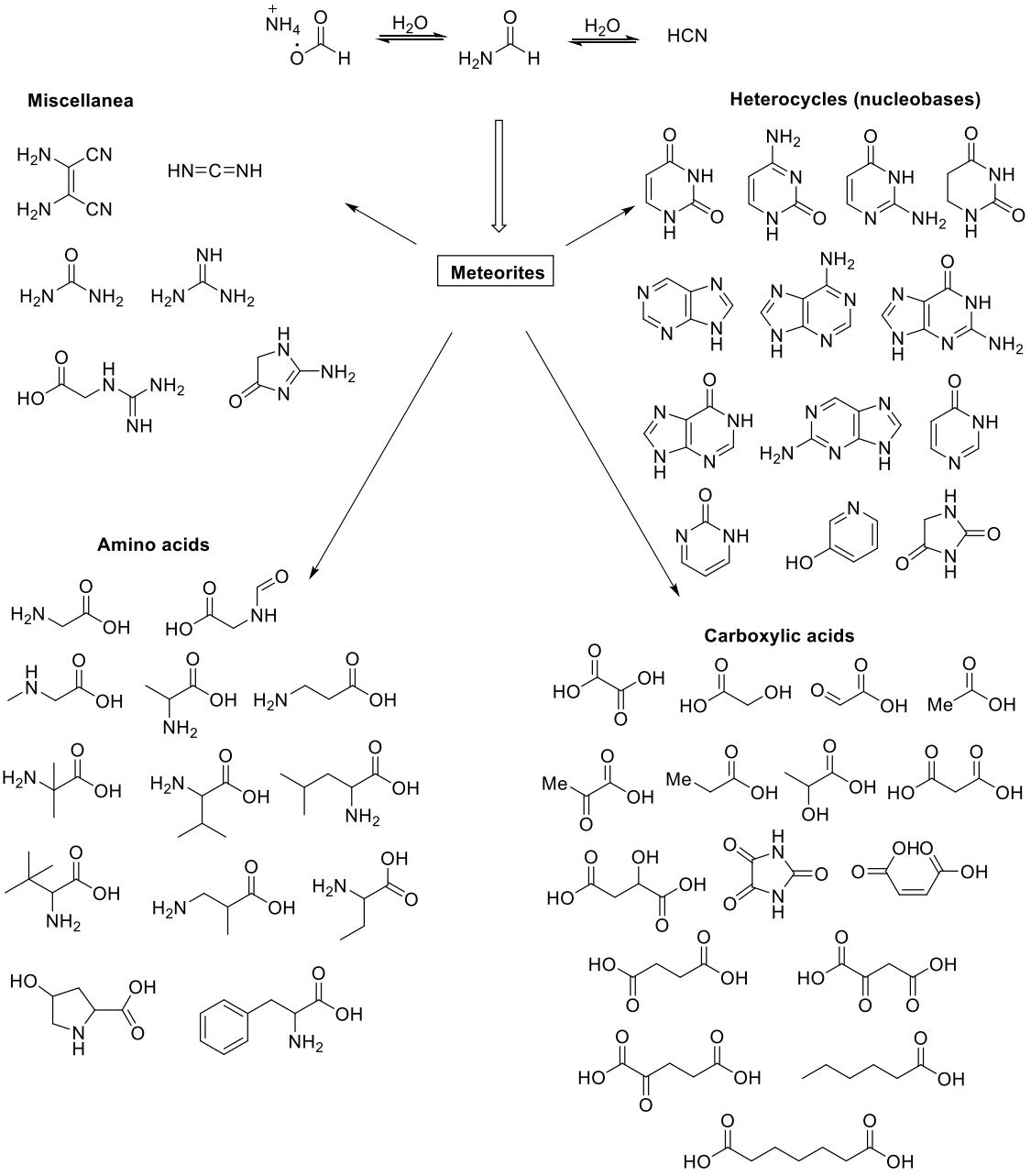

Scheme 7: Synthesis of biogenic molecules from formamide catalysed by meteorites.

The general order of reactivity of meteorites was iron and stony-iron major of achondrite and chondrite.

The yield and the composition of the products varied as a function of the meteorite, but the panel of compounds obtained was in each case a composite and representative of a potential "prebiotic soup". This may be taken as an indication that meteorite-catalysed syntheses could have occurred in several of the early Earth environments.[123]

2.1.1.1 Proton Irradiation

A set of meteorites similar to that analyzed for thermal energy-driven reactions was analyzed for reactions occurring at a low temperature under irradiation with accelerated protons, thus mimicking the solar wind/flare radiation.[124] As for thermal energy-driven reactions, the synthesis of a large panel of molecules was observed. The products isolated from the reaction mixtures were carboxylic acids as long as C20 (arachidic acid); amino acids (glycine, alanine, proline); nucleic bases (uracil, thymine, cytosine, adenine and guanine, among others); and, notably, sugars (ribose, 20-deoxyribose, glucose, 20-deoxyglucose, among others) (Scheme 8).

Most notably, four nucleosides, namely cytidine, uridine, adenosine, and thymidine, were synthesized. The detailed mechanism involved in the selective formation of the β-glycosidic bond has been reported for the reaction catalyzed by the chondrite NWA 1465.[126] In summary, sugars and nucleic bases are synthesized separately from formamide by a radical cyanide based mechanism,[124] and they can then be regio- and stereo-selectively connected through the formation of a C1 sugar-centred radical intermediate.[126] Formation of the β-glycosidic bond, that so far required complex laboratory procedures and external interventions, may thus occur in a one-pot reaction.

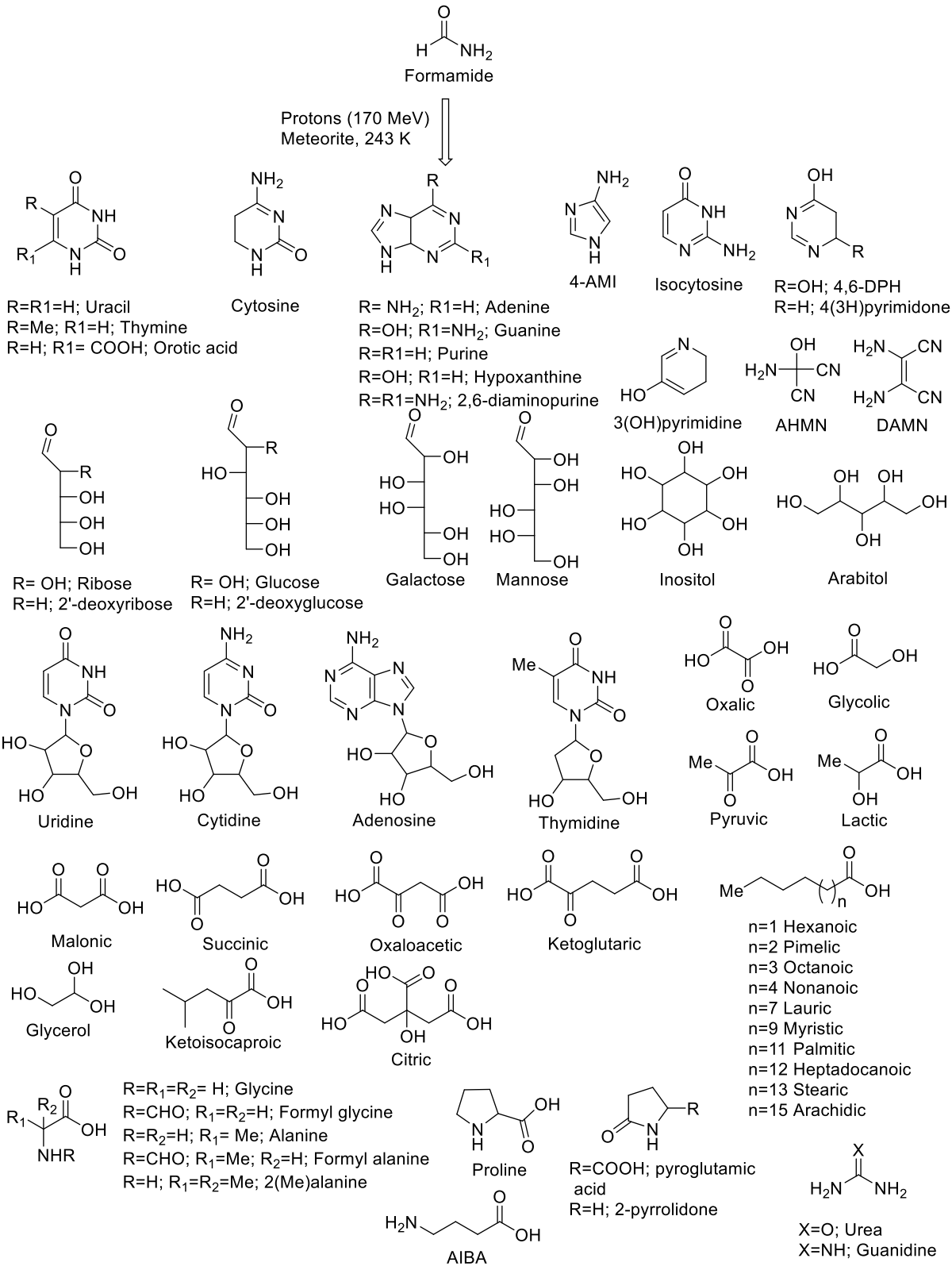

Scheme 8: Products of high energy proton irradiation of formamide in presence of meteorites.

These results show that, as an alternative to heat, radiation is a plausible and powerful energy source for prebiotic processes.[124,125,126,127] As a general trend, stony-iron, chondrite and achondrite meteorites were more active than iron meteorites. The major conclusion from this analysis is that meteorites perform as catalysts under proton irradiation conditions as exemplified by the high yields obtained, and by the one-pot synthesis of molecules as complex as ribo- and 2'-deoxy ribonucleosides.

2.1.1.2 Heavy Ion

A large panel of compounds was also observed in the case of ^{11}B-boron beams as energy source that was studied because of the interstellar abundance of boron in our Galaxy, and because of its presence in cosmic rays near the Earth.[127,128]

Compounds including purine and pyrimidine nucleic bases (uracil, cytosine, adenine, and guanine), nucleic base analogues, heterocycles, and carboxylic acids involved in metabolic pathways.[125] The presence of amino imidazole carbonitrile (AICN), 4,6-diamino purine (4,6-DAP), and 2,4-diamino pyrimidine (2,4-DAPy) among the observed products suggested the occurrence of unified mechanisms based on the generation of radical cyanide species. The case of differential purine versus pyrimidine nucleobase synthesis depending on the type of meteorite and of radiation used is noteworthy. With ^{11}B beams, a lower variety of products was detected relative to heat and protons, amino acids, and nucleosides not being observed in the reaction mixtures, probably due to the different penetration depth of the ions.

The overall result of the meteorite-catalysed condensations of formamide[121,122,129,123,130,125,126] is that in each condition tested, independent of the type of meteorite involved, the panel of compounds obtained is variegate and abundant. In addition, formamide in the presence of meteorites condenses into a plethora of prebiotic compounds, independent of the type of energy driving the reactions.

Part 1: Development and application of catalytic procedure to natural substances

Catalysis is one of the most valuable principles out of twelve of Green Chemistry. Catalysis is the science and technology of influencing the rates of chemical reactions. A catalyst is a material that changes the path of a chemical reaction without itself being expended. In this way a small amount of catalyst material can convert a large quantity of reactants and this happens preferentially under milder conditions than would be required by the stoichiometric reaction pathway. If more than one reaction product is possible, the catalyst may change the distribution of these products compared to stoichiometric conversion and thereby allow control of the selectivity of a chemical reaction.[131]

In particular, heterogeneous catalysis is crucial to chemical technology. Chemical bonds are broken and new chemical bonds are formed during the catalytic process. These events occur repeatedly, usually without a significant change of the catalyst. Heterogeneous catalysis allows for the easy separation of products making possible their recycling and reuse, with environmental and economic advantages. Great attention was due to methyltrioxorhenium (CH_3ReO_3, MTO) for the high reactivity and versatility: in combination with H_2O_2, has been demonstrated in recent years as a good catalyst in the oxidative functionalization of several organic substrates.[132,133,134]

1.1 Rhenium based catalysts.

Methyltrioxorhenium, CH_3ReO_3 abbreviated as MTO, is one of the best examined catalysts for the activation of H_2O_2 in oxidation reactions.[135]

MTO is considered a biomimetic of peroxidase, oxide-reductase and cytochrome-p-450.

Peroxidases show a hemoprotein structure and catalyse the oxidation of numerous organic and inorganic compounds, generally with the addition of oxygen, using H_2O_2 as oxidant, which is reduced to H_2O. The oxide-reductase family catalyse the reaction from aldehyde to carboxylic acids or from thiol groups to sulfonic and sulfoxides. Other enzymes such as cytochrome-p-450 are able to perform epoxidation reactions in very specific positions.

The MTO manages to catalyse all the same reactions.

With but eight atoms, the small MTO molecule functions as a versatile catalyst for a considerable breadth of reactions. The essence of its chemistry is the transfer of an oxygen atom from one species to another. The oxygen source is often hydrogen peroxide; molecular oxygen is not activated.

Among reactive rhenium (VII) species, methyltrioxorhenium (VII) (MTO) is an electrophilic homogeneous catalyst largely applied in the activation of environmental friendly hydrogen peroxide

(H_2O_2) by formation of two reactive intermediates, namely monoperoxo [$MeRe(O_2)O_2$] or bis (peroxo) [$MeRe(O_2)_2O$] η2-metal complexes (Figure 1).[136]

The chemistry of MTO is larlegy reviewed[137] including the synthetic applications including oxygen atom insertion in the sigma C-H bond,[138] oxyfunctionalization of bioactive substances,[139] epoxidations, olefin metathesis and aldehyde olefinations, oxidative nucleophilic substitution,[140] oxidative desulfurization (ODS),[141] synthesis of quinone derivatives,[142] Baeyer–Villiger rearrangement,[143] metathesis,[144] methanolysis of glycols[145] and epoxidation of olefins in both traditional[146] and non-conventional medium, such as chiral aliphatic amines,[142] fluorinated solvent[147] and ionic liquids.[148]

The most relevant drawback for the MTO catalyzed epoxidation is the concomitant nucleophilic ring opening of the oxirane ring to corresponding diol, as a consequence of the acidic property and high affinity for the oxygen atom shown by Re (VII).

For this reason, Lewis bases bearing one or more nitrogen atoms, such as pyridine, pyridine derivatives,[134,149] and bipyridines[150,151] are used as additives to inhibit the formation of diols by tuning the electronic properties of MTO.

The real efficacy of these Lewis bases in the control of the selectivity of the epoxidation is related to the stability of the MTO/additive complex, as well as to physical and chemical properties of the reaction medium. As an alternative, anhydrous reaction medium and urea hydrogen peroxide adduct (UHP) can be used to avoid the undesired nucleophilic ring opening of the oxirane ring.[152]

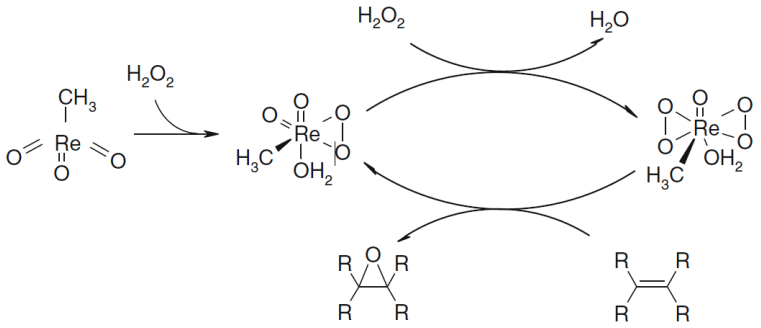

Figure 1: Mechanism of formation of mono and bi-peroxoadducts of MTO and subsequent epoxidation of olefins.

1.1.0 MTO as heterogeneous catalysts.

Very important is the development of heterogeneous catalysts, widely used in the development of new synthetic green chemistry procedures.

Procedures for the immobilization of MTO on appropriate solid supports have been reported by our group in order to overcomes the major problem of selectivity, stability and recyclability of the catalyst.

These procedures were based on the use of both oxygen and nitrogen bearing organic polymers, such as:

- chitin and chitosan;[153] natural polysaccharides are of industrial interest due to their strong absorption capabilities and affinity for transition metals, low toxicity, and versatile biotechnological and biocompatible properties.

  Saladino et al., have been described the preparation and structural characterization of novel rhenium catalysts based on the immobilization of MTO on chitosan, chitin and modified chitosan-bearing N-substituted acyl and alkyl pyridine moieties. Moreover, to further improve the specific surface area and mechanical properties, chitosan and chitin were also adsorbed on silica gel to generate silica–polysaccharide hybrid composites. Their ability to act as MTO supports was then evaluated. The reactivity of these catalysts was studied in the activation of UHP for the epoxidation of alkenes, including acid-sensitive styrene derivatives.[153]

- poly(4-vinylpyridine);[154] the poly-4 vinyl pyridine / MTO system was prepared starting from poly-4-vinylpyridine 2% cross-linked with divinylbenzene (PVP 2%), poly-4 vinylpyridine 25% cross-linked with divinylbenzene (PVP 25%) and poly-4vinylpyridine -N-oxide25% cross-linked (PVPN-25%) as supports.

  The catalysts of the poly-4-vinylpyridine family have been used in the selective epoxidation of different cyclic monoterpenes. The terpenes are the basis of numerous perfumes, detergents, agrochemicals and substances active from a therapeutic point of view, whose oxidative functionality starts with a selective epoxidation.[155]

- MTO/nitrogen ligand complexes microencapsulated in polystyrene;[156] technique that consists of introducing the active species into a polymer capsule. The polystyrene with a low degree of cross-linking (2% cross-linked with divinylbenzene, PS2%) was used to coat and isolate Lewis acids on the basis of a physical entrapment by the polymer and on the electronic interaction between the electrons π of the benzene ring and the metal center.[157] In

principle, the reactivity and selectivity of MTO in these compounds can be tuned by the chemical–physical properties of the ligand and of the support showing the advantages of the ligand accelerated catalysis and the environmental benefits of heterogeneous systems.

Saladino et al., have been reported the preparation and applicability of novel microencapsuled Lewis base adducts of MTO with monodentate and bidentate, aromatic and aliphatic nitrogen containing ligands, for the epoxidation of olefins and monoterpene derivatives, including acid-sensitive substrates.

Microencapsulated Lewis base adducts of MTO were more reactive than their homogeneous parent compounds even in the absence of the excess of ligand. They were also stable catalytic systems for several oxidations.[157]

Inorganic supports, such as niobia,[158] zeolites,[159] and alumina,[160] have been also reported in literature.

More recently, MWCNTs wrapped with poly(4-vinylpyridine)/MTO heterogeneous systems showed high reactivity in the oxidation of recalcitrant sulfur derivatives during oxidative desulfurization of synthetic diesel fuel,[161] suggesting the benign role that MWCNTs can play in MTO chemistry. Heterogenous supports increased the stability of MTO towards the decomposition to low reactive perrhenate species, the presence of Lewis-bases being particularly favorable for the epoxidation of olefins.[162,163]

However, irrespective to the applied procedure, drawbacks relative to toxicity of the Lewis base additives (e.g. pyridine and pyridine derivatives), partial selectivity, low reactivity and leaching of rhenium have yet to be completely solved.

1.2 Synthesis and application of new MWCNTs MTO catalysts.

In this part, the work is focused on the preparation, characterization and application of rhenium based heterogenous catalysts. The new heterogeneous MWCNTs-based catalysts are characterized by the presence of benzo-15-crown-5 ether (B15C5) as a ligand recognition site for the rhenium species and are applied on olephinic systems were evaluated.

Multi-wall carbon nanotubes (MWCNTs) are efficient supports for the immobilization of reactive organometallic species thanks to their high surface area to volume ratio value, chemical stability, and unique redox, rheological and structural properties.[164,165]

They show surface defect sites for the anchoring of spacer chains and selective recognition sites, as for example for crown ethers.[166] Different applications of MWCNTs-crown ether functionalized systems are reported,[167] including dispersive microsolid phase extraction procedures,[168] exchange reaction in quasi-solid-state processes,[168] absorption of metals and organic pollutants,[169] and ion-detection.[170]In these latter cases, MWCNT-crown ether tethered poly(amidoamine) (PAMAM) dendrimers received increasing attention.[171] These supramolecular aggregates are characterized by recognition sites on both the dendrimer core and the end-termination of the system.[172] The divergent methodology for the preparation of PAMAM dendrimers encompasses the grafting of 1,3-diamino propane intermediates with methyl acrylate and ethylenediamine, followed by linkage of the crown ether moiety. The chemical complexity of PAMAM dendrimers (number of dendrimer sidechains and type of ramification) depends on the successive methyl acrylate/ethylenediamine treatments, and controls the distribution of the recognition sites, the leaching of the active species,[173,174,175] and the dispersibility of MWCNTs in organic solvents.[176]

Crown ethers are potent ligand for metal atoms, thanks to high chelating properties associated to the capability of the macrocycle to chelate host of different dimension.[166] Examples of MWCNTs functionalized by crown ethers are reported,[167] they include the application in dispersive micro solid-phase extraction procedures,[168] exchange reaction in quasi-solid-state dye-sensitized solar cell,[177] absorption of metals and organic pollutant,[178] and nanostructured assemblies for ion-sensors.[170]

Crown ethers, including benzo-15-crown-5 ether (B15C5), are able to coordinate rhenium (I) and rhenium (VII) species with high efficacy, showing selective and specific binding properties by variation of the cavity size and nature of ligand atoms.[179] Compared to other crown ether, such as 18-crown-6-ether, B15C5 seems to have the space inside the cavity perfect in terms of dimensions to establish the distances of optimal bonds, so that the MTO maintains its catalytic capacity.

Following, I reported the preparation and structural characterization of novel heterogeneous catalysts based on the immobilization of MTO on MWCNTs functionalized with benzo-15- crown-5 ether (B15C5) in the presence of tethered PAMAM dendrimers. Up to first and second generation of B15C5 PAMAM aggregates were obtained by applying the divergent methodology. The variety of catalysts was increased by the use of alkyl-diamino linkers of various length (from C-2 to C-6

atoms, respectively). FT-IR, ICP-MS and XRD analyses confirmed the coordination of MTO by the B15C5 moiety after immobilization on MWCNTs. The novel catalysts were applied in the epoxidation of a large panel of olefins using H_2O_2 (35% water solution) as green oxidant in the absence of Lewis bases additives to yield epoxides in high yield and selectivity. As a general trend, alkyl-diamino linkers with longer carbon atom chain afforded the most reactive systems in PAMAM aggregates. Diols were obtained as the main reaction products in the absence of the dendrimer structure, highlighting the role of PAMAM in the selectivity of the reaction.

1.2.1 Preparation of MWCNTs-B15C5/MTO catalysts IV A-D.

MWCNTs-B15C5/MTO catalysts **IV A-D** were prepared by immobilization of MTO on previously functionalized MWCNTs-B15C5 support. Briefly, MWCNTs I were treated with different alkyl-diamino linkers, ethylene diamine (EDA), propylene diamine (PDA), cadaverine (CV), and hexamethylene diamine (HAD) (from C-2 to C-6 atoms, respectively), in the presence of N,N-di-isopropylcarbodiimide (DIC), 1-hydroxybenzotriazole (HOBt), and N,N-diisopropyl ethylamine (DIPEA) in DMF at 25°C for 24 h, to yield intermediates **II A-D**.[180] The coupling procedure was repeated with 4'-carboxy-benzo-15-crown-5 (B15C5) as electrophilic reagent, to afford MWCNTs-B15C5 **III A-D** (Scheme 1). The FT-IR analysis of intermediates **II A-D** and **III A-D** showed the shift of the peak at 1730 cm^{-1} (stretching vibration of the carboxylic group in native MWCNTs **I**) at 1637 cm^{-1}**,** confirming the formation of the amide bond.[181] Moreover, intermediates **III A-D** showed the characteristic peaks at 1120 cm^{-1} and 1210 cm^{-1}, corresponding to C–O stretching vibrational mode of B15C5.[170] MWCNTs-B15C5 **III A–D** were successively treated with MTO in THF under gentle stirring at 25°C for 6 h, to afford MWCNTs-B15C5/MTO catalysts **IV A-D**.[161] Catalysts **IV A-D** showed the typical Re=O stretching vibrational mode at 953 cm^{-1}.

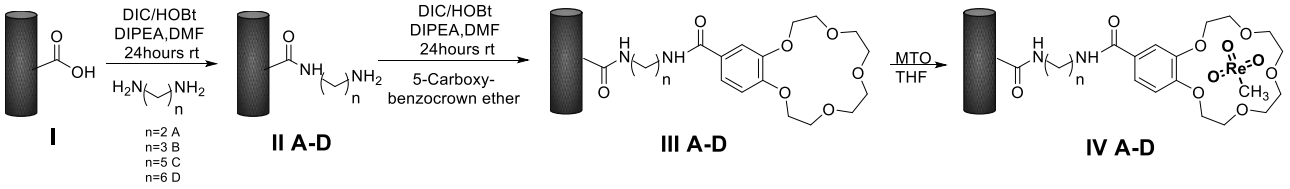

Scheme 1. Synthesis of catalysts **IV A-D.**

Scanning Electron Microscopy (SEM) analysis of **IV A-D** (Figure 2) confirmed the integrity of MWCNTs after the functionalization procedure. Powder X-ray analysis (XRD) was applied to evaluate the coordination geometry of MTO in representative intermediate **III D** and catalyst **IV D**.[182,183,184] The X-ray data of **III D** and **IV D** were treated by the difference method of neutron diffraction and isotopic substitution (NDIS)[154,185,186] in order to solve the contemporary presence of highly structured MWCNTs and amorphous B15C5 (generally indicated as support in the next discussion). Assuming that the general structure of **III D** was not significantly altered during the MTO loading, structural data for MTO/B15C15 complex were obtained by subtracting the radial distribution D(r) function of **III D** to that of

IV D (Figure 3, panels A and B).[187] The structure and distribution functions of **III D** and **IV D** are reported in materials and methods.

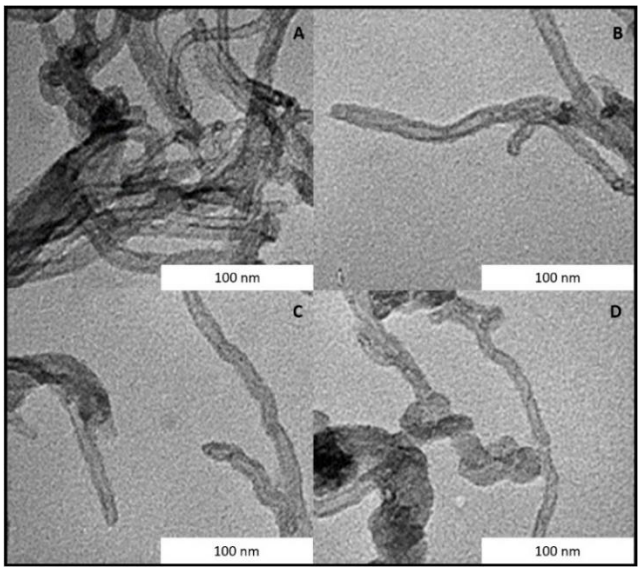

Figure 2. SEM images of catalyst **IV A-D**. The structure of MWCNTs is not modified after the functionalization procedure with B15C5.

Note that the oscillation pattern in the D(r) function of the two samples remain almost the same, confirming the hypothesis that the MTO loading didn't alter the structural order of the support. The D(r) function showed three peaks, set at about 1.80, 2.45, and 3.00 Å, respectively (Figure 3, Panel C). The first coordination sphere of the Re atom consists of six interactions assuming a quite octahedral conformation around the metal. The first peak was fitted by three metal-oxygen interaction lengths of exactly 1.80 Å and one metal-carbon interaction of 1.75 Å, respectively. The second peak at 2.45 Å is due to the other two interactions Re-O necessary to complete the octahedral coordination sphere. These interactions are also responsible for the peak at 3.00 Å (mutual interactions). The carbon atoms of the crown ether moiety might also contribute to this peak. The successive signals in the D(r) function were not further considered, since they derived from long-range MTO-MWCNTs interactions. In Figure 3 (Panel C) the function is compared with the theoretical peak shape function calculated for the octahedral model represented in Figure 3 (Panel D). The Re-O and Re-C bond distance values are quite in accord with the mean values

previously reported for MTO/Ln complexes.[188] As shown by the model (Figure 3, Panel D), the Re atom is coordinated by two adjacent oxygen atoms of the B15C5 ring. The model refers to the couple of oxygen atoms bonded to the aromatic ring, but the possibility that another couple of adjacent oxygen atoms is involved in the interaction with the metal cannot be completely ruled-out.

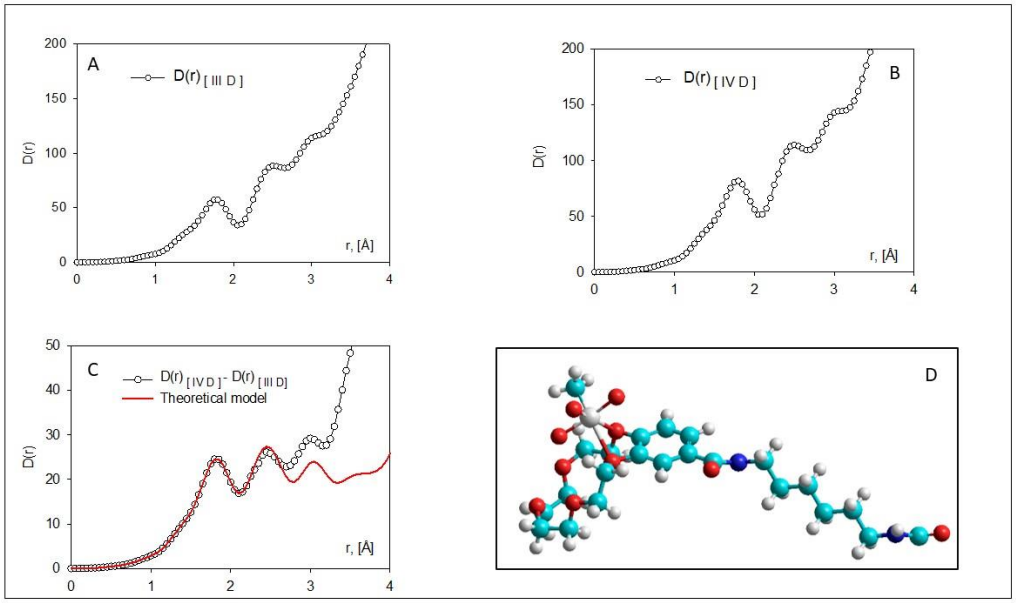

Figure 3. Red line represents the theoretical model. Panel A: Weighted experimental radial distribution function D(r) of **III D**. Panel B: experimental radial distribution function D(r) of **IV D**. Panel C: Difference curve for the two radial distribution functions, D(r)[**IVD**] - D(r)[**IIID**] [__○__]. Panel D: balls and sticks view of the complex between MTO and B15C5.

Moreover, the first Re coordination sphere analysis does not allow to determine the relative position of the methyl group with respect to the crown-ether oxygen atoms, due to the small electron differences between this group and the oxygen ones.

The distances between Re atom and ligands in the octahedral arrangement are reported in Table 1.

Table 1. Distances between Re atom and ligands in the octahedral arrangement of the complex.

Atoms	r, Å[a]
Re-O1	1.80
Re-O2	1.80
Re-O3	1.80
Re-O4	2.45
Re-O5	2.45
Re-C	1.75

[a] The mean square deviation was σ_{ij}= 0.06.

1.2.2 Preparation of MWCNTs-B15C5/PAMAM/MTO catalysts V E-H.

We prepared first and second-generation dendrimer catalysts **V E-F** and **V G-H**, respectively. As a general procedure, intermediates **II A** and **II D** were treated with methyl acrylate in MeOH at 25°C for three days, followed by addition of alkyl-diamino linkers EDA and HAD, to yield **III E-F**, respectively (Scheme 2, pathway A). The reaction of **III E-F** with B15C5 in the presence of DIC, HOBT, and DIPEA, in DMF at 25°C for 24h, afforded **IV E-F**. These latter intermediates were further converted to first-generation MWCNTs-B15C5/PAMAM/MTO catalysts **V E-F** by treatment with MTO in THF at 25°C. In a similar way, two successive treatments of **II A** and **II D** with methyl acrylate and alkyl-diamino linkers afforded **III G-H** (Scheme 2, pathway B), successively converted into **IV G-H** under previously reported experimental conditions.

Treatment of **IV G-H** with MTO in THF at 25°C yielded the second-generation MWCNTs-B15C5/PAMAM/MTO catalysts **IV G-H**.

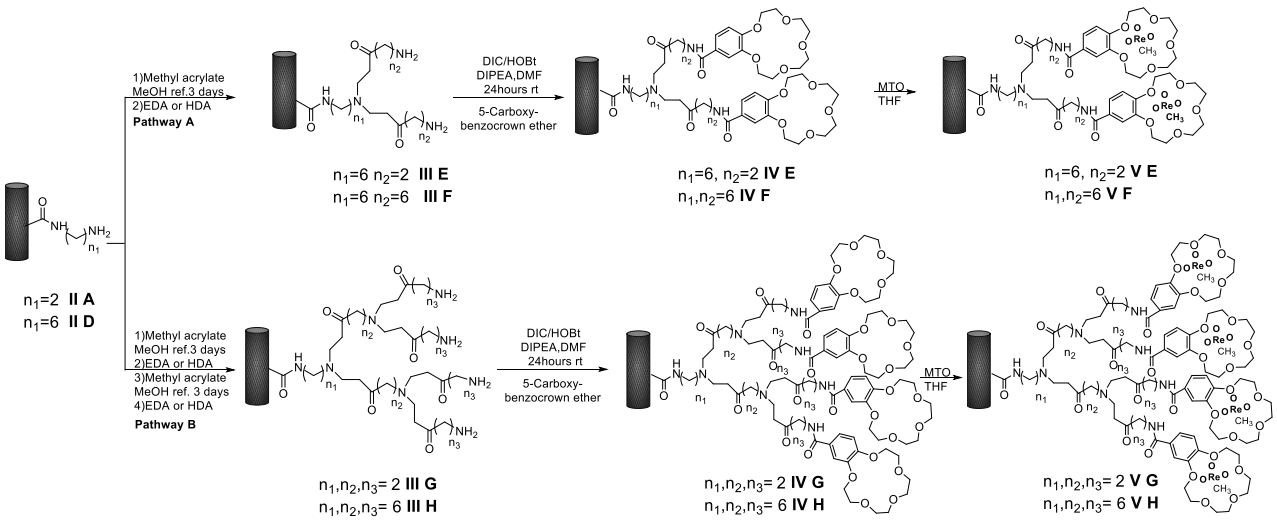

Scheme 2. Synthesis of MWCNTs-B15C5/PAMAM/MTO catalysts **V E-H**. Pathway A: preparation of the first-generation of dendrimer hybrids **V E-F**. Pathway B: preparation of the second-generation of dendrimer hybrids **V G-H**.

FT-IR analyses of catalysts **V E-H** are reported in materials and methods. Irrespective from the sample, the characteristic Re=O stretching vibrational mode at 950 cm^{-1}, and the CONH stretching vibrational mode at 1630 cm^{-1}, were always observed, besides to B15C5 C-O stretching signals at 1120, 1210, and 1250 cm^{-1}, respectively. The integrity of MWCNTs in catalysts **V E-H** after the PAMAM functionalization was confirmed by SEM analysis (Figure 4). Moreover, some sections of the MWCNTs in catalysts **V F** and **V H**, as representative examples, showed the presence of the PAMAM coating in TEM images.

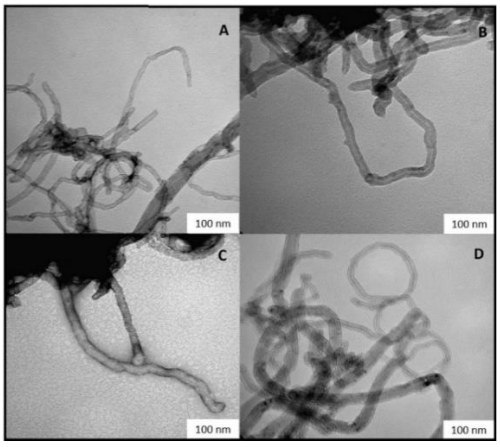

Figure 4. Scanning Electron Microscopy images of catalysts **V E-H**. Panel A: Catalyst **V E**. Panel B: Catalyst **V F**. Panel C: Catalyst **V G**. Panel D: Catalyst **V H.**

The loading factor of catalysts **IV A-D** and **V E-H** was evaluated by Inductively Coupled Plasma Mass-Spectrometry (ICP-MS) analysis (Table 2, entries 1-8). Catalysts **V E-F** showed loading factors of the same order of magnitude than **IV A-D** (Table 2, entries 5-6 versus entries 1-4). As a general trend, a slight decrease of the loading factor was observed for catalysts **V G-H** (Table 2, entries 7-8). Note that, among PAMAM catalysts, the higher value of the loading factor was obtained in the presence of the longest linker in terminal position (Table 2, entry 6 versus entry 5, and entry 8 versus entry 7).

Examples of the decreased accessibility to coordinative sites into higher generation dendrimer systems have been reported as a consequence of conformational changes, steric hindrance and encapsulation processes.[189]

Table 2. ICP-MS analyses of catalysts **IV A-D** and **V E-H**.

Entry	Catalyst	Re(%)[a]	Loading factor[b]
1	**IV A** (n=2)[c]	29.9 ± 0.3	1.6
2	**IV B** (n=3)	16.4 ± 0.3	0.9
3	**IV C** (n=5)	30.6± 0.4	1.7
4	**IV D** (n=6)	8.3 ± 0.3	0.5
5	**V E** (n_1=6, n_2=2)	22.3 ± 0.5	1.2
6	**V F** (n_1=6, n_2=6)	26.4 ± 0.4	1.4
7	**V G** (n_1=n_2=n_3=2)	3.7± 0.2	0.2
8	**V H** (n_1=n_2=n_3=6)	4.1 ± 0.3	0.3

[a]Values are expresses as wt/% with respect to the total weight of the sample. Measurements were repeated in triplicate. [b]Amount of mg of MTO per gram of support. [c]The n value represents the number of carbon atoms in the linker as reported in Scheme 2.

1.2.3 Epoxidation of olefins with catalysts IV A-D and V E-H.

Catalysts **IV A-D** and **V E-H** have been evaluated for the epoxidation of a large panel of aliphatic and aromatic olefins, including 1-hexene **1**, 1-octene **2**, trans-3-octene **3**, vinyl-cyclohexane **4**, styrene **5**, cis-stilbene **6**, and allylbenzene **7**. The oxidation was performed by treating the selected

olefin (0.05 mmol) with H_2O_2 (35% water solution, 0.5 mmol) and the appropriate amount of catalyst (containing 0.0025 mmol of MTO) at 25°C, in the absence of Lewis base additives as resumed in scheme 3.

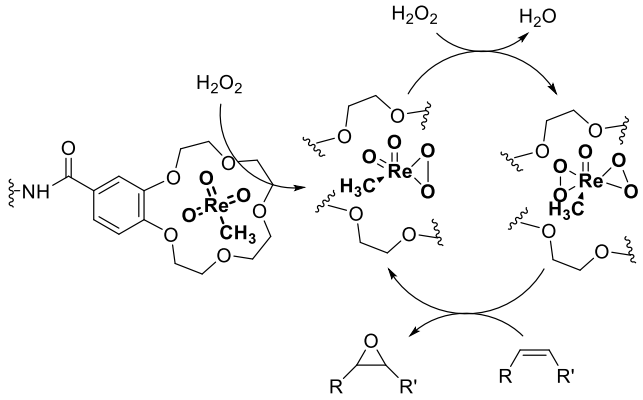

Scheme 3. Schematic representation for the MTO/H_2O_2 epoxidation of olefins. The reaction proceeds through the formation of monoperoxo [$MeRe(O_2)O_2$] and bis (peroxo) [$MeRe(O_2)O_2$] η2-metal complexes.[136]

The reaction products have been detected by gas-chromatography associated to mass-spectrometry (GC-MS) and nuclear magnetic resonance (NMR) analysis after chromatographic purification. The oxidation with MTO alone was used as reference. Irrespective from the experimental conditions, the oxidation of **1** with MTO and catalysts **IV A-D** afforded the diol **9** as the only recovered product (Table 3, entries 1-5), **IV B** being the most efficient catalyst (Table 3, entry 3) The corresponding epoxide was not detected in the reaction mixture, confirming the detrimental effect of the Lewis acidity of MTO in the ring-opening of the oxirane ring, even in the presence of B15C5. As a general trend, the catalytic activity was improved by increasing the number of carbon atoms in the alkyl-diamino spacer, as in the case of IV C-D (Table 3, entries 4 and 5), the lowest reactivity being observed with IV A, characterized by a linker with only two carbon atoms. MWCNTs-B15C5/PAMAM/MTO catalysts **V E-H** showed a different selectivity in the oxidation of compound **1**, the epoxide **8** being obtained as the only recovered product in quantitative yield and high conversion of the substrate (Table 3, entries 6-9). In particular, the second-generation of PAMAM catalysts **V G-H** was more reactive than the first-generation counterpart **V E-F** (Table 3, entries 6-7 versus entries 8-9). It is reasonable to suggest that the high selectivity toward the synthesis of the epoxide in the oxidation of **1** with PAMAM catalysts may be associated to the occurrence of additional interactions between MTO and nitrogen atoms in the dendrimer structure,

acting as internal Lewis base sites. In accordance with this hypothesis, the vibrational mode at 492 cm^{-1}, corresponding to stretching of the Re-N group, was detected for **V G**, as representative example, by Far Infrared analysis (FIR). The ligand properties of tertiary amine atoms in PAMAM dendrimer are reported.[190] For example, octahedral Co(II)-PAMAM dendrimer complexes showed a slight distorted octahedral coordination of the metal atom by the polymeric matrix.[191,192] Moreover, atomistic molecular dynamics (MD) simulations on ethylenediamine (EDA) PAMAM dendrimer wrapped on MWCNTs (up to 11th generation) showed the high mobility and the low distance occurring between tertiary nitrogen atoms and the terminal amino groups of the structure, where the metal coordinative sites are expected to be located.[191] The oxidation of aliphatic olefins 1-octene **2**, trans-3-octene **3** and vinyl-cyclohexane **4** proceeded in a similar way. The epoxides **10**, **12** and **14** were obtained in quantitative yield in the presence of catalysts **V E-H** (Table 3, entries 15-18, 24-27, and 33-36, respectively), while diols **11**, **13** and **15** were isolated as the main recovered products with MTO alone and catalysts **IV A-D** (Table 3). In this latter case, only small amounts of epoxides were detected.

The second generation of PAMAM catalysts was slightly more reactive than the first-generation counterpart in the conversion of substrate. Catalysts **V E-H** efficiently catalyzed the epoxidation of low reactive aromatic olefins, styrene **5**, cis-stilbene **6**, and allylbenzene **7**, affording the corresponding epoxides **16**, **18**, and **20**, as the only recovered products in quantitative yield, from acceptable (52%) to high (89%) conversion of substrate (Table 3, entries 42-45, 51-54, 60-63, respectively).

Instead, diols **17**, **19**, and **21**, largely prevailed in the oxidation performed with MTO and catalysts **IVA-D**.

Table 3. Oxidation of olefins **1-6** with catalysts **IV A-D** and **V E-H**.[a]

Entry	Substrate	Catalyst	Product	Conversion (%)	Yield of epoxide[b] (%)	Yield of diol[b] (%)	TON[c]
1	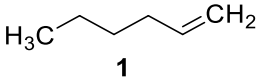 1	**MTO**	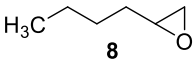 8 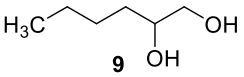 9	94	n.d.[c]	>98	
2		**IV A**		16	n.d.	>98	-
3		**IV B**		84	n.d.	>98	-
4		**IV C**		68	n.d.	>98	-
5		**IV D**		58	n.d	>98	-
6		**V E**		89	>98	n.d.	178
7		**V F**		91	>98	n.d.	182
8		**V G**		>98	>98	n.d.	200
9		**V H**		>98	>98	n.d.	200
10	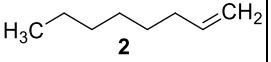 2	**MTO**	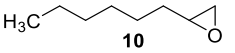 10 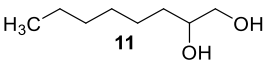 11	80	n.d	>98	-
11		**IV A**		12	n.d	>98	-
12		**IV B**		83	4	96	8
13		**IV C**		64	11	87	22
14		**IV D**		58	n.d.	n.d.	-
15		**V E**		80	>98	n.d.	160
16		**V F**		77	>98	n.d.	154
17		**V G**		>98	>98	n.d.	200
18		**V H**		>98	>98	n.d.	200
19	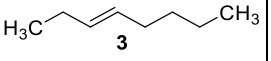 3	**MTO**	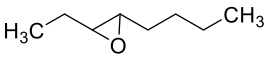 12 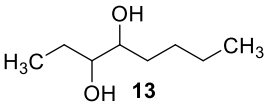 13	84	n.d.	>98	0
20		**IV A**		18	3	97	6
21		**IV B**		79	12	85	24
22		**IV C**		69	12	88	24
23		**IV D**		62	>98	n.d	124
24		**V E**		85	>98	n.d	170
25		**V F**		89	>98	n.d	178
26		**V G**		>98	>98	n.d	200
27		**V H**		>98	>98	n.d	200
28	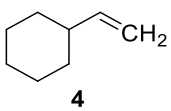 4	**MTO**	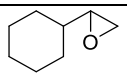 14 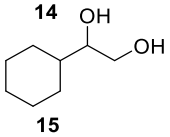 15	88	n.d.	>98	-
29		**IV A**		16	n.d.[b]	>98	-
30		**IV B**		83	14	85	28
31		**IV C**		64	3	97	6

32		**IV D**		58	n.d.[b]	>98	-
33		**V E**		93	>98	n.d	186
34		**V F**		90	>98	n.d	180
35		**V G**		>98	>98	n.d	200
36		**V H**		>98	>98	n.d	200
37	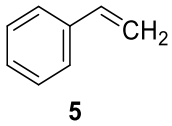 **5**	**MTO**	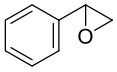 **16** 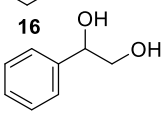 **17**	70	n.d.[b]	>98	-
38		**IV A**		31	n.d.[b]	>98	-
39		**IV B**		48	5	90	10
40		**IV C**		36	8	92	16
41		**IV D**		29	11	89	22
42		**V E**		64	>98	n.d	128
43		**V F**		67	>98	n.d	134
44		**V G**		72	>98	n.d	144
45		**V H**		74	>98	n.d	148
46	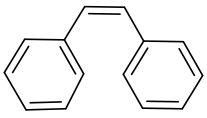 **6**	**MTO**	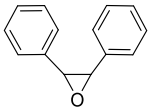 **18** 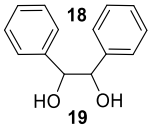 **19**	80	n.d.[b]	>98	-
47		**IV A**		18	n.d.[b]	>98	-
48		**IV B**		35	5	95	10
49		**IV C**		36	7	93	14
50		**IV D**		34	4	96	8
51		**V E**		65	>98	n.d	130
52		**V F**		61	>98	n.d	122
53		**V G**		74	>98	n.d	148
54		**V H**		77	>98	n.d	154
55	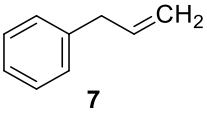 **7**	**MTO**	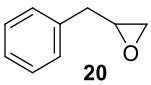 **20** 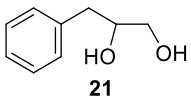 **21**	69	n.d.[b]	>98	-
56		**IV A**		21	n.d.[b]	>98	-
57		**IV B**		40	10	90	20
58		**IV C**		37	7	93	14
59		**IV D**		39	9	91	18
60		**V E**		52	>98	n.d	104
61		**V F**		48	>98	n.d	96
62		**V G**		62	>98	n.d	124
63		**V H**		89	>98	n.d	178

[a]The reaction was performed by treating the selected olefin (0.5 mmol) with a stoichiometric amount of H_2O_2 (35%, water solution) in the presence of the appropriate catalyst (0.5 mol/% with respect to loaded MTO) in CH_2Cl_2 (5.0 mL) at 25°C for 5h. Experiments were performed in triplicate. **A:** ethylene diamine $NH_2(CH_2)_2NH_2$. **B:** propylene diamine $NH_2(CH_2)_3NH_2$. **C:** cadaverine $NH_2(CH_2)_5NH_2$. **D:** hexamethylene diamine $NH_2(CH_2)_6NH_2$. [b]The product yield is calculated with respect to converted substrate. N.d. not determined. [c] [c]Turn over number expressed as the ratio between the mmol of epoxide versus the mmol of MTO in the heterogeneous catalyst.

The recyclability of catalysts **V F** and **V H** in the oxidation of compound **1** was studied as representative example (Table 4). After the first run, the catalyst was recovered by filtration, washed with CH_2Cl_2, and used without any further purification. Catalysts **V F** and **V H** showed a slight decrease in the conversion of substrate (Table 4, entries 2-6 and entries 7-12, respectively) yielding the epoxide **8** in quantitative yield for at least six successive reactions. In accordance with these data, a low decrease of the loading factor of the catalyst was observed by ICP-MS analysis of the sample at the end of any run (Table 4).

Table 4. Recyclability and stability of catalysts **V E** and **V H** in the oxidation of compound **1.**

Run	Substrate	Catalyst	Conversion (%)	Yield of epoxide (%)[a]	Re(%)[b]
1	**1**	**V F**	91	>98	26.4 ± 0.4
2			90	>98	26.1 ± 0.3
3			90	>98	26.0 ± 0.2
4			85	>98	24.3 ± 0.4
5			84	>98	23.9 ± 0.3
6			82	>98	21.6 ± 0.2
7		**V H**	>98	>98	4.1 ± 0.3
8			>98	>98	4.0 ± 0.2
9			>98	>98	4.0 ± 0.2
10			97	>98	4.0 ± 0.3
11			95	>98	3.5± 0.2
12			92	>98	3.3± 0.1

[a]The reactions were performed by treating the olefin 1 (0.5 mmol) with H_2O_2 (0.5 mmol) and the appropriate quantity of MTO catalyst (containing 0.0025 mmol of active rhenium species) calculated with respect to the MTO loading value. After each reaction, the catalyst was recovered by filtration, washed with CH_2Cl_2, and used without any further purification for the successive run. [b] Values are expresses as wt/% with respect to the total weight of the sample. Measurements were repeated in triplicate.

1.3 Conclusions

MTO was efficiently supported on B15C5 and PAMAM functionalized MWCNTs. The novel catalysts showed a different selectivity in the oxidation of olefins depending on the chemical complexity of the system. Epoxides were synthesized in quantitative yield and high conversion of substrate in the presence of PAMAM catalysts, while diols largely prevailed when B15C5 was directly linked to the surface of MWCNTs. XRD analysis showed that the Re atom was coordinated by an octahedral structure through interaction with a couple of oxygen atoms of the B15C5 ring. The high selectivity observed in the synthesis of epoxides with PAMAM catalysts was probably due to the Lewis base property of the nitrogen atoms present in the dendrimer aggregate in buffering the Lewis acidic character of Re(VII) atom. The reactivity of the dendrimer-based catalysts increased by increasing the order of complexity of the structure, the PAMAM of second-generation affording higher yield of epoxide with respect to the first-generation counterpart. In the PAMAM series, terminal alkyl-diamino spacer bearing carbon atoms (cadaverine) afforded the most reactive catalysts. Note that PAMAM catalysts **V E-H** afforded styrene epoxide in yield higher than poly(4-vinylpyridine) and microencapsulated polystyrene MTO based systems,[154] highlighting the beneficial role of the dendrimer structure in the selectivity of the reaction. In the absence of PAMAM, the Lewis acidity of MTO was responsible for the ring-opening of epoxides to diols. In this latter case, the reactivity decreased in the presence of alkyl-diamino spacer bearing more than three carbon atoms (propyl diamine). Finally, catalyst **V H** retained the catalytic activity for at least six successive runs without any appreciable leaching of the metal.

1.4 Materials and methods

1-hexene **1**, 1-octene **2**, trans-3-octene **3**, vinyl-cyclohexane **4**, styrene **5,** cis-stilbene **6**, allylbenzene **7**, organic solvents, MTO, methyl acrylate, ethylene diamine (EDA), propylene diamine (PDA), cadaverine (CV), hexamethylene diamine (HDA), diisopropylcarbodiimide (DIC), hydroxybenzothriazole (HOBt), N,N-diisopropyl ethylamine (DIPEA), 4'-carboxy-benzo-15-crown-5, and GH Polypro membrane filters were purchased from Sigma-Aldrich-Merch (Germany)

and used without further purification. Gas chromatography associated to mass spectrometry (GC–MS) was recorded on a Varian 410 GC-320 MS (Palo Alto, CA, USA) using a VF-5 ms column (30 m, 0.25 mm, 0.25 μm), and an electron beam of 70 eV. All experiments were done in triplicate. Ultrapure HNO_3 and HCl obtained from a sub-boiling system (DuoPUR, Milestone, Bergamo, Italy) and ultrapure 18.2 MΩ water from a Milli-Q (Millipore, Burlington, MA, USA) were used for the sample dissolution. ^{1}H-NMR and ^{13}C-NMR spectra were recorded on a Bruker (400 MHz) spectrometer.

1.4.1 Preparation of oxidized MWCNTs I.

In a round-bottomed flask, MWCNTs (1.0 g) and sulphonitric mixture [H_2SO_4–HNO_3 (3:1), 500 mL] were kept under magnetic stirring for 4.0 h at 25°C, sonicated for 1h and heated for 12 h at 40 °C. The reaction mixture was cooled down to 25°C and the suspension was washed with cold H_2O (400 mL). The supernatant was removed by centrifugation (4000× g rpm, 30 min). The residue was washed with deionized H_2O (200 mL) and filtered using GH polypro membrane filters 0.2 (μm). The resulting MWCNTs **I** were dried under reduced pressure and used without further purification.

1.4.2 Preparation of MWCNTs-B15C5/MTO catalysts IV A-D.

MWCNTs **I** (400 mg) were suspended in dimethyl formamide (500mL) and treated with N,N-diisopropylcarbodiimide (DIC; 250 mg, 2.0 mmol), hydroxybenzothriazole (HOBt; 270 mg, 2.0 mmol), and N,N-diisopropyl ethylamine (DIPEA; 700 μL, 4.0 mmol) in a round-bottomed flask with an egg-shaped magnetic stirring bar for 15 min at 25°C. Thereafter, the appropriate diamine (ethylene diamine for **IIA**, propylene diamine for **IIB**, cadaverine for **IIC**, and hexamethylene diamine for **IID**; 2.0 mmol) was added to the solution under gentle stirring for 12 h at 30 °C. The resulting solution was washed with DMF (5 × 5.0 mL), centrifugated (4000× g rpm, 20 min), and filtered using GH polypro membrane filters (0.2 μm). The resulting intermediates **II A–D** were dried under reduced pressure. Successively, 4'-carboxy-benzo-15-crown-5 (1.5 g, 6.0 mmol) was dissolved in DMF (250 mL), followed by treatment with DIC (790 mg, 6.0 mmol) and DIPEA (2.1 mL, 12 mmol), in a 500 mL round-bottomed flask under stirring for 4 h at 25°C. Thereafter **II A–D** (200 mg) were added to the solution and the mixture stirred for 8 h at 30 °C. The resulting intermediates **III A–D** were washed with DMF and H_2O, centrifugated (4000 × g rpm, 20 min), and filtered using GH polypro membrane filters (0.2 μm). Intermediates **III A–D** (125 mg) were suspended in

THF (50 mL) in a round-bottomed flask, and MTO (25 mg) in THF (25 mL) was added dropwise. After 1h the suspension was concentrated under reduced pressure, washed with THF (5 × 5.0 mL) and filtered using GH polypro membrane filters (0.2 μm) to afford MTO catalysts **IV A–D**.

1.4.3 Preparation of MWCNTs-B15C5/PAMAM/MTO catalysts V E-H.

The grafting of MWCNTs **I** with PAMAM was performed by applying a slightly modified procedure from the literature.[8] Methyl acrylate (10 mL) was added to a suspension of the appropriate intermediate **II D** in methanol (10 mL), and the resulting mixture was stirred at 80°C for 3 days. Thereafter, ethylene diamine (EDA, 0.15 mol, 400 mg), and in alternative, hexamethylene diamine (HAD, 0.15 mol, 775 mg), was added to the suspension in order to prepare the first-generation PAMAM intermediates **III E-F**, respectively. Two successive treatments of **II A** and **II D** with methyl acrylate and the appropriate alkyl-diamino linker afforded **III G-H**, respectively. Next, the appropriate PAMAM intermediate **III E-H** (100 mg) in DMF (50 mL) was added to a mixture of 4'-carboxybenzo-15-crown-5 (2.0 mmol, 624 mg), DIC (2.0 mmol, 406 mg), and HOBt (2.0 mmol, 270 mg) in dry CH_2Cl_2 (20 mL). The reaction mixture was stirred for 48 h at room temperature and then filtered on GH polypro membrane filters (0.2 μm) to afford PAMAM intermediates **IV E-H**, respectively. The black solid was washed several times with DMF (3x 2.0 mL) and CH_2Cl_2 (5 x 10 mL) and dried under vacuum. PAMAM intermediates **IV E-H** (100 mg) were than suspended in THF (25 mL) and a solution of MTO (25 mg) in THF (25 mL) was added dropwise. After 1h the suspension was concentrated under reduced pressure, washed with THF (5 × 5.0 mL) and filtered using GH polypro membrane filters (0.2 μm) to afford catalysts **V E–H**.

1.4.4 FT-IR analysis

FT-IR analyses were performed, at room temperature, with a Perkin–Elmer Spectrum One and a BRUKER VERTEX 70V spectrometers, respectively, both equipped with an ATR unit. Mid Infrared spectra were recorded by averaging 32 scans, with a resolution of 4 cm^{-1}. In the case of FIR (Far Infrared) configuration, spectra were registered within the (600 cm^{-1}-50 cm^{-1}) interval. Below, FT-IR of intermediates **II A-D**, **III A-D**, catalysts **IV A-D** and catalyst **V E-H**.

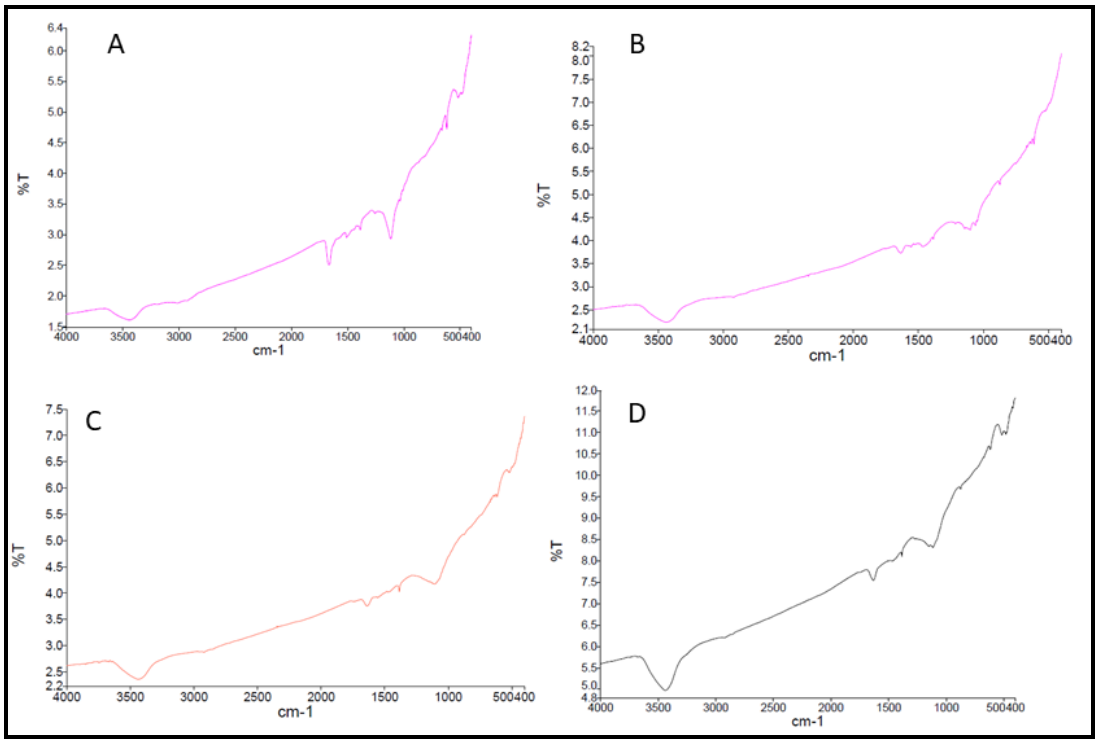

Figure 4. FT-IR of intermediates **II A-D.** Panel A: intermediate **II A**. Panel B: intermediates **II B**. Panel C: intermediates **II C**. Panel D: intermediates **II D**.

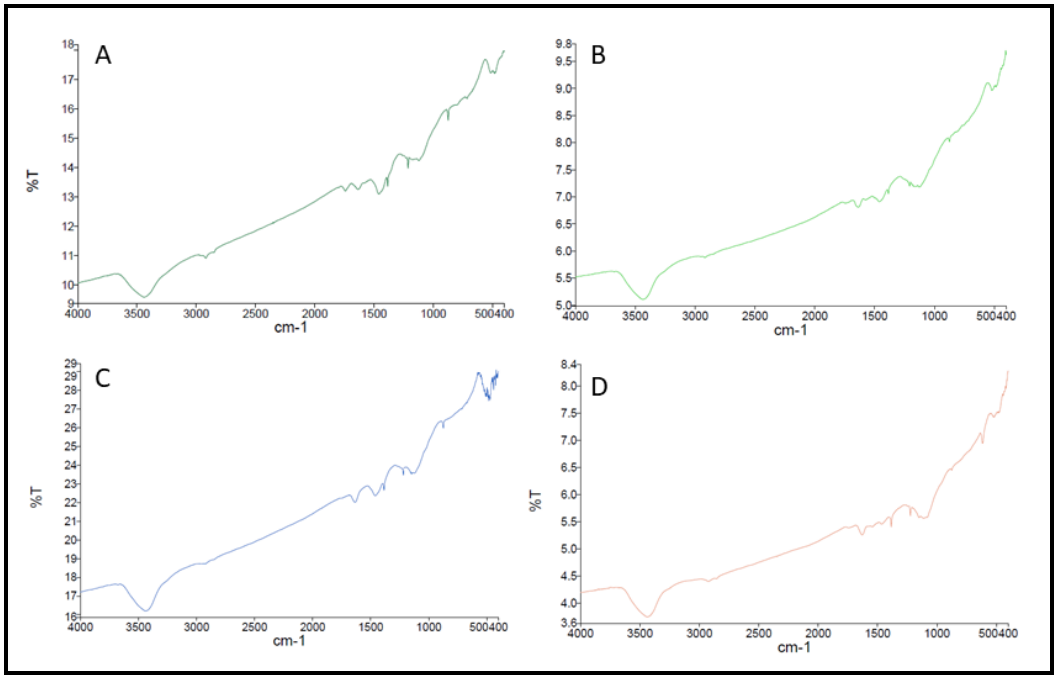

Figure 5. FT-IR of intermediates **III A-D.** Panel A: intermediate **III A**. Panel B: intermediates **III B**. Panel C: intermediates I**II C**. Panel D: intermediates **III D**.

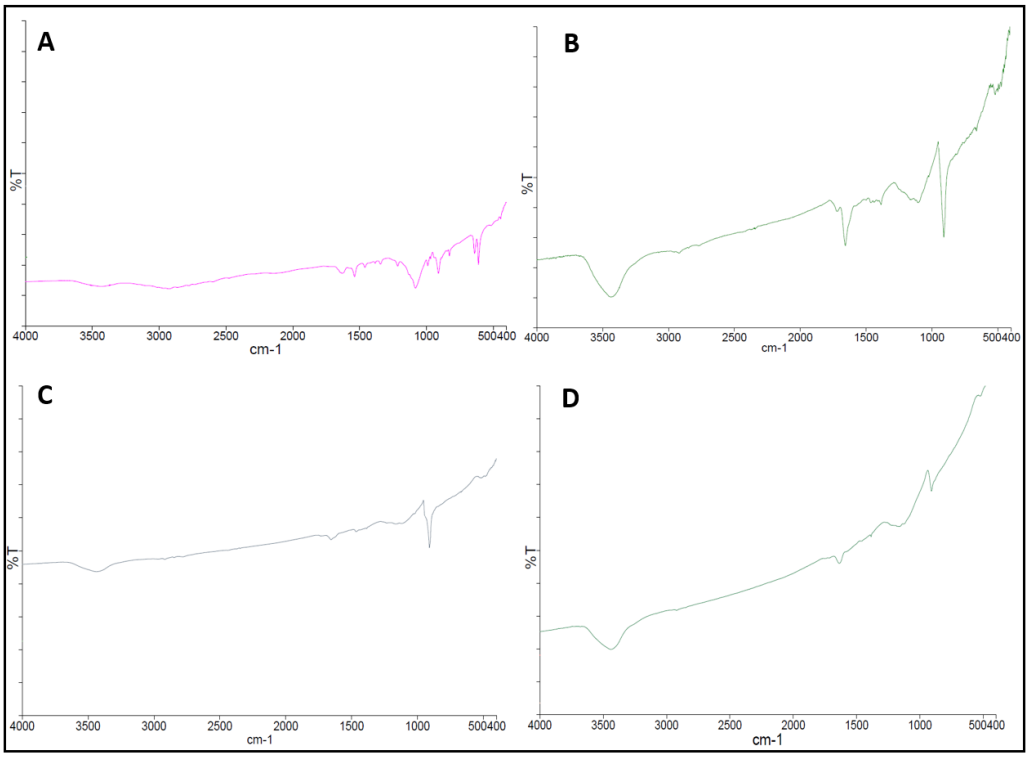

Figure 6. FT-IR of catalysts **IV A-D.** Panel A: catalyst **IV A**. Panel B: catalyst **IV B**. Panel C: catalyst **IV C**. Panel D: catalyst **IV D**.

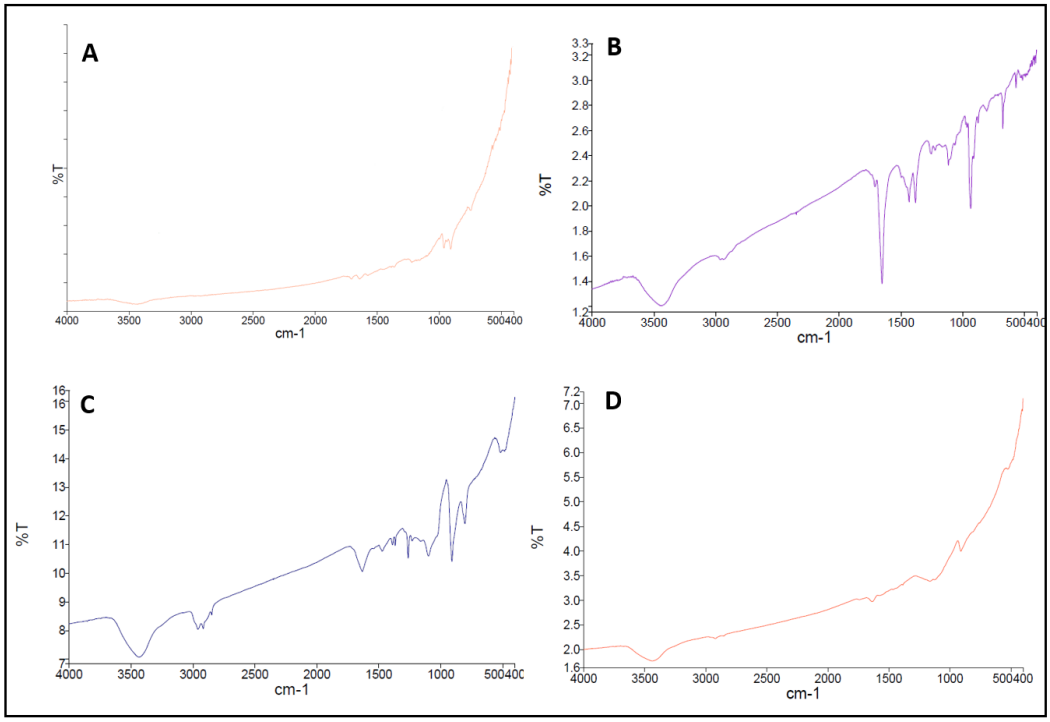

Figure 7. FT-IR of catalysts **V E-H.** Panel A: catalyst **V E**. Panel B: catalyst **V F**. Panel C : catalyst V **G**. Panel D: catalyst **V H**.

Far IR of IVD and VG compared to the reference MTO-1,2-cyclohexanediamine complex

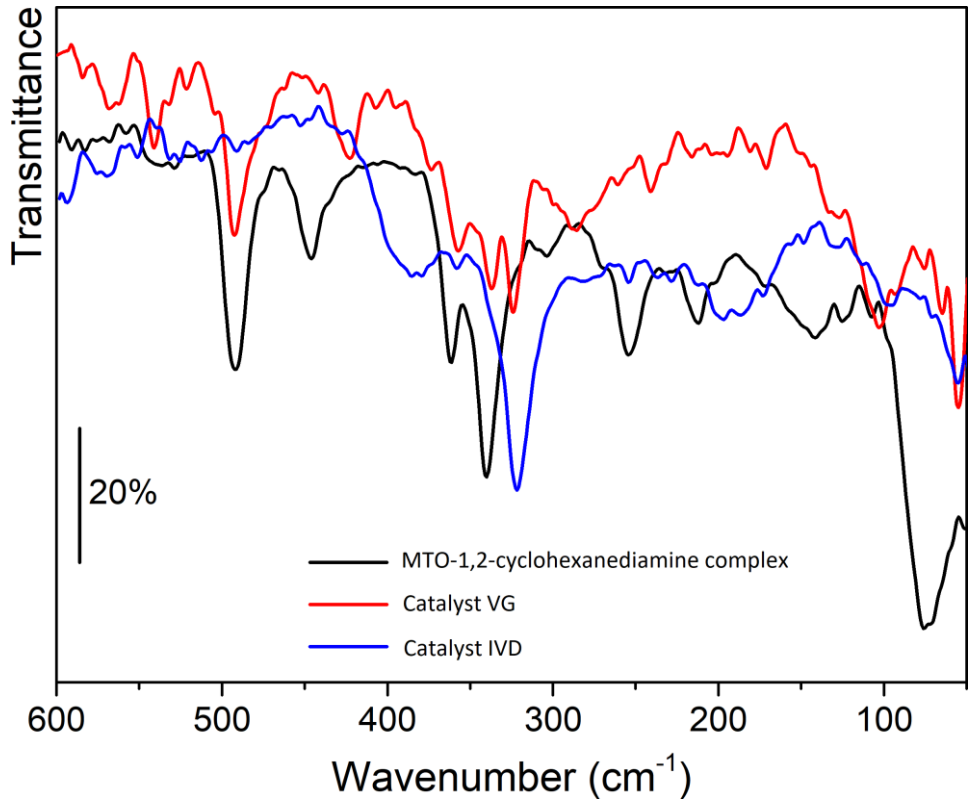

Figure 8. Far IR of IVD (blue) and VG (red) compared to the reference MTO-1,2-cyclohexanediamine complex (black)

1.4.5 Scanning Electron Microscopy (SEM) and Transmission Electron Microscopy (TEM)

For the scanning electron microscopy (SEM), the sample suspensions (50 L) were let to adsorb onto carbon tape attached to aluminum stubs and air dried at 25°C. The observation was made by a JEOL JSM 6010LA electron microscope (Waltham, MA, USA) using Scanning Electron (SE) and Back Scattered Electrons (BSE) detectors. Energy Dispersive Spectroscopy (EDS) analysis was carried out to reveal the chemical elements. Transmission electron microscopy (TEM) analysis was carried out by JEM-1200 EXII Transmission Electron Microscope. For this aim one drop of nanocomposite was put on copper lace coated with carbon and dried at 25 °C.

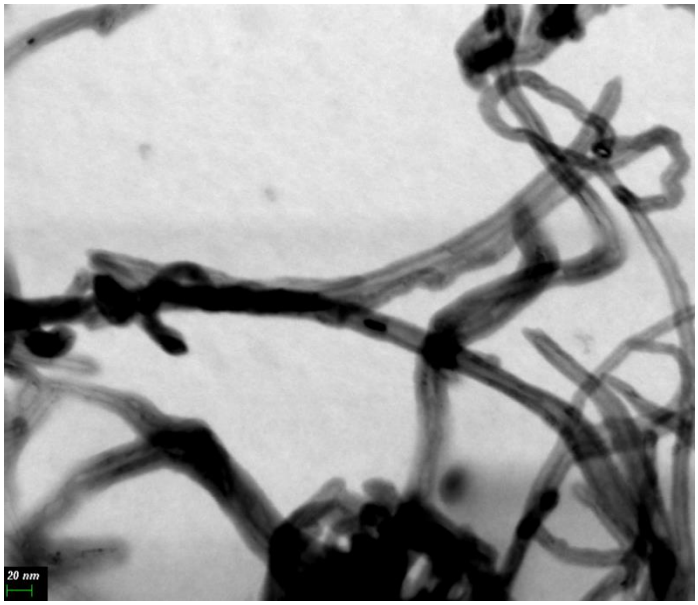

Figure 9. Transmission electron microscopy (TEM) of **V F**

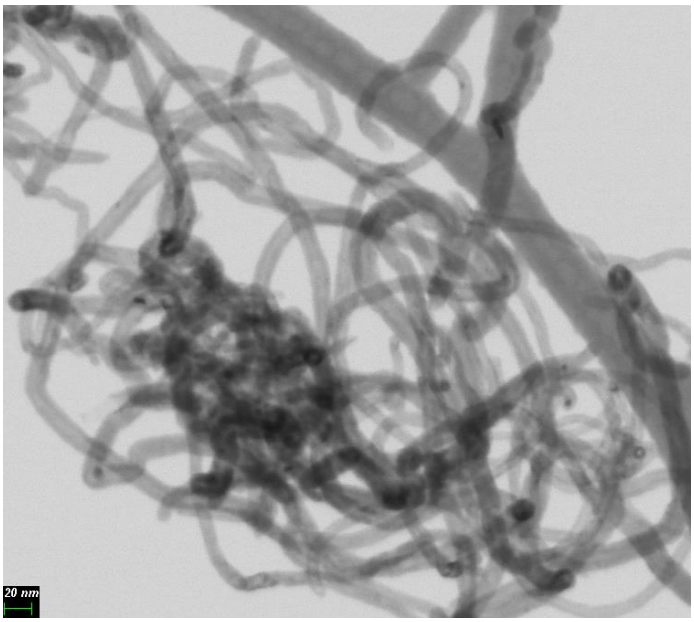

Figure 10. Transmission electron microscopy (TEM) of **V H**

1.4.6 XRD analysis

The X-ray diffraction data were collected by a Bruker D8 Advance with DaVinci design located at CNIS - La Sapienza University of Rome diffractometer with a molybdenum source. The angle dispersive instrument is equipped with a Mo KαX-Ray tube (λ = 0.7107

Å), whose radiation was focused onto the sample with Göbel mirrors. The 2θ angle range available was 2.75–142° with a step of 0.25° within Bragg-Brentano para-focusing geometry. The scattered intensity was collected with the Lynxeye XE Energy-Dispersive 1-D detector.

1.4.7 Inductively Coupled Plasma Mass-Spectrometry (ICP–MS) Analysis

The samples were weighed (from 1.0 mg to 10 mg) and transferred in fluorinated ethylene propylene (FEP) vials, previously washed to avoid any kind of external contamination. Regia solution was chosen for the mineralization. In particular, 750 µL of HCl and 150 µL HNO_3 were added and the solution was heated to 80° C for 3 hours. The volume was adjusted to 5.0 mL and then diluted another 10 times before the ICP–MS analysis. The analysis was performed with ultrahigh vacuum PHI 1257 system and an Agilent 7500 ICP–MS instrument under clean room ISO6 (Santa Clara, CA, USA), respectively.

1.4.8 Oxidation of olefins 1-7

A 5.0 mL flask equipped with a magnetic bar was charged with CH_2Cl_2 (5.0 mL), the olefins **1-7** (0.5 mmol), the appropriate amount of selected MTO catalyst (0.0025 mmol of MTO calculated with respect to the MTO loading value) and H_2O_2 (35% water solution, 50 mL, 0.5 mmol). The two-phase mixture was stirred vigorously at room temperature for 5 h. The progress of the reaction was monitored at half-hour intervals by gas chromatography associated to mass spectrometry (GC-MS) analysis of small aliquots of the organic phase. The conversion of olefins and yield of corresponding products were determined by GC-MS using n-octane as internal standard and by comparison with commercially available standards. GC–MS was recorded on a Varian 410 GC-320 MS (Palo Alto,CA, USA) using a VF-5 ms column (30 m, 0.25 mm, 0.25 m), and an electron beam of 70 eV. Helium was used as the carrier gas at a constant flow of 1.5 ml min^{-1}. The GC oven temperature was started at 50 °C (1 min hold) ramped at 20 °C min^{-1} to 115 °C (10 min hold), then ramped 5 °C min^{-1} to 280 °C (10 min hold). All the compounds **1-21** were characterized by nuclear magnetic resonance.

1.4.9 Mass spectrometry profiles of compounds 1-21

Mass spectrometry profiles of Hexene (1).

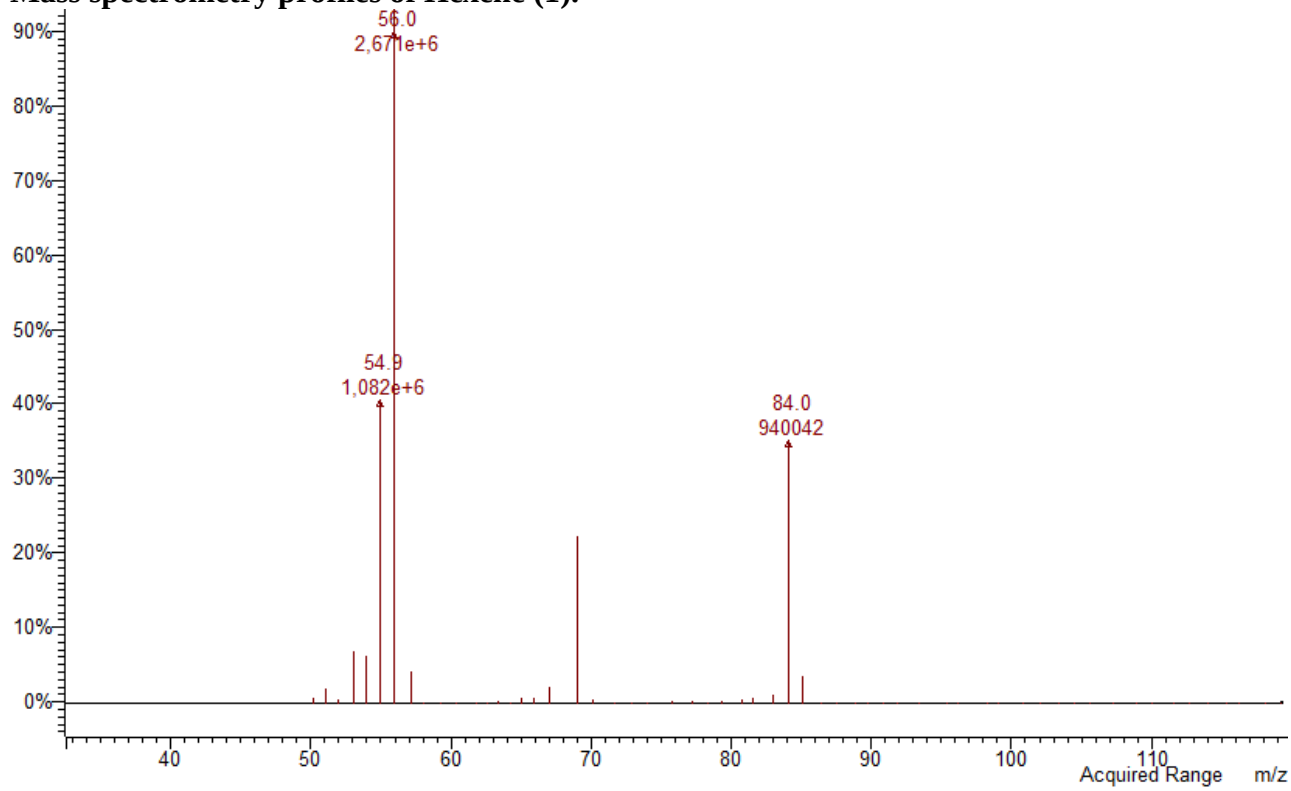

Mass spectrometry profiles of Octene (2).

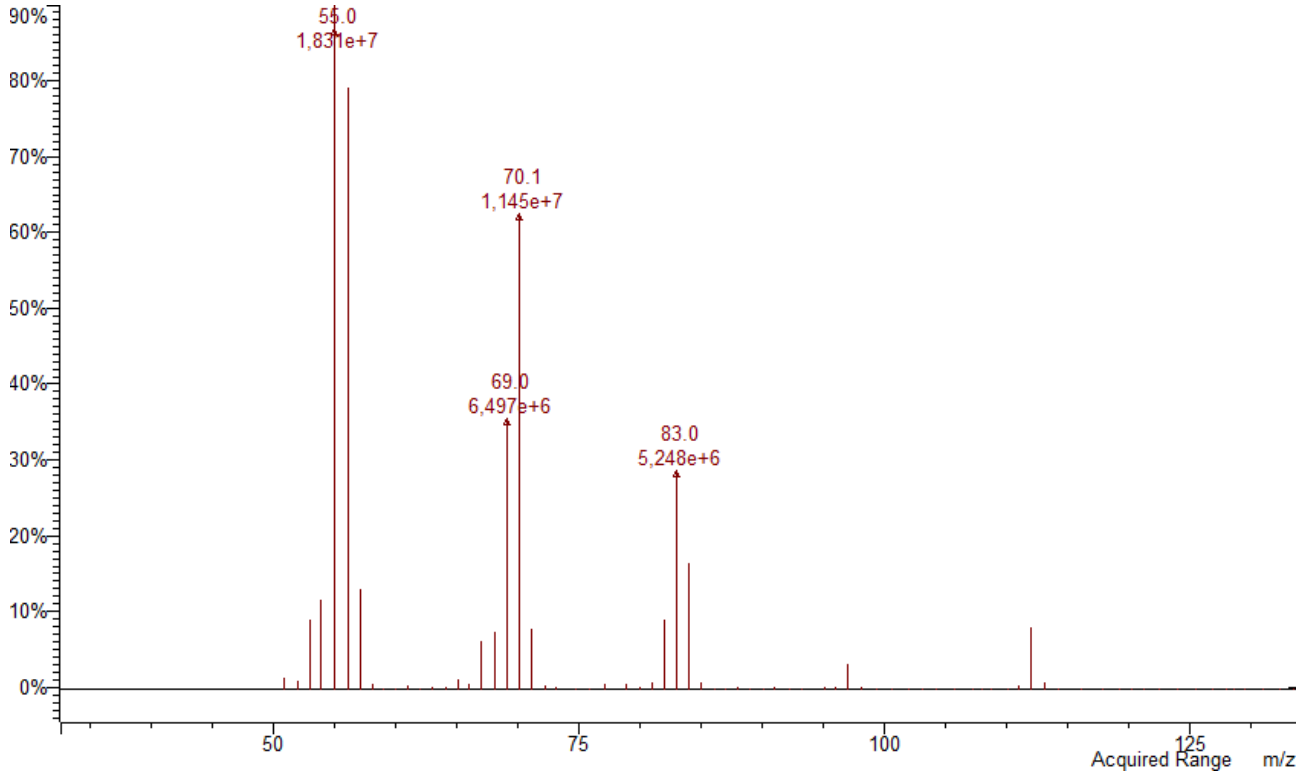

Mass spectrometry profiles of Trans-3-Octene (3).

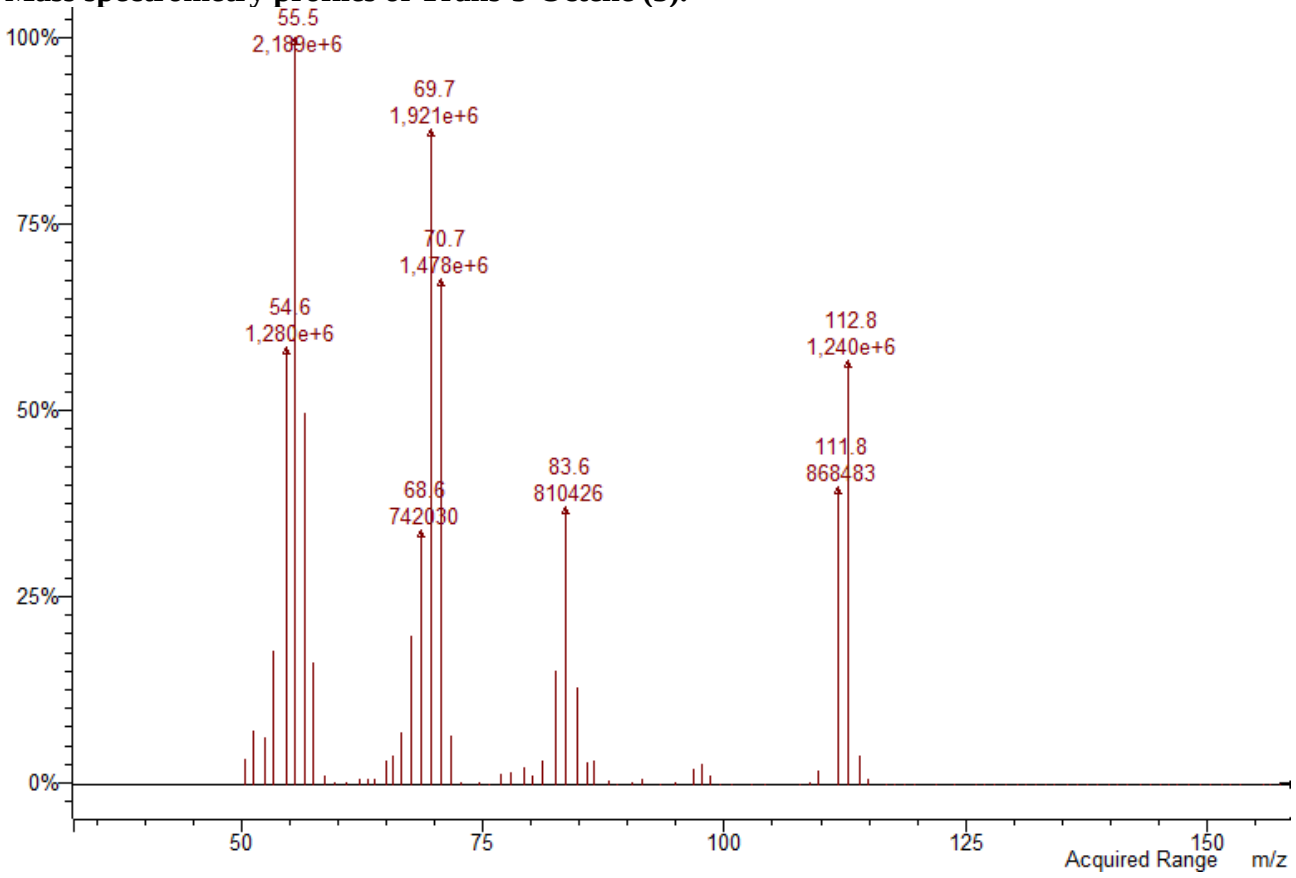

Mass spectrometry profiles of Vinylcyclohexane (4).

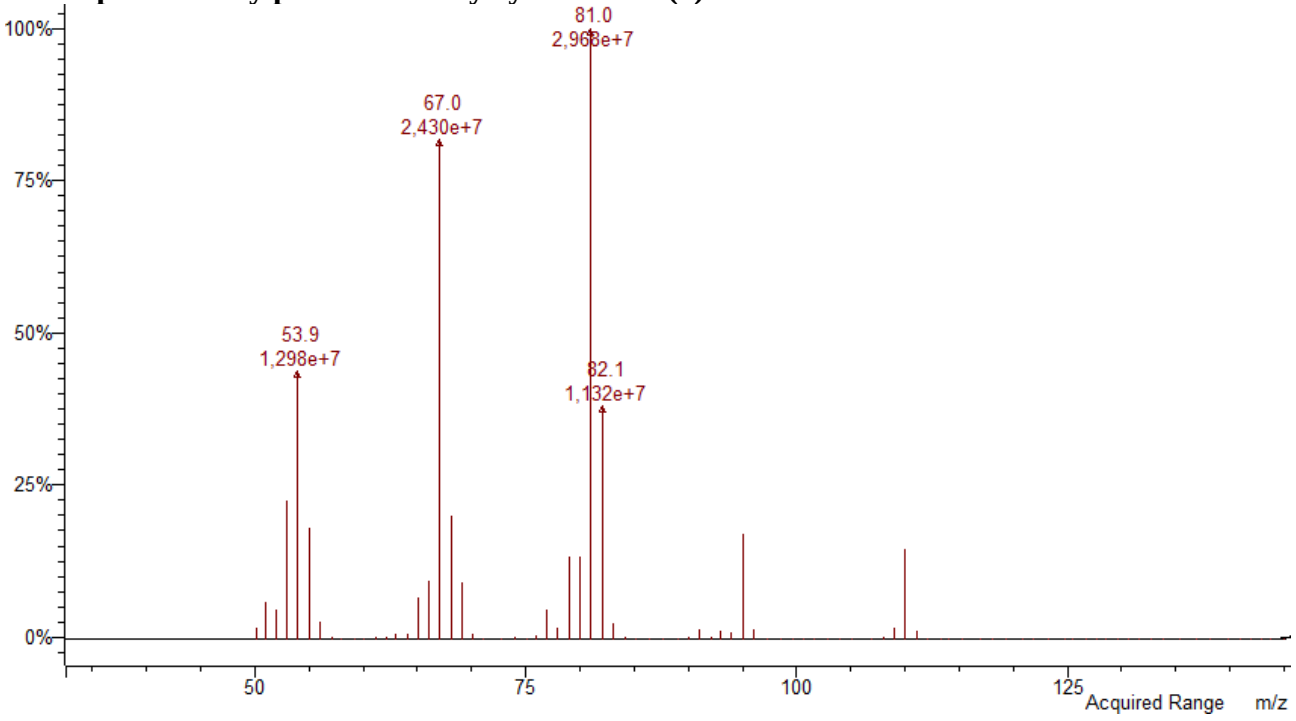

Mass spectrometry profiles of Styrene (5).

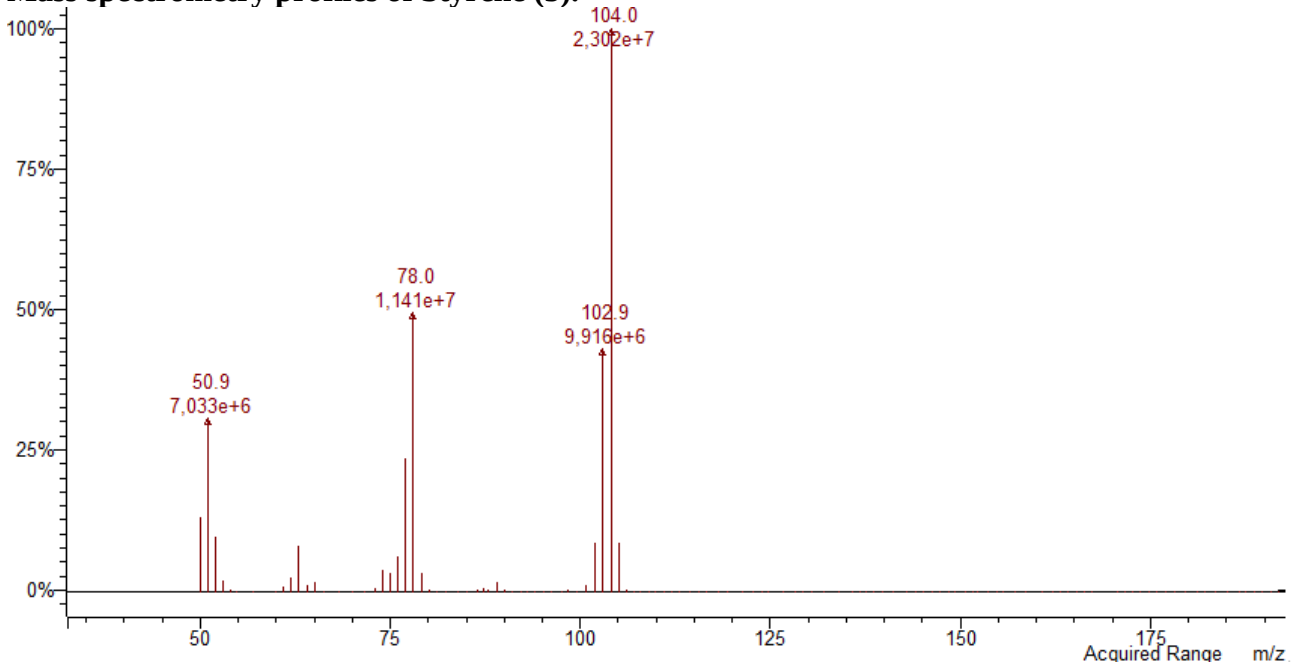

Mass spectrometry profiles of Cis-stilbene (6).

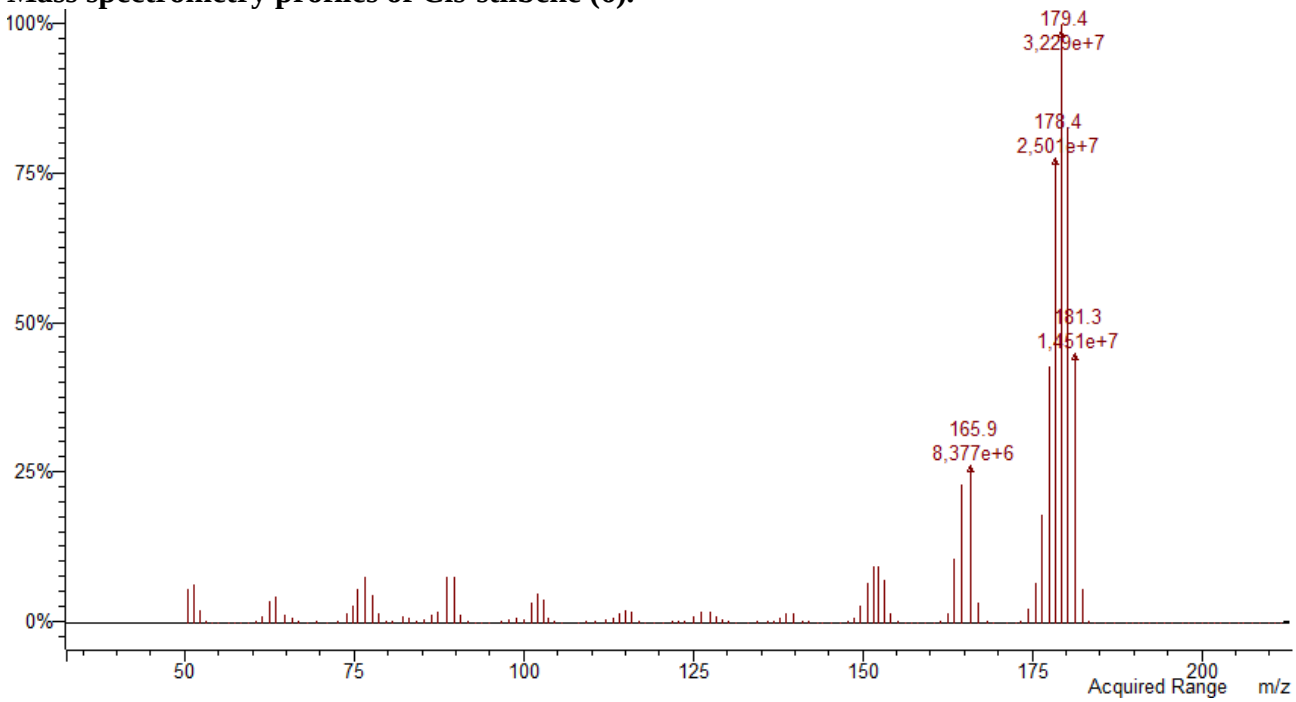

Mass spectrometry profiles of Allylbenzene (7).

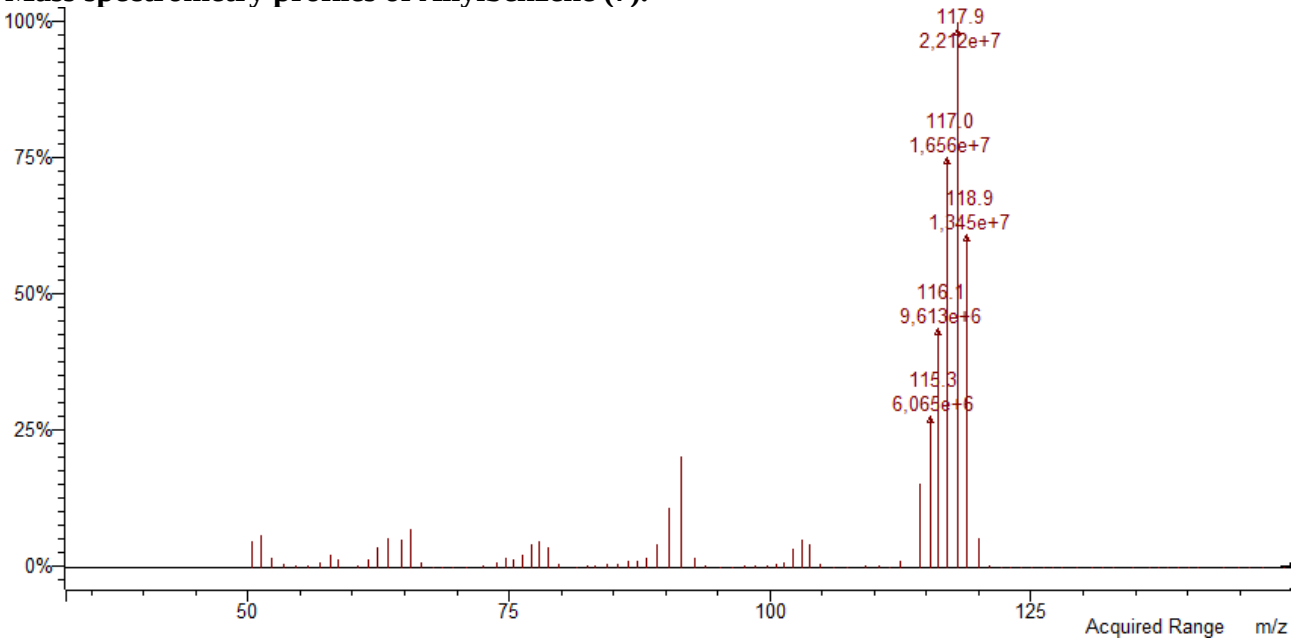

Mass spectrometry profiles of 1,2-Epoxyhexane (8).

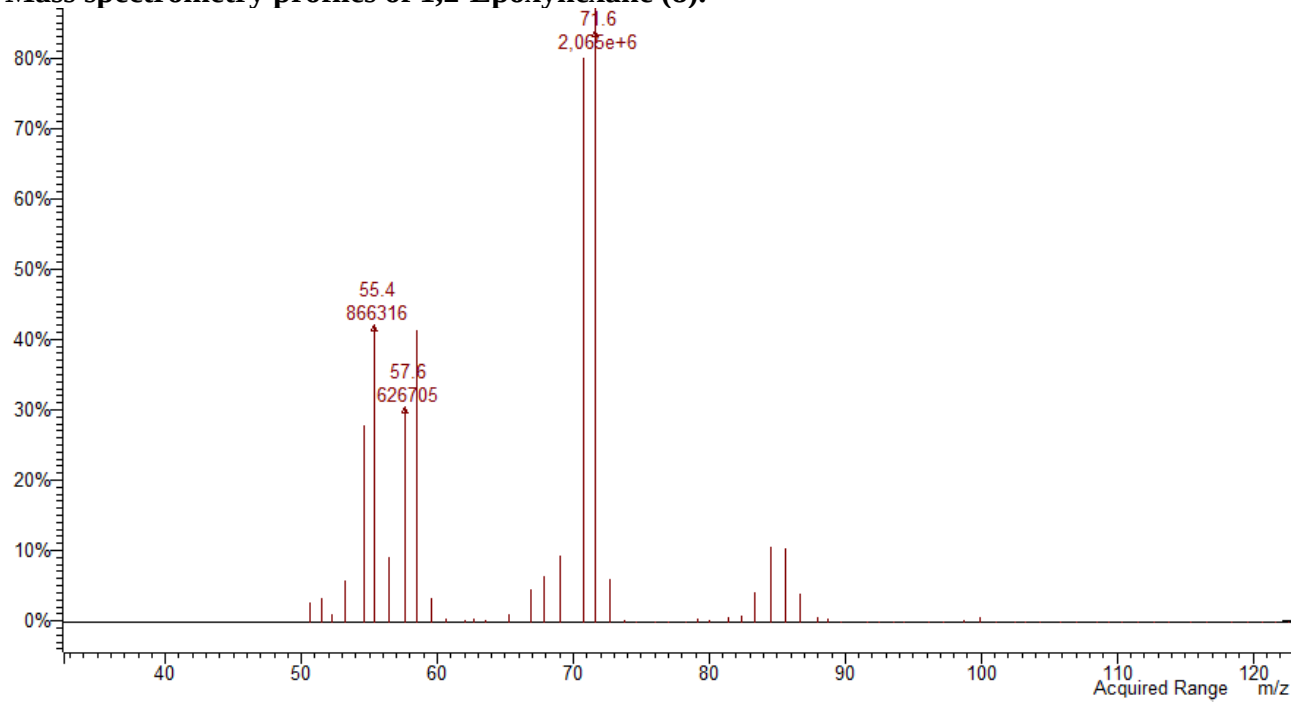

Mass spectrometry profiles of Hexane-1,2-diol (9).

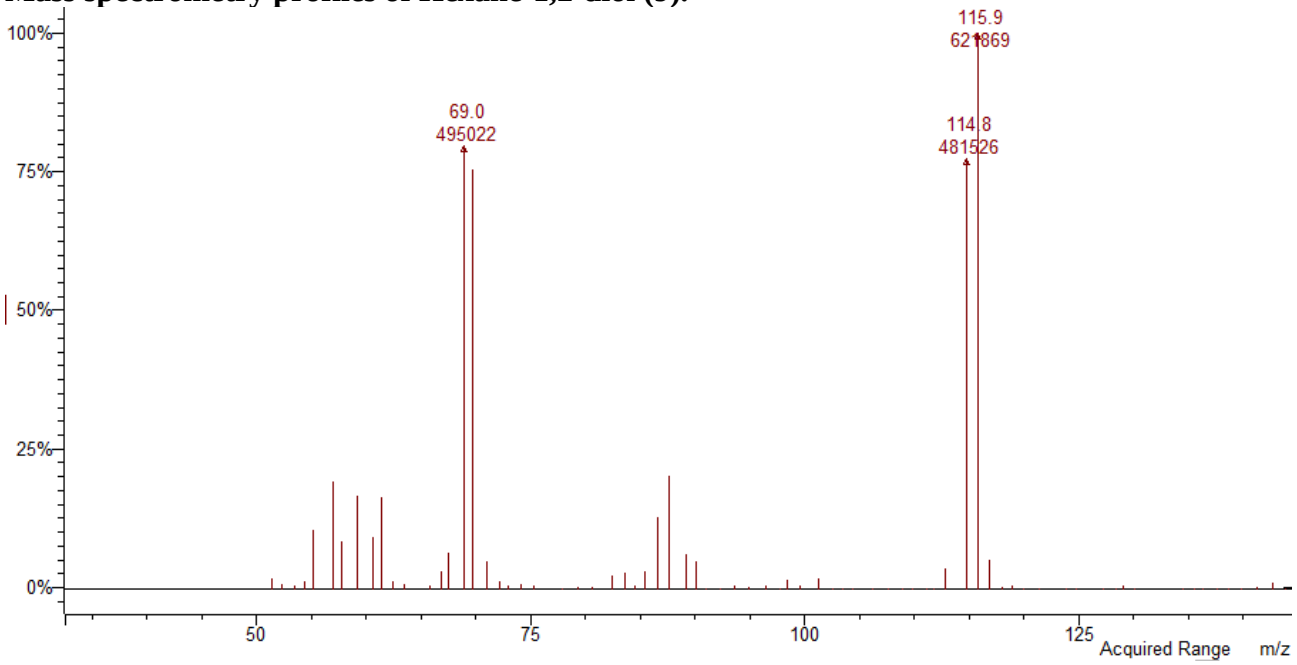

Mass spectrometry profiles of 1,2-Epoxyoctane (10).

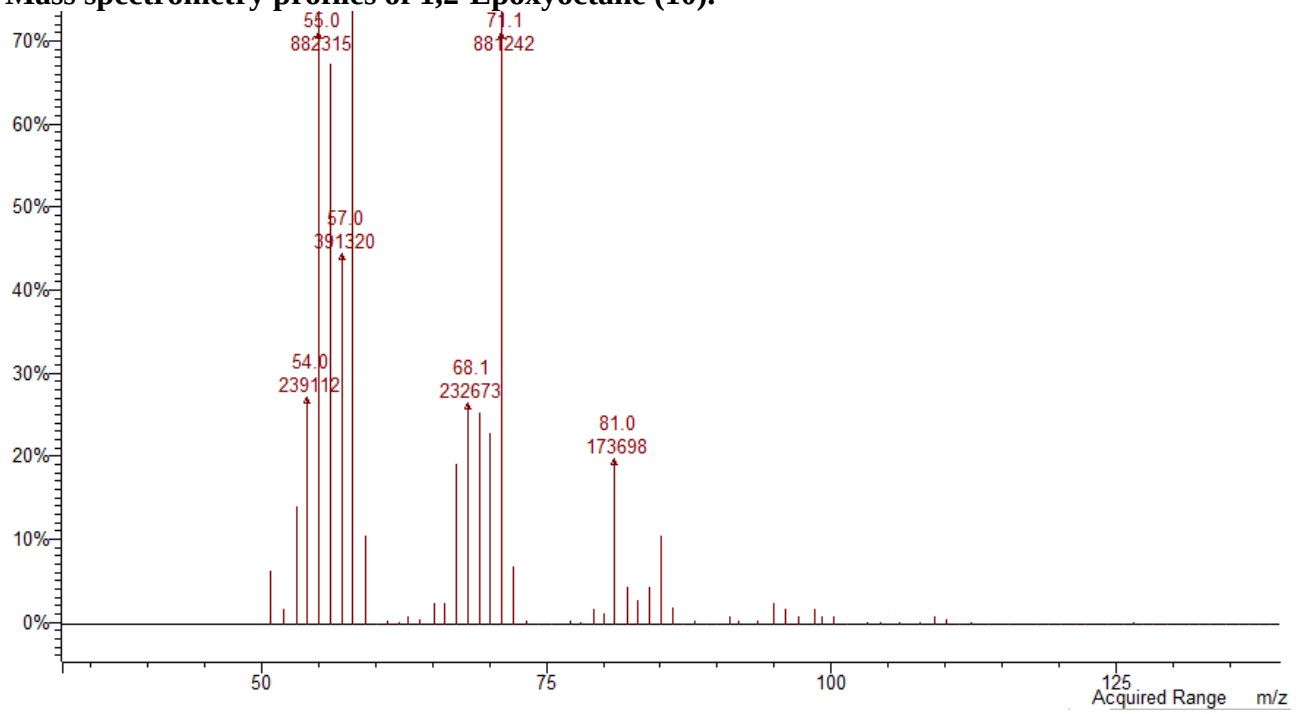

Mass spectrometry profiles of Octane-1,2-diol (11).

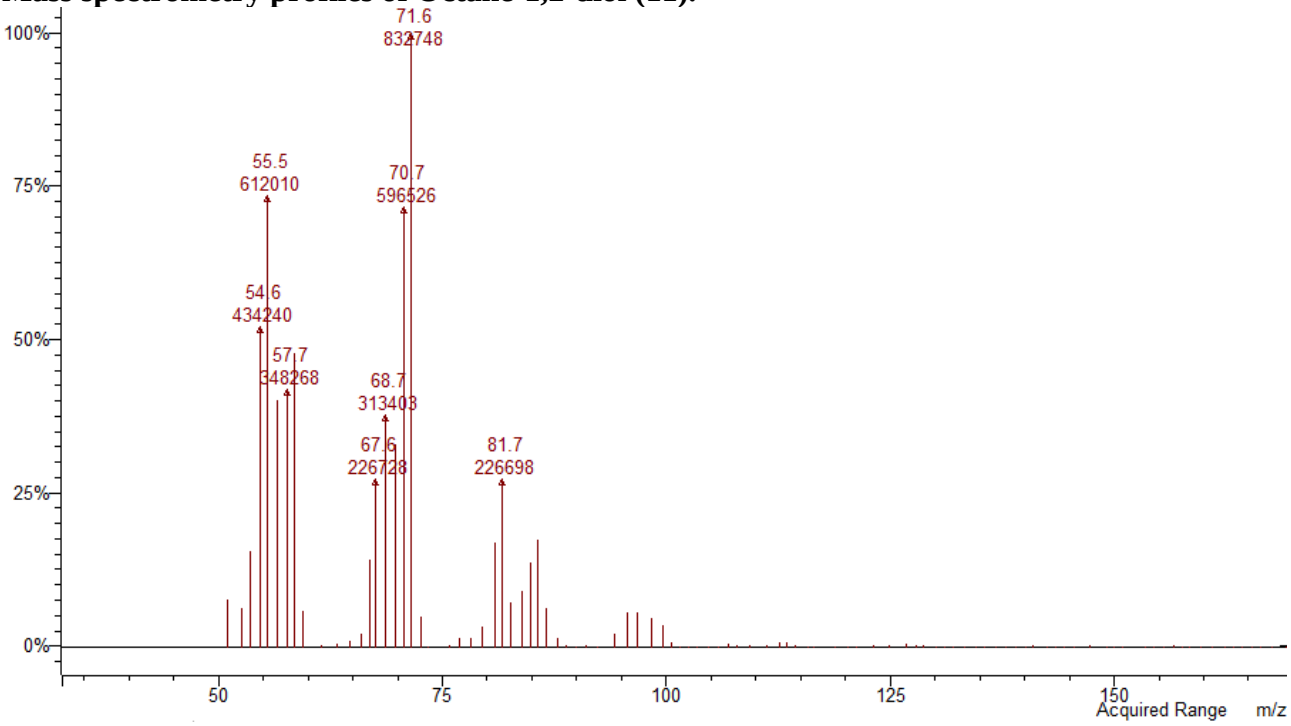

Mass spectrometry profiles of Trans-3,4-Epoxyoctane(12).

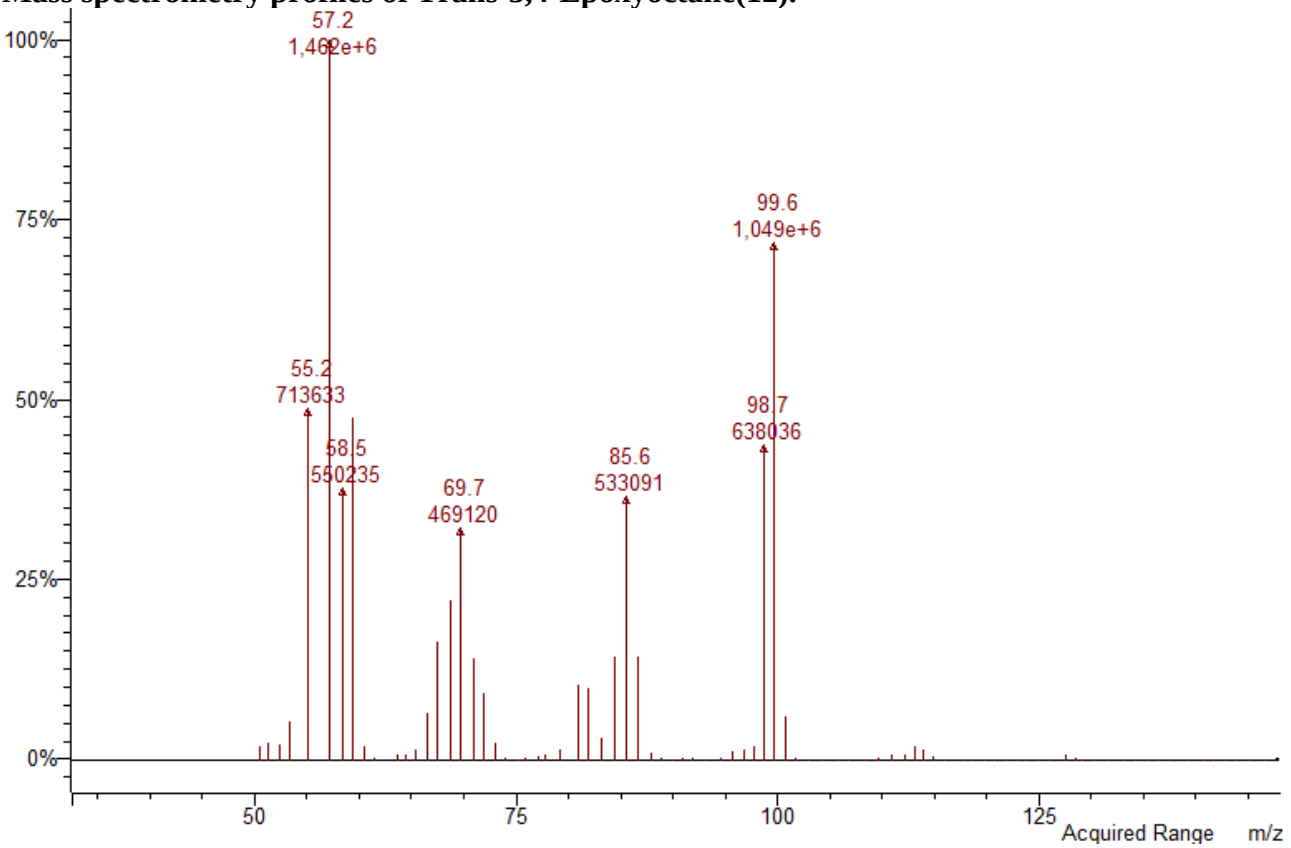

Mass spectrometry profiles of Octane-3,4-diol (13).

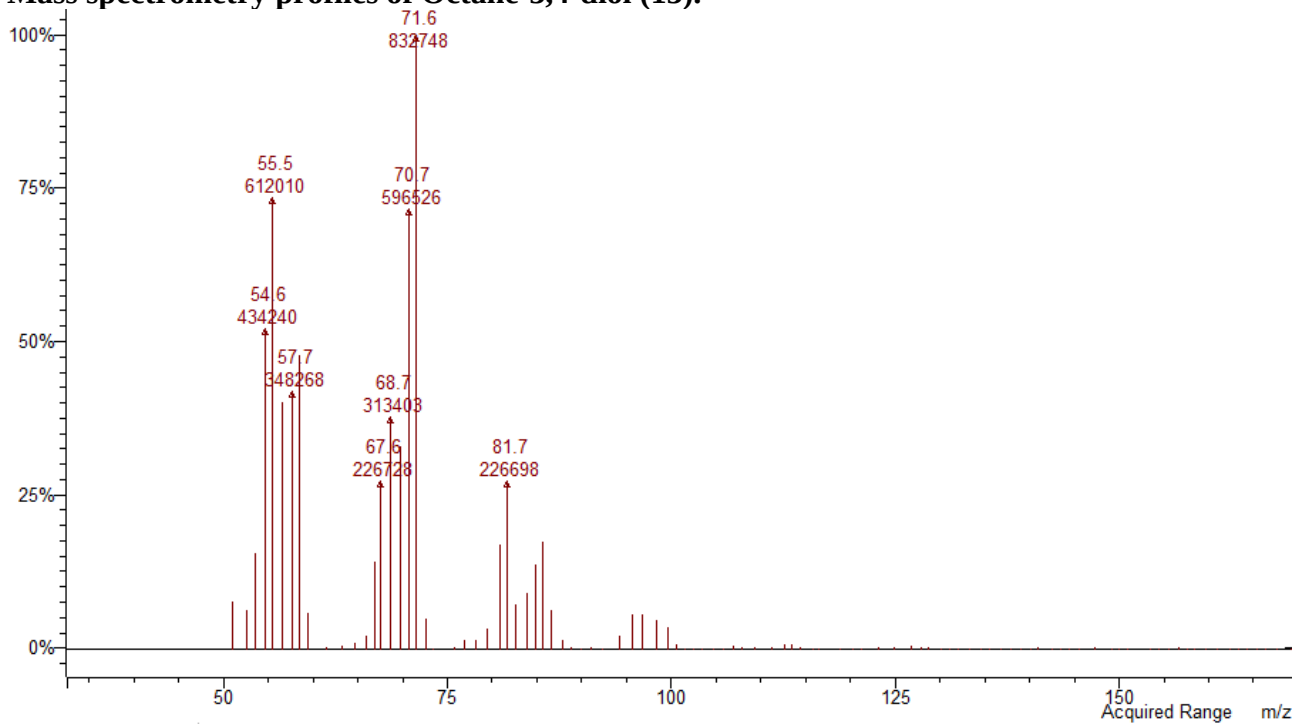

Mass spectrometry profiles of 2-Cyclohexyloxirane (14).

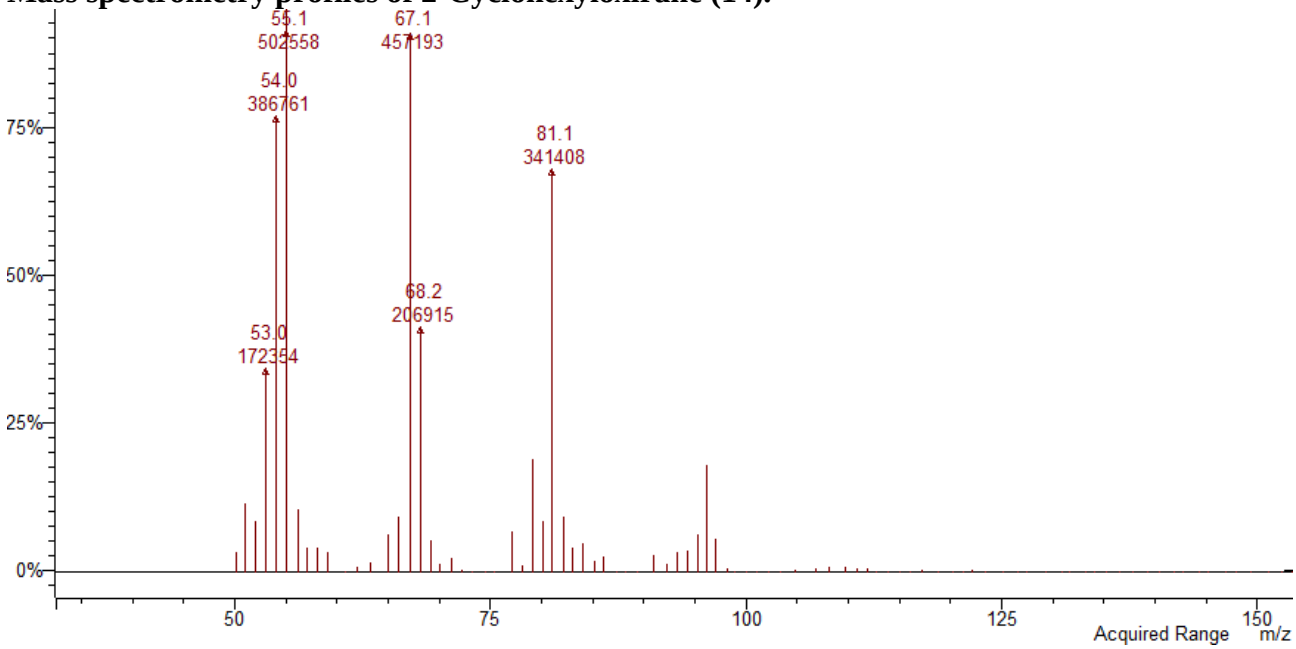

Mass spectrometry profiles of 1-Cyclohexylethane-1,2-diol (15).

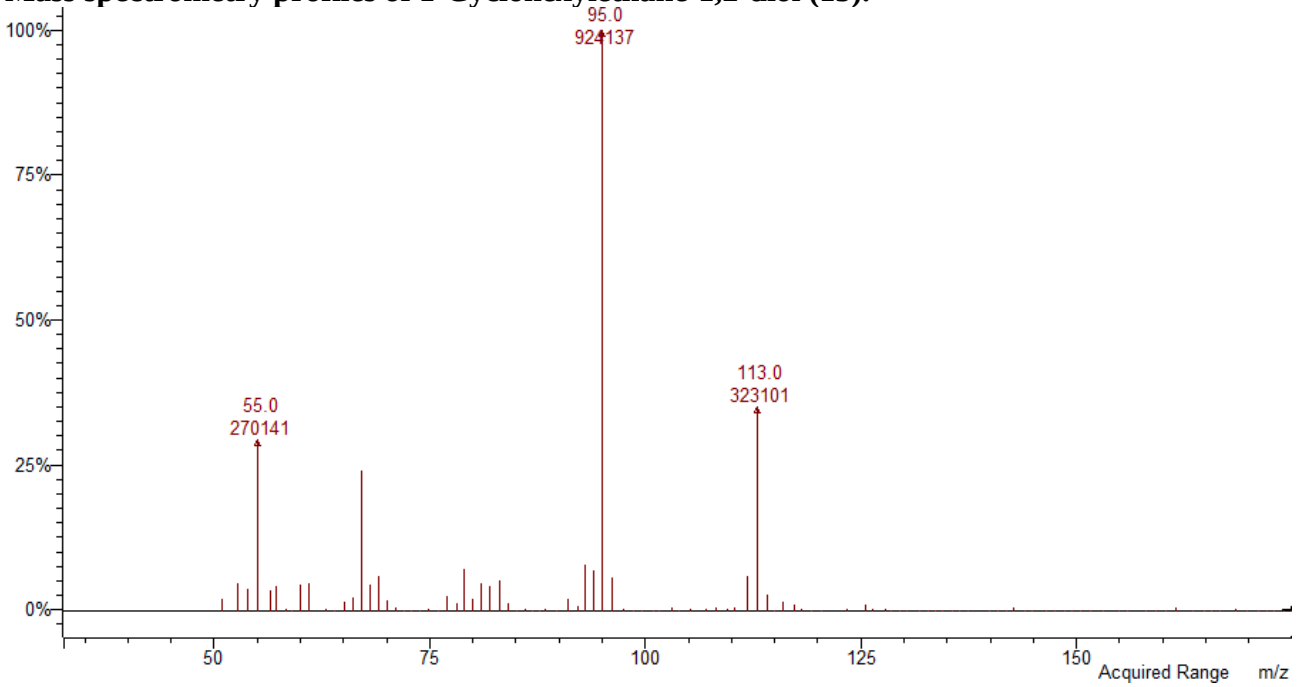

Mass spectrometry profiles of 2-Phenyloxirane (16).

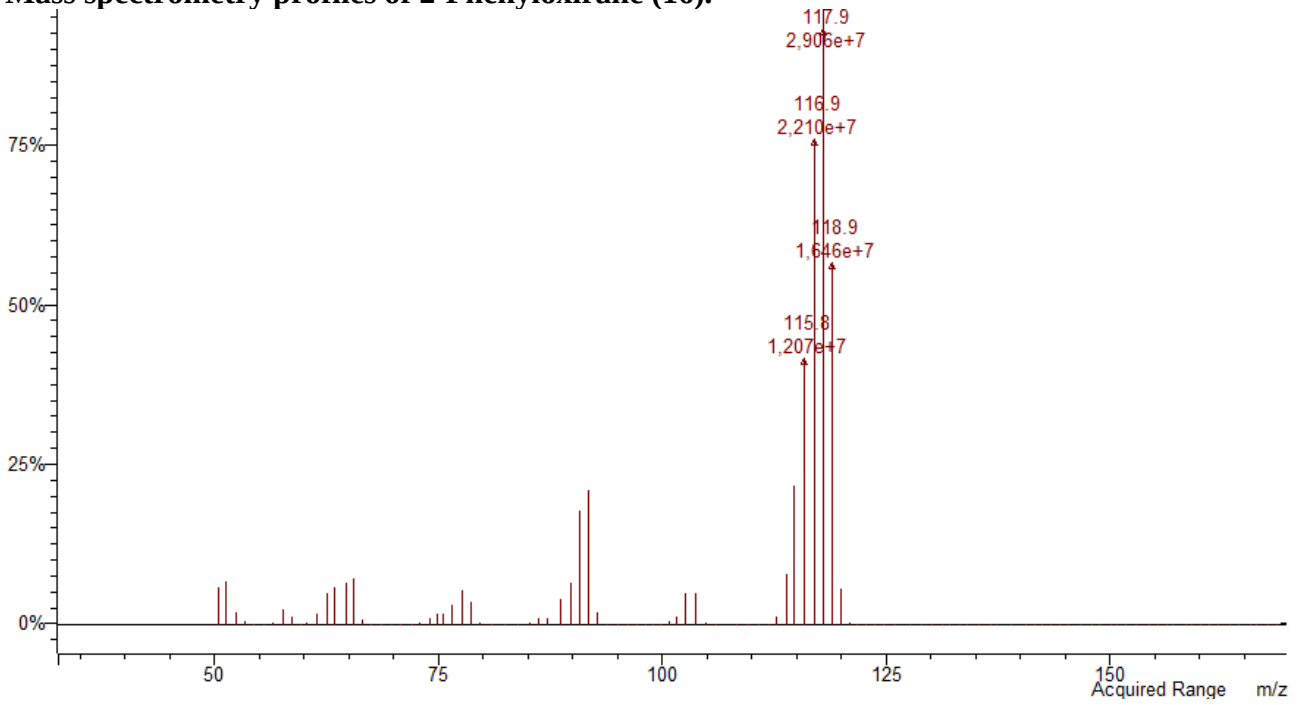

Mass spectrometry profiles of 1-Phenylethane-1,2-diol (17).

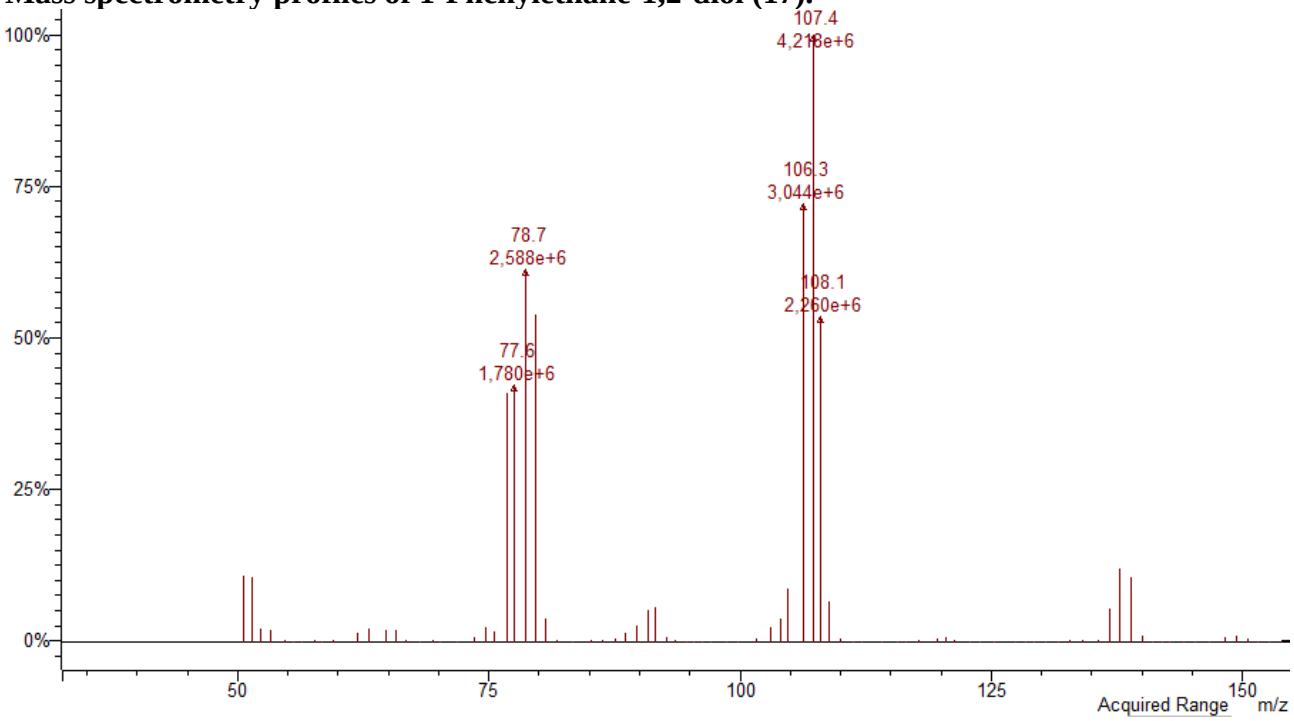

Mass spectrometry profiles of 2,3-Diphenyloxirane (18).

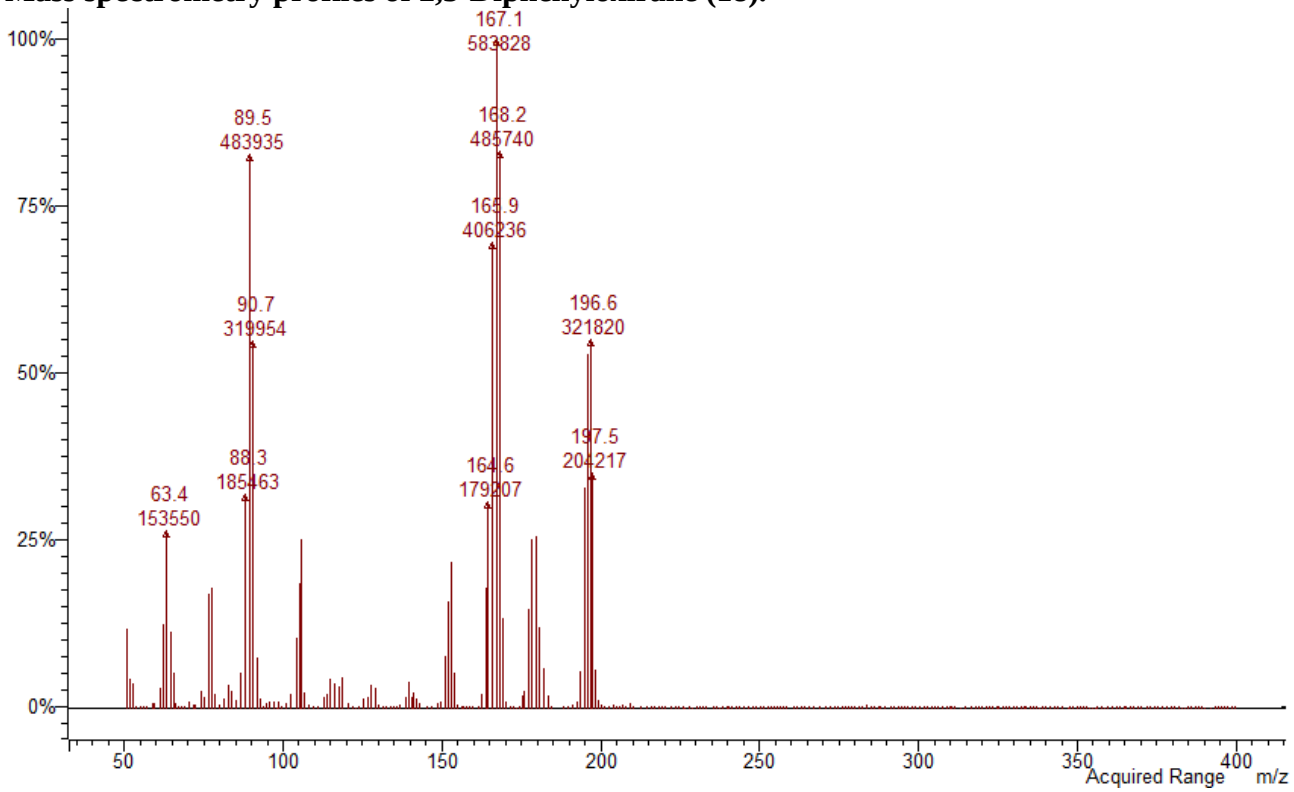

Mass spectrometry profiles of 1,2-Diphenylethane-1,2-diol (19).

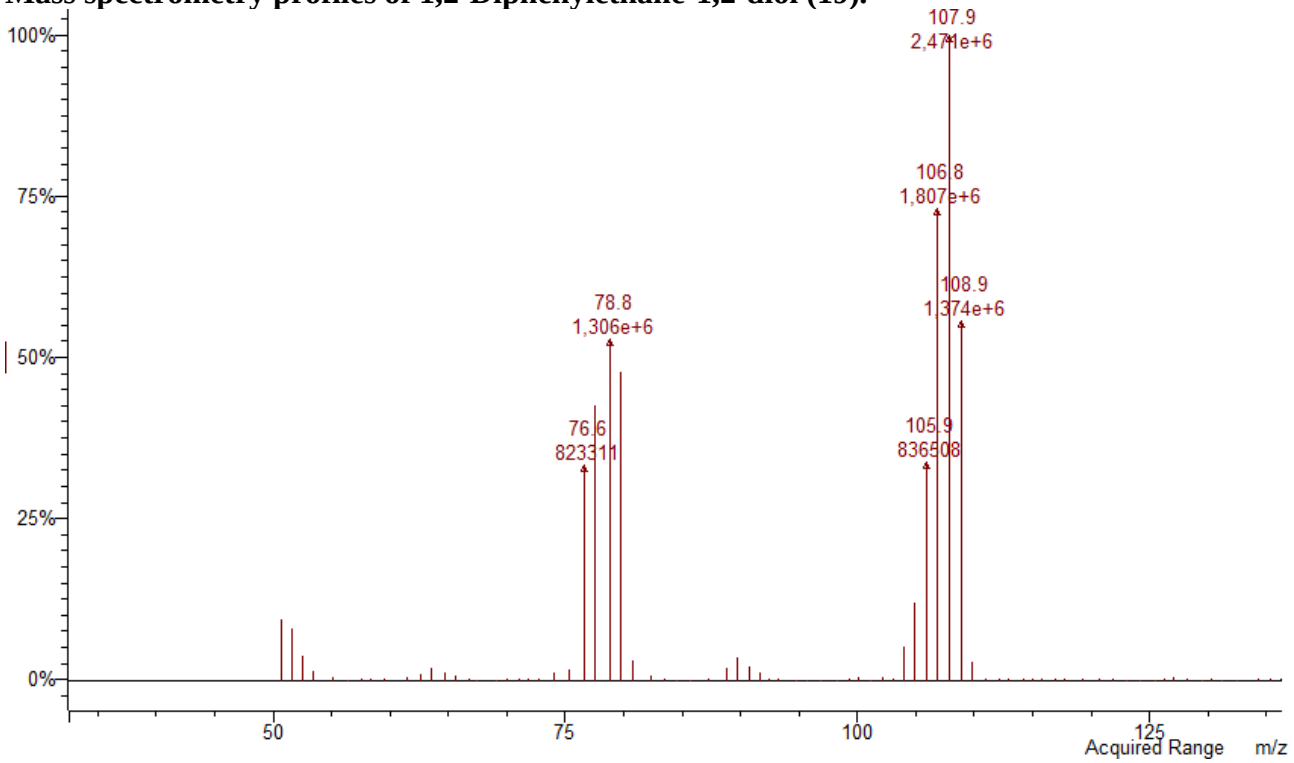

Mass spectrometry profiles of 2-benzyloxirane (20).

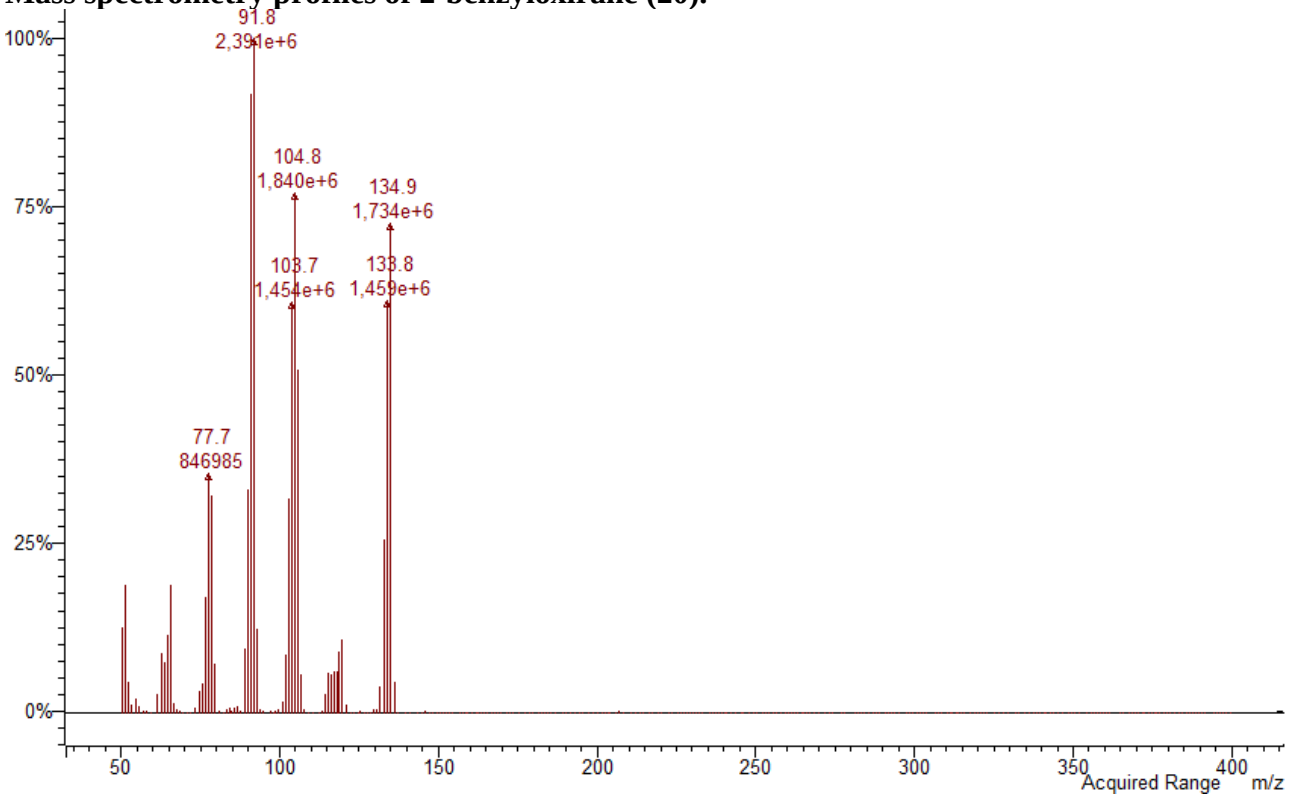

Mass spectrometry profiles of 3-phenylpropane-1,2-diol (21).

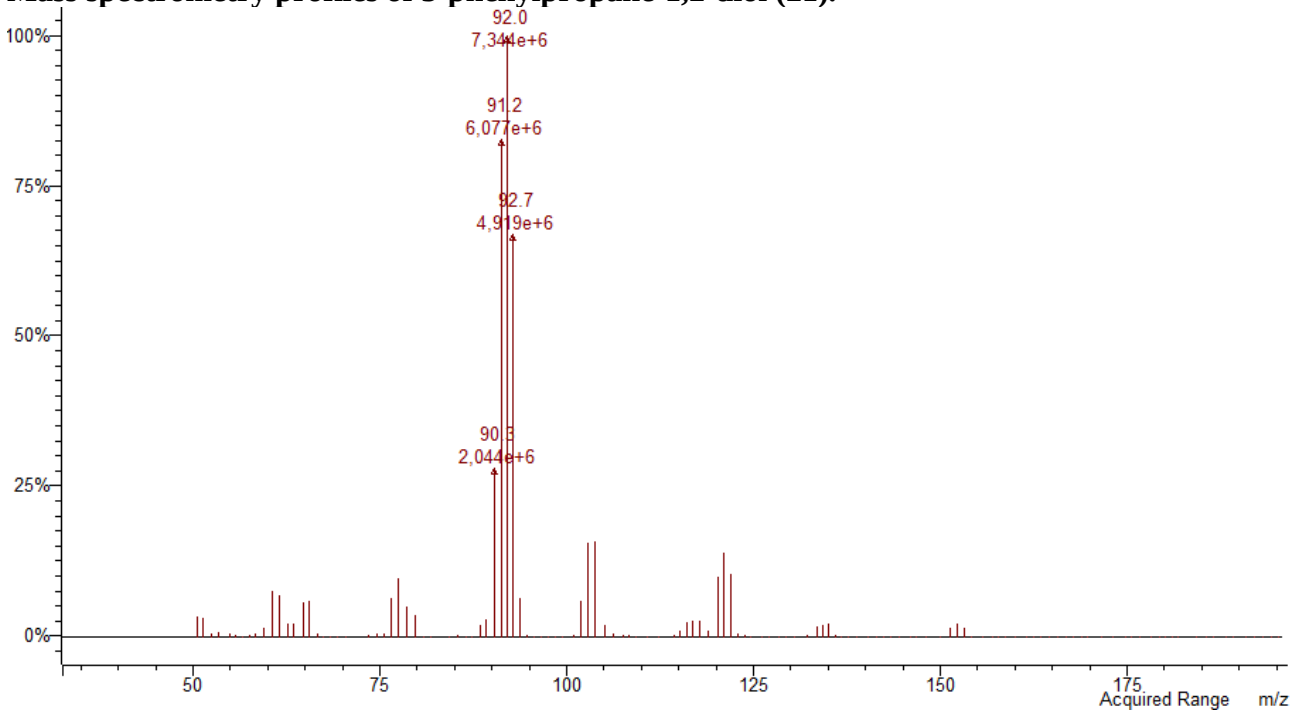

1.4.10 Nuclear magnetic resonance of compounds 1-21.

^{1}H NMR of 1-hexene (1)

^{1}H NMR ($CDCl_3$, 400 MHz): δ= 5.79-5.89 (m, 1H, -CH=), 4.93-5.04 (m, 2H, $=CH_2$), 2.07 (m, 2H,-CH_2-), 1.36-1.43 (m, 4H, 2 x-CH_2-), 0.90(m, 3H, CH_3-).

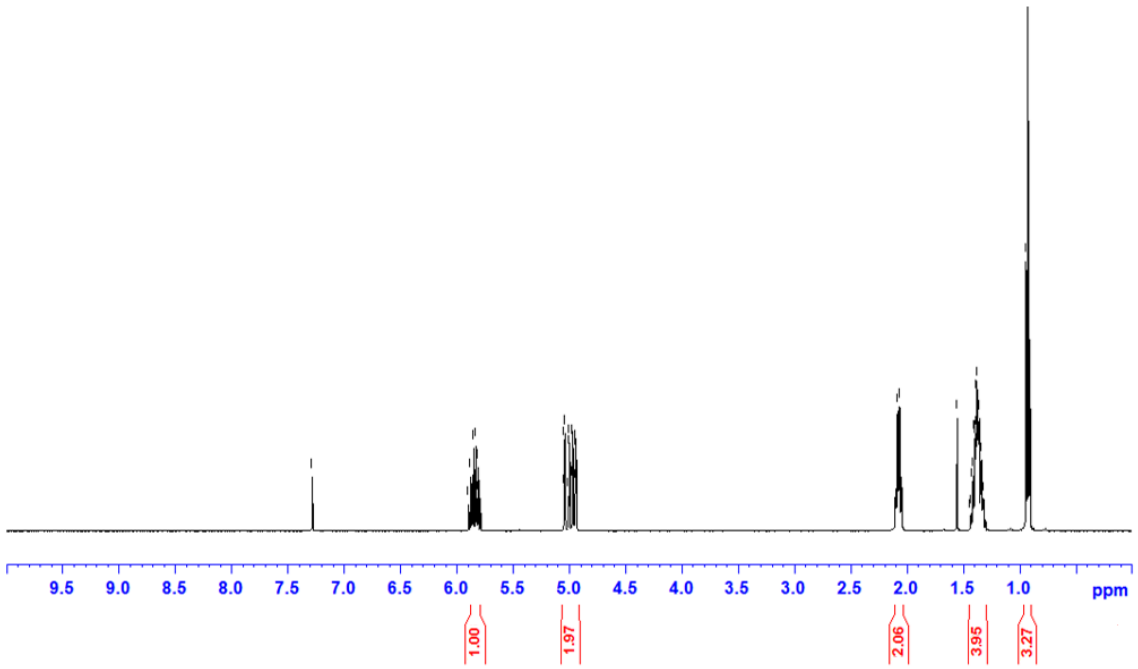

^{13}C NMR of 1-hexene (1)

^{13}C NMR ($CDCl_3$, 100 MHz): δ= 139.1 (-CH=), 115.7 ($=CH_2$), 32.5, 28.4, 22.8 (-CH_2-), 14.1 (CH_3-).

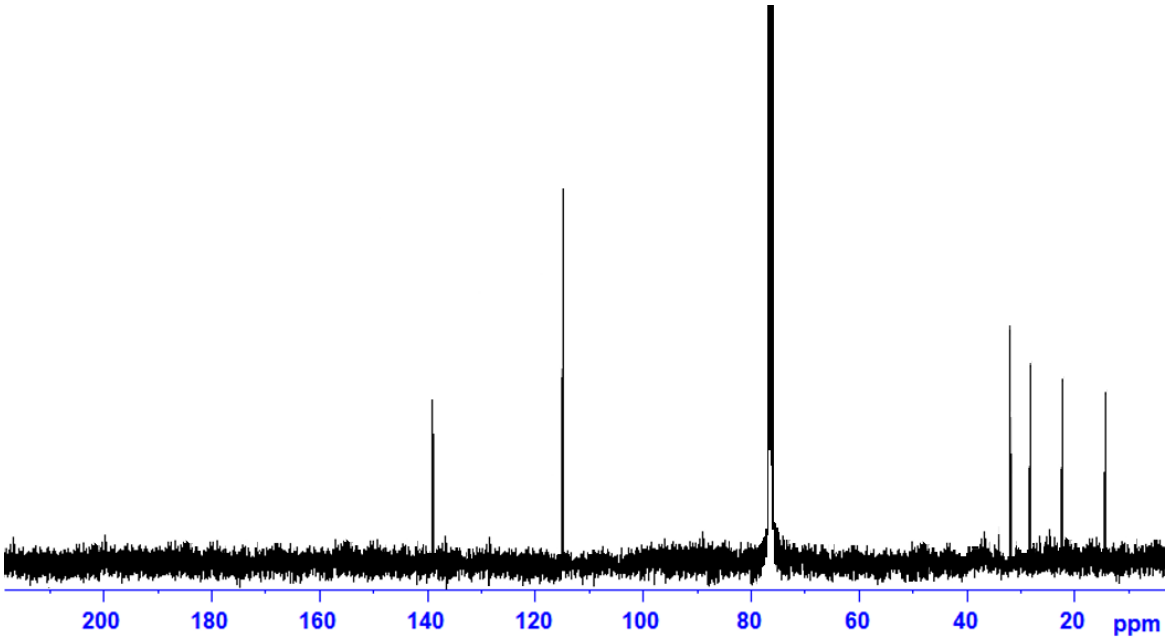

^{1}H NMR of 1-octene (2)

^{1}H NMR ($CDCl_3$, 400 MHz): δ= 5.79-5.87 (m,1H, -CH=), 4.93-5.04 (m, 2H, $=CH_2$), 2.06 (m, 2H,-CH_2-), 1.28-1.42 (m, 8H, 4 x-CH_2-), 0.91(m, 3H, CH_3-).

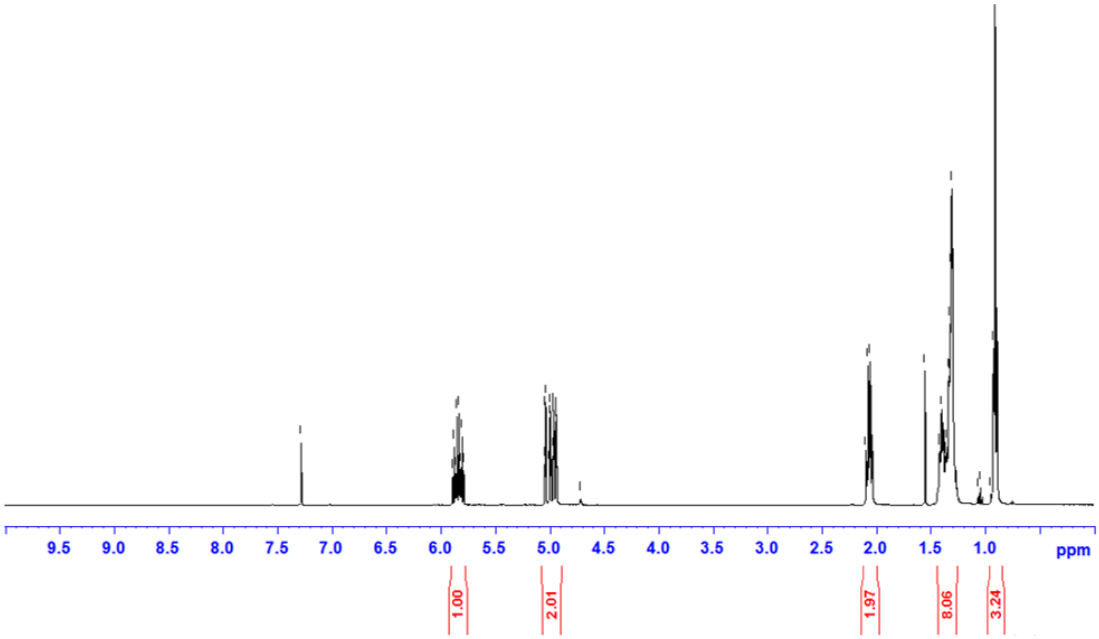

^{13}C NMR of 1-Octene (2)

^{13}C NMR ($CDCl_3$, 100 MHz): δ= 139.1 (-CH=), 115.7 ($=CH_2$), 33.9, 31.9, 29.6, 29.4, 22.7 (-CH_2-), 14.1 (CH_3-).

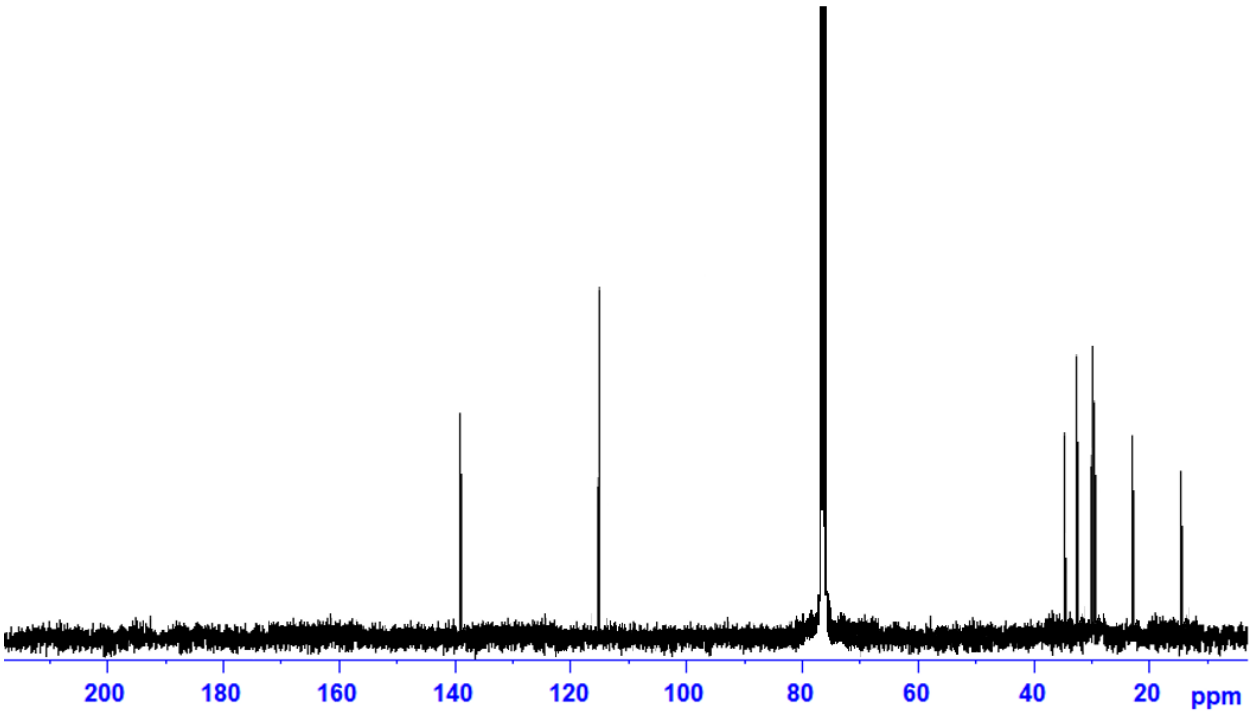

^{1}H NMR of trans-3-octene (3)

^{1}H NMR ($CDCl_3$, 400 MHz): δ= 5.37-5.50 (m, 2H, 2x -CH=), 1.97-2.05 (m, 4H, 2x -CH_2-), 1.30-1.37 (m, 4H, 2x -CH_2-), 1.00(m, 3H, -CH_3) 0.90(m, 3H, -CH_3).

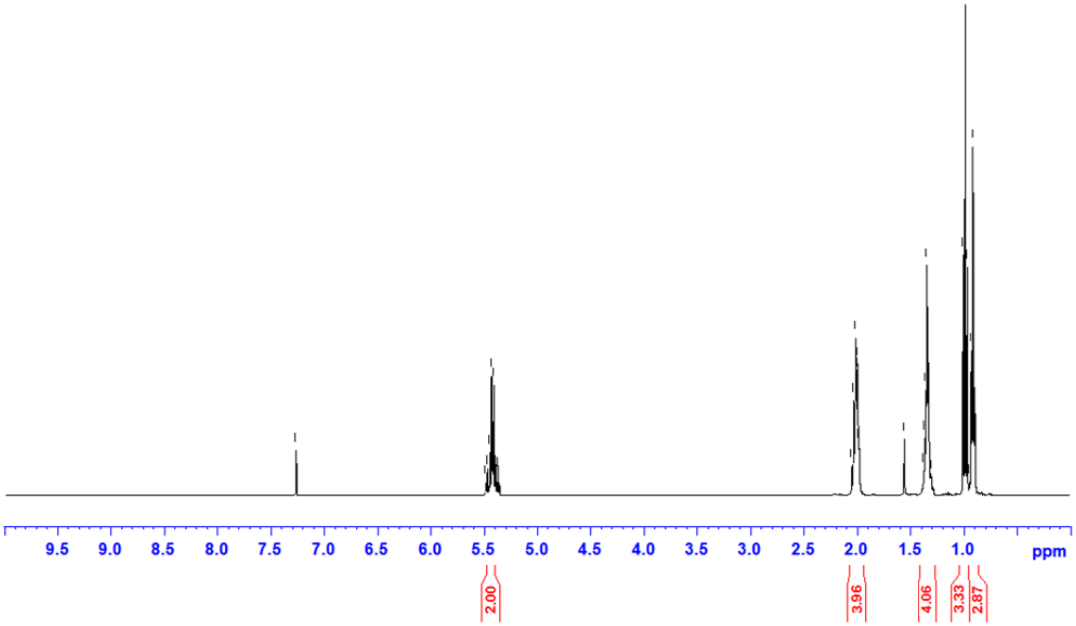

^{13}C NMR of trans-3-octene (3)

^{13}C NMR ($CDCl_3$, 100 MHz): δ= 133.7 (-CH=), 131.3 (-CH=), 33.4, 32.1, 26.5, 22.8 (-CH_2-), 14.3 (2 x CH_3-).

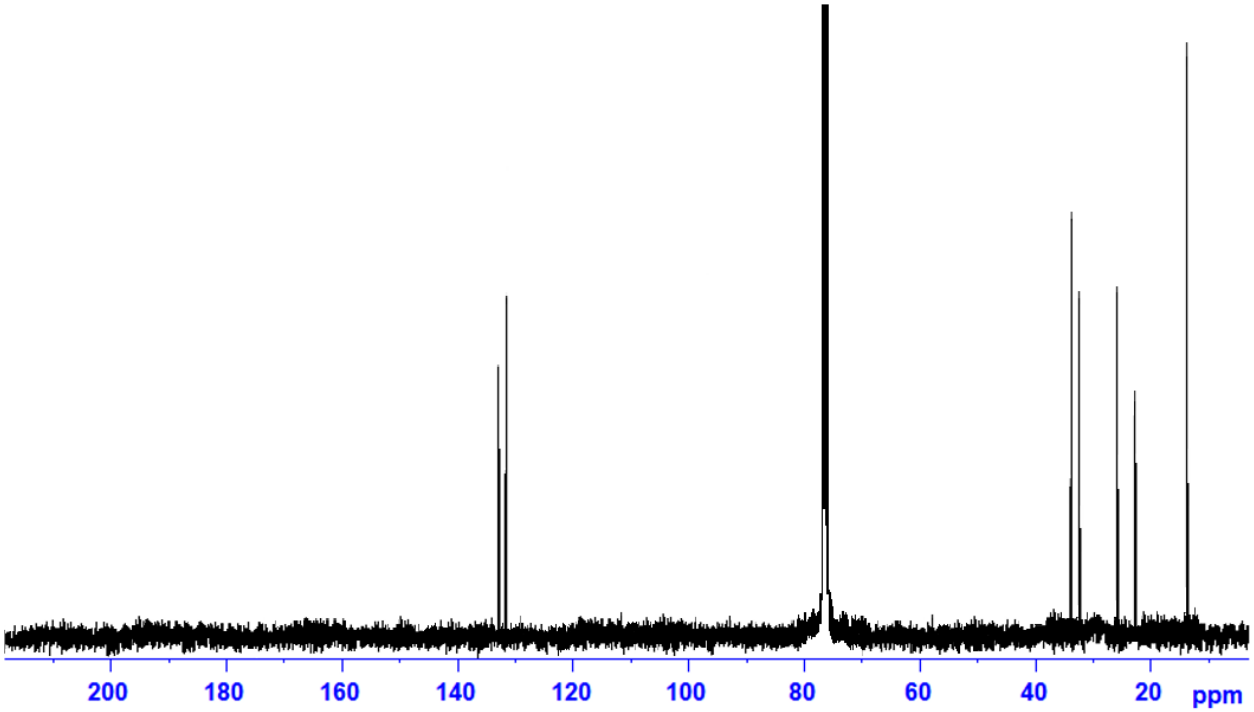

^{1}H NMR of Vinylcyclohexane (4)

^{1}H NMR ($CDCl_3$, 400 MHz): δ= 5.80 (m, 1H, -CH=), 4.88-5.00 (m, 2H, $=CH_2$), 1.97 (m, 1H, -CH), 1.09-1.76(m, 10 H, CH_2).

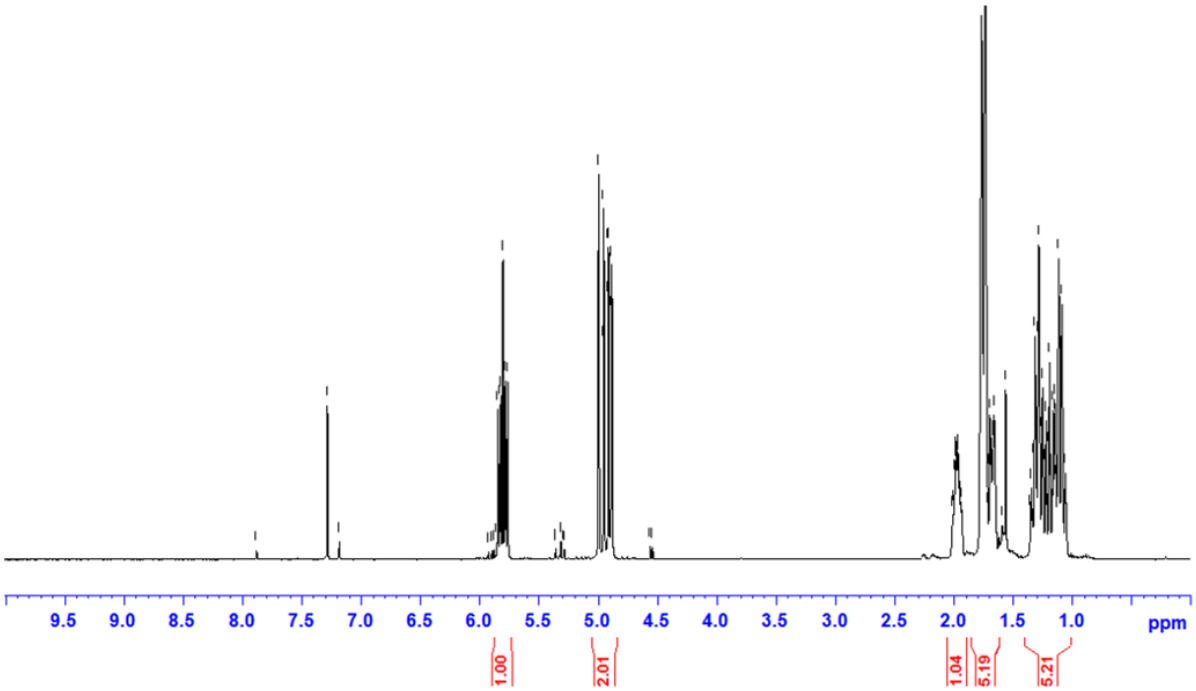

^{13}C NMR of Vinylcyclohexane (4)

^{13}C NMR ($CDCl_3$, 100 MHz): δ= 143.5 (-CH=), 112.7 ($=CH_2$), 41.8 (-CH-), 33.4 (2 x $-CH_2-$), 26.1 (2 x $-CH_2-$), 25.9 ($-CH_2-$).

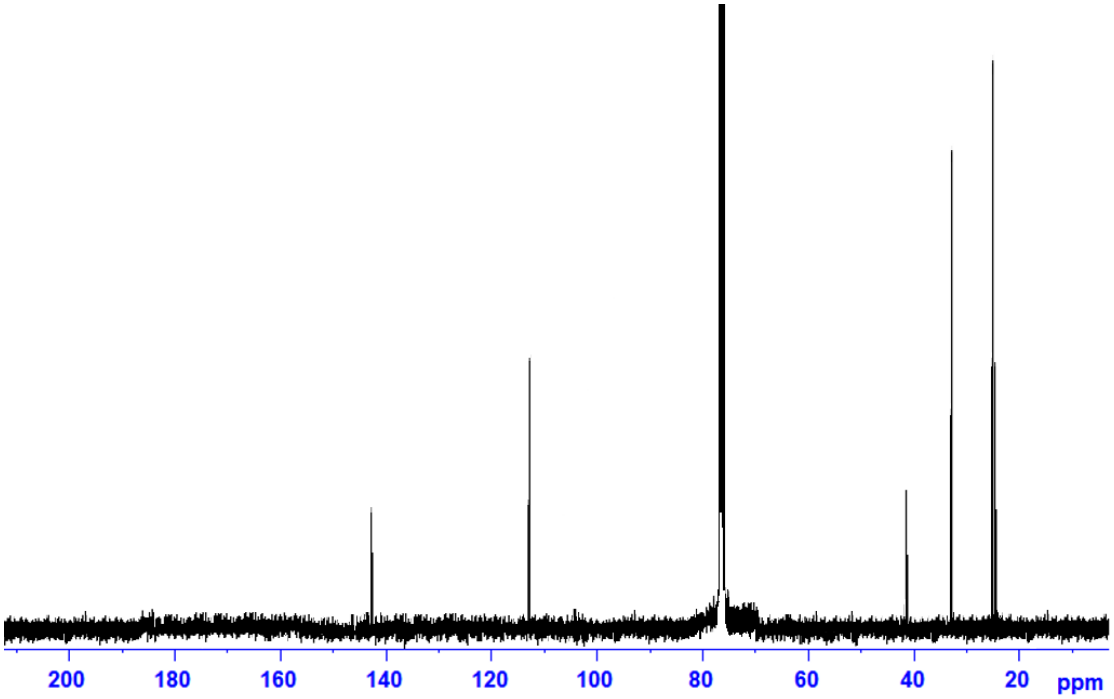

^{1}H NMR of Styrene (5)

^{1}H NMR ($CDCl_3$, 400 MHz): δ= 7.27-7.46 (m, 5H, CH Ar), 6.77 (m, 1H, -CH=), 5.79 (d, *J*= 16, 1H, $=CH_2$), 5.28 (d, *J*= 10, 1H, $=CH_2$).

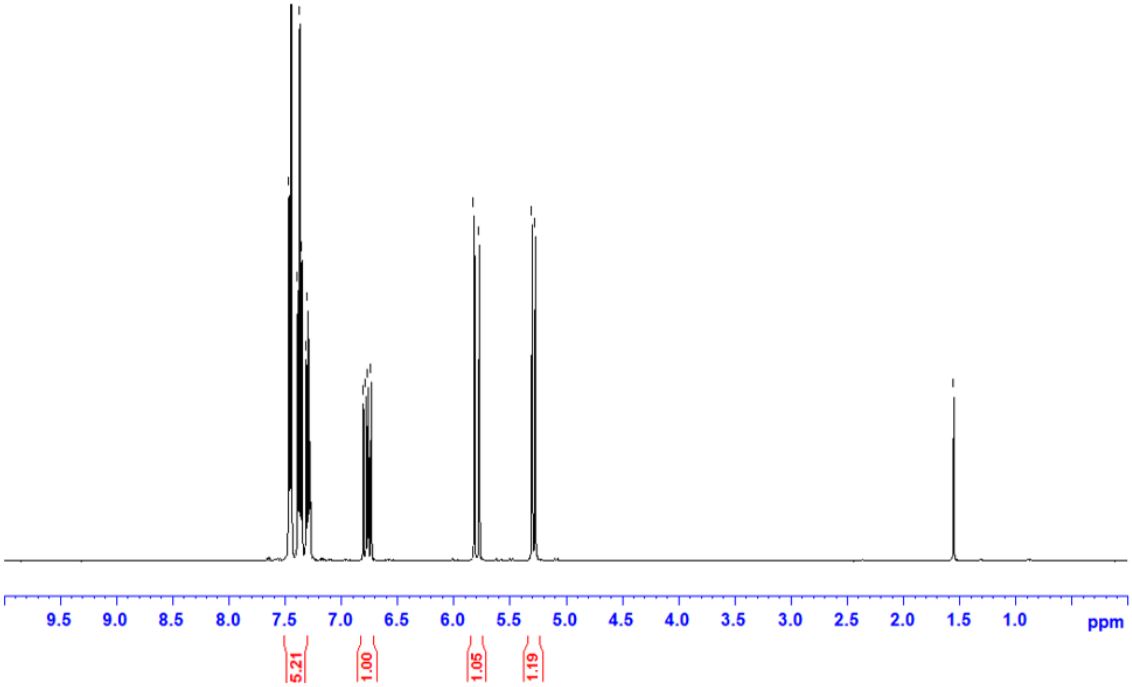

^{13}C NMR of styrene (5)

^{13}C NMR ($CDCl_3$, 100 MHz): δ=137.9 (-C-), 136.1 (-CH=), 128.6 (2 x -CH-), 128.5 (2 x -CH-), 127.9 (-CH-), 114.7 ($=CH_2$).

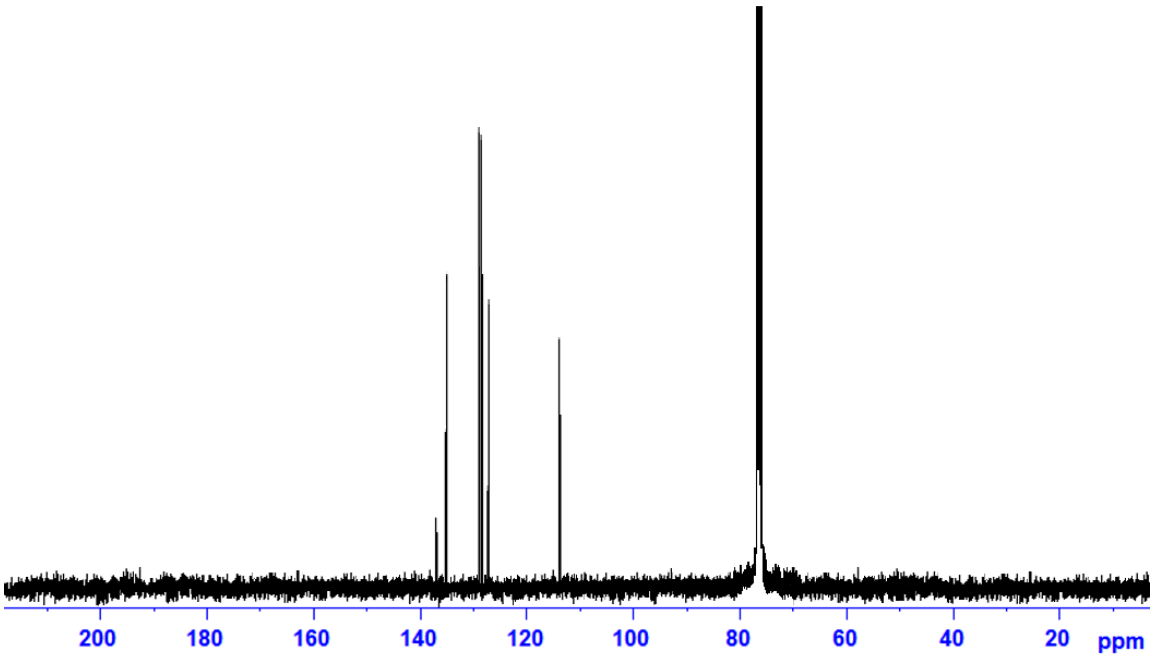

^{1}H NMR of cis-stilbene (6)

^{1}H NMR ($CDCl_3$, 400 MHz): δ= 7.20-7.30 (m, 10H, CH Ar), 6.64 (s,2H, 2x -CH=).

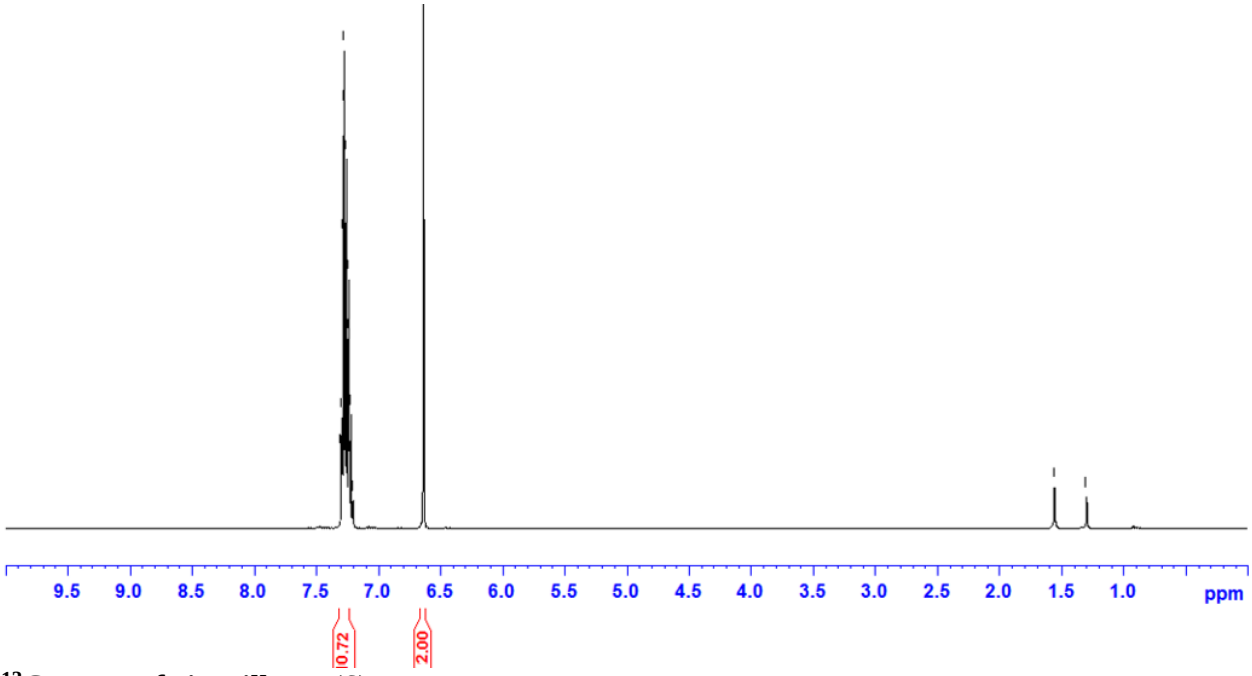

^{13}C NMR of cis-stilbene (6)

^{13}C NMR ($CDCl_3$, 100 MHz): δ= 137.5 (2 x -C-), 128.6 (4 x -CH-),128.5 (4 x -CH-), 127.9 (2 x -CH-),127.4 (2 x -CH=).

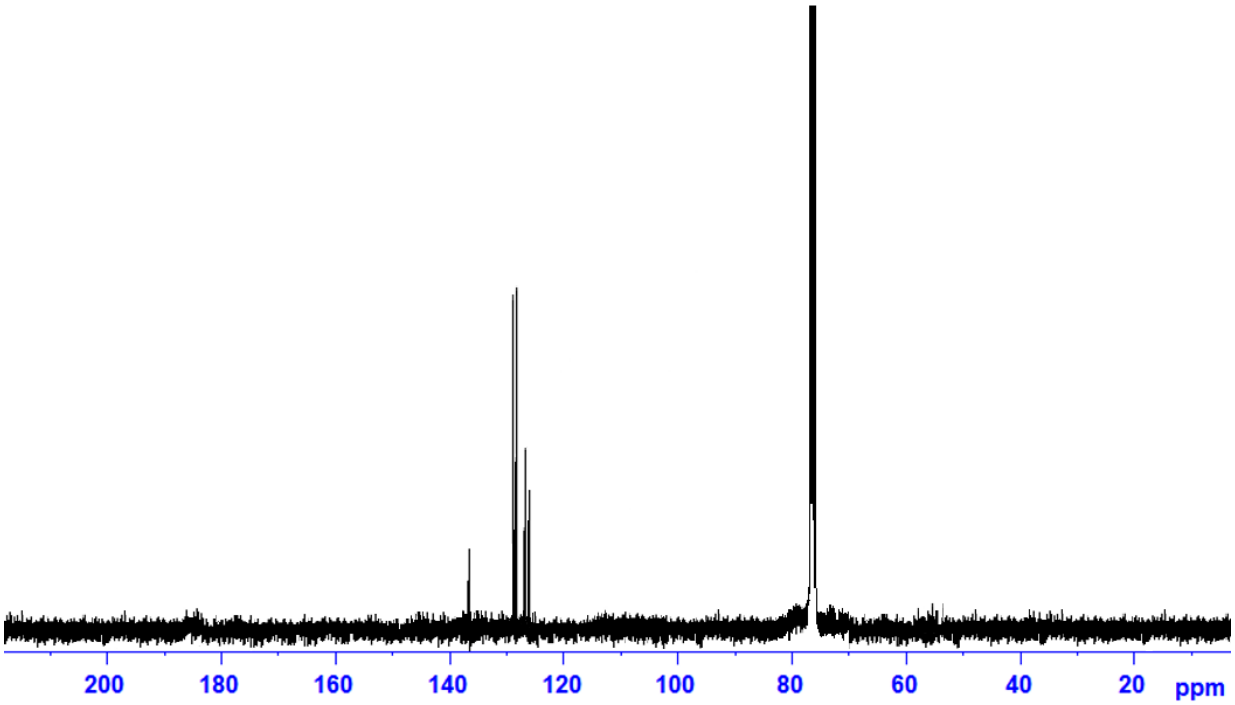

^{1}H NMR of allylbenzene (7)

^{1}H NMR ($CDCl_3$, 400 MHz): δ= 7.22-7.35 (m, 5H, CH Ar), 6.01 (m,1H, -CH=), 5.12 (m, 2H, $=CH_2$), 3.43(s, 2H, $-CH_2-$).

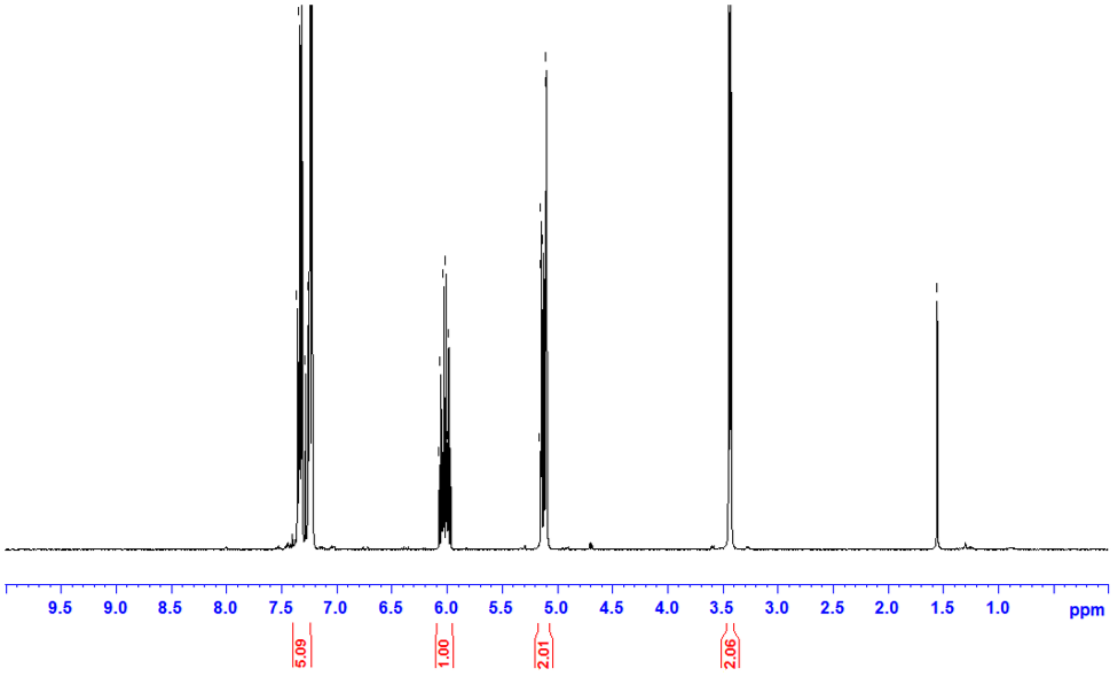

^{13}C NMR of allylbenzene (7)

^{13}C NMR ($CDCl_3$, 100 MHz): δ= 141.4 (-C-), 136.5 (-CH=), 129.0 (2 x -CH-),128.6 (2 x -CH-), 125.7 (-CH-), 115.9 ($=CH_2$), 39.5 ($-CH_2-$).

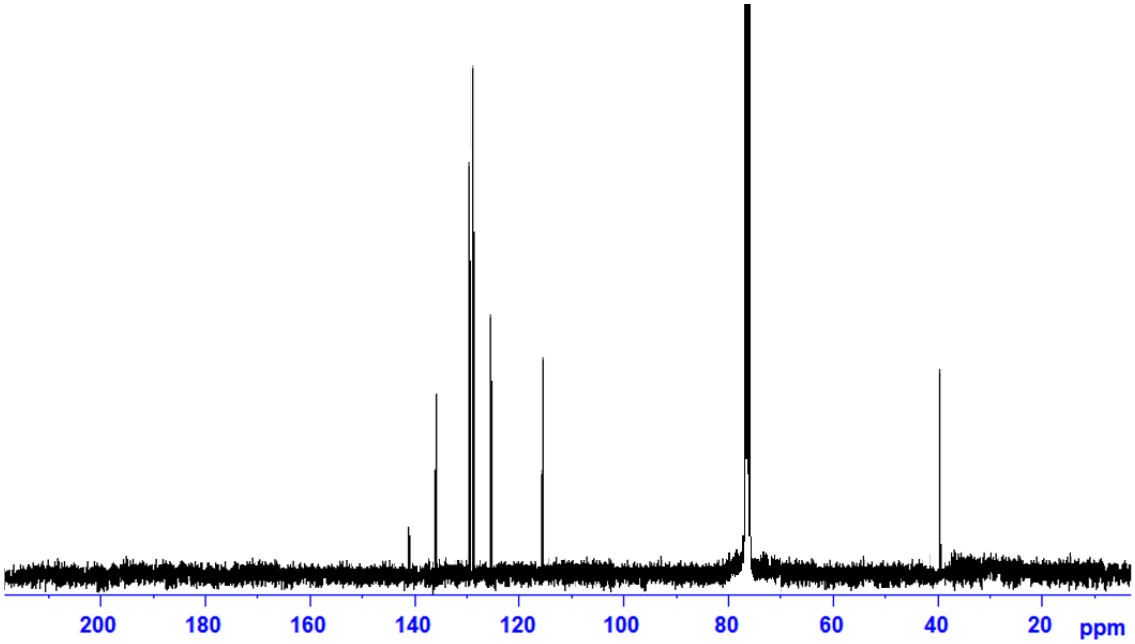

^{1}H NMR of 1,2-epoxyhexane (8)

^{1}H NMR ($CDCl_3$, 400 MHz): δ= 2.63-2.78 (m, 2H, O-CH), 2.15-2.37 (m, 1H, O-CH_2), 1.20-1.65 (m, 6H, 3 x-CH_2), 0.85-0.94 (m, 3H, CH_3-).

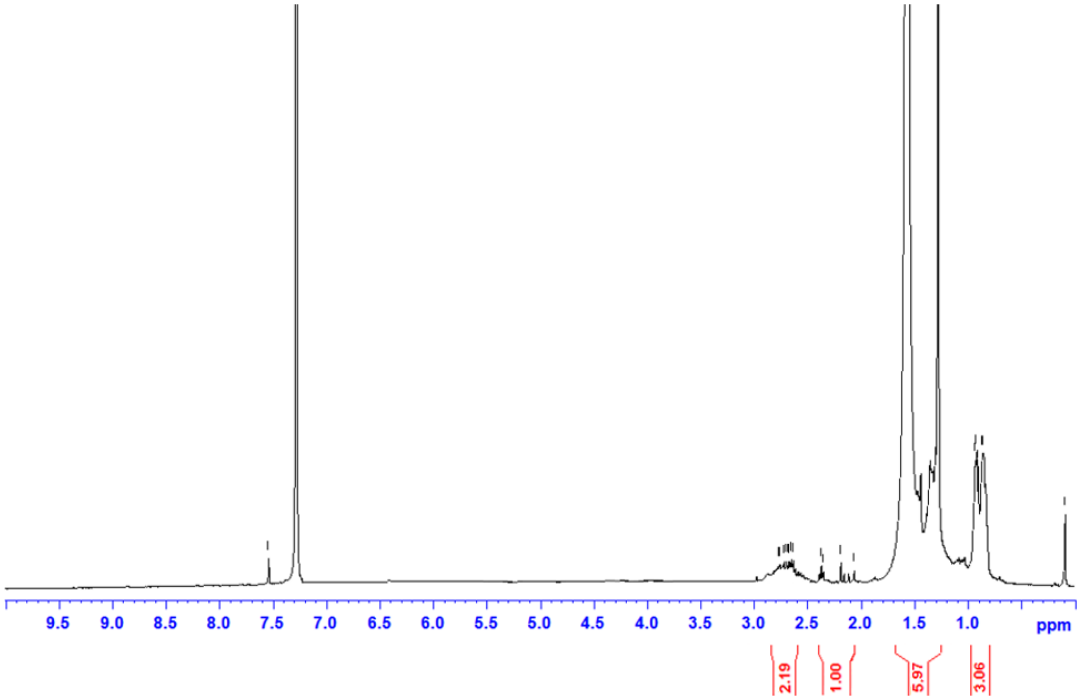

^{13}C NMR of 1,2-epoxyhexane (8)

^{13}C NMR ($CDCl_3$, 100 MHz): δ= 51.8 (O-CH), 46.4 (O-CH_2), 32.5, 28.4, 22.8 (-CH_2-), 14.1 (CH_3-).

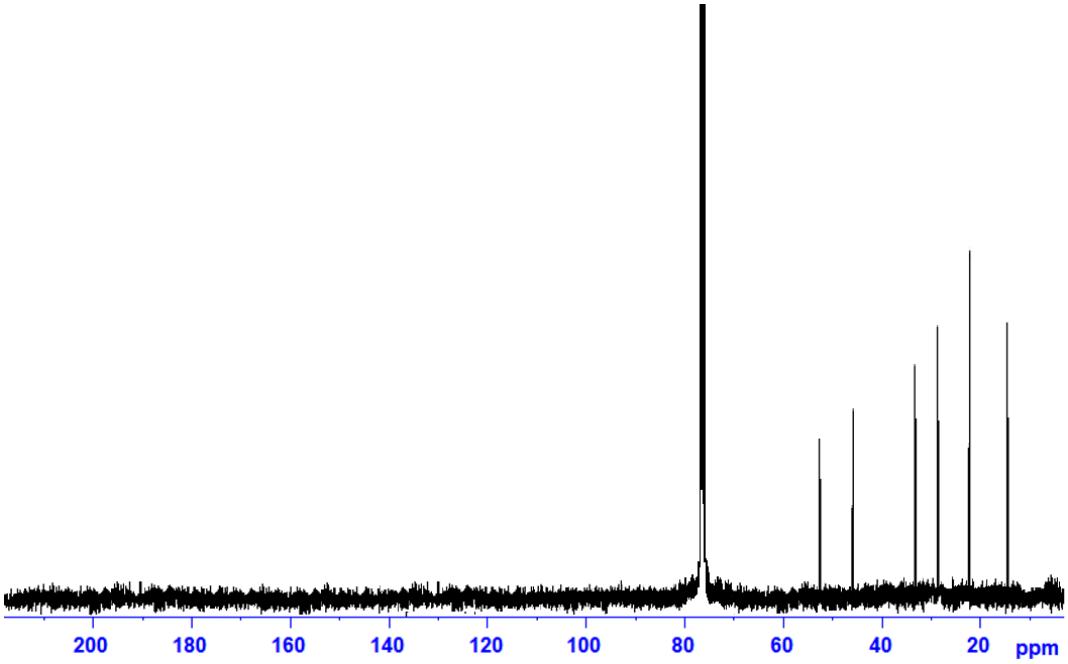

^{1}H NMR of hexane-1,2-diol (9)

^{1}H NMR ($CDCl_3$, 400 MHz): δ= 3.70 – 3.74 (m, 1H, CH-OH), 3.47-3.53 (m, 2H, CH_2-OH), 1.34 – 1.65 (m, 6H, 3 x-CH_2-), 0.91 (m, 3H, CH_3-).

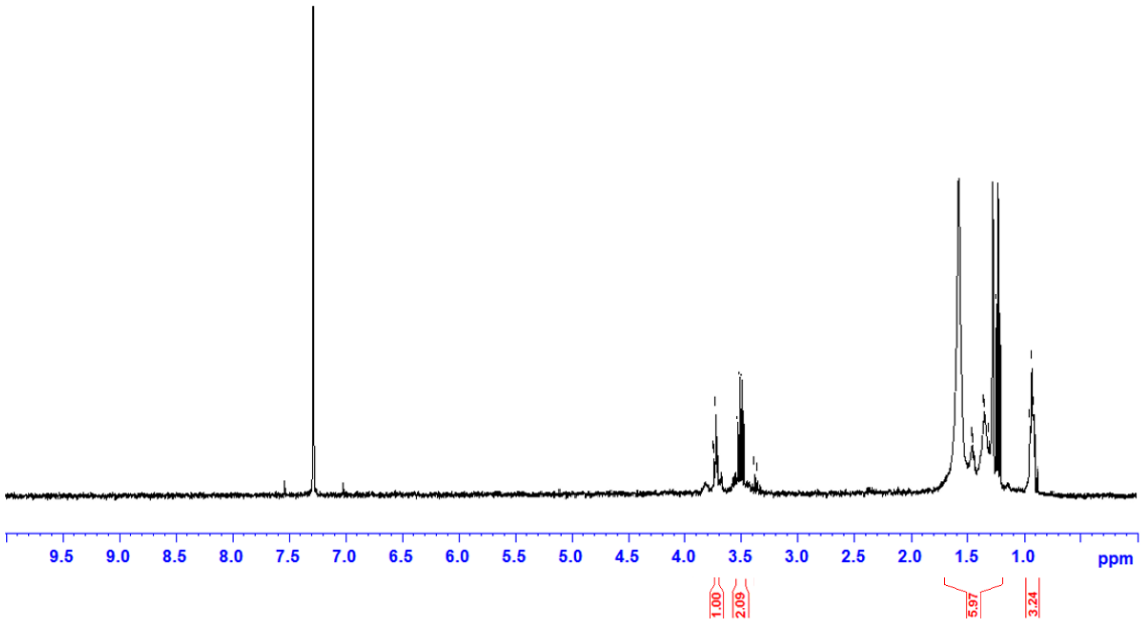

^{13}C NMR of hexane-1,2-diol (9)

^{13}C NMR ($CDCl_3$,100 MHz,): δ= 72.3 (CH-OH), 66.7 (CH_2-OH), 32.7, 27.7, 22.7 (-CH_2-), 14.0 (CH_3-).

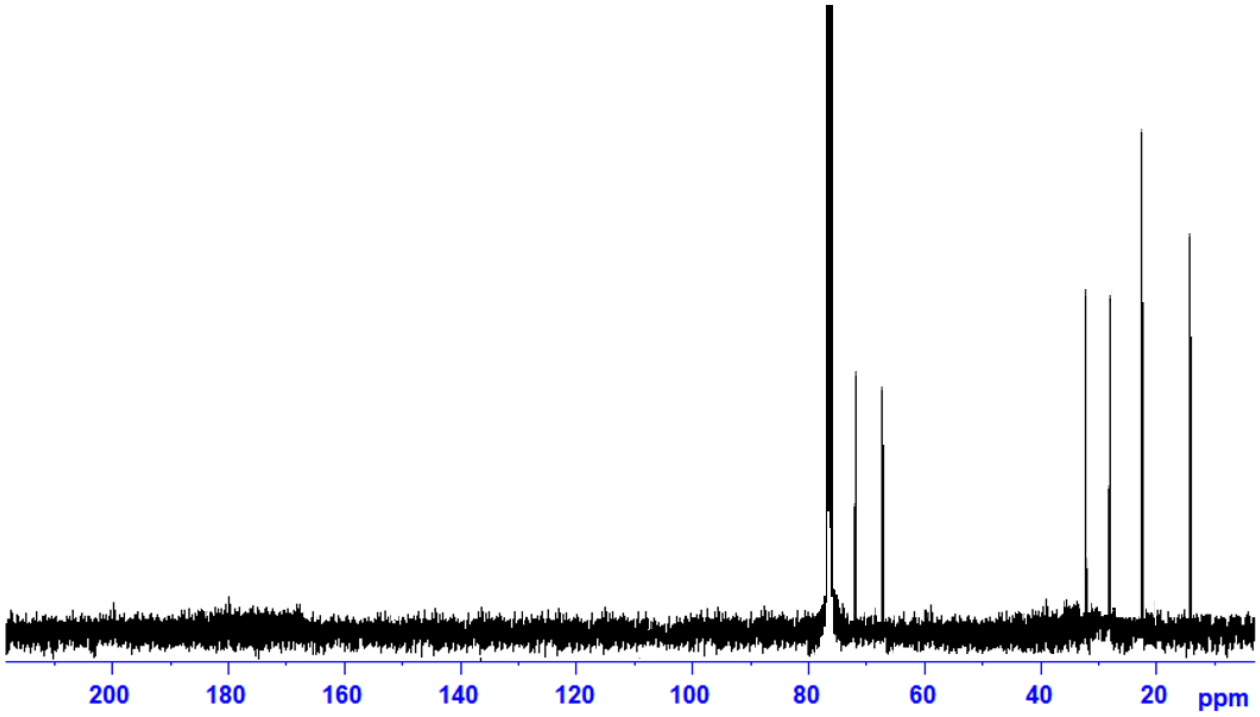

^{1}H NMR of 1,2-Epoxyoctane (10)

^{1}H NMR ($CDCl_3$,400 MHz): δ = 2.61-2.74 (m, 1H, CH-O), 2.38-2.44 (m, 2H, CH_2-OH), 1.27 - 1.90 (m, 10H, 5 x CH_{2-}), 0.85-0.90(m, 3H, CH_3-).

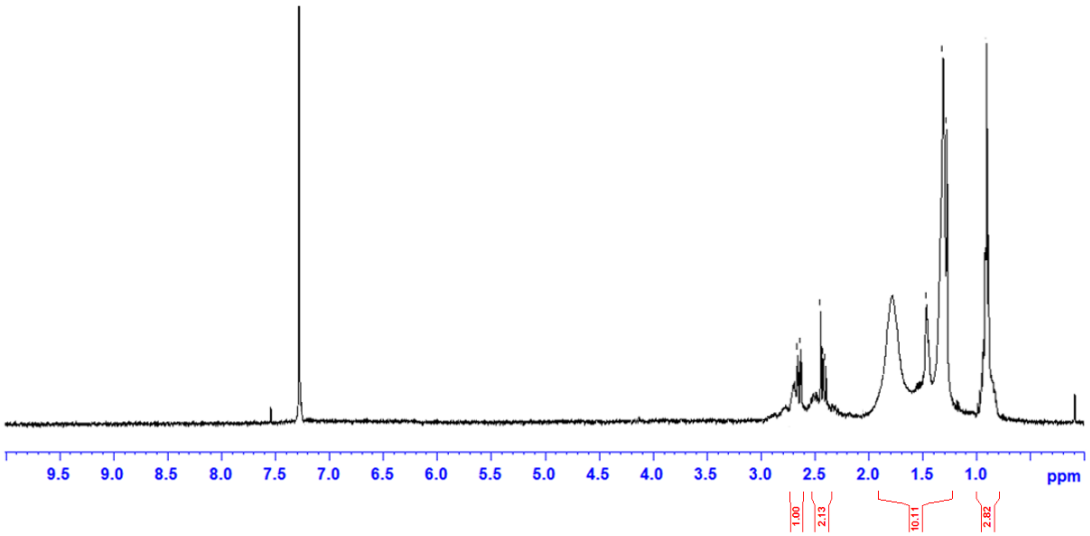

^{13}C NMR of 1,2-Epoxyoctane (10)

^{13}C NMR ($CDCl_3$, 100 MHz): δ= 52.3 (O-CH), 47.0 (O-CH_2), 32.5,31.7, 29.1, 25.9, 22.5 (-CH_2-), 14.0 (CH_3-).

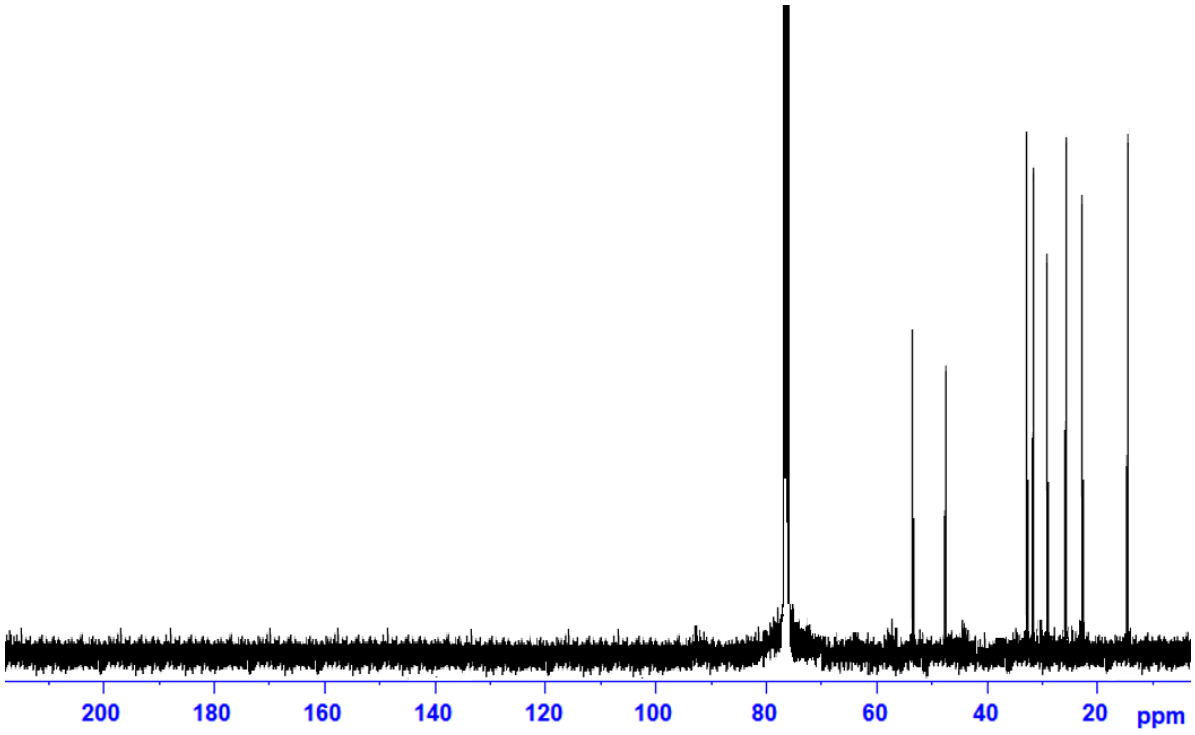

^{1}H NMR of octane-1,2-diol (11)

^{1}H NMR ($CDCl_3$,400 MHz): δ= 3.62 – 3.70 (m, 2H, CH_2-OH), 3.43-3.48 (m, 1H, CH-OH),1.45-1.50 (m, 2H,-CH_2-) 1.25-1.35 (m, 8H,-CH_2-), 0.90 (m, 3H, CH_3-).

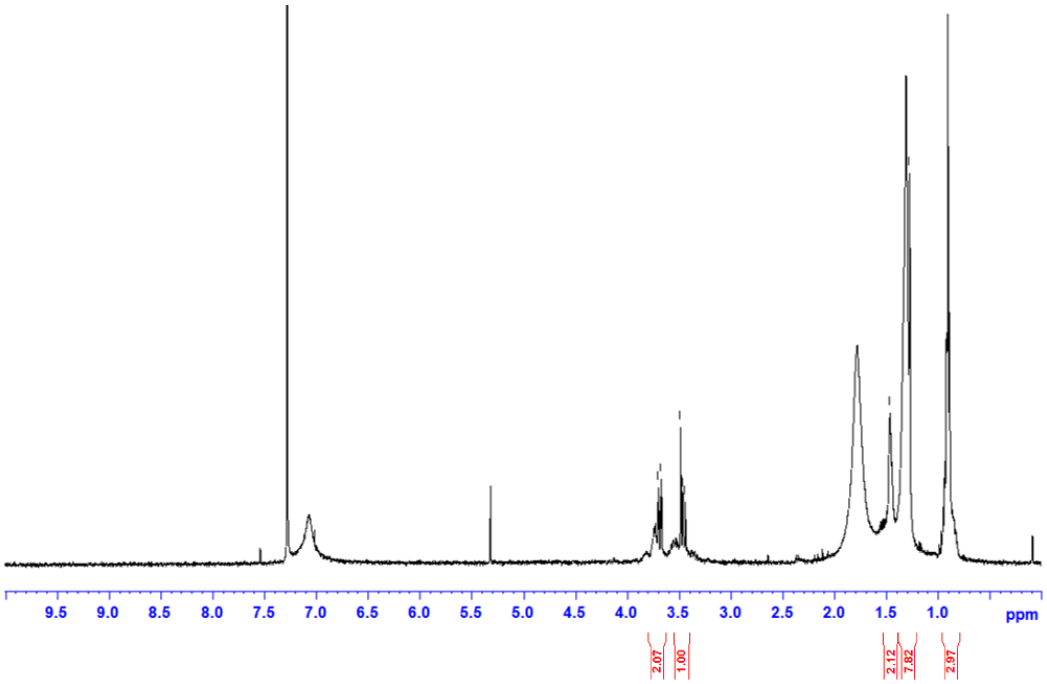

^{13}C NMR of octane-1,2-diol (11)

^{13}C NMR ($CDCl_3$,100 MHz,): δ= 72.4 (CH-OH), 66.8 (CH_2-OH), 33.1, 31.7, 29.3, 25.5, 22.6 (-CH_2-), 14.1 (CH_3-).

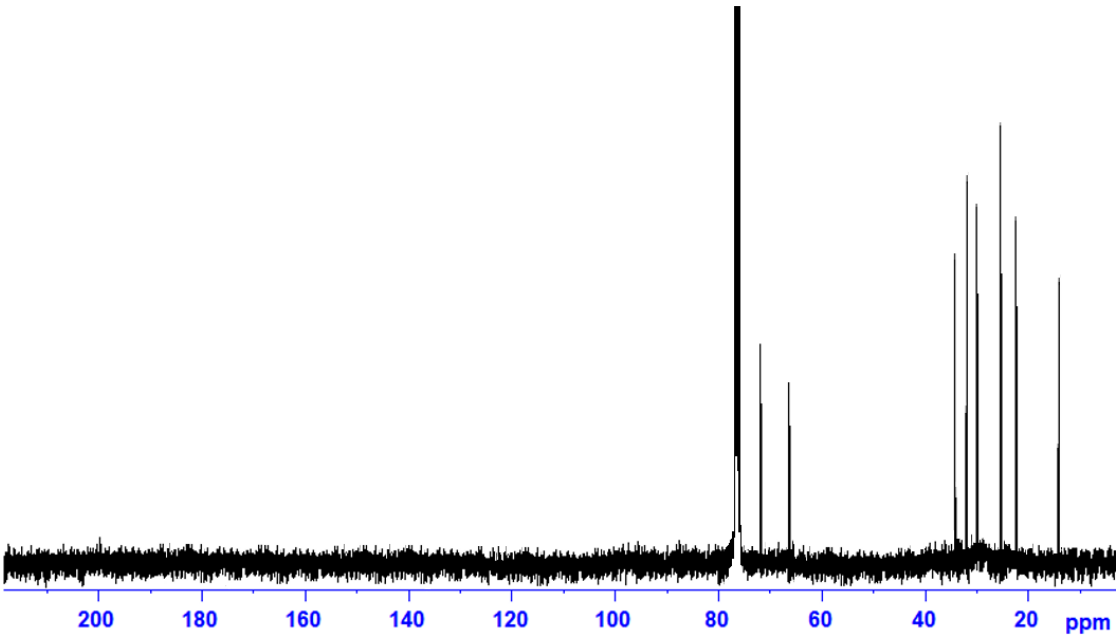

^{1}H NMR of trans-3,4-epoxyoctane (12)

^{1}H NMR ($CDCl_3$,400 MHz) δ=2.60-2.73 (m,2H, 2 x CH-O),1.28-1.62 (m, 8H, ,4 x-CH_2-), 0.98 (m, 3H, CH_3-), 0.88 (m, 3H, CH_3-).

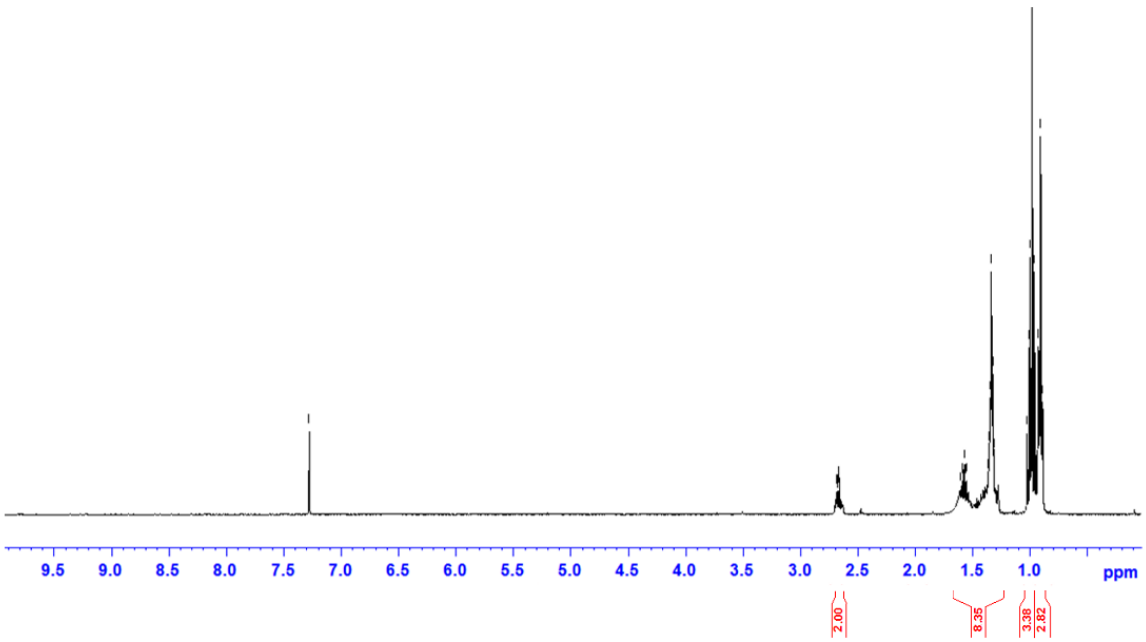

^{13}C NMR of trans-3,4-epoxyoctane (12)

^{13}C NMR ($CDCl_3$, 100 MHz): δ= 58.3 (O-CH), 57.3 (O-CH), 28.7, 27.3, 22.6, 21.0, (-CH_2-), 13.9 (CH_3-), 10.5 (CH_3-).

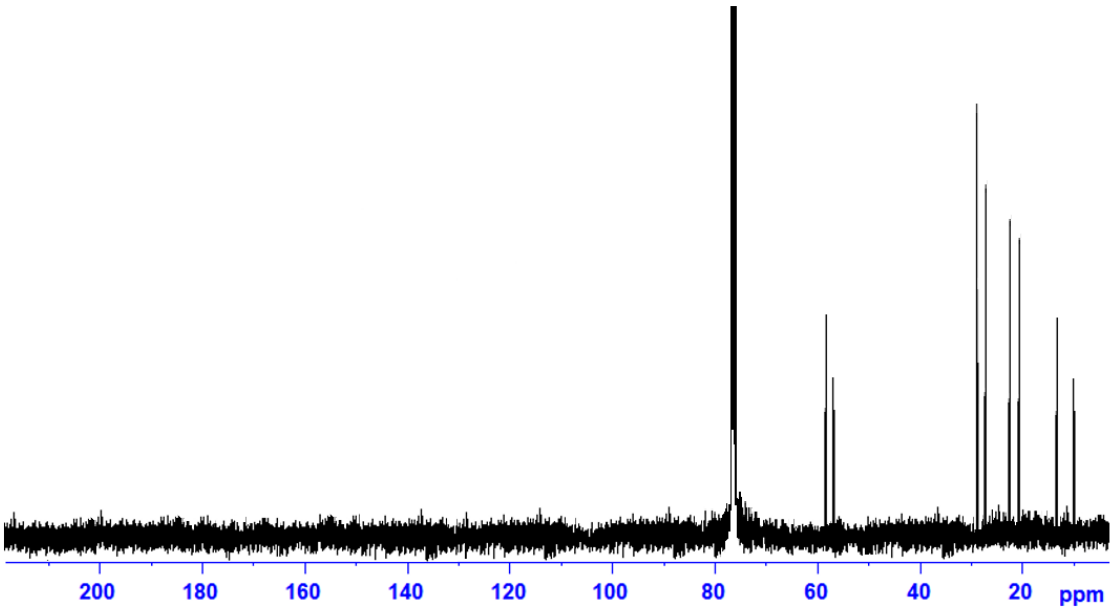

^{1}H NMR of octane-3,4-diol (13)

^{1}H NMR ($CDCl_3$,400 MHz): δ= 3.43-3.55 (m, 2H, 2 x CH-OH),1.21-1.55 (m, 8H, 4 x-CH_2-), 1.08 (m, 3H, CH_3-), 0.83-0.95 (m, 3H, CH_3-).

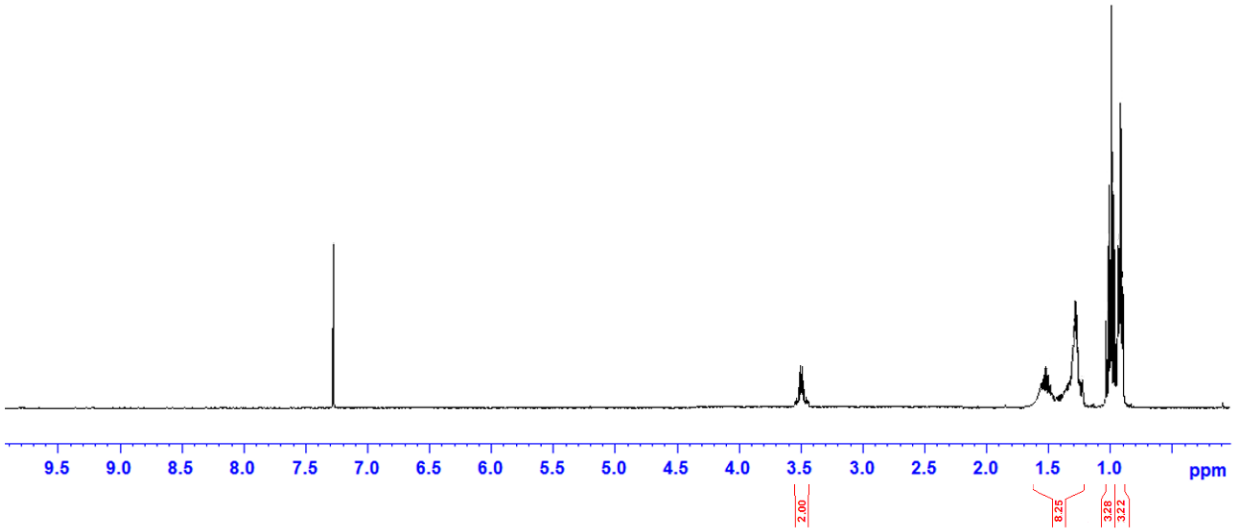

^{13}C NMR of octane-3,4-diol (13)

^{13}C NMR ($CDCl_3$ 100 MHz,): δ= 76.2 (CH-OH), 75.3 (CH-OH), 33.8, 31.7, 25.2, 22.5 (-CH_2-), 13.9 (CH_3-),10.5 (CH_3-).

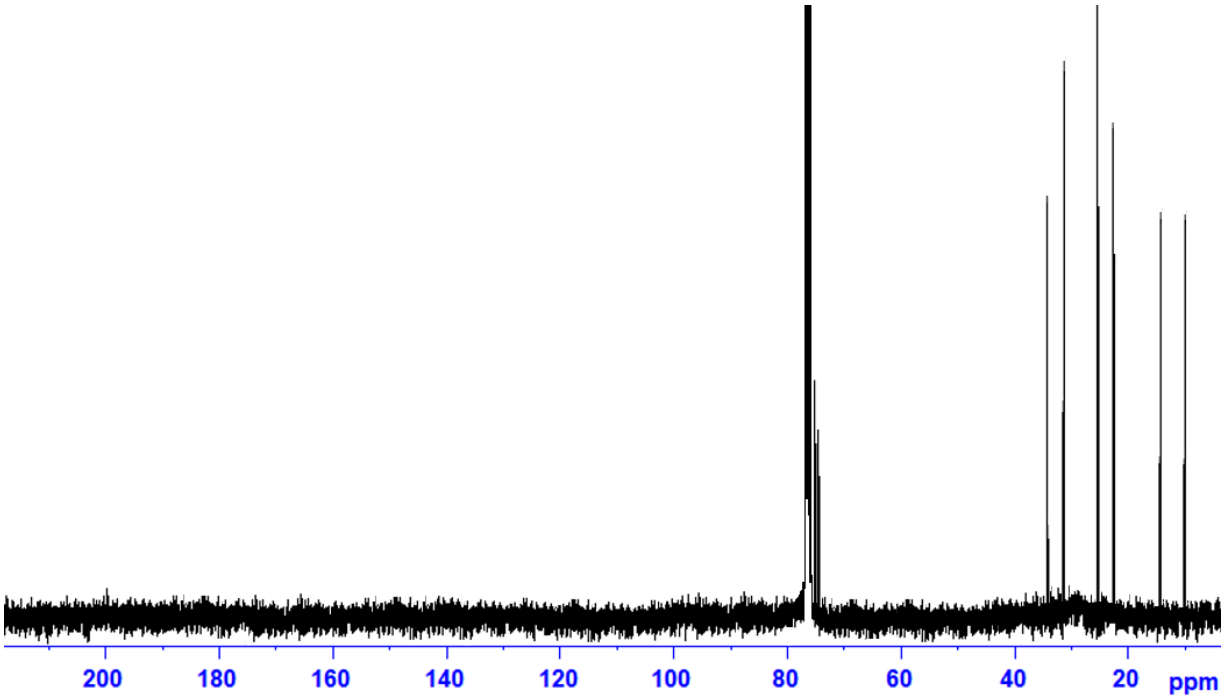

^{1}H NMR of 2-cyclohexyloxirane (14)

^{1}H NMR ($CDCl_3$,400 MHz): δ = 2.60–2.72 (m, 2H, CH_2-O), 2.51–2.54 (m, 1H, CH-O), 1.84-1.89 (m, 1H, CH), 1.53-1.72 (m, 4H, 2 x CH_2), 1.20-1.52 (m, 6H, 3 x CH_2).

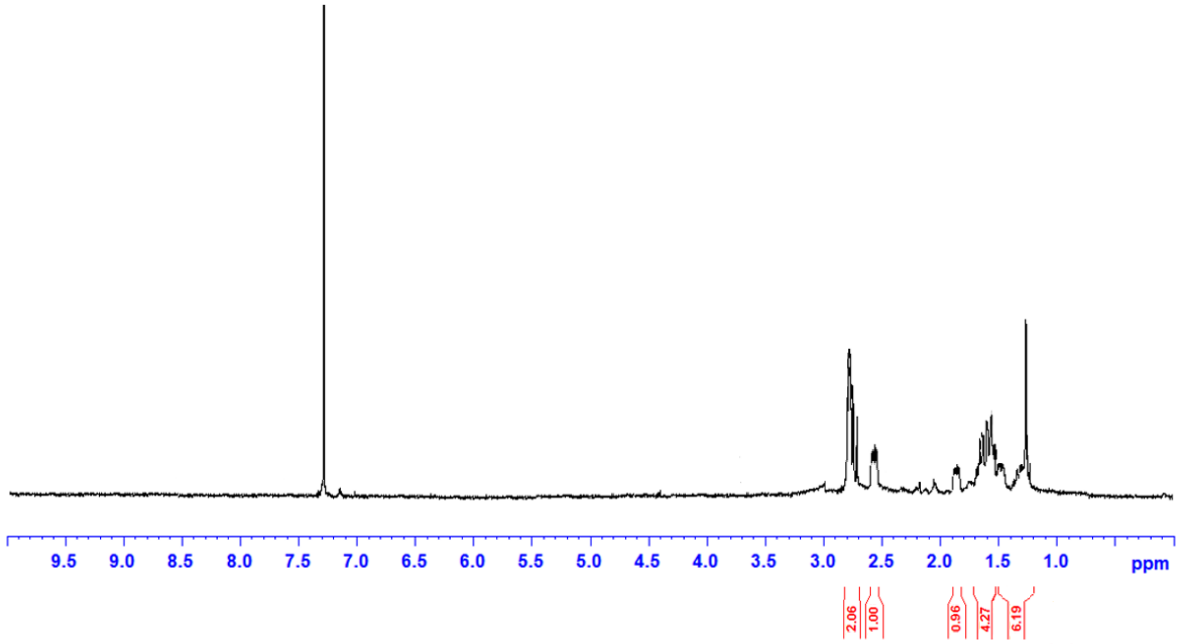

^{13}C NMR of 2-cyclohexyloxirane (14)

^{13}C NMR ($CDCl_3$, 100 MHz): δ= 56.6 (O-CH), 46.0 (O-CH_2), 40.4 (-CH-), 29.7, 28.8, 26.3, 25.7, 25.5 (-CH_2-).

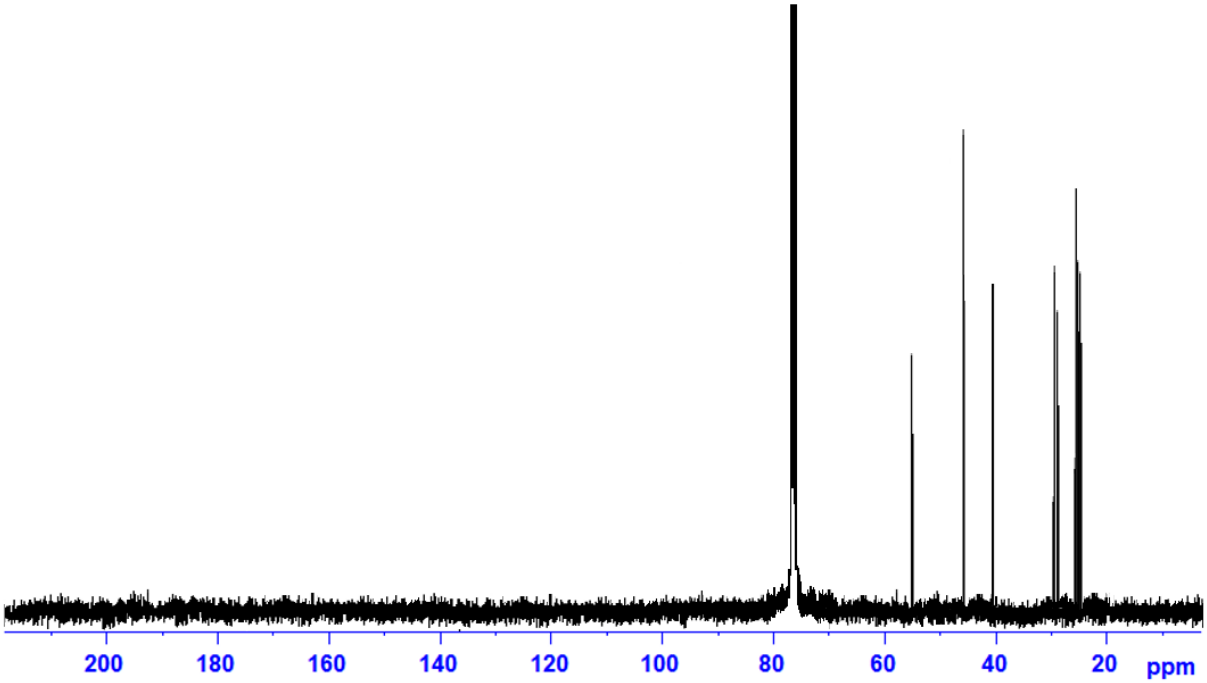

^{1}H NMR of 1-cyclohexylethane-1,2-diol (15)

^{1}H NMR ($CDCl_3$, 400 MHz): δ= 3.76-3.93 (m, 1H, CH-OH), 3.47-3.75 (m, 2H, CH_2-OH), 0.85-1.88 (m, 11H).

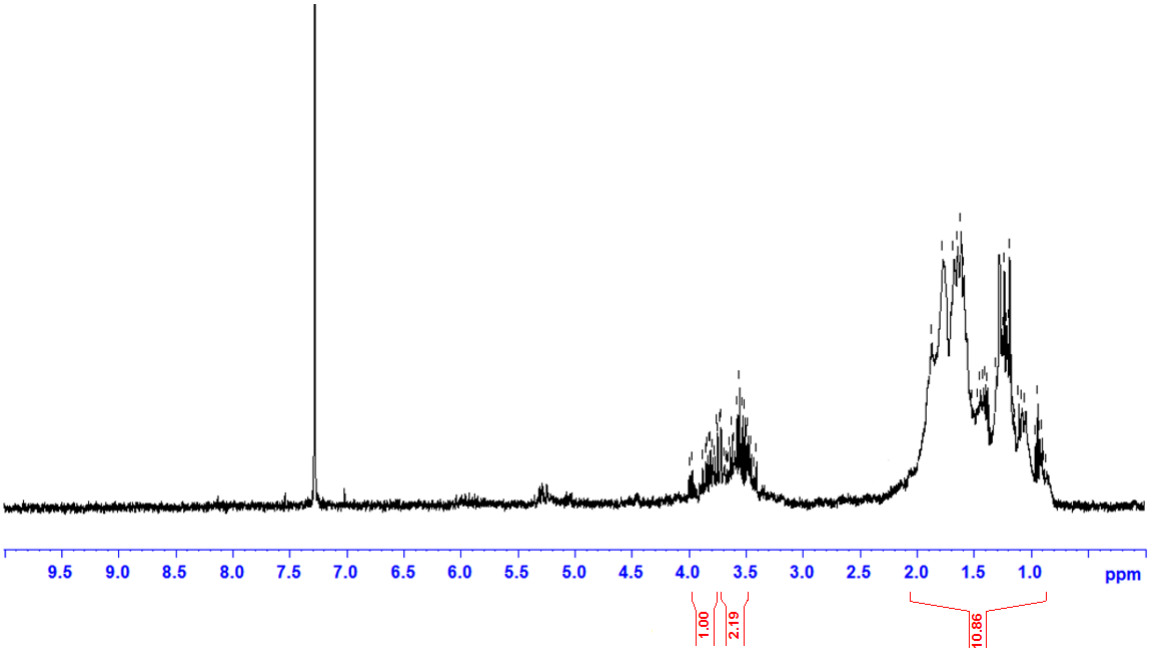

^{13}C NMR of 1-cyclohexylethane-1,2-diol (15)

^{13}C NMR ($CDCl_3$,100 MHz,): δ= 76.5 (CH-OH), 64.7 (CH_2-OH), 40.7 (-CH-), 29.0, 28.6, 26.3, 26.1, 26.0 (-CH_2-).

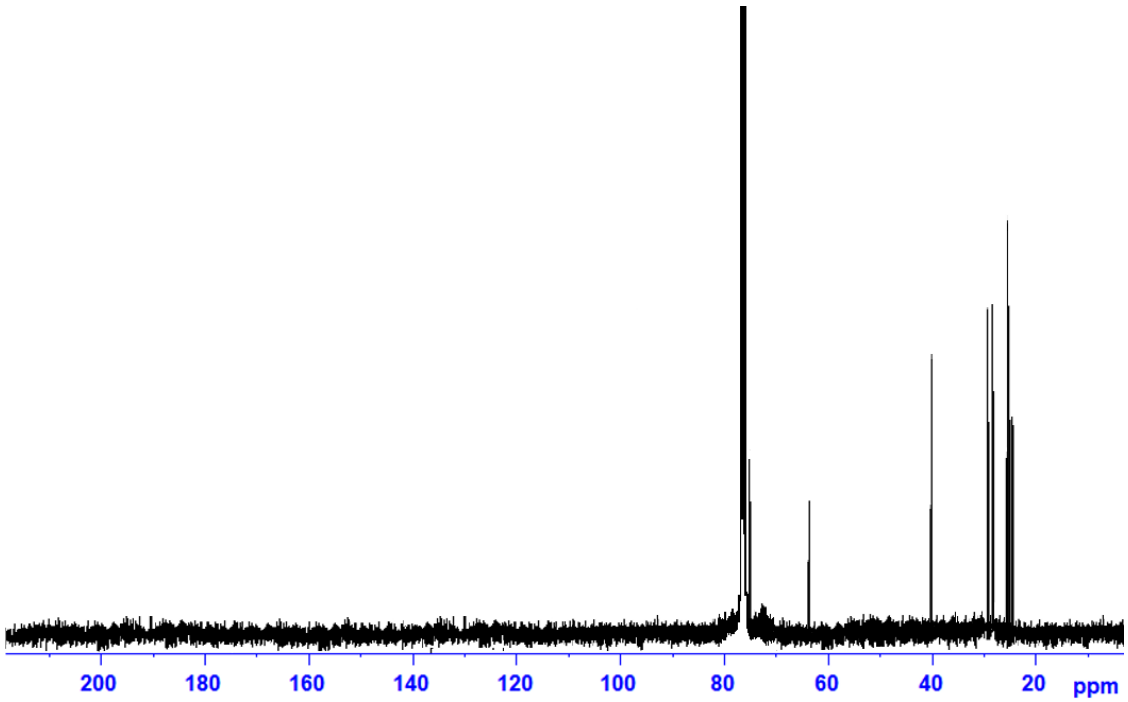

^{1}H NMR of 2-phenyloxirane (16)

^{1}H NMR ($CDCl_3$, 400 MHz): δ = 7.29–7.38 (m, 5H, CH-Ar), 3.88 (m, 1H, CH-O), 2.82-3.16(dd, 2H, *J* = 4.0 Hz, CH_2-O).

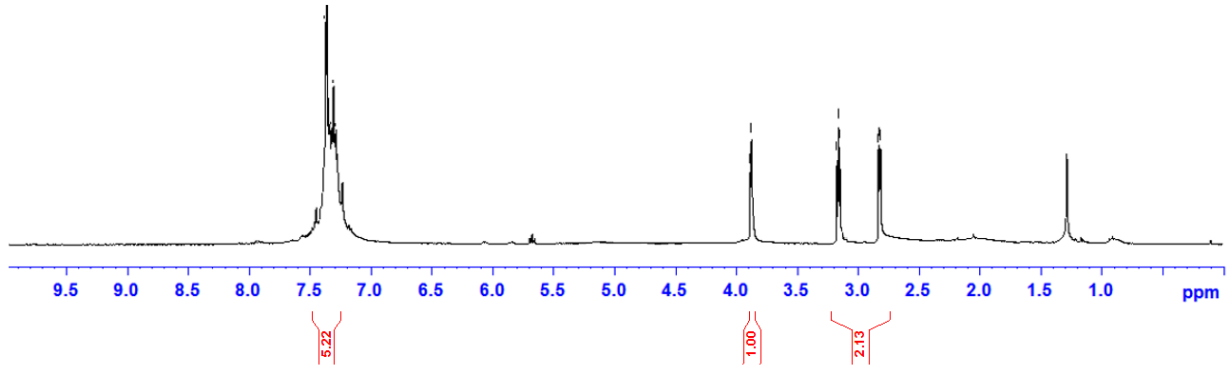

^{13}C NMR of 2-phenyloxirane (16)

^{13}C NMR ($CDCl_3$,100 MHz): δ=137.5 (-C-), 128.4 (-CH-), 128.1 (2 x -CH-), 125.4 (2 x -CH-), 52.2 (O-CH), 51.1 (O-CH_2).

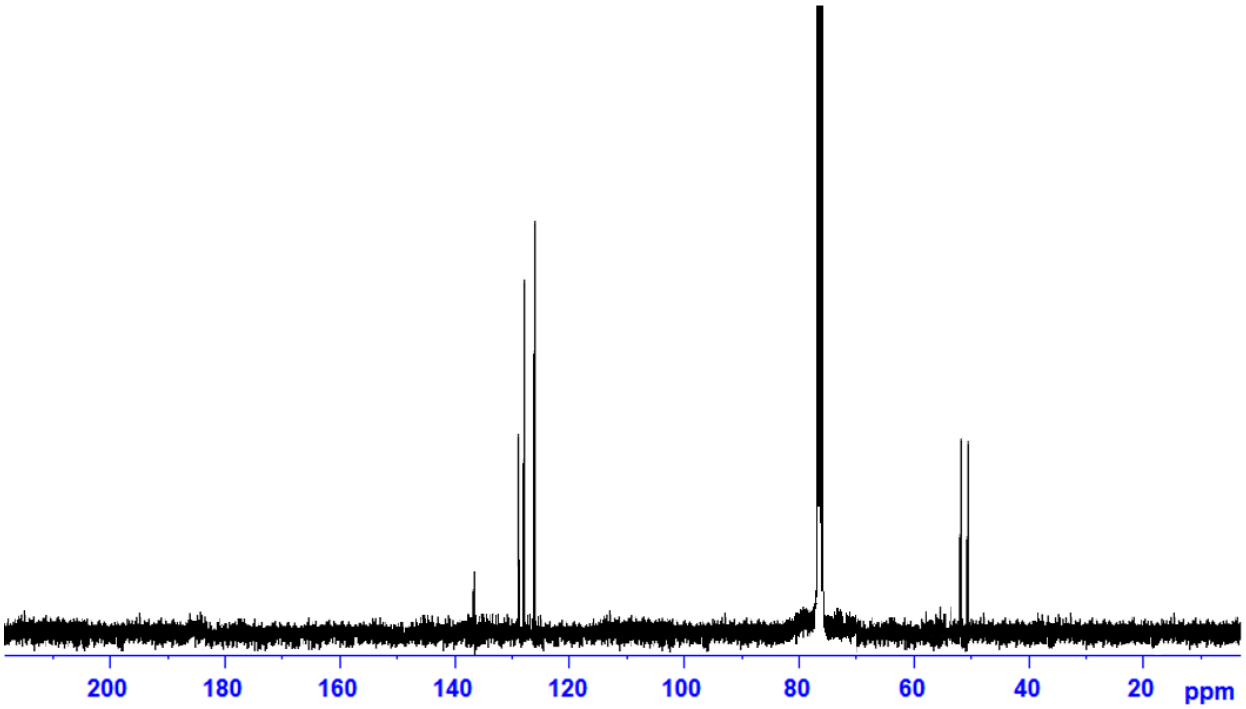

^{1}H NMR of 1-phenylethane-1,2-diol (17)

^{1}H NMR ($CDCl_3$, 400 MHz): δ= 7.29 – 7.38 (m, 5H, CH-Ar), 4.80-4.85 (m, 1H, CH-OH), 3.62-3.79 (m, 2H, CH_2-OH).

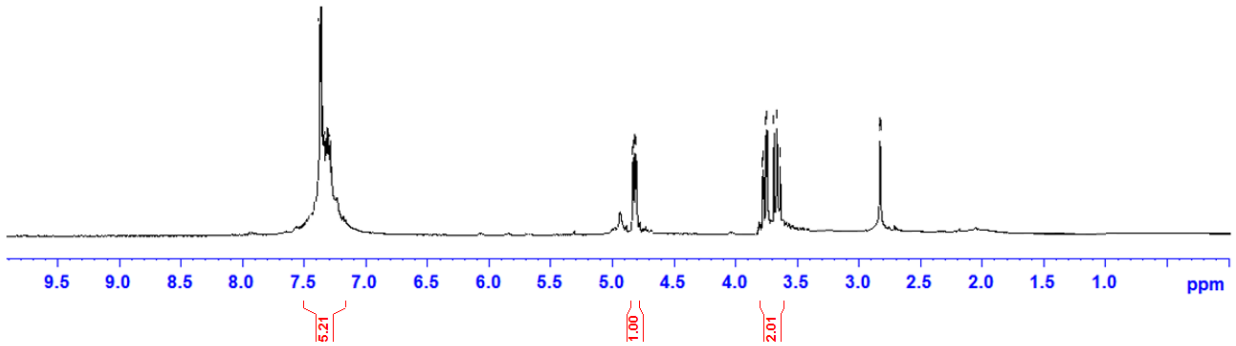

^{13}C NMR of 1-phenylethane-1,2-diol (17)

^{13}C NMR ($CDCl_3$,100 MHz,): δ= 140.4 (-C-), 128.5 (-CH-),128.0 (2 x -CH-),126.1(2 x -CH-), 74.7 (CH-OH), 68.71 (CH_2-OH).

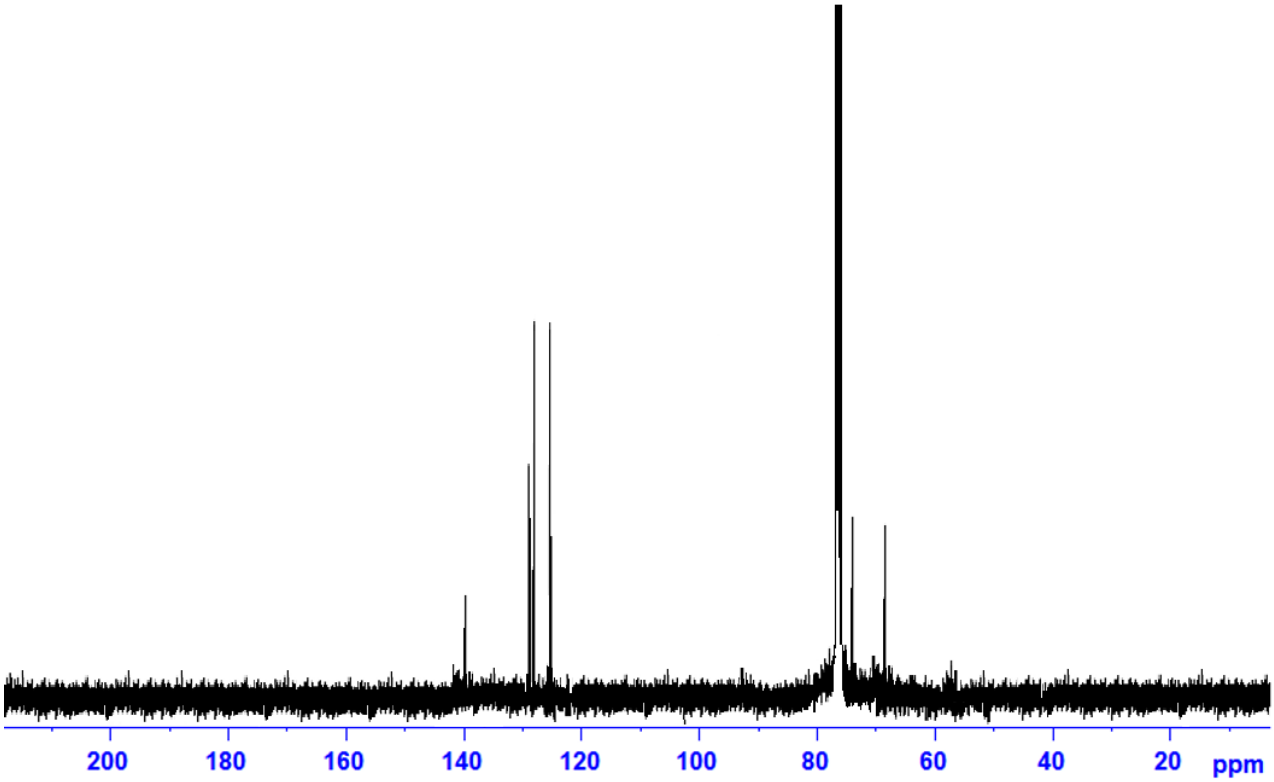

^{1}H NMR of 2,3-Diphenyloxirane (18)

^{1}H NMR ($CDCl_3$, 400 MHz): δ= 7.18-7.32 (m, 10H, CH-AR), 4.40 (s, 2H, 2 x CH-O).

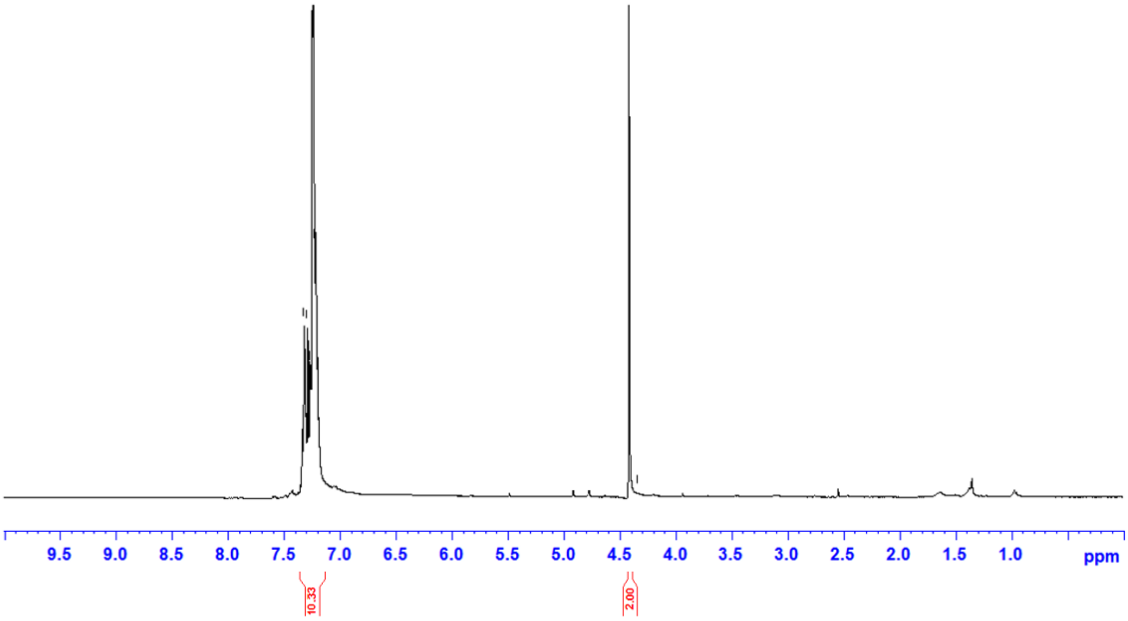

^{13}C NMR of 2,3-Diphenyloxirane (18)

^{13}C NMR ($CDCl_3$, 100 MHz): δ= 134.5 (2 x -C-),127.9 (2 x -CH-),127.6 (4 x -CH-),127.0 (4 x -CH-), 59.9 (O-CH).

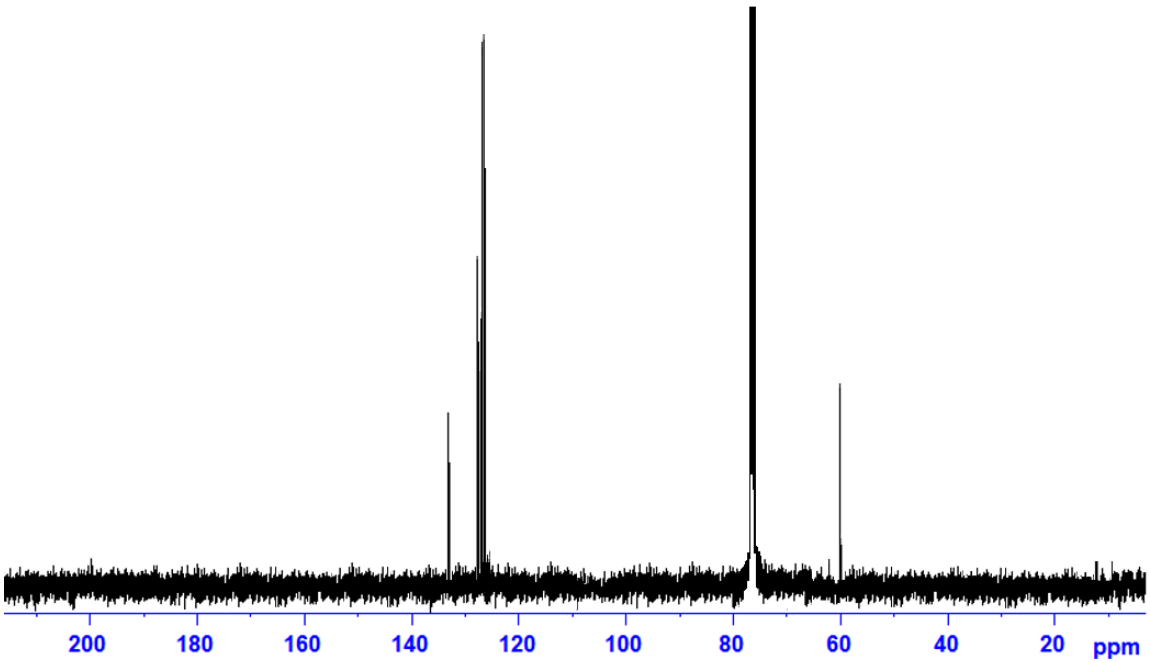

^{1}H NMR of 1,2-diphenylethane-1,2-diol (19)

^{1}H NMR ($CDCl_3$,400 MHz): δ= 8.21-8.27 (m, 2H, CH-Ar),7.15-7.35 (m, 8H, CH-Ar), 4.78 (s, 2H, 2 x CH-OH).

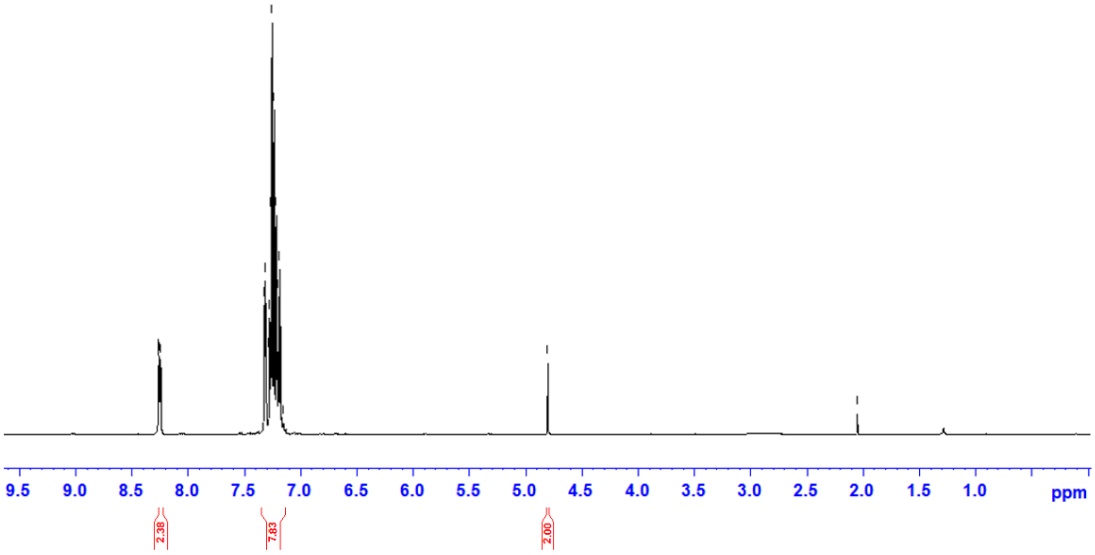

^{13}C NMR of 1,2-diphenylethane-1,2-diol (19)

^{13}C NMR ($CDCl_3$,100 MHz,): δ= 139.8 (2 x -C-),128.2 (2 x -CH-),128.1 (4 x -CH-), 127.0 (4 x -CH-), 78.1 (2 x CH-OH).

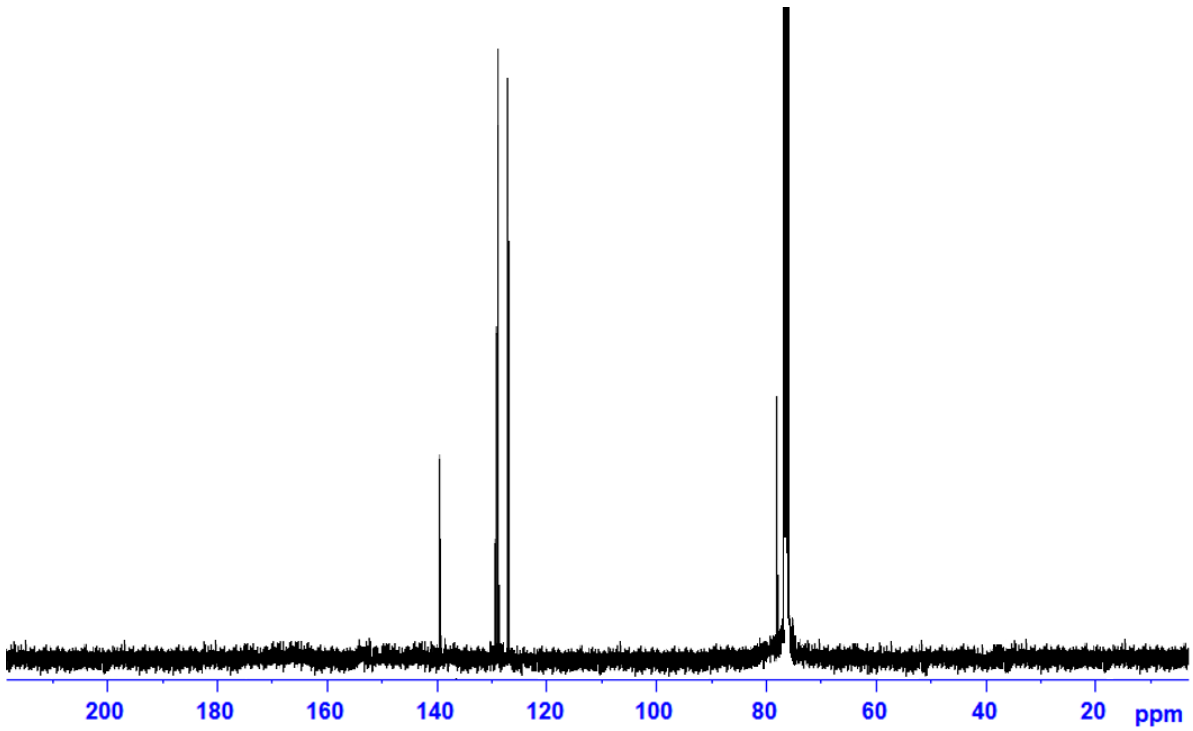

^{1}H NMR of 2-benzyloxirane (20)

^{1}H NMR ($CDCl_3$,400 MHz): δ= 7.2–7.38 (m, 5H, CH-Ar), 2.93-3.07 (m,1H, CH-O),2.79–2.81 (m, 2H, CH_2-), 2.64 (m, 2H, CH_2-O).

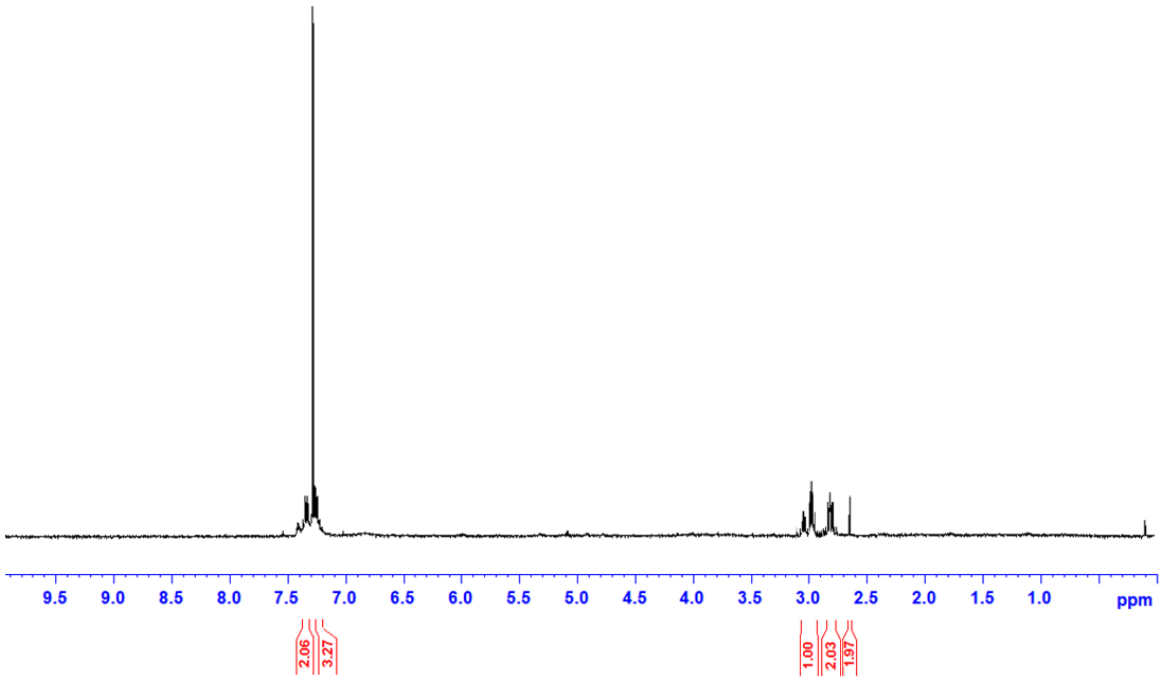

^{13}C NMR of 2-benzyloxirane (20)

^{13}C NMR ($CDCl_3$, 100 MHz): δ= 138.0 (-C-), 128.8 (2 x -CH-), 128.1 (2 x -CH-), 126.0 (-CH-), 54.5 (O-CH), 47.5 (O-CH_2), 39.6 (-CH_2-).

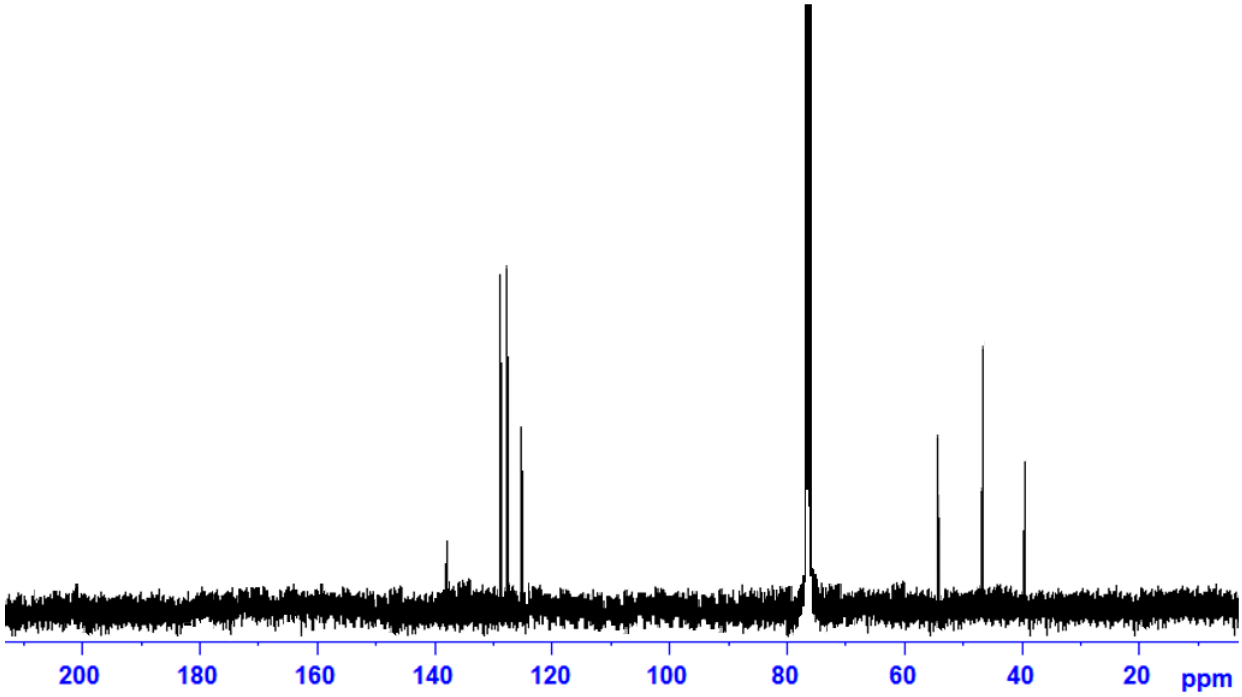

^{1}H NMR of 3-phenylpropane-1,2-diol (21)

^{1}H NMR ($CDCl_3$,400 MHz): δ= 7.23- 7.38 (m, 5H, CH-Ar), 3.70-3.75 (m, 1H, CH-OH), 3.54-3.58 (m, 2H, CH_2-OH), 2.80-2.83 (m, 2H, CH_2-).

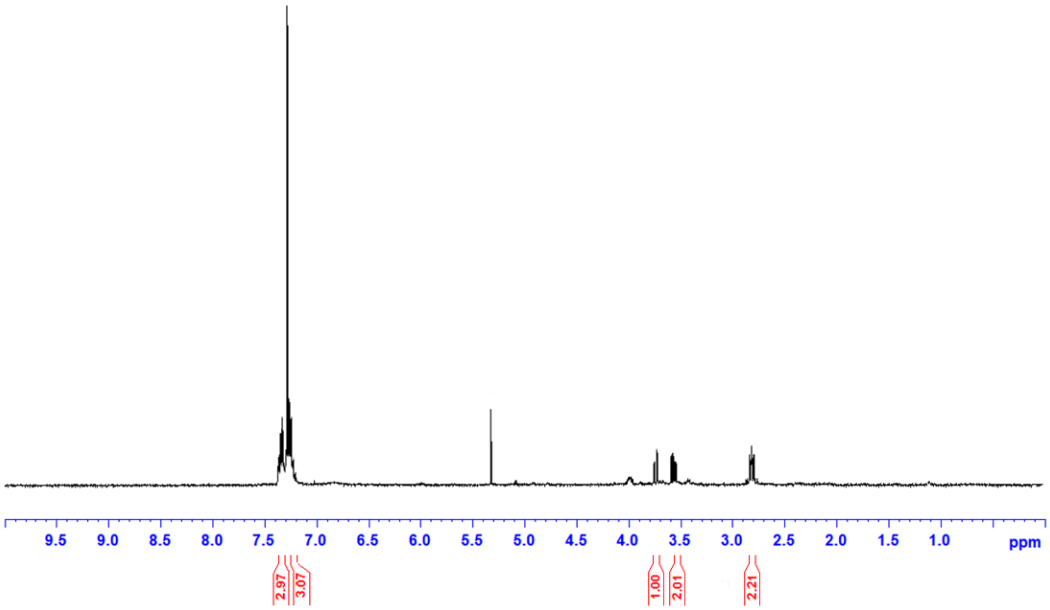

^{13}C NMR of 3-phenylpropane-1,2-diol (21)

^{13}C NMR ($CDCl_3$,100 MHz,): δ= 137.7 (-C-), 129.6 (-CH-), 128.6 (2 x -CH-), 126.6(2 x -CH-), 73.0 (CH-OH), 66.0 (CH_2-OH), 39.8 (-CH_2-).

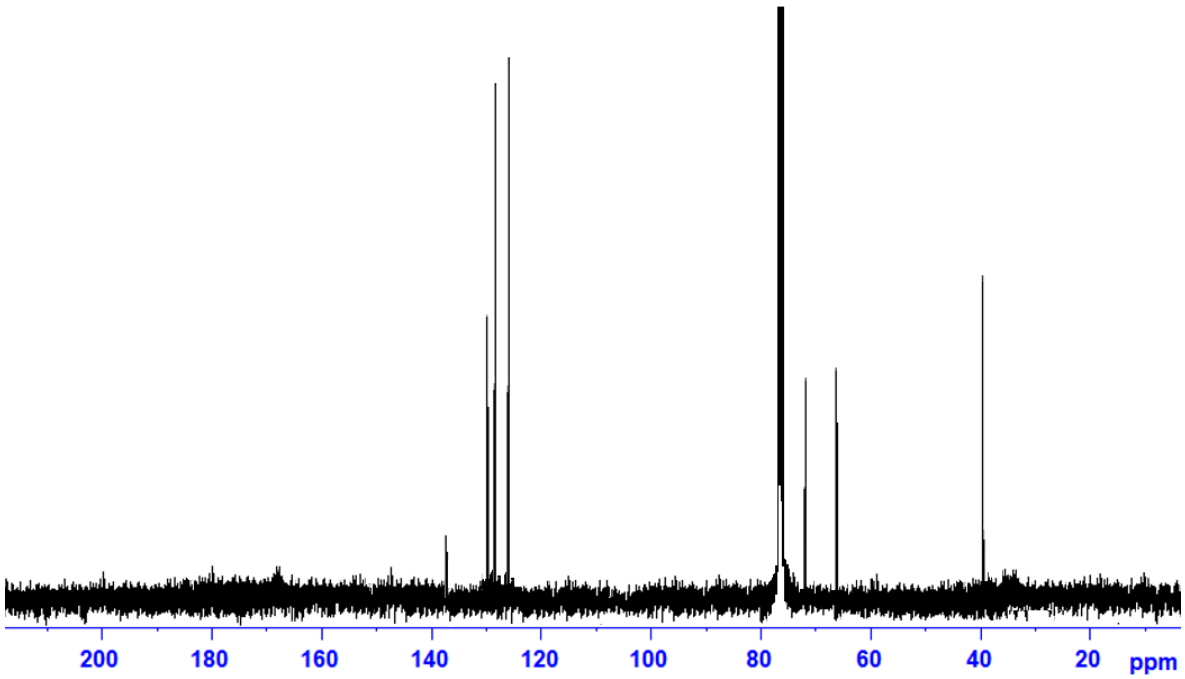

2.1 Application of heterogeneous catalysis in the prebiotic trans-glycosylation process.

Catalysis in prebiotic chemistry has been applied to trans-glycosylation processes. What is trans-glycosylation?

It is a biological process that leads to the formation of glycosidic bonds, during the synthesis of polysaccharides; nucleoside phosphate derivatives act as donor compounds in which the energies of their glycosidic bonds are partially conserved in the reaction products. Glycosyltransferases, transglycosidases and phosphorylases are the enzymes responsible for the formation of the glycosyl bond.

The formation of the glycosyl bond between sugar and nucleobase is a critical process in the abiotic origin of nucleosides,[193] since both reagents are thermodynamically stable compounds and no further stabilization is expected to occur after the linkage, especially in aqueous medium.[194] In addition, nucleosides lack of the n-σ* hyper-conjugation effect that is characteristic of the free sugar.[195] Multi-steps prebiotic syntheses of nucleosides have been reported,[196] encompassing the construction of the sugar on the nucleobase, as in the case of the formamido-pyrimidine chemistry[197,198,199,200,201] or, in alternative, the construction of the nucleobase on pre-formed amino-sugar (oxazoline chemistry).[202,203,204] These syntheses yield nucleosides in high regio- and stereoselectivity but suffer from the disadvantages of a large number of reaction steps involving protection and de-protection procedures. As an alternative, the one-step synthesis of nucleosides involves the direct formation of the glycosyl bond between the nucleobase and the sugar from both pre-formed substrates[126,205] or, in alternative, generated *in situ* reagents from simple chemical precursors. Example of this latter procedure is the synthesis of three ribonucleosides (adenosine, uridine and cytidine) and one 2'-deoxy ribonucleoside (thymidine) by proton beam irradiation of formamide and meteorites, mimicking the solar wind conditions.[124] The efficacy of formamide in the synthesis of biomolecules is evident in a large panel of physical-chemical conditions fueled by mineral catalysis and different energy sources, as reviewed and reported in introduction.[206,70,122,207,208,209] In addition, formamide is the optimal solvent for the thiolysis step in the oxazoline chemistry,[204] as well as the effective formylating agent in the formamido-pyrimidine procedure.[210] The formation of the glycosyl bond under proton beam irradiation occurred by a radical mechanism,[211] the observed β-stereoselectivity being due to the interaction of the sugar with the surface of the mineral.[204] In this latter case, di-glycosylated adenines **1** were detected as a mixture of the corresponding pyranose (**p**) and furanose (**f**) isomers, having β- and α-configuration at

the anomeric position, namely N^6-(2-deoxy-D-ribopyranosyl)-2'-deoxyadenosine(**1pα/β**), and N^6-(2-deoxy-D-ribofuranosyl)-2'-deoxyadenosine(**1fα/β**) (Figure 11).[126,212,213]

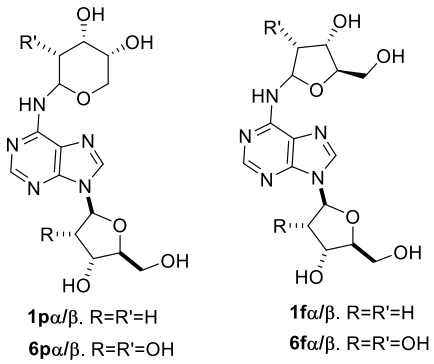

Figure 11. N^6-(2-deoxy-D-ribopyranosyl)-2'-deoxyadenosine **1pα/β**, N^6-(2-deoxy-D-ribofuranosyl)-2'-deoxyadenosine **1fα/β**, N^6-(-D-ribopyranosyl)-2'-deoxyadenosine **6pα/β**, N^6-(-D-ribofuranosyl)-2'-deoxyadenosine **6fα/β.**

The phosphorylation of adenosine to corresponding nucleotides, including reactive cyclic adenosine monophosphates,[214] was also reported in similar conditions.[215] Remarkably, di-glycosylated adenines have been identified as a "remnant" structural motif in damaged DNA sites (e.g. abasic sites), where the 2'-deoxyadenosine residue of one helix links the opposite site of the double helix (Figure 12).[216]

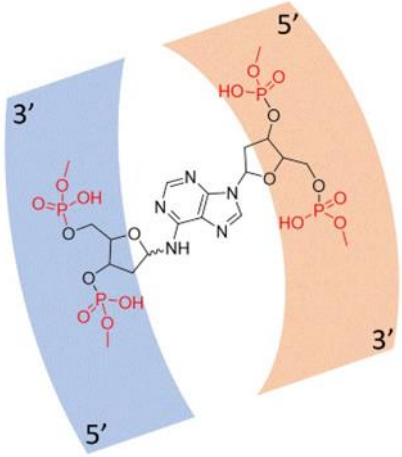

Figure 12. Structural motif in damaged DNA sites. N^6-(2'-deoxy-D-ribofuranosyl)-2'-deoxyadenosine (black) was selected as a representative case of the four possible isomeric forms of the sugar bonded at

the N^6-exocyclic position of the adenosine residue.[217] The sugar-phosphate backbone is reported in a red code.

The DNA cross-links are stable at neutral pH and room temperature, but they decompose at relatively high temperature (half-life, 65 days at 37°C) to yield 2'-deoxyadenosine with release of the N6-glycosyl moiety.[217] This implies that di-glycosylated adenines are potential reagents for intermolecular trans-glycosylation processes, during which the starting nucleoside can perform as the donor of the glycosyl residue when the appropriate nucleobase is provided.[218,219] This process is a valuable entry for the synthesis of a large panel of nucleosides, favouring the easy conversion of purine nucleosides into the pyrimidine counterpart (and vice-versa).[220]

Trans-glycosylation is also relevant in the prebiotic scenario, avoiding independent synthetic for the formation of purine and pyrimidine nucleosides.[221] Chemically-driven trans-glycosylation occurs at elevated temperature, or in the presence of heavy metals, usually starting from protected substrates in multi-step conditions.[222] Herein, we report the one-pot glycosylation of un-protected pyrimidine nucleobases by the selective intermolecular transfer of the N^6-glycosyl moiety from di-glycosylated adenines under proton beam irradiation. The reaction works at low temperature in solid state condition or, in alternative, in formamide and in the presence of the chondrite meteorite Northwest Africa NWA 1465. The complete set of pyrimidine nucleosides in RNA molecules was obtained, the yield and regio- and stereoselectivity of the glycosylation being increased in the presence of formamide and NWA 1465. The reported experimental conditions are similar to those effective during the one-pot synthesis of nucleobases and sugars from a chemical precursor as simple as formamide, furnishing a robust framework for the prebiotic formation of nucleic acid precursors.[206]

2.1.1 Synthesis of pyrimidine nucleosides 3.

Di-glycosylated adenines were prepared as previously described.[216,217] Briefly, 2'-deoxyadenosine **4** (0.57 mmol) and 2-deoxy-D-ribose (2.62 mmol) were dissolved in glacial acetic acid and methanol (1:3 v/v) and the reaction stirred at 40 °C for 72 h to afford **1** in 50% total yield as a mixture of the four corresponding α/β-pyranose and furanose isomers, compounds **1pα, 1pβ**, **1fα,** and **1fβ,** respectively. The relative percentage of the four isomers, their synthesis, NMR data and UHPLC-MS analyses are reported in materials and methods. Data were in accordance with those reported in the literature.[217]

Three types of experiments were performed for the trans-glycosylation of thymine **2** with **1** under proton beam irradiation. One of the experiments was performed in dry-film condition starting from a solid layer mixture of **1** (0.1 mmol) and **2** (0.1 mmol) (condition A).

A second was performed in previous experimental conditions in the presence of formamide (NH_2CHO, 1.0 mL) (condition B), while the third experiment was different from the second only for the presence of NWA 1465 (3.6 mg; 10% in weight with respect to **1**) (condition C). NWA 1465 is a meteorite representative of the chondrite family[122] (preparation of powdered sample, elemental composition and cosmo-origin data of NWA 1465 are reported in materials and methos) which was previously applied in the synthesis of adenosine derivatives from adenine and sugar in the presence of formamide.[126] The samples were irradiated with 170 MeV proton beam for 3.0 min at 243K (the proton field was bounded to 10×10 cm^2 by the collimator system). The averaged linear energy transfer (LET), representing the distribution of the energy in the sample with respect to the track of the proton beam, was kept at 0.57 keV/μm, while the total radiation absorbed dose was 6.0 Gy (Scheme 4).

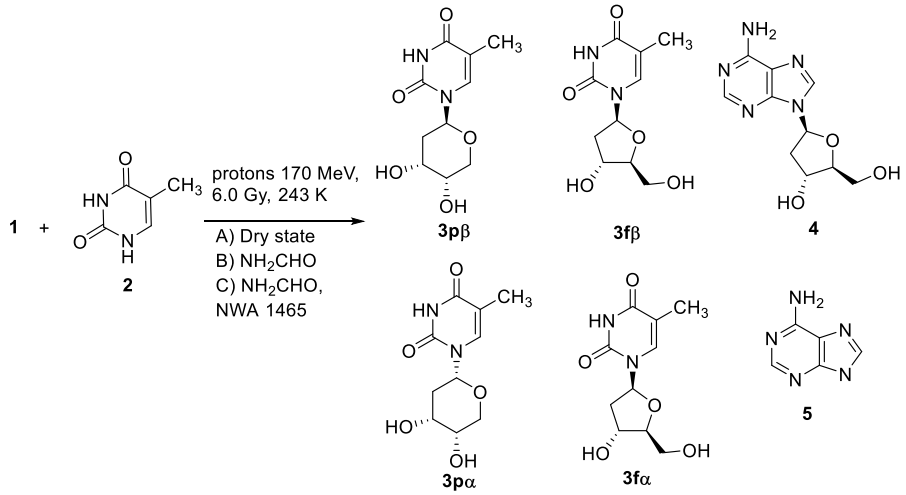

Scheme 4. Synthesis of nucleoside **3** from **1** and thymine **2**.

The UHPLC-MS analyses of the reactions are reported in Figure 13 (Panels A-C).

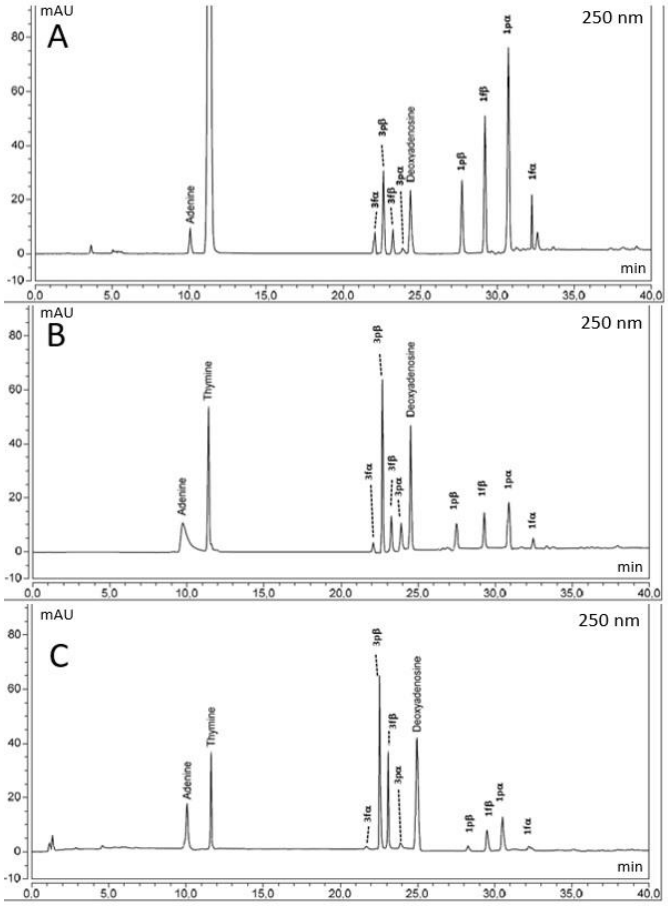

Figure 13. UHPLC analyses of the reaction between **1** and thymine **2** under different experimental conditions. Panel A: dry-film condition (condition A). Panel B: formamide (condition B). Panel C: formamide + NWA 1465 (condition C). Spectra were recorded at 250 nm.

The reactions were purified by semi-preparative HPLC and the reaction products characterized by NMR and MS analyses by comparison with data previously reported.[223,224,225] The yield of reaction products was calculated as percentage of the isolated nucleoside (mmol) with respect to converted **1**. 1-(β-D-2'-deoxyribopyranosyl) thymine **3pβ**, thymidine **3fβ**, 1-(α-D-2'-deoxyribopyranosyl) thymine **3pα**, and 1-(α-D-2'-deoxyribofuranosyl) thymine **3fα** were detected in low but appreciable amount (the total yield of **3** is reported in Table 1, entry 1), besides to 2'-deoxyadenosine **4**, adenine **5** and unreacted **1**. The relative percentage of **3pβ, 3fβ, 3pα**, and **3fα** is reported in Table 6. Adenine **5** was probably formed by partial degradation of adenosine. The mass to charge (m/z) ratio values, relative MS peak abundances of products and the original m/z fragmentation spectra are reported in material and

methods. Compounds **3pβ** and thymidine were obtained as the major isomers (Table 6, materials and methods), **3pβ** being isolated in the highest yield (the β/α ratio value of isolated anomers is reported in Table 5).

The prevalence of the pyranose form is in accordance with data previously reported for the glycosylation of pyrimidine nucleobases with unprotected ribose.[226] The possible role of pyranose nucleosides and of other sugar analogues in the prebiotic origin of nucleic acids has been reported and discussed.[226] The transfer of the glycosyl moiety from **1** to **2** selectively involved the N^6-glycosyl group as a donor and proceeded with high regioselectivity, the N^1-glycosylated pyrimidine (thermodynamic product) being the only detected regioisomer. A similar selectivity was reported during the glycosylation of **2** with ribose in the presence of 1,8-diazabicyclo[5.4.0]undec-7-ene (DBU), diisopropyl azodicarboxylate (DIAD), and tri-*n*-butylphosphine [P(*n*-Bu)$_3$], as a consequence of the higher nucleophilicity of the N^1 nitrogen atom in the pyrimidine ring.[227]

Table 5. Intermolecular trans-glycosylation of nucleobases **2**, and **7**-**8** by di-glycosylated adenines **1** and **6** under proton beam irradiation.

Entry	Method	Di-glycosylated adenine	Nucleobase	Conv. (%)	Product(s)	β/α ratio[a]	Yield (%)
1	A			25	**3**(**4**)[**5**]	68:32	18(10)[4]
2	B	**1**	**2**	71	**3**(**4**)[**5**]	85:15	61(31)[10]
3	C			82	**3**(**4**)[**5**]	98:2	70(39)[14]
4	A			21	**9**(**11**)[**5**]	70:30	16 (10)[4]
5	B	**6**	**7**	70	**9**(**11**)[**5**]	86:14	60 (38)[10]
6	C			78	**9**(**11**)[**5**]	94:6	65(39)[12]
7	A			14	**10**(**11**)[**5**]	68:32	10(5)[2]
8	B	**6**	**8**	62	**10**(**11**)[**5**]	82:18	45(25)[11]
9	C			70	**10**(**11**)[**5**]	93:7	49(34)[13]

Reactions were performed in the presence of di-glycosylated adenines **1** and **6** (0.1 mmol) and equimolar amount of the appropriate pyrimidine nucleobase **2**, **7** and **8**. The yield was calculated as percentage (%) of reaction product with respect to converted reagent. The round and square brackets represent the yield of recovered 2'-deoxyadenosine **4** and adenosine **11**, and adenine **5**, respectively. The data are the mean value of three experiments with standard deviation equal to or less than 0.1 %. [a] Ratio between the β and α anomers including both pyranose and furanose forms have been determined after semi-preparative HPLC purification and comparison with standard compounds.

In addition, *N*-glycosylates are thermodynamically stable products with respect to *O*-glycosylate counterpart during the trans-glycosylation of pyrimidine nucleobases.[228] The glycosyl transfer from **1** probably occurred through the formation of a sugar open-ring imine intermediate at the N^6-anomeric position of the donor molecule.[217] Note that the regioselectivity was different from that of metal catalyzed conditions, in which case the N^3-isomer largely predominate, as a consequence of the formation of the metal σ-complex in the N^1-position of the heterocycle ring (e.g. HgX and SnX_4 complexes).[229] Better results were obtained in condition B, in which case **3** was isolated in 61% total yield with a preferred β-stereochemistry (Table 5, entry 2), **3pβ** and thymidine being again the major isomers (Table 6, materials and methods). The increase of the yield of **3** was probably due to the high solubilizing effect of formamide.[126] Other possible products derived from the formamide condensation pathway[15] were not detected in our experimental conditions since they are expected to be synthesized in a negligible amount (μg scale) with respect to that of nucleosides (mg scale). NWA 1465 (condition C) further improved the yield of **3**, showing the highest stereoselectivity in the synthesis of the β-anomer (Table 5, entry 3; Table 6, materials and methods).

This reaction pattern is in accordance with the preferential attack of the nucleobase from the less hindered side of the sugar once adsorbed on the meteorite surface.[130]

2.1.2 Synthesis of nucleosides 9 and 10.

Due to the relevance of ribonucleosides in the "RNA world" hypothesis of the Origin of Life,[230] we successively evaluated the efficacy of the trans-glycosylation procedure in the case of ribose. N^6-(D-ribos-1-yl)-adenosine **6** (Figure 11) was prepared as a mixture of the four possible isomers by the procedure previously reported for the synthesis of **1**. Adenosine **11** (0.57 mmol) and-D-ribose (2.62 mmol) were dissolved in glacial acetic acid and methanol (1:3 v/v) and the reaction was stirred at 40°C for 72 h to afford **6** in 25% total yield. Synthesis, NMR data and UHPLC-MS analysis of **6** are in materials and methods. The chromatographic profile of **6** showed four peaks corresponding to the

formation of expected isomers **6pα, 6pβ**, **6fα** and **6fβ** (Table 6, materials and methods). The irradiation experiments were repeated in conditions A-C by reaction of **6** with uracil **7** and cytosine **8** as pyrimidine acceptors. The crudes were analyzed by UHPLC-MS analyses and purified by semi-preparative HPLC to yield pyrimidine nucleosides **9** and **10**, respectively, as a mixture of the corresponding pyranose and furanose isomers (Table 6, materials and methods), besides to unreacted **6**, adenosine **11** and adenine **5** (Scheme 6).

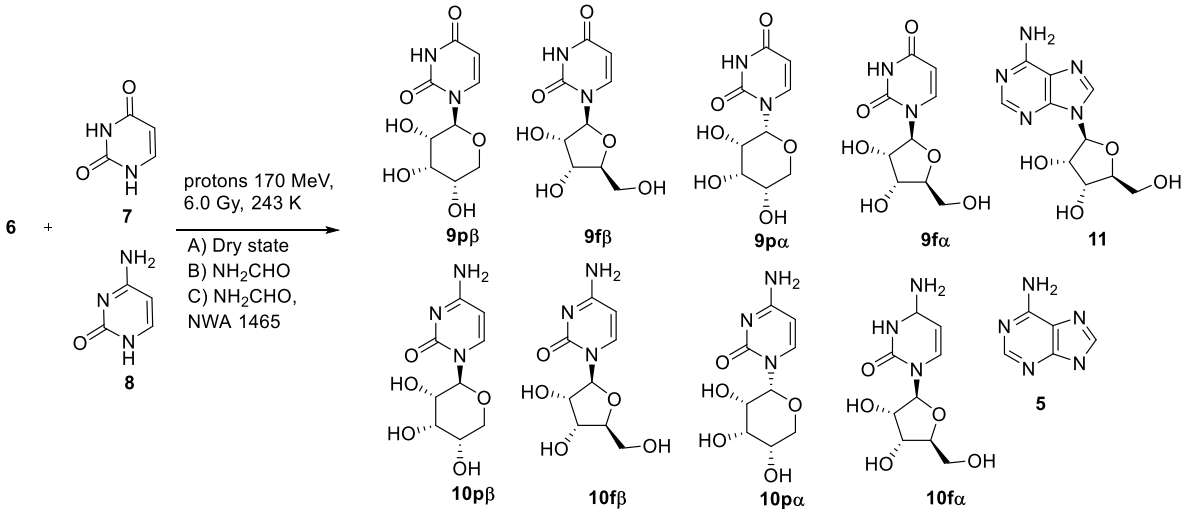

Scheme 6. Synthesis of nucleoside **9**-**10** from **6** and nucleobase **7**-**8.**

The isolated products were analyzed by NMR and MS, and the structural data were in accordance with authentical samples or with data reported in the literature.[231,232,233] The results confirmed the high regioselectivity in the formation of N^1-pyrimidine isomers, including canonical uridine **9fβ** and cytidine **10fβ**, from low to acceptable yield (Table 5, entries 4-9). Conditions B-C afforded the highest conversion of substrate and yield of nucleoside (Table 5, entry 4 versus entries 5-6, and entry 7 versus entries 8-9). Irrespective from the experimental conditions, **9pβ** and uridine, and **10pβ** and cytidine, were isolated as the major isomers (Table 6, materials and methods), the β-pyranose derivatives being isolated in the highest yield. In accordance with the Baker's rule (that is the neighboring group participation of the 2'-OH of ribose in the formation of the glycosyl bond), nucleosides **9** and **10** were largely obtained as the corresponding β-anomers, with the only exception of condition A, in which case an appreciable amount of the α-isomer was also detected (Table 5).

2.2 Conclusions

The prebiotic synthesis of nucleosides is a relevant process in the bottom-up model for the origin of pristine nucleic acid molecules. Phosphorylation[234,235,236] and trans-phosphorylation processes[237] are available for the successive formation of nucleotides and oligonucleotides, and different mechanisms for the polymerization of these building blocks to larger molecules are reported, encompassing both template and un-template conditions.[238,195,214] Two different levels of chemical complexity are operative in the synthesis of nucleosides: i) the correct regioselectivity in the linkage between the nucleobase and the sugar (that is N^1-position for pyrimidines); and ii) the control of the β-stereochemistry of the glycosyl bond. Multi-steps procedures solved this hurdle by application of scaffold oriented strategies, including the neighboring assistance as in the amino-oxazoline pathway[203] or, in alternative, the controlled addition of the 3-OH group of the sugar on the Re-face of the imine intermediate in the formamido pyrimidine chemistry.[239] In this latter case, a careful tuning of the pH overcome the regioselectivity problem.[239] Irrespective from the synthetic strategy, no-convergent procedures are proposed for the contemporary formation of purine and pyrimidine nucleosides.[240] The occurrence of a trans-glycosylation process simplifies this scenario, since the complete set of purine and pyrimidine nucleosides with the correct regio- and stereochemistry can be in principle obtained from only one di-glycosylated derivative, when the appropriate nucleobase is available as glycosyl acceptor. The very fact that di-glycosylated adenine is obtained as a by-product from formamide during the one-pot synthesis of canonical nucleosides and nucleobases, and that they are a "remnant" structural motif in damaged DNA, further suggests that the trans-glycosylation can act as a chemiomimetic process[226] in expanding the panel of biologically relevant molecules obtainable from a C-1 chemical precursor as simple as formamide. In this chemistry, NWA 1465 shows a relevant effect in the control of the stereochemistry of the transformation, expanding the possible role of meteorites as effective prebiotic chemical factories.[114] In this latter case, meteorites represent a clear-cut case for the necessity of high catalyst complexity in prebiotic process.[241] The contemporary presence in meteorites of different minerals and metal oxides in both crystalline and amorphous states, which depends on the cosmo-origin, furnish a large variety of catalytic sites[242] to improve the glycosylation process, in accordance with the role played by organometallic species in this kind of reaction.[220]

2.3 Materials and Methods.

All reagents and solvents were purchased from Aldrich and used without further purification. NWA 1465 from Sahara-Naizak was used after previous treatment as described in following paragraph. All reactions were performed under an inert argon atmosphere. Glassware was dried with a flame under a stream of argon gas and allowed to cool under an inert atmosphere prior to use. Flash chromatography was performed on 230−400 mesh silica gel, and thin-layer chromatography was performed on alumina plates coated with silica gel (Merck 60 F254 plates). TLC plates were performed by UV absorbance at 254 nm or staining with bromo cresol. The analysis of the samples was performed by using the Ultimate 3000 Rapid Resolution UHPLC system (DIONEX, Sunnyvale, USA) equipped with C18 REPROSIL-PUR BASIC column (2,5 um x 150 mm x2mm) or, in alternative, a Phenomenex Gemini AXIA PA C18 reversed-phase semi-preparative column (21 mm × 250 mm, 10 µm). Chromatographic separations were achieved using the following conditions: column temperature 30 °C, flow rate 0.2 mL/min or 2 mL/min, gradient elution with phase A (H_2O, 0.05 % formic acid) and phase B (acetonitrile, CH_3CN). The 0-18% linear gradient of phase A to phase B was employed over 50 min, returning to 100% A in 10 min. Products were detected by their absorbance at 250 nm. The UHPLC system was coupled with a mass spectrometer Q-Extractive (Thermo). The instrument was used in positive ionization mode with a full scan program (FS). Nuclear magnetic resonance spectra (^{1}H-NMR, ^{13}C-NMR) were recorded on Bruker 400 MHz spectrometer.

2.3.1 Preparation of the powdered sample, elemental composition and cosmo-origin data of meteorite NWA 1465

NWA 1465 was from Sahara-nayzak, Asnieres sur Seine, France. Dust (approximately 100 mg) was extracted by a two-steps procedure to remove possible organics. The first consisted in the addition of 1.0 mL 0.1 N NaOH and 3.0 mL of 2:1 chloroform-methanol, the second step in the addition of 1.0 mL 0.1 N sulphuric acid and 3.0 mL of 2:1 chloroform-methanol. Between steps the powder was recovered by centrifugation (6000 rpm, 10 min) and the supernatant phase was decanted.

NWA 1465 was found in 2001 in the Western Saharan desert. NWA 1465 (shock stage, S4) is classified as a carbonaceous chondrite (type 3) with flattened chondrules, mineral fragments, and refractory objects in a compact anhydrous matrix of Fe-rich olivine, Ca-rich pyroxene, enstatite, forsterite, troilite, magnetite, FeNi-metal, and weathering products (degree of weathering, W3). NWA 1465 also contains Ca in the order of cm dimension, Al-rich inclusions and large inclusions of dark material). The oxygen isotope composition of the bulk of NWA 1465is: $\delta 18O$ = 4.89‰, $\delta 17O$ =0.71‰. The oxygen isotope

composition of dark material (δ18O =13.08‰, δ17O = 5.83‰) is not in equilibrium with that of the host meteorite.

2.3.2 Synthesis of N^6-(D-2'-deoxyribos-1-yl)-2'-deoxyadenosine 1.

Compound **1** was prepared as previously reported in the literature.[217] 2'-Deoxyadenosine **4**(144 mg, 0.57 mmol) and 2'-deoxy-D-ribose (343 mg, 2.62 mmol) were dissolved in glacial acetic acid (300 μl) and methanol (700μl). The mixture was stirred at 40°C for 72 h. At the end of the reaction the solvent was removed under reduced pressure to afford a dark yellow residue successively purified by flash chromatography (95/5.0 v/v dichloromethane/methanol) to yield **1** as a mixture of the four corresponding α/β pyranose and furanose isomers **1pα, 1pβ**, and **1fα, 1fβ** (105 mg, 0.28 mmol 50% total yield). The assignment of the structure of different isomers was carried out by comparison of recorded chromatograms with HPLC-UV analysis previously reported in the literature,[217] and the relative percentage of α/β-pyranose and furanose isomers was calculated by comparison of the relative percentage of the peaks' area. In the successive transformations compound **1** was used as a mixture.

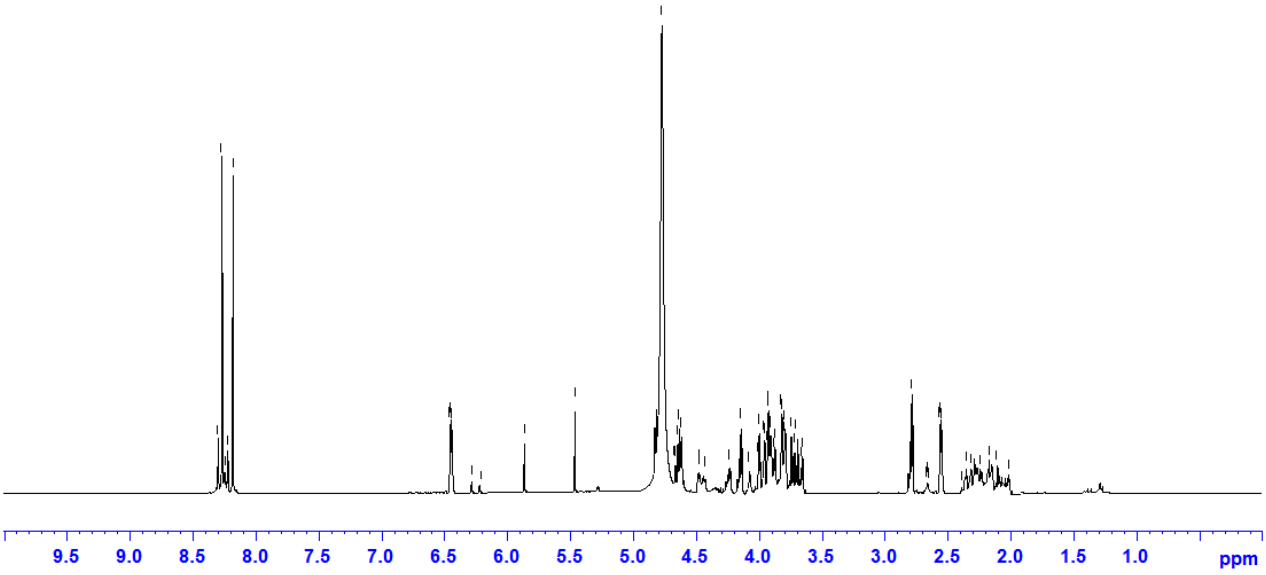

^{1}H-NMR spectrum of compound **1** in D_2O.

^{1}H-NMR (400 MHz, D_2O) 8.30 (s, CH, H8), 8.29 (s, CH,H8), 8.27 (s, CH H8), 8.26 (s, CH, H2), 8.25 (s, CH, H2), 8.20 (s, CH, H2), 6.43 (t, *J*=8Hz CH, H1'), 6.28 (s, CH, H1''),6.21 (s, CH, H1''), 5.81 (s, CH, H1''), 5.48 (s, CH, H1''), 4.64 (m, CH, H3'), 4.47 (m, CH, H3''), 4.44(m, CH, H3''), 4.29 (m, CH, H3''), 4.17 (m, CH, H4'), 4.10 (m, CH, H4''), 4.07 (m, CH, H3''), 4.02 (m, CH, H4''), 3.94 (m, CH_2, H5''), 3.90 (m, CH, H4''), 3.84(m, CH_2, H5''), 3.83 (m, CH_2, H5'), 3.79 (m, CH_2, H5''), 3.77 (m, CH_2, H5'), 3.76 (m, CH_2, H5''), 3.70 (m, CH_2, H5''), 3.69 (m, CH_2, H5''), 3.65 (m, CH, H5''), 3.64 (m, CH_2, H5''), 2.80 (m, CH_2, H2'), 2.66 (m, CH_2, H2''), 2.55 (m, CH_2, H2'), 2.39 (m, CH_2, H2''), 2.33 (m, CH_2, H2''), 2.24 (m, CH_2, H2''), 2.16 (m, CH_2, H2''), 2.13 (m, CH_2, H2''), 2.08 (m, CH_2, H2''), 2.07 (m, CH_2, H2'').

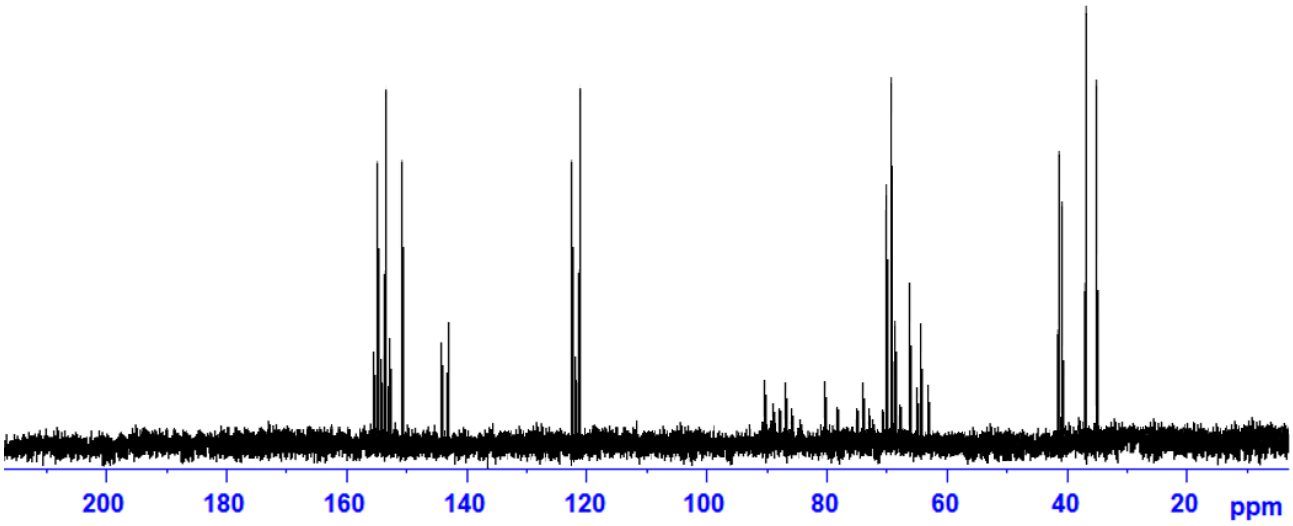

^{13}C-NMR spectrum of compound **1** in D_2O.

^{13}C-NMR (100 MHz, D_2O) 156.1 (C6), 156.0 (C6), 155.9 (C6), 154.9 (C2), 154.8 (C2), 154.7 (C2),151.3 (C4), 143.5 (C8), 143.3 (C8), 122.2 (C5), 122.1(C5), 122.0(C5), 90.1 (C4'), 88.6 (C4''), 87.9 (C4''), 87.4 (C1'), 87.3 (C1''), 84,5 (C1''), 80.3 (C1''), 77.9(C1''), 74.3(C3''), 73.9 (C3'), 73.8 (C3''), 70.3 (C3''), 69.6 (C5''), 69.3 (C4''), 69.2 (C4''), 68.5 (C3''), 66.1 (C5''), 64.7(C5''),64.4 (C5'), 63.9 (C5''), 41.7 (C2'), 41.6 (C2''), 37.1 (C2''), 35.6 (C2''). ESI-MS: m/z: 368.16 $[M + H]^+$. Elemental Analysis for $C_{15}H_{21}N_5O_6$ calculated: C, 49.04; H, 5.76; N, 19.06; O, 26.13, found: C, 48.94; H, 5.94; N, 18.98; O, 27.15.

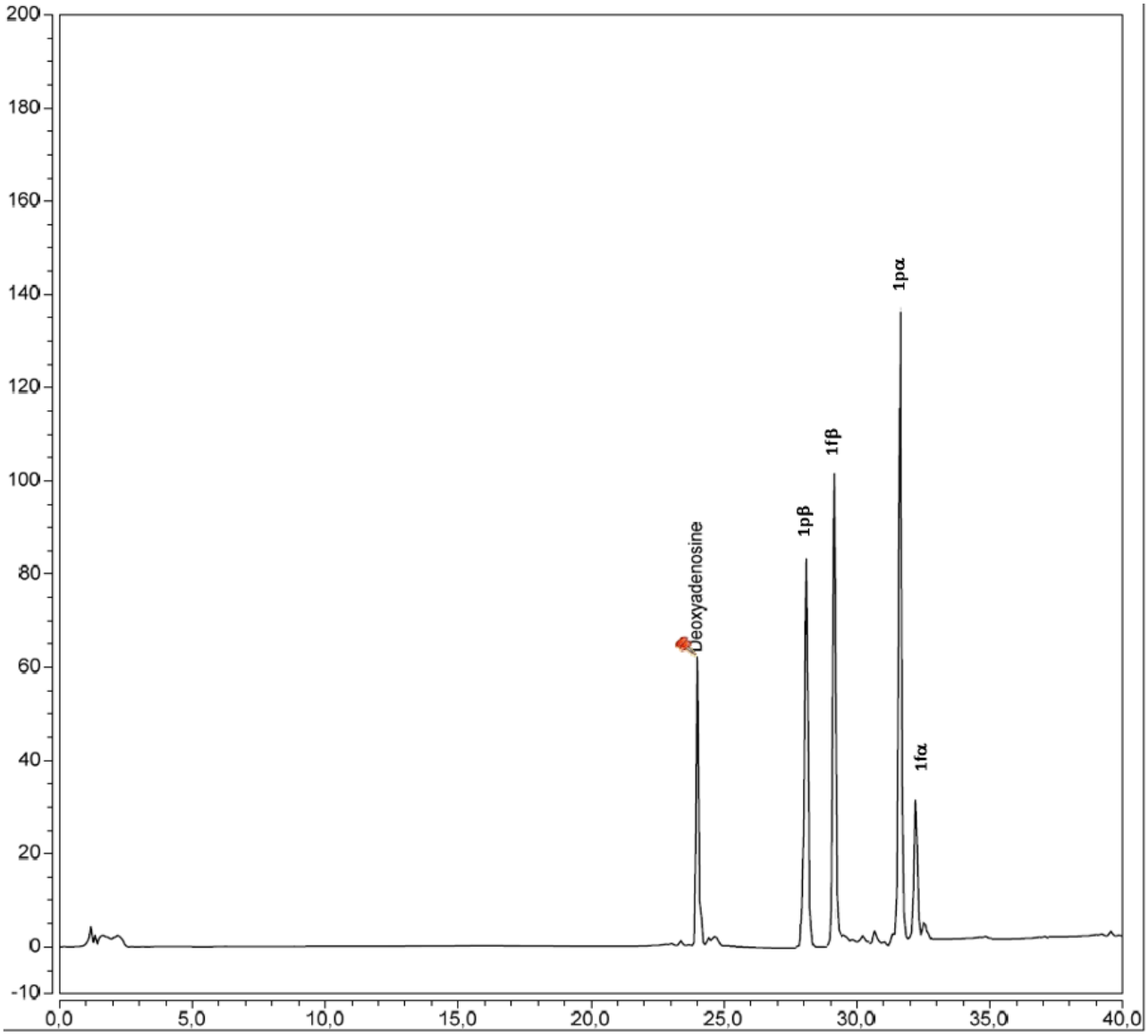

UHPLC chromatogram of compound **1**. The assignment of peaks of isomers **1pα**, **1pβ**, **1fα**, and **1fβ**, was performed on the basis of reference 218.

Original m/z fragmentation spectra of compound 1.

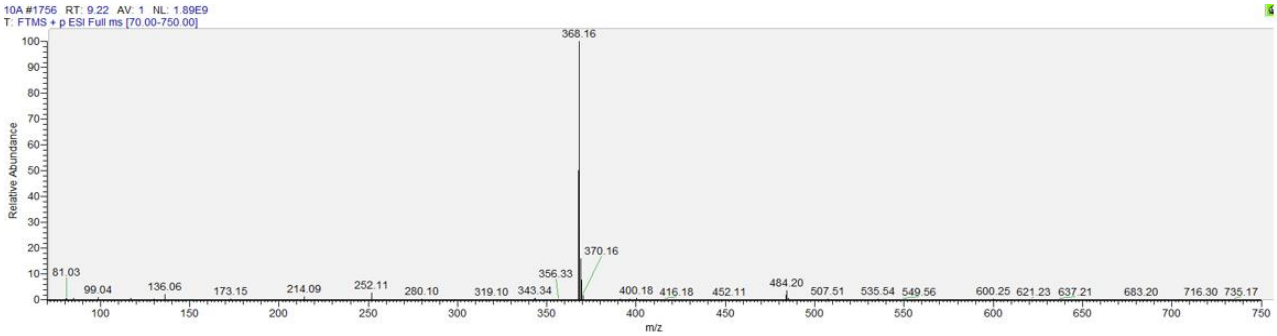

2.3.3 Synthesis of N^6-(D-ribos-1-yl)-adenosine 6

Compounds **6** was prepared by applying the procedure previously applied for the synthesis of **1**. [217] Briefly, adenosine **11** (152 mg 0.57 mmol) and D-ribose (393 mg 2.62 mmol) were dissolved in glacial acetic acid and methanol (1:3 v/v) and the reaction was stirred at 40◦C for 72 h. Thereafter the solvent was removed under reduced pressure and the resulting dark yellow residue purified by flash chromatography (95/5.0 v/v dichloromethane/methanol) to afford **6** (57 mg, 0.14 mmol 25% total yield) as a mixture of the four possible isomers (**6pα, 6pβ**, **6fα** and **6fβ**). UHPLC-MS analyses of **6** were in accordance with reported data (Table 6). In the successive transformations compound **6** was used as a mixture.

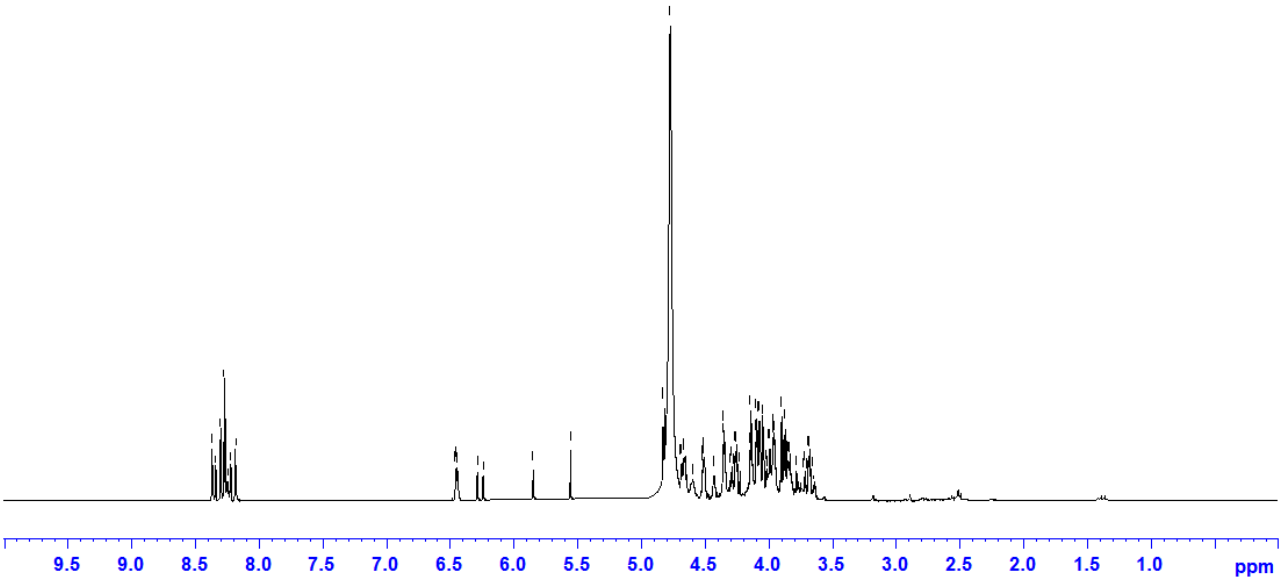

^{1}H-NMR spectrum of compound **6** in D_2O.

^{1}H-NMR (400 MHz, D_2O) 8.37 (s, CH, H8), 8.35 (s, CH,H8), 8.30 (s, CH H8), 8.29 (s, CH, H2), 8.27 (s, CH, H2), 8.23 (s, CH, H2), 8.19 (s, CH, H2), 6.45 (t, *J*=8Hz CH, H1'), 6.27 (s, CH, H1''),6.24 (s, CH, H1''), 5.85 (s, CH, H1''), 5.56 (s, CH, H1''), 4.82 (m, CH, H3'), 4.70 (m, CH, H2') 4.67 (m, CH, H3''),4.62 (m, CH, H2''), 4.52 (m, CH, H3''), 4.46 (m, CH, H2''), 4.34 (m, CH, H3''), 4.29 (m, CH, H2''), 4.25 (m, CH, H4'), 4.22 (m, CH, H4''), 4.15 (m, CH, H3''), 4.10 (m, CH, H2'') 4.02 (m, CH, H4''), 4.00 (m, CH_2, H5''), 3.92 (m, CH, H4''), 3.87(m, CH_2, H5''), 3.83 (m, CH_2, H5'), 3.78 (m, CH_2,

H5''), 3.77 (m, CH_2, H5'), 3.75 (m, CH_2, H5''), 3.72 (m, CH_2, H5''), 3.70 (m, CH_2, H5''), 3.68 (m, CH, H5''), 3.65(m, CH_2, H5'').

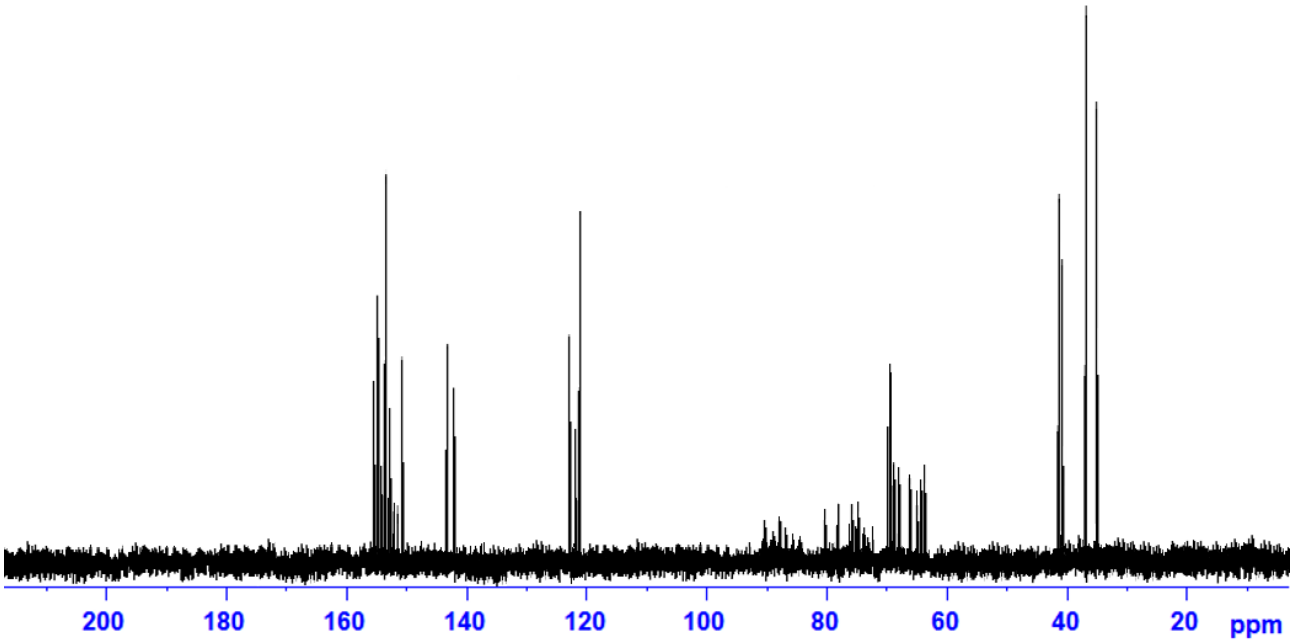

^{13}C-NMR spectrum of compound **6** in D_2O.

^{13}C-NMR (100 MHz, D_2O) 156.3 (C6), 156.0 (C6), 155.5 (C6), 154.9 (C2), 154.8 (C2), 154.7 (C2),151.8 (C4), 143.0 (C8), 142.0 (C8), 122.5 (C5), 122.0 (C5), 120.8 (C5), 90.3 (C4'), 88.7 (C4''), 87.9 (C4''), 86.2 (C1'), 85.4 (C1''), 84,5 (C1''), 80.5 (C1''), 77.9 (C1''), 75.8 (C3''), 75.6 (C3'), 75.4 (C3''), 75.1 (C2''), 74.7 (C2'), 74.2 (C2''), 73.3 (C3''), 72.2 (C2''), 69.8 (C5''), 69.4 (C4''), 69.3 (C4''), 68.7 (C3''), 66.3 (C5''), 64.8 (C5''), 64.5 (C5'), 64.0 (C5''). ESI-MS: m/z: 400.16 $[M+H]^+$. Elemental Analysis for $C_{15}H_{21}N_5O_8$ calculated: C, 45.11; H, 5.30; N, 17.54; O, 32.05, found: C, 45.05; H, 5.41; N, 17.52; O, 32.84.

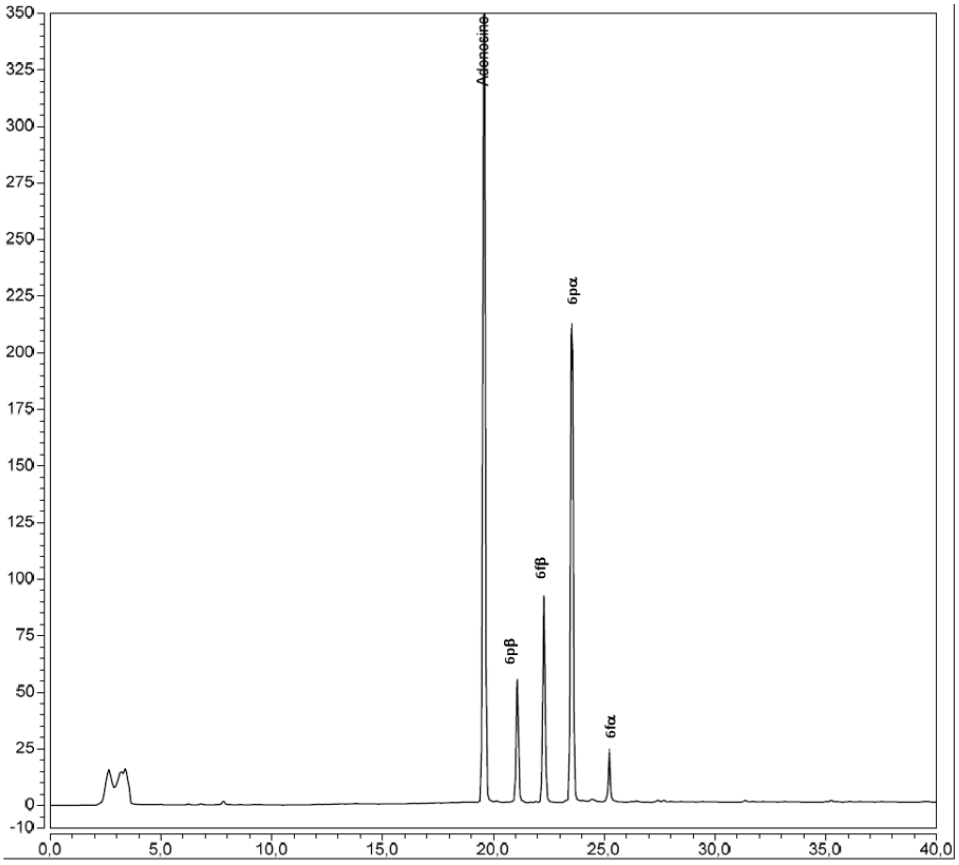

UHPLC chromatogram of compound **6**. The assignment of peaks of isomers **6p**□, **6p**□, **6f**□, and **6f**□, was performed on the basis of reference 218.

Original m/z fragmentation spectra of compound 6.

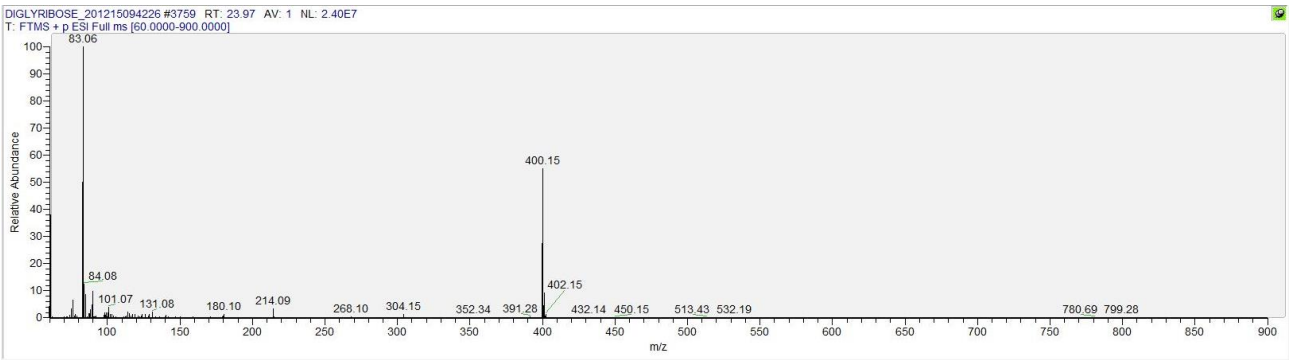

2.3.4 Synthesis of pyrimidine nucleosides 3, 9 and 10 in dry-film condition (condition A).

Compounds **1** or **6** (0.1 mmol) and the appropriate pyrimidine nucleobase (0.1 mmol) were solubilized in 2.0 mL of water, stirred for 1 min and successive dried under nitrogen and high vacuum until complete solvent evaporation. Thereafter, the mixture was irradiated at 243 K with 170 MeV protons for 3.0 min at the Phasatron accelerator facility of the Joint Institute for Nuclear Research of Dubna (Moscow region, Russia). The uniform proton field was bounded to 10x10 cm^2 by the collimator system. The averaged linear energy transfer (LET) was 0.57 keV/mm and the calculated absorbed dose was 6.0 Gy. Thereafter the sample was analyzed by UHPLC-MS detection without any further purification. To unambiguously assign the structures of nucleoside isomers, the reaction mixtures were purified by semi-preparative HPLC and the isolated products analyzed by ^{1}H-^{13}C-NMR and MS. Structures were assigned by comparison with commercially available samples and data in the literature.[232,233]

Characterization data of products 3,9-10.

1-(β-D-2'-deoxyribopyranosyl) thymine 3pβ. White solid. ^{1}H-NMR (400 MHz, D_2O, ppm): δ 7.61 (s, CH, H6), 5.96 (dd, *J* = 4.0Hz, 8.0 Hz, CH, H1'), 4.40-3.80 (m, CH, H3'-H4', CH_2, H5'), 2.11 (m, CH_2, H2'), 1.90 (s, CH_3). ^{13}C-NMR (100 MHz, D_2O, ppm): δ 163.7 (C4), 150.8 (C2), 136.0 (C6), 110.9 (C5), 92.8 (C1'), 67.3 (C3'), 67.0 (C4'), 64.5 (C5'), 27.8 (C2'), 12.4 (CH_3). ESI-MS: m/z: 242,09 $[M + H]^+$ Elemental Analysis for $C_{10}H_{14}N_2O_5$ calculated: C, 49.58; H, 5.83; N, 11.56; O, 33.02 found: C, 49.51; H, 5.80; N, 11.52; O, 32.98.

Thymidine 3fβ. White solid. ^{1}H-NMR (400 MHz, CD_3OD, ppm): δ 7.83 (d, *J* = 0.5 Hz, CH, H6), 6.29 (t, *J* = 8.0 Hz, CH, H1'), 4.61 (s, 3'-OH), 4.42 (ddd, *J* = 6.0 Hz, 3.5 Hz, 3.0 Hz, CH, H3'), 3.93 (dd, *J* = 7.0, Hz 3.5 Hz, CH, H4'), 3.82 (dd, *J* = 12 Hz, 3 Hz, 5'-OH), 3.75 (dd, *J* = 12.0 Hz, 1.5 Hz, CH_2, H5'), 2.25 (m, CH_2, H2'), 1.90 (d, *J* = 1.0 Hz, CH_3). ^{13}C-NMR (100 MHz, CD_3OD, ppm): δ 166.4 (C4), 152.4 (C2), 138.2 (C6), 111.6 (C5), 88.8 (C1'), 86.3 (C3'), 72.2 (C4'), 62.8 (C5'), 41.2 (C2'), 12.4 (CH_3). ESI-MS: m/z: 242,09 $[M + H]^+$ Elemental Analysis for $C_{10}H_{14}N_2O_5$ calculated: C, 49.58; H, 5.83; N, 11.56; O, 33.02 found: C, 49.53; H, 5.79; N, 11.54; O, 32.97.

1-(α-D-2'-deoxyribopyranosyl) thymine 3pα. White solid. ^{1}H-NMR (400 MHz, D_2O, ppm): δ 7.69 (s, CH, H6), 5.69 (dd, *J* = 4.0 Hz, 9.0 Hz, CH, H1'), 4.20-3.60 (m, CH, H3'-H4', CH_2, H5'), 2.09 (m, CH_2, H2'), 1.93 (s, CH_3). ^{13}C-NMR (100 MHz, D_2O, ppm): δ 163.7 (C4), 150.8 (C2), 136.0 (C6), 110.9 (C5), 92.8 (C1'), 67.3 (C3'), 67.0 (C4'), 64.5 (C5'), 27.8 (C2'), 12.4 (CH_3). ESI-MS: m/z: 242,09 $[M + H]^+$ Elemental Analysis for $C_{10}H_{14}N_2O_5$ calculated: C, 49.58; H, 5.83; N, 11.56; O, 33.02 found: C, 49.52; H, 5.79; N, 11.53; O, 32.99.

1-(α-D-2'-deoxyribofuranosyl) thymine 3fα. White solid.^{1}H-NMR (400 MHz, DMSO, ppm): δ 11.27 (s, NH), 7.69 (s, CH, H6), 6.16 (t, *J* = 7.3 Hz, CH, H1'), 5.22 (d, *J* = 4.2 Hz, 3'-OH), 5.01 (t, *J* = 5.2 Hz, 5'-OH), 4.22 (m, CH, H4'), 3.92 (m, CH, H3'), 3.56 (m, CH_2, H5'), 2.07 (m, CH_2, H2'), 1.76 (s, CH_3). ^{13}C-NMR (100 MHz, DMSO, ppm): δ 163.5 (C6), 150.6 (C2), 139.4 (C4), 110.7 (C5), 94.3 (C1'), 87.1 (C4'), 70.2 (C3'), 61.1 (C5'), 40.3 (C2'), 13.2 (5-CH_3). ESI-MS: m/z: 242,09 $[M + H]^+$ Elemental Analysis for $C_{10}H_{14}N_2O_5$ calculated: C, 49.58; H, 5.83; N, 11.56; O, 33.02 found: C, 49.55; H, 5.77; N, 11.49; O, 32.96.

1-(β-D-Ribopyranosyl) uracil 9pβ. White solid. ^{1}H NMR (400 MHz, DMSO, ppm): δ 11.25 (s, NH_2), 7.66 (d, *J* = 8.1 Hz, CH, H6), 5.60 (d, *J* = 8.1 Hz, CH, H5), 5.58 (d, *J* = 9.4 Hz, CH, H1'), 5.11 (OH), 5.09 (OH), 4.84 (OH), 3.97 (d, *J* = 3.2 Hz, CH, H3'), 3.68 (d, *J* = 9.5 Hz, CH, H2'), 3.63 (ddd, *J* = 7.4, 6.0, 2.3 Hz, CH, H4'), 3.58 – 3.53 (m, CH_2, H_a5', H_b5'). ^{13}C NMR (100 MHz, DMSO, ppm): δ 163.0 (C4), 151.1 (C2), 141.4 (C6), 101.67 (C5), 79.6 (C1'), 71.2 (C3'), 67.6 (C2'), 66.4 (C4'), 65.2 (C5'). ESI-MS: m/z: 245.07 $[M + H]^+$ Elemental Analysis for $C_9H_{12}N_2O_6$ calculated: C, 44.27; H, 4.95; N, 11.47; O, 39.31 found: C, 44.22; H, 4.91; N, 11.42; O, 38.97.

Uridine 9fβ. White solid.^{1}H-NMR (400 MHz, CD_3OD, ppm): δ 8.00 (d, *J* = 8.0 Hz, CH, H6), 5.90 (d, *J* = 4.4 Hz, CH, H1′), 5.69 (d, *J* = 8.0 Hz, CH, H5), 4.18 (t, *J* = 4.8 Hz, CH, H2′), 4.14 (t, *J* = 4.8 Hz, CH, H3′), 4.00 (m, CH, H4') 3.83-3.73 (m, CH_2, H5′). ^{13}C-NMR (100 MHz, CD_3OD, ppm): d 166.2 (C4), 152.5 (C2), 142.8 (C6), 102.7 (C5), 90.8 (C1′), 86.4 (C4′), 75.8 (C2′), 71.4 (C3′), 62.3 (C5′). ESI-MS: m/z: 245.07 $[M + H]^+$ Elemental Analysis for $C_9H_{12}N_2O_6$ calculated: C, 44.27; H, 4.95; N, 11.47; O, 39.31 found: C, 44.20; H, 4.88; N, 11.39; O, 38.95.

1-(α-D-Ribopyranosyl) uracil 9pα. White solid. ^{1}H-NMR (400 MHz, DMSO, ppm): δ 11.34 (s, NH_2), 7.70 (d, *J* = 8.2 Hz, CH, H6), 5.57 (d, *J* = 8.1 Hz, CH, H5), 5.47 (d, *J* = 1.2 Hz, CH, H1'), 5.27 (2'-OH), 5.17 – 5.12 (3'-OH), 5.10 (4'-OH), 3.96 (dd, *J* = 12.4 Hz, 1.6 Hz, CH, H_a5'), 3.75 (d, *J* = 12.2 Hz, CH, H_b5'), 3.72 (d, *J* = 7.4 Hz, CH, H2'), 3.70 – 3.66 (m, CH, H3', H4'). ^{13}C (100 MHz, DMSO): 163.1 (C4), 150.0 (C2), 142.5 (C6), 100.1 (C5), 81.6 (C1'), 70.9 (C2'), 70.3 (C5'), 68.6 (C4'), 67.2 (C3'). ESI-MS: m/z: 245.07 $[M + H]^+$ Elemental Analysis for $C_9H_{12}N_2O_6$ calculated: C, 44.27; H, 4.95; N, 11.47; O, 39.31 found: C, 44.22; H, 4.87; N, 11.38; O, 38.94.

1-(α-D-Ribofuranosyl) uracil 9fα. White solid. ^{1}H-NMR (400 MHz, DMSO, ppm): δ 11.18 (s, NH) 7.61 (d, *J* = 8.1 Hz, CH, H6), 6.01 (d, *J* = 4.6 Hz, CH, H1'), 5.56 (d, *J* = 8.1 Hz, CH, H5), 5.49 (OH), 5.12 (OH), 4.80 (OH), 4.16 (t, *J* = 4.5 Hz, CH, H2'), 4.06 – 3.98 (m, CH, H3', H4'), 3.58 (dd, *J* = 12.0 Hz, 2.7 Hz, CH, H_a5), 3.42 (dd, *J* = 12.2 Hz, 4.1 Hz, CH, H_b5). ^{13}C-NMR (100 MHz, DMSO): δ 163.3 (C4),

150.6 (C2), 142.8 (C6), 99.8 (C5), 85.1 (C1'), 84.0 (C4'), 70.4 (C3'), 70.3 (C2'), 61.2 (C7). ESI-MS: m/z: 245.07 $[M + H]^+$ Elemental Analysis for $C_9H_{12}N_2O_6$ calculated: C, 44.27; H, 4.95; N, 11.47; O, 39.31 found: C, 44.19; H, 4.83; N, 11.35; O, 38.91.

1-(β-D-ribopyranosyl) cytosine 10pβ. White solid.^{1}H-NMR (400 MHz, DMSO, ppm): δ 7.54 (d, *J* = 7.4 Hz, CH, H6), 7.16-7.05 (NH_2), 5.70 (d, *J* = 9.6 Hz, CH, H1'), 5.68 (d, *J* = 7.5 Hz, CH, H5), 5.01 (OH), 4.83 (OH), 4.78 (OH), 3.96 (s, CH, H3'), 3.64 – 3.57 (m, CH, H4', H2'), 3.54 (d, *J* = 10.2 Hz, CH, H_a5'), 3.50 (dd, *J* = 10.3 Hz, 5.0 Hz, CH, H_b5'). ^{13}C-NMR (100 MHz, DMSO): δ 165.3 (C4), 155.7 (C2), 141.8 (C6), 93.9 (C5), 79.8 (C1'), 71.2 (C3'), 68.0 (C2'), 66.7 (C4'), 65.2 (C5'). ESI-MS: m/z: 244,09 $[M + H]^+$ Elemental Analysis for $C_9H_{13}N_3O_5$ calculated: C, 44.45; H, 5.39; N, 17.28; O, 32.89 found: C, 44.42; H, 5.36; N, 17.25; O, 32.87

Cytidine 10fβ. White solid.^{1}H-NMR (400 MHz, CD_3OD, ppm): δ 7.45 (d, *J* = 7.2 Hz, CH, H6), 5.91 (d, *J* = 5.2 Hz, CH, H1′), 5.81 (d, *J* = 7.2 Hz, CH, H5), 5.00–3.52 (m, CH, H2′, CH, H3', CH, H4', CH_2, H5′). ^{13}C-NMR (400 MHz, CD_3OD, ppm): δ 166.8 (C4), 158.2 (C2), 142.4 (C6), 96.9 (C5), 91.2 (C1′), 84.6 (C4′), 74.8 (C2′), 70.1 (C3′), 61.6 (C5′). ESI-MS: m/z: 244,09 $[M + H]^+$ Elemental Analysis for $C_9H_{13}N_3O_5$ calculated: C, 44.45; H, 5.39; N, 17.28; O, 32.89 found: C, 44.41; H, 5.35; N, 17.24; O, 32.85.

1-(α-D-ribopyranosyl) cytosine 10pα. White solid ^{1}H-NMR (400 MHz, DMSO, ppm): δ 7.61 (d, *J* = 7.4 Hz, CH, H6), 7.18 -7.02 (NH_2), 5.67 (d, *J* = 7.4 Hz, CH, H5), 5.47 (s, CH, H1'), 5.13 (d, *J* = 6.0 Hz, OH), 5.10 (d, *J* = 5.8 Hz, OH), 5.07 (d, *J* = 7.7 Hz, OH), 3.95 (dd, *J* = 12.2 Hz, 1.8 Hz, CH, H_a5'), 3.75 – 3.63 (m, CH, 4H, H2, H3, H4, H_b5'). ^{13}C-NMR (100 MHz, DMSO): δ 165.5 (C4), 154.4 (C2), 143.1 (C6), 92.5 (C5), 82.3 (C1'), 70.6 (C2'), 70.3 (C5'), 68.7 (C4'), 67.4 (C3'). ESI-MS: m/z: 244,09 $[M + H]^+$ Elemental Analysis for $C_9H_{13}N_3O_5$ calculated: C, 44.45; H, 5.39; N, 17.28; O, 32.89 found: 44.40; H, 5.34; N, 17.23; O, 32.84.

1-(α-D-ribofuranosyl) cytosine 10fα. White solid ^{1}H-NMR (400 MHz, DMSO, ppm): δ 7.52 (d, *J* = 7.4 Hz, CH, H6), 7.05-6.96 (NH_2), 6.01 (d, *J* = 3.7 Hz, CH, H1'), 5.66 (d, *J* = 7.4 Hz, CH, H5), 5.27 (OH), 4.97 (OH), 4.77 (OH), 4.07 – 4.01 (m, CH, H2', H3'), 3.98 – 3.92 (m, CH, H4'), 3.61 (dd, *J* = 12.1 Hz, 2.6 Hz, CH, H_a5'), 3.42 (dd, *J* = 12.2 Hz, 4.6 Hz, CH, H_b5'). ^{13}C NMR (100 MHz, DMSO, ppm): δ 165.6 (C4), 155.2 (C2), 143.1 (C6), 92.3 (C5), 85.6 (C1'), 83.1 (C4'), 70.6 (C2'), 70.1 (C3'), 61.1 (C5'). ESI-MS: m/z: 244,09 $[M + H]^+$ Elemental Analysis for $C_9H_{13}N_3O_5$ calculated: C, 44.45; H, 5.39; N, 17.28; O, 32.89 found: C, 44.39; H, 5.32; N, 17.23; O, 32.83.

2.3.5 Synthesis of pyrimidine nucleosides 3, 9 and 10 in formamide and NWA 1465 (conditions B and C).

Compounds **1** or **6** (0.1 mmol) and the appropriate nucleobase (0.1 mmol) were solubilized in 2.0 mL of formamide (in the case of condition C, 10% w/w of NWA 1465 were added in the mixture), stirred for 1.0 min and irradiated as previously reported. In the case of condition C, the samples were filtered at the end of the irradiation to remove NWA 1465. Thereafter the samples were analyzed as described in condition A.

2.3.6 Relative percentage of the α/β–pyranose and furanose isomers of compounds 1, 3, 6, 9, and 10

Table 6. Relative percentage of the isomers of compounds **1**, **3**, **6**, **9**, and **10.**

Entry	Nucleobases	Condition[b]	Amount of products (%)[a]			
1	-	-	**1pβ**	**1fβ**	**1pα**	**1fα**
			23	30	38	9
2	2	A	**3pβ**	**3fβ**	**3pα**	**3fα**
			56	19	10	15
3		B	70	14	11	5
4		C	61	34	3	2
5	-	-	**6pβ**	**6fβ**	**6pα**	**6fα**
			16	24	54	6
6	7	A	**9pβ**	**9fβ**	**9pα**	**9fα**
			57	17	23	3
7		B	77	14	5	4
8		C	51	40	6	3
9	8	A	**10pβ**	**10fβ**	**10pα**	**10fα**
			66	10	20	4
10		B	61	19	14	6
11		C	55	35	8	2

[a]The relative percentage of α/β-pyranose and furanose isomers was calculated after isolation by semi-preparative HPLC analysis. The data are the mean value of three experiments with a standard deviation equal to or less than 0.1 %.[b] Panel A: dry-film condition (condition A). Panel B: formamide (condition B). Panel C: formamide + NWA 1465 (condition C).

2.3.7 Mass to charge (m/z) ratio values and relative MS peak abundances of products of 1-11.

Product	m/z
1	368.16 $[M+H]^+$ (100), 252.11$[M-116+H]^+$ (4), 136.06 $[M-232+H]^+$ (3)
2	127.05 $[M+H]^+$ (8), 91.05 (100)
3	243.10 $[M+H]^+$ (16), 127.05 $[M-116+H]^+$ (36), 83.06 (100)
4	252.11 $[M+H]^+$ (100), 136.06 $[M-116+H]^+$ (18)
5	136.06 $[M+H]^+$ (100)
6	400.15 $[M+H]^+$ (56), 268.10 $[M-132+H]^+$ (2), 83.06 (100)
7	113.03 [M+H]+ (12), 91.05 (100)
8	112.05 $[M+H]^+$ (100)
9	245.08 $[M+H]^+$ (48), 113.03 $[M-132+H]^+$ (50), 61.04 (100)
10	244.09 $[M+H]^+$ (100), 112.05 $[M-132+H]^+$ (36)
11	268.10 $[M+H]^+$ (100), 136.06 $[M-132+H]^+$ (4)

2.3.8 Original m/z fragmentation spectra of compounds 2-5, 7-11.

m/z fragmentation spectra of compound **2**.

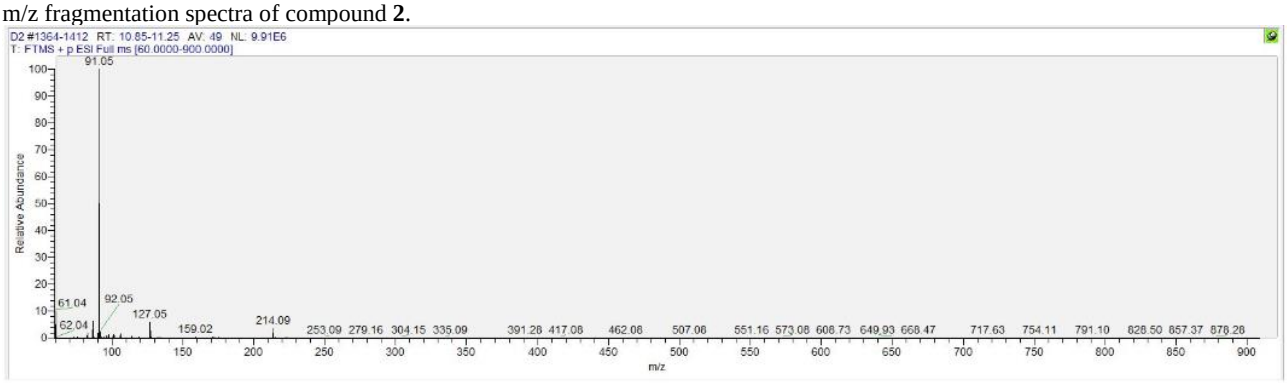

m/z fragmentation spectra of compound **3**.

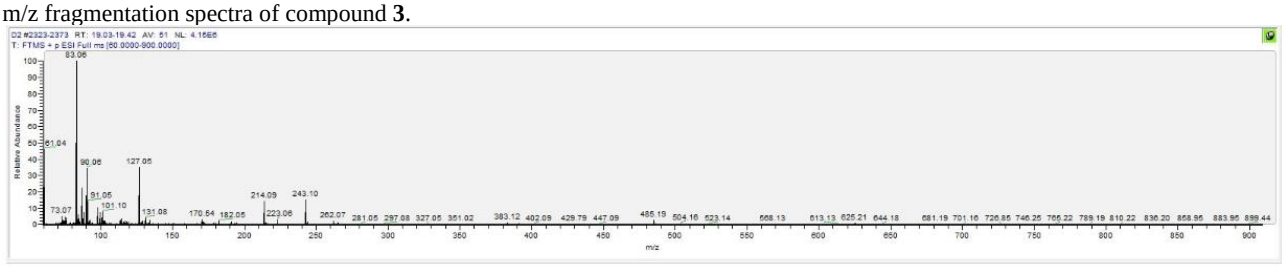

m/z fragmentation spectra of compound **4**.

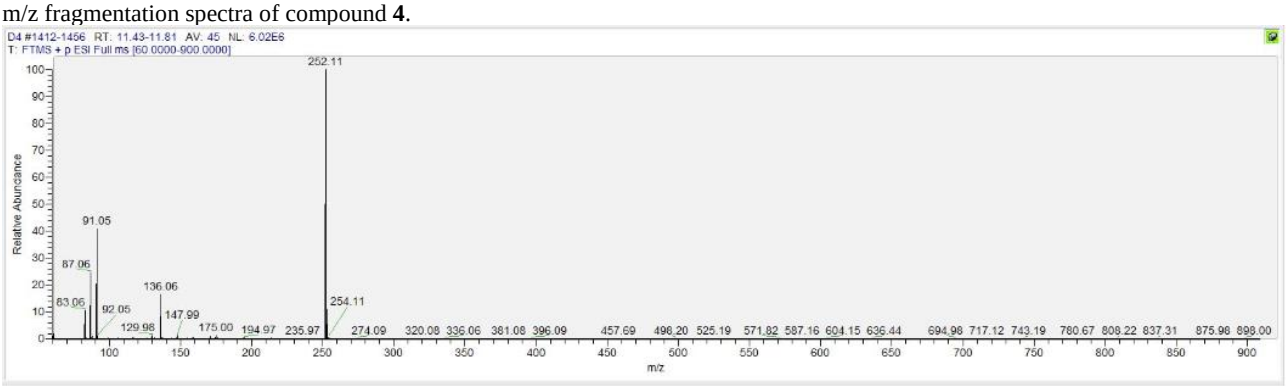

m/z fragmentation spectra of compound **5**.

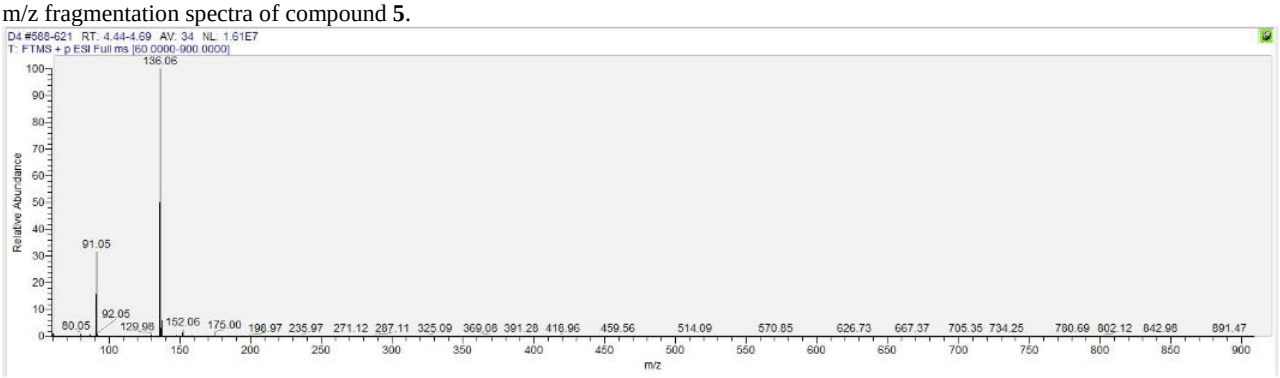

m/z fragmentation spectra of compound **7**.

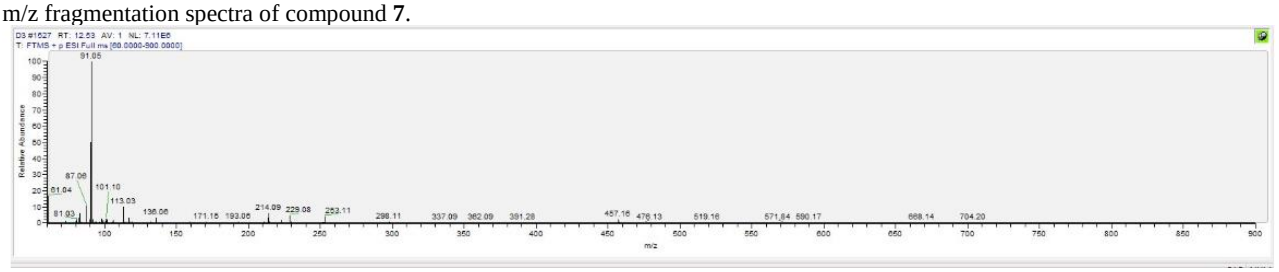

m/z fragmentation spectra of compound **8**.

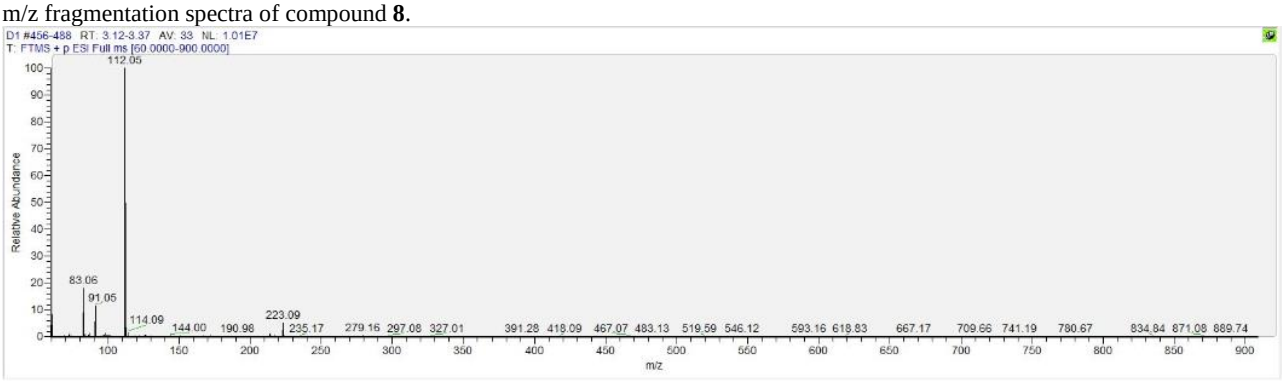

m/z fragmentation spectra of compound **9**.

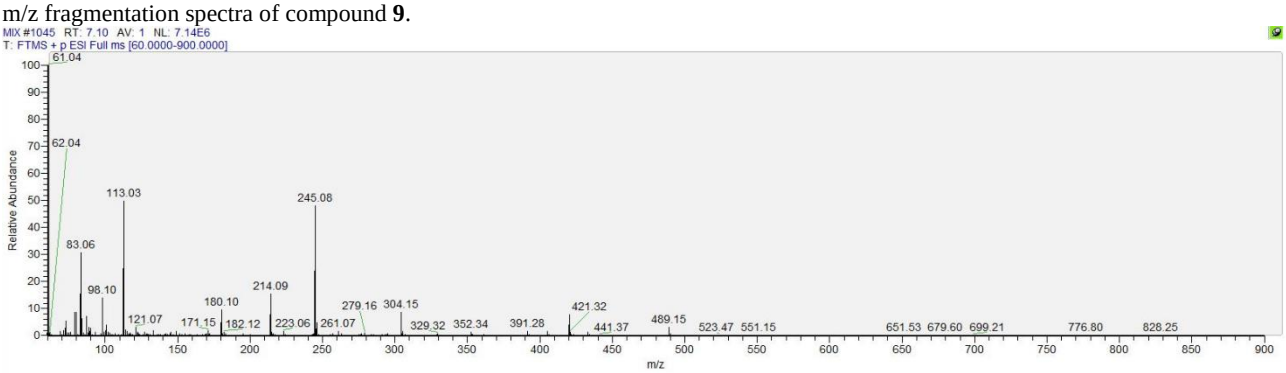

m/z fragmentation spectra of compound **10**.

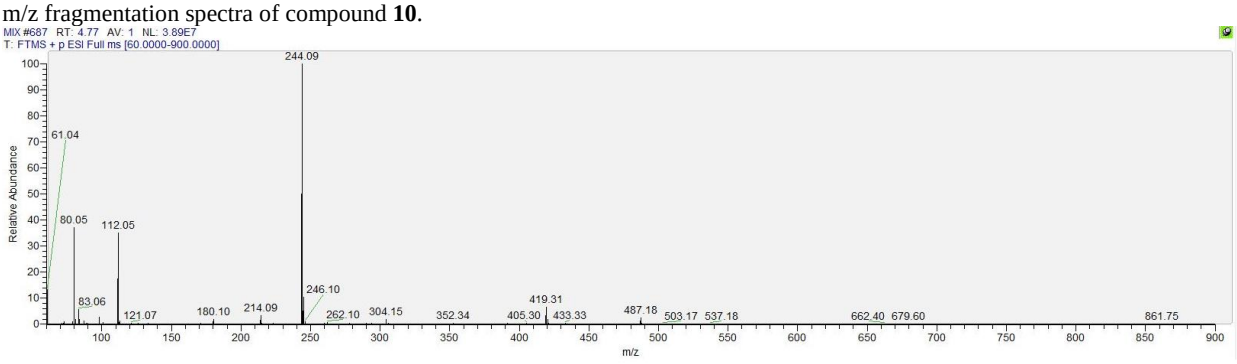

m/z fragmentation spectra of compound **11**.

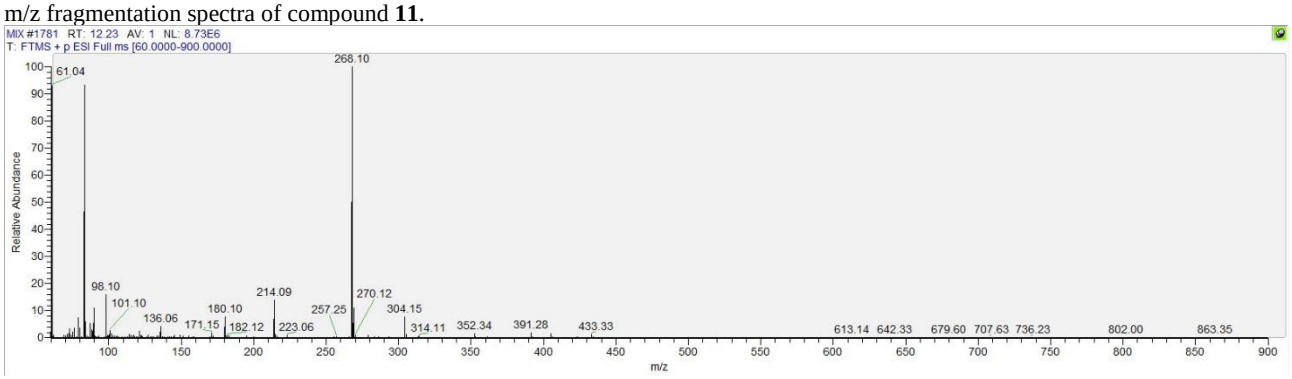

2.3.9 UHPLC of compounds 9-10.

Synthesis of uridine **9** from **6** and uracil **7** in dry film (condition A).

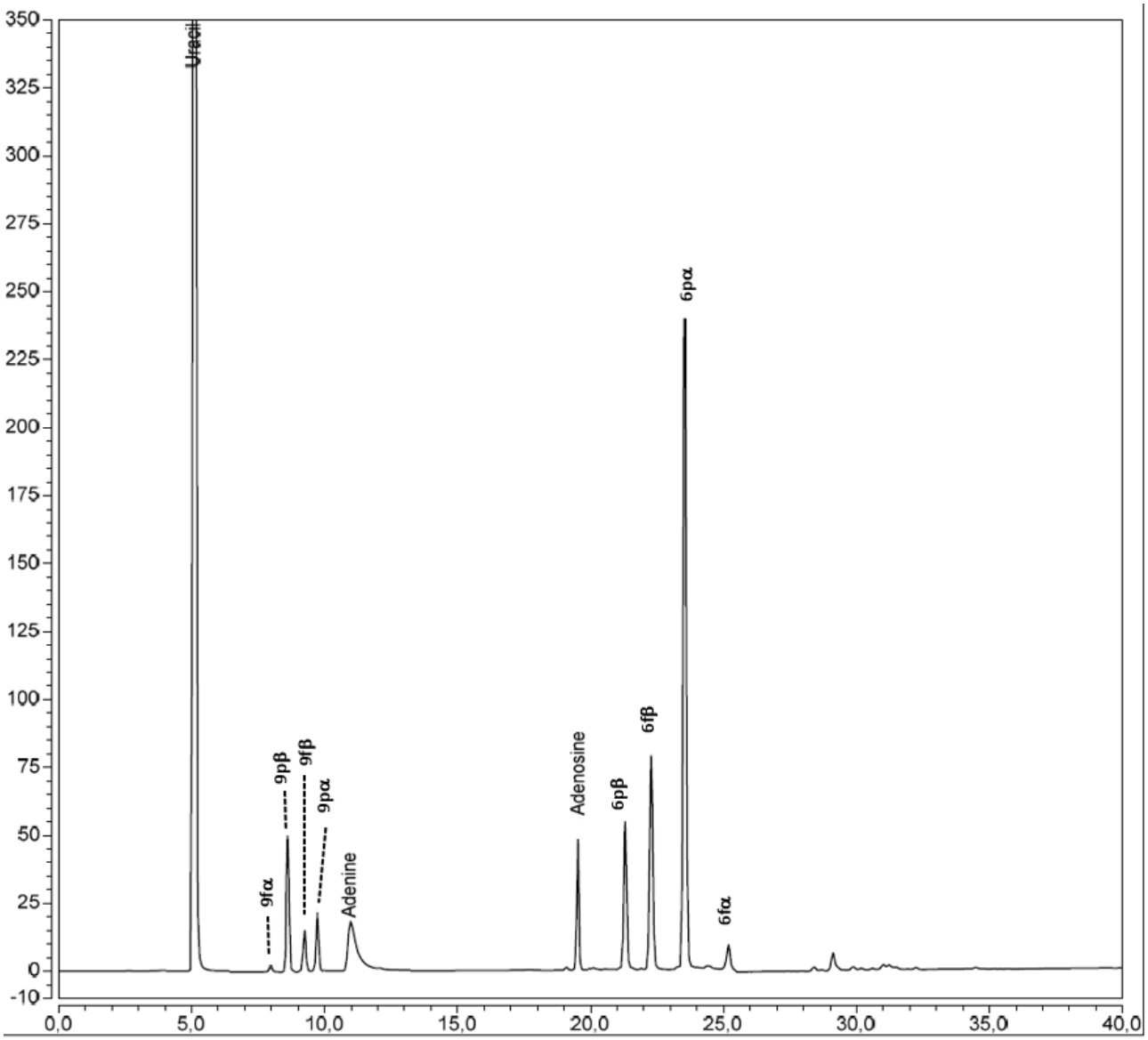

Synthesis of uridine **9** from **6** and uracil **7** in formamide solution (condition B).

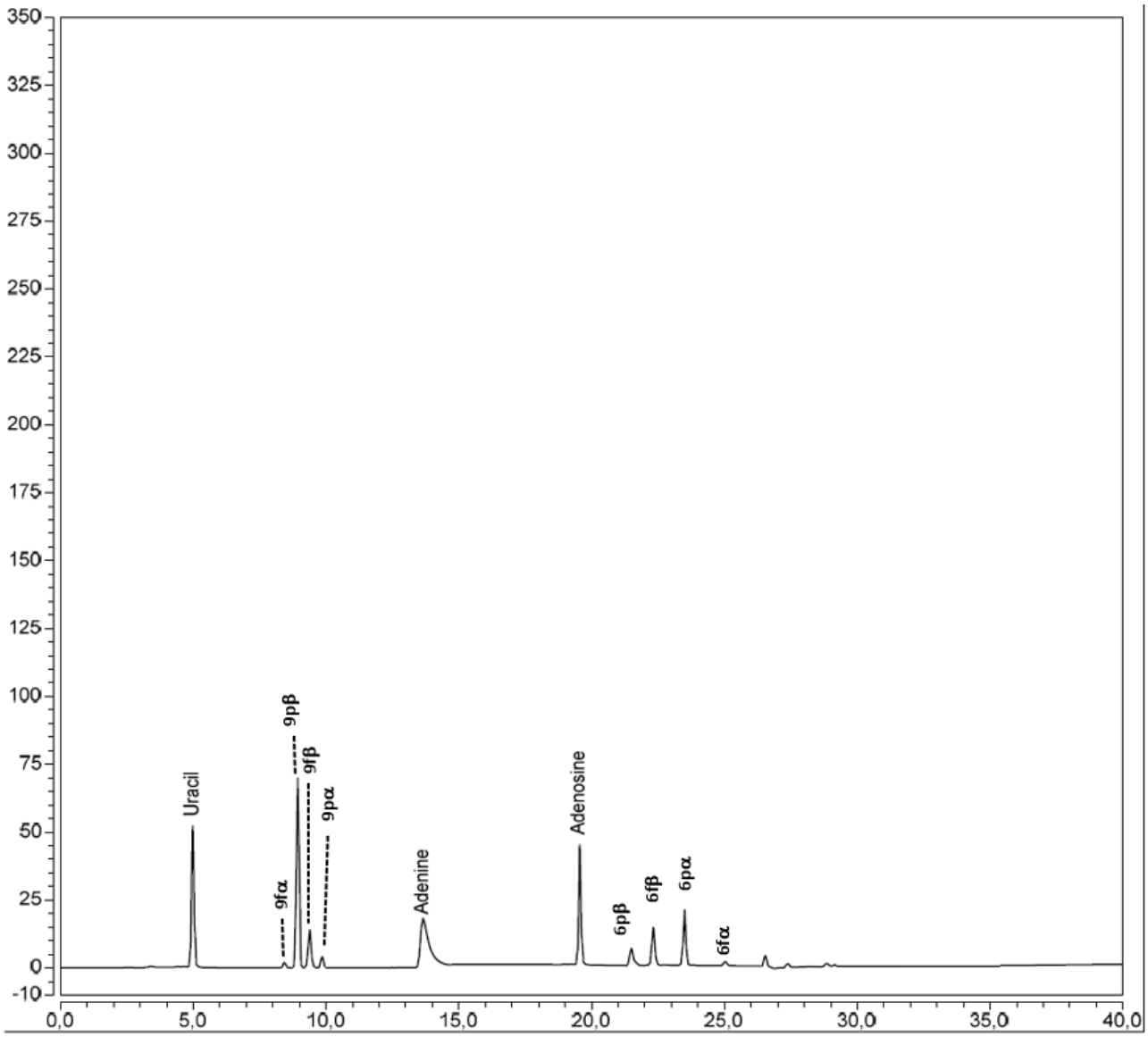

Synthesis of uridine **9** from **6** and uracil **7** in the presence of formamide and NWA 1465 (condition C).

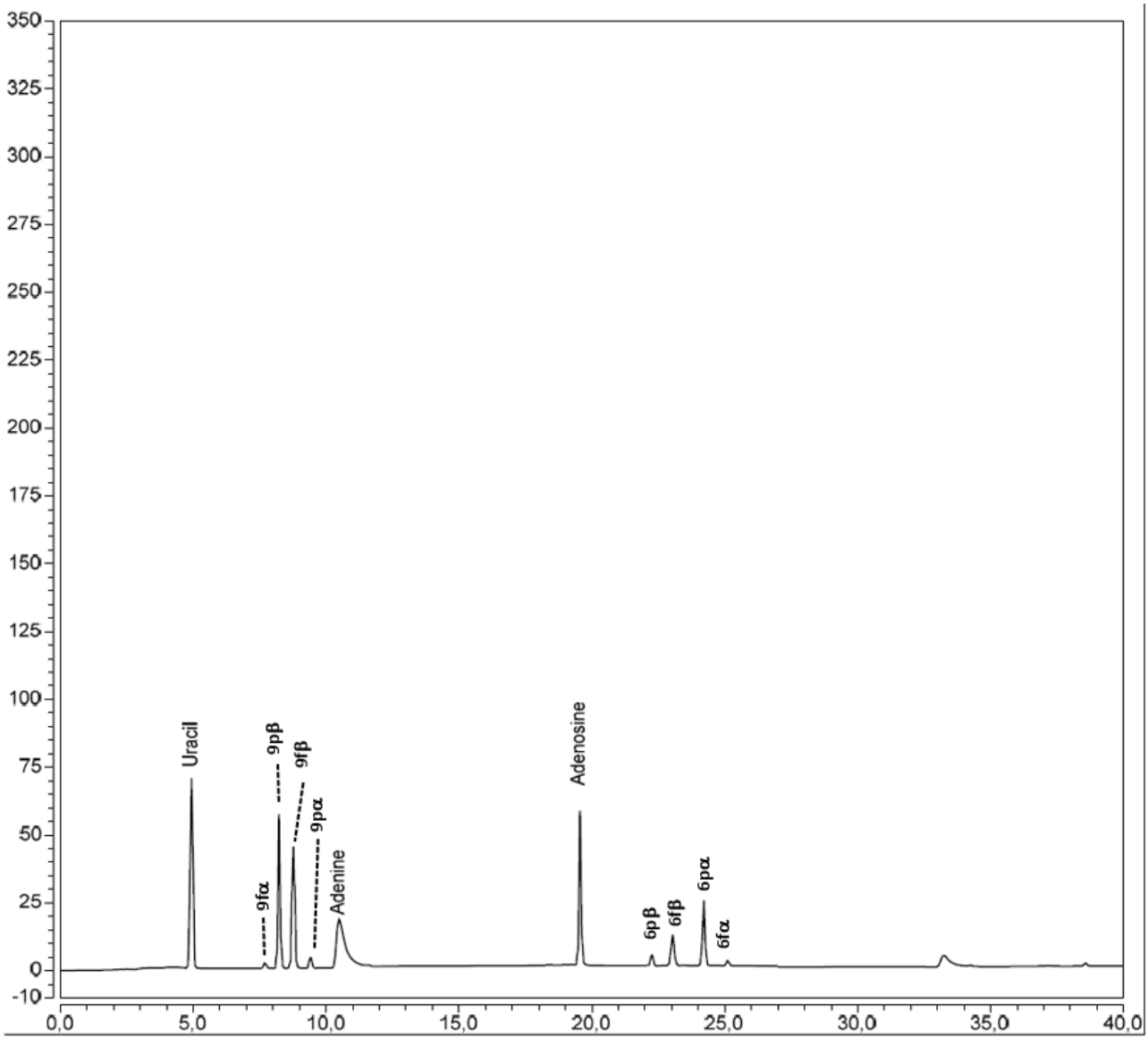

Synthesis of cytidine **10** from **6** and cytosine **8** in dry film (condition A).

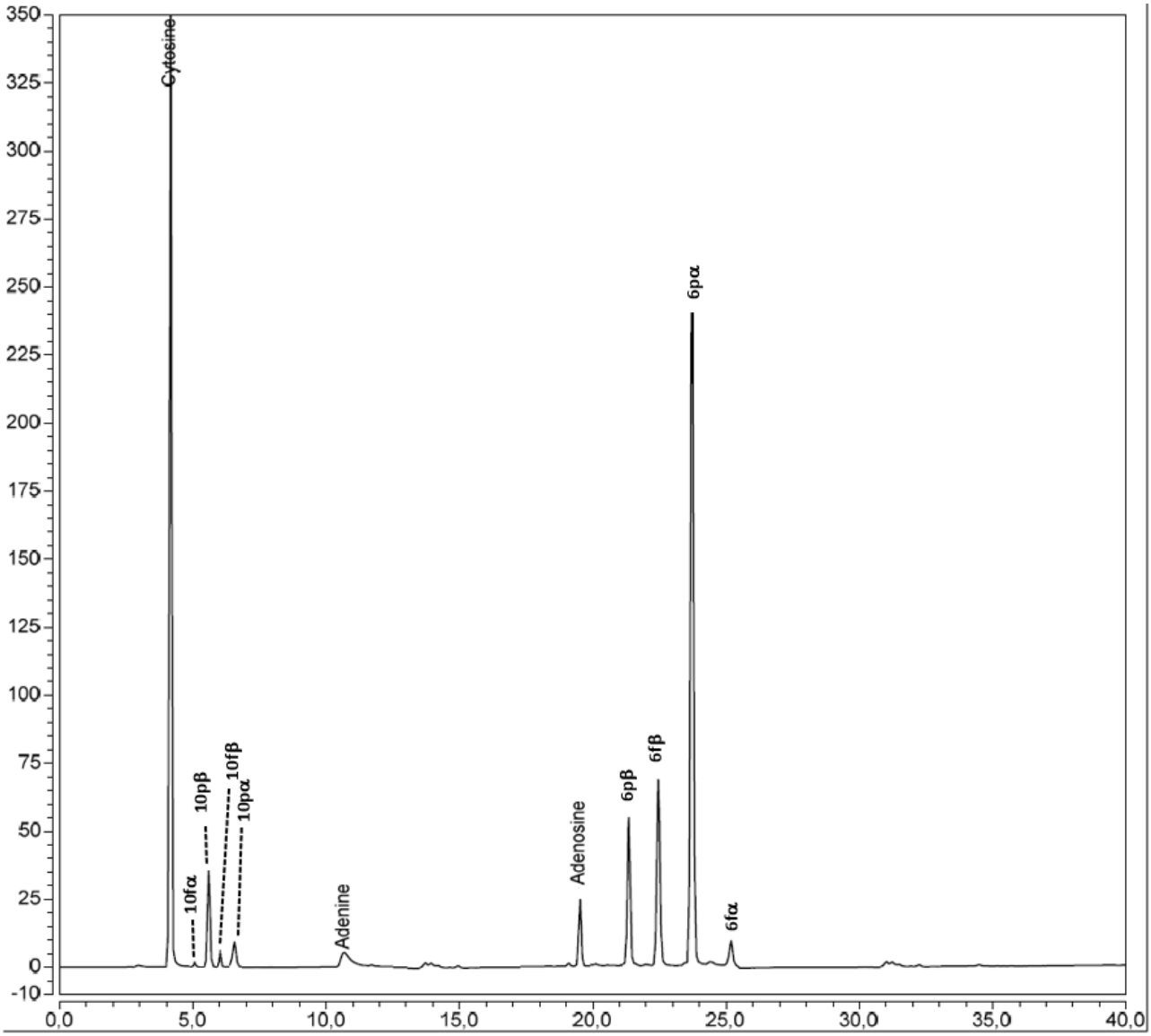

Synthesis of cytidine **10** from **6** and cytosine **8** in formamide solution (condition B).

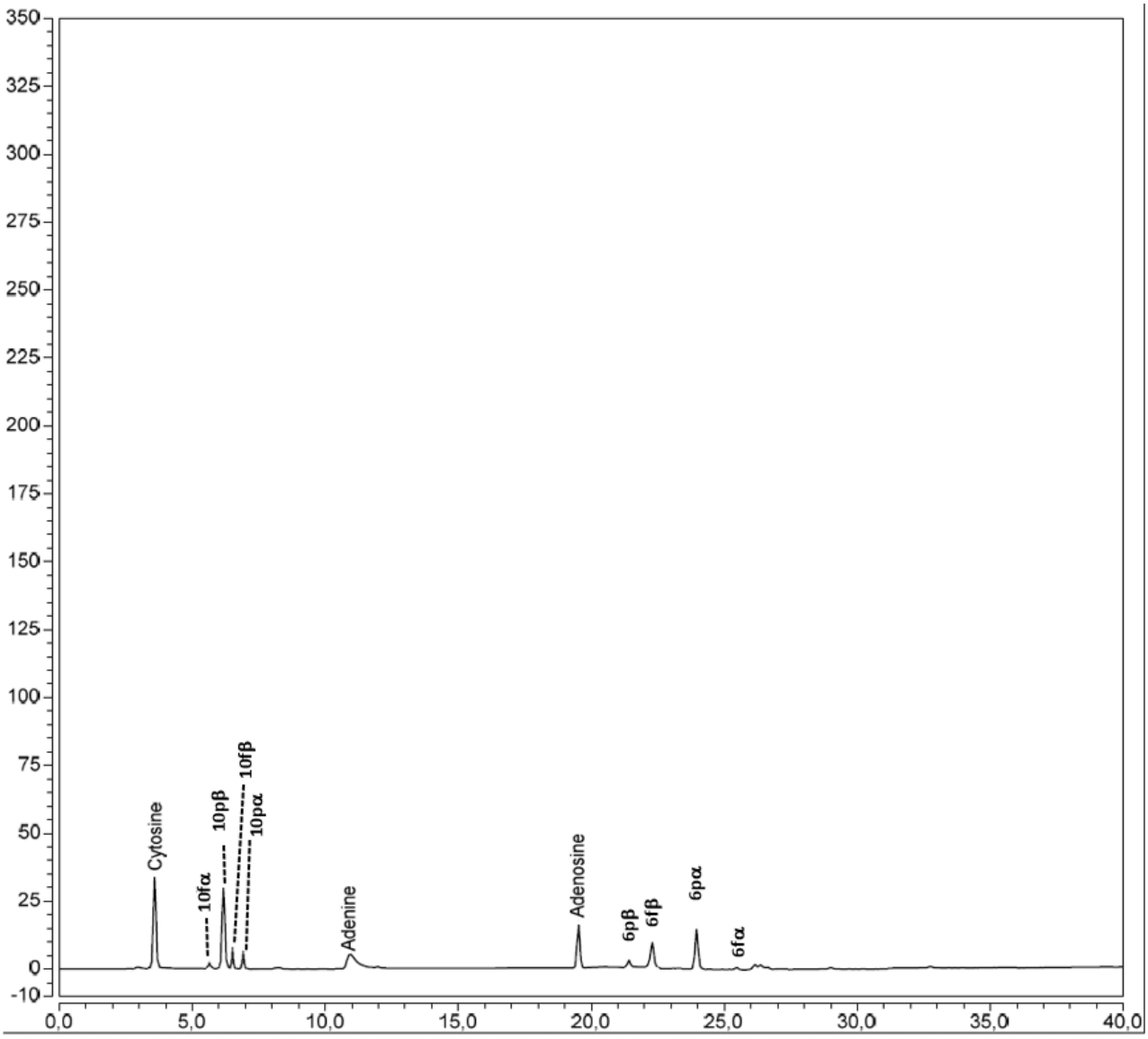

Synthesis of cytidine **10** from **6** and cytosine **8** in the presence of formamide and NWA 1465 (condition C).

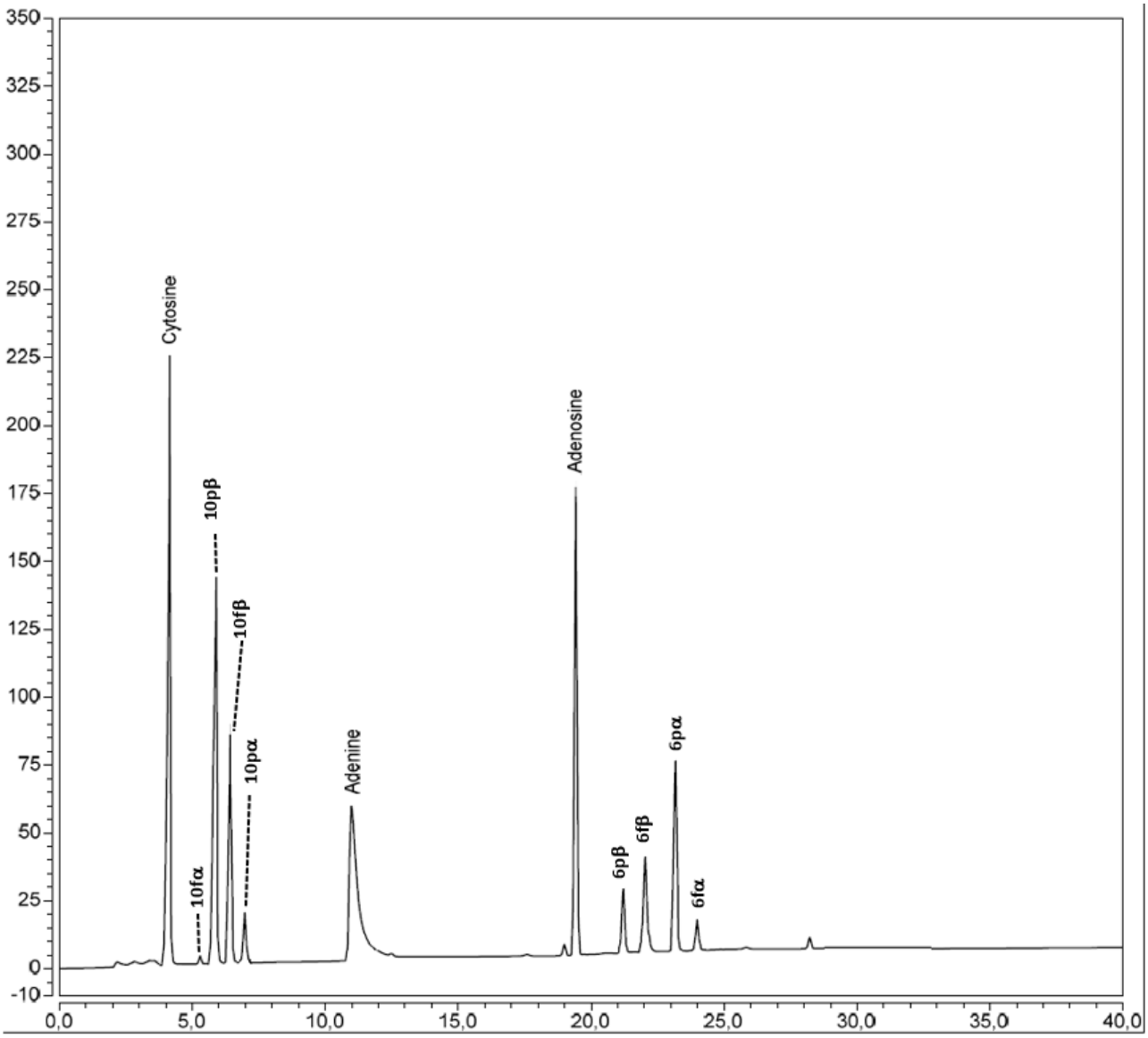

Part 2: Application of prebiotic multicomponent chemistry for the synthesis of bioactive compounds

It is well recognized that Multi-Component Chemistry (MCC) played a key role in molecular evolution generating high chemical diversity from two or more reagents.[243] The prebiotic MCC of the Origins generated an incredible variety of organic structures in the pristine Earth, setting the molecular evolution conditions for the emergence of the Last Universal Common Ancestor (LUCA).[244] The first documented prebiotic MCC encompasses the Strecker reaction for the synthesis of amino acids,[245] the Butlerow condensation of formaldehyde to sugars,[246] and the Orò transformation of cyanuric acid (HCN) to purine nucleobases.[247] More recently, prebiotic MCC involving formamide (NH_2CHO), a product of hydrolysis of HCN,[206] afforded a robust chemical framework for the contemporary synthesis of sugars, carboxylic acids, amino acids and several types of heterocyclic compounds, including purine and pyrimidine nucleobases and nucleosides.[248,126,249,250] A number of unnatural derivatives has been also synthesized by the spontaneous combination of the original molecules, including peptide nucleic acids[102] and non-natural nucleobases and nucleosides, such as acyclic nucleosides,[251] which belong in well-known antiviral drug families.[252] In particular, peptide nucleic acid derivatives showed high antiviral activity against Influenza A, HIV and HBV viruses.[253,254] Examples of the synthesis of PNA's building blocks in prebiotic chemistry are reported, and the emergence of structural complexity associated to chemical modification of the nucleobase and sugar discussed in detail.[221,255] The possible role of PNA in the origin of life prior to an RNA world is reviewed, and the synthesis of PNA precursors on the primitive earth, as well as the possibility of template-directed PNA chemical replication and ligation, deeply investigated.[256,257.258,259]
In addition, the synthesis of PNA derivatives bearing heterocycle analogues and modified nucleobases have been reported in order to explore hybridization processes and emergent self-assembly and biological properties.[260,261,262,263] Today, the modernization of the MCC by innovative techniques (e.g. microwave-assisted procedures) furnishes an impressive combination of tools to force and speed-up the production of complex heterocyclic derivatives encompassing the so called "Molecular Evolution-Inspired Synthesis".[264]

1.1 Synthesis of bioactive PNA's derivatives from HCN polymeric species.

The prebiotic synthesis of PNA's building blocks includes the condensation of formamide and HCN oligomers, such as aminomalononitrile (AMN) and diaminomaleonitrile (DAMN), trimer and tetramer of HCN respectively.[265,249] AMN is a key intermediate in the prebiotic synthesis of purine nucleobases in the framework of prebiotic chemistry,[208,206,96,266,100] AMN has been identified as a common intermediate in

the prebiotic chemistry of HCN and NH_2CHO.[267,268,266,100,269,270,85] AMN is involved in the formation of imidazole intermediates, such as amino imidazole carbonitrile and amino imidazole carboxyamide, which are well-recognized precursors of purine and pyrimidine nucleobases and analogues.[271] Imidazoles are important pharmacophore in natural products and drugs, including antiviral agents[272] with anti-influenza virus activity.[273,274] In addition, imidazoles are commonly used as synthons in the preparation of bioactive purines by annulation with C-1 containing compounds as simple as urea, guanidine, formic acid and NH_2CHO.[275] Besides to AMN, diaminomaleonitrile (DAMN),[276] the tetramer of HCN,[265,249] is also a well-recognized intermediate in the prebiotic synthesis of nucleobases and of other biologically relevant heterocycles.[266,277,278,279,51] The formation of DAMN under prebiotic conditions has been recently reviewed.[280,241,250]

1.1.0 Aminomalononitrile inspired prebiotic chemistry as a novel multicomponent tool for the synthesis of imidazole and purine derivatives with antiinfluenza A virus activity

Here we report that AMN inspired multicomponent prebiotic chemistry yields amino imidazole carbonitrile derivatives decorated with different α-amino acids. The reaction involves the condensation between aminomalononitrile *para*-toluenesulfonate salt (AMNS), selected α-amino acids and trimethyl orthoacetate (TOA), a well-recognized one-carbon donor reagent in multicomponent chemistry,[281,282] under microwave-assisted conditions. The rationale in the chimera between heterocycle derivatives and amino acids has been largely explored in the case of peptide-nucleic acids as alternative to RNA in the origin of life, being characterized by high informational content and important biological activities.[283] In addition, the novel imidazole derivatives were transformed into the corresponding amino purine analogues to further explore the chemical space around the imidazole scaffold by a solvent free microwave assisted pyrimidine ring-closing procedure involving formic acid. Formic acid is a ubiquitous component in the pristine Earth, often involved in the prebiotic chemistry of AMN.[283] Amino imidazole carbonitriles and the corresponding purine derivatives showed appreciable activity against influenza A virus, probably due to the block of the viral budding from the cell, impairing viral release to other cells.

1.1.0.1 Synthesis of amino imidazole carbonitrile derivatives 4a-f and 5 a-f

Amino imidazole carbonitrile derivatives were prepared by a multicomponent procedure involving the microwave assisted condensation of AMNS **1**, trimethyl orthoacetate **2** (TOA) and a panel of protected α-amino acids (as methyl ester derivatives) **3a-f**, including glycine **3a**, alanine **3b**, valine **3c**, serine **3d**,

phenylalanine **3e**, and tyrosine **3f** (Scheme 1). Trimethyl orthoacetate was preferred to simpler trimethyl orthoformate in order to avoid undesired side-reactions.[284] The reaction was performed by two sequential synthetic steps without any intermediate workup and purification as follows: a) AMNS **1** (5.9 mmol) dissolved in THF (30 mL) and triethylamine TEA (7.1 mmol, 1.0 mL) was stirred at room temperature for 30 min, followed by the addition of trimethyl orthoacetate **2** (8.3 mmol) and microwave irradiation (250 W, 250 psi) for 2.0 min at 200 °C; b) the solution was cooled down at 25°C and the crude was treated with TEA (7.1 mmol, 1.0 mL) and protected α-amino acids **3a-f** (7.1 mmol) under previously reported microwave conditions. The reaction proceeded with a quantitative conversion of **1** to yield amino imidazole carbonitrile methyl ester derivatives **4a-f** in yield ranging from 25% to 60% (Table 1, entries 1-6) depending on the nature of selected α-amino acid (Scheme 1; Pathway A). The closure of the imidazole ring must have taken place *via* an imino ether intermediate followed by the nucleophilic addition of the amino acid residue.[285] The reported procedure not represent a completely plausible prebiotic process requiring organic solvents and microwave irradiation. Compounds **4a-f** were selectively decorated by the α-amino acid residue at the N-1 position in order to explore the chemical space around the imidazole ring. Note that, the possible formation of bis-imidazole derivatives as a consequence of a further reaction of compounds **4a-f** with trimethyl orthoformate was not observed under our experimental conditions.[275] The low mass balance of the reaction was probably due to the competitive self-oligomerization of AMN to HCN polymers.[286] As a general trend, the yield of the reaction decreased by increasing the structural complexity of the α-amino acid side-chain (Table 1, entry 1 vs entries 2-3), with the only exception of aromatic derivatives phenyl alanine and tyrosine, in which cases the corresponding amino imidazole carbonitrile derivatives were isolated in relatively high yield (Table 1, entries 5-6). The beneficial effect of the aromatic moiety in the annulation of AMN with simple amine has been previously reported.[275] Compounds **4a-f** were successively de-protected (NaOH 1M for 18 h at 25°C) to afford the corresponding amino imidazole carbonitriles AICs **5a-f** (Scheme 1, Pathway B) (Table 1, entries 7-12).

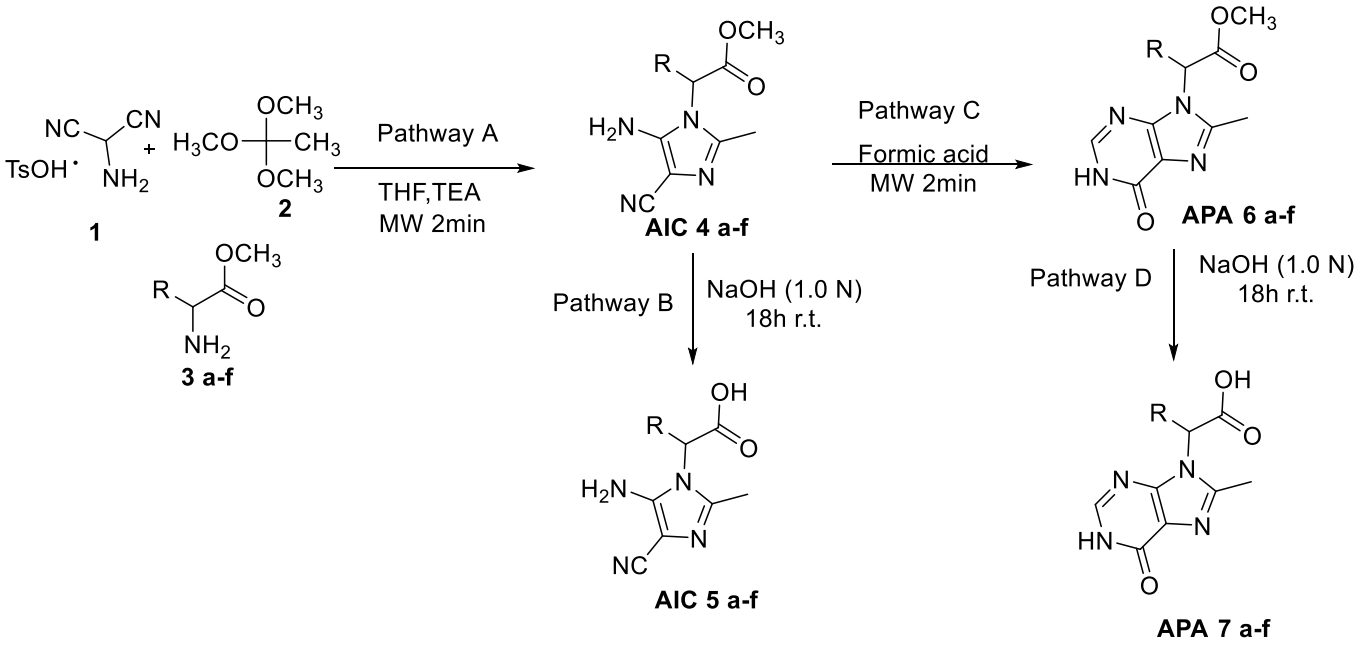

Scheme 1. Synthesis of amino imidazole carbonitrile derivatives **4a-f** and **5 a-f**, and 8,9-disubstituted-6,9-dihydro-1H-purin-6-ones **6a-f** and **7a-f.**

Table 1. Amino imidazole carbonitrile methyl esters **4 a-f** and amino imidazole carbonitriles **5a-f** from three component condensation of AMN, trimethyl orthoacetate and a-amino acids.

Entry	α-amino acid	Condition	Products	R	Yield (%)[c]
1	Glycine	THF, 2.0 min, 250 W, 250 psi at 200 °C[a]	**4a**	H	60
2	Alanine		**4b**	CH_3	34
3	Valine		**4c**	$CH(CH_3)_2$	32
4	Serine		**4d**	CH_2OH	25
5	Phenylalanine		**4e**	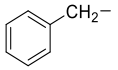	51
6	Tyrosine		**4f**	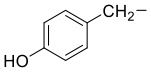	48
7	Glycine	NaOH, 18 hrs, 25 °C[b]	**5a**	H	92
8	Alanine		**5b**	CH_3	95

9	Valine		**5c**	$CH(CH_3)_2$	98
10	Serine		**5d**	CH_2OH	93[d]
11	Phenylalanine		**5e**	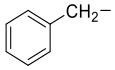	90
12	Tyrosine		**5f**	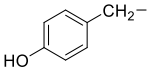	94

[a] Reaction conditions: compound **1** (5.9 mmol) in THF (30 mL) and triethylamine (7.1 mmol) for 30min at 25 °C; then compound **2** (8.3 mmol) and amino-acid (**3a-f**) (7.1 mmol) under MW irradiation. [b] NaOH (1N, 1.0mL) stirring for 18hrs at 25 °C. [c] Yield has been calculated on the basis of the amount of the recovered product. Reactions were performed in triplicate.

1.1.0.2 Synthesis of 8,9-disubstituted-6,9-dihydro-1H-purin-6-one derivatives 6a-f and 7 a-f.

The role of amino imidazole carbonitriles as annulation synthons for the synthesis of a large diversity of heterocyclic derivatives has been reported and the mechanism of their condensation discussed in detail.[287,288,289] For example, C-1 containing reagents as simple as urea, guanidine, formic acid and NH_2CHO, have been applied to yield di-amino purines, hypoxanthine, adenine, 1H-purin-2-(3H)-ones and other analogues. On the basis of these data, compounds **4 a-f** were annulated with formic acid to yield the corresponding 8,9-disubstituted-6,9-dihydro-1H-purin-6-one methyl esters **6a-f**. Briefly, compounds **4a-f** (3.8 mmol) were dissolved in formic acid (3.0 mL) under microwave irradiation (250 W, 250 psi) for 2.0 min at 200 °C (Scheme 1, Pathway C) to afford **6a-f** in quantitative conversion of substrate and yield (Table 2, entries 1-6). In addition, **6a-f** (0.1 mmol) were successively de-protected (NaOH 1M for 18 h at 25°C) to corresponding 8, 9-disubstituted-6,9-dihydro-1H-purin-6-ones **7a-f** (Scheme 1, Pathway D) (Table 2, entries 7-12).

Table 2. Synthesis of amino purine analogues **6a-f** and **7a-f.**

Entry	α-amino acid	Condition	Products	R	Yield(%)[c]
1	Glycine	Formic acid, 2.0 min, 250 W, 250 psi at 200 °C[a]	**6a**	H	88
2	Alanine		**6b**	CH_3	85
3	Valine		**6c**	$CH(CH_3)_2$	87
4	Serine		**6d**	CH_2OH	92
5	Phenylalanine		**6e**	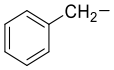	90
6	Tyrosine		**6f**	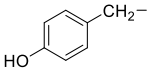	95
7	Glycine	NaOH, 18 hrs, 25 °C[b]	**7a**	H	98
8	Alanine		**7b**	CH_3	94
9	Valine		**7c**	$CH(CH_3)_2$	96
10	Serine		**7d**	CH_2OH	92

11	Phenylalanine		**7e**	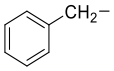	94
12	Tyrosine		**7f**	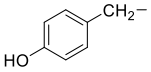	88

[a] Reaction conditions: compound **4 a-f** (3.8 mmol) was dissolved in formic acid (3.0 mL), under MW irradiation. [b] NaOH (1N, 1.0mL) stirring for 18 hrs at 25 °C. [c] Yield has been calculated on the basis of the amount of the recovered product. Reactions were performed in triplicate.

1.1.0.3. Biological assay

Influenza A virus is one of the most common infectious human respiratory pathogens associated with significant morbidity and mortality, especially in hospitalized patients. Among the influenza viruses, type A strains are responsible for annual epidemics and pandemic events. They belong to the *Orthomyxoviridae* family and are characterized by segmented, single-stranded negative RNA genome. RNA segments associate with the nucleoprotein (NP) and the viral RNA-dependent RNA polymerase (RdRp) complex in the replication and transcription cycles.[290] Three families of antiviral compounds are active against influenza A virus: a) the first one blocks the ion-channel activity of the viral Matrix (M) 2 protein involved in the virus uncoating; b) the second family includes inhibitors of the viral Neuraminidase (NA), blocking the release of viral particles from infected cells; and c) inhibitors of the polymerase complex. Among them, baloxavir, marboxil and favirapir have being licensed in Japan and United States.[291] However, the huge circulation of different influenza viruses and the emergence of drug-resistant strains lead to the search of new antiviral agents. For this reason, the novel imidazole and purine derivatives were tested against influenza A/Puerto Rico/8/34 H1N1 (PR8) virus. In the first set of experiments, A549 cells were infected with 0.001 MOI of PR8 and treated with different concentrations (range 5–80 μg/mL) of compounds **4 a-f, 5a-f, 6a-f** and **7a-f** (Table 3) for 24 h. Then, infected treated-cells were fixed and stained with antibodies specific for the viral protein Hemagglutinin (HA), as described in the experimental part. The cytotoxicity of the compounds was evaluated by standard MTT assay. Table 3 shows the values of IC50, CC50, and relative selective index (SI) obtained on A549 cells. Compounds **4e**, **5a**, **4b**, **4d**, **5e**, **7c**, **6c**, **6f**, and **7b** showed SI values more than 1.5. These compounds were further investigated to evaluate the ability in impairing viral release from infected cells. Briefly, A549 cells were infected with PR8 and treated with concentrations (100, 150 and 200 μg/mL) of selected compounds. After 24 h, infected cell monolayers were directly stained with anti-HA

antibodies as described above, while supernatants were recovered and used to newly infect fresh monolayers. We found that within the 9 most active derivatives, compounds **5a** and **7c** decreased the expression of HA on infected monolayers (Figure 1A) compared to untreated infected cells (Figure 1; Panel A, part I). The percentage of Relative Fluorescent Units (RFU) of HA was dose-dependently reduced. As a consequence, the supernatants of treated cells contained less viral particles able to infect other monolayers (Figure 1; Panel B).

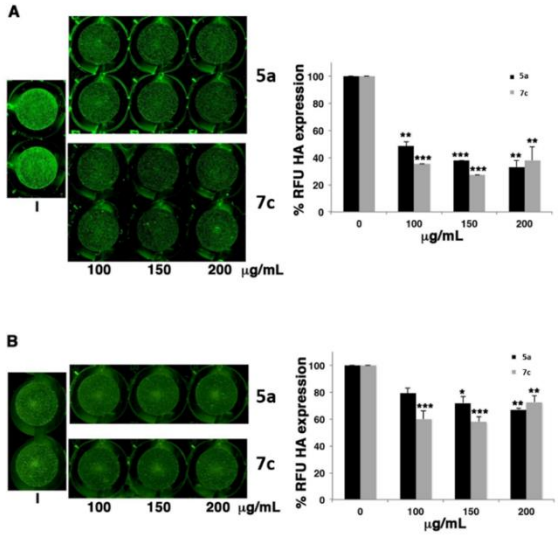

Figure 1. The expression of Hemagglutinin (HA) by means of In Cell Western (ICW) assay in the presence of most active compounds 5a and 7c. A549 cells were infected with PR8 (0.001 MOI) and treated or not (I) with different concentrations (100, 150 and 200 mg/mL) of compounds. After 24 h treatment, cells were fixed and stained for HA protein, as described in the Materials and Methods section (panel A); supernatants were recovered and used to infect a fresh monolayer of A549 cells (panel B). The expression of viral HA was analyzed by ICW assay, using LI-COR Image Studio Software. The percentage of relative fluorescence units (RFU) was calculated in comparison to untreated infected cells (considered 100%). Values are the mean ± S.D. of two replicates of one experiment of two performed (n = 2). Statistical significance of the data vs untreated infected cells was defined as * $p < 0.05$ and ** $p < 0.01$ and *** $p < 0.001$ (unpaired t-test).

Overall, the results suggest that both compounds **5a** and **7c** may block specific steps of viral replication, probably involving the viral budding from the cell, thus impairing viral release from infected cells and the spreading of virions to the other ones.

Table 3. Biological activity of compounds **4 a-f**, **5a-f**, **6a-f and 7a-f** against Influenza A virus

Entry	Class	Amino acid	R	Products	IC50[a]	CC50[b]	SI[c]
1	Amino-imidazole-carbonitrile derivatives (**AIC**)	Glycine	H	**4a**	nd	1.02	nd
2				**5a**	0.76	2.20	2.9
3		Alanine	CH_3	**4b**	0.76	2.75	3.6
4				**5b**	3.00	2.91	1
5		Valine	$CH(CH_3)_2$	**4c**	2.41	1.13	0.5
6				**5c**	0.83	0.62	0.8
7		Serine	CH_2OH	**4d**	0.68	1.99	2.9
8				**5d**	nd	nd	nd
9		Phenylalanine	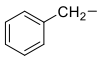	**4e**	0.39	0.84	2.1
10				**5e**	0.46	3.36	7.2
11		Tyrosine	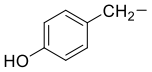	**4f**	3.20	1.45	0.5
12				**5f**	1.99	0.90	0.45
13	Amino-purine-analogues (**APA**)	Glycine	H	**6a**	6.96	2.11	0.3
14				**7a**	0.89	0.75	0.84
15		Alanine	CH_3	**6b**	nd	0.47	nd
16				**7b**	1.85	2.86	1.5
17		Valine	$CH(CH_3)_2$	**6c**	0.18	0.31	1.7
18				**7c**	0.59	1.09	1.8
19		Serine	CH_2OH	**6d**	nd	0.93	nd
20				**7d**	-	6.11	-
21		Phenylalanine	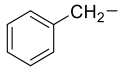	**6e**	1.87	0.51	0.3
22				**7e**	nd	6.35	nd
23		Tyrosine	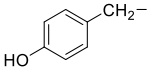	**6f**	0.48	0.80	1.7
24				**7f**	nd	nd	nd

[a] IC_{50} is the drug concentration (mmoL) causing 50% inhibition of the desired activity. Each experiment was conducted in triplicate. [b]CC_{50} is the drug concentration (mmoL) causing 50% of death of viable cell. [c] SI is the selectivity index defined as the ratio of the CC_{50} to the IC_{50}.

1.1.1 Conclusions

Aminomalononitrile inspired prebiotic chemistry furnished an efficient synthetic tool for the synthesis of a large panel of imidazole and purine derivatives decorated with a natural amino acid motif. These products resemble the first heterocycle derivatives possibly produced by an original multicomponent reaction involving some of the well-recognized prebiotic precursors, such as HCN oligomer and amino acids. The annulation of amino-imidazole-carbonitrile derivatives into the corresponding amino-purine-analogues generally reduced the activity against influenza A/Puerto Rico/8/34 H1N1 (PR8) virus, suggesting the antiviral pharmacophore role of the imidazole scaffold. The derivatives bearing a free carboxylic moiety in the amino acid residue (compounds **5** and **7**) showed an IC50 value of the same order of magnitude than the corresponding esters (compounds **4** and **6**). The comparable anti-viral activity between imidazole derivatives bearing a free or a protected carboxyl moieties has been previously reported in the case of HSV.[292] Derivatives decorated with the valine and phenylalanine structural motif showed the higher activity in both AIC and APA series, compounds **4b**, **4e**, **5a**, **5e**, **6c**, **6f** and **7a** being characterized by the highest IC50 value (Table 3 entries 2, 3, 9, 10, 14, 17, 23). Among the AIC family, the presence of the phenylalanine residue produced the most active derivatives, namely compounds **4e** and **5e**, (IC50 values of 0.39 μM and 0.46 μM). They also showed the highest selectivity index (2.1 and 7.2 respectively). On the other hand, valine derivatives **6c** and **7c** were the most active compounds in the APA series, showing IC50 value of 0.18 μM and 0.59 μM, respectively, and SI value of 1.7 and 1.8, respectively. Compounds **4b**, **4e**, **5a**, **5e**, **6c**, **6f** and **7a** showed an antiviral activity against influenza A/Puerto Rico/8/34 H1N1 (PR8) virus higher than standard antiviral agents (Oseltamivir phosphate, ribavirin and amantadine) and a selectivity index comparable to ribavirin (5.84) and higher than amantadine.[293] In addition, compounds **5a** and **7c** decreased the expression of viral HA on infected monolayers, suggesting the occurrence of inhibition of the viral budding from the cell, thus preventing the viral release from infected cells and the spreading to other cells. This hypothesis is in accordance with previous data on the capacity of imidazole derivatives to block the release of virions from infected cells.[294] The peptide nucleic acid building blocks we synthesized could also be relevant to prebiotic research, suggesting novel structural motif to be considered in pristine molecular evolution processes.

2.1.0 Multicomponent synthesis of diaminopurine and guanine PNA's analogues active against influenza A virus from prebiotic compounds.

As a continuation of the previous work,[295] an alternative synthesis of bioactive PNA's building block analogues from prebiotic compounds such as aminomalononitrile (AMN), urea and guanidine, was developed. Urea and guanidine[296] have been involved in multicomponent procedures with cyanoacetaldehyde,[297,298] malic acid,[299] acrylonitrile,[300] propionic acid,[301] and β-alanine.[302,303,304] In addition, they favored the ring-closing annulation and aromatization in the transformation of pyrimidines and purines.[280] Here, we report a new synthetic pathway for the preparation of bioactive diaminopurine and guanine PNA's building blocks by microwave assisted multicomponent synthesis of amino imidazole carbonitrile derivatives in the presence of sustainable reaction solvents. For the purpose, AMN and α-amino acids were reacted in the presence of trimethyl orthoacetate and 2-methyltetrahydrofuran (2-MeTHF), or in alternative, ethylene glycol (EG), followed by treatment of amino imidazole carbonitrile intermediates with guanidine and urea. 2-MeTHF and EG were selected since they are greener alternative to toxic organic solvents in tandem reactions, photocatalytic cascade and cyclization process.[305,306,307,308,309,310] The novel purine derivatives showed high inhibitory activity against influenza A virus, encompassing the range of nano-molar activity.

2.1.0.1 Synthesis of diaminopurine analogues (8a-f, 9a-f) and guanine analogues (10a-g, 11a-g).

As a selected case, amino imidazole carbonitrile derivatives **4a** was prepared by reaction of AMN **1** (5.9 mmol) and trimethyl orthoacetate **2** (8.3 mmol; TOA) with glycine methyl ester derivative **3a** (7.1 mmol) in the appropriate reaction solvent (2-MeTHF, or in alternative EG; 30 mL) and in the presence of triethylamine (7.1 mmol, 1.0 mL; TEA), working at room temperature for 30 min followed by microwave irradiation (250 W, 250 psi) at 200 °C for 2.0 min (Scheme 1). The reaction with tetrahydrofuran (THF) was also performed as a reference.[295] As reported in Table 1, the yield of amino imidazole carbonitrile methyl ester derivative **4a** was higher with 2-MeTHF than THF and EG, this latter solvent being the less efficient of the series (Table 1, entry 5 versus entries 1 and 4). This result was probably due to the high polarity of EG responsible for the undesired amino acid self-condensation. Note that 2-MeTHF performed better than traditional multicomponent reaction solvents such as methylene dichloride (CH_2Cl_2) and acetonitrile (CH_3CN) (Table 1, entry 5, versus entries 2 and 3). In order to generalize the procedure, the reaction was repeated using a panel of five α-amino acids methyl ester derivatives **3b**-**g** (alanine **3b**, valine **3c**, serine **3d**, phenylalanine **3e**, tyrosine **3f** and

tryptophan **3g**) to yield the corresponding amino imidazole carbonitrile methyl esters **4b-g** in yield ranging from 29% to 56% (Table 4, entries 6-11).

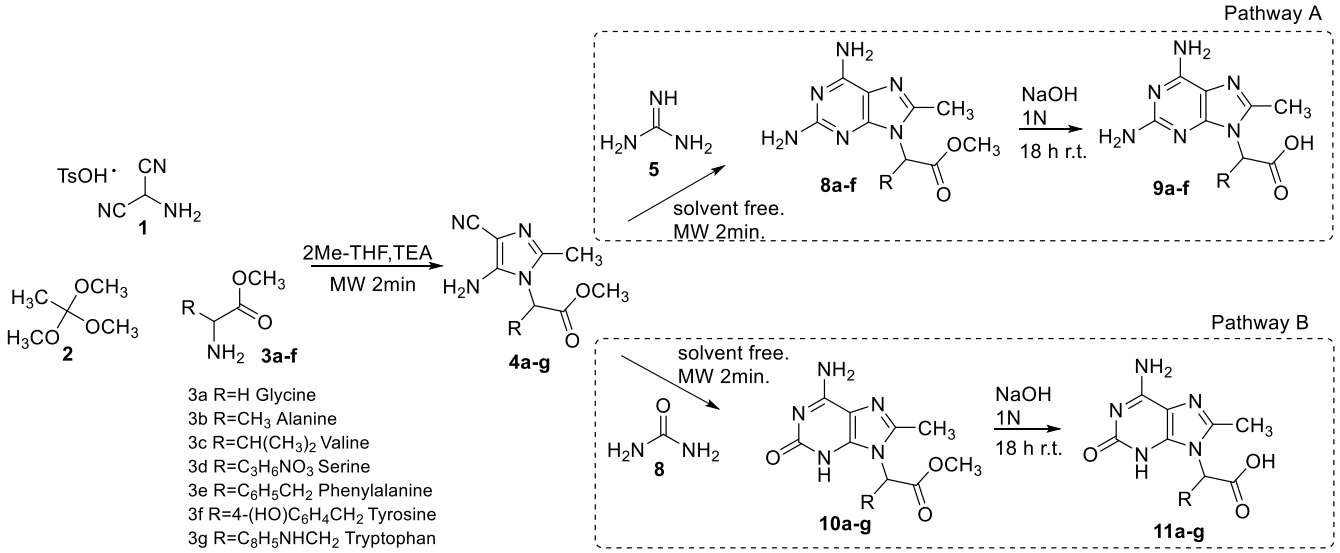

Scheme 2. Synthesis of diaminopurine analogues **8a-f, 9a-f** (Pathway A) and guanine analogues **10a-g, 11a-g** (Pathway B).

Table 4. Synthesis of aminoimidazole carbonitrile derivatives **4a-g**[a].

Entry	α-amino acid	Condition	Products	R	Yield (%)[b]
1	Glycine	THF, 2.0 min, 250 W, 250 psi at 200 °C	**4a**	H	60
2		CH_2Cl_2, 2.0 min, 250 W, 250 psi at 200 °C			20
3		CH_3CN,			50

		2.0 min, 250 W, 250 psi at 200 °C			
4		$(CH_3O)_2(CH_2)_2$, 2.0 min, 250 W, 250 psi at 200 °C			15
5		2Me-THF, 2.0 min, 250 W, 250 psi at 200 °C			66
6	Alanine		**4b**	CH_3	37
7	Valine		**4c**	$CH(CH_3)_2$	35
8	Serine		**4d**	CH_2OH	29
9	Phenylalanine		**4e**	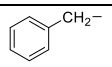	56
10	Tyrosine		**4f**	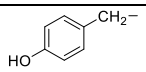	52
11	Tryptophan		**4g**	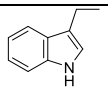	50

[a] AMN **1** (5.9 mmol), trimethyl orthoacetate **2** (8.3 mmol), amino-acid (**3a-g**) (7.1 mmol) and triethylamine (7.1 mmol) under MW irradiation. [b] Yield has been calculated on the basis of the amount of the recovered product. Reactions were performed in triplicate.

Next, the reaction was oriented toward the preparation of PNA's diaminopurine analogues (DAPAs) **8a-f** (Scheme 2, Pathway A) and guanine analogues (GAs) **10a-g** (Scheme 2, Pathway B). Imidazole derivatives **4a–g** were reacted with guanidine **5** or, in alternative urea **8**, as one-carbon donors in the annulation process (Scheme 3).

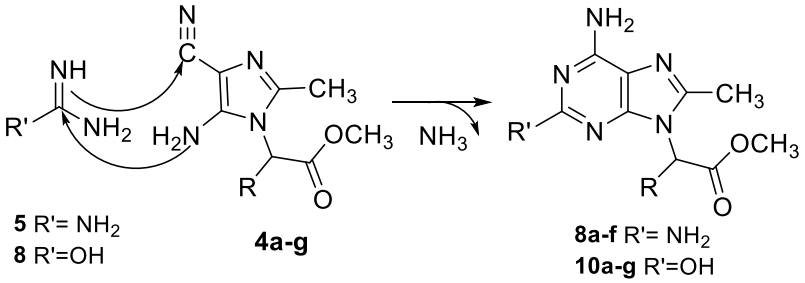

Scheme 3. Proposed mechanism for the synthesis of compounds **8a-f** and **10a-g.**

Briefly, imidazole derivatives **4a–g** (0.80 mmol) and compounds **5** and **8** (1.60 mmol, 2 eq.) were treated under solvent-free microwave irradiation (150 W, 250 psi) for 2.0 min at 250 °C (Scheme 2, Pathways A and B) to afford **8a–f** and **10a-g**, respectively, in quantitative conversion of substrate and appreciable yield of product (Table 5, entries 2–7 and Table 6, entries 2-8). The reaction of compound **4a** was carried out also under simple thermal conditions (250 °C) as a reference to yield DAPA **8a** and GA **10a** in low yield (Table 5 and 6; entry 1 versus 2), confirming the beneficial role of microwave in the annulation process. As a general trend, the selectivity of the reaction decreased by increasing the irradiation time, probably due to the occurrence of polycondensation side-reactions with formation of high polar derivatives not isolated under our experimental conditions.[311]

Table 5. Synthesis of diaminopurine analogues **8a-f** and **9a-f**.

Entry	α-amino acid	Condition	Products	R	Yield (%)[d]
1	Glycine	Solvent free, 120.0 min, at 250 °C[a]	**8a**	H	21
2		Solvent free,			38

3	Alanine	MW 2.0 min, 150 W, 250 psi at 250 °C[b]	**8b**	CH_3	25
4	Valine		**8c**	$CH(CH_3)_2$	31
5	Serine		**8d**	CH_2OH	25
6	Phenylalanine		**8e**	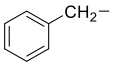	40
7	Tyrosine		**8f**	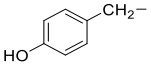	42
8	Glycine	NaOH, 18 hrs, 25 °C[c]	**9a**	H	98
9	Alanine		**9b**	CH_3	95
10	Valine		**9c**	$CH(CH_3)_2$	99
11	Serine		**9d**	CH_2OH	96
11	Phenylalanine		**9e**	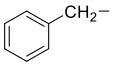	95
12	Tyrosine		**9f**	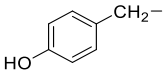	98

[a] Reaction conditions: **4a–f** (0.80 mmol), guanidine carbonate **5** (1.60 mmol, 2 eq.) under solvent-free thermal heating for 120.0 minutes at 250 °C. [b] Reaction conditions: **4a–f** (0.80 mmol), guanidine carbonate **5** (1.60 mmol, 2 eq.) under solvent-free microwave irradiation (150 W, 250 psi) for 2.0 minutes at 250 °C. [c] NaOH (1.0 N, 1.0 mL) stirring for 18hrs at 25 °C. [d] Yield has been calculated on the basis of the amount of the recovered product. Reactions were performed in triplicate.

The polycondensation of urea, guanidine and their derivatives in the presence of aromatic compound is reviewed and the relationship between this process and the energy source and the reaction time deeply investigated.[312] Even if a specific selectivity trend was not observed, it has not escaped our attention that the substitution pattern of imidazole intermediates **4a-g** played a significative role in the reaction. In particular, the presence of electron-donating aromatic amino acid residues generally increased the overall yield of the annulation process, with the only exception for the case of compound **10a** (Table 5 entries 6 and 7 and Table 6, entries 6, 7 and 8 vs Table 6 entry 2). Finally, in order to increase the solubility in water and enlarging the panel of PNA's building blocks, DAPAs **8a–f** and GAs **10a-g** (0.1 mmol) were treated with NaOH (1.0 N) at 25°C for 18 h (Scheme 2) to afford the corresponding carboxylic acid derivatives **9a–f** and **11a-g**, respectively.

Table 6. Synthesis of guanine analogues **10a-g** and **11a-g**.

Entry	α-amino acid	Condition	Products	R	Yield (%)[d]
1	Glycine	Solvent free, 120.0 min, at 250 °C[a]	**10a**	H	25
2		Solvent free, MW 2.0 min, 150 W, 250 psi at 250 °C[b]			45
3	Alanine		**10b**	CH_3	32
4	Valine		**10c**	$CH(CH_3)_2$	35
5	Serine		**10d**	CH_2OH	27
6	Phenylalanine		**10e**	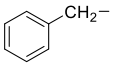	41
7	Tyrosine		**10f**	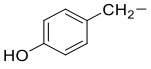	45
8	Tryptophan		**10g**	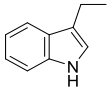	47
9	Glycine	NaOH, 18 hrs, 25 °C[c]	**11a**	H	99
10	Alanine		**11b**	CH_3	94
11	Valine		**11c**	$CH(CH_3)_2$	98
12	Serine		**11d**	CH_2OH	97
13	Phenylalanine		**11e**	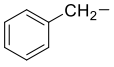	94
14	Tyrosine		**11f**	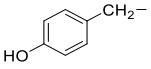	99
15	Tryptophan		**11g**	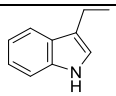	98

[a] Reaction conditions: **4a–g** (0.80 mmol), urea **8** (1.60 mmol, 2 eq.) under solvent-free thermal heating for 120.0 minutes at 250 °C. [b] Reaction conditions: **4a–g** (0.80 mmol), urea **8** (1.60 mmol, 2 eq.) under solvent-free microwave irradiation (150 W, 250 psi) for 2.0 minutes at 250 °C. [c] NaOH (1.0 N, 1.0 mL) stirring for 18hrs at 25 °C. [d] Yield has been calculated on the basis of the amount of the recovered product. Reactions were performed in triplicate.

2.1.0.2 Biological assay

Compounds **8a-f**, **9a-f**, **10a-g** and **11a-g** were tested against influenza virus A, one of the main respiratory pathogens responsible for seasonal epidemics or pandemic events. The use of vaccines and drugs in the therapy of influenza A virus, such as neuraminidase (NA), M2 channel and polymerase inhibitors is limited by the multidrug-resistant phenomenon associated with the high variability and the circulation of new influenza virus strains,[313,314] requiring a continuous effort for the search of new antiviral agents. PNA's analogues are well recognized compounds with inhibitory activity against viral infections being able to pair with viral RNA and DNA.[102,263] For example, pyrimidine-like PNA's derivatives showed selective pair with poly-purine sequences of double helical RNA,[315] while 2-amino pyridines counterpart[316] interfere with RNA editing.[317]

A549 cells were infected with 0.001 MOI of PR8 and treated with different concentrations (0.015–0.36 mMoL) of **8a-f**, **9a-f**, **10a-g** and **11a-g** (Table 7) for the following 24 h. The cytotoxicity of the compounds was evaluated by standard MTT assay. The antiviral activity was evaluated by the HAU assay from supernatants of cells infected with PR8/H1N1 virus and treated for 24 hours with the compounds. Control cells were treated with DMSO alone at the same concentration used for each compound. Table 7 shows the values of IC50, CC50, and relative selective index (SI). Compounds **8f**, **9f**, **10a**, **11a**, **10f** and **11f** showed the highest SI values and IC50 values were close related to the most-used NA inhibitor oseltamivir-carboxylate concentrations in cell cultures.[318,319] As general trend, DAPAs and GAs showed a comparable anti-viral activity, and derivatives bearing a free carboxylic moiety showed an IC50 value higher than the corresponding esters (Table 7). In addition, compounds decorated with glycine, phenylalanine, tyrosine showed the highest inhibitory activity. In both series, compounds **8f**, **9f**, **10a**, **11a**, **10f**, **11f,** showed the lower toxicity (Table 7 entries 12, 13, 14, 15, 24, 25). The presence of an aromatic residue always leads to an inhibitory activity effect, the tyrosine residue producing the most active derivatives (**8f**, **9f**, **10f** and **11f**) with IC50 values of 0.020, 0.024, 0.023 and 0.035 mM, respectively, and the highest CC50 value (0.580, 0.610, 0.582 and 0.604 mM respectively). The major activity of compounds bearing a tyrosine residue could be explained by the high radical scavenging activity and antioxidant activity reported for this catechol derivative, which can interfere in the overall redox activity of the cell, thus modulating the viral cycle.[43,320,321]

Table 7. Biological activity of compounds **8a-f**, **9a-f**, **10a-g** and **11a-g** against Influenza A virus.

Entry	Class	Amino acid	R	Products	IC50[a]	CC50[b]	SI[c]
1	-	-	-	Oseltamivir	0.180	0.350	1.95
2	Diaminopurine analogues (DAPA)	Glycine	H	**8a**	0.390	0.560	1.4
3				**9a**	0.526	0.621	1.2
4		Alanine	CH_3	**8b**	n.a	0.790	-
5				**9b**	n.a	0.846	-
6		Valine	$CH(CH_3)_2$	**8c**	n.a	0.718	-
7				**9c**	n.a	0.756	-
8		Serine	CH_2OH	**8d**	n.a	0.318	-
9				**9d**	n.a	0.350	-
10		Phenylalanine	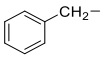	**8e**	0.039	0.420	10.5
11				**9e**	0.210	0.610	2.9
12		Tyrosine	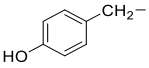	**8f**	0.020	0.580	29.0
13				**9f**	0.024	0.610	25.4
14	Guanine analogues (GA)	Glycine	H	**10a**	0.036	0.896	24.1
15				**11a**	0.039	0.764	19.2
16		Alanine	CH_3	**10b**	n.a	0.715	-
17				**11b**	n.a	0.821	-
18		Valine	$CH(CH_3)_2$	**10c**	n.a	0.650	-
19				**11c**	n.a	0.420	-
20		Serine	CH_2OH	**10d**	n.a	0.218	-
21				**11d**	n.a	0.323	-
22		Phenylalanine	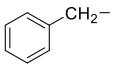	**10e**	0.340	0.710	2.1
23				**11e**	0.520	0.654	1.3
24		Tyrosine	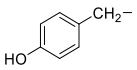	**10f**	0.023	0.582	25.3
25				**11f**	0.035	0.604	17.3
26		Tryptophan		**10g**	0.310	0.690	2.2
27				**11g**	0.510	0.673	1.3

[a] IC50 is the drug concentration (mmoL) causing 50% inhibition of the desired activity. Each experiment was conducted in triplicate. [b]CC50 is the drug concentration (mmoL) causing 50% of death of viable cell. [c] SI is the selectivity index defined as the ratio of the CC50 to the IC50. n.a: not available.

2.1.1 Conclusions

A large panel of diaminopurine and guanine PNA's analogues was synthesized from aminomalononitrile multicomponent chemistry and guanidine and urea as one-carbon annulation reagents. The process was assisted by microwave irradiation to afford amino acid decorated purine derivatives resembling the structural motif of acyclo-nucleosides. With respect to our previous study,[295] environmental sustainable 2-MeTHF was selected as the best reaction solvent as an alternative to toxic THF, affording imidazole intermediates **4a-g** in yield higher than THF and other organic solvents, such as MeCN and CH_2Cl_2. In addition, we proved for the first time that the annulation of imidazoles **4a-g** was effective also in the presence of guanidine carbonate and urea (two widely recognized prebiotic precursors,[296] affording a large variety of novel PNA's building blocks to investigate both the chemical space and the scaffold morphing. This reflect the unexpected high IC50 and SI values in the inhibition of influenza A virus and in the range of nano-molar concentration showed by compounds **8a**, **9a**, **9e**, **10e**, and **11e**. They were decorated by glycine, phenylalanine and tyrosine. In particular, compounds **8f**, **9f**, **10f** and **11f**, bearing the tyrosine residue, showed IC50 of 0.020, 0.024, 0.023 and 0.035 μM and the highest CC50, probably due to the high antioxidant activity reported for this amino acid. Interestingly, despite a detailed investigation was not carried out about the mechanism of action of novel compounds, our attention was also attracted by the repetitive difference of activity between the derivatives bearing a free carboxylic moiety in the amino acid residue and the ester counterpart, these latter being more active. The very fact that carboxylic acid derivatives showed inhibitory activity different from that of the corresponding ester derivatives suggested that these latter were enough stable to esterase activity to interact with virus pathways. Indeed, the presence of a free carboxylic moiety may alter the micro-local pH and the hemagglutinin complex of the virus, probably inducing conformational changes by protonation of histidine residues, that could favor the viral entry into the cell.[322] Therefore, we can also hypothesize that the ester compounds may inhibit specific steps of viral replication by impairing the host-cell micro-environment.

3.1.0 A Three-Way Regioselective Synthesis of Amino Acid Decorated Imidazole, Purine and Pyrimidine Derivatives by Multicomponent Chemistry Starting from Prebiotic Diaminomaleonitrile

In the previous works, it has been reported the multicomponent synthesis of imidazole derivatives decorated with amino acid residues, and their successive annulation to corresponding purines, by thermal condensation of aminomalononitrile (AMN) and trimethyl orthoacetate with α-amino acids.[295,323] Besides to AMN, diaminomaleonitrile (DAMN),[276,324] the tetramer of HCN,[265,249] is a key intermediate in the prebiotic synthesis of purine and pyrimidine nucleobases in the framework of prebiotic chemistry.[266,277,300,279,51] The formation of DAMN under prebiotic conditions has been recently reviewed.[280,241,250] This compound is characterized by the contemporary presence of electrophile and nucleophile reactive sites, which make it a useful reagent for the multicomponent synthesis of heterocycles. DAMN is easy photo-isomerized to diaminofumaronitrile (DAFN) which in turn can be cyclized to amino imidazole carbonitrile (AICN) under Thermal conditions. Selection of the energy sources which favor one of these transformations can furnish a tool for the control of the chemical complexity of the reaction products. The effect of different energy sources on the selectivity of prebiotic reactions was previously reported in the case of the thermal and photochemical condensation of formamide to RNA nucleobases, in which case purine derivatives (especially guanine) were selectively synthesized under photothermal conditions as a consequence of the preferential formation of AICN as a reactive intermediate.[271] How did energy source can affect the chemo- and regioselectivity of multicomponent chemistry of DAMN to yield PNA's building-blocks? To what extent is the coexistence of different energy sources in tuning novel and unexpected reaction pathways? This work describes the unprecedented three-way regioselective multicomponent synthesis of novel amino-acid decorated imidazole, purine and pyrimidine derivatives by condensation of DAMN with trimethyl orthoacetate and a selected panel of α-amino acids. The three synthetic pathways were independent of each other, the selectivity of the reaction being controlled by the energy source. In particular, imidazole derivatives were synthesized under thermal conditions (DAMN pathway), while pyrimidine derivatives were obtained under photoirradiation (DAFN pathway). Finally, purines were selectively isolated combining photochemical and thermal conditions (AICN pathway), further enlarging the variety of possible PNA's building blocks which can be synthesized from the same panel of starting reagents.

3.1.0.1 Synthesis of amino-acid decorated Imidazole derivatives-DAMN pathway

The synthesis of amino-acid decorated imidazole derivatives was performed by a slightly modification of the thermal procedure described for AMN.[295] Under these experimental conditions the occurrence of previously reported DAMN isomerization/annulation process was not operative. DAMN **13** (2.30 mmol, 1.0 eq.), trimethyl orthoacetate **2** (3.25 mmol, 1.4 eq.), and glycine methyl ester **3a** (2.77 mmol, 1.2 eq.) were dissolved in three alternative reaction solvents (CH_2Cl_2, THF and MeCN) in the presence of triethylamine TEA (2.77 mmol, 1.2 eq.) and reacted under dark conditions at room temperature, or in alternative, at the reflux temperature of the selected solvents (39.6 °C, CH_2Cl_2; 66 °C, THF; and 82°C, MeCN) for 15h and 24 h, respectively. The best result was obtained in the presence of MeCN at 25°C for 15h, in which case the imidazole **14a** was isolated as the only recovered product in satisfactory yield (Table 8, entry 3). Irrespective from the experimental conditions, the reaction performed at the highest temperature was less effective, producing high conversion of DAMN and low yield of imidazole 1**4a** (Table 8, entry 5). The low value of the mass balance was probably due to the formation of high molecular weight oligomers of DAMN, which precipitated from the reaction solution as an insoluble dark-matter.[206,325] In order to generalize the procedure, the reaction was repeated under the optimal experimental conditions (MeCN at 25°C for 15h) using the methyl esters of alanine **3b**, valine **3c**, serine **3d**, phenylalanine **3e**, and tyrosine **3f**. Amino-acid decorated imidazoles **14b-f** were isolated as the only recovered products from acceptable to high yield (Table 8, entries 6-10). In accordance with data previously reported for the multicomponent synthesis of imidazole derivatives bearing simple alkyl and aryl amine side-chains,[295,326] compounds **14a-f** were obtained by the concerted electrophile/nucleophile-oriented condensation of DAMN with **2** and **3a-f** to yield the intermediate **I** (not isolated), (Scheme 4) followed by ring-aromatization and internal displacement of a methanol molecule (Scheme 5).

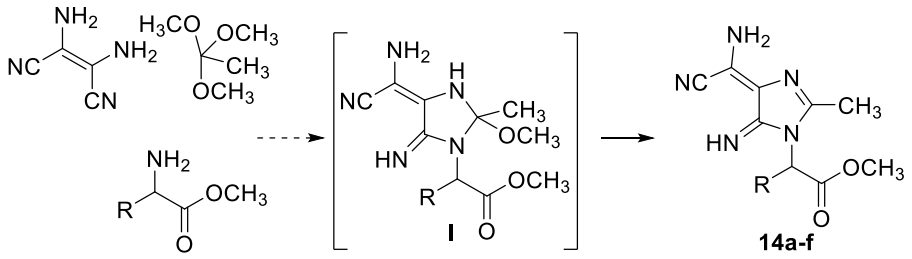

Scheme 4: Proposed mechanism for amino-acid decorated imidazole, DAMN-pathway

As a general trend, the yield of compounds **14a-f** increased in the presence of aliphatic amino acids, imidazole **14d** being isolated in the highest yield (Table 8, entries 9-10 versus 3,6-8). This trend was in

accordance with the lower pka value and the relatively higher nucleophilicity of aromatic amino acids with respect to the aliphatic counterpart.[327]

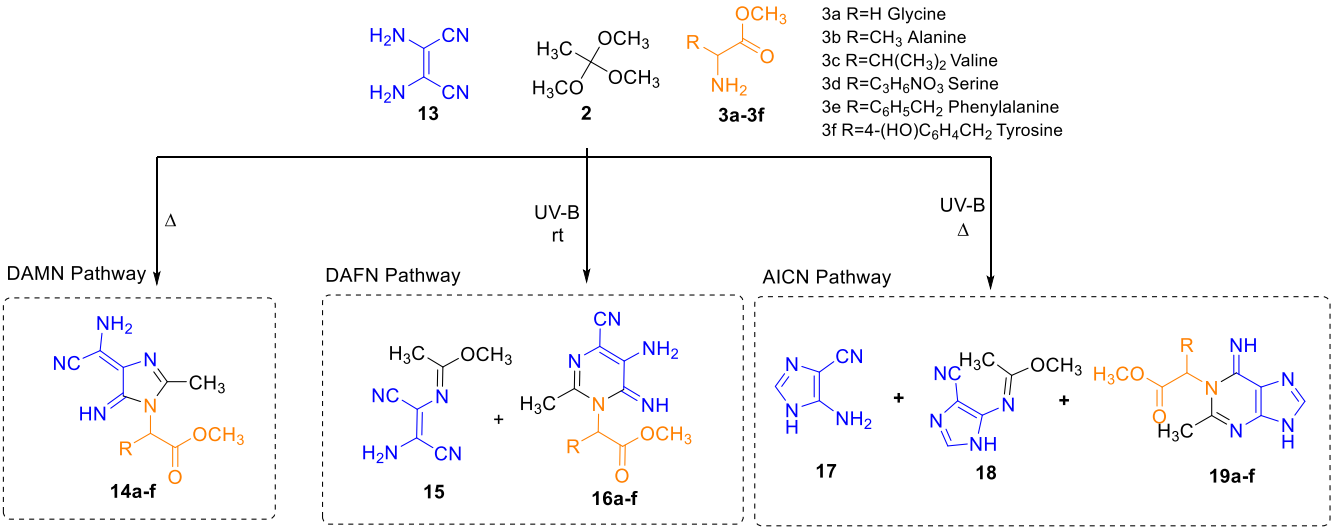

Scheme 5. Regioselective synthesis of amino-acid imidazole, purine and pyrimidine derivatives.

Table 8. Synthesis of amino-acid decorated imidazole derivatives **14a-f**[a]

Entry	α-amino acid	Solvent	Temperature (°C)	Time (h)	Products	R	Conversion(%)	Yield (%)[b]
1	Glycine	CH_2Cl_2	25	15	**14a**	H	10	5
2		THF	25	15			60	35
3		MeCN	25	15			70	62
4			25	24			72	58
5			82	15			80	21
6	Alanine	MeCN	25	15	**14b**	CH_3	65	57
7	Valine				**14c**	$CH(CH_3)_2$	68	55
8	Serine				**14d**	CH_2OH	81	73
9	Phenylalanine				**14e**	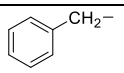	58	39
10	Tyrosine				**14f**	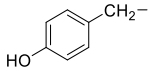	65	45

[a] DAMN **13** (2.30 mmol, 1.0 eq.), trimethyl orthoacetate **2** (3.25 mmol, 1.4 eq.), a-amino acid derivatives **3a-3f** (2.77 mmol, 1.2 eq.) and TEA (2.77 mmol, 1.2 eq.). [b] Yield have been calculated with respect to converted DAMN **13**. The conversion of the reaction was evaluated on the basis of unreacted **13**.

3.1.0.2 Synthesis of amino-acid decorated pyrimidine derivatives-DAFN pathway

We expected that the regioselectivity of the three-components condensation between DAMN, trimethyl orthoacetate and α-amino acids should be changed under photochemical conditions, due to the fast isomerization of DAMN to DAFN. To test this possibility, DAMN **13** (2.30 mmol, 1.0 eq.), trimethyl orthoacetate **2** (3.25 mmol, 1.4 eq.), and glycine methyl ester **3a** (2.77 mmol, 1.2 eq.) were dissolved in MeCN (10 mL) in the presence of TEA (2.77 mmol, 1.2 eq.) and irradiated at the optimal wavelength-range reporter for the isomerization of DAMN to DAFN (280-320 nm)[328] at 0°C, or in alternative at 25°C, for 15 h. Under these experimental conditions, the amino-acid decorated pyrimidine **16a** was recovered as the main reaction product from low to acceptable yield (Table 9, entries 1-3), besides low amount of the iminoether derivative **15** and traces amount of amino-imidazole carbonitrile (AICN) **17**

(Scheme 5). The yield of pyrimidine 1**6a** at 0 °C was higher than that at 25°C, in which case the dark insoluble residue was again observed.[206,325] The effective formation of DAFN during the synthesis of pyrimidine 1**6a** was confirmed by the presence of the bathochromic effect associated to the conversion of DAMN (λmax 295 nm) to DAFN (λmax 304 nm),[329] as well as by the appearance of characteristic IR bands at 2197 and 2242 cm^{-1} (vibrations of CN), 1602 cm^{-1} (C=C stretching band), and 3434-3000 cm^{-1} (N-H stretching bands).[330] The reaction repeated with α-amino acid derivatives **3b-3f** afforded amino-acid decorated pyrimidines 1**6b-f** from good to high yield, confirming the generality of the procedure (Table 9, entries 4-8). The formation of pyrimidine 1**6a-f** probably occurred by the initial reaction of DAFN with compound **2** to yield the iminoether derivative **15** (that we effectively isolated from the reaction mixture), followed by addition of amino acid derivatives **3a-f**, and successive internal displacement of methanol molecule, to yield the six-ring closure of the pyrimidine ring. (Scheme 6)

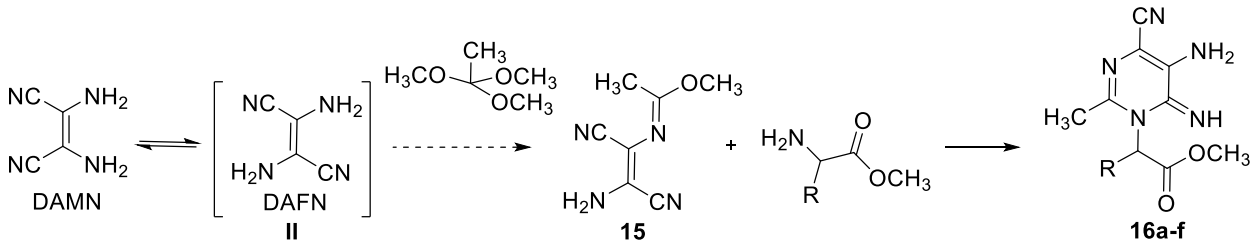

Scheme 6: Proposed mechanism for pyrimidine derivatives, DAFN-pathway.

The formation of the iminoether intermediate by reaction of AMN and compound **2** has been previously reported.[295] The effective role of iminoether 1**5** in the annulation process was confirmed by analyzing the reaction of isolated 1**5** and **3a** under reported experimental conditions, in which case pyrimidine 1**6a** was obtained in appreciable yield (Table 9, entry 2). Again, aliphatic amino acids **3a-d** afforded pyrimidine derivatives in the highest yield (Table 9 entries 3-6).

Table 9. Synthesis of pyrimidine derivatives **16a-f**[a]

Entry	α-amino acid	Solvent	Temperature (°C)	Time (h)	Products	R	Conversion (%)	Yield (%)[b]	Yield of 15 (%)[c]
1	Glycine	MeCN,	25	15	**16a**	H	80	20	5
2		MeCN[d]	25	15	**16a**	H	75	50	10
3		MeCN	0	15	**16a**	H	74	62	5

4	Alanine	MeCN	0	15	**16b**	CH_3	65	57	7
5	Valine				**16c**	$CH(CH_3)_2$	71	55	10
6	Serine				**16d**	CH_2OH	80	73	8
7	Phenylalanine				**16e**	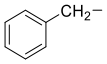	68	39	4
8	Tyrosine				**16f**	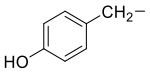	62	45	5

[a] DAMN **13** (2.30 mmol, 1.0 eq.), trimethyl orthoacetate **2** (3.25 mmol, 1.4 eq.), α–amino acid derivatives **3a-f** (2.77 mmol, 1.2 eq.) and TEA (2.77 mmol, 1.2 eq.) under UV-B lamp radiation (280-320 nm). [b] Yield have been calculated with respect to converted DAMN **13**. [c] Yield have been calculated with respect to converted 1**5**. [d] 1**5** (2.30 mmol, 1.0 eq.), **3a** (2.77 mmol, 1.2 eq.) and TEA (2.77 mmol, 1.2 eq.) under UV-B lamp radiation (280-320 nm).

3.1.0.3 Synthesis of amino-acid decorated purine derivatives-AICN Pathway

Finally, we combined thermal and photochemical conditions to further improve the complexity of the reaction pathway. In this latter case, the following transformations were expected the condensation process: A) photo driven isomerization of DAMN to DAFN; and B) cyclization of DAFN to AICN and successive thermal annulation of AICN to purine derivatives. The synthesis of AICN from DAFN is still matter of debate.[331] Data are reported to confirm the occurrence of the cyclization of DAFN to AICN *via* unstable azetidine intermediate **III**.[332] In accordance with this data, when DAMN **13** (2.30 mmol, 1.0 eq.), trimethyl orthoacetate **2** (3.25 mmol, 1.4 eq.), and α-amino acid derivatives **3a-f** (2.77 mmol, 1.2 eq.) were refluxed in MeCN (10 mL) in the presence of TEA (2.77 mmol, 1.2 eq.) under photon irradiation (290-315 nm) for 15 h, the amino-acid decorated purine derivatives **19a-f** were isolated as the main reaction products in acceptable yield (Table 3, entries 1-6), besides to 4-cyanoimidazole iminoether derivative **18** and traces amount of AICN **7** (Scheme 1, AICN pathway). The isolation of imidazole iminoether derivative **18** from the reaction mixture suggested the occurrence of the initial addition between **2** and AICN **17**, followed by annulation of 1**8** with α-amino acid derivatives to yield 1**9a-f** (Scheme 7). The efficient transformation of DAFN to compounds 1**7** and 1**8** was probably responsible for the absence of pyrimidine derivatives as possible reaction side-products, DAFN being not further available for the condensation with **2**.

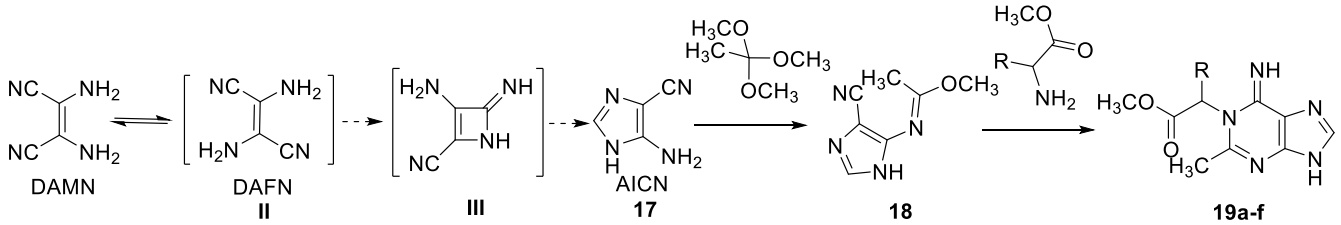

Scheme 7: proposed mechanism for purine derivatives, AICN-pathway.

Table 10. Synthesis of purine derivatives 1**9a-f**[a]

Entry	α-amino acid	Solvent	Temperature (°C)	Time (h)	Products	R	Conversion (%)	Yield (%)[b]	Yield of 18 (%)	Yield of AICN 17
1	Glycine	MeCN	Reflux	15	**19a**	H	92	64	6	3
2	Alanine				**19b**	CH_3	95	65	8	4
3	Valine				**19c**	$CH(CH_3)_2$	98	72	9	4
4	Serine				**19d**	CH_2OH	93	70	7	3
5	Phenylalanine				**19e**	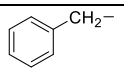	90	45	13	5
6	Tyrosine				**19f**	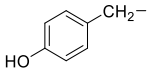	94	54	15	4

[a] DAMN **13** (2.30 mmol, 1.0 eq.), trimethyl orthoacetate **2** (3.25 mmol, 1.4 eq.), a-amino acid derivatives **3a-f** (2.77 mmol, 1.2 eq.) and TEA (2.77 mmol, 1.2 eq.) under UV-B lamp radiation (280-320 nm) [b] Yield have been calculated with respect to converted DAMN **13**.

3.1.1 Conclusions

Multicomponent chemistry is a powerful tool for the synthesis of heterocyclic compounds,[333] especially when optimal experimental conditions are selected in order to control the regioselectivity of the condensation process. They include the use of catalysts and of assisted microwave and ultra sounds conditions.[334] Previous works showed that the same reagents could react in a different manner under multicomponent conditions depending on the nature and intensity of the energy source.[335,336] In the case of DAMN, the energy source can control the selectivity of the in situ isomerization and annulation of DAMN to DAFN and AICN, respectively.[337] It is important to note that the fate of these intermediates may afford heterocycles characterized by rings of different size and chemical composition. At room temperature and in the absence of photoirradiation, DAMN is the major condensing reagent with trimethyl orthoacetate and α-amino acid derivatives to yield five-ring closure processes and formation of amino-acid decorated imidazole derivatives. Conversely, photochemical and photothermal conditions shifted the selectivity of the reaction towards DAFN and AICN intermediates, followed by selective formation of amino-acid decorated pyrimidine and purine derivatives, respectively. Taking into account the synthetic potential of these multicomponent reactions for the preparation of bioactive heterocycles, it must not escape the attention that the energetic conditions analyzed in this study were also plausible for the primitive earth. Thus, the multicomponent chemistry of DAMN involving one-carbon atom donor and α-amino acids may be (in principle) effective for the contemporary prebiotic formation of amino-acid decorated imidazole, purine and pyrimidine PNA's building blocks, improving chemical information in the primitive recognition code, the selectivity of the synthesis being simply controlled by the reaction temperature and the presence or absence of UV irradiation.

4.1.0 Materials and Methods

All solvents and reagents used were of analytical grade and were purchased from Aldrich Chemical Co. Silica gel 60 F254 plates and silica gel 60 were furnished from Merck. Chemical reactions were monitored using thin-layer chromatography on precoated aluminum silica gel Merck 60 F254 plates and a UV lamp was used for visualization. Merck silica gel 60 (230–400 mesh) was used for chromatography. All the microwave reactions were performed by a microwave synthesizer CEM Discover (CEM Corporation Italy). All products were dried in a high vacuum (10–3 mbar). NMR spectra were recorded on a Bruker Advance DRX400 (400 MHz/100 MHz) spectrometer. Chemical shifts for protonsare reported in parts per million (scale) and internally referenced to the DMSO-d_6, CD_3OD, D_2O, $CDCl_3$. Coupling constants (*J*) are reported in Hz. Multiplicities are reported in the conventional form: s = singlet, d = doublet, t = triplet, dd = doublets of doublets, m = multiplet.

The analysis of the photo-isomerization processes were performed by Varian Cary 50 UV scan (Crawley, U.K.) in the range from 190 nm to 450 nm at 25 °C under gentle stirring, and data were elaborated by standard UV−scan software. ATR-IR analyses were performed at room temperature by Agilent Cary 630 ATR-FTIR analyzer. Selected compounds were directly placed on the diamond attenuated total reflectance (ATR) crystal of the apparatus. The analyses were recorded in less than 30 seconds (64 scans at 4 cm^{-1} resolution).

4.1.0.1 General procedure for the synthesis of 5- Amino-1,2-disubstituted-1H-imidazole-4-carbonitriles (4 a-g)

To a solution of aminomalononitrile p-toluenesulfonate **1** (5.9 mmol) in THF (30 mL) was added triethylamine (7.1 mmol). The mixture was stirred at room temperature for 30 min. To this solution was added trimethyl orthoacetate **2** (8.3 mmol), and the solution was stirred under microwave condition using the following program:

N° of cycles	Temperature	Ramp Time	Hold Time	Pressure (psi)	Power (W)
1	200 °C	1 min	2 min	250	250

Thereafter, the solution was cooled at room temperature and triethylamine (7.1 mmol) and the corresponding amino-acid (protected as methyl ester) (**3a-g**) (7.1 mmol) were added. The solution stirred under microwave condition above described. At the end of the reaction, the solvent was removed under reduced pressure and the residue was dissolved in dichloromethane (30 mL) and extracted with saturated aqueous Na_2CO_3 (3 × 20 mL) and saturated aqueous NaCl (1x 20 mL). The organic layer was dried over Na_2SO_4, and the solvent was evaporated under reduced pressure. The crude was purified by flash-chromatography eluting with ethyl acetate (AcOEt): hexane (Hex) (2:1) to afford **4 a-g** from 15 to 60% of yield.

In a second step, the synthesis of 5- Amino-1,2-disubstituted-1H-imidazole-4-carbonitriles **4a-g** was improved, using 2-MeTHF as solvent instead of THF, affording compounds **4a-g** in yields ranging 29 to 66%.

4.1.0.2 General procedure for the synthesis of amino-purine-analogues (6a-f)

Compound **4 a-f** (3.8 mmol) was dissolved in formic acid (3.0 mL) and stirred under microwave condition described for the synthesis of **4a-f**. After returning to room temperature, the mixture was poured into water (30 mL). The resulting precipitate was filtered and washed with water. The crude was purified by flash-chromatography eluting with dichloromethane (CH_2Cl_2): methanol (CH_3OH) (5:1) to afford **6 a-f** in quantitative yield.

4.1.0.3 General procedure for the synthesis of diaminopurine analogues 8a-f and guanine analogues 10a-g.

Imidazole **4a-g** (0.80 mmol, 1 eq.) and guanidine carbonate **5** (for derivatives **8a-f**) or urea **8** (for derivatives **10a-g**) (1.60 mmol, 2 eq.) were irradiated under microwave condition using the program in table 11.

Table 11. Microwave condition program for the synthesis of compounds **8a-f** and **10a-g**.

N° of cycles	Temperature	Ramp Time	Hold Time	Pressure (psi)	Power (W)
1	200 °C	1 min	2	250	150

			min		

Thereafter, the solution was poured in hot water (8.0 mL), and the mixture was stirred for 10 min. After the mixture returned to room temperature, the solid residue was filtered, evaporated under reduced pressure and purified by silica gel chromatography eluting with 10% methanol in dichloromethane. Compounds **8a-f** and **10a-g** were obtained as brown solids in yield from 21 to 45%.

4.1.0.4 General procedure for the synthesis of amino-purine-analogues (5a-f and 7a-f), diaminopurine analogues (9a-f) and guanine analogues (11a-g) bearing free carboxylic acid moiety.

Compound **4 a-f, 6 a-f, 8a-f** or **10a-g** (0.1mmol) was hydrolyzed in NaOH solution (1N, 1.0 mL) stirring for 18h at room temperature. Thereafter, the solution was neutralized with HCl 1N, freeze-dried and the residue washed with CH_3OH. The organic layer was evaporated under reduced pressure to obtain **5a-f, 7a-f, 9a-f** or **11a-g** in quantitative yield.

4.1.0.5 General procedure for the synthesis of amino-acid decorated Imidazole derivatives 14a-f DAMN pathway.

DAMN **13** (2.30 mmol, 1.0 eq.), trimethyl orthoacetate **2** (3.25 mmol, 1.4 eq.), and α-amino acid derivatives **3a-f** (2.77 mmol, 1.2 eq.) were dissolved in the appropriate solvent (10mL) in the presence of TEA (2.77 mmol, 1.2 eq.) and the reaction was gently stirred at 25° C for 15 hours. At the end, the solvent was removed under reduced pressure and the crude was purified by flash-chromatography by eluting with ethyl acetate (AcOEt): petroleum ether (PET) (1:1) to afford compounds **14a-f**.

4.1.0.6 General procedure for the synthesis of amino-acid decorated pyrimidine derivatives 16a-f DAFN pathway.

DAMN **13** (2.30 mmol, 1.0 eq.), trimethyl orthoacetate **2** (3.25 mmol, 1.4 eq.), and α–amino acid derivatives **3a-f** (2.77 mmol, 1.2 eq.) were dissolved in MeCN (10 mL) in the presence of TEA (2.77 mmol, 1.2 eq.) and irradiated in the range between 290 nm and 315 nm (UV-B photons) by 3 x 100W Uv-B Philips Broadband TL at 0°C, or in alternative at 25°C, for 15 hours. At the end, the solvent was

removed under reduced pressure and the crude was purified by flash-chromatography by eluting with CH_2Cl_2: MeOH (10:0.5 v/v) to afford compounds **16a-f** as the main reaction products, besides iminoether intermediate **15**.

4.1.0.7 General procedure for the synthesis of amino-acid decorated purine derivatives 19a-f AICN pathway.

DAMN **13** (2.30 mmol, 1.0 eq.), trimethyl orthoacetate **2** (3.25 mmol, 1.4 eq.), and α-amino acid derivatives **3a-f** (2.77 mmol) were refluxed in MeCN (10 mL) in the presence of TEA (2.77 mmol, 1.2 eq.) under photon irradiation for 15 h using wavelength λ value in the range form 280 nm to 320 nm by 3 x 100W UV-B Philips Broadband TL. At the end, the solvent was removed under reduced pressure and the crude was purified by flash-chromatography by eluting with CH_2Cl_2: MeOH (5:0.5 v/v) to afford compounds **19a-f** as the main reaction products, besides to imidazole intermediate **18** and traces amount of compound **17**.

Spectroscopic data (^{1}H-NMR and ^{13}C-NMR) of all synthesized compounds are reported below.

Compound 4a Methyl 2-(5-amino-4-cyano-2-methyl-1H-imidazol-1-yl)acetate. The crude residue was recovered by crystallization as a beige solid.**^{1}H-NMR** (400 MHz, DMSO-*d_6*, ppm): δ 6.135 (s, 2H, NH_2), 4.733 (s, 2H, CH_2), 3.706 (s, 3H, O-CH_3), 2.078 (s, 3H, CH_3).**^{13}C-NMR** (100 MHz, DMSO-*d_6*, ppm): δ 168.515 (C=O), 148.883 (C), 140.104 (C), 118.080 (C), 88.533 (C), 52.912 (O-CH_3), 43.907 (CH_2), 13.297 (CH_3).MS (ESI): m/z (M + H) +195.19. Elemental Analysis for $C_8H_{10}N_4O_2$ calculated: C, 49.48; H, 5.19; N, 28.85; O, 16.48. Found: C, 49.45; H, 5.16; N, 28.81; O, 16.43.

Compound 4b Methyl 2-(5-amino-4-cyano-2-methyl-1H-imidazol-1-yl)propanoate**.** The crude residue was purified by silica gel chromatography eluting with Ethyl Acetate: Petroleum Ether (2:1). Compound **4b** was isolated as beige solid.**^{1}H-NMR** (400 MHz, $CDCl_3$, ppm): δ 4.897-4.878 (m, 1H, CH), 4.150 (s, 2H, NH_2), 3.847 (s, 3H, O-CH_3), 2.336 (s, 3H, CH_3), 1.761 (d, *J* = 7.6 Hz, 3H, CH_3). **^{13}C-NMR** (100 MHz, $CDCl_3$, ppm): δ 170.573 (C=O), 145.708 (C), 140.664 (C), 115.587 (C), 96.244 (C), 53.373 (CH), 53.297(O-CH_3), 15.965 (CH_3), 14.096 (CH_3).MS (ESI): m/z (M + H) +209.22. Elemental Analysis for $C_9H_{12}N_4O_2$ calculated: C, 51.92; H, 5.81; N, 26.91; O, 15.37. Found: C, 51.89; H, 5.77; N, 26.87; O, 15.32.

Compound 4c Methyl 2-(5-amino-4-cyano-2-methyl-1H-imidazol-1-yl)-3-methylbutanoate. The crude residue was purified by silica gel chromatography eluting with Ethyl Acetate:Hexane (2:1). Compound

4c was isolated as orange solid. **^{1}H-NMR** (400 MHz, DMSO-d_6, ppm): δ 6.042 (s, 2H, NH_2), 4.577 (d, J = 10.8 Hz, 1H, CH), 3.705 (s, 3H, O-CH_3), 2.597-2.553 (m, 1H, CH), 2.123 (s, 3H, CH_3), 1.113 (d, J = 6.4 Hz, 3H, CH_3), 0.639 (d, J = 6.4 Hz, 3H, CH_3).**^{13}C-NMR** (100 MHz, DMSO-d_6, ppm): δ 169.805 (C=O), 148.935 (C), 139.722 (C), 117.724 (C), 89.925 (C), 61.883(CH), 53.198 (O-CH_3), 28.372 (CH), 20.673 (CH_3), 18.860 (CH_3), 14.716 (CH_3). MS (ESI): m/z (M + H) +238.28. Elemental Analysis for $C_{11}H_{16}N_4O_2$ calculated: C, 55.92; H, 6.83; N, 23.71; O, 13.54. Found: C, 55.86; H, 6.78; N, 23.65; O, 13.49.

Compound 4d Methyl 2-(5-amino-4-cyano-2-methyl-1H-imidazol-1-yl)-3-hydroxypropanoateThe crude residue was purified by silica gel chromatography eluting with Ethyl Acetate. Compound **4d** was isolated as beige solid. **^{1}H-NMR** (400 MHz, DMSO-d_6, ppm): δ 6.890 (s, 1H, OH), 5.872 (s, 2H, NH_2), 5.473-5.092 (m, 2H, CH_2), 3.689 (s, 3H, O-CH_3), 3.666-3.615 (m, 1H, CH), 2.114 (s, 3H, CH_3). **^{13}C-NMR** (100 MHz, DMSO-d_6, ppm): δ 168.27 (C=O), 148.98 (C), 140.56 (C), 117.99 (C), 90.09 (C), 62.85 (CH_2), 59.86 (CH), 53.09(O-CH_3), 14.55 (CH_3).MS (ESI): m/z (M + H) +225.22. Elemental Analysis for $C_9H_{12}N_4O_3$ calculated: C, 48.21; H, 5.39; N, 24.99; O, 21.41. Found: C, 48.17; H, 5.35; N, 24.94; O, 21.38.

Compound 4e Methyl 2-(5-amino-4-cyano-2-methyl-1H-imidazol-1-yl)-3-phenylpropanoate. The crude residue was purified by silica gel chromatography eluting with Ethyl Acetate:Hexane (3:1). Compound **4e** was isolated as yellow oil.**^{1}H-NMR** (400 MHz, $CDCl_3$, ppm): δ 7.283-7.254 (m, 3H, CH-Ar), 6.995-6.973 (m, 2H, CH-Ar), 4.837-4.799 (dd, J = 4.0, 11.2 Hz, 1H, CH_2), 4.323 (s, 2H, NH_2), 3.877 (s, 3H, O-CH_3), 3.569 (t, J = 12.8 Hz, 1H, CH), 3.385-3.340 (dd, J = 4.4, 13.6 Hz, 1H, CH_2), 1.809 (s, 3H, CH_3).**^{13}C-NMR** (100 MHz, $CDCl_3$, ppm): δ 169.934 (C=O), 146.094 (C), 141.435 (C), 135.347 (C), 129.080 (C-Ar x2), 128.757(C-Ar x2), 127.768 (C-Ar), 115.833 (C), 95.757 (C), 60.286 (CH), 53.498 (O-CH_3), 35.296 (CH_2), 13.456 (CH_3).MS (ESI): m/z (M + H) +285.32. Elemental Analysis for $C_{15}H_{16}N_4O_2$ calculated: C, 63.37; H, 5.67; N, 19.71; O, 11.25. Found: C, 63.31; H, 5.62; N, 19.68; O, 11.20.

Compound 4f Methyl 2-(5-amino-4-cyano-2-methyl-1H-imidazol-1-yl)-3-(4-hydroxyphenyl)propanoate. The crude residue was purified by silica gel chromatography eluting with Ethyl Acetate: Petroleum Ether (4:1). Compound **4f** was isolated as yellow solid.**^{1}H-NMR** (400 MHz, DMSO-d_6, ppm): δ 9.249 (s, 1H, OH), 6.846 (d, J = 8.4 Hz, 2H, CH-Ar),6.593 (d, J = 8.4 Hz, 2H, CH-Ar), 5.700 (s, 2H, NH_2) 5.199-5.160 (m, 1H, CH), 3.724 (s, 3H, O-CH_3), 3.266-3.219 (m,2H, CH_2),

1.794 (s, 3H, CH_3). **^{13}C-NMR** (100 MHz, DMSO-d_6, ppm): δ 169.44 (C=O), 156.59 (C-OH), 148.22 (C), 140.24 (C), 130.41 (C-Ar x2), 126.71 (C-Ar), 117,83 (C), 115.60 (C-Ar x2), 90.92 (C), 60.22 (CH), 53.26 (O-CH_3), 34.19 (CH_2), 14.56 (CH_3).MS (ESI): m/z (M + H) + 301.32. Elemental Analysis for $C_{15}H_{16}N_4O_3$ calculated: C, 59.99; H, 5.37; N, 18.66; O, 15.98. Found: C, 59.95; H, 5.29; N, 18.61; O, 15.94.

Compound 4g Methyl 2-(5-amino-4-cyano-2-methyl-1H-imidazol-1-yl)-3-(1H-indol-3-yl)propanoate. The crude residue was purified by silica gel chromatography eluting with Ethyl Acetate: Petroleum Ether (2:1). Compound **4g** was isolated as yellow solid.**^{1}H-NMR** (400 MHz, DMSO-d_6, ppm): δ 10.85 (s, 1H, NH), 7.52 (d, *J* = 8.0 Hz, 1H, CH-Ar), 7.32 (d, *J* = 8.0 Hz, 1H, CH-Ar), 7.08 (t, *J* = 7.6 Hz, 1H, CH-Ar), 6.99 (t, *J* = 7.6 Hz, 1H, CH-Ar), 6.89 (d, *J* = 2.0 Hz, 1H, CH-Ar), 5.75 (s, 2H, NH_2), 5.30 (t, *J* = 7.8 Hz, 1H, CH), 3.77 (s, 3H, O-CH_3), 3.54 (d, *J* = 8 Hz, 2H, CH_2), 1.74 (s, 3H, CH_3). **^{13}C-NMR** (100 MHz, DMSO-d_6, ppm): δ 169.67 (C=O), 145.05 (C), 140.26 (C), 136.39 (C-Ar), 127.23 (C-Ar), 124.21 (C-Ar), 121.55 (C-Ar), 118.99 (C-Ar), 118.36 (C-Ar), 115.14 (C), 111.91 (C-Ar), 109.00 (C-Ar), 95.22 (C), 57.37 (CH), 53.27 (O-CH_3), 25.27 (CH_2), 14.16 (CH_3). MS (ESI): m/z (M + H) + 324.14. Elemental Analysis for $C_{17}H_{17}N_5O_2$ calculated: C, 63.15; H, 5.30; N, 21.66; O, 9.90. Found: C, 63.12; H, 5.29; N, 21.64; O, 9.89.

Compound 5a 2-(5-amino-4-cyano-2-methyl-1H-imidazol-1-yl)acetic acid**.** Compound **5a** was isolated as beige solid.**^{1}H-NMR** (400 MHz, D_2O, ppm): δ 4.285 (d, *J* = 8.8 Hz, 2H, CH_2), 2.112 (d, *J* = 11.2 Hz, 3H, CH_3).**^{13}C-NMR** (100 MHz, D_2O, ppm): δ 174.50 (C=O), 144.50 (C), 141.60 (C), 109.61 (C), 95.61(C), 45.88 (CH_2), 12.00 (CH_3). MS (ESI): m/z (M + H) +181.17. Elemental Analysis for $C_7H_8N_4O_2$ calculated: C, 46.67; H, 4.48; N, 31.10; O, 17.76. Found: C, 46.62; H, 4.43; N, 31.05; O, 17.71.

Compound 5b 2-(5-amino-4-cyano-2-methyl-1H-imidazol-1-yl)propanoic acid. Compound **5b** was isolated as beige solid. **^{1}H-NMR** (400 MHz, MeOD, ppm): δ 4.260 (d, *J* = 7.6 Hz, 1H, CH), 1.747 (s, 3H, CH_3), 1434 (s, 3H, CH_3). **^{13}C-NMR** (100 MHz, MeOD, ppm): δ 167.11 (C=O), 142.78 (C), 139.26 (C), 117.28 (C), 93.45(C), 58.05 (CH), 22.48 (CH_3), 14.60 (CH_3). MS (ESI): m/z (M + H) +195.19. Elemental Analysis for $C_8H_{10}N_4O_2$ calculated: C, 49.48; H, 5.19; N, 28.85; O, 16.48. Found: C, 49.43; H, 5.15; N, 28.79; O, 16.41.

Compound 5c 2-(5-amino-4-cyano-2-methyl-1H-imidazol-1-yl)-3-methylbutanoic acid**.** Compound **5c** was isolated as beige solid.**^{1}H-NMR** (400 MHz, D_2O, ppm): δ 4.384 (d, *J* = 2.8 Hz, 1H, CH), 2.409-2.340 (m, 1H, CH), 2.229 (s, 3H, CH_3), 0.937 (d, *J* = 6.8 Hz, 3H, CH_3), 0.756 (d, *J* = 6.8 Hz, 3H, CH_3).**^{13}C-NMR** (100 MHz, D_2O, ppm): δ 181.50 (C=O), 148.33 (C), 141.22 (C), 117.46 (C), 92.58 (C), 67.34 (CH), 29.76 (CH), 16.76 (CH_3), 16.17 (CH_3), 13.25 (CH_3).MS (ESI): m/z (M + H) +223.25. Elemental Analysis for $C_{10}H_{14}N_4O_2$ calculated: C, 54.04; H, 6.35; N, 25.21; O, 14.40. Found: C, 53.97; H, 6.31; N, 25.17; O, 14.35.

Compound 5d 2-(5-amino-4-cyano-2-methyl-1H-imidazol-1-yl)-3-hydroxypropanoic acid. Compound **5d** was isolated as beige solid.**^{1}H-NMR** (400 MHz, D_2O, ppm): δ 4.489-4.415 (m, 1H, CH), 3.119 (s, 2H, CH_2), 2.625 (s, 3H, CH_3). **^{13}C-NMR** (100 MHz, D_2O, ppm): δ 168.62 (C=O), 145.80 (C), 140.76 (C), 116.44 (C), 94.79 (C), 64.43 (CH_2), 61.41 (CH), 12.92 (CH_3). MS (ESI): m/z (M + H) +211.19. Elemental Analysis for $C_8H_{10}N_4O_3$ calculated: C, 45.71; H, 4.80; N, 26.66; O, 22.83. Found: C, 45.66; H, 4.75; N, 26.61; O, 22.78.

Compound 5e 2-(5-amino-4-cyano-2-methyl-1H-imidazol-1-yl)-3-phenylpropanoic acid Compound **5e** was isolated as beige solid. **^{1}H-NMR** (400 MHz, D_2O, ppm): δ 7.160 -7.129 (m, 3H, CH-Ar), 6.930-6.925 (m, 2H, CH-Ar), 3.405-3.358 (dd, *J* = 4.4, 14.4 Hz, 2H, CH_2), 3.204 (d, *J* = 14.4 Hz, 1H, CH), 2.275 (s, 3H, CH_3). **^{13}C-NMR** (100 MHz, D_2O, ppm): δ 166.90 (C=O), 154.94 (C), 139.62 (C), 134.76 (C), 129.24 (C-Ar x2), 128.38 (C-Ar x2), 127.08 (C-Ar), 108.66 (C), 95.90 (C), 60.23 (CH), 34.70 (CH_2), 12.80 (CH_3). MS (ESI): m/z (M + H) +271.29. Elemental Analysis for $C_{14}H_{14}N_4O_2$ calculated: C, 62.21; H, 5.22; N, 20.73; O, 11.84. Found: C, 62.16; H, 5.28; N, 20.69; O, 11.79.

Compound 5f 2-(5-amino-4-cyano-2-methyl-1H-imidazol-1-yl)-3-(4-hydroxyphenyl)propanoic acid**.** Compound **5f** was isolated as yellow solid. **^{1}H-NMR** (400 MHz, MeOD, ppm): δ 6.797 (d, *J* = 2.0 Hz, 2H, CH-Ar),6.494 (d, *J* = 6.4 Hz, 2H, CH-Ar), 4.004-3.961(m, 1H, CH), 2.885-2.848 (m, 2H, CH_2), 1.9876 (s, 3H, CH_3). **^{13}C-NMR** (100 MHz, MeOD, ppm): δ 167.02 (C=O), 156.01 (C-OH), 147.00 (C), 137.88 (C), 129.61 (C-Ar x2), 120.47 (C-Ar), 118.54 (C-Ar x2), 108.95 (C), 95.90 (C), 59.81 (CH), 35.99 (CH_2), 12.47 (CH_3). MS (ESI): m/z (M + H) +287.29. Elemental Analysis for $C_{14}H_{14}N_4O_3$ calculated: C, 58.74; H, 4.93; N, 19.57; O, 16.77. Found: C, 58.69; H, 4.88; N, 19.52; O, 16.71.

Compound 6a Methyl 2-(8-methyl-6-oxo-1,6-dihydro-9H-purin-9-yl)acetate. Compound **6a** was isolated as brown solid. **^{1}H-NMR** (400 MHz, D_2O, ppm): δ 8.067 (s, 1H, CH-Ar), 5.051 (s, 2H, CH_2),

3.744 (s, 3H, O-CH_3), 2.438 (s, 3H, CH_3). **^{13}C-NMR** (100 MHz, D_2O, ppm): δ 169.76 (C=O), 155.96 (C), 151.77 (C), 149.80 (C), 145.45 (C), 122.02 (C), 53.42 (O-CH_3), 43.91 (CH_2), 12.49 (CH_3). MS (ESI): m/z (M + H) +221.20. Elemental Analysis for $C_9H_{10}N_4O_3$ calculated: C, 48.65; H, 4.54; N, 25.21; O, 21.60. Found: C, 48.61; H, 4.48; N, 25.16; O, 21.55.

Compound 6b Methyl 2-(8-methyl-6-oxo-1,6-dihydro-9H-purin-9-yl)propanoate. Compound **6b** was isolated as brown solid. **^{1}H-NMR** (400 MHz, DMSO-*d_6*, ppm): δ 8.159 (s, 1H, CH-Ar), 4.714-4.697 (m, 1H, CH), 3.652 (s, 3H, O-CH_3), 2.265 (s, 3H, CH_3), 1.506 (d, *J* = 7.2 Hz, 3H, CH_3). **^{13}C-NMR** (100 MHz, DMSO-*d_6*, ppm): δ 169.21 (C=O), 163.66 (C), 156.83 (C), 145.26 (C), 136.91 (C), 111.34 (C), 54.79 (O-CH_3), 50.28 (CH), 15.96 (CH_3), 13.40 (CH_3). MS (ESI): m/z (M + H) +237.23. Elemental Analysis for $C_{10}H_{12}N_4O_3$ calculated: C, 50.84; H, 5.12; N, 23.72; O, 20.32. Found: C, 50.79; H, 5.06; N, 23.67; O, 20.27.

Compound 6c Methyl 3-methyl-2-(8-methyl-6-oxo-1,6-dihydro-9H-purin-9-yl)butanoate. Compound **6c** was isolated as brown solid. **^{1}H-NMR** (400 MHz, DMSO-*d_6*, ppm): δ 7.970 (s, 1H, CH-Ar), 4.970 (d, *J* = 10.0 Hz, 1H, CH), 3.629 (s, 3H, O-CH_3), 2.851-2.793 (m, 1H, CH), 2.268 (s, 3H, CH_3), 1.120 (d, *J* = 6.8 Hz, 3H, CH_3), 0.744 (d, *J* = 6.8 Hz, 3H, CH_3). **^{13}C-NMR** (100 MHz, DMSO-*d_6*, ppm): δ 175.20 (C=O), 163.69 (C), 145.67 (C), 138.57 (C), 136.98 (C), 111.13 (C), 63.61 (CH), 52.92 (O-CH_3), 29.96 (CH), 17.52(CH_3), 16.57 (CH_3), 13.88 (CH_3). MS (ESI): m/z (M + H) +265.29. Elemental Analysis for $C_{12}H_{16}N_4O_3$ calculated: C, 54.54; H, 6.10; N, 21.20; O, 18.16. Found: C, 54.49; H, 6.05; N, 21.16; O, 18.11.

Compound 6d Methyl 3-hydroxy-2-(8-methyl-6-oxo-1,6-dihydro-9H-purin-9-yl)propanoate**.** Compound **6d** was isolated as brown solid. **^{1}H-NMR** (400 MHz, DMSO-*d_6*, ppm): δ 8.090 (s, 1H, CH-Ar), 5.473-5.092 (m, 2H, CH_2), 3.689 (s, 3H, O-CH_3), 3.666-3.615 (m, 1H, CH), 2.141 (s, 3H, CH_3). **^{13}C-NMR** (100 MHz, DMSO-*d_6*, ppm): δ 168.07 (C=O), 162.93 (C), 150.65 (C), 146.34(C), 143.51 (C), 115.97(C), 63.38 (CH), 61.55 (CH_2), 52.59 (O-CH_3),13.11 (CH_3). MS (ESI): m/z (M + H) +253.23. Elemental Analysis for $C_{10}H_{12}N_4O_4$ calculated: C, 47.62; H, 4.80; N, 22.21; O, 25.37. Found: C, 47.57; H, 4.76; N, 22.18; O, 25.32.

Compound 6e Methyl 2-(8-methyl-6-oxo-1,6-dihydro-9H-purin-9-yl)-3-phenylpropanoate. Compound **6e** was isolated as brown solid. **^{1}H-NMR** (400 MHz, DMSO-*d_6*, ppm): δ 8.147 (s, 1H, CH-Ar), 7.223-7.197 (m, 3H, CH-Ar), 7.030-7.006 (m, 2H, CH-Ar), 5.068 (t, *J* = 4.8 Hz, 1H, CH), 3.689 (s, 3H, O-

CH_3), 3.238 (dd, *J* = 6.2, 13.6 Hz, 2H, CH_2), 2.239 (s, 3H, CH_3). **^{13}C-NMR** (100 MHz, DMSO-d_6, ppm): δ 175.70 (C=O), 164.18 (C), 147.50 (C), 143.35 (C), 137.09 (C), 135.10 (C), 129.86 (C-Ar x2), 128.82(C-Ar x2), 127.58 (C-Ar), 111.35 (C), 59.98 (CH), 53.16 (O-CH_3), 35.30 (CH_2), 13.72 (CH_3). MS (ESI): m/z (M + H) +314.33. Elemental Analysis for $C_{16}H_{16}N_4O_3$ calculated: C, 61.53; H, 5.16; N, 17.94; O, 15.37. Found: C, 61.51; H, 5.12; N, 17.89; O, 15.34.

Compound 6f Methyl 3-(4-hydroxyphenyl)-2-(8-methyl-6-oxo-1,6-dihydro-9H-purin-9-yl)propanoate. Compound **6f** was isolated as brown solid. **^{1}H-NMR** (400 MHz, DMSO-d_6, ppm): δ 8.142 (s, 1H, CH-Ar), 6.789 (d, *J* = 8.4 Hz, 2H, CH-Ar), 6.576 (d, *J* = 8.4 Hz, 2H, CH-Ar), 4.962 (t, *J* = 4.8 Hz, 1H, CH), 3.724 (s, 3H, O-CH_3), 3.094 (dd, *J* = 4.4, 10.4 Hz, 2H, CH_2), 2.211 (s, 3H, CH_3). **^{13}C-NMR** (100 MHz, DMSO-d_6, ppm): δ 175.71 (C=O), 163.64 (C), 156.81(C), 149.99 (C), 144.34 (C), 138.70 (C), 137.05 (C-Ar), 130.80 (C-Ar x2), 124.93(C-Ar x2), 115.62 (C), 60.25 (CH), 54.42 (O-CH_3), 34.56 (CH_2), 13.72 (CH_3). MS (ESI): m/z (M + H) +329.33. Elemental Analysis for $C_{16}H_{16}N_4O_3$ calculated: C, 61.53; H, 5.16; N, 17.94; O, 15.37. Found: C, 61.48; H, 5.11; N, 17.89; O, 15.32.

Compound 7a 2-(8-methyl-6-oxo-1,6-dihydro-9H-purin-9-yl)acetic acid. Compound **7a** was isolated as beige solid. **^{1}H-NMR** (400 MHz, D_2O, ppm): δ 7.944 (s, 1H, CH-Ar), 4.556 (s, 2H, CH_2), 2.325 (s, 3H, CH_3). **^{13}C-NMR** (100 MHz, D_2O, ppm): δ 174.45 (C=O), 166.79 (C), 152.78 (C), 150.80 (C), 149.80 (C), 121.56 (C) 45.46 (CH_2), 12.61 (CH_3). MS (ESI): m/z (M + H) +209.18. Elemental Analysis for $C_8H_8N_4O_3$ calculated: C, 46.16; H, 3.87; N, 26.91; O, 23.06. Found: C, 46.11; H, 3.82; N, 26.86; O, 23.00.

Compound 7b 2-(8-methyl-6-oxo-1,6-dihydro-9H-purin-9-yl)propanoic acid**.** Compound **7b** was isolated as beige solid. **^{1}H-NMR** (400 MHz, D_2O, ppm): δ 8.326 (s, 1H, CH-Ar), 5.034-4.978 (m, 1H, CH), 2.180 (s, 3H, CH_3), 1.386 (s, 3H, CH_3). **^{13}C-NMR** (100 MHz, MeOD, ppm): δ 169.10 (C=O), 160.03 (C), 155.38 (C), 151.92 (C), 137.16 (C), 109.13 (C), 51.58 (CH), 15.11 (CH_3), 11.94 (CH_3). MS (ESI): m/z (M + H) +223.20. Elemental Analysis for $C_9H_{10}N_4O_3$ calculated: C, 48.65; H, 4.54; N, 25.21; O, 21.60. Found: C, 48.61; H, 4.49; N, 25.17; O, 21.54.

Compound 7c 3-methyl-2-(8-methyl-6-oxo-1,6-dihydro-9H-purin-9-yl)butanoic acid. Compound **7c** was isolated as beige solid. **^{1}H-NMR** (400 MHz, D_2O, ppm): δ 7.857(s, 1H, CH-Ar), 4.401 (d, *J* = 10.8 Hz, 1H, CH), 2.236-2.202 (m, 1H, CH), 2.087 (s, 3H, CH_3), 0.786 (d, *J* = 6.8 Hz, 3H, CH_3), 0.614 (d, *J* = 6.8 Hz, 3H, CH_3). **^{13}C-NMR** (100 MHz, D_2O, ppm): δ 175.56 (C=O), 167.15 (C=O), 152.73 (C),

149.48 (C), 139.90 (C), 108.48 (C), 65.44 (CH), 29.60 (CH), 16.99 (CH_3), 16.20 (CH_3), 13.29 (CH_3). MS (ESI): m/z (M + H) +251.26. Elemental Analysis for $C_{11}H_{14}N_4O_3$ calculated: C, 52.79; H, 5.64; N, 22.39; O, 19.18. Found: C, 52.73; H, 5.58; N, 22.33; O, 19.13.

Compound 7d 3-hydroxy-2-(8-methyl-6-oxo-1,6-dihydro-9H-purin-9-yl)propanoic acid. Compound **7d** was isolated as brown solid. **^{1}H-NMR** (400 MHz, CD_3OD, ppm): δ 8.563 (s, 1H, CH-Ar), 5.422-5.404 (m, 2H, CH_2), 3.625-3.500 (m, 1H, CH), 1.190 (s, 3H, CH_3). **^{13}C-NMR** (100 MHz, CD_3OD, ppm): δ 165.54 (C=O), 155.45 (C), 149.92 (C), 145.68 (C), 142.10 (C), 116.06 (C), 65.92 (CH), 62.67 (CH_2), 14.65 (CH_3). MS (ESI): m/z (M + H) +239.07. Elemental Analysis for $C_9H_{10}N_4O_4$ calculated: C, 45.38; H, 4.23; N, 23.52; O, 26.87. Found: C, 45.32; H, 4.19; N, 23.47; O, 26.82.

Compound 7e 2-(8-methyl-6-oxo-1,6-dihydro-9H-purin-9-yl)-3-phenylpropanoic acid. Compound **7e** was isolated as yellow solid. **^{1}H-NMR** (400 MHz, CD_3OD, ppm): δ 8.557 (s, 1H, CH-Ar), 7.183-7.120 (m, 5H, CH-Ar), 4.620 (t, *J* = 4.8 Hz, 1H, CH), 3.489 (dd, *J* = 14.4, 13.6 Hz, H, CH_2), 2.146 (s, 3H, CH_3). **^{13}C-NMR** (100 MHz, CD_3OD, ppm): δ 174.11 (C=O), 166.77 (C), 155.80 (C), 147.79 (C), 137.50 (C), 135.78 (C), 129.15 (C-Ar x2), 127.98 (C-Ar x2), 126.54 (C-Ar), 109.04 (C), 66.73 (CH), 35.65 (CH_2), 12.28 (CH_3). MS (ESI): m/z (M + H) +299.30. Elemental Analysis for $C_{15}H_{14}N_4O_3$ calculated: C, 60.40; H, 4.73; N, 18.78; O, 16.09. Found: C, 60.35; H, 4.68; N, 18.71; O, 16.01.

Compound 7f 3-(4-hydroxyphenyl)-2-(8-methyl-6-oxo-1,6-dihydro-9H-purin-9-yl)propanoic acid. Compound **7f** was isolated as orange solid. **^{1}H-NMR** (400 MHz, D_2O, ppm): δ 8.349 (s, 1H, CH-Ar), 6.640 (d, *J* = 8.0 Hz, 2H, CH-Ar), 6.325 (d, *J* = 8.0 Hz, 2H, CH-Ar), 5.150-5.145 (m, 1H, CH), 3.225 (dd, *J* = 4.4, 14.8 Hz, 2H, CH_2), 2.014 (s, 3H, CH_3). **^{13}C-NMR** (100 MHz, CD_3OD, ppm): δ 174.77 (C=O), 169.08 (C), 151.65 (C), 148.17 (C), 137.93 (C), 129.59 (C-Ar x2), 128.89 (C-Ar), 120.59 (C), 118.55 (C-Ar x2), 108.94 (C), 63.40 (CH), 36.14 (CH_2), 12.38 (CH_3). MS (ESI): m/z (M + H) +315.30. Elemental Analysis for $C_{15}H_{14}N_4O_4$ calculated: C, 57.32; H, 4.49; N, 17.83; O, 20.36. Found: C, 57.27; H, 4.43; N, 17.77; O, 20.31.

Compound 8a. Methyl 2-(2,6-diamino-8-methyl-9H-purin-9-yl) acetate. The crude residue was purified by silica gel chromatography eluting with 10% methanol in dichloromethane. **^{1}H-NMR** (400 MHz, DMSO-*d_6*, ppm): δ 6.89 (s, 2H, NH_2), 6.12 (s, 2H, NH_2), 4.71 (s, 2H, CH_2), 3.68 (s, 3H, O-CH_3), 2.24 (s, 3H, CH_3). **^{13}C-NMR** (100 MHz, DMSO-*d_6*, ppm): δ 171.78 (C=O), 160.09 (C), 155.33 (C), 152.94 (C), 146.03 (C), 115.53 (C), 52.46 (O-CH_3), 48.81 (CH_2), 13.15 (CH_3). MS (ESI): m/z (M+H) +

237,24. Elemental analysis for $C_9H_{12}N_6O_2$ calculated: C, 45.76; H, 5.12; N, 35.58; O, 13.54. Found: C, 45.73; H, 5.11; N, 35.56; O, 13.53.

Compound 8b. Methyl 2-(2,6-diamino-8-methyl-9H-purin-9-yl) propanoate. The crude residue was purified by silica gel chromatography eluting with 10% methanol in dichloromethane. **^{1}H-NMR** (400 MHz, DMSO-*d_6*, ppm): δ 6.90 (s, 2H, NH_2), 6.27 (s, 2H, NH_2), 4.52-4.51 (m, 1H, CH), 3.75 (s, 3H, O-CH_3), 2.13 (s, 3H, CH_3), 1.29 (d, *J* = 7.2 Hz, 3H, CH_3). **^{13}C-NMR** (100 MHz, DMSO-*d_6*, ppm): δ 169.92 (C=O), 158.08 (C), 155.58 (C), 152.03 (C), 145.06 (C), 118.00 (C), 53.36 (CH) 52.77 (O-CH_3), 22.86 (CH_3), 13.02 (CH_3). MS (ESI): m/z (M+H) + 251,26. Elemental analysis for $C_{10}H_{14}N_6O_2$ calculated: C, 47.99; H, 5.64; N, 33.58; O, 12.79. Found: C, 47.96; H, 5.63; N, 35.56; O, 12.77.

Compound 8c. Methyl 2-(2,6-diamino-8-methyl-9H-purin-9-yl)-3-methylbutanoate. The crude residue was purified by silica gel chromatography eluting with 10% methanol in dichloromethane.**^{1}H-NMR** (400 MHz, DMSO-*d_6*, ppm): δ 6.76 (s, 2H, NH_2), 6.06 (s, 2H, NH_2), 5.00 (d, *J* = 9.6 Hz, 1H, CH), 3.72 (s, 3H, O-CH_3), 2.71-2.67 (m, 1H, CH), 2.12 (s, 3H, CH_3), 1.18 (d, *J* = 6.4 Hz, 3H, CH_3), 0.88 (d, *J* = 6.4 Hz, 3H, CH_3). **^{13}C-NMR** (100 MHz, DMSO-*d_6*, ppm): δ 168.88 (C=O), 158.13 (C), 153.93 (C), 151.48 (C), 147.00 (C), 116.82 (C), 67.32 (CH), 53.29 (O-CH_3), 25.02 (CH), 20.00 (CH_3), 16.36 (CH_3), 14.57 (CH_3). MS (ESI): m/z (M+H) + 279,32. Elemental analysis for $C_{12}H_{18}N_6O_2$ calculated: C, 51.79; H, 6.52; N, 30.20; O, 11.50. Found: C, 51.76; H, 6.51; N, 30.18; O, 11.48.

Compound 8d. Methyl 2-(2,6-diamino-8-methyl-9H-purin-9-yl)-3-hydroxypropanoate. The crude residue was purified by silica gel chromatography eluting with 10% methanol in dichloromethane.**^{1}H-NMR** (400 MHz, DMSO-*d_6*, ppm): δ 6.97 (s, 2H, NH_2), 6.46 (s, 1H, OH), 6.05 (s, 2H, NH_2), 4.41-4.39 (m, 2H, CH_2), 3.77 (s, 3H, O-CH_3), 3.64-3.62 (m, 1H, CH), 2.13 (s, 3H, CH_3). **^{13}C-NMR** (100 MHz, DMSO-*d_6*, ppm): δ 170.62 (C=O), 160.87 (C), 156.47 (C), 153.03 (C), 146.78 (C), 117.65 (C), 68.00 (CH), 61.21 (CH_2) 52.40 (O-CH_3), 14.12 (CH_3). MS (ESI): m/z (M+H) + 267,26. Elemental analysis for $C_{10}H_{14}N_6O_3$ calculated: C, 45.11; H, 5.30; N, 31.56; O, 18.03. Found: C, 45.08; H, 5.29; N, 31.54; O, 18.02.

Compound 8e. Methyl 2-(2,6-diamino-8-methyl-9H-purin-9-yl)-3-phenylpropanoate. The crude residue was purified by silica gel chromatography eluting with 10% methanol in dichloromethane. **^{1}H-NMR** (400 MHz, DMSO-*d_6*, ppm): δ 7.22-7.02 (m, 5H, CH-Ar), 6.63 (s, 2H, NH_2), 6.21 (s, 2H, NH_2), 5.22-5.20 (m, 1H, CH), 3.63 (s, 3H, O-CH_3), 3.23-3.18 (dd, *J* = 4.0, 14.0 Hz, 1H, CH_2), 2.95-2.92 (dd, *J*

= 6.8, 9.0 Hz, 1H, CH_2), 2.22 (s, 3H, CH_3). **^{13}C-NMR** (100 MHz, DMSO-*d*$_6$, ppm): δ 167.62 (C=O) 157.88 (C), 155.01 (C), 153.06 (C), 150.64 (C), 141.10 (C), 129.41 (C-Ar x2), 128.66 (C-Ar x2), 126.67 (C-Ar), 111.70 (C), 64.39 (CH), 53.79 (O-CH_3), 34.88 (CH_2), 13.09 (CH_3). MS (ESI): m/z (M+H) +327.36. Elemental analysis for $C_{16}H_{18}N_6O_2$ calculated: C, 58.88; H, 5.56; N, 25.75; O, 9.80. Found: C, 58.85; H, 5.55; N, 25.73; O, 9.78.

Compound 8f. Methyl 2-(2,6-diamino-8-methyl-9*H*-purin-9-yl)-3-(4-hydroxyphenyl) propanoate. The crude residue was purified by silica gel chromatography eluting with 10% methanol in dichloromethane. **^{1}H-NMR** (400 MHz, DMSO-*d*$_6$, ppm): δ 9.29 (s, 1H, OH), 7.11 (s, 2H, NH_2), 6.77 (d, *J* = 8.8 Hz, 2H, CH-Ar), 6.61 (d, *J* = 8.4 Hz, 2H, CH-Ar), 5.95 (s, 2H, NH_2), 5.19-5.17 (m, 1H, CH), 3.71 (s, 3H, O-CH_3), 2.89-2.85 (dd, *J* = 6.0, 14.0 Hz, 1H, CH_2), 2.77-2.72 (dd, *J* = 9.2, 14.0 Hz, 1H, CH_2), 2.08 (s, 3H, CH_3). **^{13}C-NMR** (100 MHz, DMSO-*d*$_6$, ppm): δ 169.03 (C=O), 159.38 (C), 157.04 (C), 155.86 (C), 153.71 (C), 145.29 (C), 131.20 (C-Ar), 130.36 (C-Ar x2), 120.12 (C), 115.59 (C-Ar x2), 67.81 (CH), 53.62 (O-CH_3), 34.73 (CH_2), 13.71 (CH_3). MS (ESI): *m/z* (M+H) + 343,36. Elemental analysis for $C_{16}H_{18}N_6O_3$ calculated: C, 56.13; H, 5.30; N, 24.55; O, 14.02. Found: C, 56.10; H, 5.29; N, 24.53; O, 14.00.

Compound 9a. 2-(2,6-diamino-8-methyl-9*H*-purin-9-yl) acetic acid. The crude residue was purified by silica gel chromatography eluting with 10% methanol in dichloromethane. **^{1}H-NMR** (400 MHz, CD_3OD, ppm): δ 4.45 (s, 2H, CH_2), 2.17 (s, 3H, CH_3). **^{13}C-NMR** (100 MHz, CD_3OD, ppm): δ 169.03 (C=O), 160.05 (C), 155.87 (C), 152.92 (C), 147.19 (C), 115.74 (C), 49.74 (CH_2), 13.32 (CH_3). MS (ESI): *m/z* (M+H) + 223,21. Elemental analysis for $C_8H_{10}N_6O_2$ calculated: C, 43.24; H, 4.54; N, 37.82; O, 14.40. Found: C, 43.21; H, 4.53; N, 37.80; O, 14.39.

Compound 9b. 2-(2,6-diamino-8-methyl-9H-purin-9-yl)propanoic acid. The crude residue was purified by silica gel chromatography eluting with 10% methanol in dichloromethane.**^{1}H-NMR** (400 MHz, CD_3OD, ppm): δ 4.61-4.55 (m, 1H, CH), 2.08 (s, 3H, CH_3), 1.77 (s, 3H, CH_3). **^{13}C-NMR** (100 MHz, CD_3OD, ppm): δ 168.05 (C=O), 159.15 (C), 156.27 (C), 153.19 (C), 146.24 (C), 114.96 (C), 59.32 (CH), 22.33 (CH_3), 13.43 (CH_3). MS (ESI): *m/z* (M+H) + 237,24. Elemental analysis for $C_9H_{12}N_6O_2$ calculated: C, 45.76; H, 5.12; N, 35.58; O, 13.54. Found: C, 45.73; H, 5.11; N, 35.56; O, 13.53.

Compound 9c. 2-(2,6-diamino-8-methyl-9H-purin-9-yl)-3-methylbutanoic acid. The crude residue was purified by silica gel chromatography eluting with 10% methanol in dichloromethane. **^{1}H-NMR** (400

MHz, CD_3OD, ppm): δ 4.55 (d, *J* = 3.6 Hz, 1H, CH), 2.41-2.37 (m, 1H, CH), 2.17 (s, 3H, CH_3), 0.99 (d, *J* = 6.4 Hz, 3H, CH_3), 0.81 (d, *J* = 6.8 Hz, 3H, CH_3). **^{13}C-NMR** (100 MHz, CD_3OD, ppm): δ 169.15 (C=O), 159.19 (C), 155.96 (C), 152.24 (C), 145.22 (C), 116.46 (C), 66.23 (CH), 24.43 (CH), 21.11 (CH_3), 16.31 (CH_3), 13.55 (CH_3). MS (ESI): *m/z* (M+H) + 265.29. Elemental analysis for $C_{11}H_{16}N_6O_2$ calculated: C, 49.99; H, 6.10; N, 31.80; O, 12.11. Found: C, 49.96; H, 6.09; N, 31.78; O, 12.10.

Compound 9d. 2-(2,6-diamino-8-methyl-9H-purin-9-yl)-3-hydroxypropanoic acid. The crude residue was purified by silica gel chromatography eluting with 10% methanol in dichloromethane.**^{1}H-NMR** (400 MHz, CD_3OD, ppm): δ 5.45-5.41 (m, 1H, CH), 4.18-4.15 (m, 2H, CH_2), 2.12 (s, 3H, CH_3). **^{13}C-NMR** (100 MHz, CD_3OD, ppm): δ 169.87 (C=O), 159.75 (C), 156.11 (C), 153.30 (C), 146.42 (C), 117.18 (C), 64.82 (CH), 61.01 (CH_2), 13.31 (CH_3). MS (ESI): *m/z* (M+H) + 253,23. Elemental analysis for $C_9H_{12}N_6O_3$ calculated: C, 42.86; H, 4.80; N, 33.32; O, 19.03. Found: C, 42.83; H, 4.79; N, 33.30; O, 19.02.

Compound 9e. 2-(2,6-diamino-8-methyl-9H-purin-9-yl)-3-phenylpropanoic acid. The crude residue was purified by silica gel chromatography eluting with 10% methanol in dichloromethane. **^{1}H-NMR** (400 MHz, CD_3OD, ppm): δ 7.36-7.23 (m, 5H, CH-Ar), 5.21-5.16 (m, 1H, CH), 3.15-3.11 (dd, *J* = 4.4, 14.0 Hz, 1H, CH_2), 3.03-2.97 (dd, *J* = 4.4, 14.0 Hz, 1H, CH_2), 2.16 (s, 3H, CH_3). **^{13}C-NMR** (100 MHz, CD_3OD, ppm): δ 169.04 (C=O), 156.95 (C), 154.78 (C), 152.15 (C), 149.98 (C), 141.92 (C), 129.58 (C-Ar x2), 127.82 (C-Ar x2), 124.88 (C-Ar), 112.64 (C), 64.45 (CH), 34.40 (CH_2), 14.41 (CH_3). MS (ESI): *m/z* (M+H) + 313,33. Elemental analysis for $C_{15}H_{16}N_6O_2$ calculated: C, 57.68; H, 5.16; N, 26.91; O, 10.24. Found: C, 57.65; H, 5.15; N, 26.89; O, 10.23.

Compound 9f. 2-(2,6-diamino-8-methyl-9H-purin-9-yl)-3-(4-hydroxyphenyl) propanoic acid. The crude residue was purified by silica gel chromatography eluting with 10% methanol in dichloromethane. **^{1}H-NMR** (400 MHz, CD_3OD, ppm): δ 7.15 (d, *J* = 8.0 Hz, 2H, CH-Ar), 6.75 (d, *J* = 7.6 Hz, 2H, CH-Ar), 5.26-5.20 (m, 1H, CH), 3.20-3.14 (m, 2H, CH_2), 2.06 (s, 3H, CH_3). **^{13}C-NMR** (100 MHz, CD_3OD, ppm): δ 169.81 (C=O), 159.74 (C), 157.11 (C), 154.16 (C), 152.30 (C), 146.42 (C), 134.18 (C), 130.77 (C-Ar x2), 121.01 (C), 116.82 (C-Ar x2), 60.43 (CH), 34.71 (CH_2), 13.79 (CH_3). MS (ESI): *m/z* (M+H) + 329,33. Elemental analysis for $C_{15}H_{16}N_6O_3$ calculated: C, 54.87; H, 4.91; N, 25.60; O, 14.62. Found: C, 54.84; H, 4.90; N, 25.58; O, 14.60.

Compound 10a. Methyl 2-(6-amino-8-methyl-2-oxo-2,3-dihydro-9H-purin-9-yl) acetate. The crude residue was purified by silica gel chromatography eluting with 10% methanol in dichloromethane. **^{1}H-NMR** (400 MHz, DMSO-d_6, ppm): δ 11.28 (s, 1H, NH), 6.13 (s, 2H, NH_2), 4.15 (s, 2H, CH_2), 3.70 (s, 3H, O-CH_3), 2.07 (s, 3H, CH_3). **^{13}C-NMR** (100 MHz, DMSO-d_6, ppm): δ 168.44 (C=O), 156.91 (C), 152.04 (C), 150.07 (C), 148.88 (C), 110.81 (C), 52.44 (O-CH_3), 45.08 (CH_2), 13.52 (CH_3). MS (ESI): *m/z* (M+H) + 238,22. Elemental analysis for $C_9H_{11}N_5O_3$ calculated: C, 45.57; H, 4.67; N, 29.52; O, 20.23. Found: C, 45.54; H, 4.66; N, 29.50; O, 20.22.

Compound 10b. Methyl 2-(6-amino-8-methyl-2-oxo-2,3-dihydro-9H-purin-9-yl)propanoate. The crude residue was purified by silica gel chromatography eluting with 10% methanol in dichloromethane. **^{1}H-NMR** (400 MHz, DMSO-d_6, ppm): δ 10.22 (s, 1H, NH), 6.16 (s, 2H, NH_2), 4.72 -4.68 (m, 1H, CH), 3.65 (s, 3H, O-CH_3), 2.26 (s, 3H, CH_3), 1.81 (d, J = 7.2 Hz, 3H, CH_3). **^{13}C-NMR** (100 MHz, DMSO-d_6, ppm): δ 169.49 (C=O), 159.83 (C), 154.84 (C), 150.51 (C), 147.34 (C), 112.21 (C), 58.27 (CH), 53.44 (O-CH_3), 21.48 (CH_3), 13.32 (CH_3). MS (ESI): *m/z* (M+H) + 252,25. Elemental analysis for $C_{10}H_{13}N_5O_3$ calculated: C, 47.81; H, 5.22; N, 27.88; O, 19.10. Found: C, 47.78; H, 5.21; N, 27.86; O, 19.09.

Compound 10c. Methyl 2-(6-amino-8-methyl-2-oxo-2,3-dihydro-9H-purin-9-yl)-3-methylbutanoate. The crude residue was purified by silica gel chromatography eluting with 10% methanol in dichloromethane. **^{1}H-NMR** (400 MHz, DMSO-d_6, ppm): δ 11.11 (s, 1H, NH), 6.16 (s, 2H, NH_2), 4.69 (d, J = 3.6 Hz, 1H, CH), 3.65 (s, 3H, O-CH_3), 2.85-2.79 (m, 1H, CH), 2.26 (s, 3H, CH_3), 1.15 (d, J = 6.4 Hz, 3H, CH_3), 0.76 (d, J = 6.8 Hz, 3H, CH_3). **^{13}C-NMR** (100 MHz, DMSO-d_6, ppm): δ 168.99 (C=O), 157.83 (C), 152.17 (C), 149.34 (C), 147.68 (C), 110.72 (C), 64.10 (CH), 52.61 (O-CH_3), 26.14 (CH), 19.81(CH_3), 17.48 (CH_3), 13.82 (CH_3). MS (ESI): *m/z* (M+H) + 280,30. Elemental analysis for $C_{12}H_{17}N_5O_3$ calculated: C, 51.60; H, 6.14; N, 25.08; O, 17.18. Found: C, 51.57; H, 6.13; N, 25.06; O, 17.16.

Compound 10d. Methyl 2-(6-amino-8-methyl-2-oxo-2,3-dihydro-9H-purin-9-yl)-3-hydroxypropanoate. The crude residue was purified by silica gel chromatography eluting with 10% methanol in dichloromethane. **^{1}H-NMR** (400 MHz, DMSO-d_6, ppm): δ 10.09 (s, 1H, NH), 6.89 (s, 1H, OH), 6.17 (s, 2H, NH_2), 5.45- 5.43 (m, 1H, CH), 5.02-4.99 (m, 1H, CH_2), 3.68 (s, 3H, O-CH_3), 3.66-3.61 (m, 1H, CH_2), 2.14 (s, 3H, CH_3). **^{13}C-NMR** (100 MHz, DMSO-d_6, ppm): δ 169.49 (C=O), 158.67

(C), 154.17 (C), 151.34 (C), 148.18 (C), 111.55 (C), 62.93 (CH), 60.94 (CH_2), 53.11 (O-CH_3), 13.65 (CH_3). MS (ESI): *m/z* (M+H) + 268,25. Elemental analysis for $C_{10}H_{13}N_5O_4$ calculated: C, 44.94; H, 4.90; N, 26.21; O, 23.95. Found: C, 51.57; H, 6.13; N, 25.06; O, 17.16.

Compound 10e. Methyl 2-(6-amino-8-methyl-2-oxo-2,3-dihydro-9H-purin-9-yl)-3-phenylpropanoate. The crude residue was purified by silica gel chromatography eluting with 10% methanol in dichloromethane. **^{1}H-NMR** (400 MHz, DMSO-d_6, ppm): δ 11.00 (s, 1H, NH), 7.19-7.12 (m, 3H, CH-Ar), 7.05-7.03 (m, 2H, CH-Ar), 6.44 (s, 2H, NH_2), 5.10-5.06 (m, 1H, CH), 3.69 (s, 3H, O-CH_3), 3.22-3.17 (dd, *J* = 5.6, 14.0 Hz, 1H, CH_2), 3.13-3.07 (dd, *J* =7.6, 14.0 Hz, 1H, CH_2), 2.05 (s, 3H, CH_3). **^{13}C-NMR** (100 MHz, DMSO-d_6, ppm): δ 170.49 (C), 158.88 (C), 154.19 (C), 151.15 (C), 145.13 (C), 138.15 (C-Ar), 129.17 (C-Ar x2), 128.66 (C-Ar x2), 126.89 (C-Ar), 107.61 (C), 66.22 (CH), 56.49 (O-CH_3), 35.01 (CH_2), 14.35 (CH_3). MS (ESI): *m/z* (M+H) + 328,34. Elemental analysis for $C_{16}H_{17}N_5O_3$ calculated: C, 58.71; H, 5.23; N, 21.39; O, 14.66. Found: C, 58.68; H, 5.22; N, 21.37; O, 14.65.

Compound 10f. Methyl 2-(6-amino-8-methyl-2-oxo-2,3-dihydro-9H-purin-9-yl)-3-(4-hydroxyphenyl) propanoate. The crude residue was purified by silica gel chromatography eluting with 10% methanol in dichloromethane. **^{1}H-NMR** (400 MHz, DMSO-d_6, ppm): δ 11.11 (s, 1H, NH), 9.16 (s, 1H, OH), 6.82 (d, *J* = 8.0 Hz, 2H, CH-Ar), 6.55 (d, *J* = 8.0 Hz, 2H, CH-Ar), 6.33 (s, 2H, NH_2), 4.99-4.95 (m, 1H, CH), 3.74 (s, 3H, O-CH_3), 2.89-2.85 (dd, *J* = 6.0, 14.0 Hz, 1H, CH_2), 2.77-2.72 (dd, *J* = 9.2, 14.0 Hz, 1H, CH_2), 2.03 (s, 3H, CH_3). **^{13}C-NMR** (100 MHz, DMSO-d_6, ppm): δ 170.66 (C=O), 156.23 (C), 155.03 (C), 152.67 (C), 150.65 (C), 143.77 (C), 130.07 (C-Ar), 128.04 (C-Ar x2), 115.48 (C-Ar x2), 108.72 (C), 63.48 (CH), 54.11 (O-CH_3), 34.20 (CH_2), 15.04 (CH_3). MS (ESI): *m/z* (M+H) + 344,34. Elemental analysis for $C_{16}H_{17}N_5O_4$ calculated: C, 55.97; H, 4.99; N, 20.40; O, 18.64. Found: C, 55.94; H, 4.98; N, 20.38; O, 18.62.

Compound 10g. Methyl 2-(6-amino-8-methyl-2-oxo-2,3-dihydro-9H-purin-9-yl)-3-(1H-indol-3-yl)propanoate. The crude residue was purified by silica gel chromatography eluting with 10% methanol in dichloromethane. **^{1}H-NMR** (400 MHz, DMSO-d_6, ppm): δ 11.81 (s, 1H, NH), 10.92 (s, 1H, NH), 7.07 (t, *J* = 7.0 Hz, 1H, CH-Ar), 6.98 (t, *J* = 7.2 Hz, 1H, CH-Ar), 6.87 (d, *J* = 2.0 Hz, 1H, CH-Ar), 6.78 (d, J = 2.0 Hz, 1H, CH-Ar), 6.58 (d, *J* = 2.0 Hz, 1H, CH-Ar), 6.53 (s, 2H, NH_2), 5.25 (t, *J* = 4.6 Hz, 1H, CH), 3.64 (s, 3H, O-CH_3), 3.45 (d, *J* = 4.0 Hz, 2H, CH_2), 1.99 (s, 3H, CH_3). **^{13}C-NMR** (100 MHz, DMSO-d_6, ppm): δ 169.82 (C=O), 159.78 (C), 154.59 (C), 145.39 (C), 140.54 (C), 136.35 (C-Ar),

128.88 (C-Ar), 123.30 (C-Ar), 121.63 (C-Ar), 119.12 (C-Ar), 116.99 (C-Ar), 111.92 (C-Ar), 110.89 (C-Ar), 106.57 (C), 61.03 (CH), 52.20 (O-CH_3), 26.94 (CH_2), 13.55 (CH_3). MS (ESI): *m/z* (M+H) + 367,14. Elemental analysis for $C_{18}H_{18}N_6O_3$ calculated: C, 59.01; H, 4.95; N, 22.94; O, 13.10. Found: C, 58.98; H, 4.94; N, 22.92; O, 13.09.

Compound 11a. 2-(6-amino-8-methyl-2-oxo-2,3-dihydro-9H-purin-9-yl) acetic acid. The crude residue was purified by silica gel chromatography eluting with 10% methanol in dichloromethane. **^{1}H-NMR** (400 MHz, CD_3OD, ppm): δ 4.55 (s, 2H, CH_2), 2.16 (s, 3H, CH_3). **^{13}C-NMR** (100 MHz, CD_3OD, ppm): δ 169.61 (C=O), 157.66 (C),153.33 (C), 151.25 (C), 147.96 (C), 110.88 (C), 43.83 (CH_2), 13.17 (CH_3). MS (ESI): *m/z* (M+H) + 224,19. Elemental analysis for $C_8H_9N_5O_3$ calculated: C, 43.05; H, 4.06; N, 31.38; O, 21.50. Found: C, 43.02; H, 4.05; N, 31.36; O, 21.48.

Compound 11b. 2-(6-amino-8-methyl-2-oxo-2,3-dihydro-9H-purin-9-yl) propanoic acid. The crude residue was purified by silica gel chromatography eluting with 10% methanol in dichloromethane. **^{1}H-NMR** (400 MHz, CD_3OD, ppm): δ 4.72-4.66 (m, 1H, CH), 2.18 (s, 3H, CH_3), 1.88 (s, 3H, CH_3). **^{13}C-NMR** (100 MHz, CD_3OD, ppm): δ 169.65 (C=O), 158.83 (C),153.50 (C), 150.34 (C), 147.84 (C), 109.88 (C), 59.44 (CH), 20.14 (CH_3), 13.48 (CH_3). MS (ESI): *m/z* (M+H) + 238,22. Elemental analysis for $C_9H_{11}N_5O_3$ calculated: C, 45.57; H, 4.67; N, 29.52; O, 20.23. Found: C, 45.54; H, 4.66; N, 29.50; O, 20.21.

Compound 11c. 2-(6-amino-8-methyl-2-oxo-2,3-dihydro-9H-purin-9-yl)-3-methylbutanoic acid. The crude residue was purified by silica gel chromatography eluting with 10% methanol in dichloromethane. **^{1}H-NMR** (400 MHz, CD_3OD, ppm): δ 4.40 (d, *J* = 10.8 Hz, 1H, CH), 2.24-2.20 (m, 1H, CH), 2.08 (s, 3H, CH_3), 0.78 (d, *J* = 6.8 Hz, 3H, CH_3), 0.61 (d, *J* = 6.8 Hz, 3H, CH_3). **^{13}C-NMR** (100 MHz, CD_3OD, ppm): δ 169.32 (C=O), 157.66 (C), 154.67 (C), 150.84 (C), 146.68 (C), 111.22 (C), 63.60 (CH), 26.31 (CH), 19.47 (CH_3), 16.82 (CH_3), 14.15 (CH_3). MS (ESI): *m/z* (M+H) + 266,27. Elemental analysis for $C_{11}H_{15}N_5O_3$ calculated: C, 49.81; H,5.70; N, 26.40; O, 18.09. Found: C, 49.78; H, 5.69; N, 26.38; O, 18.08.

Compound 11d. 2-(6-amino-8-methyl-2-oxo-2,3-dihydro-9H-purin-9-yl)-3-hydroxypropanoic acid. The crude residue was purified by silica gel chromatography eluting with 10% methanol in dichloromethane. **^{1}H-NMR** (400 MHz, CD_3OD, ppm): δ 5.42-5.40 (m, 1H, CH), 3.62-3.50 (m, 2H, CH_2), 2.01 (s, 3H, CH_3). **^{13}C-NMR** (100 MHz, CD_3OD, ppm): δ 170.65 (C=O), 159.49 (C), 154.34 (C),

152.17 (C), 149.51 (C), 113.21 (C), 64.76 (CH), 61.60 (CH_2), 13.48 (CH_3). MS (ESI): *m/z* (M+H) + 254,22. Elemental analysis for $C_9H_{11}N_5O_4$ calculated: C, 42.69; H, 4.38; N, 27.66; O, 25.27. Found: C, 42.66; H, 4.37; N, 27.64; O, 25.25.

Compound 11e. 2-(6-amino-8-methyl-2-oxo-2,3-dihydro-9H-purin-9-yl)-3-phenylpropanoic acid**.** The crude residue was purified by silica gel chromatography eluting with 10% methanol in dichloromethane. **^{1}H-NMR** (400 MHz, CD_3OD, ppm): δ 7.18-7.12 (m, 5H, CH-Ar), 5.05- 4.99 (m, 1H, CH), 3.24-3.17 (dd, *J* =4.4, 18.8 Hz, 2H, CH_2), 2.12 (s, 3H, CH_3). **^{13}C-NMR** (100 MHz, CD_3OD, ppm): δ 169.79 (C=O), 158.18 (C), 155.45 (C), 151.60 (C), 145.68 (C), 137.22 (C- Ar), 129.59 (C-Ar x2), 127.86 (C-Ar x2), 125.78 (C-Ar), 108.46 (C), 65.92 (CH), 35.52 (CH_2), 14.65 (CH_3). MS (ESI): *m/z* (M+H) + 314,32. Elemental analysis for $C_{15}H_{15}N_5O_3$ calculated: C, 57.50; H, 4.83; N, 22.35; O, 15.32. Found: C, 57.47; H, 4.82; N, 22.33; O, 15.30.

Compound 11f. 6-amino-9-(1-(4-hydroxyphenyl)-3-oxobutan-2-yl)-8-methyl-3,9-dihydro-2*H*-purin-2-one. The crude residue was purified by silica gel chromatography eluting with 10% methanol in dichloromethane. **^{1}H-NMR** (400 MHz, D_2O, ppm): δ 6.82 (d, *J* = 7.6 Hz, 2H, CH-Ar), 6.63 (d, *J* = 6.4 Hz, 2H, CH-Ar), 5.19-5.16 (m, 1H, CH), 3.22 (d, *J* = 14.8 Hz, 1H, CH_2), 2.98 (d, *J* =14.8 Hz, 1H, CH_2) 2.12 (s, 3H, CH_3). **^{13}C-NMR** (100 MHz, D_2O, ppm): δ 168.32 (C=O), 158.70 (C), 155.36 (C-Ar), 153.85 (C), 148.30 (C), 142.41 (C), 132.88 (C-Ar), 129.69 (C-Ar x2), 117.95 (C-Ar x2), 110.36 (C), 61.50 (CH), 35.86 (CH_2), 15.27 (CH_3). MS (ESI): *m/z* (M+H) + 330.32. Elemental analysis for $C_{15}H_{15}N_5O_4$ calculated: C, 54.71; H, 4.59; N, 21.27; O, 19.43. Found: C, 54.68; H, 4.58; N, 21.25; O, 19.42.

Compound 11g. 2-(6-amino-8-methyl-2-oxo-2,3-dihydro-9H-purin-9-yl)-3-(1H-indol-3-yl)propanoic acid. The crude residue was purified by silica gel chromatography eluting with 10% methanol in dichloromethane. **^{1}H-NMR** (400 MHz, D_2O, ppm): δ 7.56 (d, *J* = 8.0 Hz, 1H, CH-Ar), 7.47 (d, *J* = 8.0 Hz, 1H, CH-Ar), 7.24 (s, 1H, CH-Ar), 7.21 (t, *J* = 7.2 Hz, 1H, CH-Ar), 7.13 (t, *J* = 7.2 Hz, 1H, CH-Ar), 5.40 (t, *J* = 6.2 Hz,1H, CH), 3.43 (t, *J* = 6.8 Hz, 2H, CH_2), 1.99 (s, 3H, CH_3). **^{13}C-NMR** (100 MHz, D_2O, ppm): δ 169.31 (C=O), 158.44 (C), 153.98 (C), 144.22 (C), 139.03 (C), 135.52 (C-Ar), 127.49 (C-Ar), 123.81 (C-Ar), 122.13 (C-Ar), 119.62 (C-Ar), 117.92 (C-Ar), 111.76 (C-Ar), 110.17 (C-Ar), 106.91 (C), 59.56 (CH), 31.12 (CH_2), 13.89 (CH_3). MS (ESI): *m/z* (M+H) + 353.13. Elemental analysis

for $C_{17}H_{16}N_6O_3$ calculated: C, 57.95; H, 4.58; N, 23.85; O, 13.62. Found: C, 57.92; H, 4.57; N, 23.83; O, 13.61.

Compound 14a. Methyl 2-(4-(amino(cyano)methylene)-5-imino-2-methyl-4,5-dihydro-1H-imidazol-1-yl)acetate. Brown solid, m.p. 201.8°C. **^{1}H-NMR** (400 MHz, DMSO-*d*$_6$, ppm): δ 8.29 (s, 1H, NH), 6.82 (s, 2H, NH_2), 3.82 (d, *J* = 6.0 Hz, 2H, CH_2), 3.63 (s, 3H, OCH_3), 1.86 (s, 3H, CH_3).**^{13}C-NMR** (100 MHz, DMSO-*d*$_6$, ppm): δ 170.96 (C=O), 151.72 (C), 143.44 (C), 130.11(C), 122.57 (C), 111.90 (C), 52.09 (OCH_3), 43.35 (CH_2), 22.68 (CH_3). MS (ESI): m/z (M + H) +222.09. Elemental Analysis ($C_9H_{11}N_5O_2$) calculated: C, 48.86; H, 5.01; N, 31.66; O, 14.46. Found: C, 48.83; H, 5.00; N, 31.64; O, 14.44.

Compound 14b. Methyl 2-(4-(amino(cyano)methylene)-5-imino-2-methyl-4,5-dihydro-1H-imidazol-1-yl)propanoate. Brown solid, m.p.198.1°C. **^{1}H-NMR** (400 MHz, DMSO-*d*$_6$, ppm): δ 9.03 (s, 1H, NH), 6.12 (s, 2H, NH_2), 4.36-4.31 (m, 1H, CH), 3.63 (s, 3H, OCH_3), 1.94 (s, 3H, CH_3), 1.35 (d, *J* = 7.2 Hz, 3H, CH_3). **^{13}C-NMR** (100 MHz, DMSO-*d*$_6$, ppm): δ 170.26 (C=O), 151.58 (C), 147.14 (C), 132.57 (C), 127.00 (C), 111.77(C), 52.44 (CH), 48.67 (OCH_3), 17.04 (CH_3), 14.37 (CH_3). MS (ESI): m/z (M + H) +236.11. Elemental Analysis ($C_{10}H_{13}N_5O_2$) calculated: C, 51.06; H, 5.57; N, 29.77; O, 13.60. Found: C, 51.03; H, 5.56; N, 29.75; O, 13.58.

Compound 14c. Methyl 2-(4-(amino(cyano)methylene)-5-imino-2-methyl-4,5-dihydro-1H-imidazol-1-yl)-3-methylbutanoate. Brown solid, m.p. 205.7°C. **^{1}H-NMR** (400 MHz, DMSO-*d*$_6$, ppm): δ 8.15 (s, 1H, NH), 6.86 (s, 2H, NH_2), 4.16-4.13 (m, 1H, CH), 3.63 (s, 3H, OCH_3), 2.04-1.96 (m, 1H, CH), 1.88 (s, 3H, CH_3), 0.89 (d, *J* = 7.2 Hz, 6H, 2xCH_3).**^{13}C-NMR** (100 MHz, DMSO-*d*$_6$, ppm): δ 170.09 (C=O), 151.57 (C), 146.13 (C), 137.71 (C), 124.76 (C), 111.74 (C), 57.91 (CH), 52.04 (O-CH_3), 30.27 (CH), 22.68 (CH_3), 19.42 (CH_3), 18.76 (CH_3). MS (ESI): m/z (M + H) +264.14. Elemental Analysis for $C_{12}H_{17}N_5O_2$ calculated: C, 54.74; H, 6.51; N, 26.60; O, 12.15. Found: C, 54.71; H, 6.50; N, 26.58; O, 12.14.

Compound 14d. Methyl 2-(4-(amino(cyano)methylene)-5-imino-2-methyl-4,5-dihydro-1H-imidazol-1-yl)-3-hydroxypropanoate. Brown solid, m.p. 258.9°C. **^{1}H-NMR** (400 MHz, DMSO-*d*$_6$, ppm): δ 9.13 (s, 1H, NH), 6.83 (s, 2H, NH_2), 4.97 (s, 1H, OH), 4.06-4.00 (m, 2H, CH_2), 3.72 (s, 3H, OCH_3), 3.66 (d, *J* = 3.6 Hz, 1H, CH), 2.11 (s, 3H, CH_3). **^{13}C-NMR** (100 MHz, DMSO-*d*$_6$, ppm): δ 170.26 (C=O), 151.53

(C), 141.73 (C), 132.07 (C), 121.10 (C), 111.71 (C), 63.74 (CH), 58.34 (CH_2), 51.62 (OCH_3), 14.34 (CH_3). MS (ESI): m/z (M + H) +252.10. Elemental Analysis ($C_{10}H_{13}N_5O_3$) calculated: C, 47.81; H, 5.22; N, 27.88; O, 19.10. Found: C, 47.78; H, 5.21; N, 27.86; O, 19.08.

Compound 14e. Methyl 2-(4-(amino(cyano)methylene)-5-imino-2-methyl-4,5-dihydro-1H-imidazol-1-yl)-3-phenylpropanoate. Brown solid, m.p. 292.2°C. **^{1}H-NMR** (400 MHz, DMSO-d_6, ppm): δ 8.34 (s, 1H, NH), 7.29-7.20 (m, 5H, CH-Ar), 6.06 (s, 2H, NH_2), 4.47-4.42 (m, 1H, CH), 3.59 (s, 3H, OCH_3), 3.03-2.98 (dd, *J* = 5.6, 13.6 Hz, 1H, CH_2), 2.89-2.84 (dd, *J* = 9.2, 13.6 Hz, 1H, CH_2), 1.79 (s, 3H, CH_3).**^{13}C-NMR** (100 MHz, DMSO-d_6, ppm): δ 172.67 (C=O), 151.58 (C), 144.78 (C), 137.73 (C), 130.27 (C), 129.46 (C-Ar x2), 128.70 (C-Ar x2), 128.44 (C-Ar), 127.00 (C), 111.76 (C), 54.07 (CH_2), 52.25 (OCH_3), 37.20 (CH), 22.69 (CH_3). MS (ESI): m/z (M + H) +312.14. Elemental Analysis ($C_{16}H_{17}N_5O_2$) calculated: C, 61.72; H, 5.50; N, 22.49; O, 10.28. Found: C, 61.68; H, 5.49; N, 22.47; O, 10.26.

Compound 14f. Methyl 2-(4-(amino(cyano)methylene)-5-imino-2-methyl-4,5-dihydro-1H-imidazol-1-yl)-3-(4-hydroxyphenyl)propanoate. Brown solid, m.p. 403.9°C. **^{1}H-NMR** (400 MHz, DMSO-d_6, ppm): δ 9.24 (s, 1H, NH), 8.26 (s, 1H, OH), 6.99 (d, *J* = 8.4 Hz, 2H, CH-Ar), 6.67 (d, *J* = 8.0 Hz, 2H, CH-Ar), 6.15 (s, 2H, NH_2), 4.38-4.32 (m, 1H, CH), 3.72 (s, 3H, OCH_3), 2.89-2.85 (dd, *J* = 6.0, 14.0 Hz, 1H, CH_2), 2.78-2.72 (dd, *J* = 9.2, 13.6 Hz, 1H, CH_2), 1.80 (s, 3H, CH_3).**^{13}C-NMR** (100 MHz, DMSO-d_6, ppm): δ 172.81 (C=O), 156.43 (C), 152.38 (C), 146.79 (C), 132.40 (C), 130.40 (C-Ar x2), 127.68 (C-Ar), 119.66 (C), 116.50 (C-Ar x2), 113.15 (C), 60.23 (CH), 52.19 (OCH_3), 36.51 (CH_2), 22.70 (CH_3). MS (ESI): m/z (M + H) +328.13. Elemental Analysis ($C_{16}H_{17}N_5O_3$) calculated: C, 58.71; H, 5.23; N, 21.39; O, 14.66. Found: C, 58.68; H, 5.22; N, 21.37; O, 14.64.

Compound 15. Methyl N-2-amino-1,2-dicyanovinyl)acetimidate. Brown solid, m.p. 149.9°C. **^{1}H-NMR** (400 MHz, DMSO-d_6, ppm): *δ* 6.69 (s, 2H, NH_2), 3.74 (s, 3H, OCH_3), 2.03 (s, 3H, CH_3). **^{13}C-NMR** (100 MHz, DMSO-d_6, ppm): *δ* 171.71 (C), 121.54 (C), 119.33 (C),117.48 (C), 106.56 (C), 55.37 (OCH_3), 20.45 (CH_3). MS (ESI): m/z (M + H) +314.32. Elemental Analysis ($C_7H_8N_4O$) calculated: C, 51.21; H, 4.91; N, 34.13; O, 9.75. Found: C 51.18; H, 4.90; N, 34.11, O, 9.73.

Compound 16a. Methyl 2-(5-amino-4-cyano-6-imino-2-methylpyrimidin-1(6H)-yl)acetate. Yellow oil. **^{1}H-NMR** (400 MHz, DMSO-d_6, ppm): δ 9.31 (s, 1H, NH), 6.69 (s, 2H, NH_2), 4.76 (s, 2H, CH_2), 3.73 (s, 3H, OCH_3), 2.03 (s, 3H, CH_3) ppm. **^{13}C-NMR** (100 MHz, DMSO-d_6, ppm): δ 166.48 (C=O), 162.81 (C), 160.24 (C), 144.02 (C), 121.51 (C), 99.77 (C), 55.37 (OCH_3), 49.06 (CH_2), 17.71 (CH_3). MS (ESI): m/z (M + H) +222.09. Elemental Analysis ($C_9H_{11}N_5O_2$) calculated: C, 48.86; H, 5.01; N, 31.66; O, 14.46. Found: C, 48.83; H, 4.99; N, 31.64; O, 14.45.

Compound 16b. Methyl 2-(5-amino-4-cyano-6-imino-2-methylpyrimidin-1(6H)-yl) propanoate. Brown oil. **^{1}H-NMR** (400 MHz, DMSO-d_6, ppm): δ 9.02 (s, 1H, NH), 6.69 (s, 2H, NH_2), 5.69 (d, J = 7.6 Hz, 1H, CH), 3.67 (s, 3H, OCH_3), 2.69 (s, 3H, CH_3), 1.82 (s, 3H, CH_3). **^{13}C-NMR** (100 MHz, DMSO-d_6, ppm): δ 169. 92 (C=O), 161.40 (C), 159.58 (C), 133.03 (C), 127.06 (C), 114.84 (C), 53.37 (CH), 52.77 (OCH_3), 25.87 (CH_3), 16.03 (CH_3). MS (ESI): m/z (M + H) +298.32. Elemental Analysis ($C_{10}H_{13}N_5O_2$) calculated: C, 51.06; H, 5.57; N, 29.77; O, 13.60. Found: C, 51.03; H, 5.56; N, 29.75, O, 13.58.

Compound 16c. Methyl 2-(5-amino-4-cyano-6-imino-2-methylpyrimidin-1(6H)-yl)-3-methylbutanoate. Brown oil. **^{1}H-NMR** (400 MHz, DMSO-d_6, ppm): δ 8.51 (s, 1H, NH), 6.75 (s, 2H, NH_2), 5.09 (d, J = 9.6 Hz, 1H, CH), 3.54 (s, 3H, OCH_3), 2.63(d, J = 5.2 Hz, 1H, CH), 2.00 (s, 3H, CH_3) 1.09 (d, J = 6.4 Hz, 3H, CH_3), 0.59 (d, J = 6.4 Hz, 3H, CH_3). **^{13}C-NMR** (100 MHz, DMSO-d_6, ppm): δ 166.48 (C=O), 158.54 (C), 121.51 (C), 117.24 (C), 115.38 (C), 99.78 (C), 69.39 (CH), 54.46 (OCH_3), 28.73 (CH), 23.13 (CH_3), 19.74 (CH_3), 17.71 (CH_3). MS (ESI): m/z (M + H) +264.30. Elemental Analysis ($C_{12}H_{17}N_5O_2$) calculated: C, 54.74; H, 6.51; N, 26.60; O, 12.15. Found: C, 54.71; H, 6.50; N, 26.58; O, 12.13.

Compound 16d Methyl 2-(5-amino-4-cyano-6-imino-2-methylpyrimidin-1(6H)-yl)-3-hydroxypropanoate. Brown oil. **^{1}H-NMR** (400 MHz, DMSO-d_6, ppm): δ 9.14 (s, 1H, NH), 7.56 (s, 2H, NH_2), 4.97 (s, 1H, OH), 4.24-4.21 (m, 2H, CH_2), 3.66 (s, 3H, OCH_3), 3.46-3.43 (m, 1H, CH), 2.01 (s, 3H, CH_3). **^{13}C-NMR** (100 MHz, DMSO-d_6, ppm): δ 171.78 (C=O), 162.75 (C), 158.48 (C), 145.99 (C), 119.06 (C), 98.04 (C), 61.74 (CH), 55.37 (OCH_3), 49.06 (CH_2), 22.83 (CH_3). MS (ESI): m/z (M + H) +314.32. Elemental Analysis ($C_{10}H_{13}N_5O_3$) calculated: C, 47.81; H, 5.22; N, 27.88; O, 19.10. Found: C, 47.78; H, 5.21; N, 27.86: O, 19.08.

Compound 16e. Methyl 2-(5-amino-4-cyano-6-imino-2-methylpyrimidin-1(6H)-yl)-3-phenylpropanoate. Yellow oil. **^{1}H-NMR** (400 MHz, DMSO-d_6, ppm): δ 9.13 (s, 1H, NH), 7.28-7.19 (m, 5H, CH-Ar), 6.69 (s, 2H, NH_2), 4.06-3.97 (m, 1H, CH), 3.73 (s, 3H, OCH_3), 3.18-3.12 (dd, J = 5.2, 16.4 Hz, 1H, CH_2), 3.09-3.05 (dd, J = 2.8, 9.6 Hz, 1H, CH_2) 2.03 (s, 3H, CH_3). **^{13}C-NMR** (100 MHz, DMSO-d_6, ppm): δ 169.44 (C=O), 164.14 (C), 158.83 (C), 143.36 (C), 136.58 (C), 127.89 (C-Ar x2), 126.59 (C-Ar x2), 125.39 (C-Ar), 114.11 (C), 99.45(C), 64.09 (CH), 53.80 (OCH_3), 36.54 (CH_2), 17.19 (CH_3). MS (ESI): m/z (M + H) +298.32. Elemental Analysis ($C_{16}H_{17}N_5O_2$) calculated: C, 61.72; H, 5.50; N, 22.49; O, 10.28. Found: C, 61.68; H, 5.49; N, 22.47; O, 10.26.

Compound 16f. Methyl 2-(5-amino-4-cyano-6-imino-2-methylpyrimidin-1(6H) -yl)-3-(4-hydroxyphenyl)propanoate. Yellow oil. **^{1}H-NMR** (400 MHz, DMSO-d_6, ppm): δ 10.52 (s, 1H, OH) 9.23 (s, 1 H, NH), 7.00 (d, J = 8.4 Hz, 2H, CH-Ar), 6.67 (d, J = 8.4 Hz, 2H, CH-Ar), 5.67 (s, 2H, NH_2), 4.38-4.32 (m, 1H, CH), 3.58 (s, 3H, OCH_3), 2.89-2.85 (dd, J = 7.2, 14.4 Hz, 1H, CH_2), 2.78-2.72 (dd, J = 8.8, 13.6, Hz, 1H, CH_2), 1.79 (s, 3H, CH_3). **^{13}C-NMR** (100 MHz, DMSO-d_6, ppm): δ 172.93 (C=O), 169.81 (C), 156.51 (C), 152.88 (C), 143.89 (C), 130.40 (C-Ar x2), 127.60 (C-Ar), 117.90 (C), 115.50 (C-Ar x2), 97.98 (C), 54.44 (CH), 52.18 (OCH_3), 36.51 (CH_2), 22.71 (CH_3). MS (ESI): m/z (M + H) +314.32. Elemental Analysis ($C_{16}H_{17}N_5O_3$) calculated: C, 58.71; H, 5.23; N, 21.39; O, 14.66. Found: C, 58.68; H, 5.22; N, 21.36, O, 14.65.

Compound 18. Methyl N-(4-cyano-1H-imidazol-5-yl)acetimidate. Yellow solid, m.p. 184.5°C. **^{1}H-NMR** (400 MHz, DMSO-d_6, ppm): δ 12.78 (s, 1H, NH), 7.67 (s, 1H, CH), 3.78 (s, 3H, OCH_3), 2.04 (s, 3H, CH_3).**^{13}C-NMR** (100 MHz, DMSO-d_6, ppm): δ 167.34 (C=O), 135.66 (C), 128.92 (C), 116.08 (C), 88.35 (C), 54.51 (O-CH_3), 17.63 (CH_3). MS (ESI): m/z (M + H) +165.07. Elemental Analysis ($C_7H_8N_4O$) calculated: C, 51.21; H, 4.91; N, 34.13; O, 9.75. Found: C, 51.18; H, 4.90; N, 34.11; O, 9.73.

Compound 19a. Methyl 2-(6-imino-2-methyl-6,9-dihydro-1H-purin-1-yl) acetate. Yellow solid m.p. 210.6°C. **^{1}H-NMR** (400 MHz, DMSO-d_6, ppm): δ 12.67 (s, 1H, NH), 7.67 (s, 1H, CH), 7.11 (s, 1H, NH), 3.78 (s, 3H, OCH_3), 3.69 (d, J = 3.6 Hz, 2H, CH_2), 2.04 (s, 3H, CH_3).**^{13}C-NMR** (100 MHz, DMSO-d_6, ppm): δ 167.44 (C=O), 154.80 (C), 151.94 (C), 149.61 (C), 135.90 (C), 117.40 (C), 54.52

(OCH_3), 48.66 (CH_2), 17.62 (CH_3). MS (ESI): m/z (M + H) +222.09. Elemental Analysis ($C_9H_{11}N_5O_2$) calculated: C, 48.86; H, 5.01; N, 31.66; O, 14.46. Found: C, 48.83; H, 5.00; N, 31.64; O, 14.44.

Compound 19b. Methyl 2-(6-imino-2-methyl-6,9-dihydro-1H-purin-1-yl)propanoate. Yellow solid, m.p. 206.9°C. **^{1}H-NMR** (400 MHz, DMSO-*d_6*, ppm): δ 12.66 (s, 1H, NH), 9.05 (s, 1H, NH), 7.68 (s, 1H, CH), 4.83-4.80 (m, 1H, CH), 3.69 (s, 3H, OCH_3), 2.01 (s, 3H, CH_3), 1.44 (d, *J* = 7.2 Hz, 3H, CH_3).**^{13}C-NMR** (100 MHz, DMSO-*d_6*, ppm): δ 170.19 (C=O), 156.77 (C), 152.48 (C), 149.97 (C), 144.07 (C), 118.83 (C), 54.58 (CH), 50.65 (OCH_3), 23.09 (CH_3), 14.49 (CH_3). MS (ESI): m/z (M + H) +236.11. Elemental Analysis ($C_{10}H_{13}N_5O_2$) calculated: C, 51.06; H, 5.57; N, 29.77; O, 13.60. Found: C, 51.03; H, 5.56; N, 29.75; O, 13.58.

Compound 19c. Methyl 2-(6-imino-2-methyl-6,9-dihydro-1H-purin-1-yl)-3-methylbutanoate. Brown solid, m.p. 214.4°C. **^{1}H-NMR** (400 MHz, DMSO-*d_6*, ppm): δ 12.78 (s, 1H, NH), 9.21 (s, 1H, NH), 7.62 (s, 1H, CH), 4.65 (d, *J* =3.6 Hz, 1H, CH), 3.78 (s, 3H, OCH_3), 2.58-2.55 (m, 1H, CH), 2.08 (s, 3H, CH_3), 1.25 (d, *J* = 5.6 Hz, 3H, CH_3), 0.98 (d, *J* = 5.6 Hz, 3H, CH_3).**^{13}C-NMR** (100 MHz, DMSO-*d_6*, ppm): δ 172.54 (C=O), 155.19 (C), 152.83 (C), 150.69 (C), 145.68 (C), 117.76 (C), 70.24 (CH) 55.35 (OCH_3), 29.71 (CH), 23.44 (CH_3), 21.56 (CH_3), 19.51 (CH_3). MS (ESI): m/z (M + H) +264.14. Elemental Analysis ($C_{12}H_{17}N_5O_2$) calculated: C, 54.74; H, 6.51; N, 26.60; O, 12.15. Found: C, 54.71; H, 6.50; N, 26.58; O, 12.13.

Compound 19d. Methyl 3-hydroxy-2-(6-imino-2-methyl-6,9-dihydro-1H-purin-1-yl)propanoate. Brown solid, m.p. 267.7°C. **^{1}H-NMR** (400 MHz, DMSO-*d_6*, ppm): δ 12.81 (s, 1H, NH), 9.18 (s, 1H, NH), 7.47 (s, 1H, CH), 4.93 (s, 1H, OH), 4.05-4.01 (m, 2H, CH_2), 3.75 (s, 3H, OCH_3), 3.63 (s, 1H, CH), 2.04 (s, 3H, CH_3).**^{13}C-NMR** (100 MHz, DMSO-*d_6*, ppm): δ 168.22 (C=O), 156.41 (C), 152.48 (C), 150.69 (C), 142.63 (C), 118.47 (C), 66.39 (CH), 59.06 (CH_2), 52.79 (O-CH_3), 22.73 (CH_3). MS (ESI): m/z (M + H) +252.10. Elemental Analysis ($C_{10}H_{13}N_5O_3$) calculated: C, 47.81; H, 5.22; N, 27.88; O, 19.10. Found: C, 47.78; H, 5.21; N, 27.86; O, 19.08.

Compound 19e. Methyl 2-(6-imino-2-methyl-6,9-dihydro-1H-purin-1-yl)-3 phenylpropanoate. Yellow solid, m.p. 300.9°C. **^{1}H-NMR** (400 MHz, DMSO-*d_6*, ppm): δ 12.21 (s, 1H, NH), 9.39 (s, 1H, NH), 7.28-7.19 (m, 5H, CH-Ar), 6.92 (s, 1H, CH), 4.22-4.20 (m, 1H, CH), 3.67 (s, 3H, OCH_3), 3.12-2.91 (m,

2H, CH_2), 2.01 (s, 3H, CH_3).**^{13}C-NMR** (100 MHz, DMSO-*d_6*, ppm): δ 169.64 (C=O), 155.88 (C), 151.58 (C), 149.26 (C), 137.26 (C), 135.30 (C-Ar), 129.93 (C-Ar x2), 129.03 (C-Ar x2), 127.42 (C-Ar), 117.58 (C), 67.47 (CH), 52.97 (OCH_3), 36.87 (CH_2), 15.57 (CH_3). MS (ESI): m/z (M + H) +312.14. Elemental Analysis ($C_{16}H_{17}N_5O_2$) calculated: C, 61.72; H, 5.50; N, 22.49; O, 10.28. Found: C, 61.68; H, 5.49; N, 22.47; O, 10.27.

Compound 19f. Methyl 3-(4-hydroxyphenyl)-2-(6-imino-2-methyl-6,9-dihydro-1H-purin-1-yl)propanoate. Yellow solid, m.p. 412.6°C. **^{1}H-NMR** (400 MHz, DMSO-*d_6*, ppm): δ 13.16 (s, 1H, NH), 9.06 (s, 1H, NH), 8.27 (s, 1H, OH), 7.43 (s, 1H, CH), 6.99 (d, *J* = 8.4 Hz, 2H, CH-Ar), 6.67 (d, *J* = 8.4 Hz, 2H, CH-Ar), 4.38-4.32 (m, 1H, CH), 3.74 (s, 3H, OCH_3), 2.89-2.85 (dd, *J* =6.0, 14.0 Hz, 1H, CH_2), 2.78-2.72 (dd, *J* = 9.2, 14.0 Hz, 1H, CH_2), 2.04 (s, 3H, CH_3).**^{13}C-NMR** (100 MHz, DMSO-*d_6*, ppm): δ 169.65 (C=O), 156.46 (C), 154.09 (C), 152.48 (C), 150.33 (C), 137.83 (C), 130.36 (C-Ar x2), 127.81 (C-Ar), 120.08 (C), 115.55 (C-Ar x2), 54.41 (CH), 52.12 (OCH_3), 36.58 (CH_2), 22.70 (CH_3). MS (ESI): m/z (M + H) +328.13. Elemental Analysis ($C_{16}H_{17}N_5O_3$) calculated: C, 58.71; H, 5.23; N, 21.39; O, 14.66. Found: C, 58.68; H, 5.22; N, 21.37; O, 14.64.

Compound 4a Methyl 2-(5-amino-4-cyano-2-methyl-1H-imidazol-1-yl)acetate.

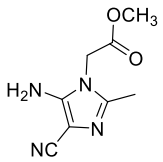

^{1}H-NMR

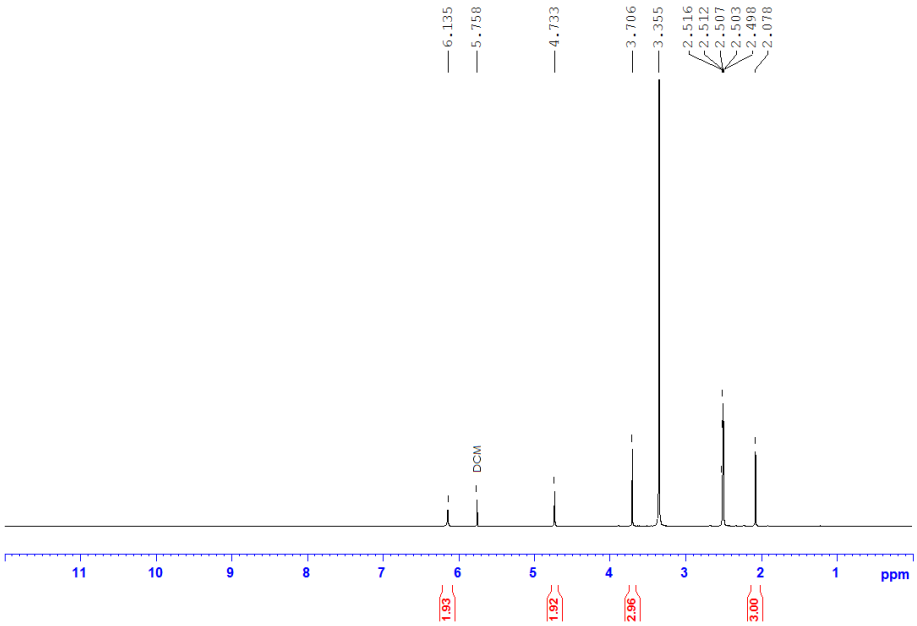

^{13}C-NMR

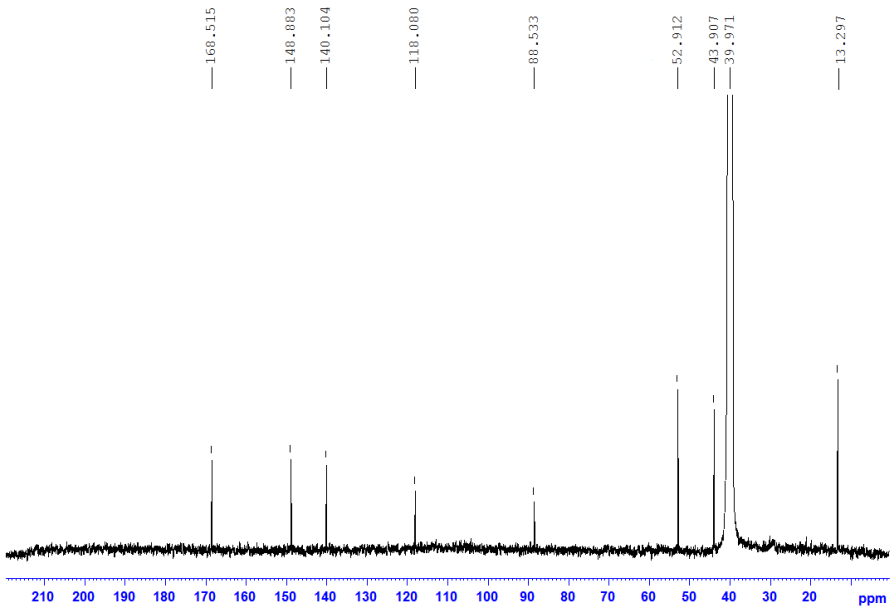

Compound 4b Methyl 2-(5-amino-4-cyano-2-methyl-1H-imidazol-1-yl)propanoate.

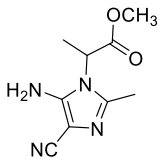

^{1}H-NMR

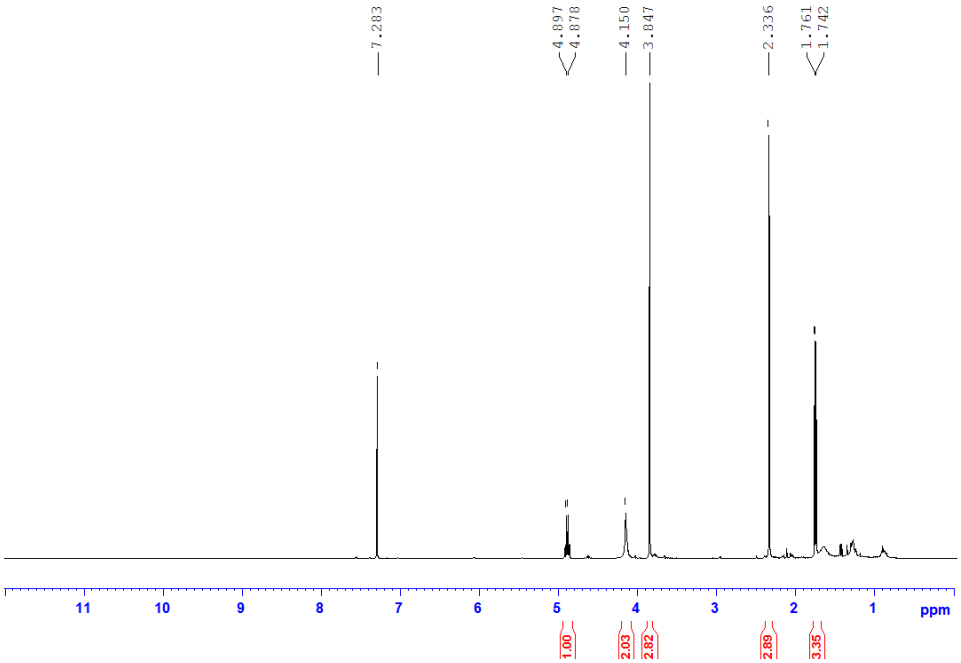

^{13}C-NMR

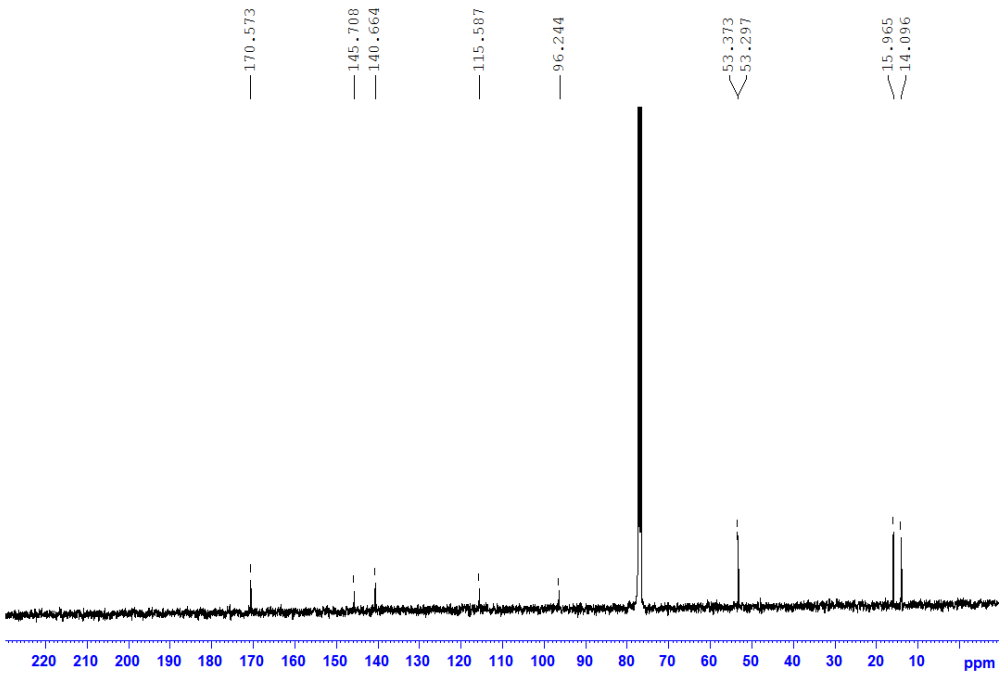

Compound 4c Methyl 2-(5-amino-4-cyano-2-methyl-1H-imidazol-1-yl)-3-methylbutanoate.

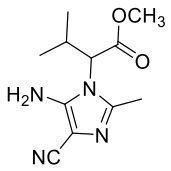

^{1}H-NMR

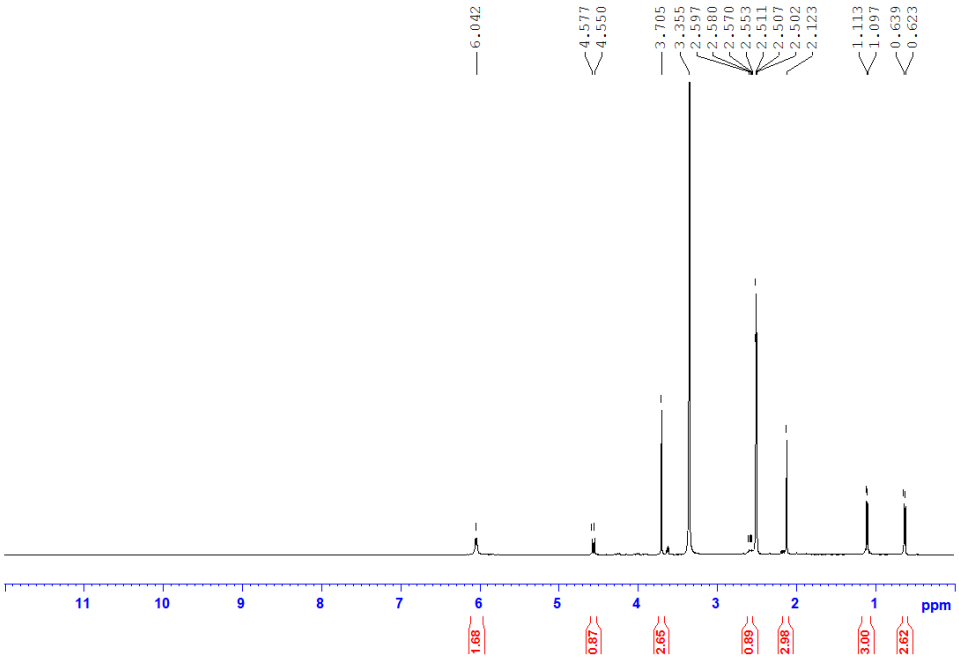

^{13}C-NMR

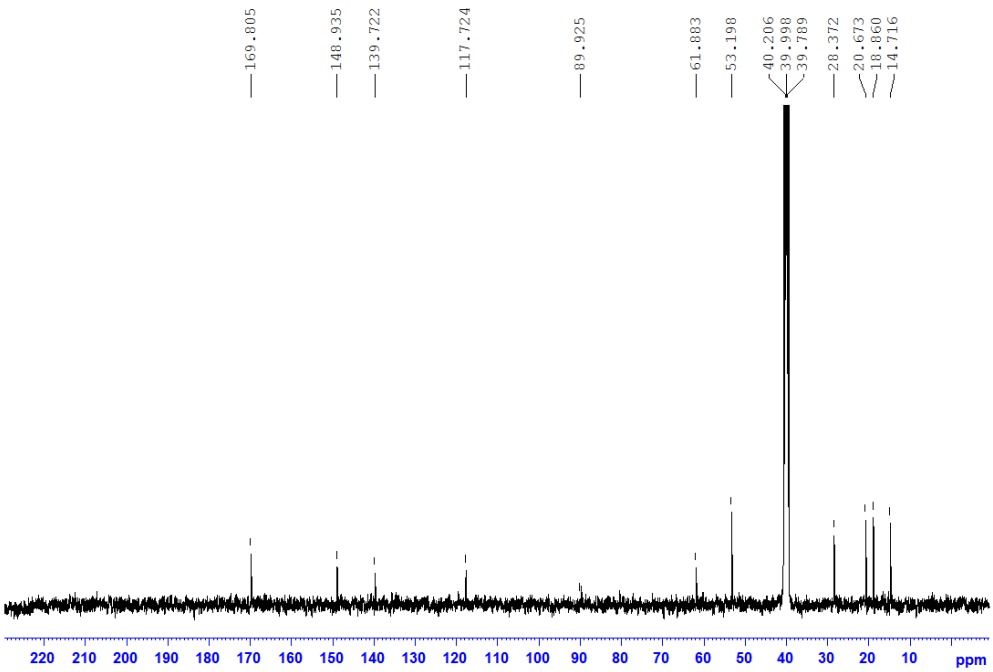

Compound 4d Methyl 2-(5-amino-4-cyano-2-methyl-1H-imidazol-1-yl)-3-hydroxypropanoate.

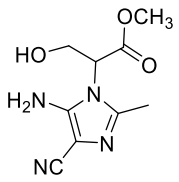

^{1}H-NMR

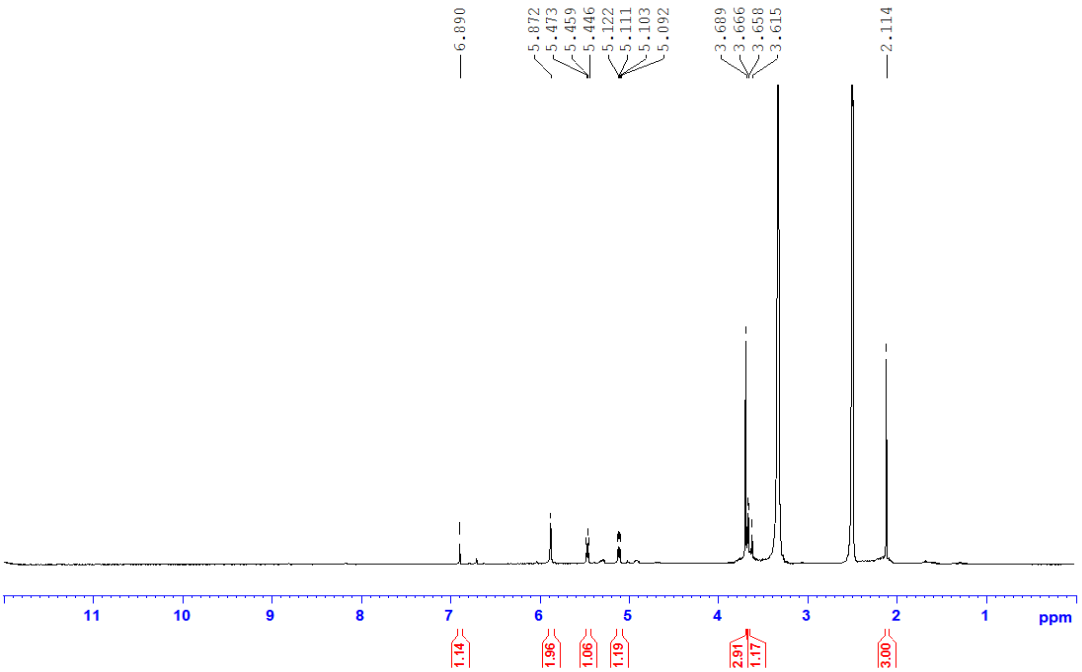

^{13}C-NMR

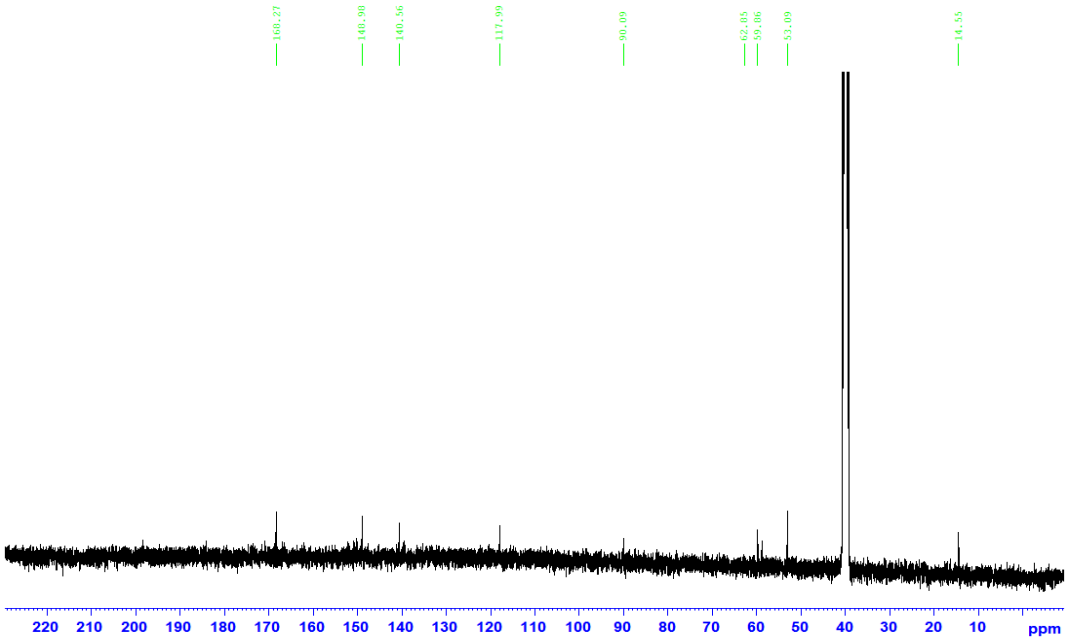

Compound 4e Methyl 2-(5-amino-4-cyano-2-methyl-1H-imidazol-1-yl)-3-phenylpropanoate.

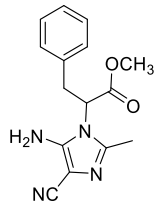

^{1}H-NMR

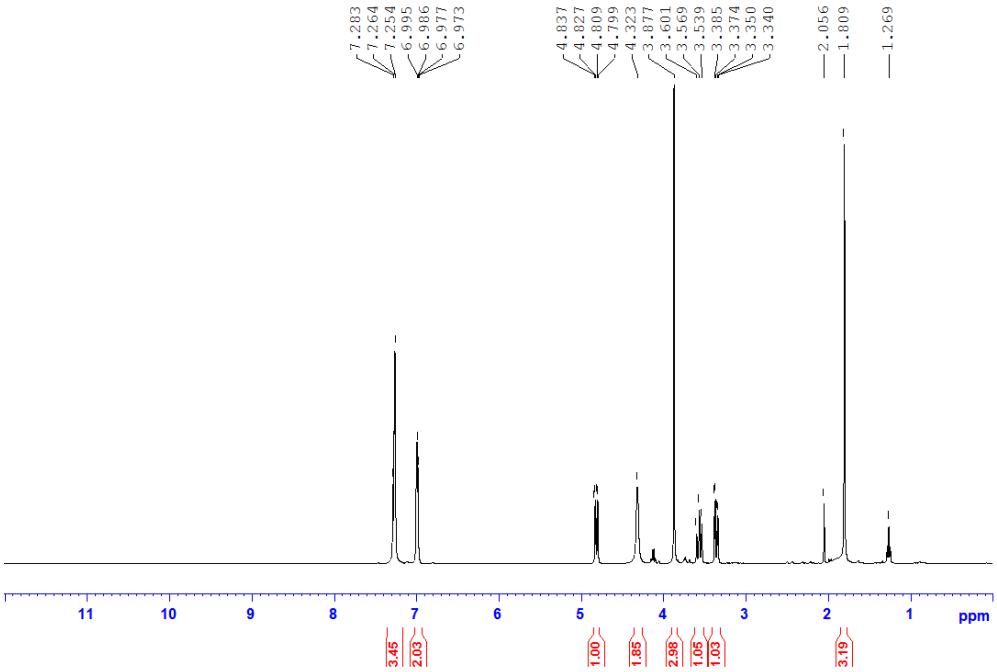

^{13}C-NMR

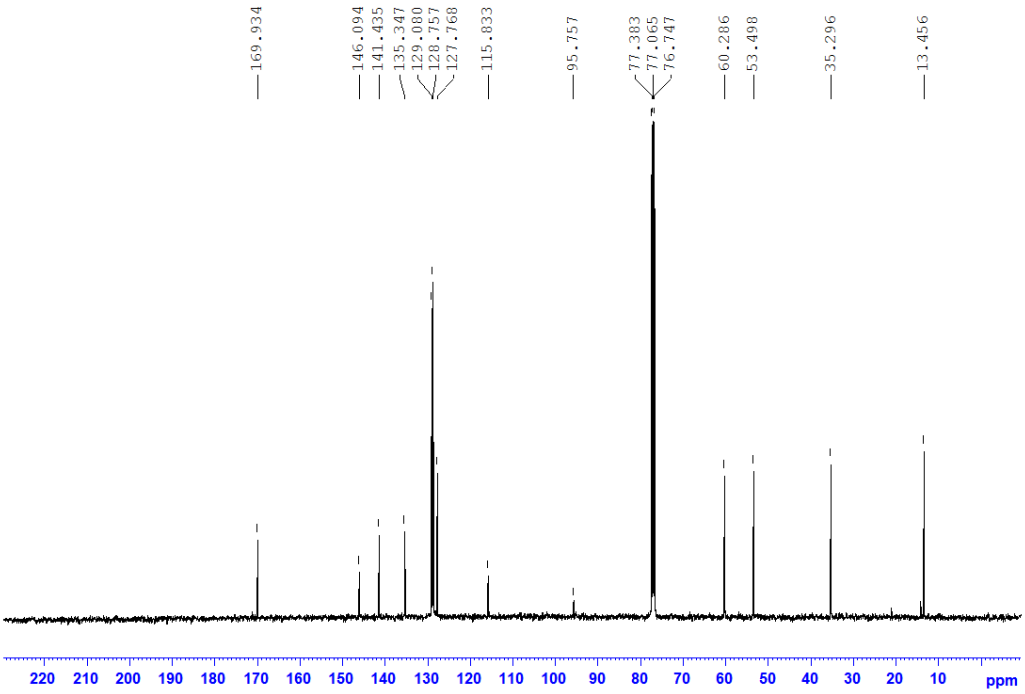

Compound 4f Methyl 2-(5-amino-4-cyano-2-methyl-1H-imidazol-1-yl)-3-(4-hydroxyphenyl)propanoate.

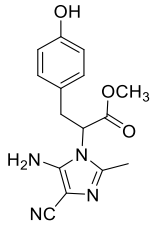

^{1}H-NMR

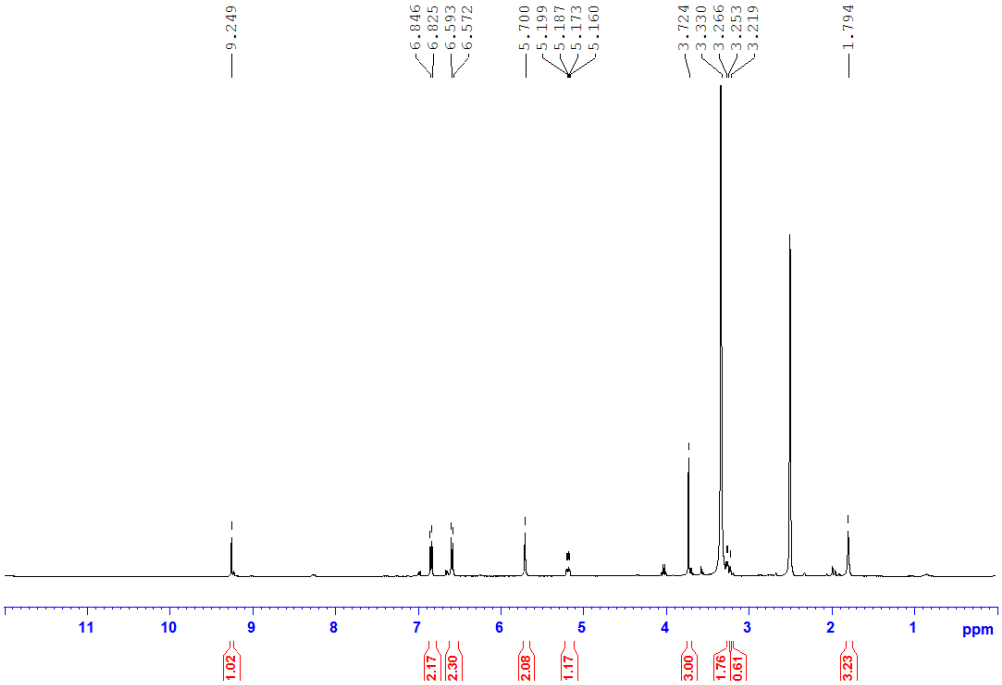

^{13}C-NMR

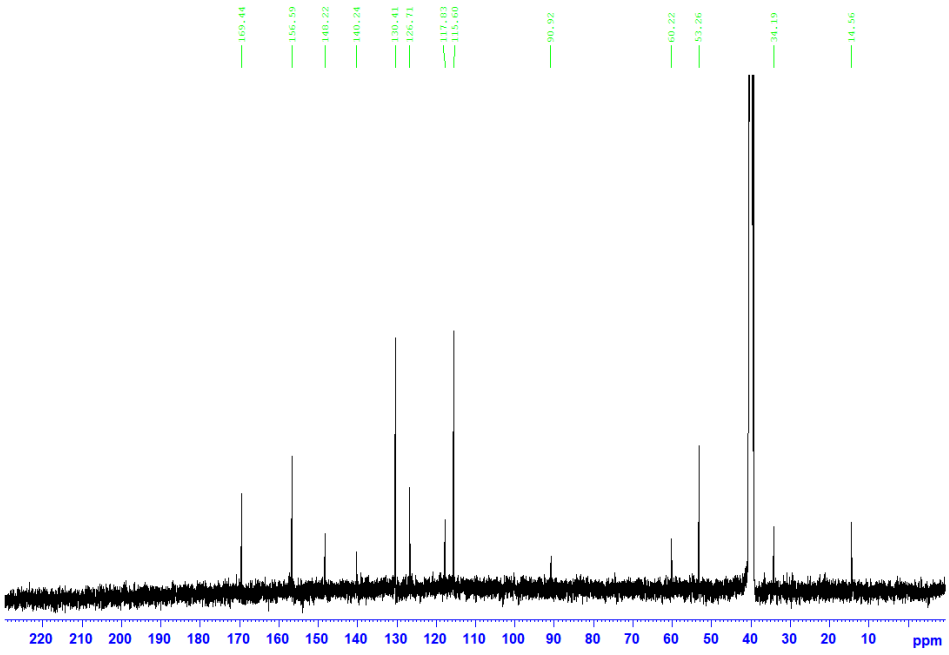

Compound 4g Methyl 2-(5-amino-4-cyano-2-methyl-1H-imidazol-1-yl)-3-(1H-indol-3-yl)propanoate

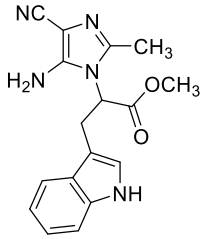

^{1}H-NMR

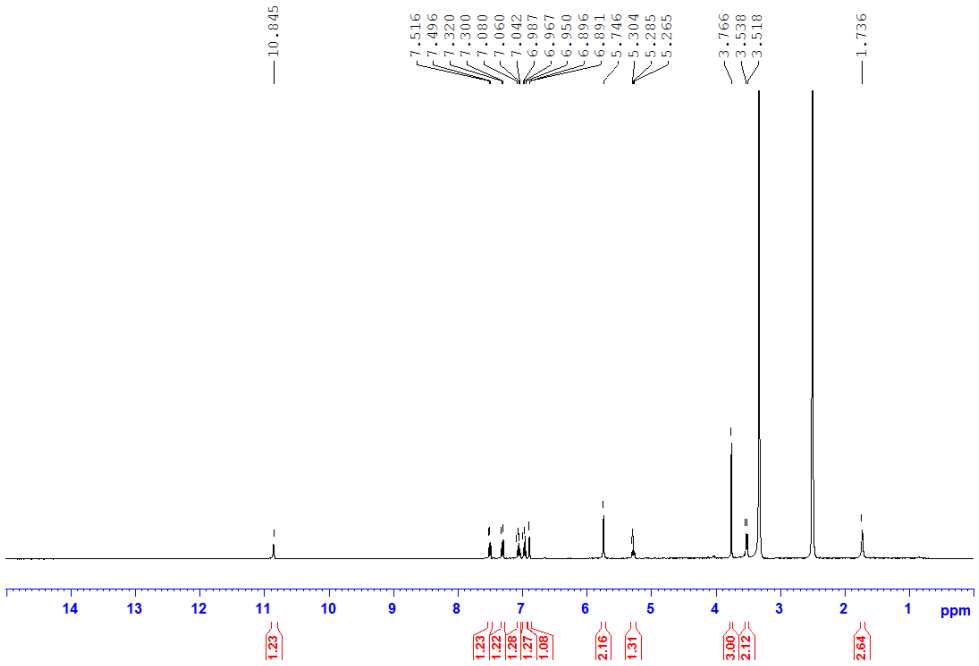

^{13}C-NMR

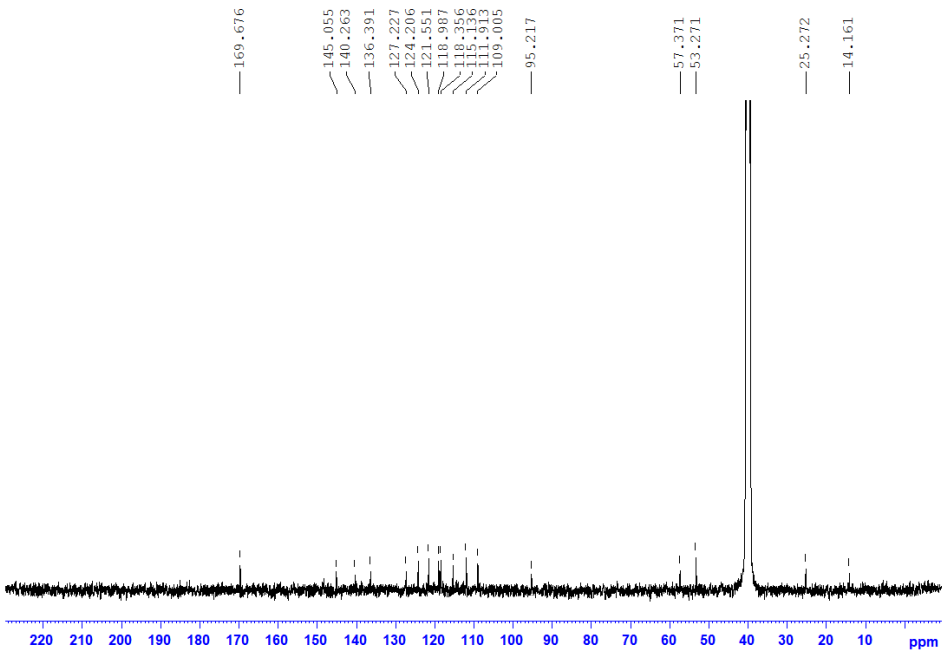

Compound 5a 2-(5-amino-4-cyano-2-methyl-1H-imidazol-1-yl)acetic acid**.**

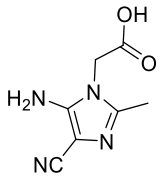

^{1}H-NMR

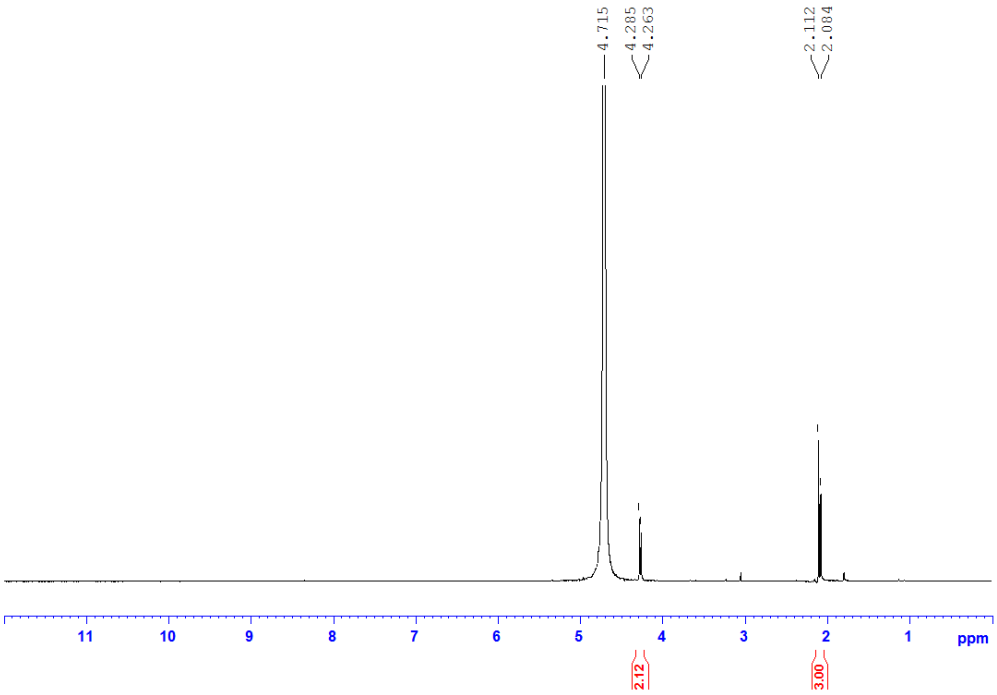

^{13}C-NMR

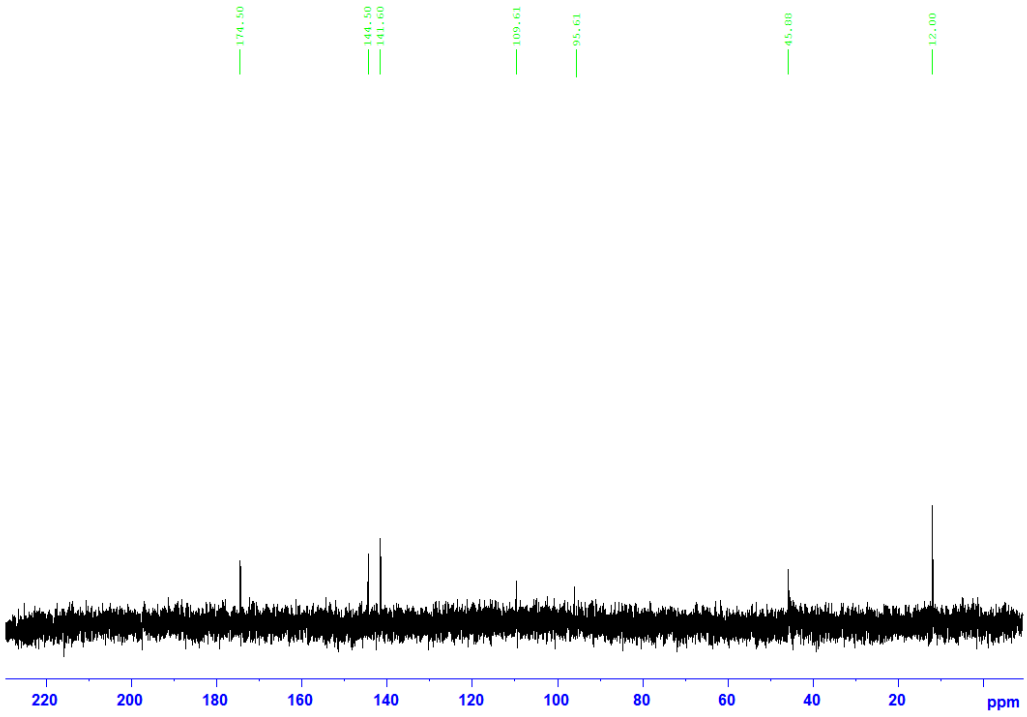

Compound 5b 2-(5-amino-4-cyano-2-methyl-1H-imidazol-1-yl)propanoic acid.

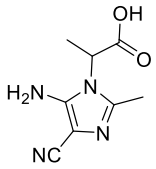

^{1}H-NMR

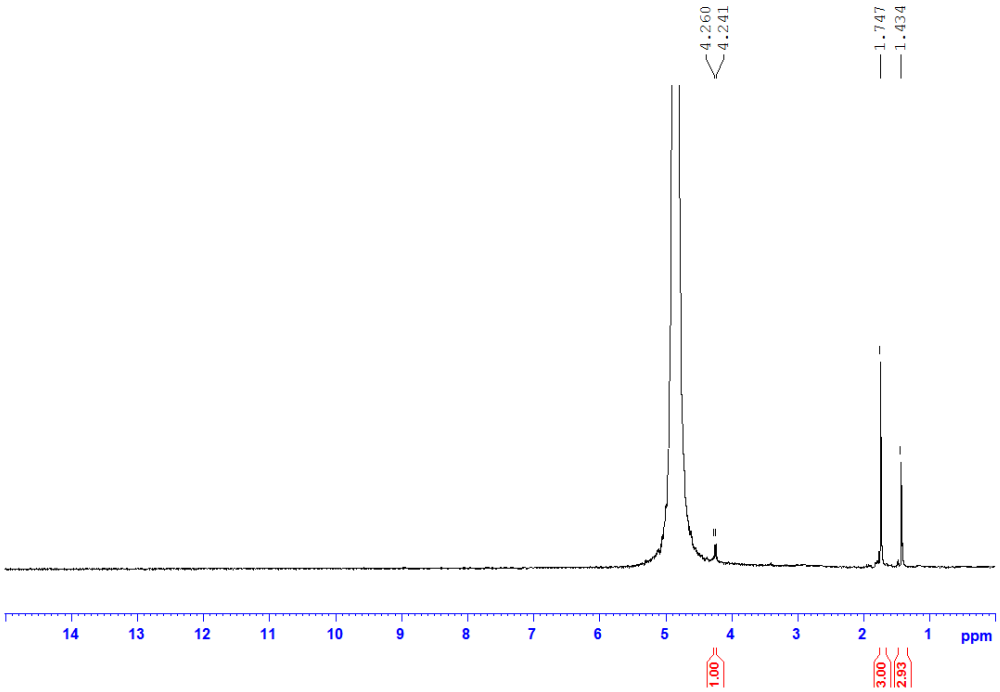

^{13}C-NMR

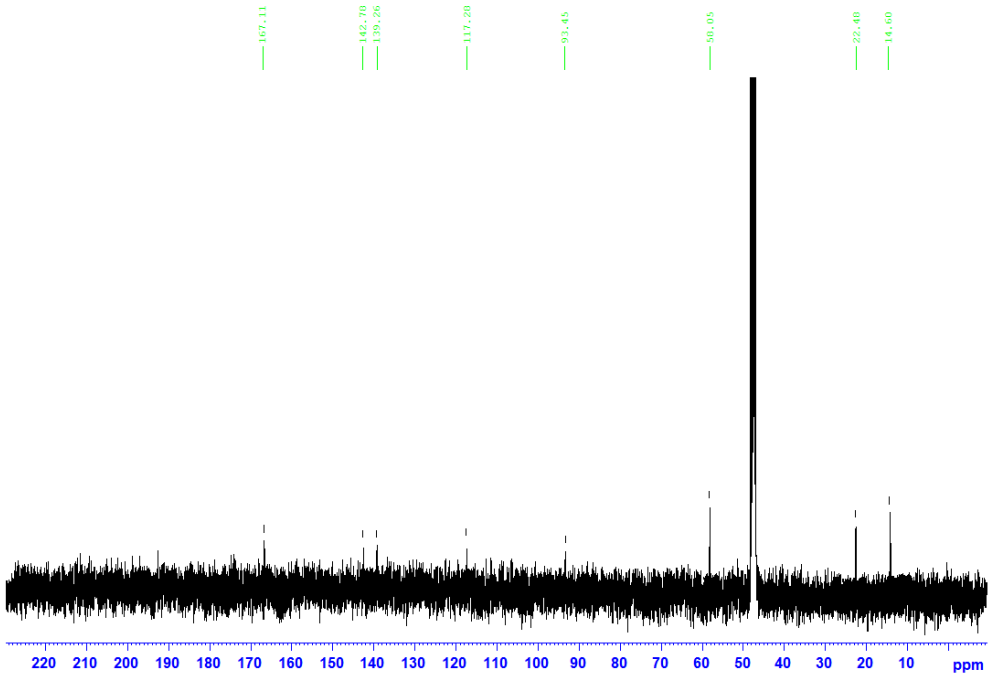

Compound 5c 2-(5-amino-4-cyano-2-methyl-1H-imidazol-1-yl)-3-methylbutanoic acid.

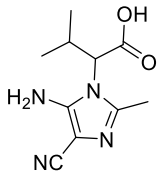

^{1}H-NMR

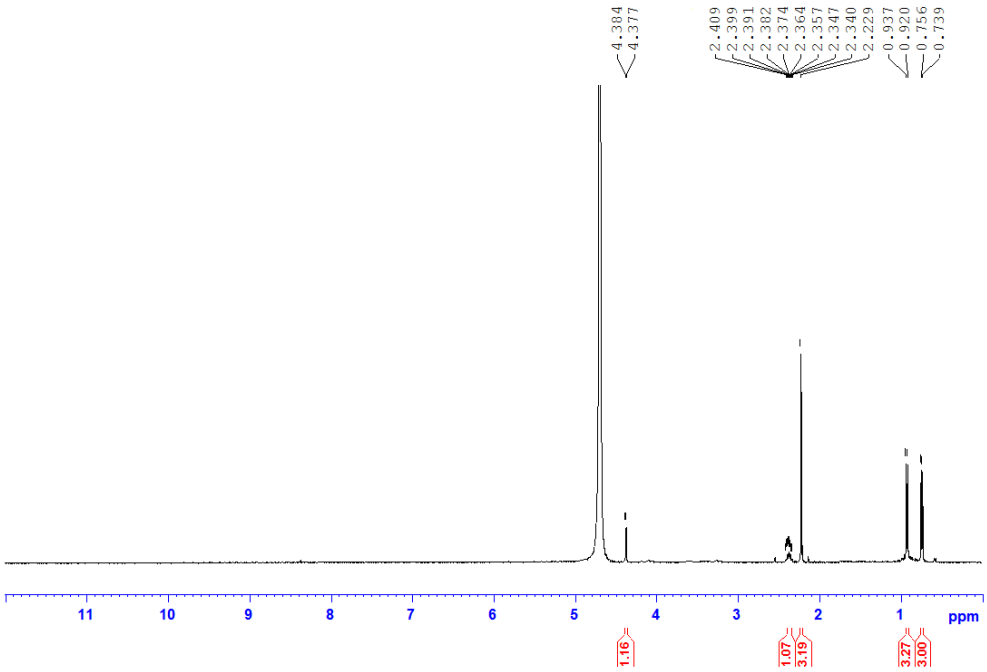

^{13}C-NMR

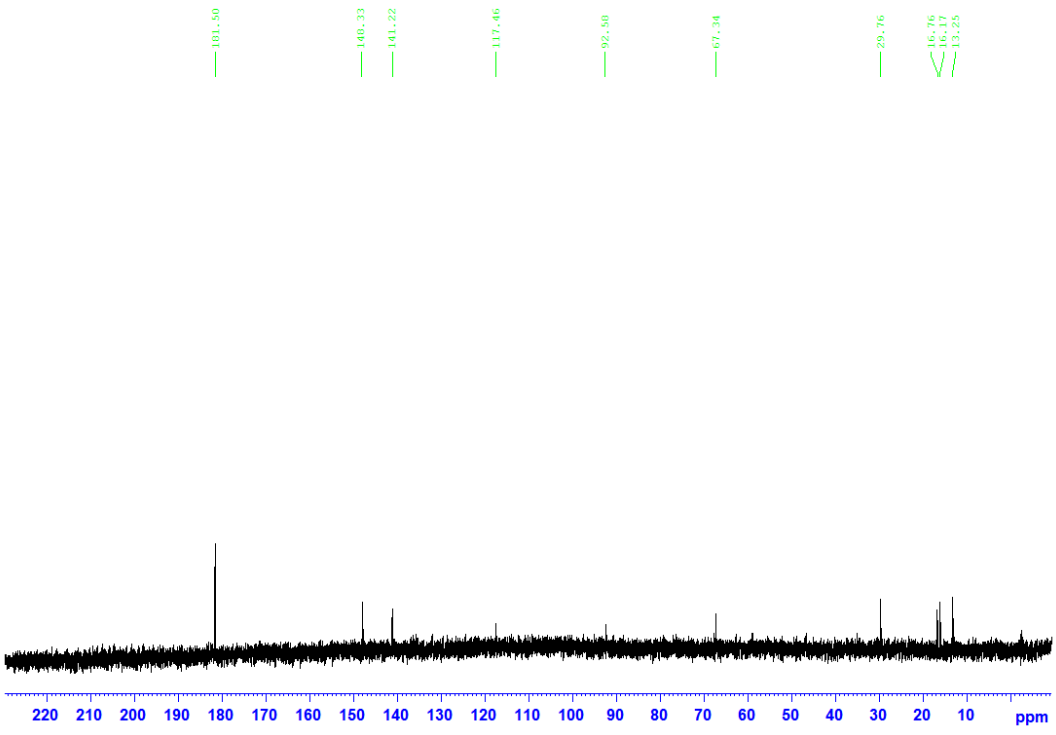

Compound 5d 2-(5-amino-4-cyano-2-methyl-1H-imidazol-1-yl)-3-hydroxypropanoic acid.

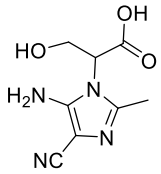

^{1}H-NMR

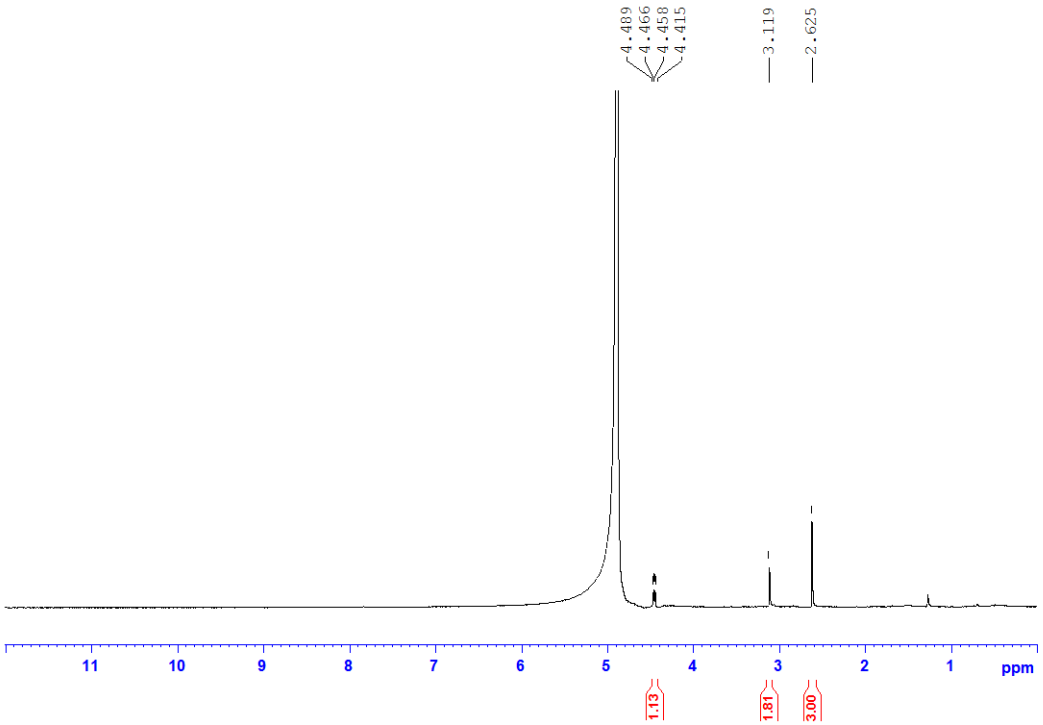

^{13}C-NMR

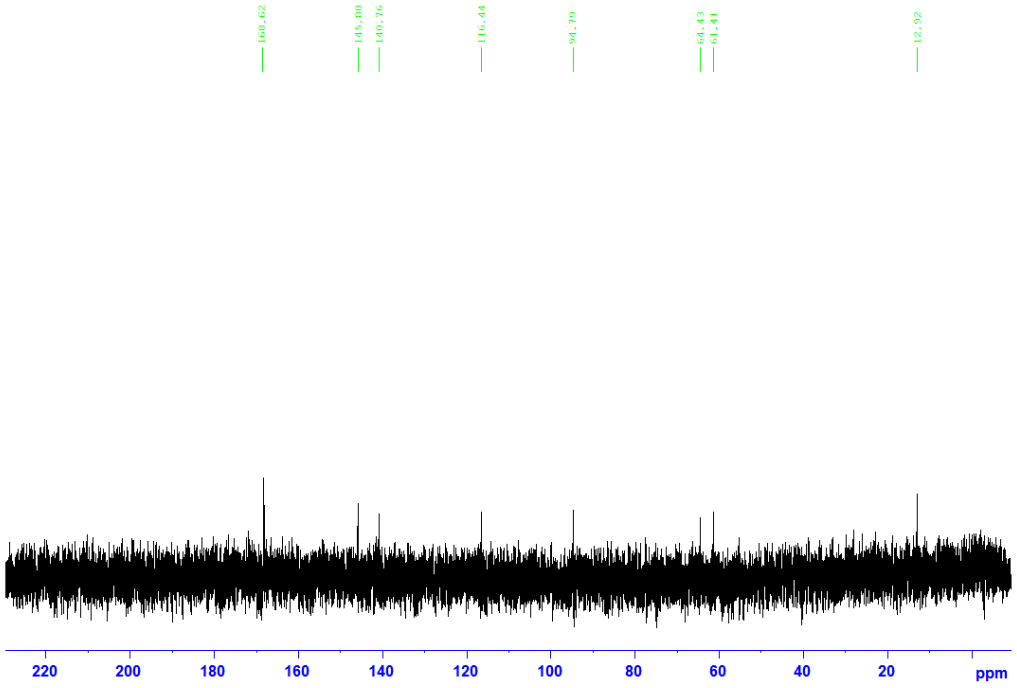

Compound 5e 2-(5-amino-4-cyano-2-methyl-1H-imidazol-1-yl)-3-phenylpropanoic acid.

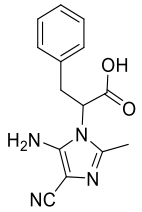

^{1}H-NMR

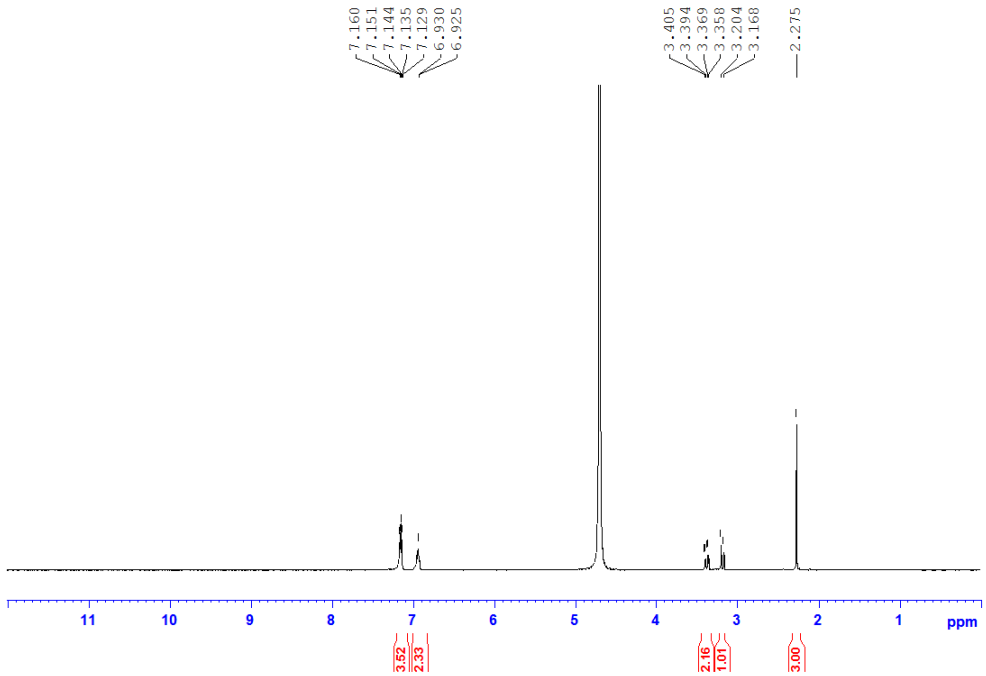

^{13}C-NMR

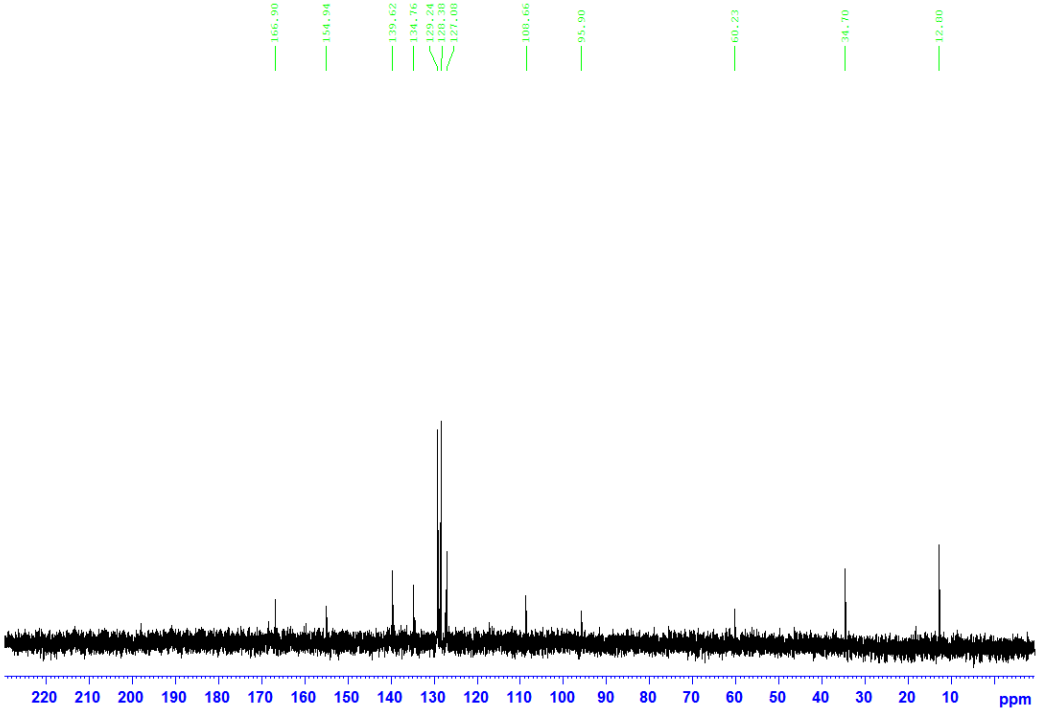

Compound 5f 2-(5-amino-4-cyano-2-methyl-1H-imidazol-1-yl)-3-(4-hydroxyphenyl)propanoic acid**.**

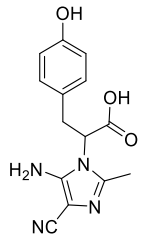

^{1}H-NMR

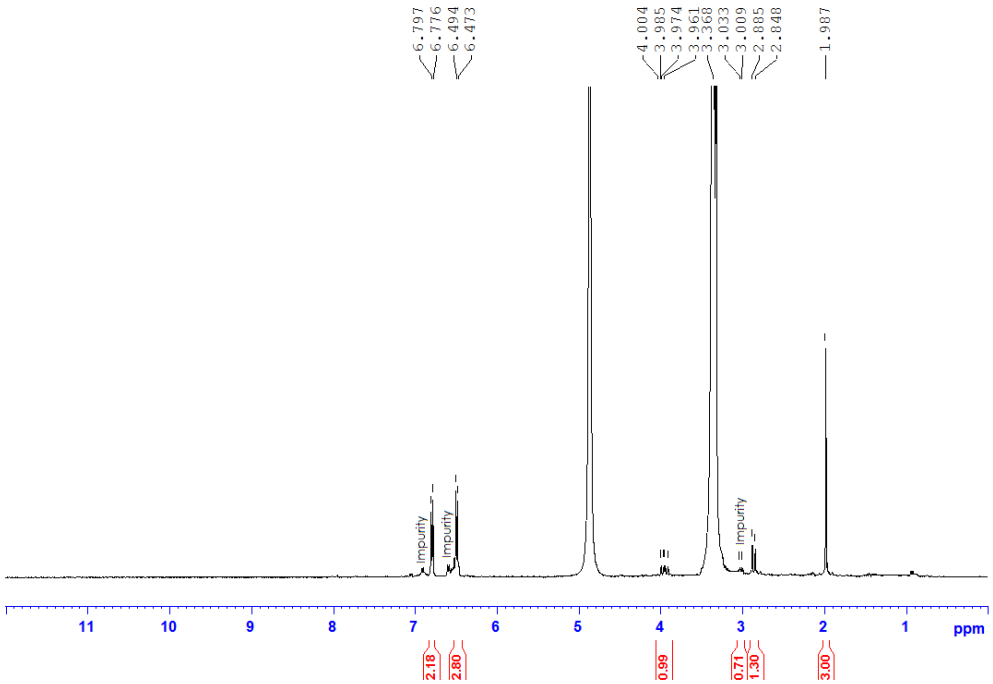

^{13}C-NMR

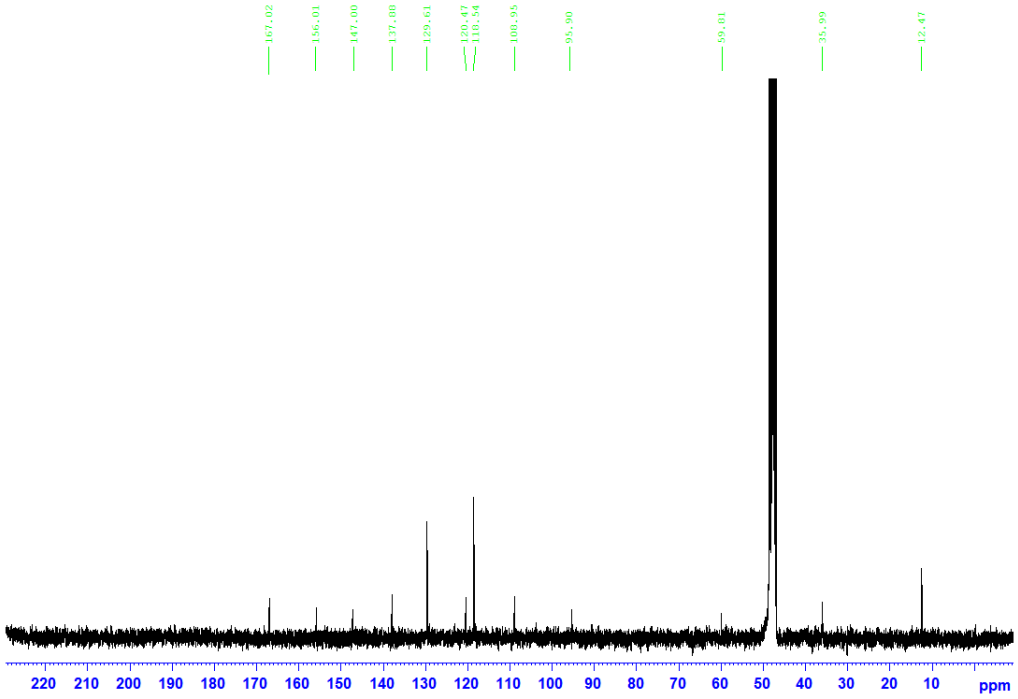

Compound 6a Methyl 2-(8-methyl-6-oxo-1,6-dihydro-9H-purin-9-yl)acetate.

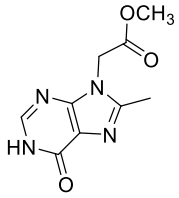

^{1}H-NMR

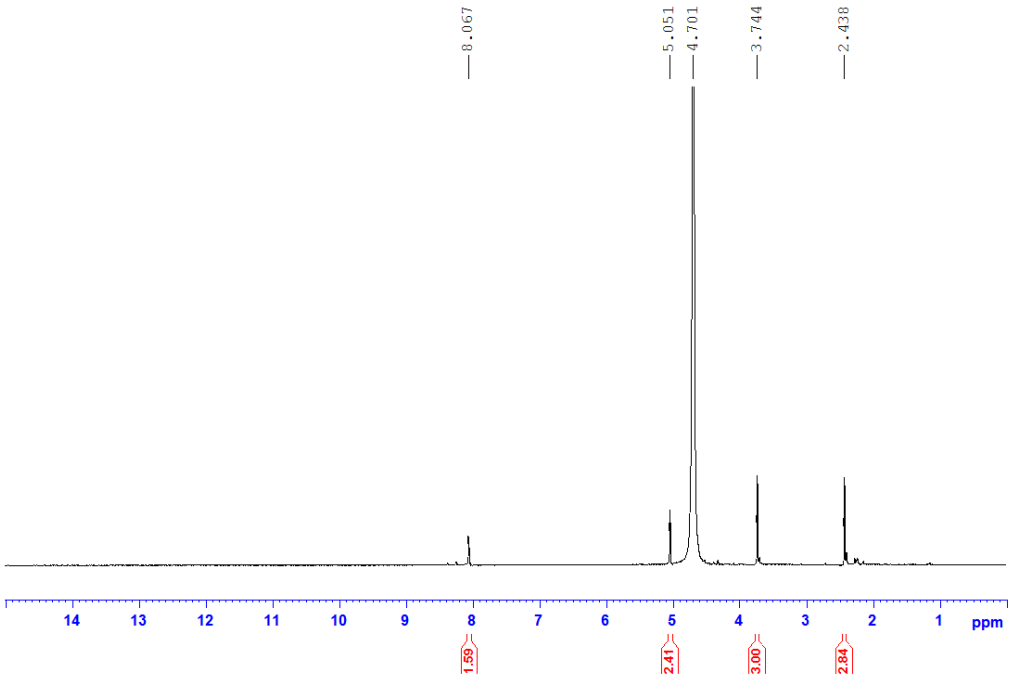

^{13}C-NMR

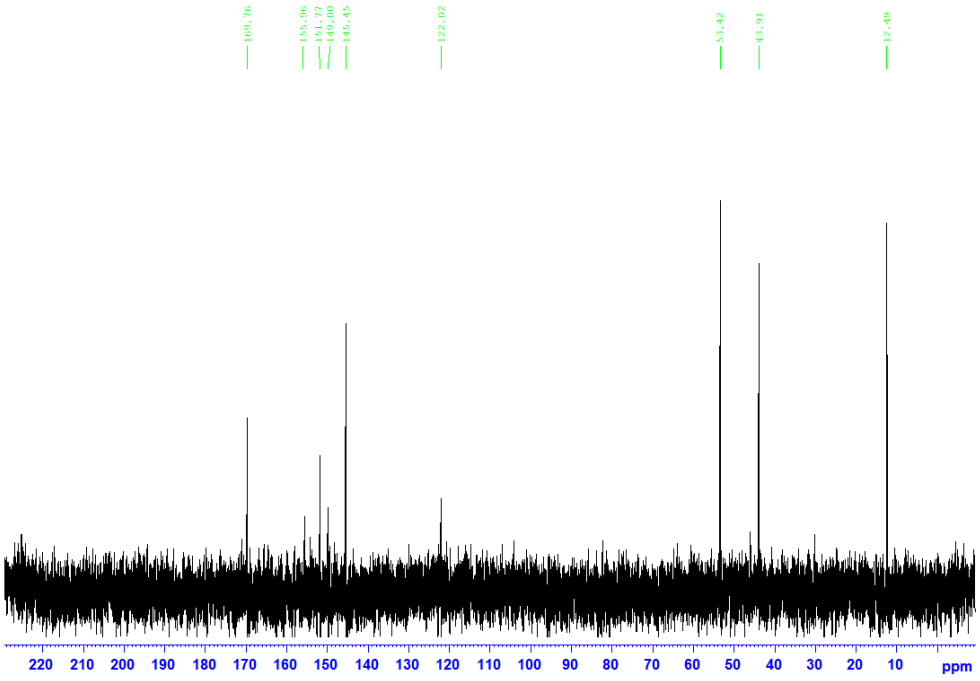

Compound 6b Methyl 2-(8-methyl-6-oxo-1,6-dihydro-9H-purin-9-yl)propanoate.

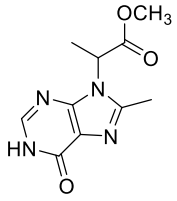

^{1}H-NMR

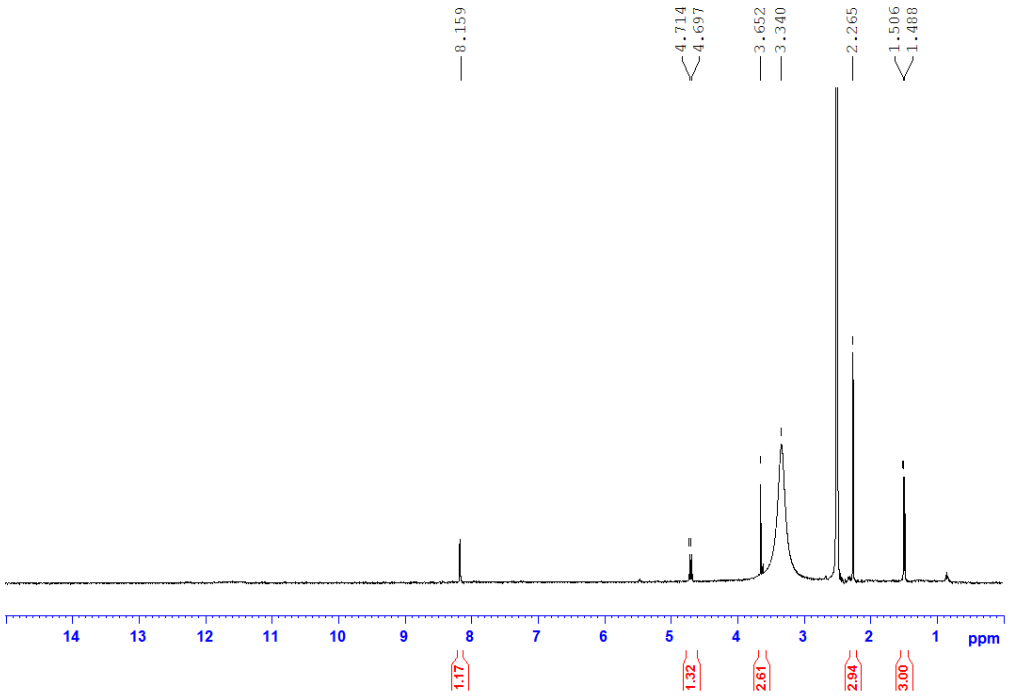

^{13}C-NMR

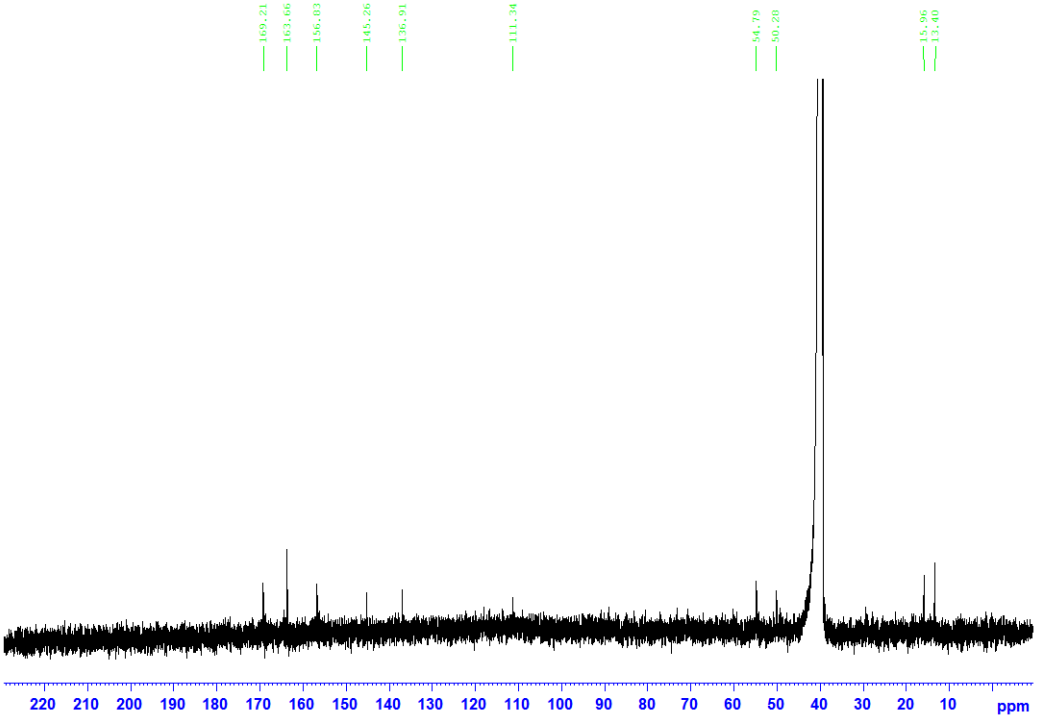

Compound 6c Methyl 3-methyl-2-(8-methyl-6-oxo-1,6-dihydro-9H-purin-9-yl)butanoate.

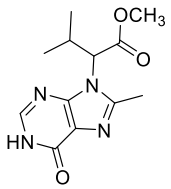

^{1}H-NMR

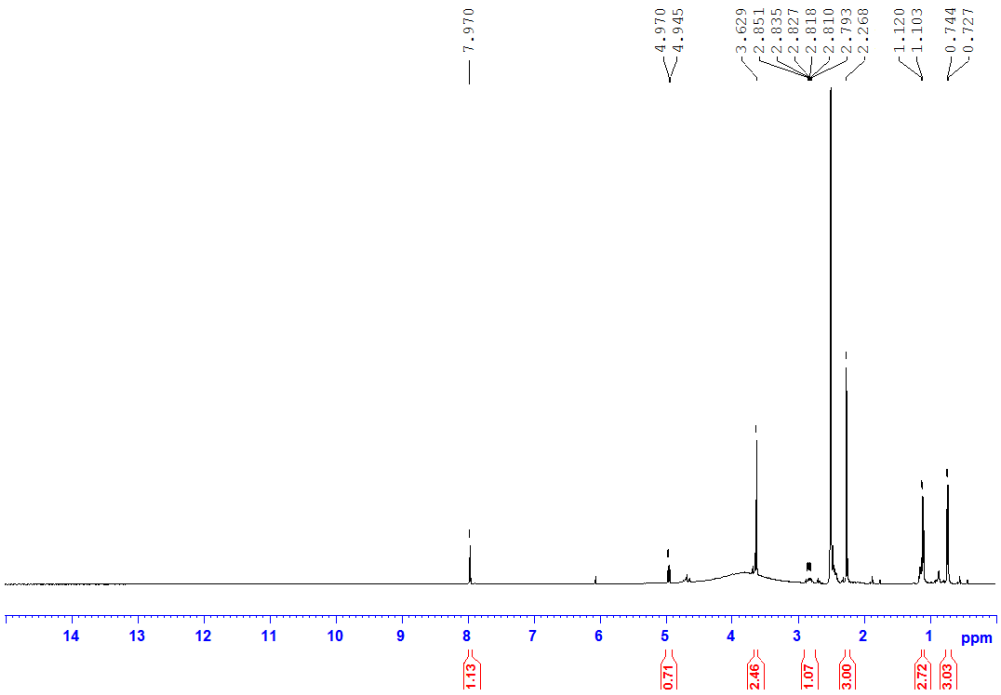

^{13}C-NMR

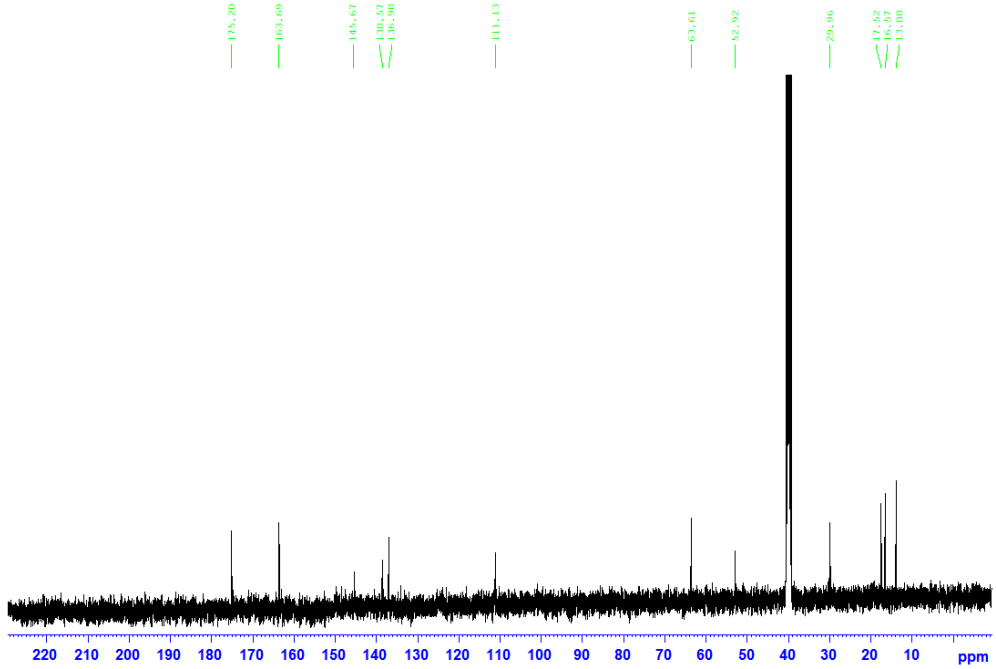

Compound 6d Methyl 3-hydroxy-2-(8-methyl-6-oxo-1,6-dihydro-9H-purin-9-yl)propanoate**.**

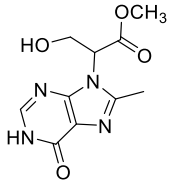

^{1}H-NMR

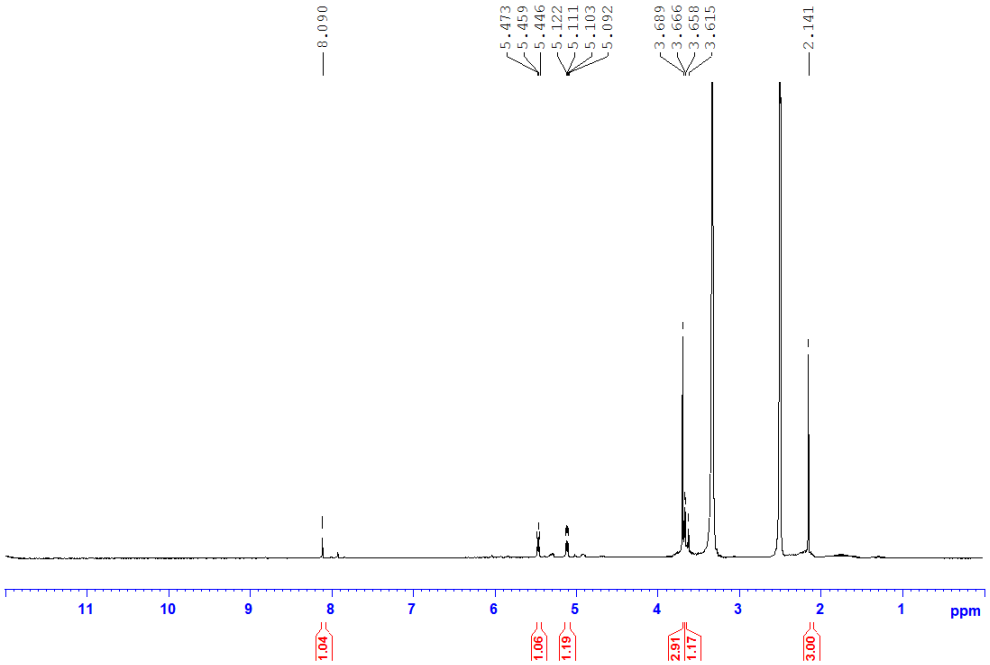

^{13}C-NMR

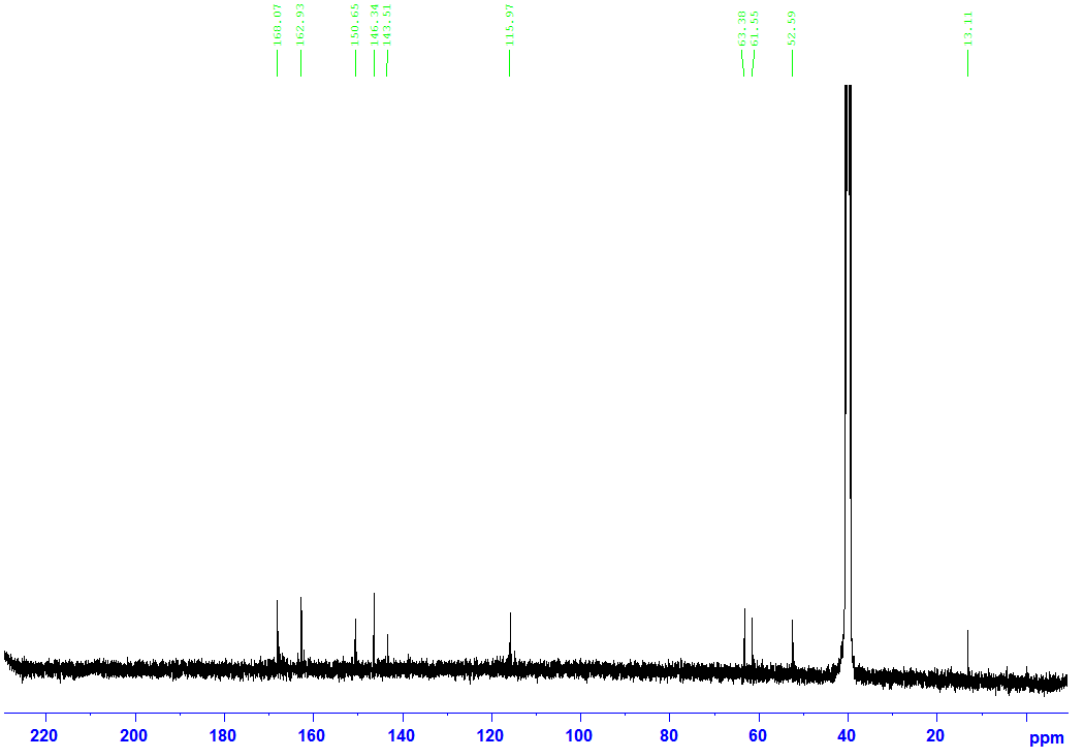

Compound 6e Methyl 2-(8-methyl-6-oxo-1,6-dihydro-9H-purin-9-yl)-3-phenylpropanoate.

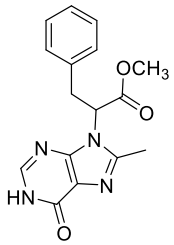

^{1}H-NMR

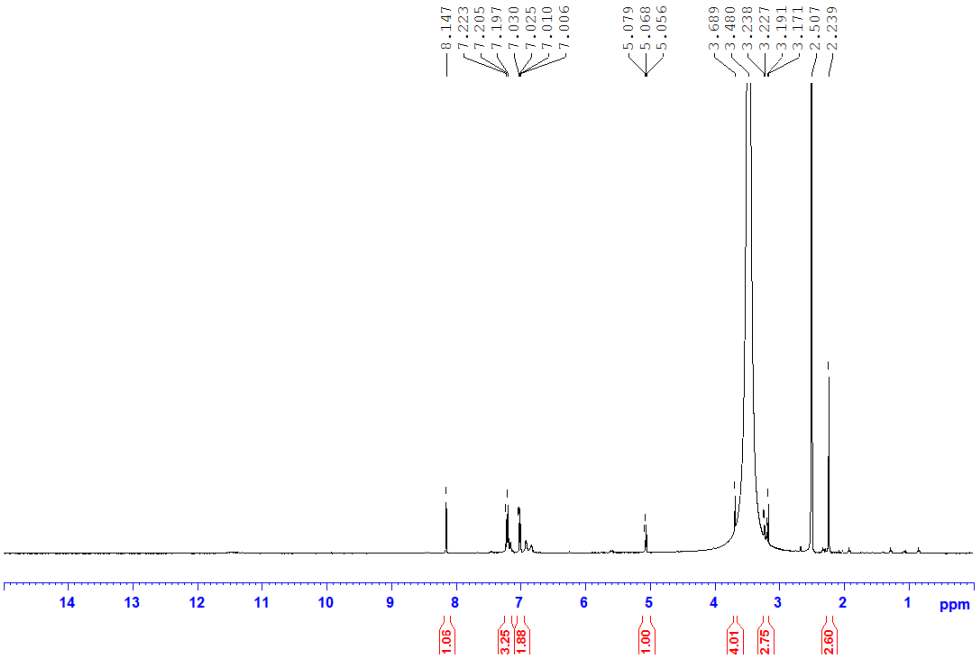

^{13}C-NMR

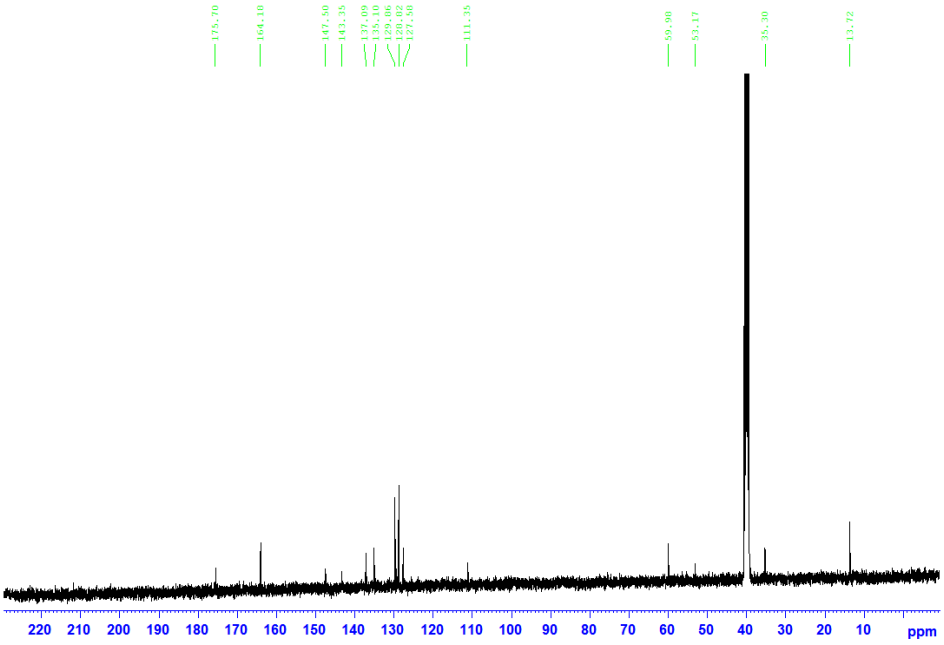

Compound 6f Methyl 3-(4-hydroxyphenyl)-2-(8-methyl-6-oxo-1,6-dihydro-9H-purin-9-yl)propanoate.

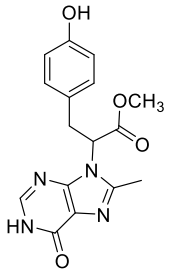

^{1}H-NMR

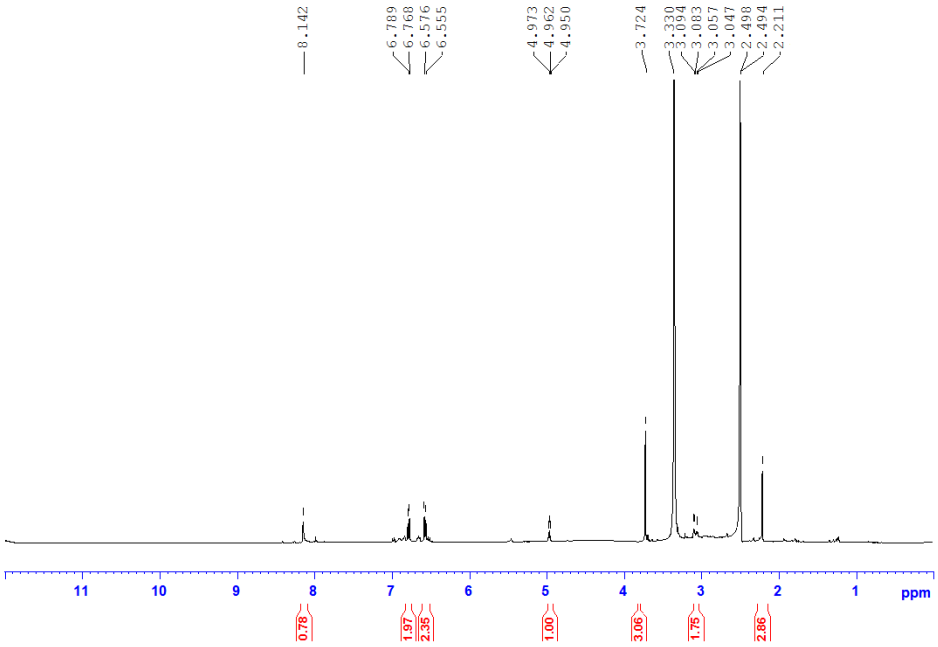

^{13}C-NMR

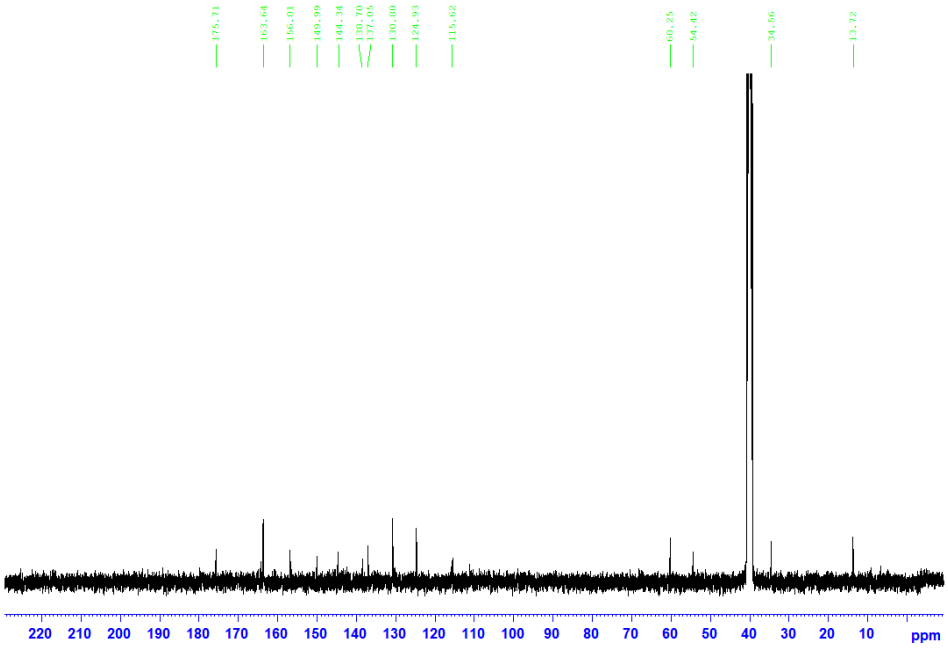

Compound 7a 2-(8-methyl-6-oxo-1,6-dihydro-9H-purin-9-yl)acetic acid.

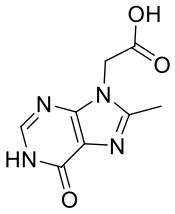

^{1}H-NMR

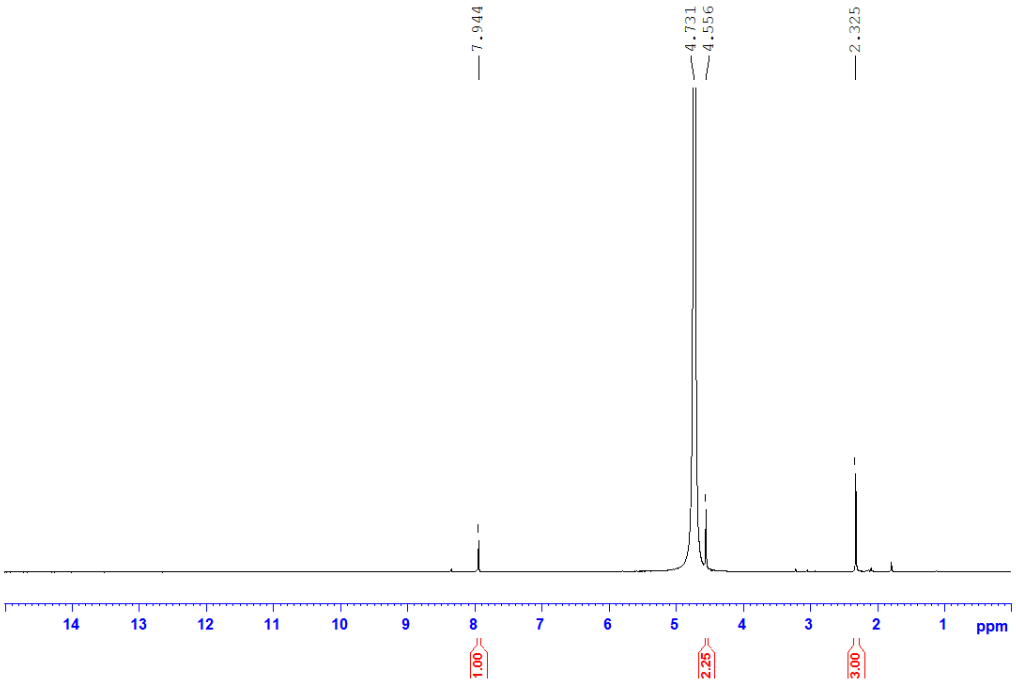

^{13}C-NMR

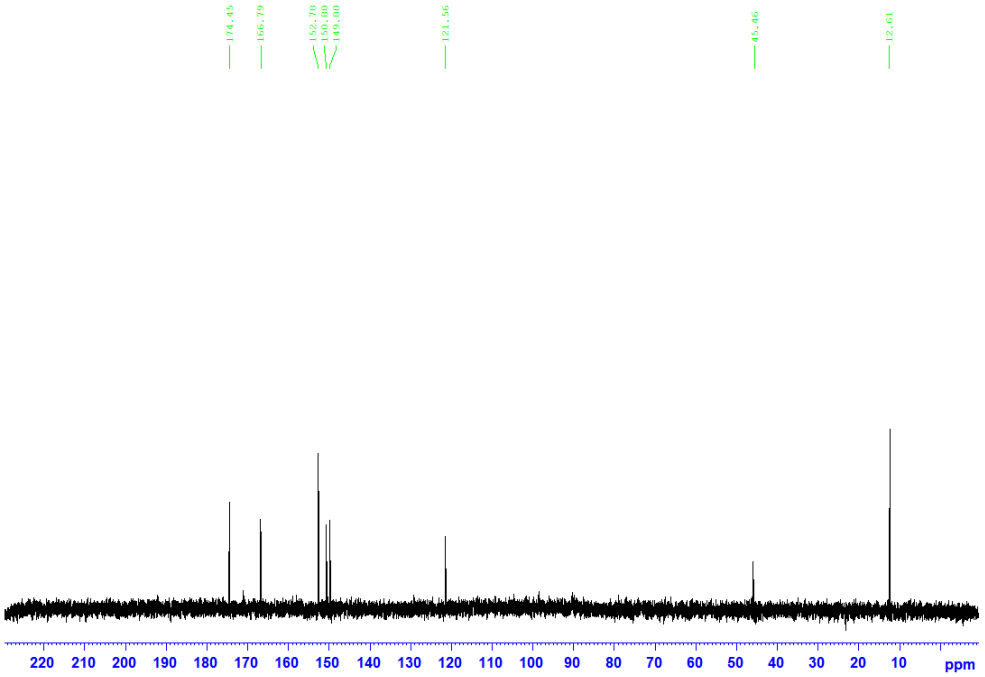

Compound 7b 2-(8-methyl-6-oxo-1,6-dihydro-9H-purin-9-yl)propanoic acid**.**

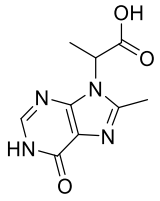

^{1}H-NMR

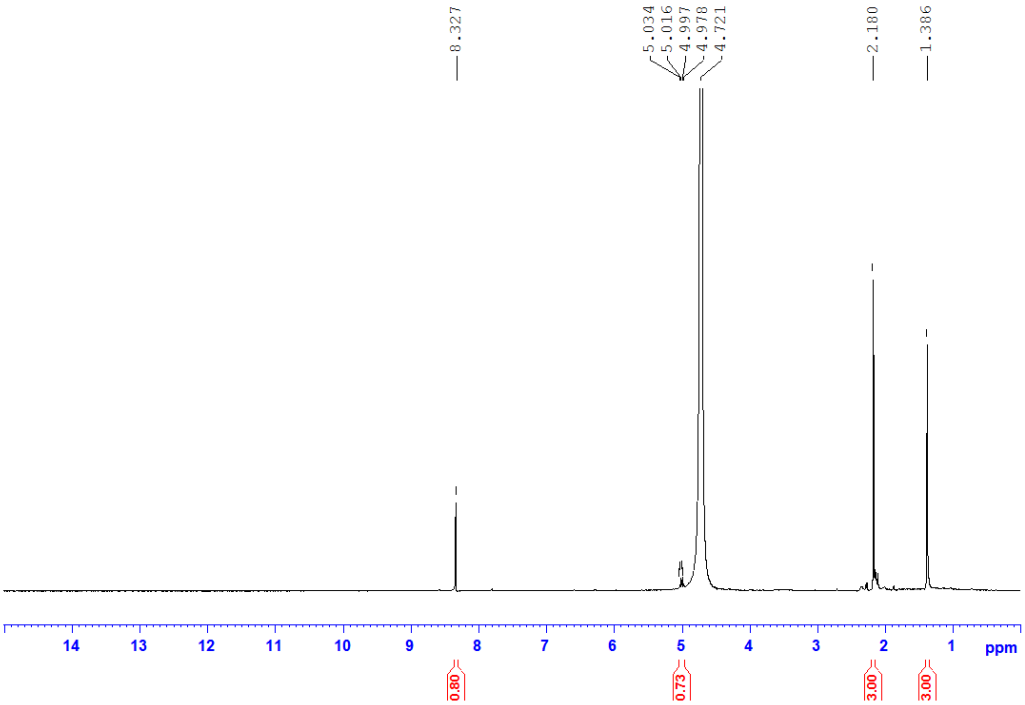

^{13}C-NMR

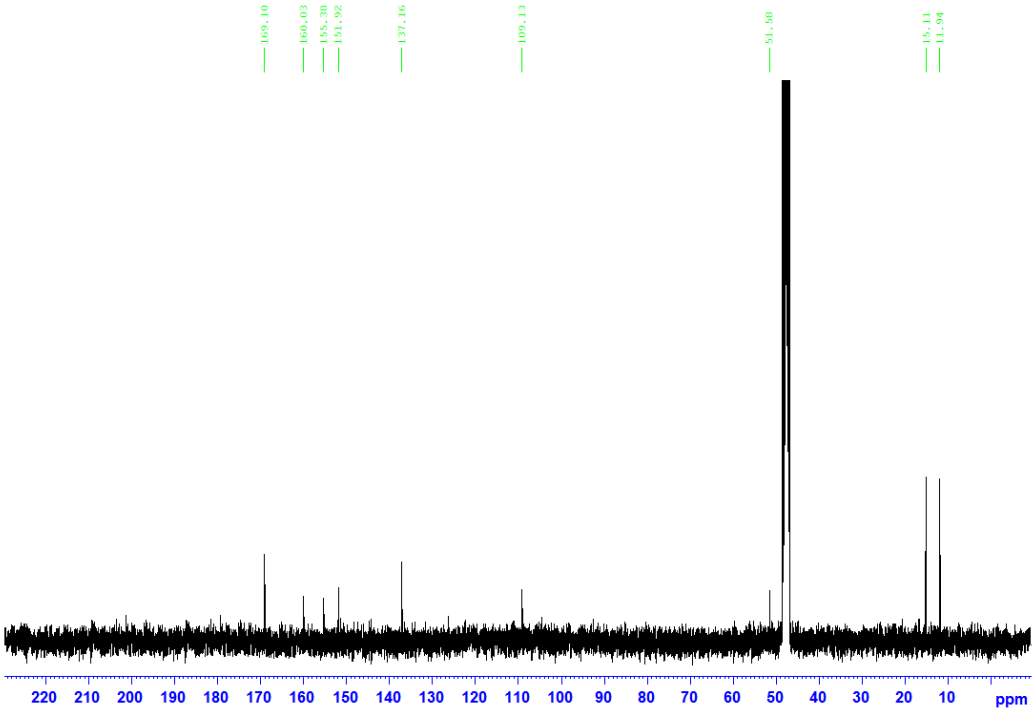

Compound 7c 3-methyl-2-(8-methyl-6-oxo-1,6-dihydro-9H-purin-9-yl)butanoic acid.

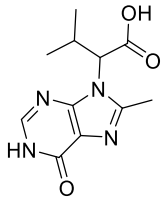

^{1}H-NMR

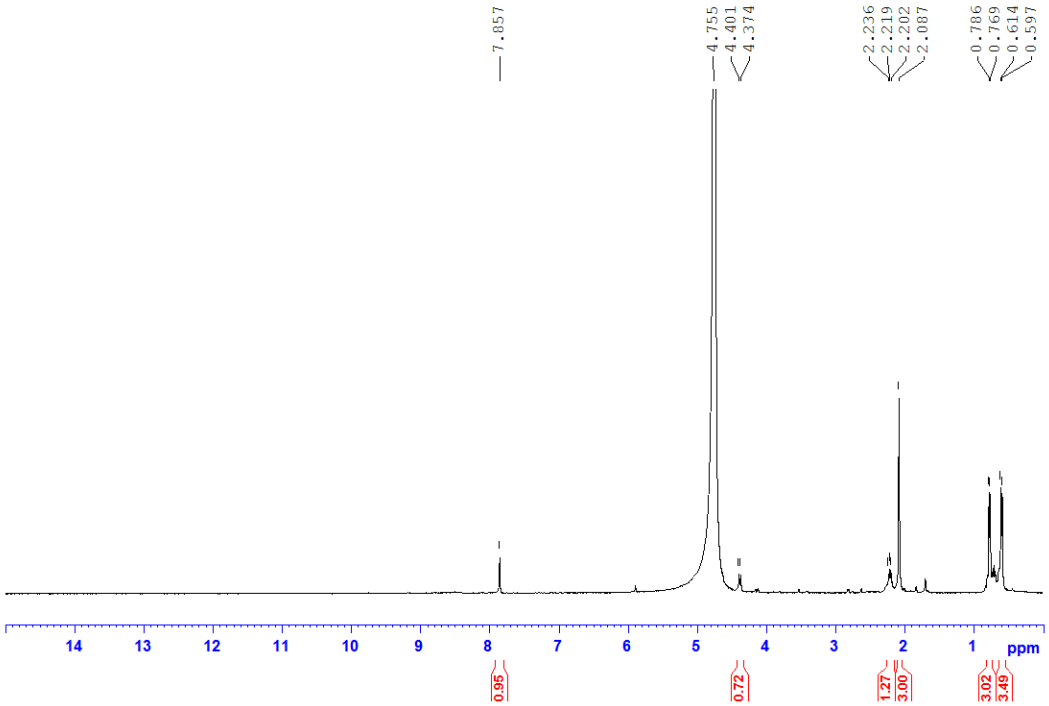

^{13}C-NMR

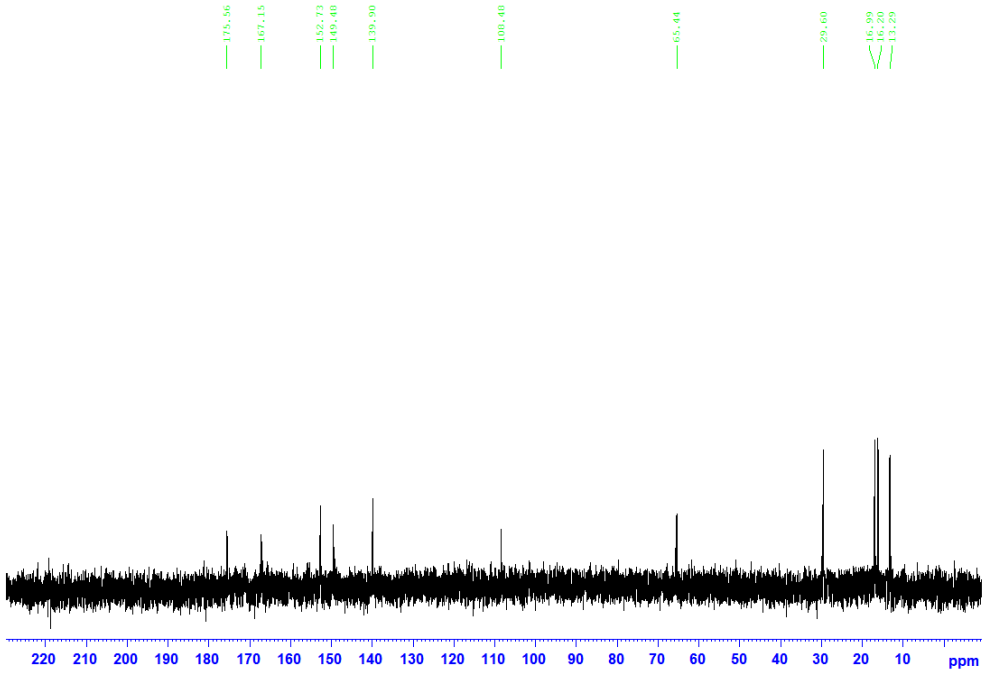

Compound 7d 3-hydroxy-2-(8-methyl-6-oxo-1,6-dihydro-9H-purin-9-yl)propanoic acid.

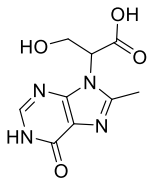

^{1}H-NMR

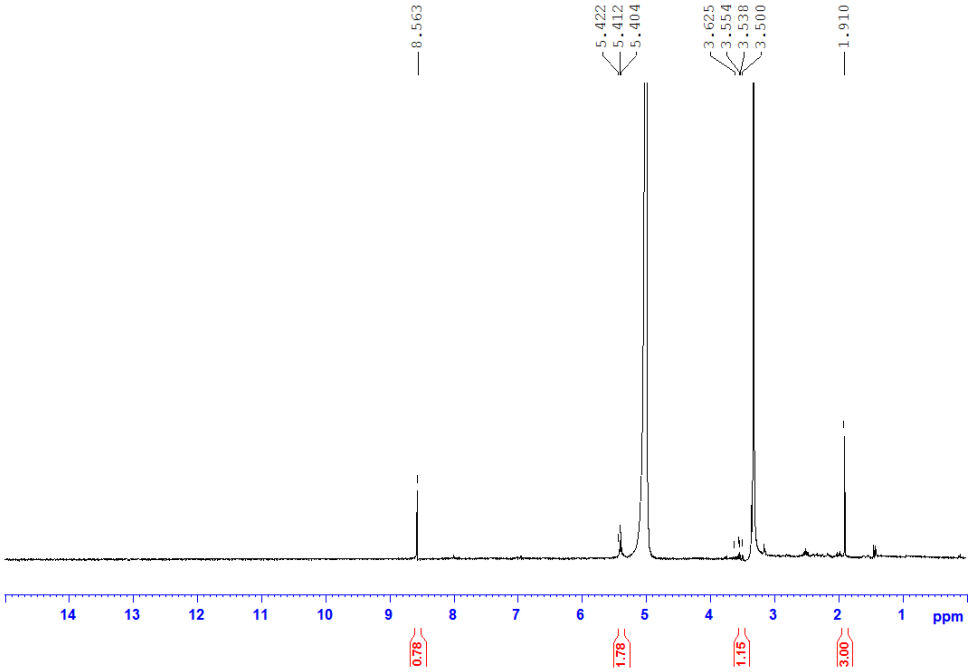

^{13}C-NMR

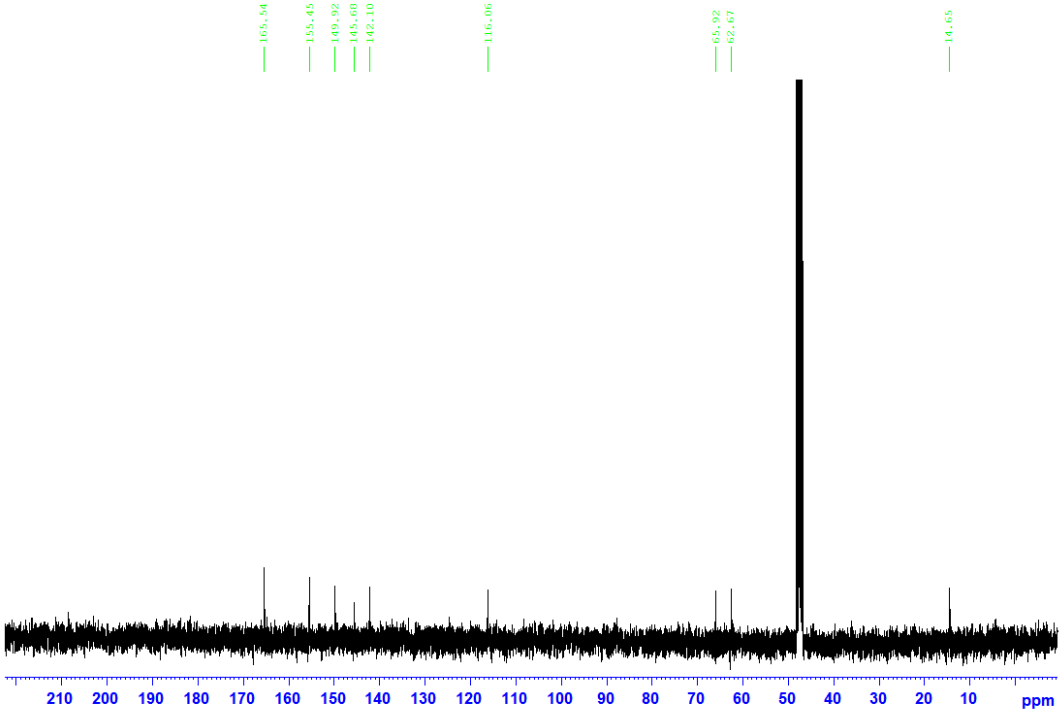

Compound 7e 2-(8-methyl-6-oxo-1,6-dihydro-9H-purin-9-yl)-3-phenylpropanoic acid.

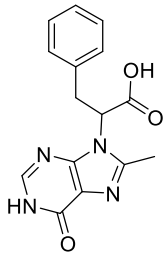

^{1}H-NMR

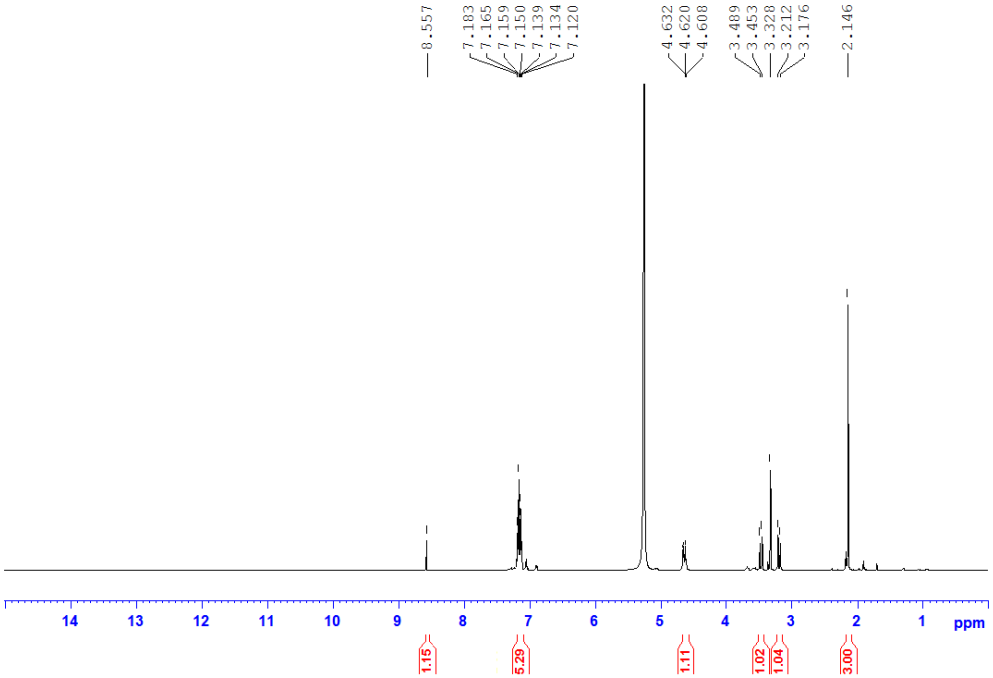

^{13}C-NMR

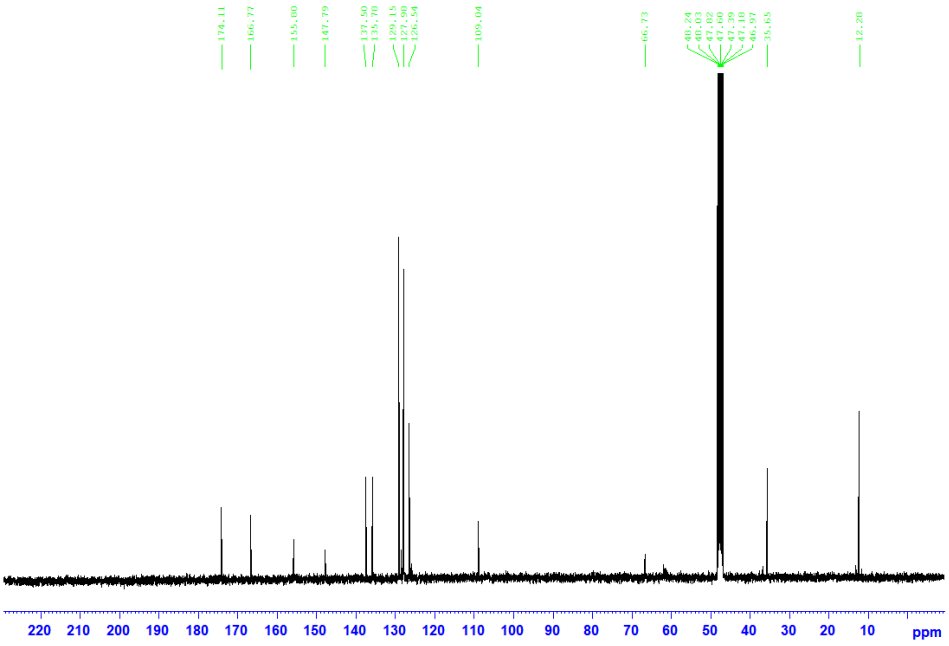

Compound 7f 3-(4-hydroxyphenyl)-2-(8-methyl-6-oxo-1,6-dihydro-9H-purin-9-yl)propanoic acid.

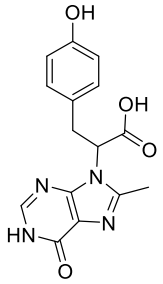

^{1}H-NMR

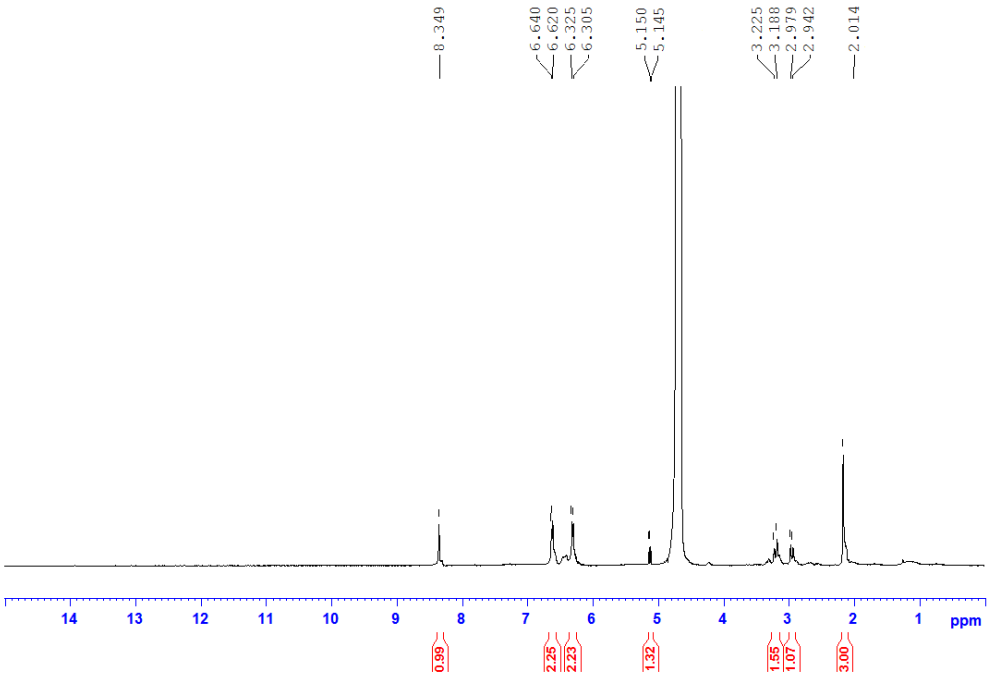

^{13}C-NMR

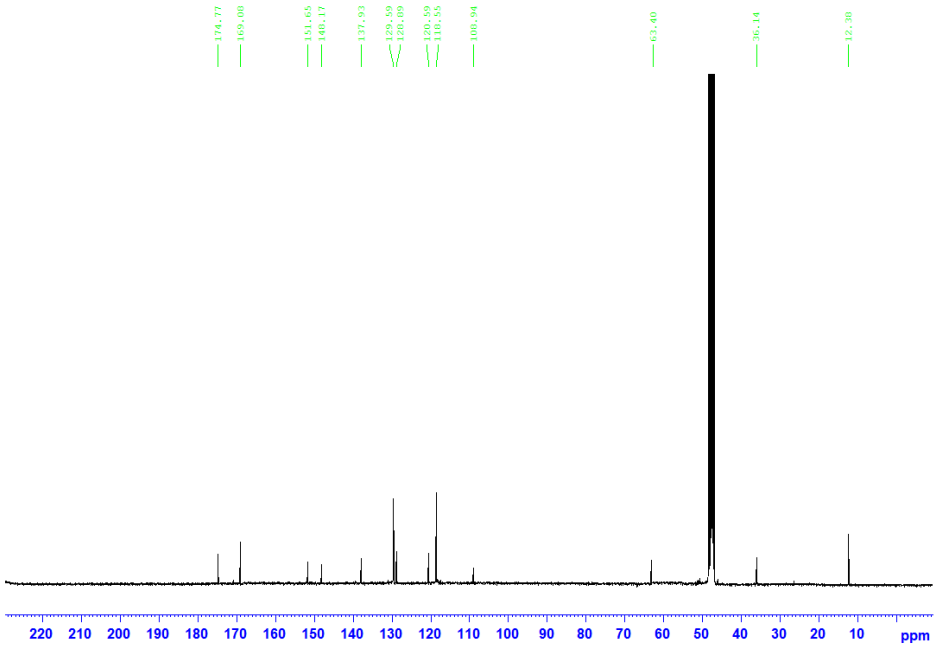

Compound 8a Methyl 2-(2,6-diamino-8-methyl-9H-purin-9-yl) acetate.

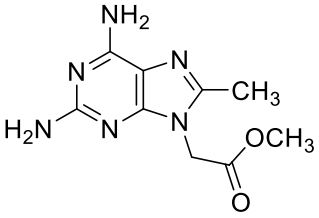

^{1}H-NMR

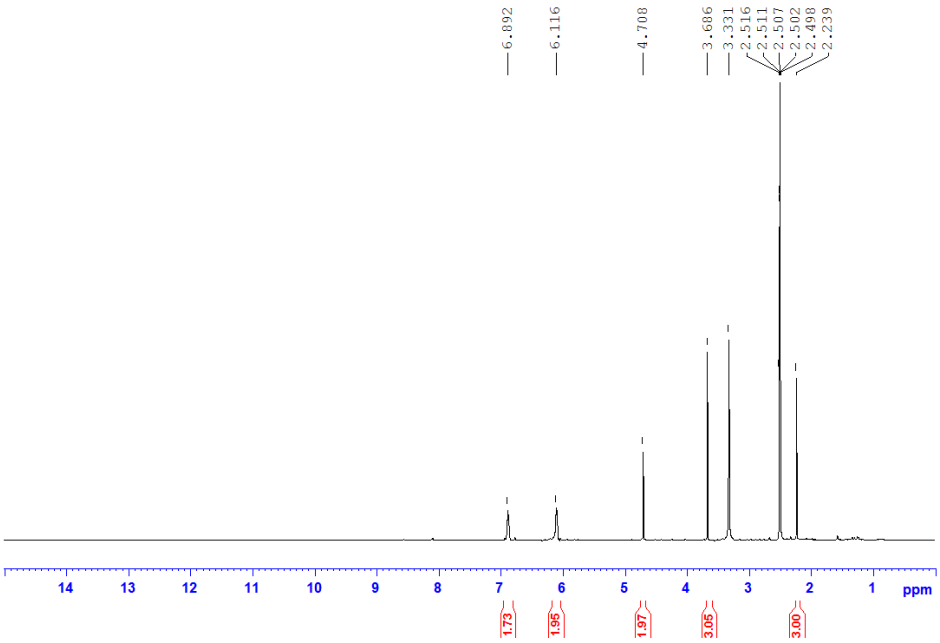

^{13}C-NMR

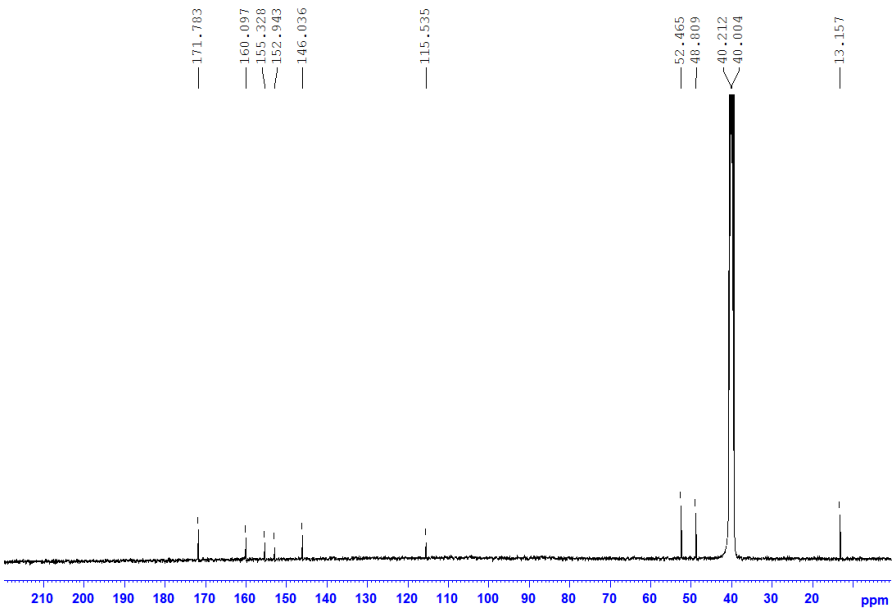

Compound 8b Methyl 2-(2,6-diamino-8-methyl-9H-purin-9-yl) propanoate.

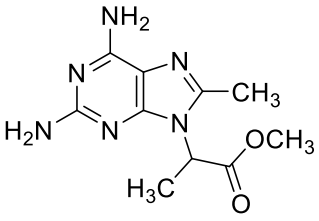

^{1}H-NMR

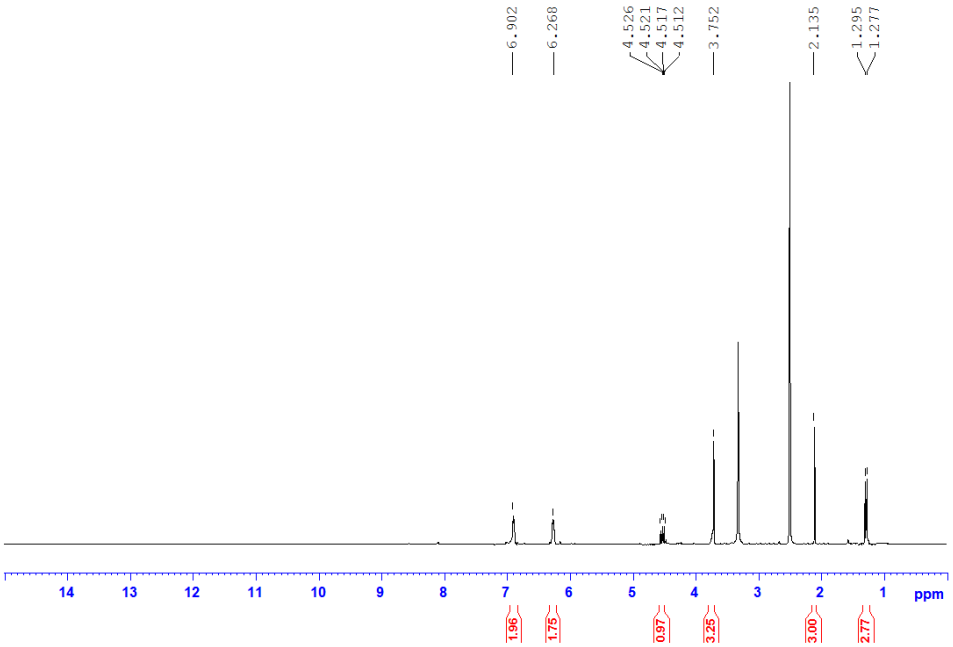

^{13}C-NMR

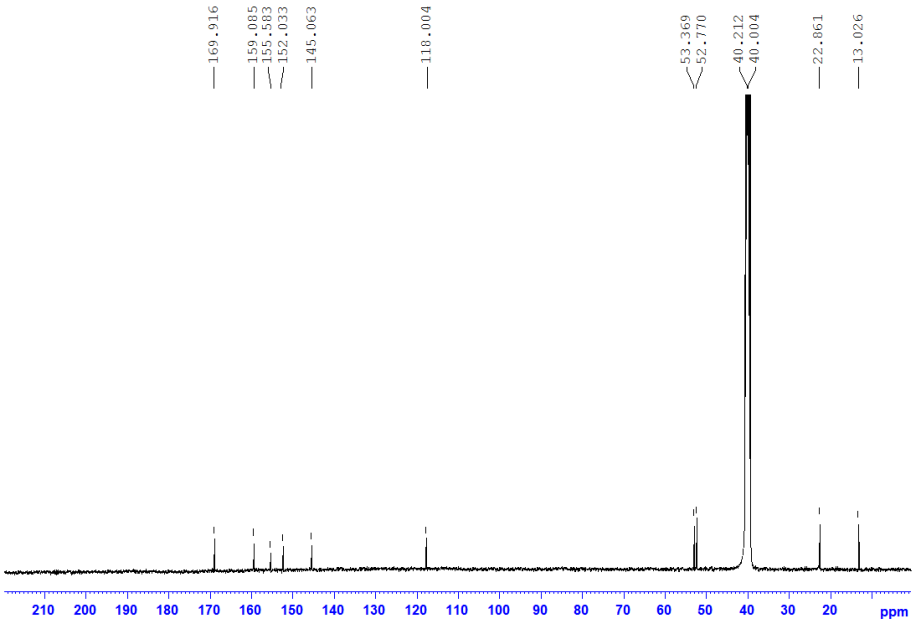

Compound 8c Methyl 2-(2,6-diamino-8-methyl-9H-purin-9-yl)-3-methylbutanoate.

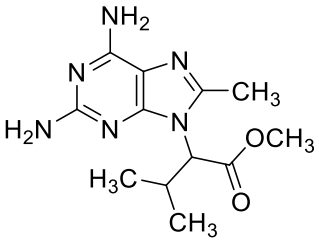

^{1}H-NMR

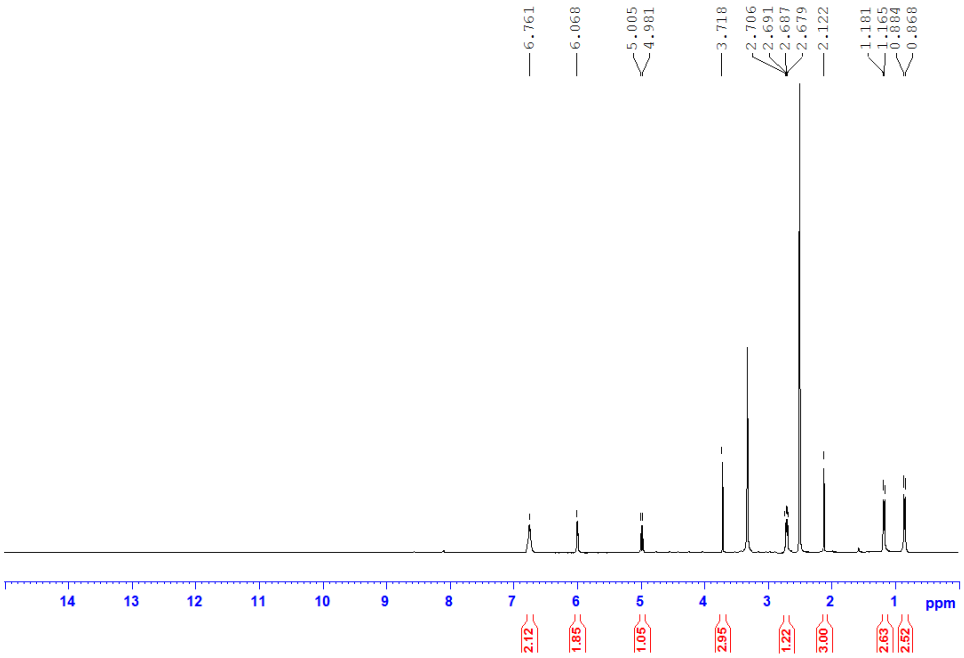

^{13}C-NMR

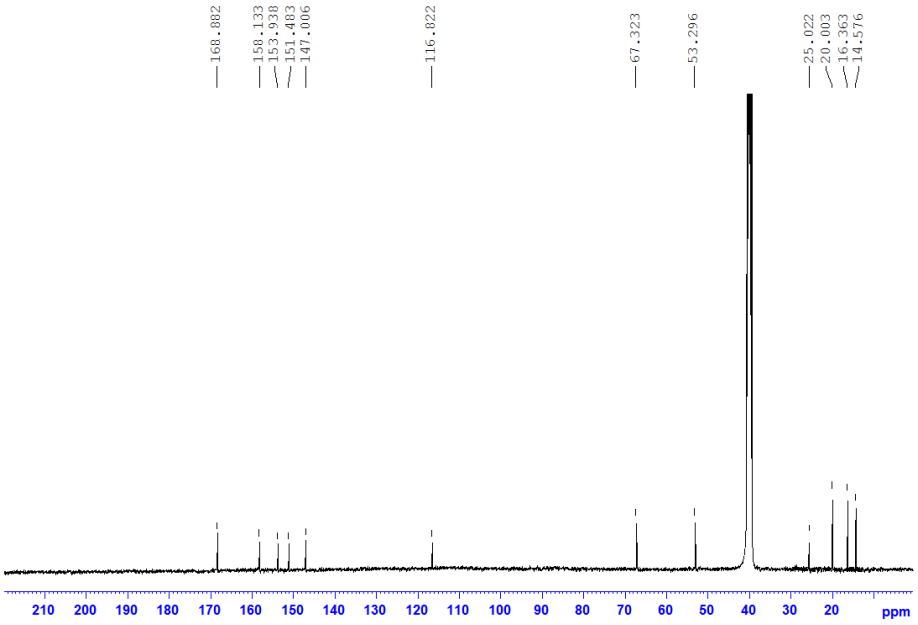

Compound 8d Methyl 2-(2,6-diamino-8-methyl-9H-purin-9-yl)-3-hydroxypropanoate.

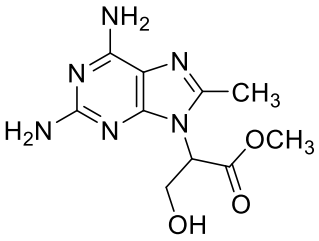

^{1}H-NMR

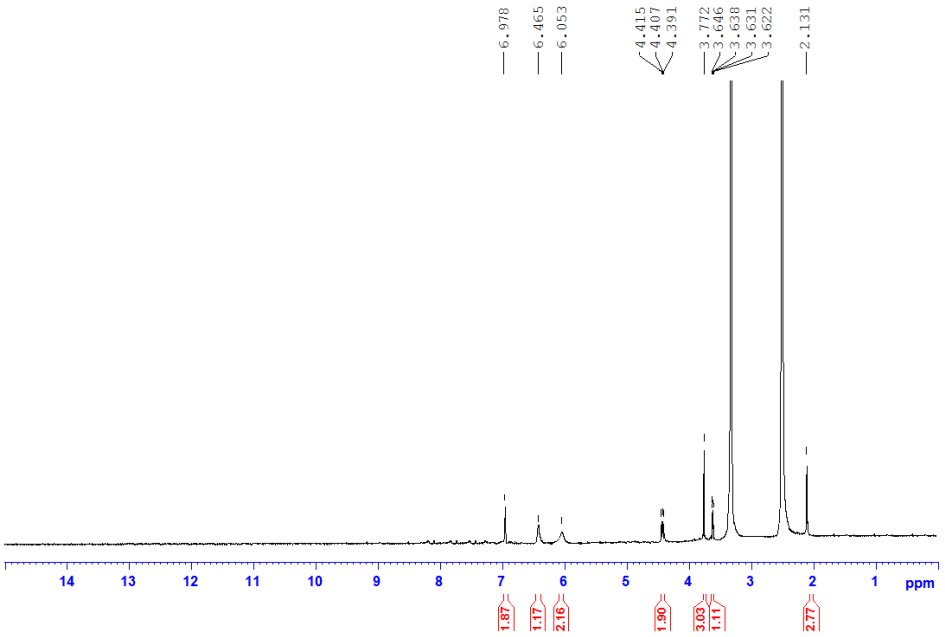

^{13}C-NMR

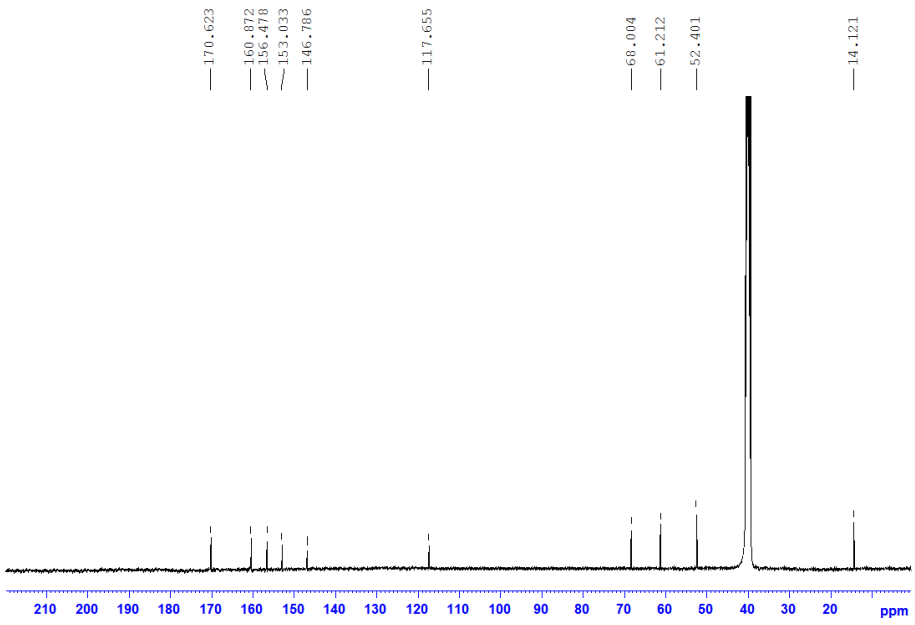

Compound 8e Methyl 2-(2,6-diamino-8-methyl-9H-purin-9-yl)-3-phenylpropanoate.

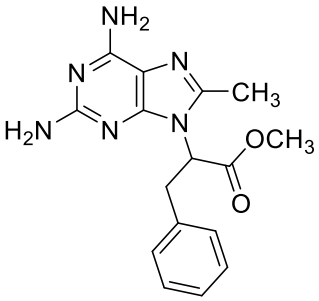

^{1}H-NMR

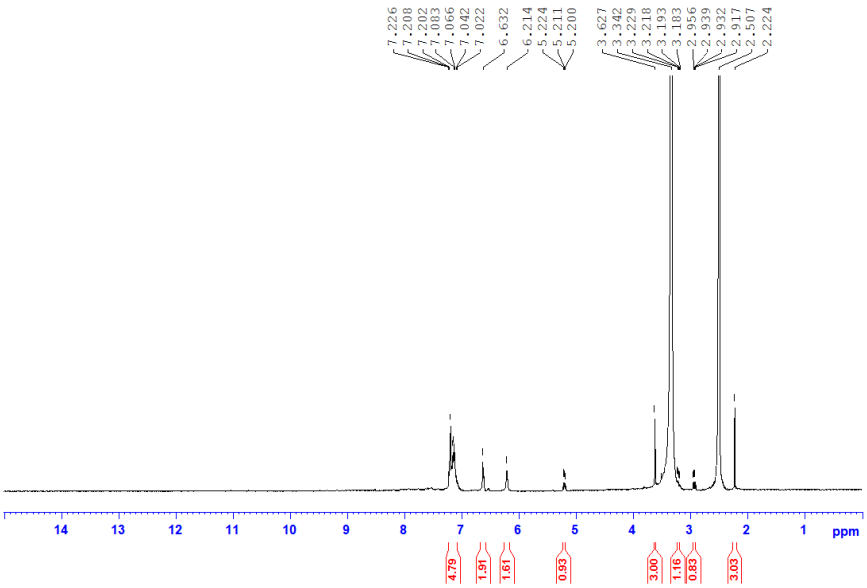

^{13}C-NMR

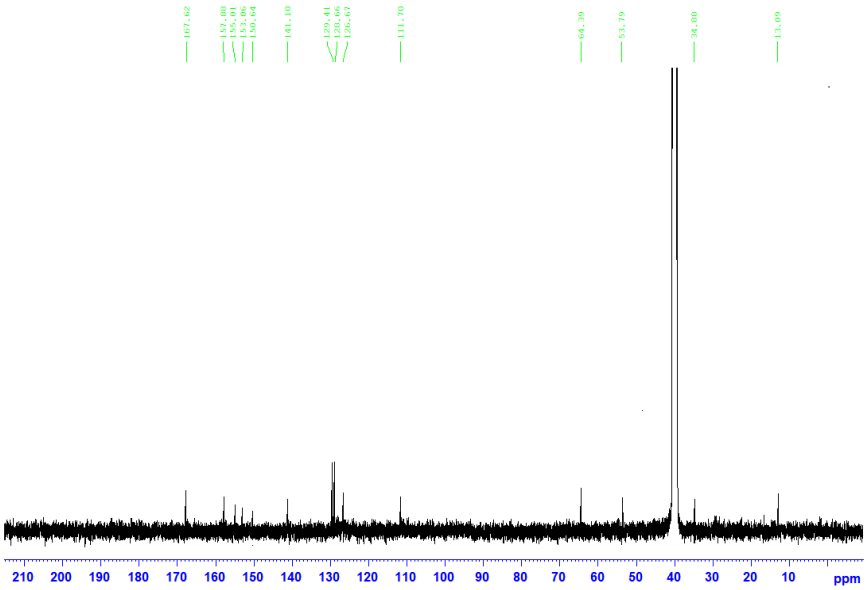

Compound 8f Methyl 2-(2,6-diamino-8-methyl-9H-purin-9-yl)-3-(4-hydroxyphenyl) propanoate.

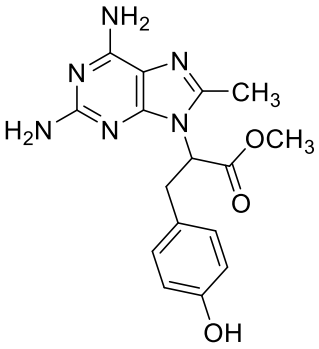

^{1}H-NMR

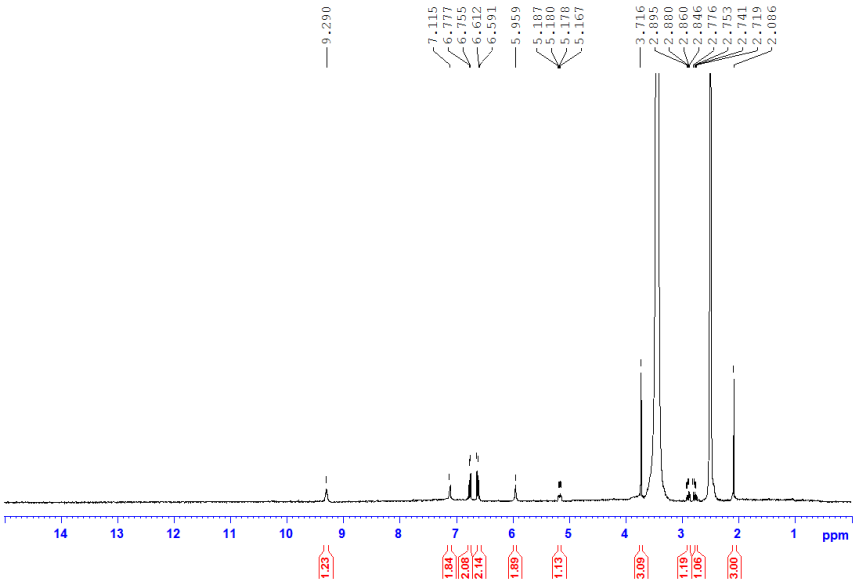

^{13}C-NMR

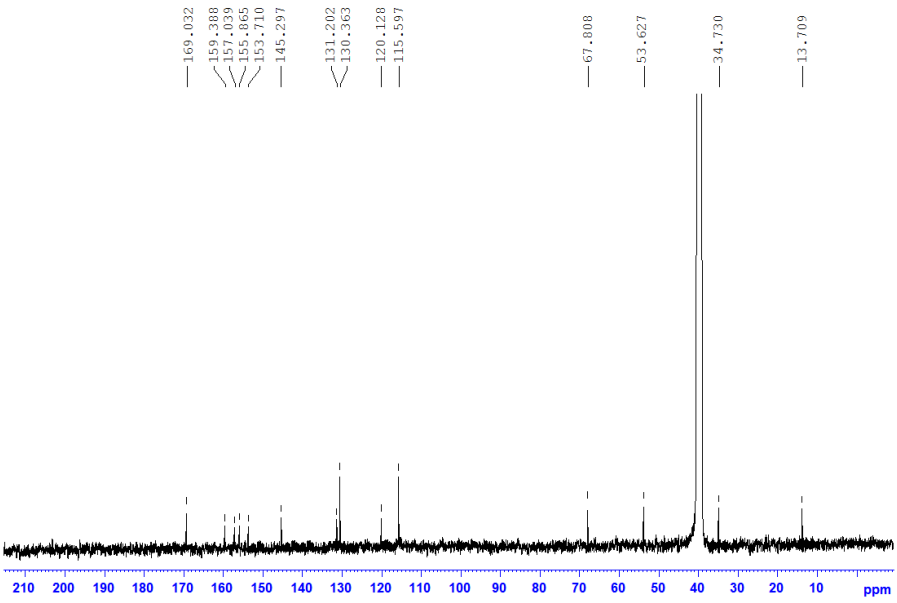

Compound 9a 2-(2,6-diamino-8-methyl-9H-purin-9-yl) acetic acid.

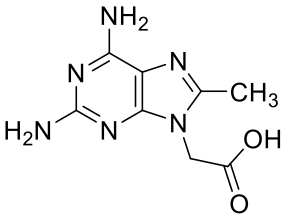

^{1}H-NMR

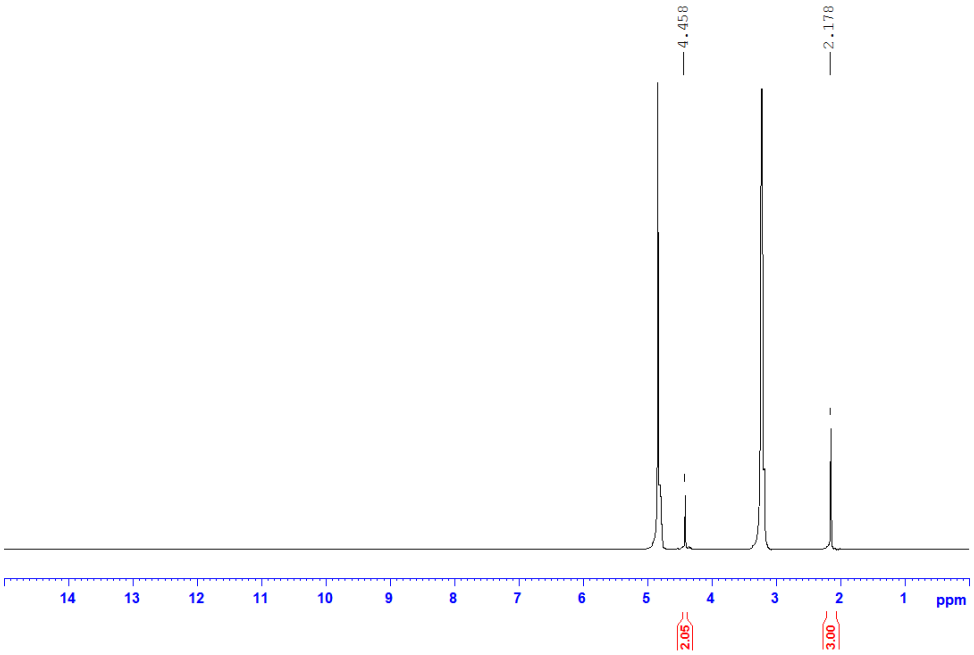

^{13}C-NMR

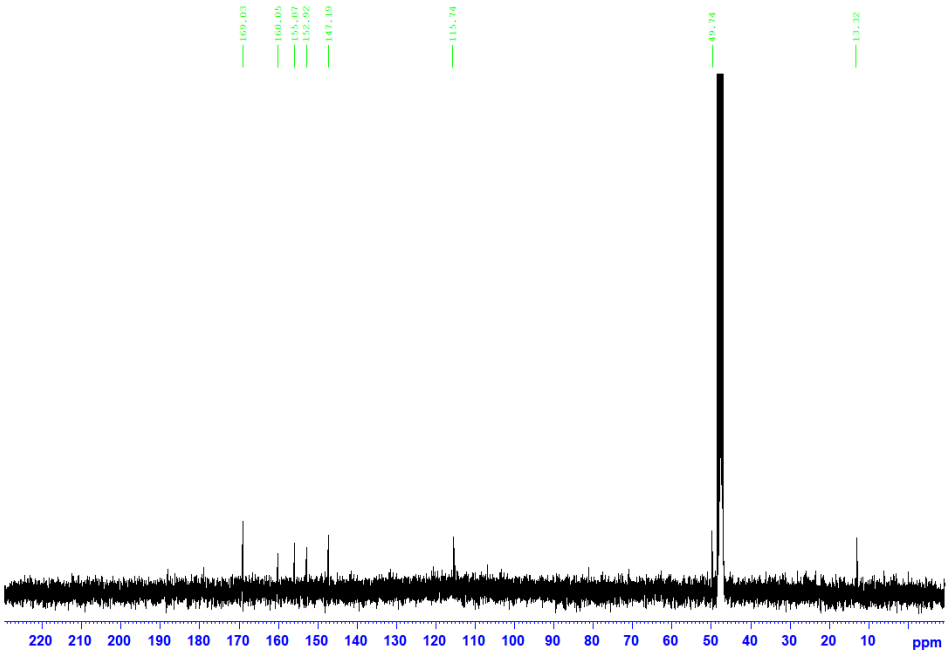

Compound 9b 2-(2,6-diamino-8-methyl-9H-purin-9-yl)propanoic acid.

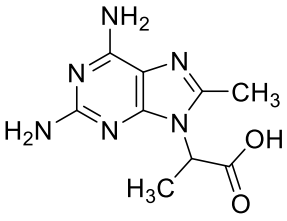

^{1}H-NMR

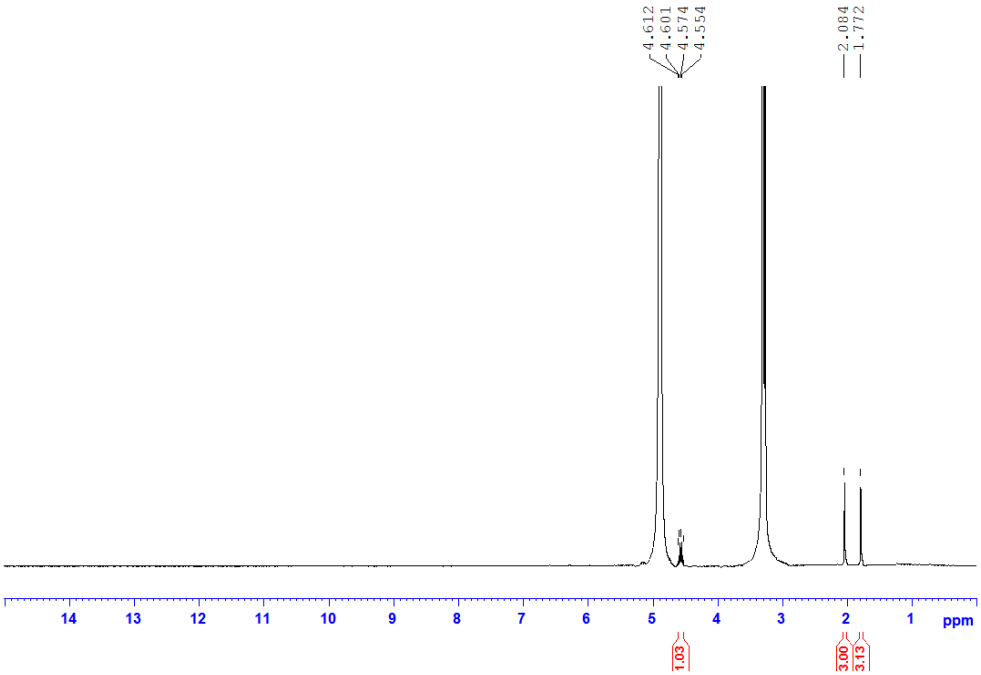

^{13}C-NMR

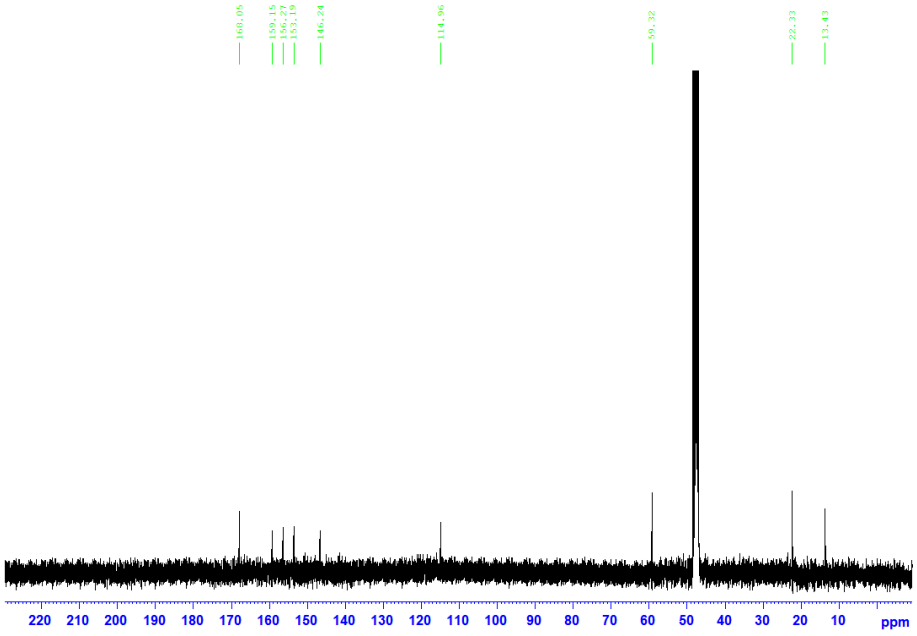

Compound 9c 2-(2,6-diamino-8-methyl-9H-purin-9-yl)-3-methylbutanoic acid.

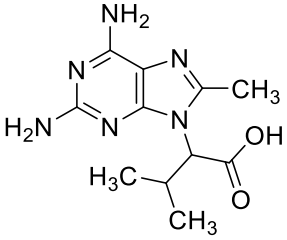

^{1}H-NMR

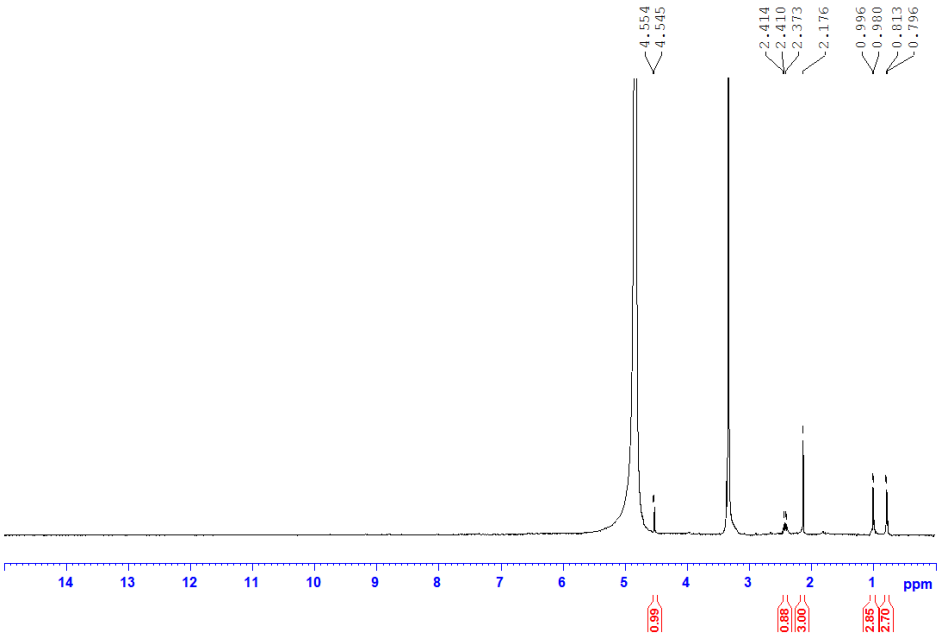

^{13}C-NMR

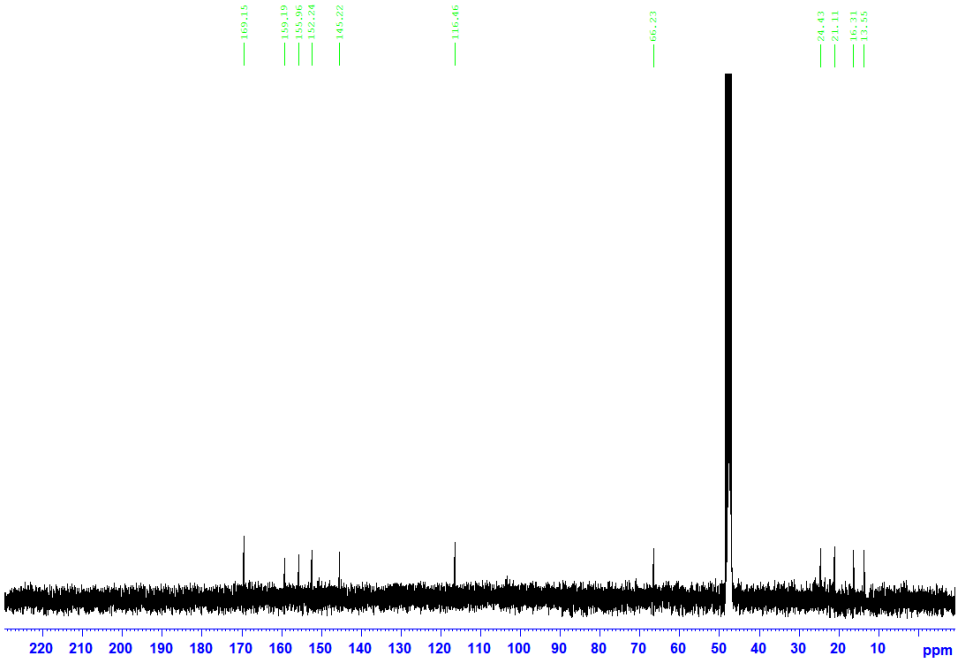

Compound 9d 2-(2,6-diamino-8-methyl-9H-purin-9-yl)-3-hydroxypropanoic acid.

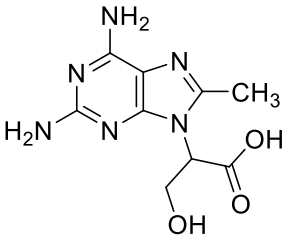

^{1}H-NMR

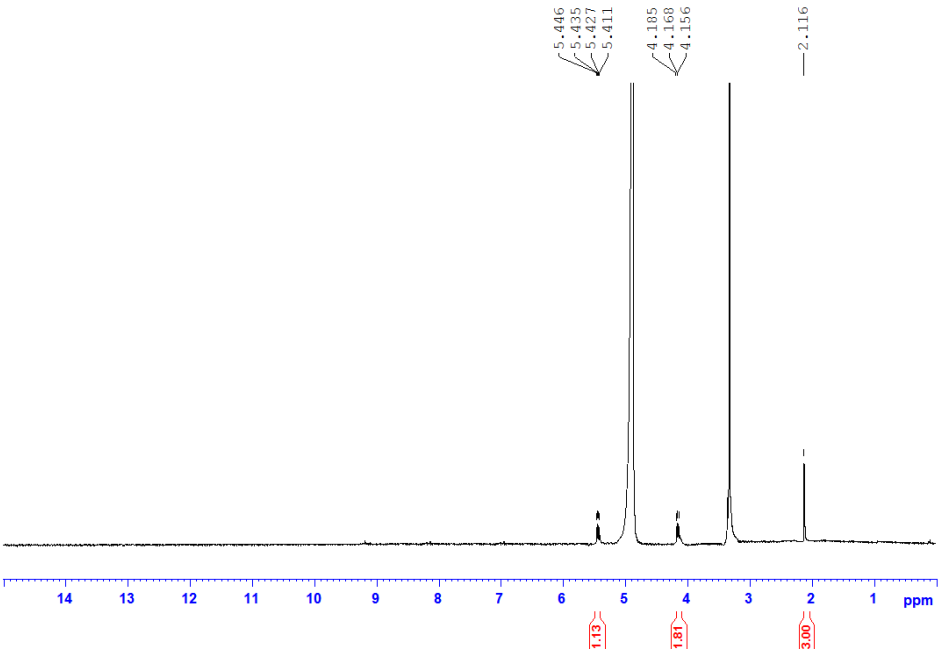

^{13}C-NMR

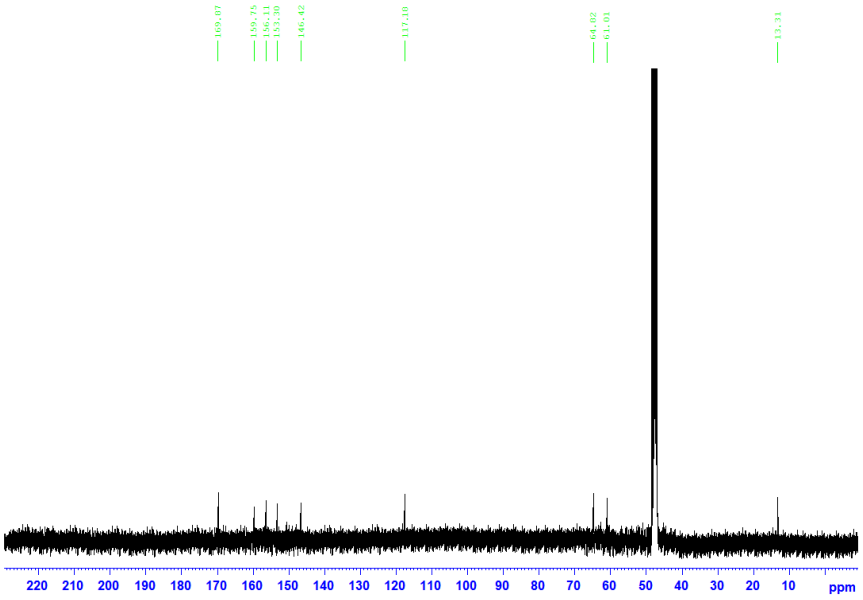

Compound 9e 2-(2,6-diamino-8-methyl-9H-purin-9-yl)-3-phenylpropanoic acid.

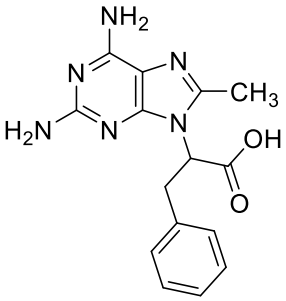

^{1}H-NMR

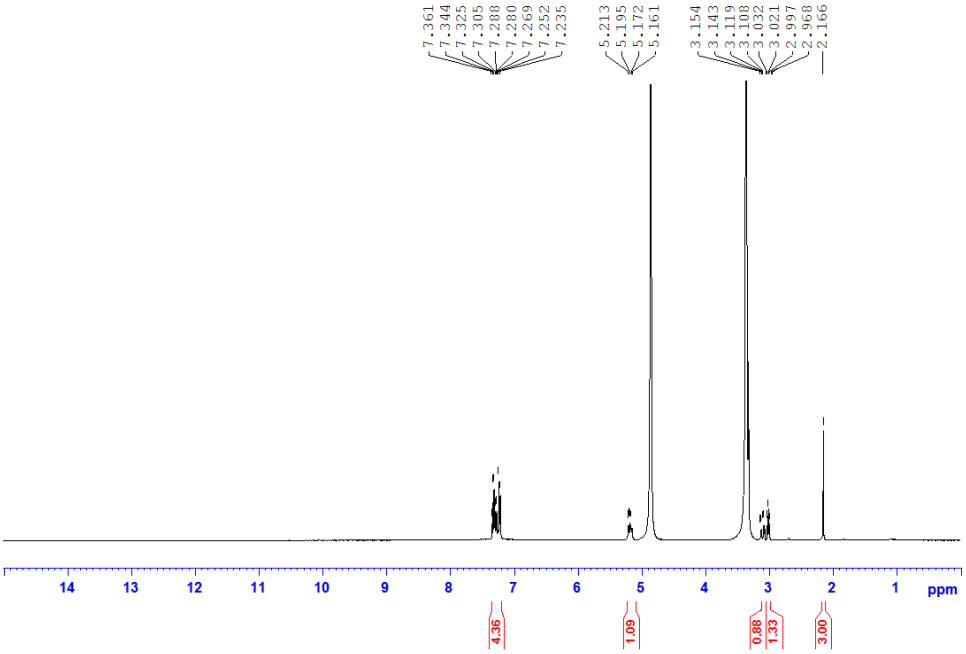

^{13}C-NMR

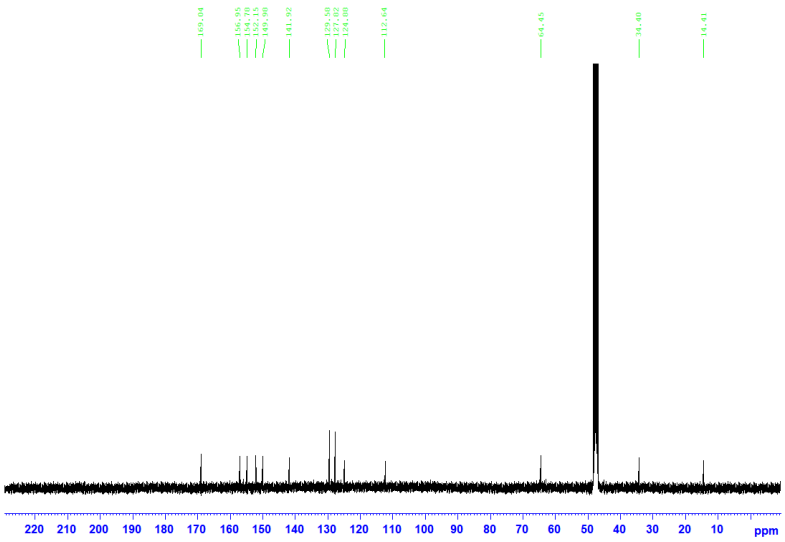

Compound 9f 2-(2,6-diamino-8-methyl-9H-purin-9-yl)-3-(4-hydroxyphenyl) propanoic acid.

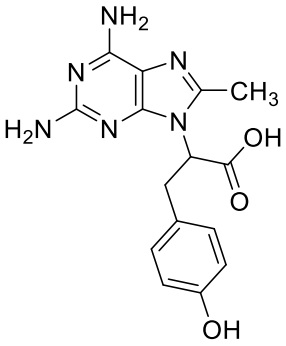

^{1}H-NMR

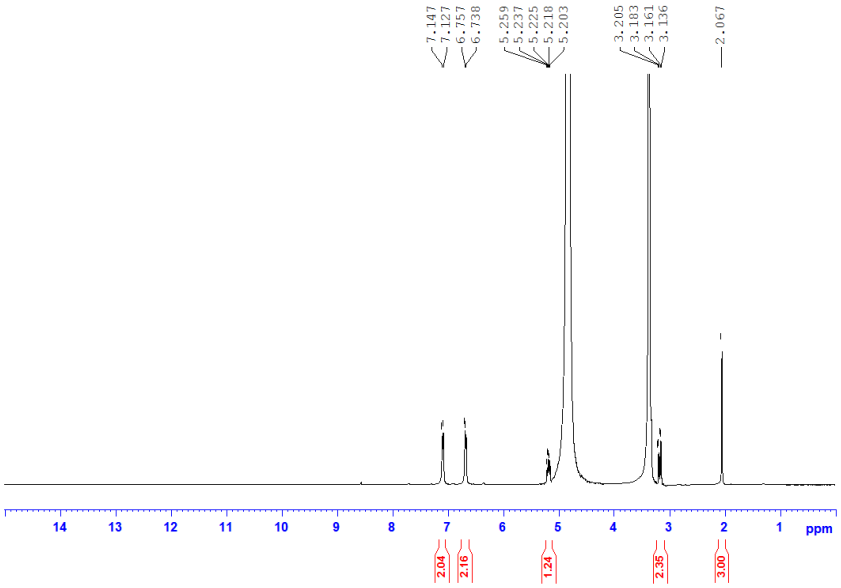

^{13}C-NMR

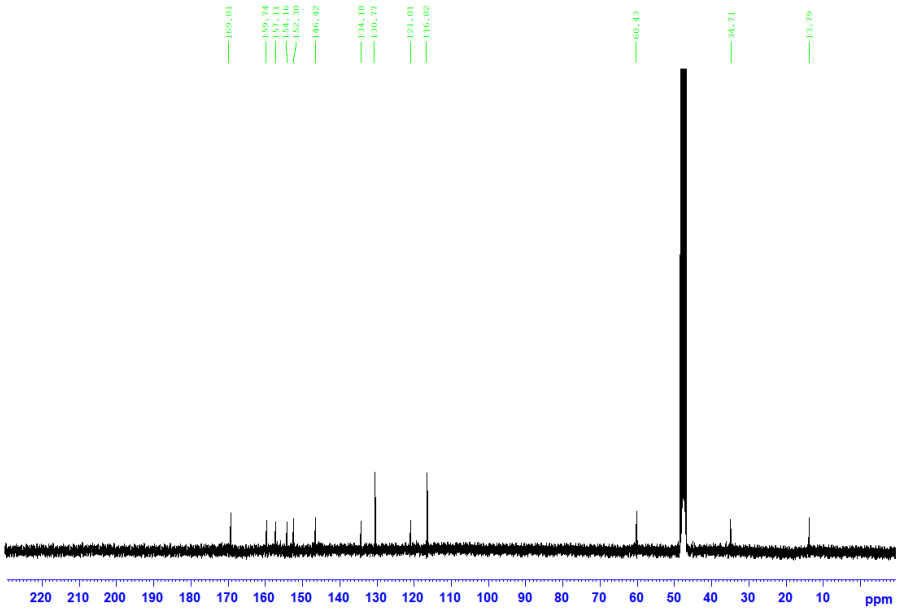

Compound 10a Methyl 2-(6-amino-8-methyl-2-oxo-2,3-dihydro-9H-purin-9-yl) acetate.

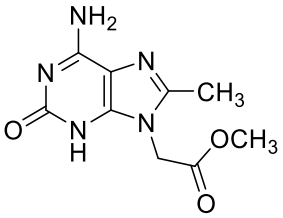

^{1}H-NMR

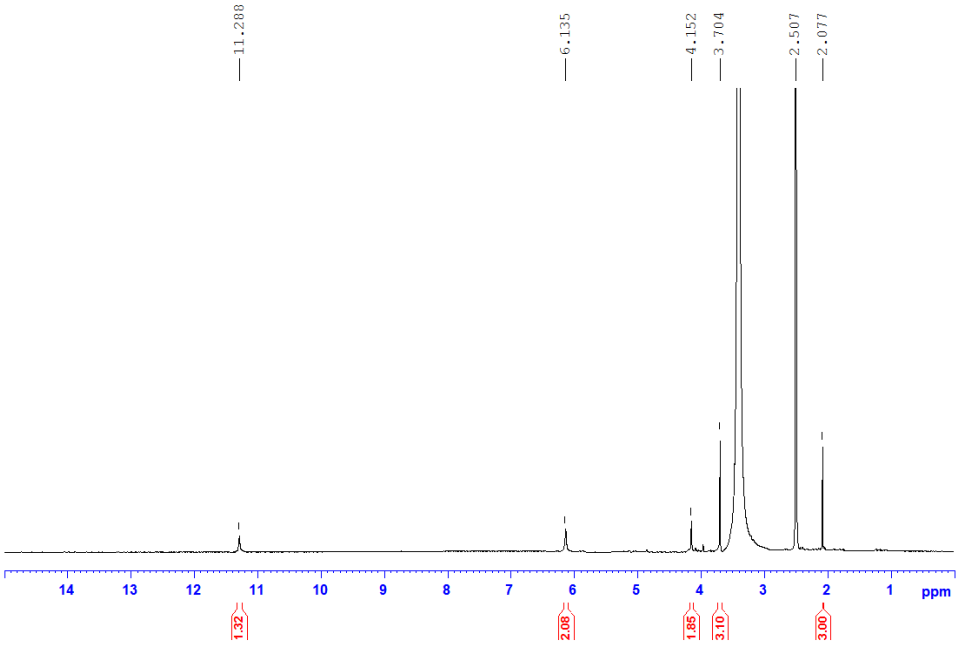

^{13}C-NMR

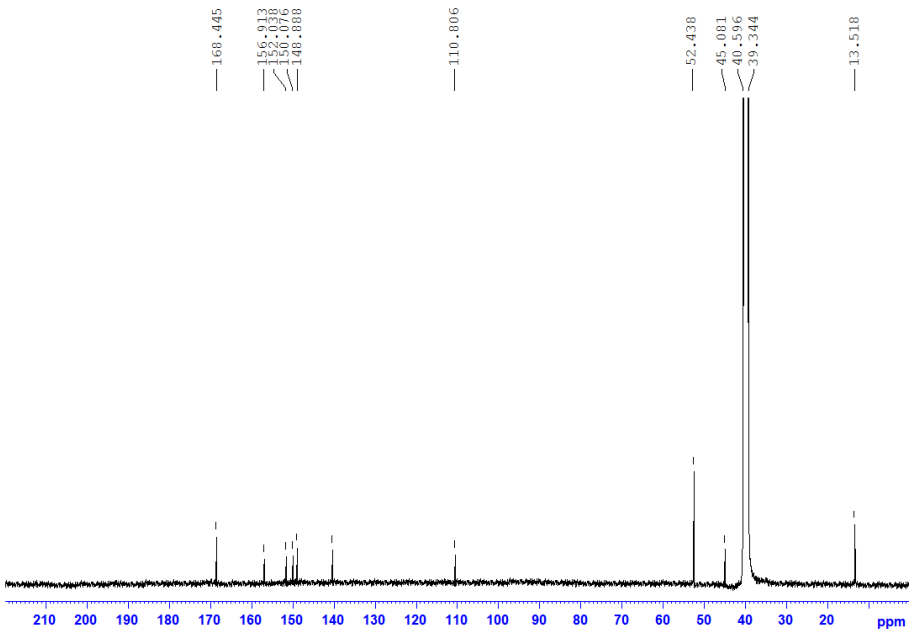

Compound 10b Methyl 2-(6-amino-8-methyl-2-oxo-2,3-dihydro-9H-purin-9-yl)propanoate.

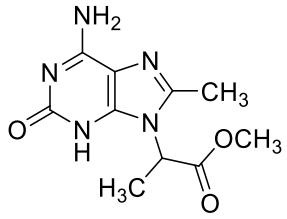

^{1}H-NMR

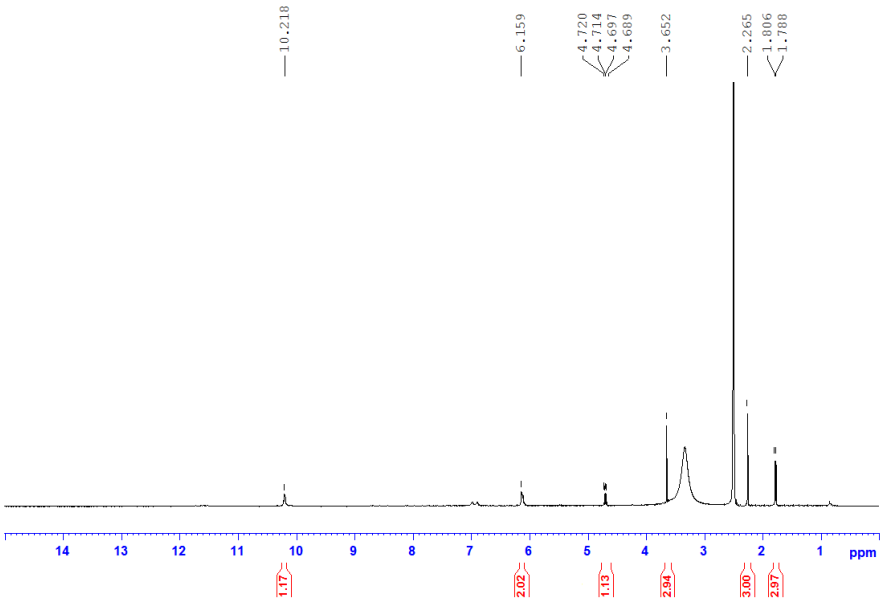

^{13}C-NMR

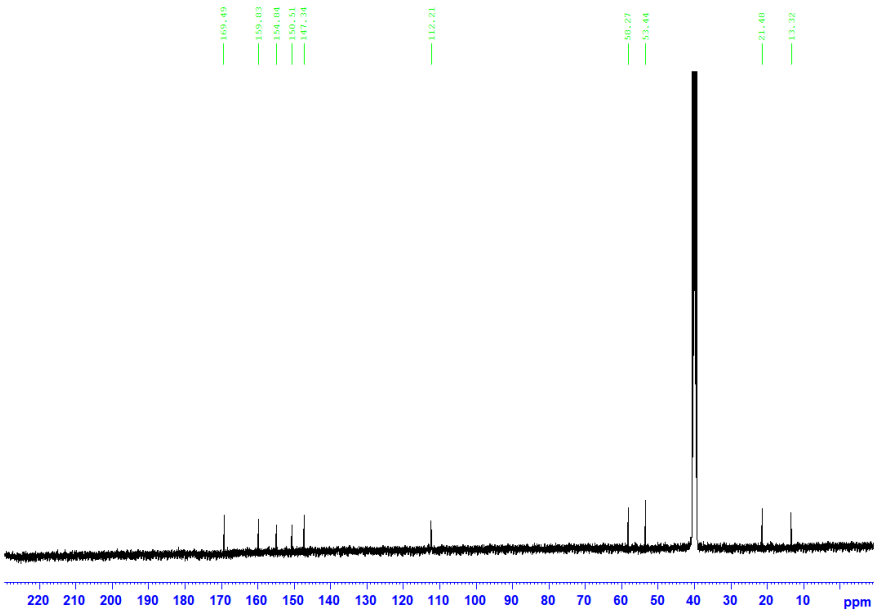

Compound 10c Methyl 2-(6-amino-8-methyl-2-oxo-2,3-dihydro-9H-purin-9-yl)-3-methylbutanoate.

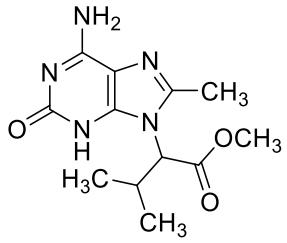

^{1}H-NMR

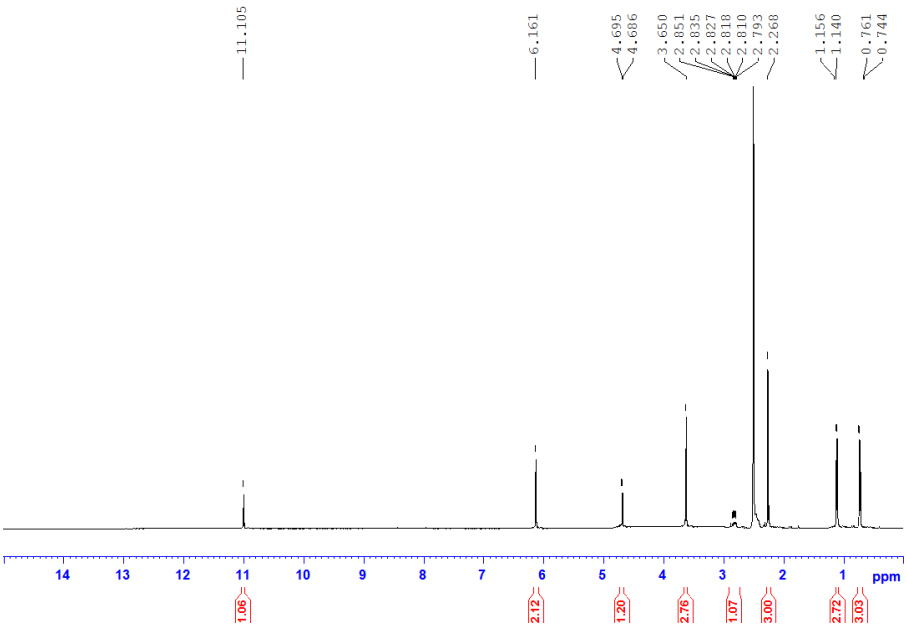

^{13}C-NMR

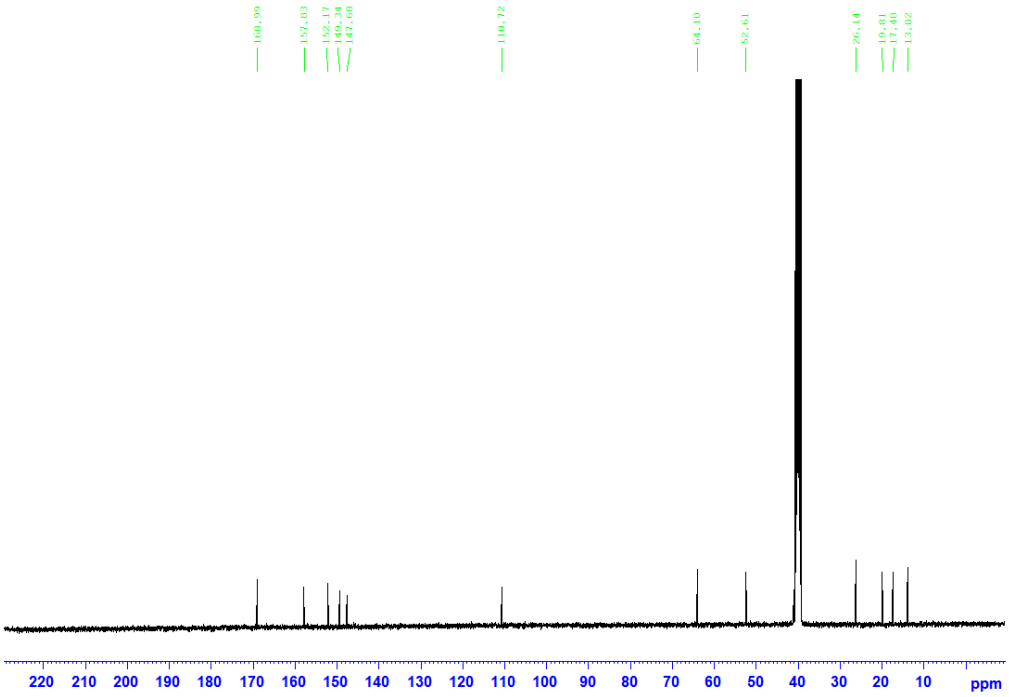

Compound 10d Methyl 2-(6-amino-8-methyl-2-oxo-2,3-dihydro-9H-purin-9-yl)-3-hydroxypropanoate.

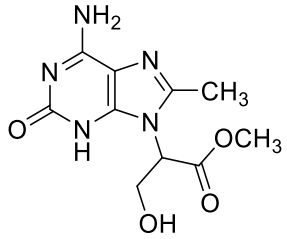

^{1}H-NMR

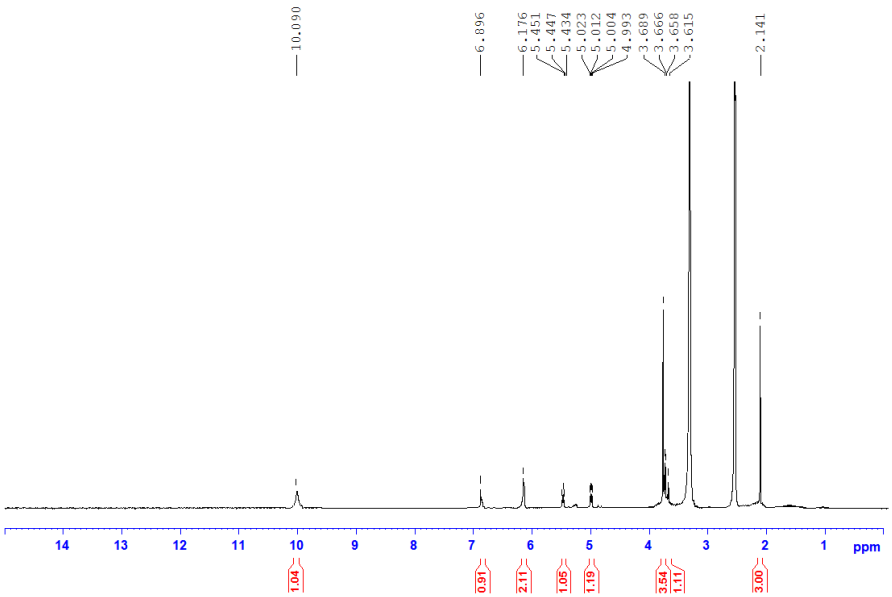

^{13}C-NMR

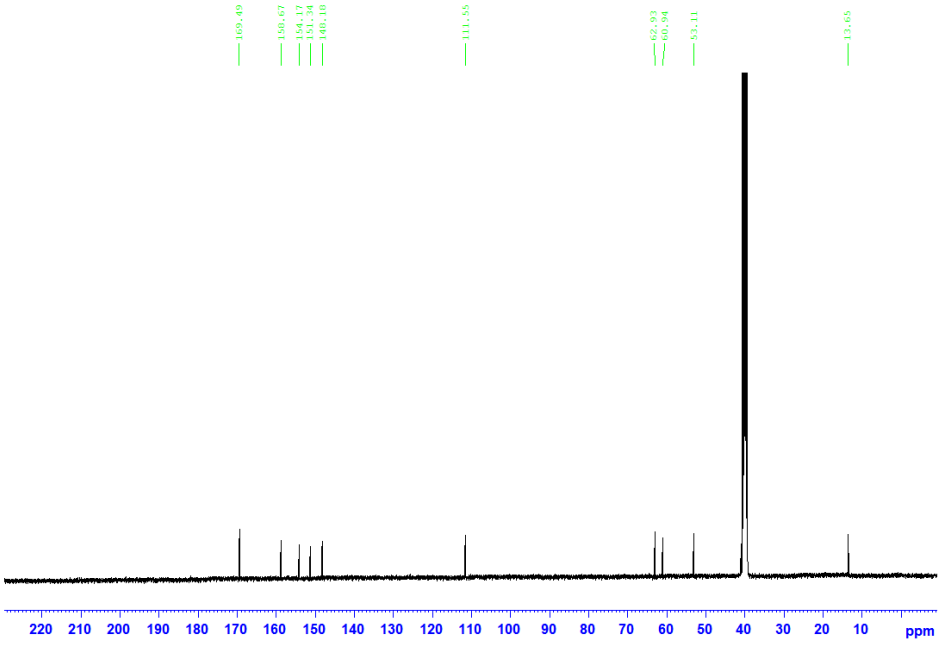

Compound 10e Methyl 2-(6-amino-8-methyl-2-oxo-2,3-dihydro-9H-purin-9-yl)-3-phenylpropanoate.

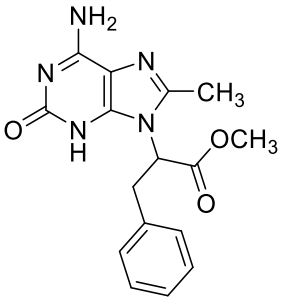

^{1}H-NMR

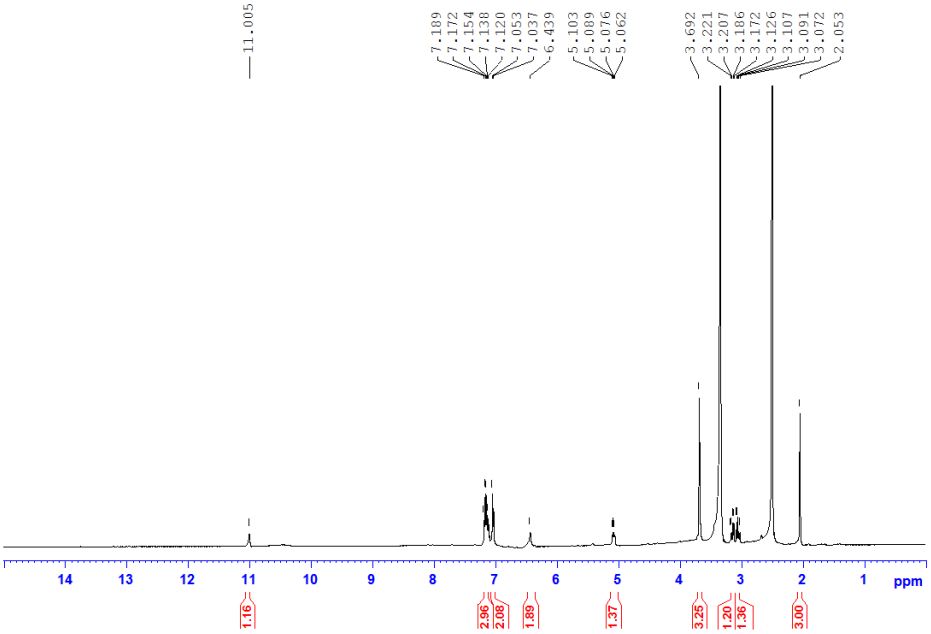

^{13}C-NMR

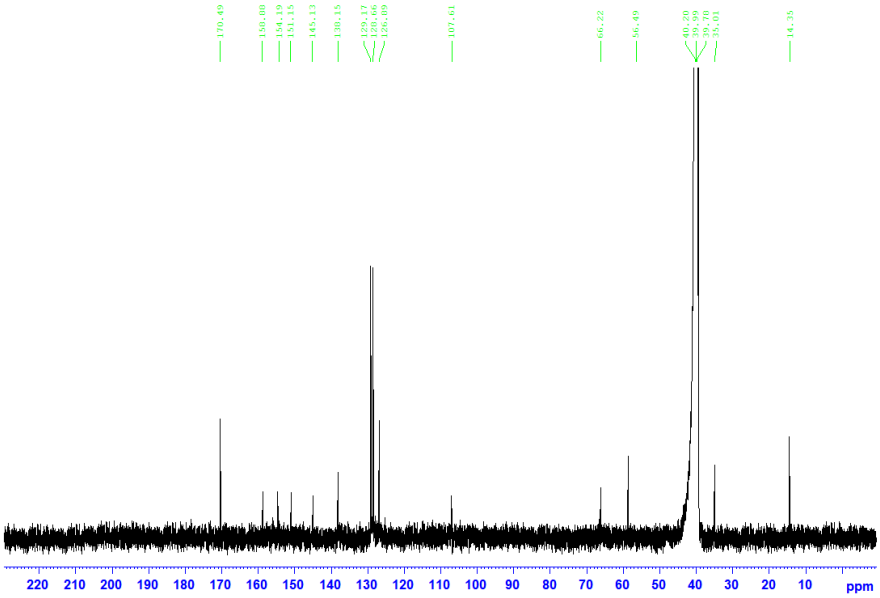

Compound 10f Methyl 2-(6-amino-8-methyl-2-oxo-2,3-dihydro-9H-purin-9-yl)-3-(4-hydroxyphenyl) propanoate.

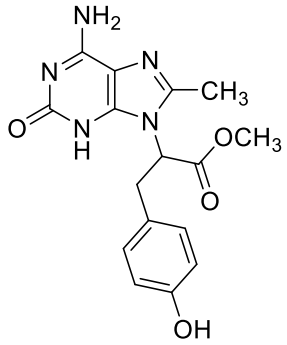

^{1}H-NMR

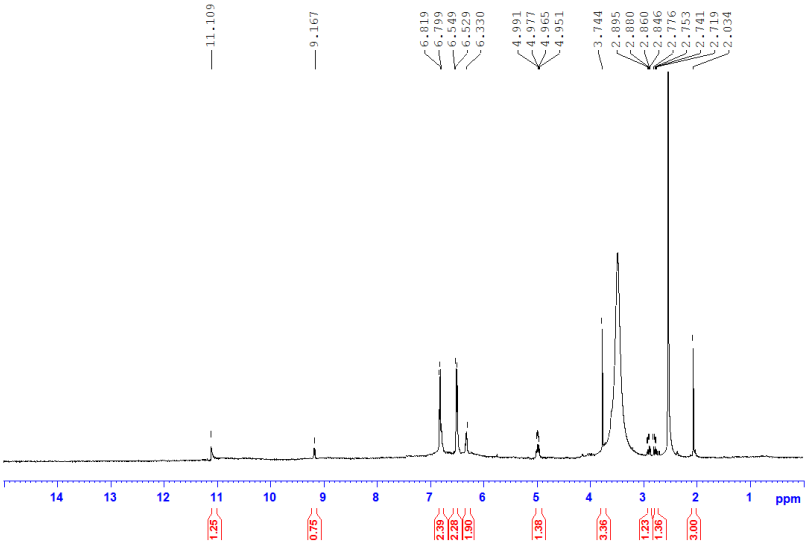

^{13}C-NMR

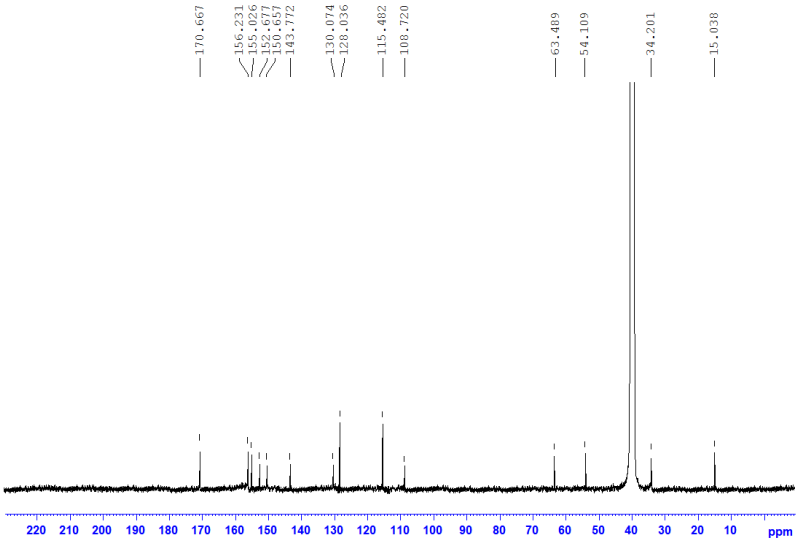

Compound 10g Methyl 2-(6-amino-8-methyl-2-oxo-2,3-dihydro-9H-purin-9-yl)-3-(1H-indol-3-yl)propanoate.

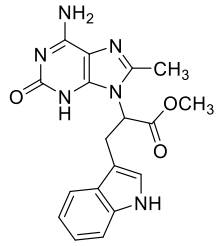

^{1}H-NMR

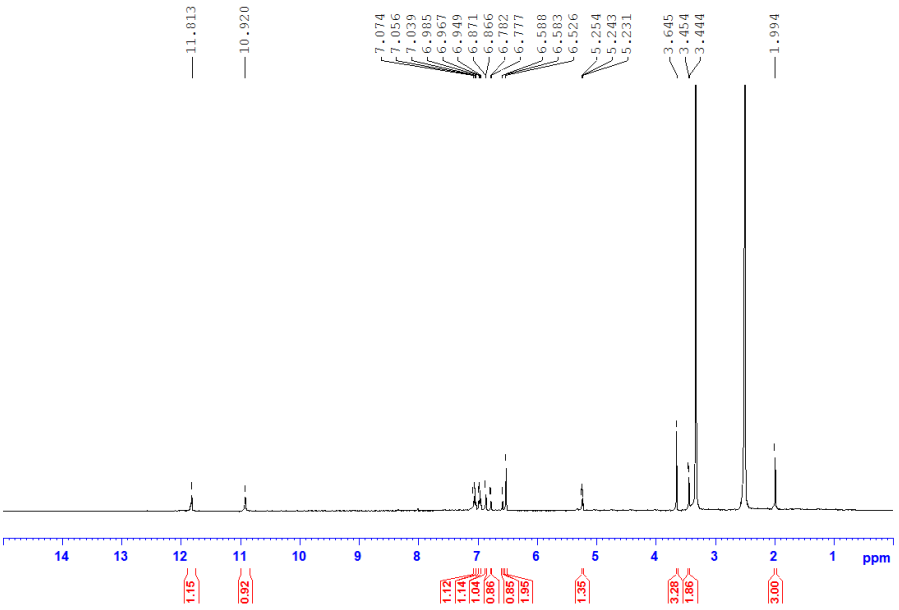

^{13}C-NMR

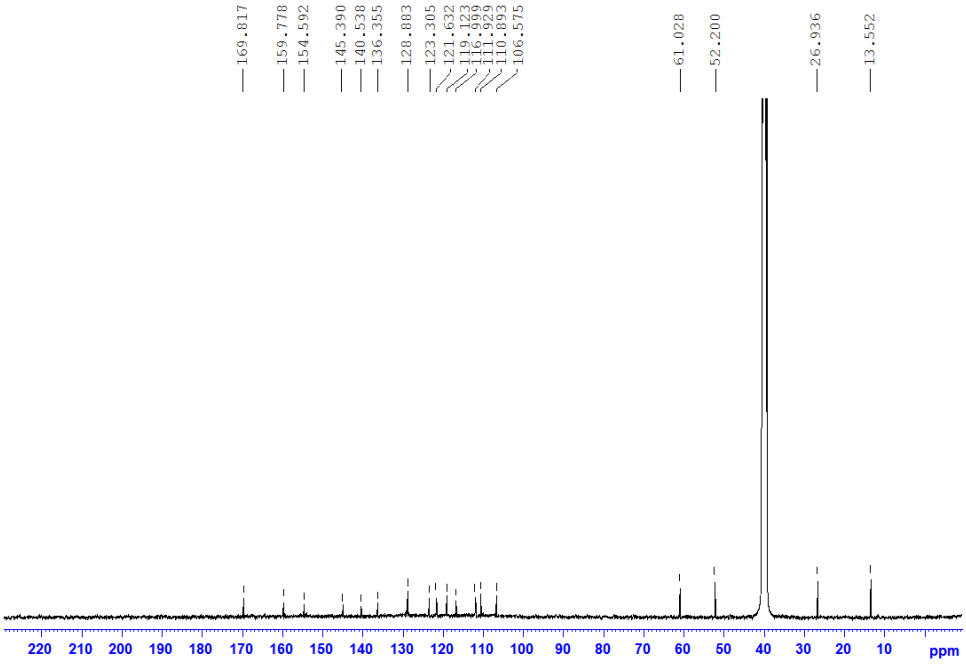

Compound 11a 2-(6-amino-8-methyl-2-oxo-2,3-dihydro-9H-purin-9-yl) acetic acid.

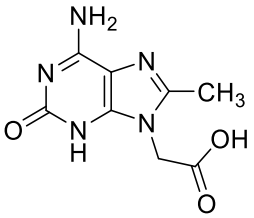

^{1}H-NMR

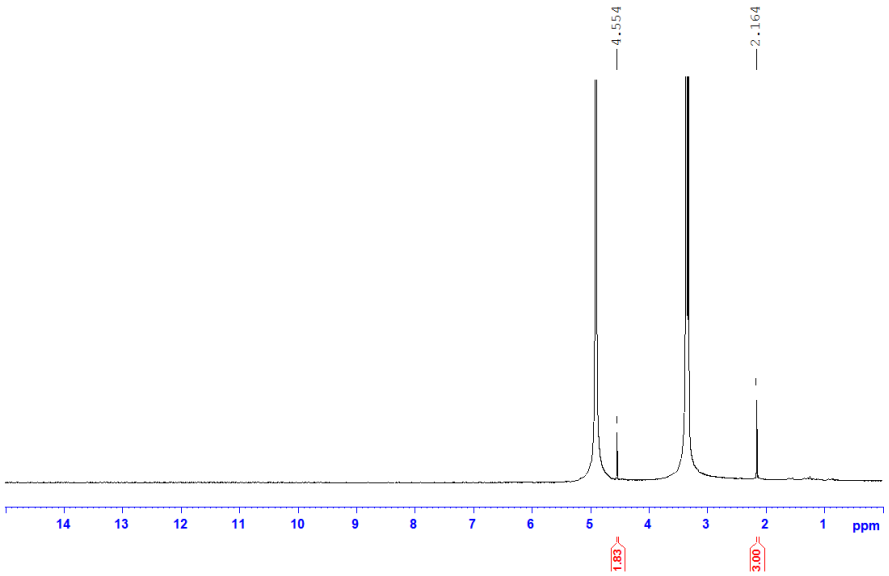

^{13}C-NMR

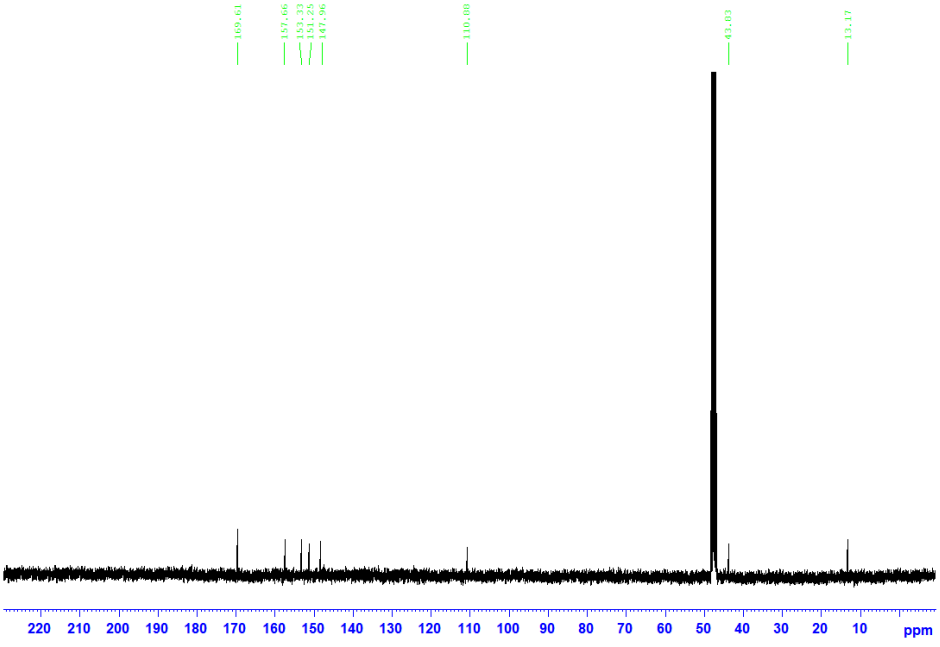

Compound 11b 2-(6-amino-8-methyl-2-oxo-2,3-dihydro-9H-purin-9-yl) propanoic acid.

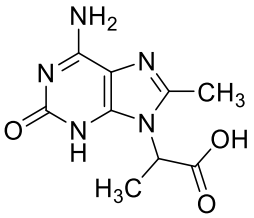

^{1}H-NMR

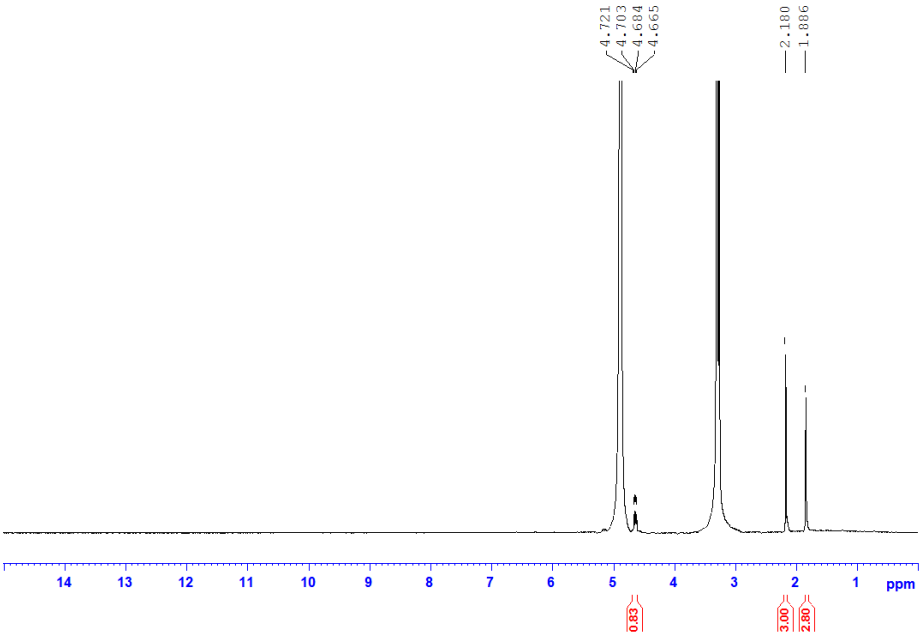

^{13}C-NMR

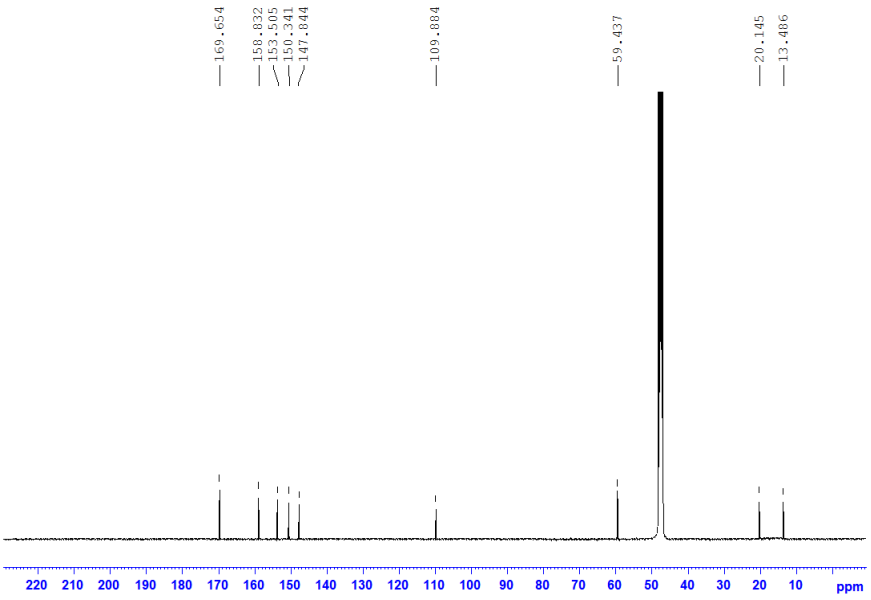

Compound 11c 2-(6-amino-8-methyl-2-oxo-2,3-dihydro-9H-purin-9-yl)-3-methylbutanoic acid.

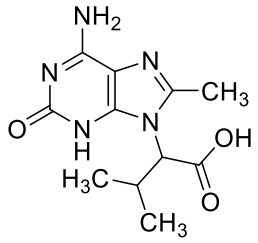

^{1}H-NMR

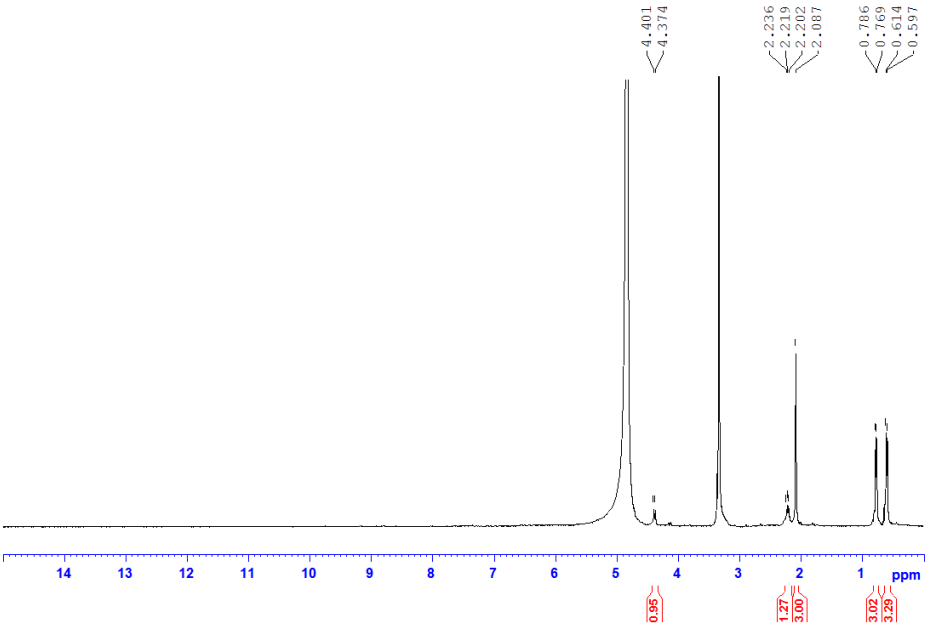

^{13}C-NMR

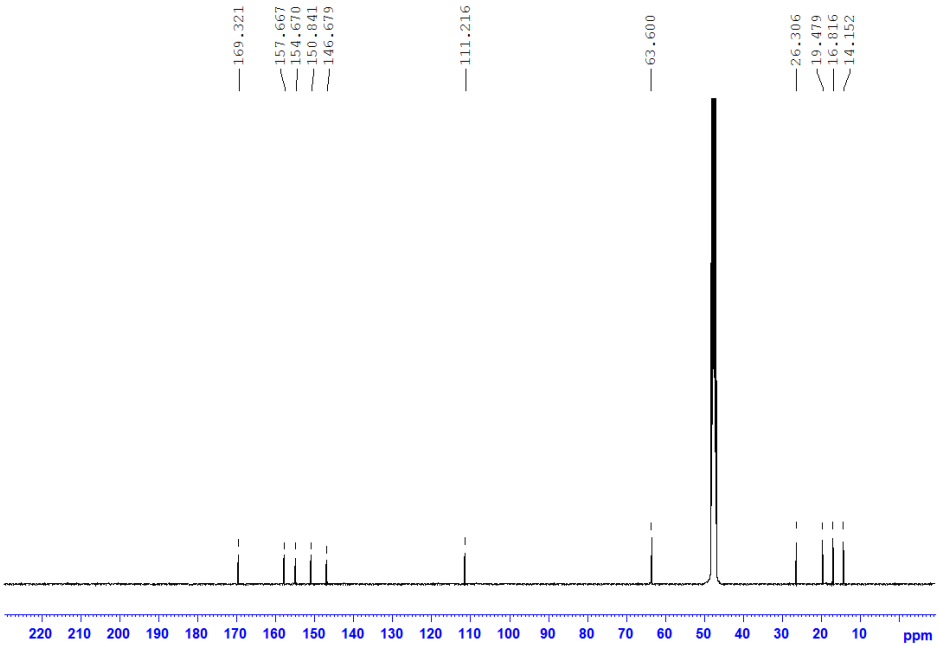

Compound 11d 2-(6-amino-8-methyl-2-oxo-2,3-dihydro-9H-purin-9-yl)-3-hydroxypropanoic acid.

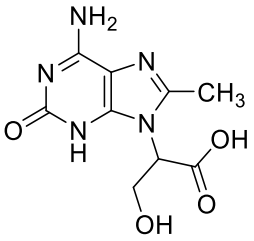

^{1}H-NMR

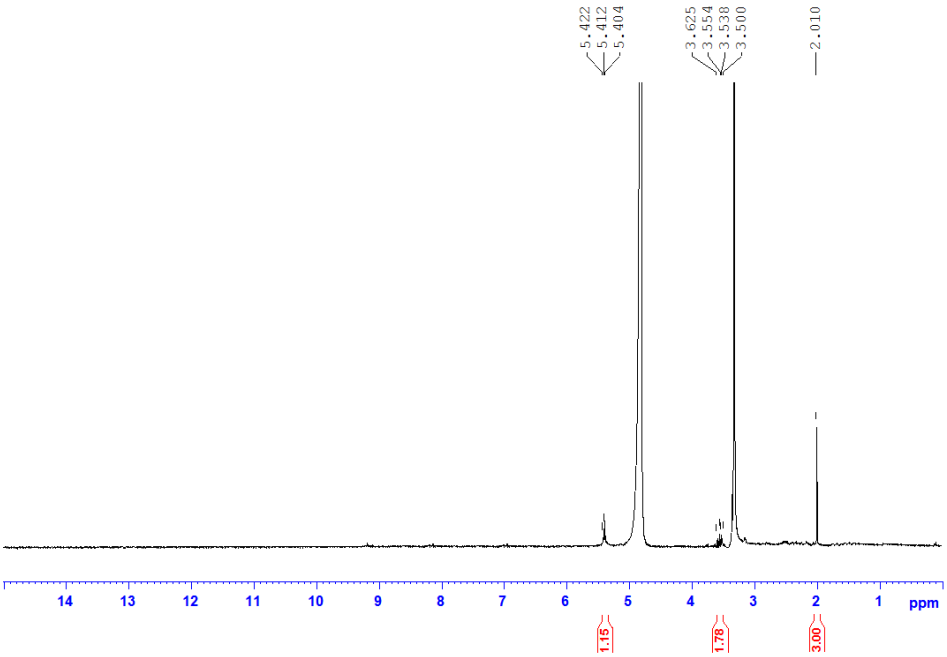

^{13}C-NMR

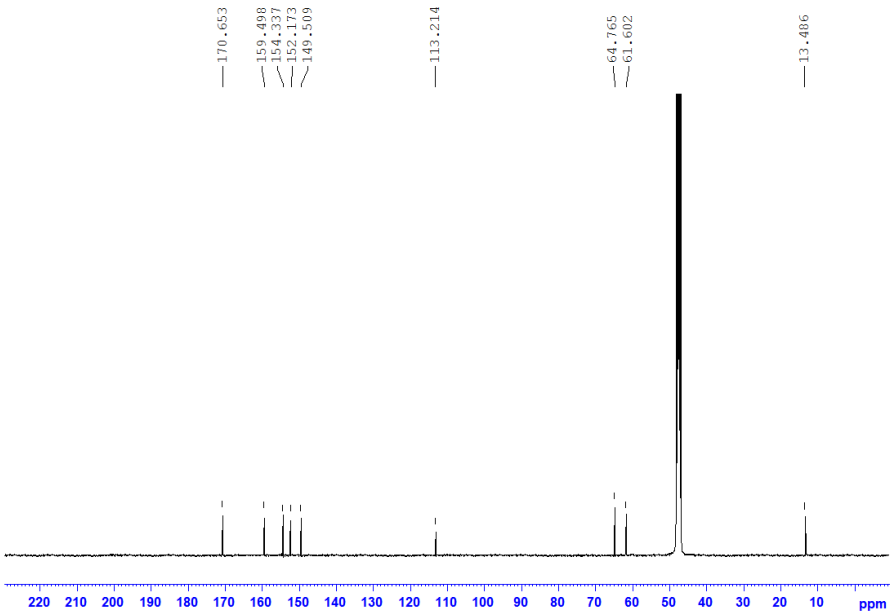

Compound 11e 2-(6-amino-8-methyl-2-oxo-2,3-dihydro-9H-purin-9-yl)-3-phenylpropanoic acid.

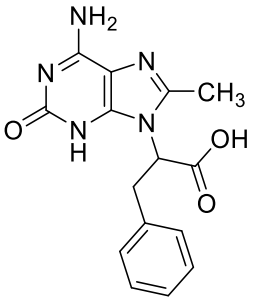

^{1}H-NMR

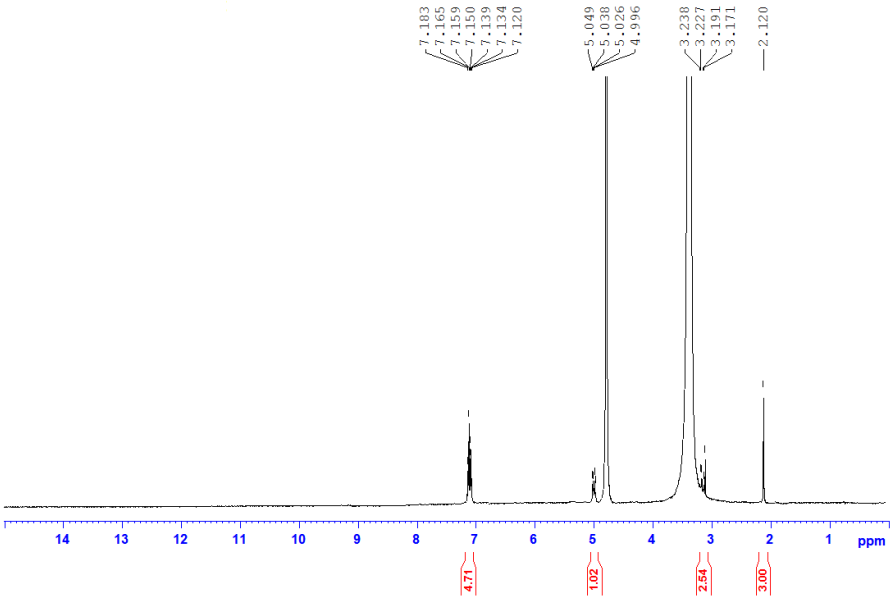

^{13}C-NMR

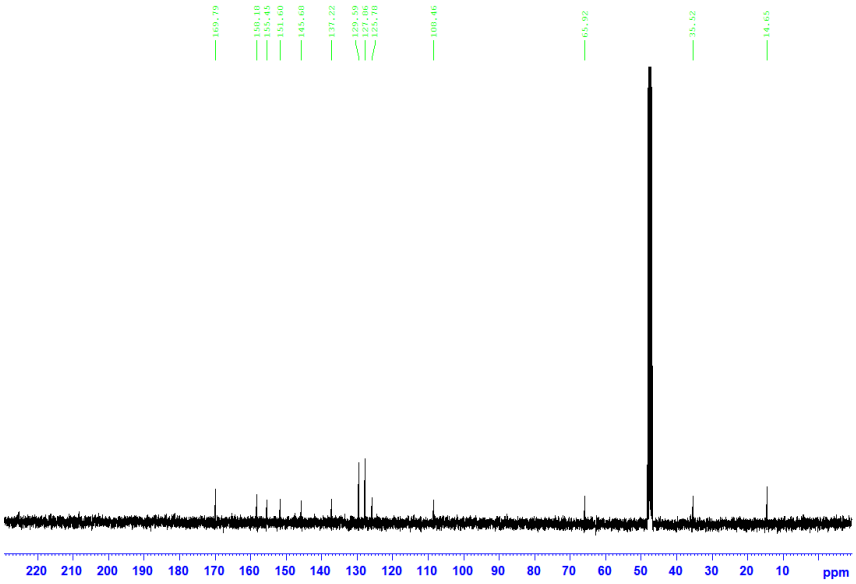

Compound 11f 6-amino-9-(1-(4-hydroxyphenyl)-3-oxobutan-2-yl)-8-methyl-3,9-dihydro-2H-purin-2-one.

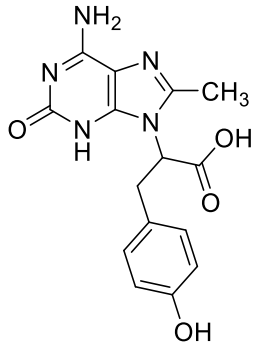

^{1}H-NMR

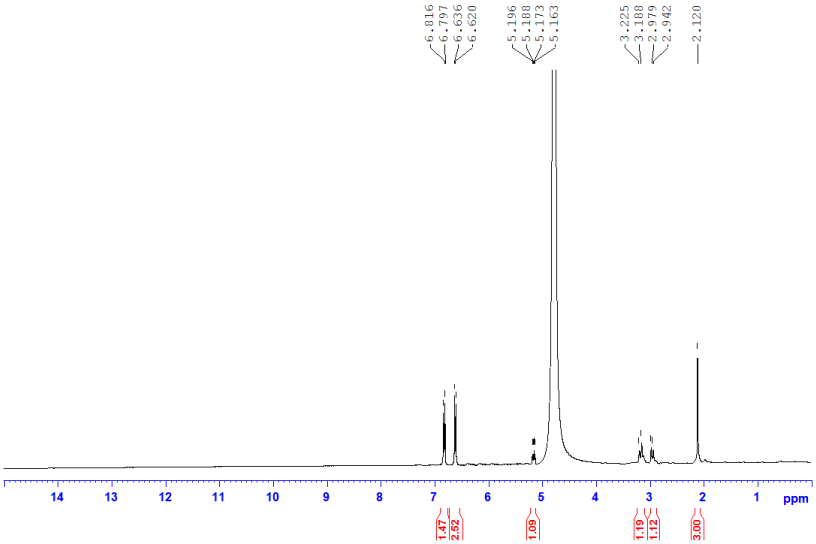

^{13}C-NMR

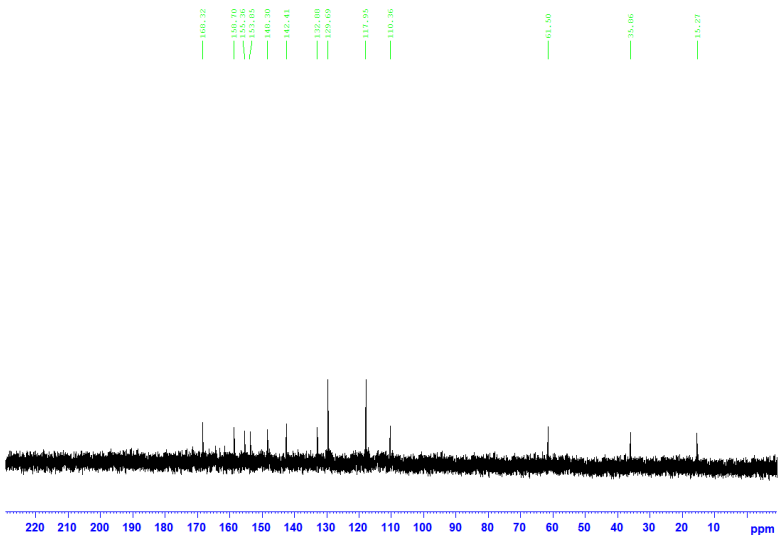

Compound 11g 2-(6-amino-8-methyl-2-oxo-2,3-dihydro-9H-purin-9-yl)-3-(1H-indol-3-yl)propanoic acid.

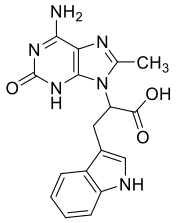

^{1}H-NMR

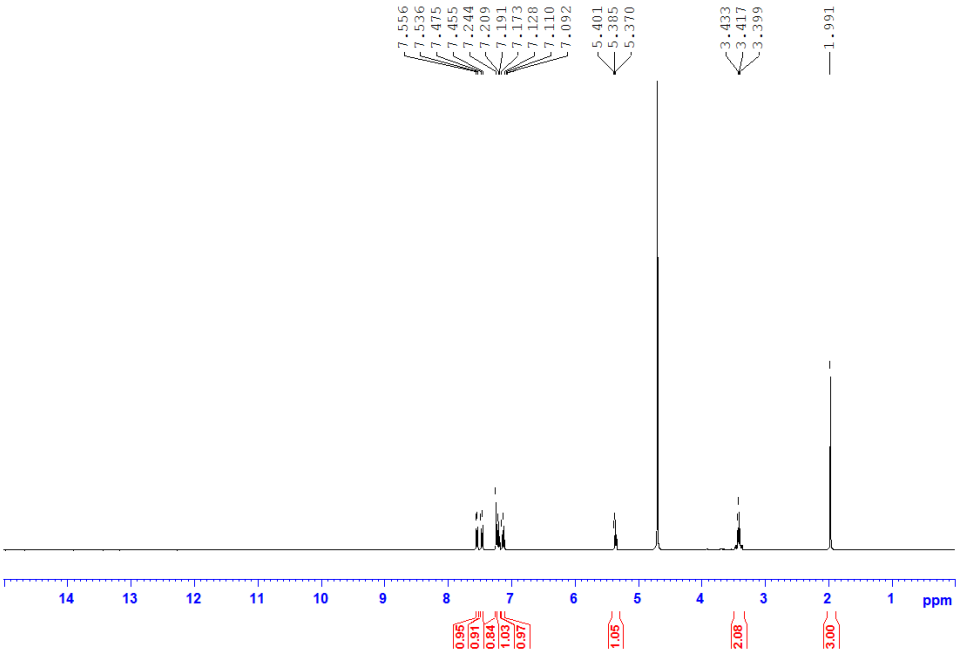

^{13}C-NMR

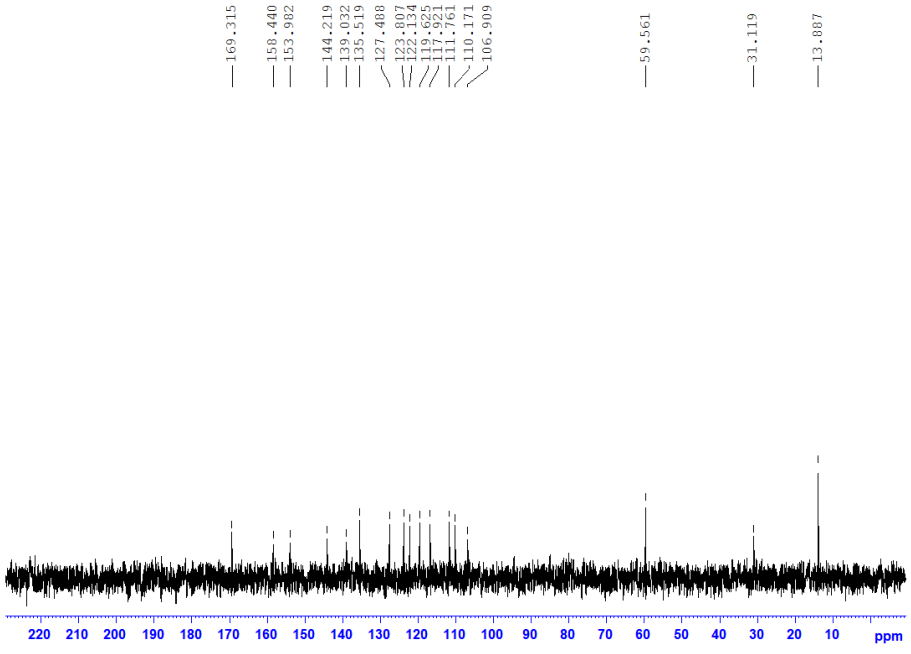

Compound 14a Methyl 2-(4-(amino(cyano)methylene)-5-imino-2-methyl-4,5-dihydro-1H-imidazol-1-yl)acetate.

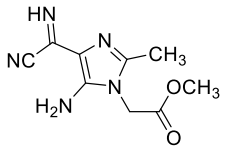

^{1}H-NMR

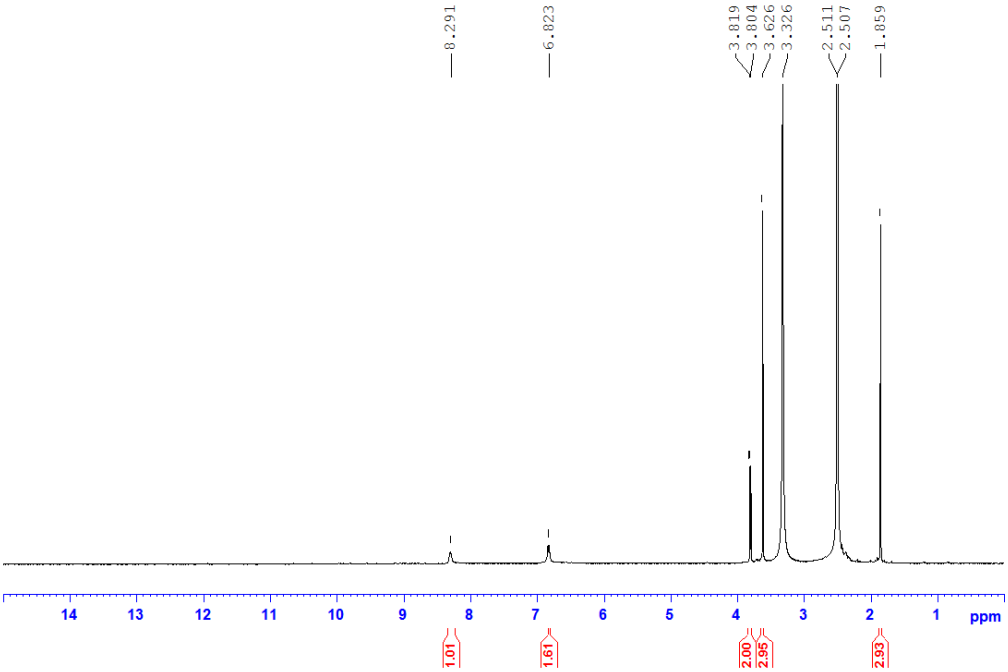

^{13}C-NMR

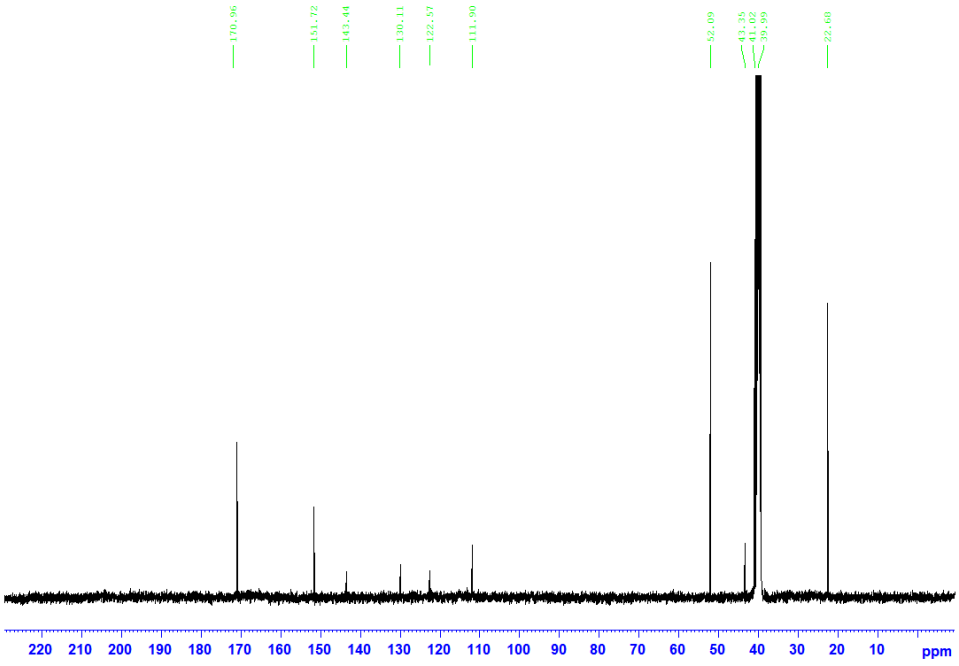

Compound 14b Methyl 2-(4-(amino(cyano)methylene)-5-imino-2-methyl-4,5-dihydro-1H-imidazol-1-yl)propanoate.

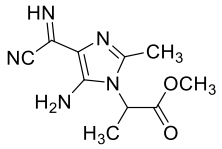

^{1}H-NMR

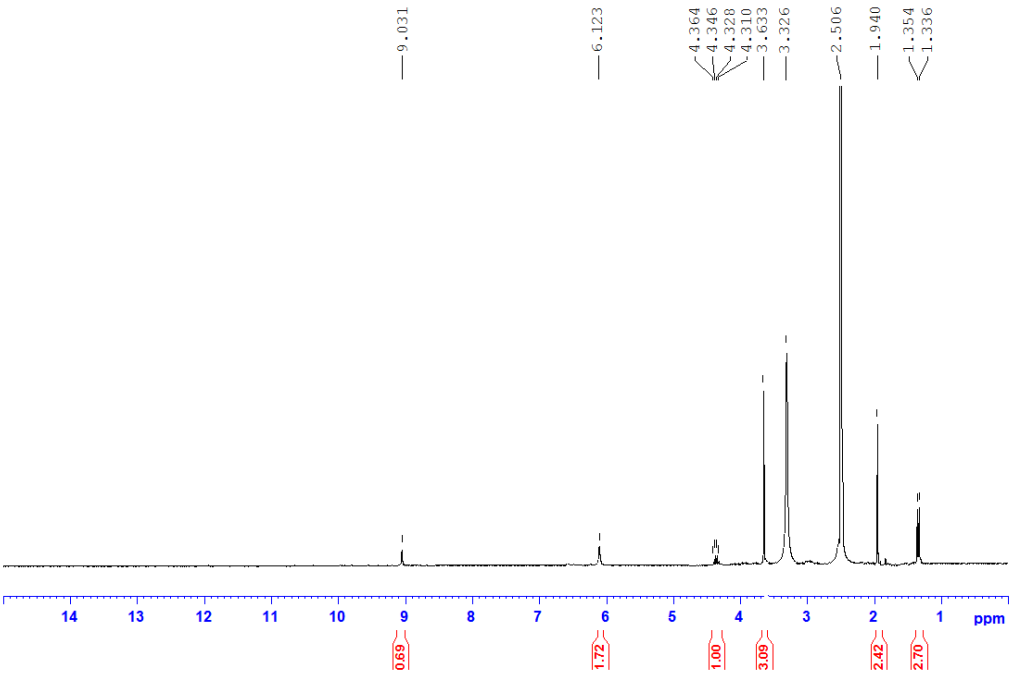

^{13}C-NMR

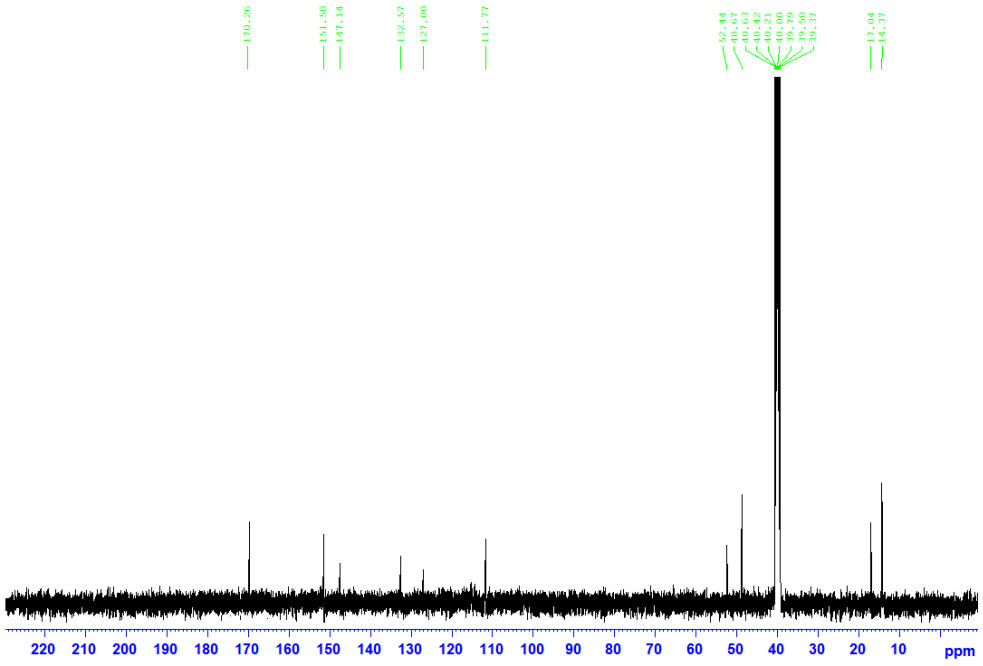

Compound 14c Methyl 2-(4-(amino(cyano)methylene)-5-imino-2-methyl-4,5-dihydro-1H-imidazol-1-yl)-3-methylbutanoate.

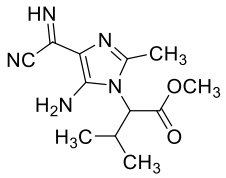

^{1}H-NMR

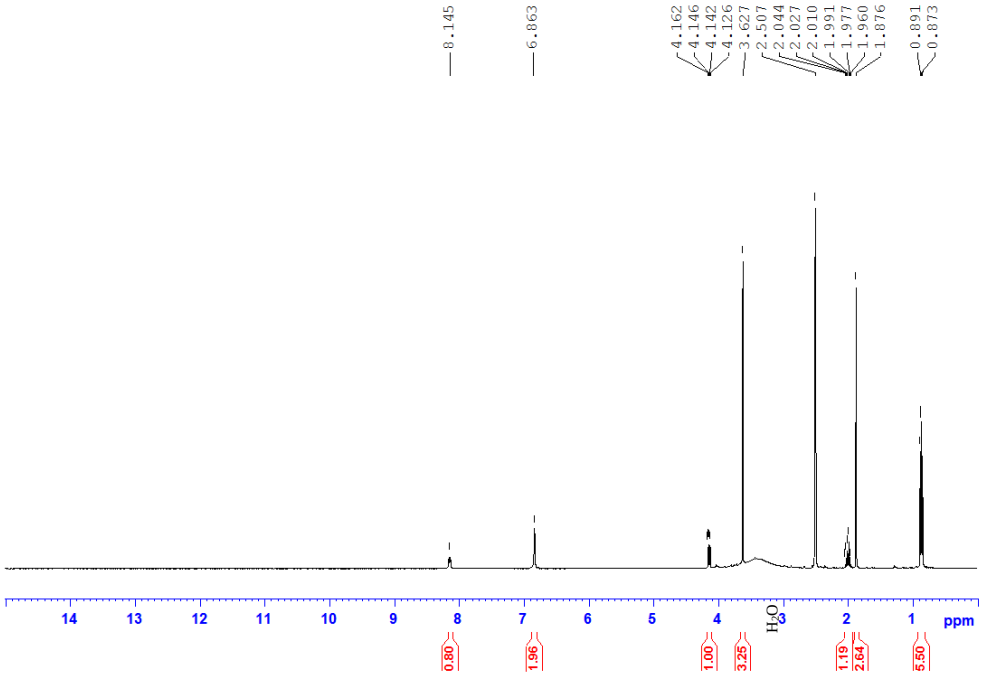

^{13}C-NMR

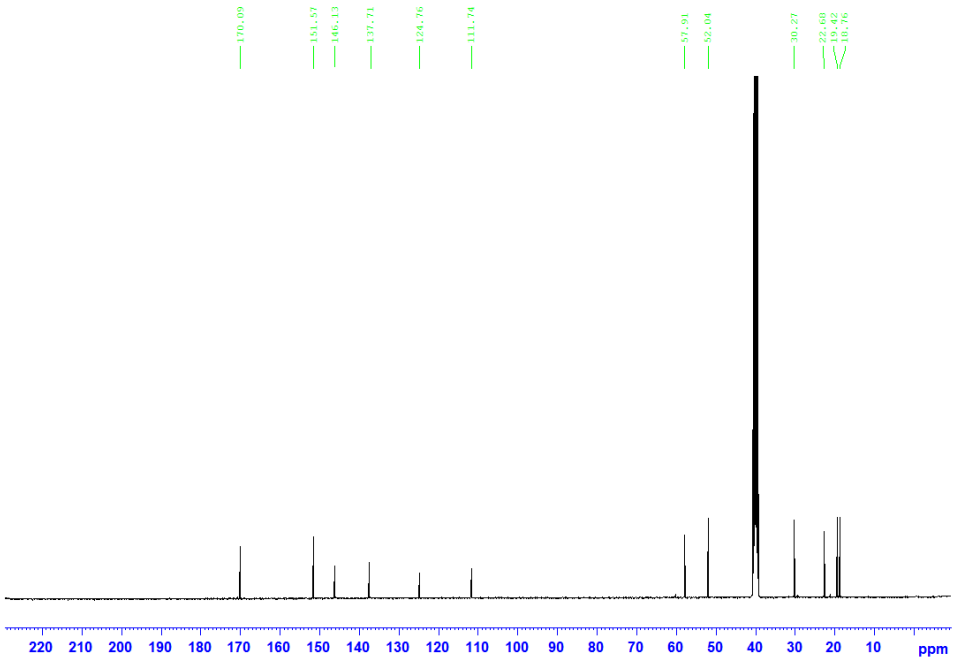

Compound 14d Methyl 2-(4-(amino(cyano)methylene)-5-imino-2-methyl-4,5-dihydro-1H-imidazol-1-yl)-3-hydroxypropanoate.

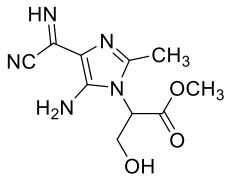

^{1}H-NMR

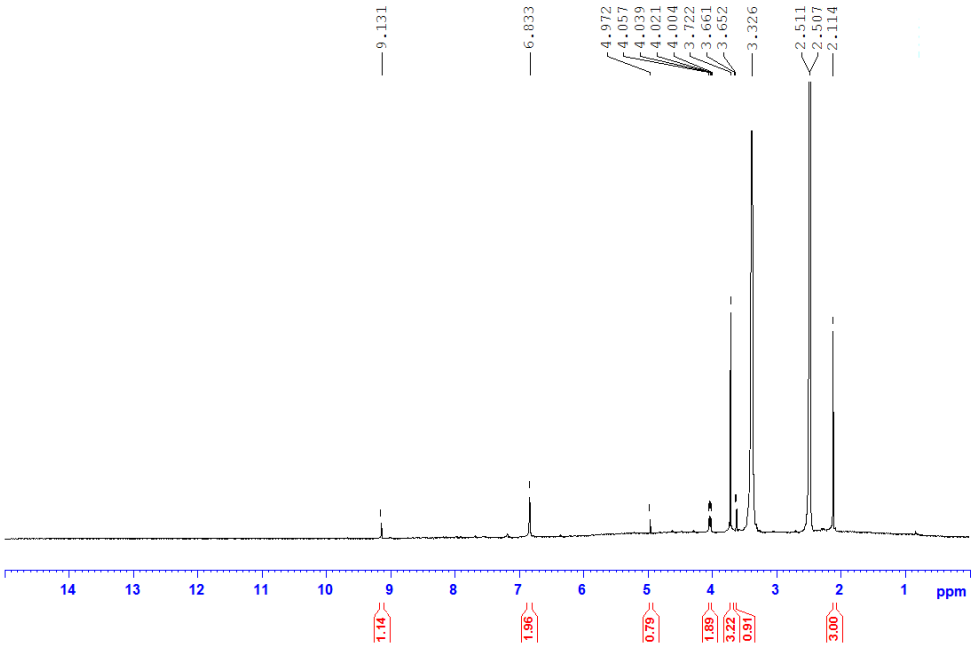

^{13}C-NMR

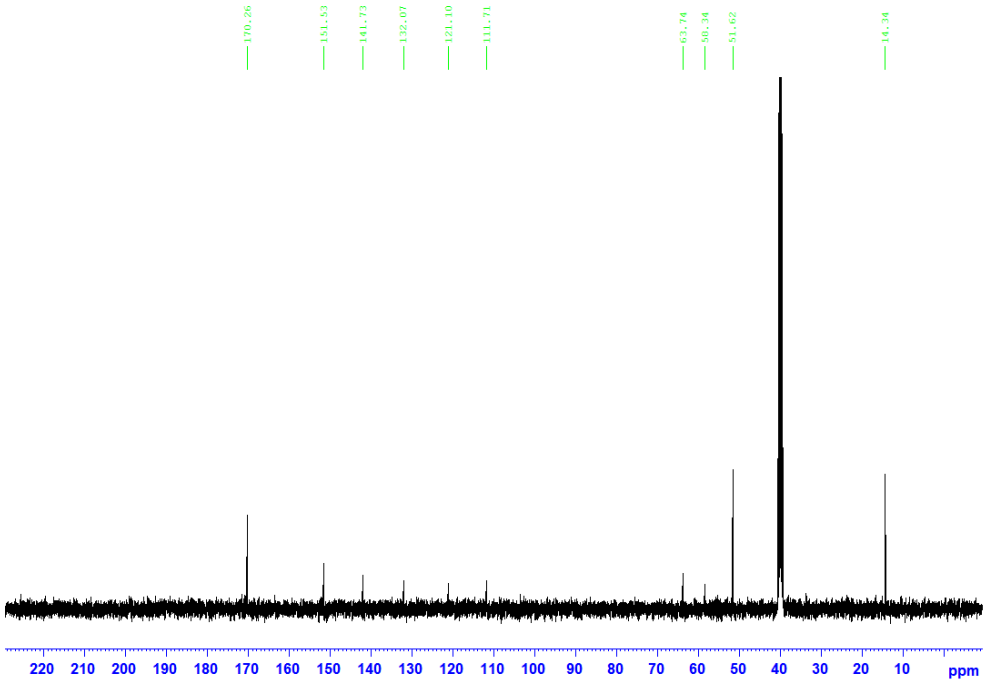

Compound 14e Methyl 2-(4-(amino(cyano)methylene)-5-imino-2-methyl-4,5-dihydro-1H-imidazol-1-yl)-3-phenylpropanoate.

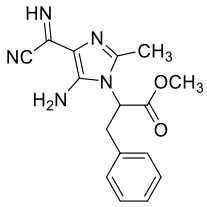

^{1}H-NMR

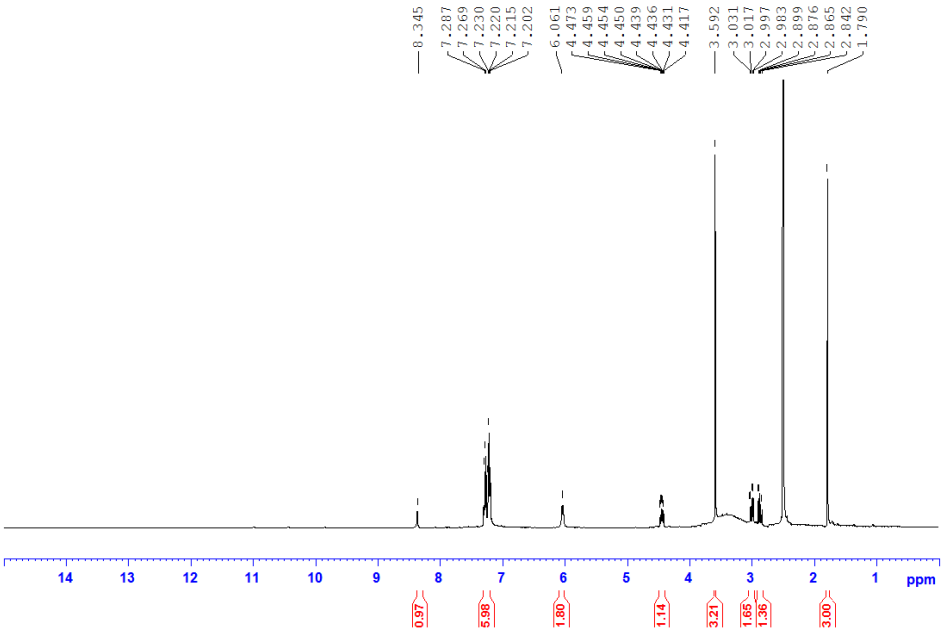

^{13}C-NMR

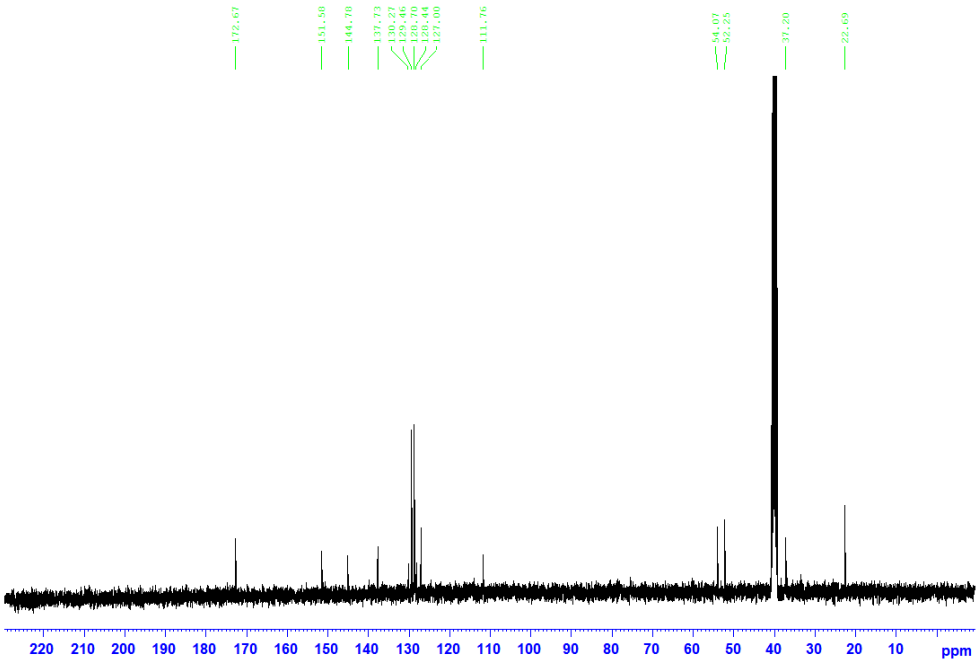

Compound 14f Methyl2-(4-(amino(cyano)methylene)-5-imino-2-methyl-4,5-dihydro-1H-imidazol-1-yl)-(4hydroxyphenyl)propanoate.

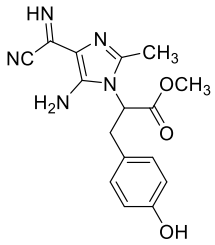

^{1}H-NMR

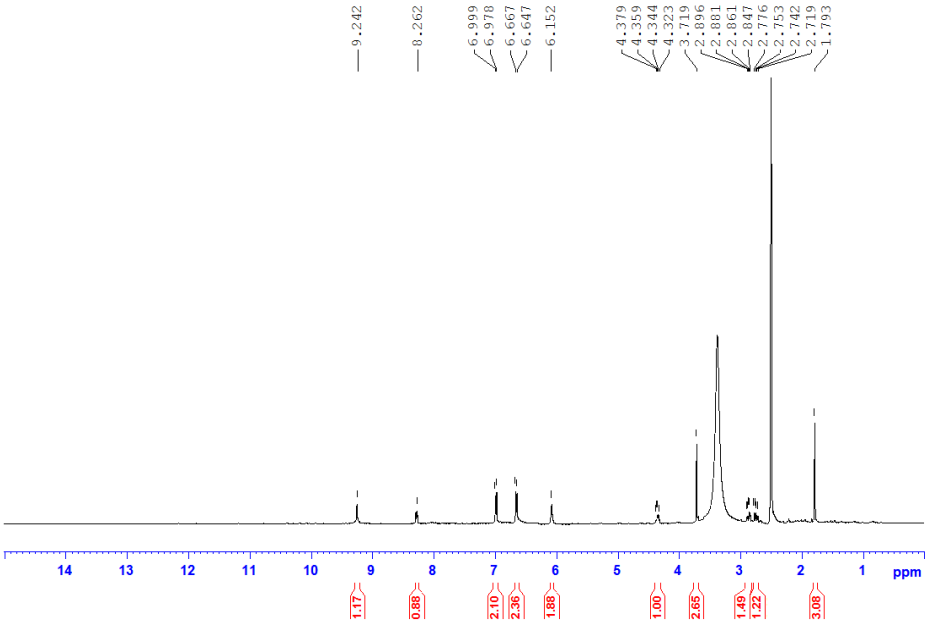

^{13}C-NMR

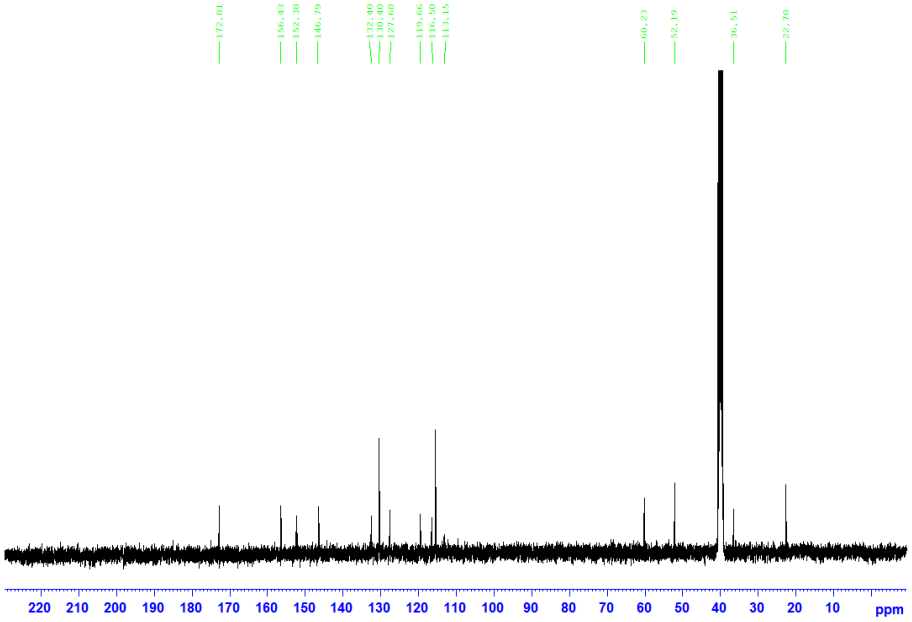

Compound 15 Methyl N-2-amino-1,2-dicyanovinyl)acetimidate.

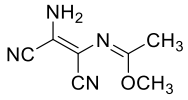

^{1}H-NMR

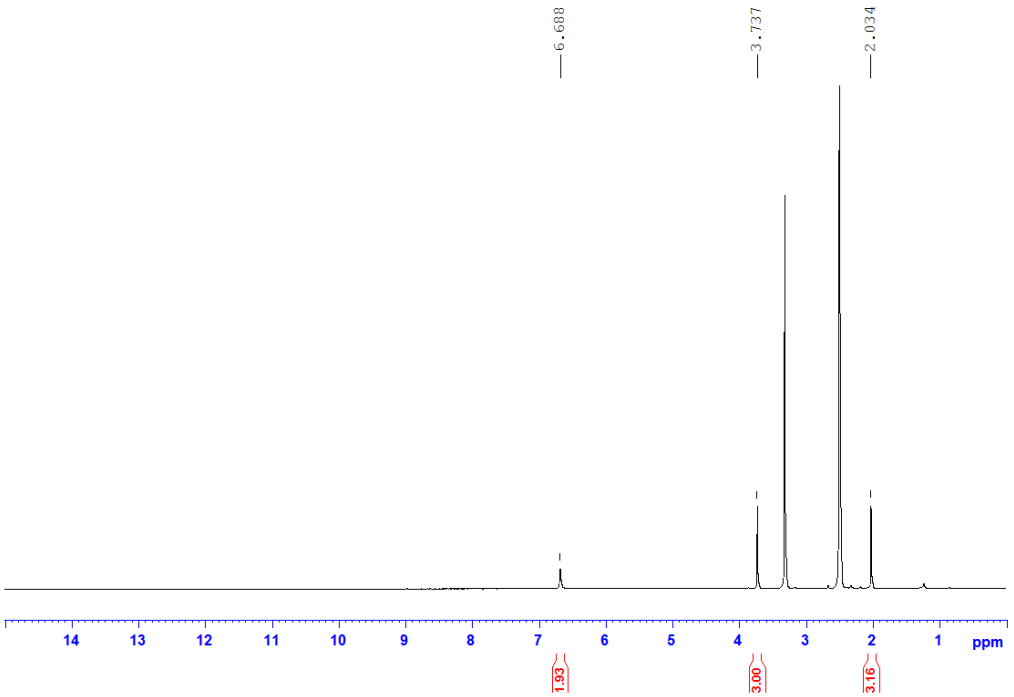

^{13}C-NMR

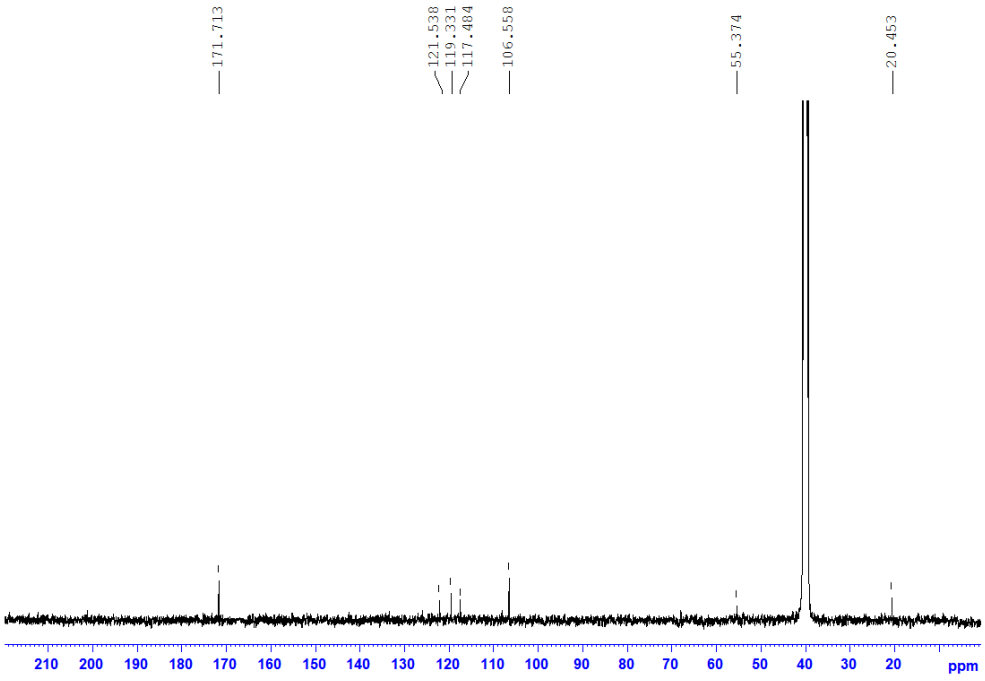

Compound 16a Methyl 2-(5-amino-4-cyano-6-imino-2-methylpyrimidin-1(6H)-yl)acetate.

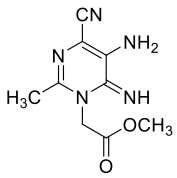

^{1}H-NMR

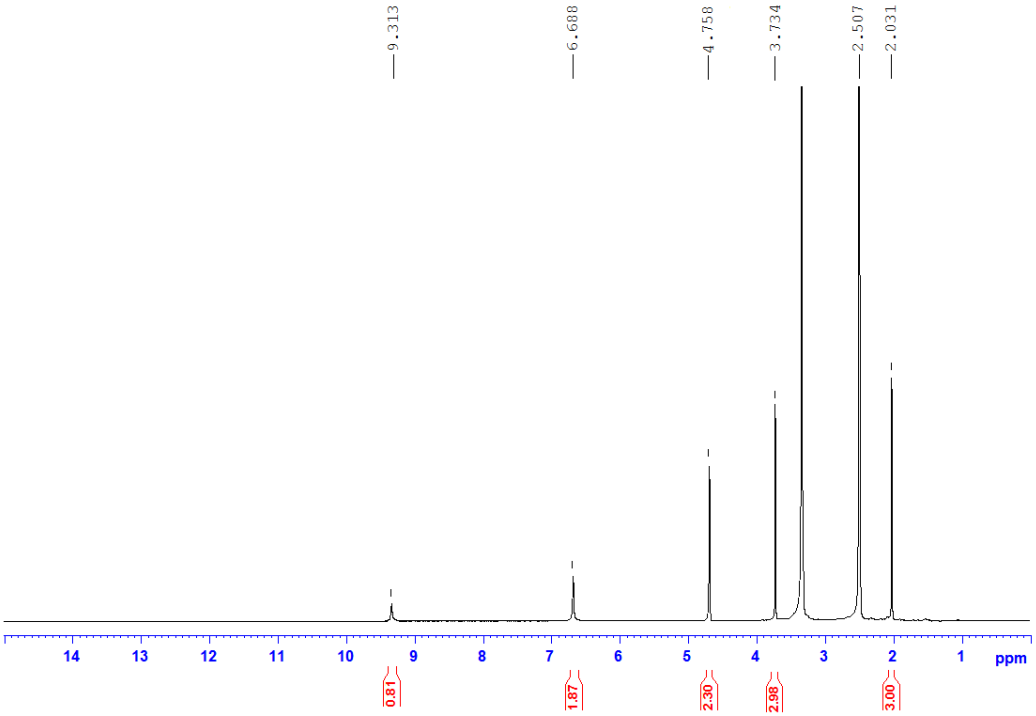

^{13}C-NMR

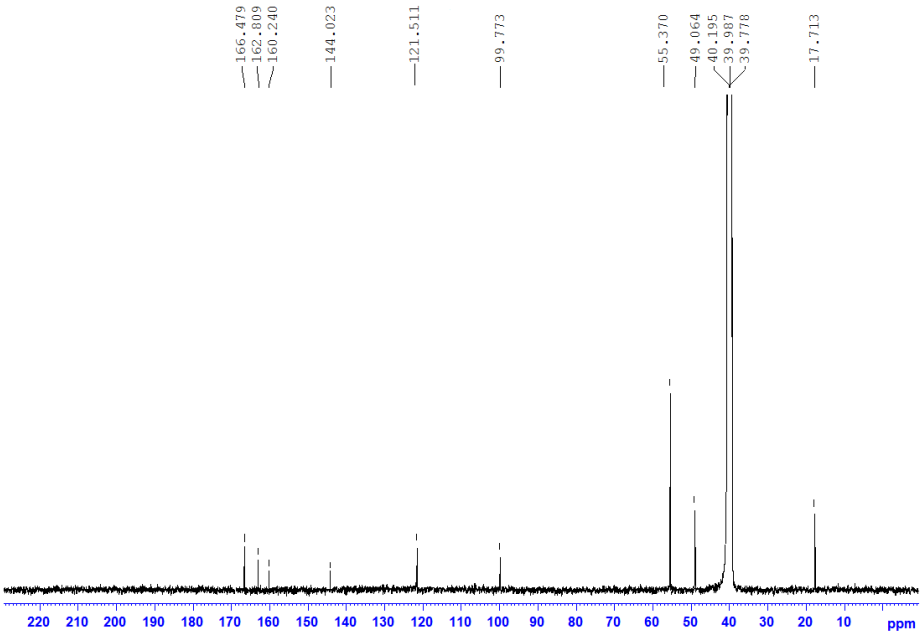

Compound 16b Methyl 2-(5-amino-4-cyano-6-imino-2-methylpyrimidin-1(6H)-yl)propanoate.

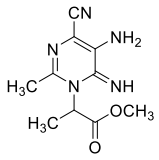

^{1}H-NMR

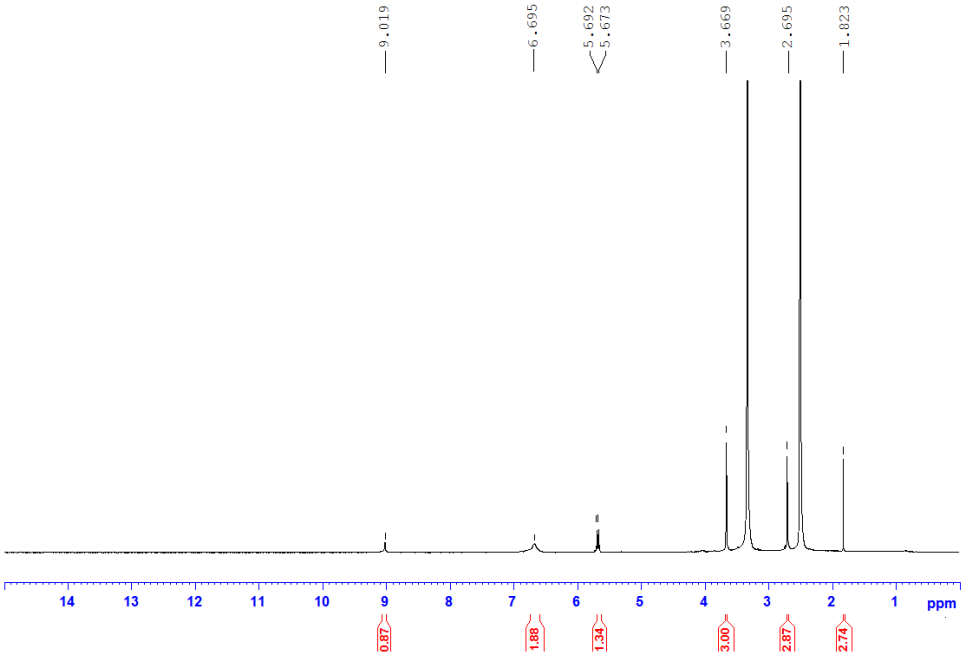

^{13}C-NMR

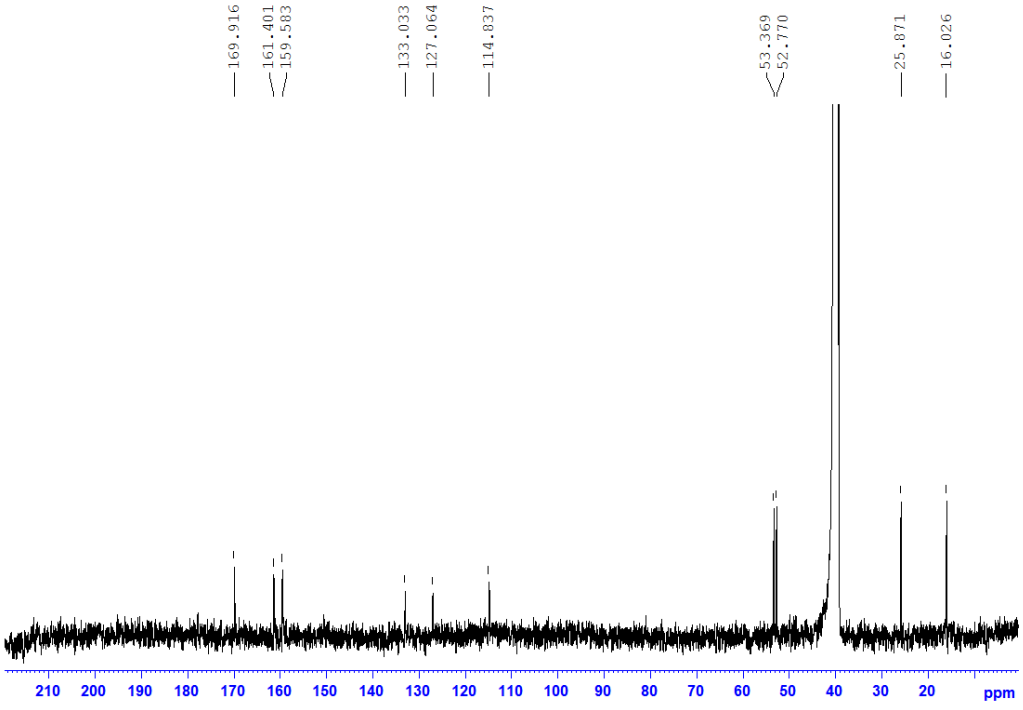

Compound 16c Methyl 2-(5-amino-4-cyano-6-imino-2-methylpyrimidin-1(6H)-yl)-3-methylbutanoate.

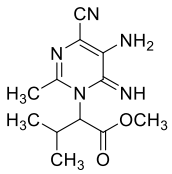

^{1}H-NMR

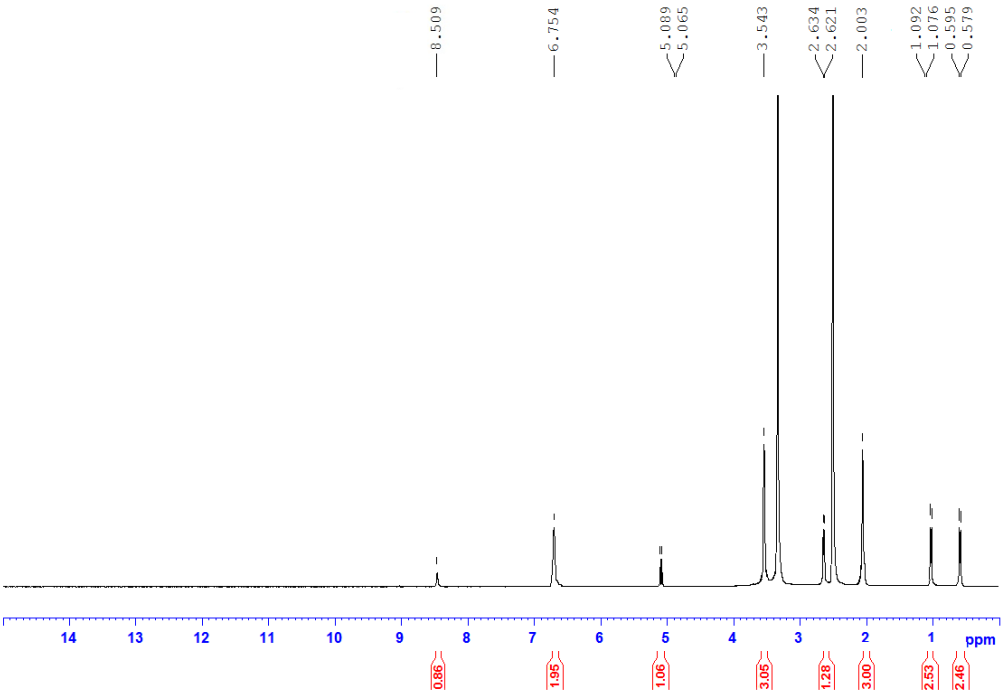

^{13}C-NMR

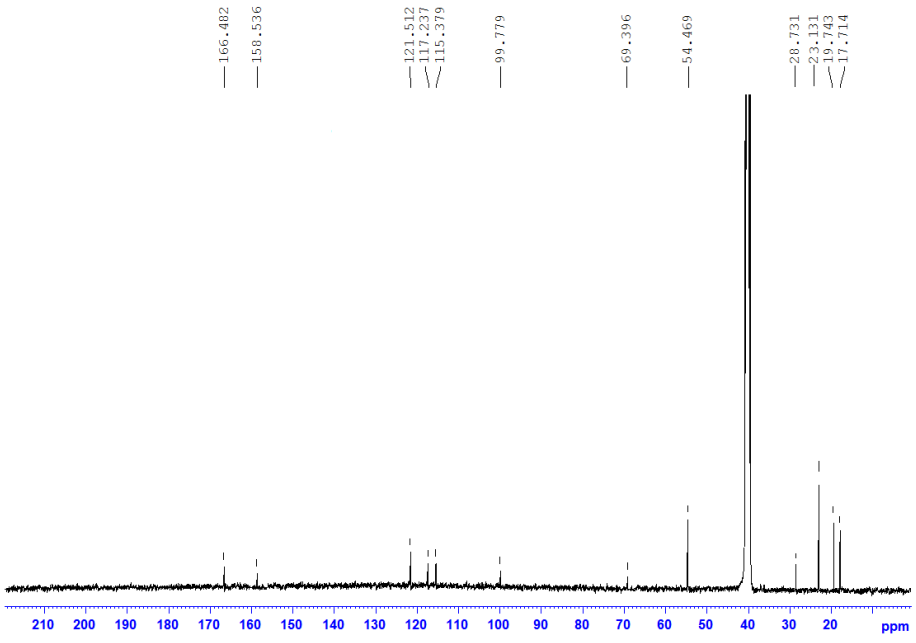

Compound 16d Methyl 2-(5-amino-4-cyano-6-imino-2-methylpyrimidin-1(6H)-yl)-3-hydroxypropanoate.

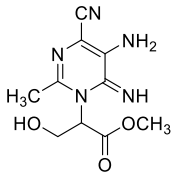

^{1}H-NMR

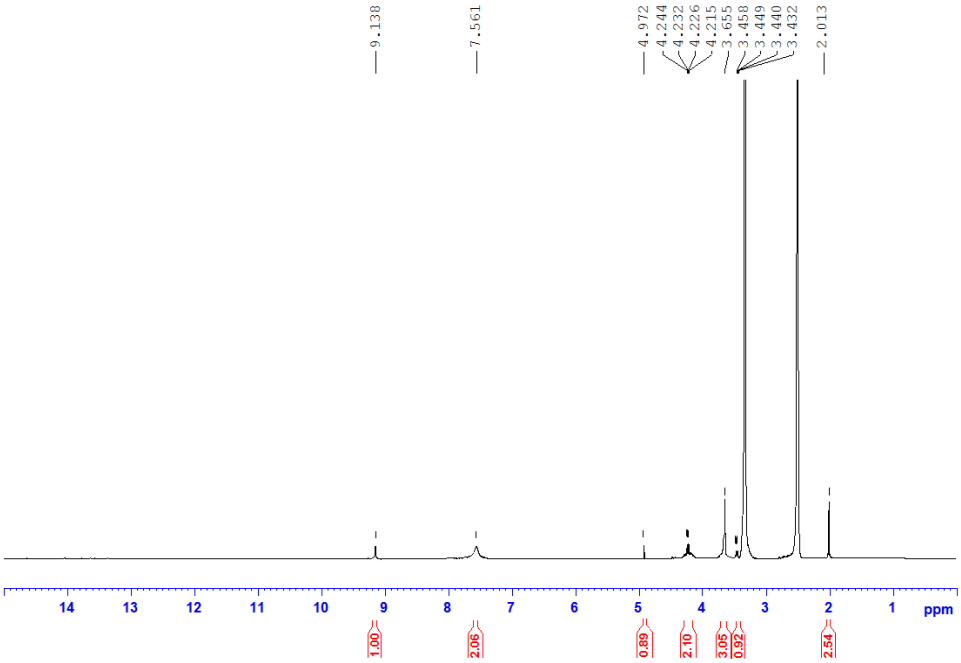

^{13}C-NMR

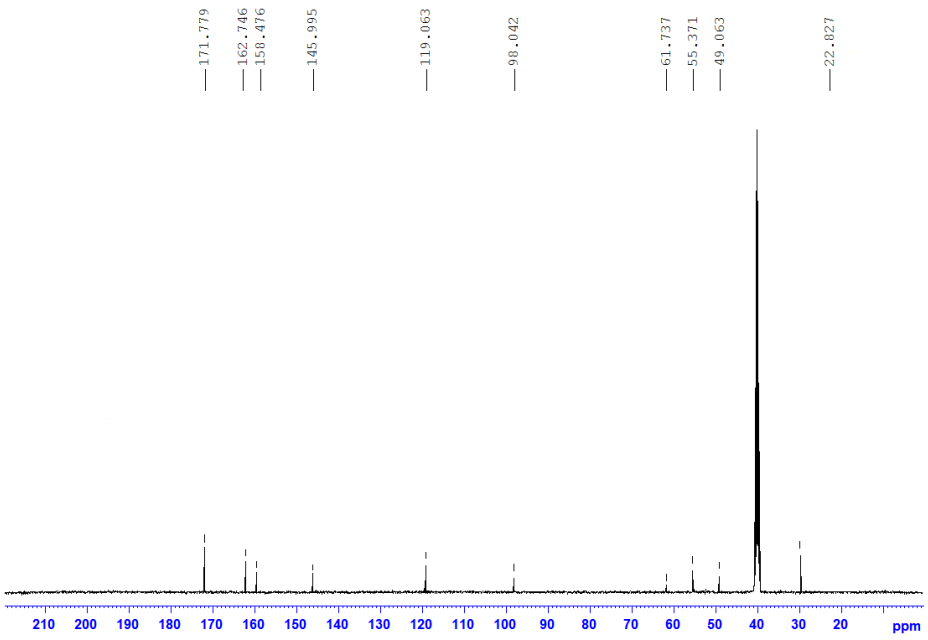

Compound 16e Methyl 2-(5-amino-4-cyano-6-imino-2-methylpyrimidin-1(6H)-yl)-3-phenylpropanoate.

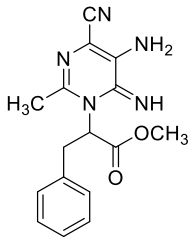

^{1}H-NMR

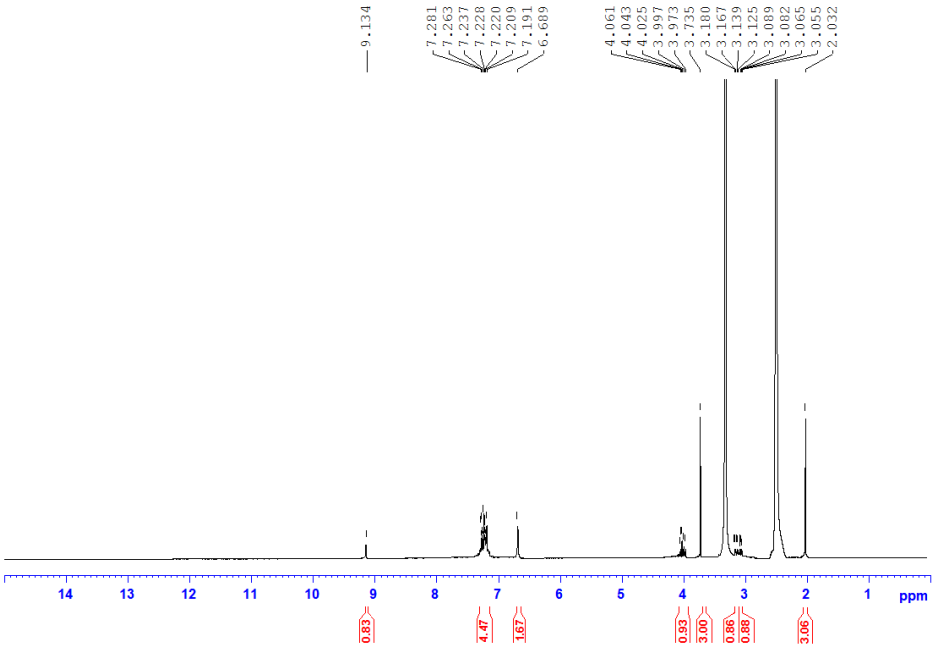

^{13}C-NMR

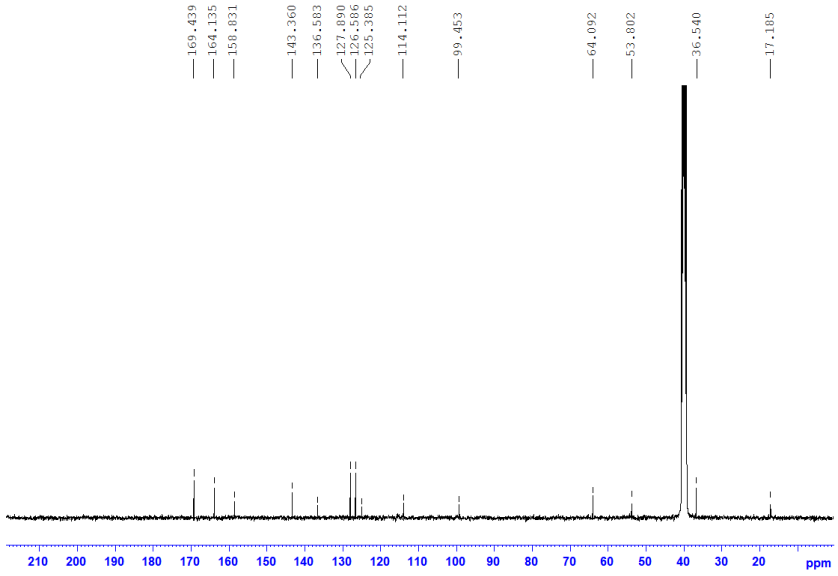

Compound 16f Methyl 2-(5-amino-4-cyano-6-imino-2-methylpyrimidin-1(6H)-yl)-3-(4-hydroxyphenyl)propanoate.

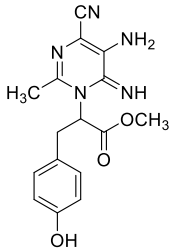

^{1}H-NMR

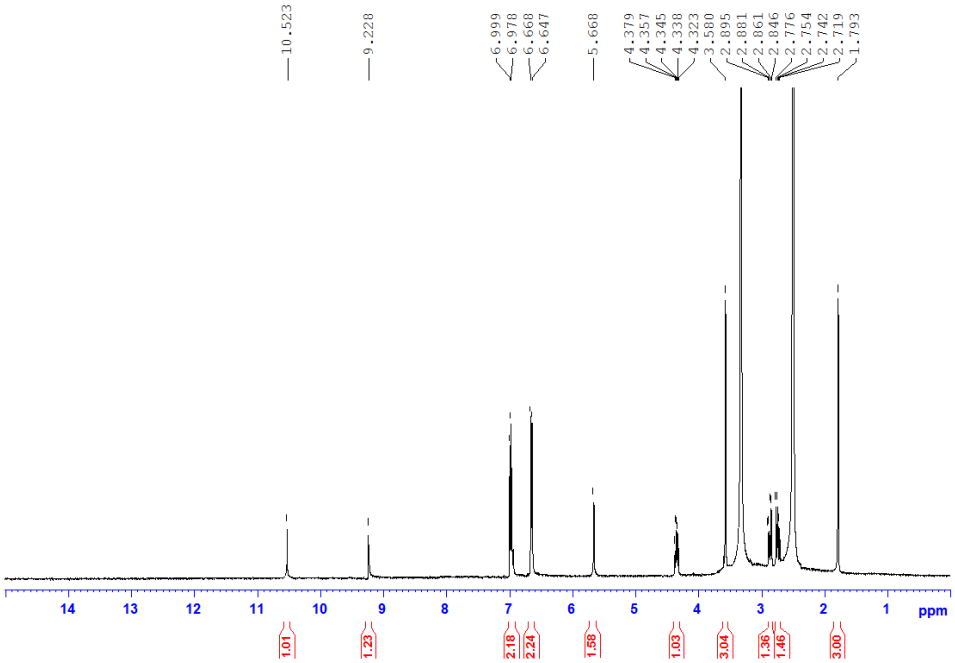

^{13}C-NMR

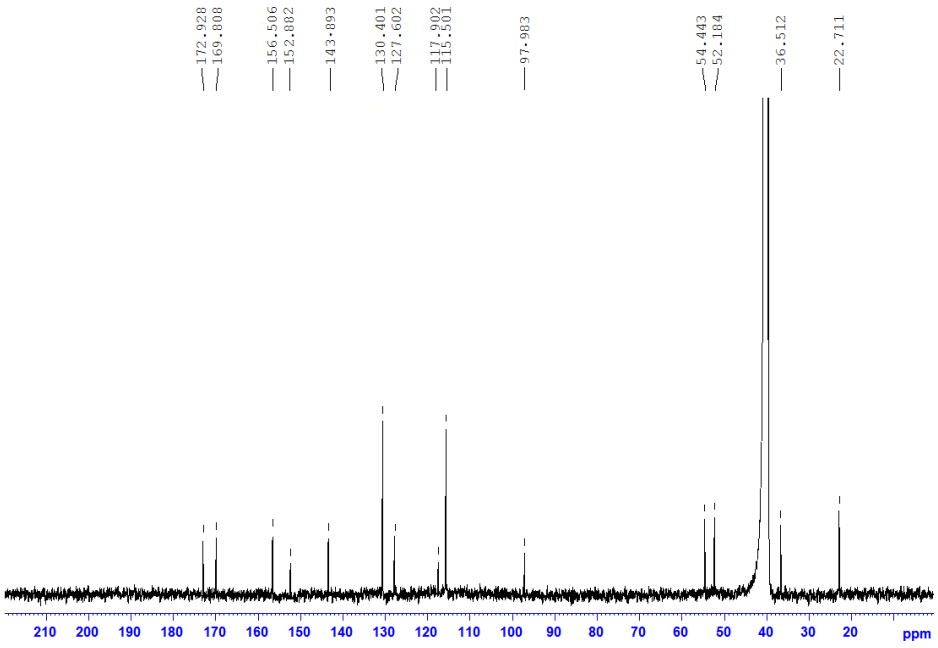

Compound 18 Methyl N-(4-cyano-1H-imidazol-5-yl)acetimidate.

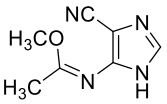

^{1}H-NMR

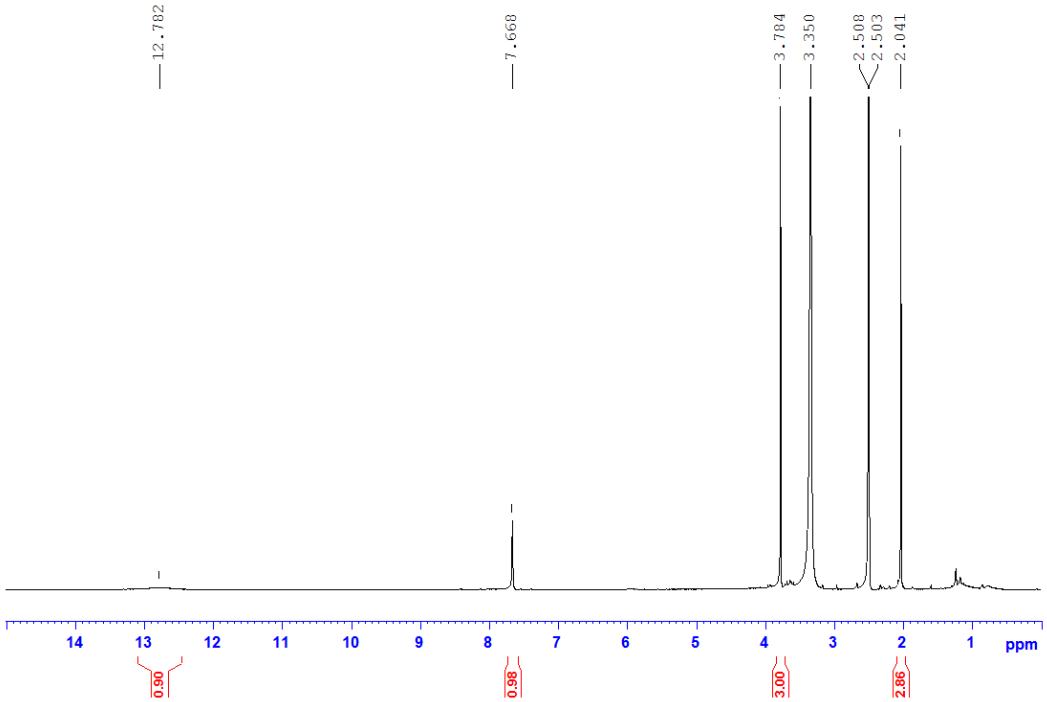

^{13}C-NMR

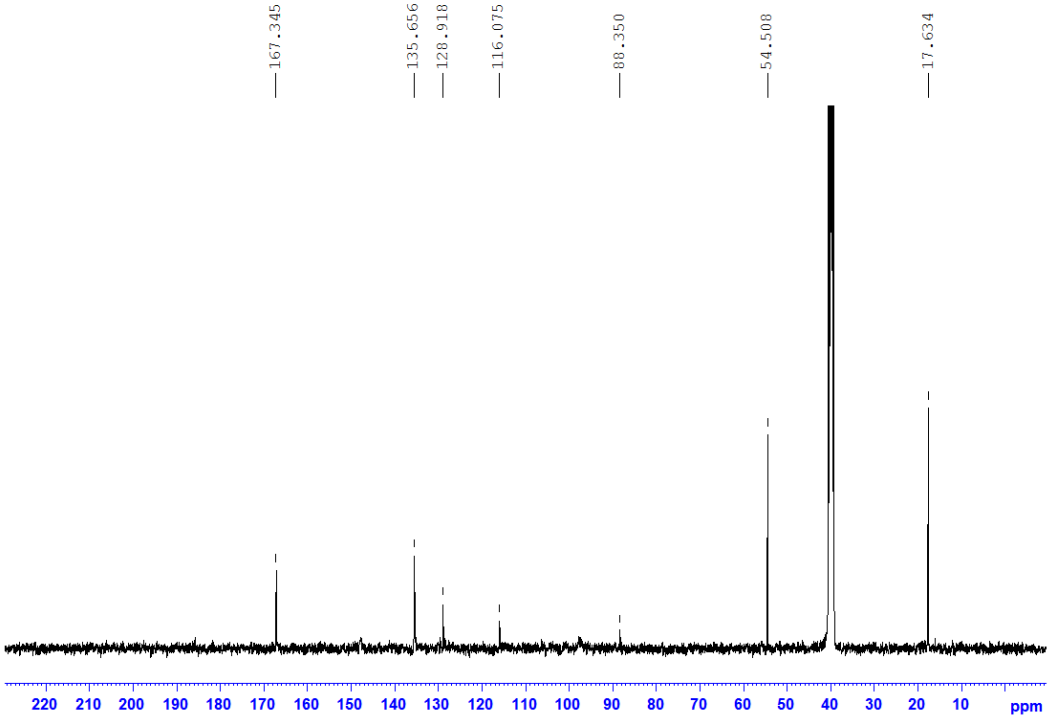

Compound 19a Methyl 2-(6-imino-2-methyl-6,9-dihydro-1H-purin-1-yl)acetate.

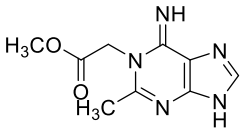

^{1}H-NMR

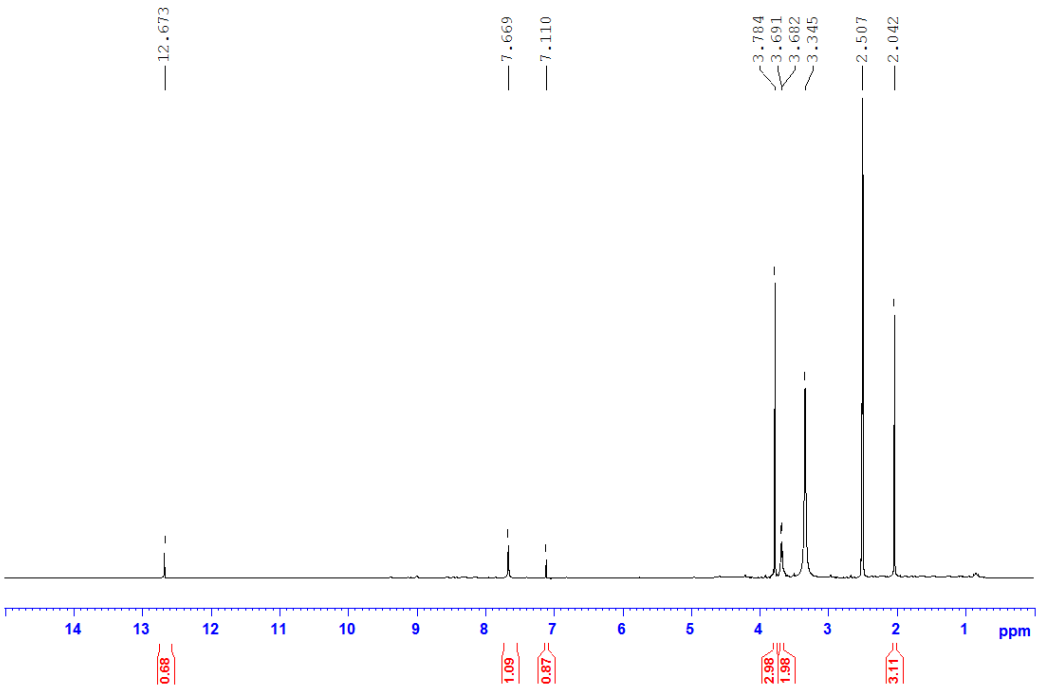

^{13}C-NMR

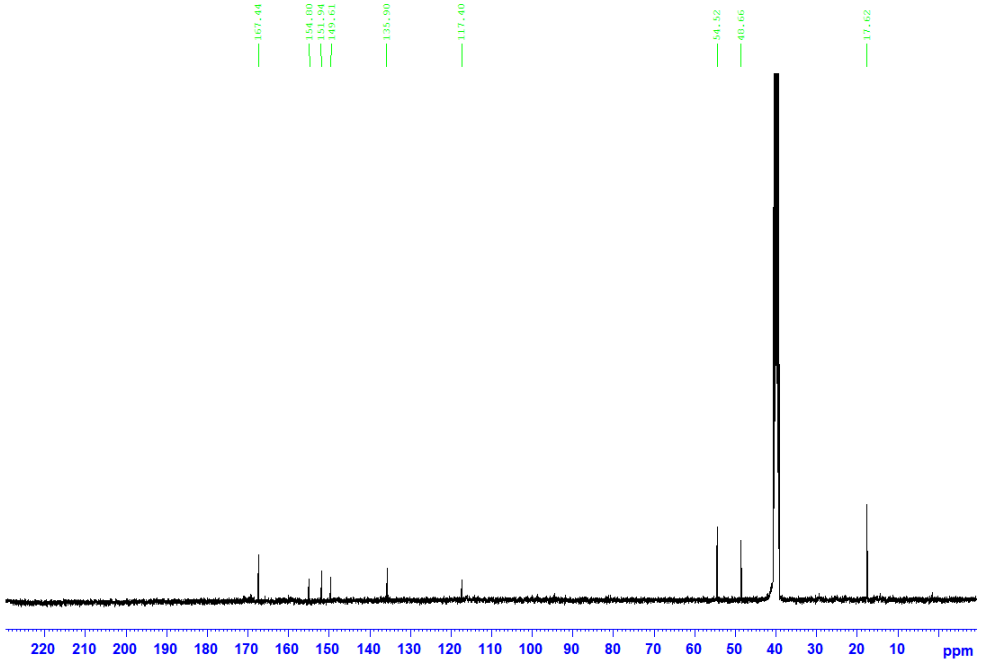

Compound 19b Methyl 2-(6-imino-2-methyl-6,9-dihydro-1H-purin-1-yl)propanoate.

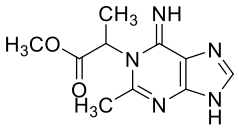

^{1}H-NMR

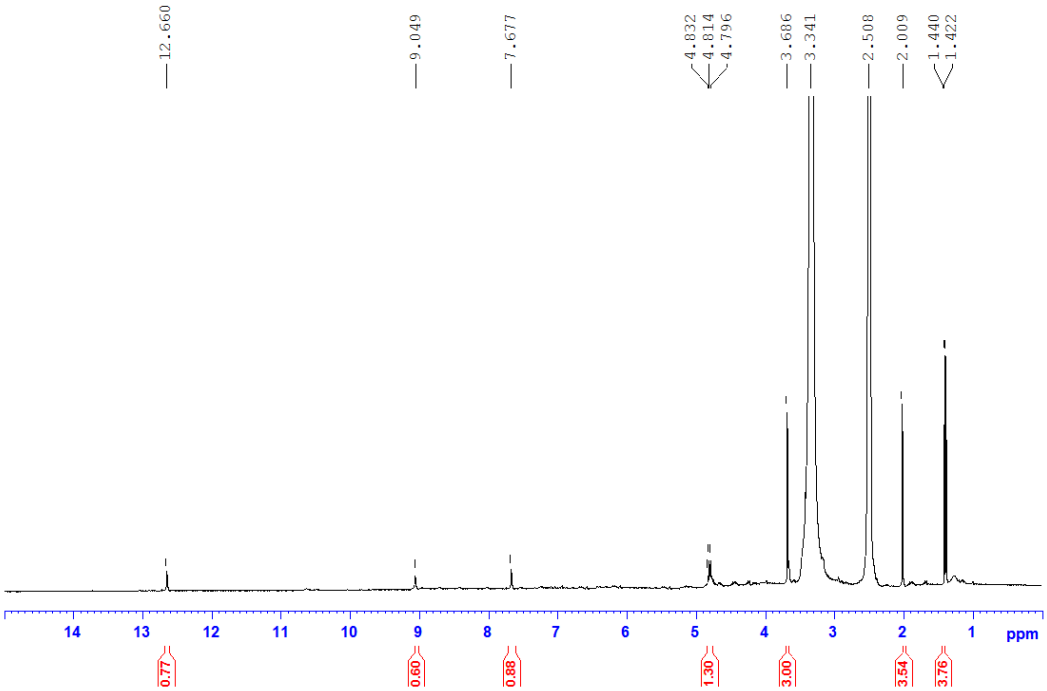

^{13}C-NMR

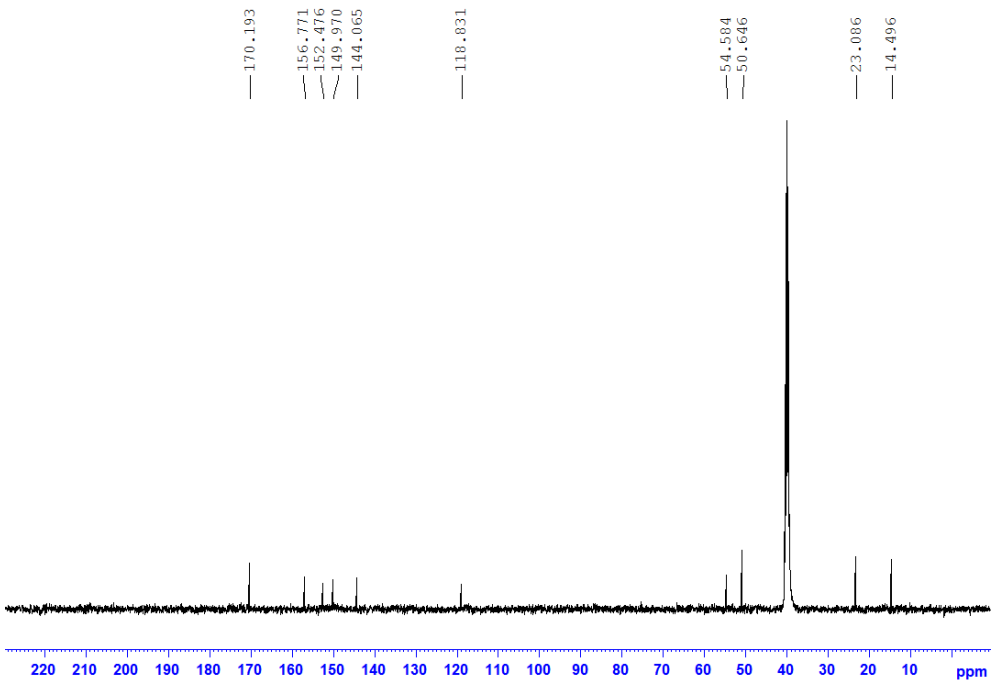

Compound 19c Methyl 2-(6-imino-2-methyl-6,9-dihydro-1H-purin-1-yl)-3-methylbutanoate.

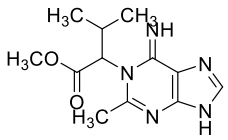

^{1}H-NMR

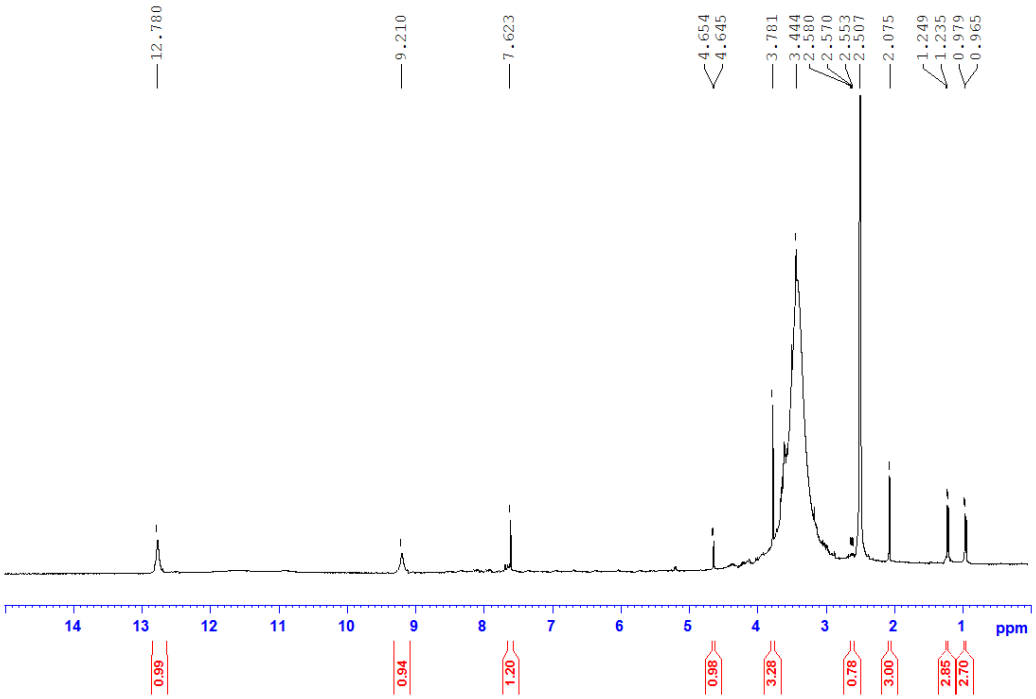

^{13}C-NMR

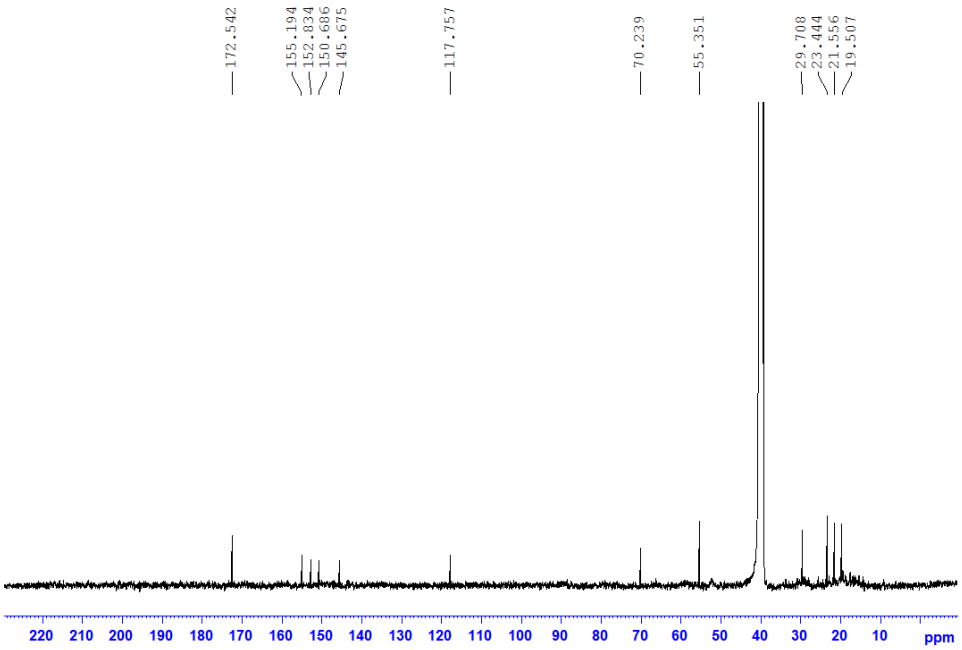

Compound 19d Methyl 3-hydroxy-2-(6-imino-2-methyl-6,9-dihydro-1H-purin-1-yl)propanoate.

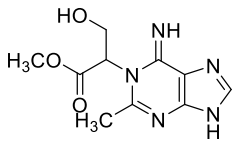

^{1}H-NMR

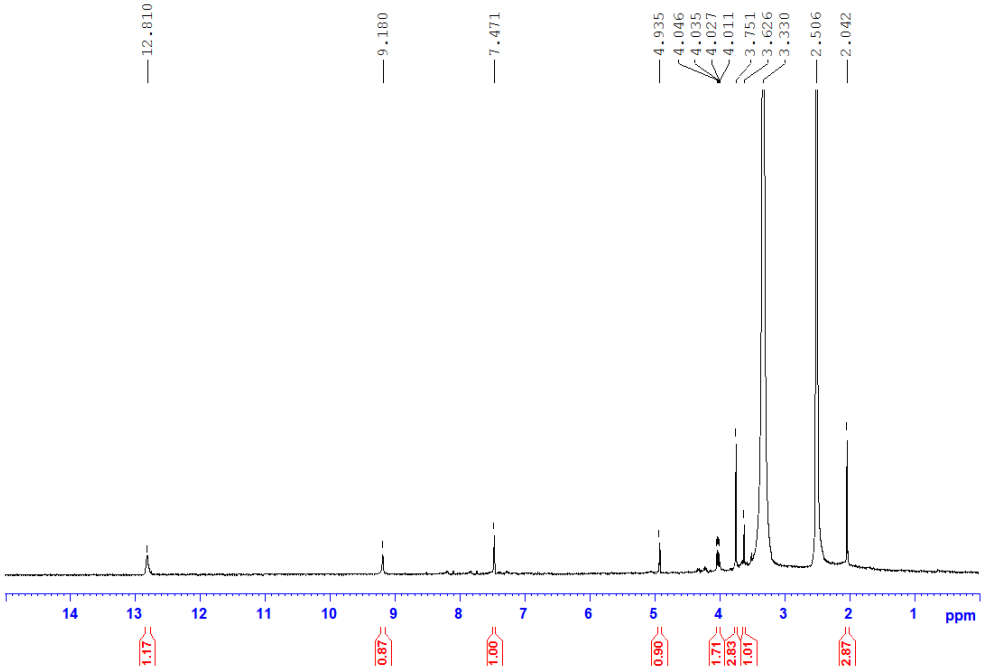

^{13}C-NMR

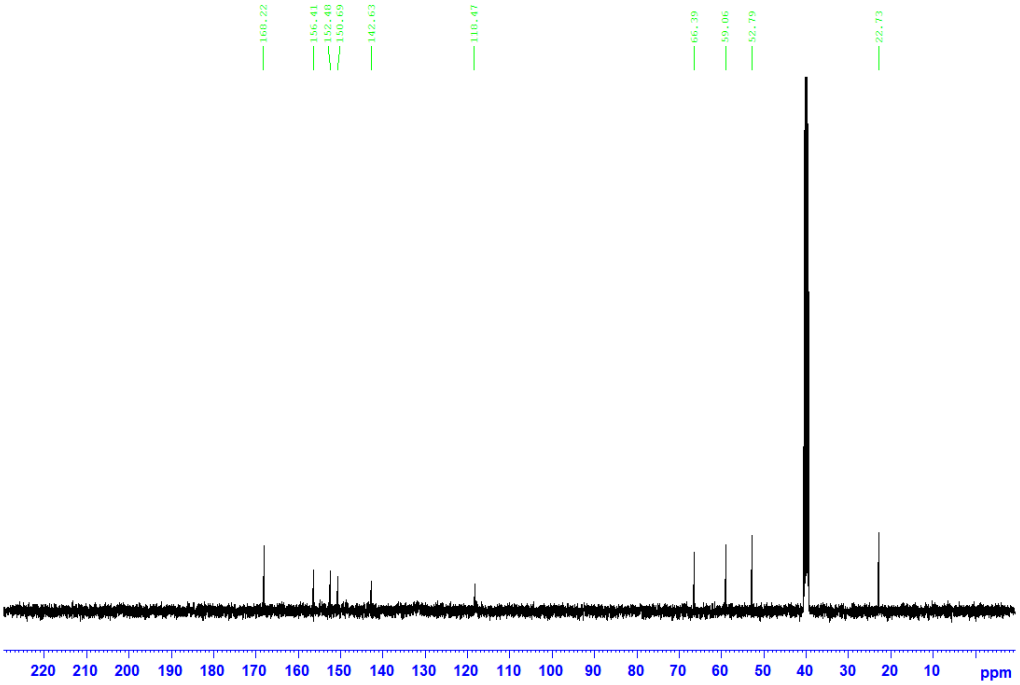

Compound 19e Methyl 2-(6-imino-2-methyl-6,9-dihydro-1H-purin-1-yl)-3-phenylpropanoate.

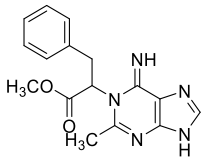

^{1}H-NMR

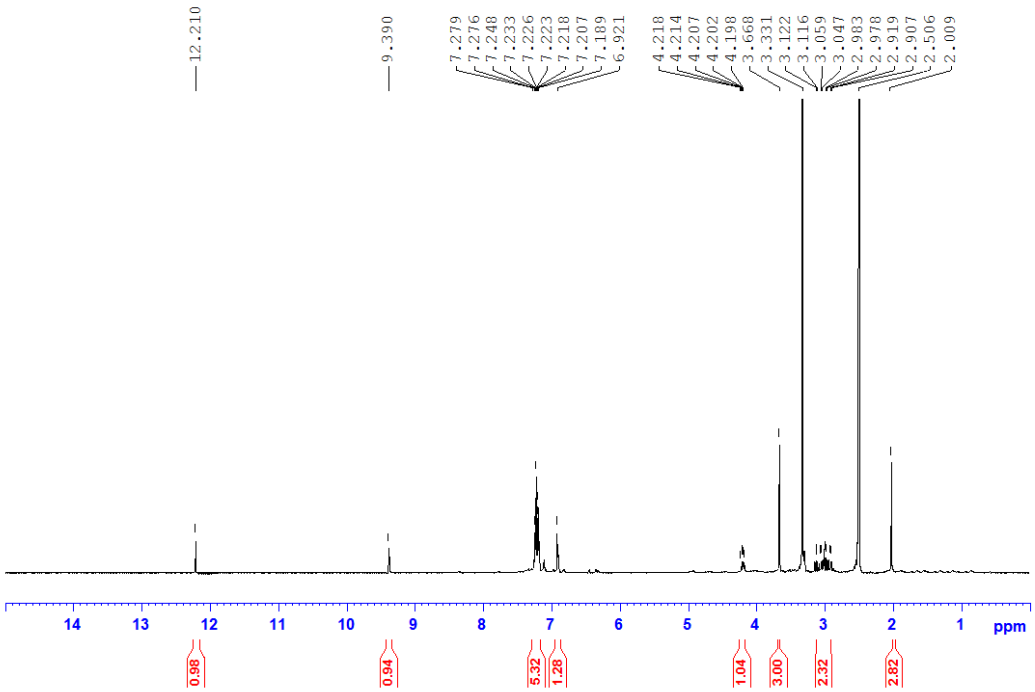

^{13}C-NMR

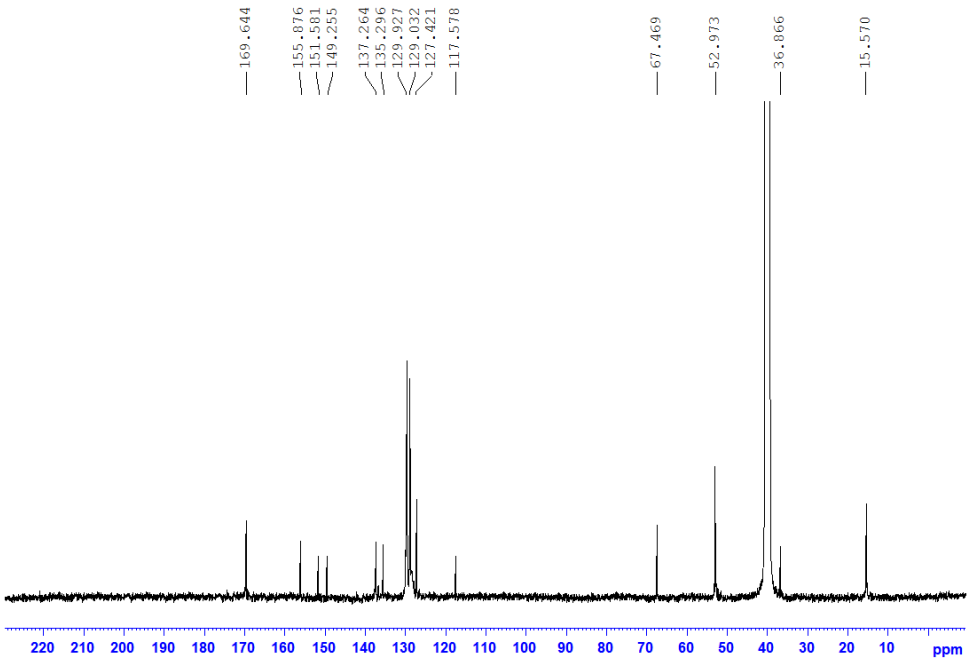

Compound 19f Methyl 3-(4-hydroxyphenyl)-2-(6-imino-2-methyl-6,9-dihydro-1H-purin-1-yl)propanoate.

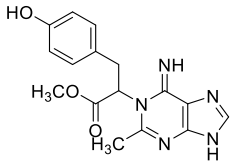

^{1}H-NMR

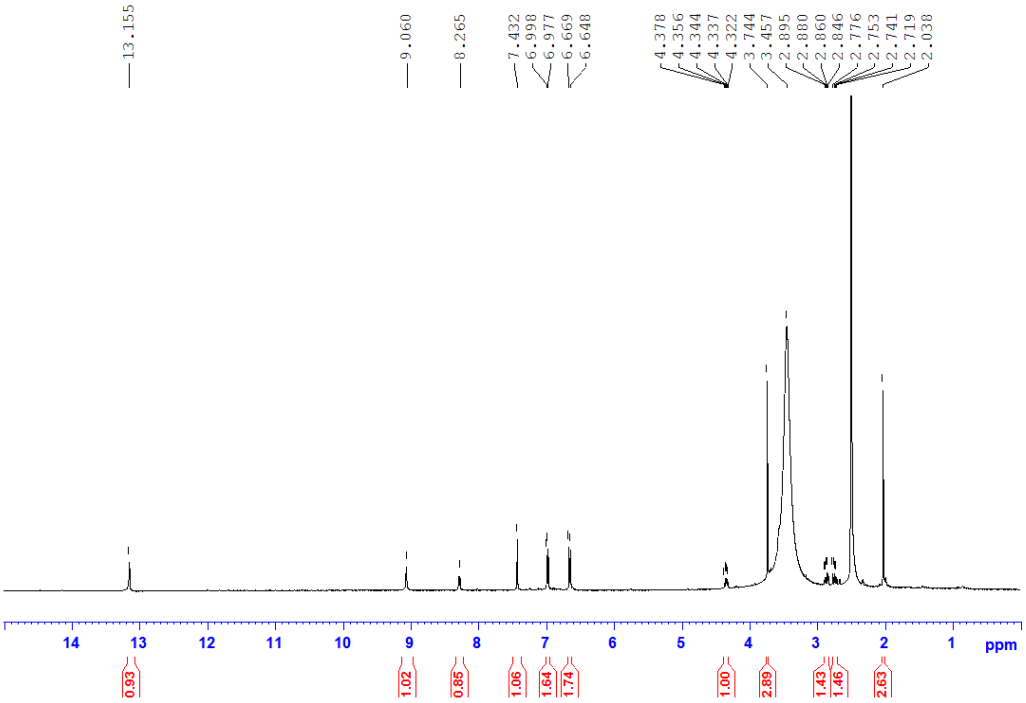

^{13}C-NMR

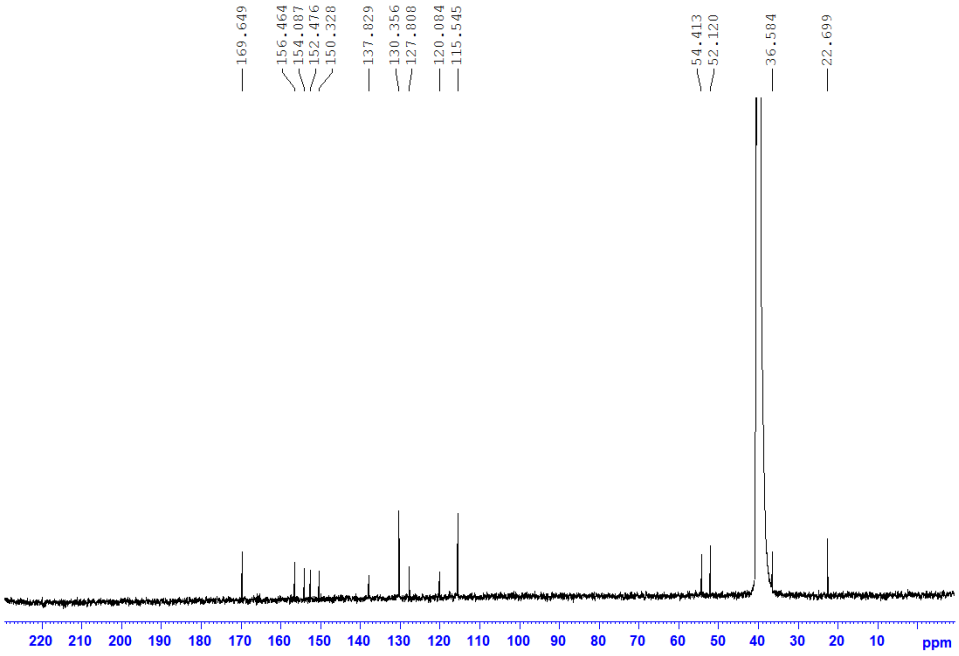

4.1.0.8 UV-visible analyses of compound 13, 15, 16a, 17, 18 and 19a.

Accurately weighed 10 mg of the powdered compounds **13**, **15**, **16a**, **17**, **18** and **19a** were taken in a 10 mL volumetric flask and 10 mL of MeCN were added to reach the concentration of 1 mg/mL. 1 mL of each stock solution was pipetted into quartz cuvette and diluted with 2 mL of MeCN and the absorbance measured in the range from 190 nm to 450 nm. Following, original UV-visible spectra are reported.

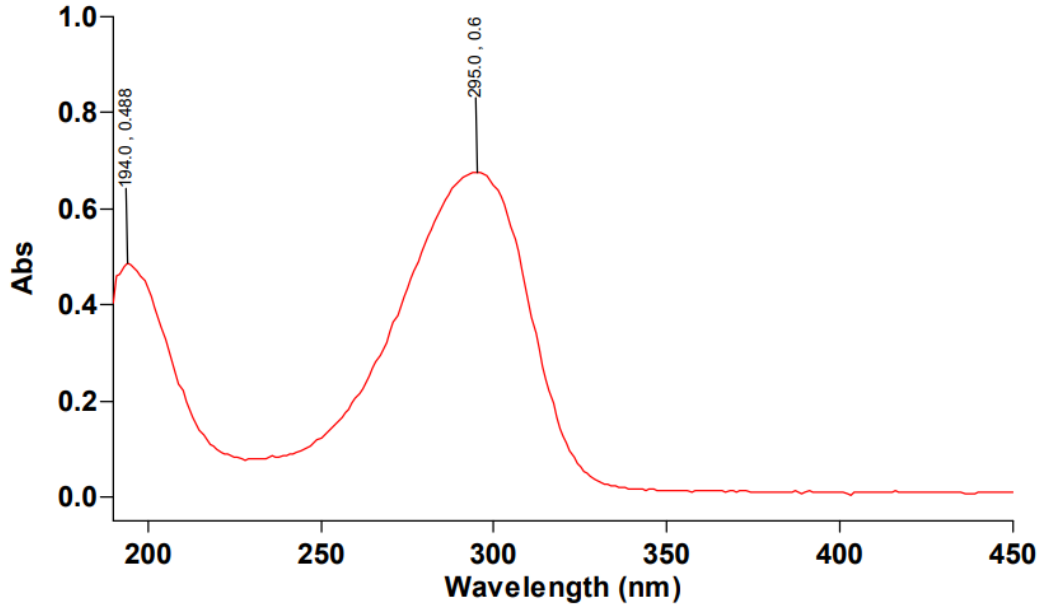

Figure 2: UV-Vis spectrum of **DAMN 13**.

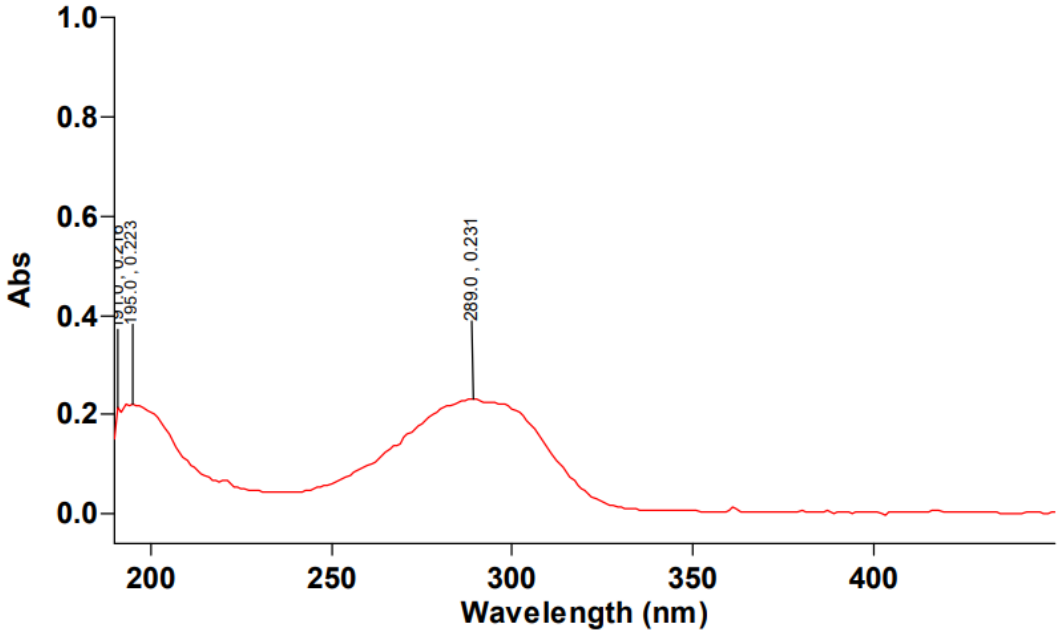

Figure 3: UV-Vis spectrum of **intermediate 15**.

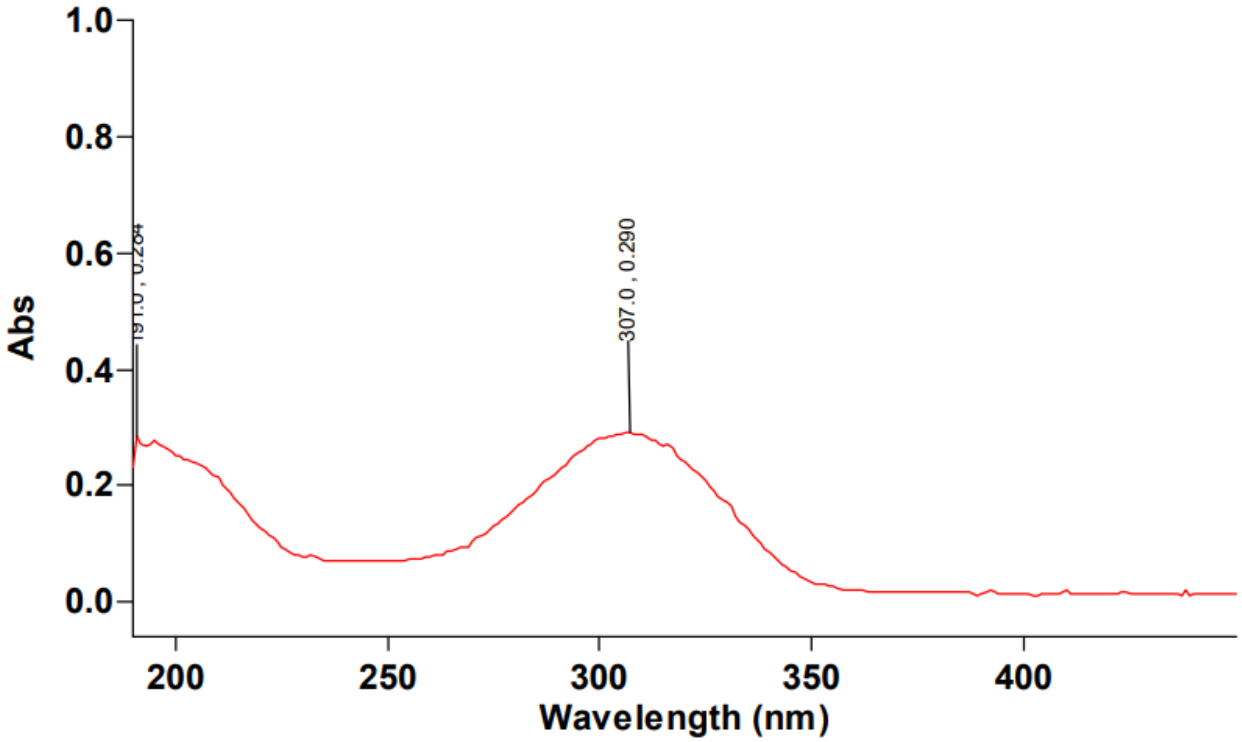

Figure 4: UV-Vis spectrum of **16a**.

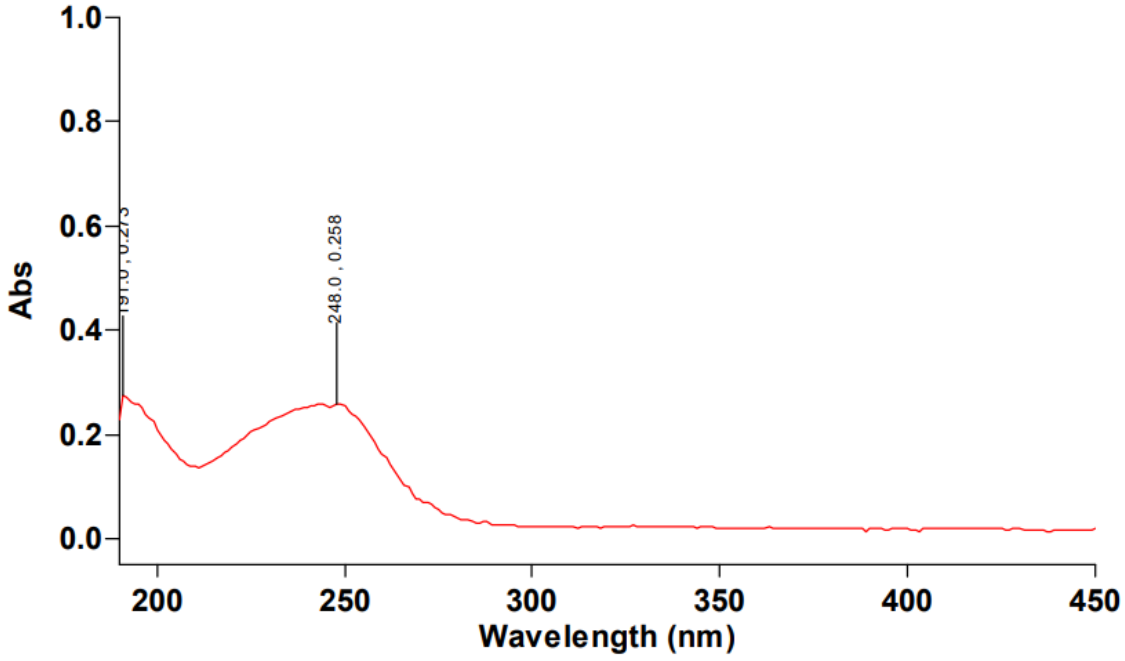

Figure 5: UV-Vis spectrum of **AICN 17**.

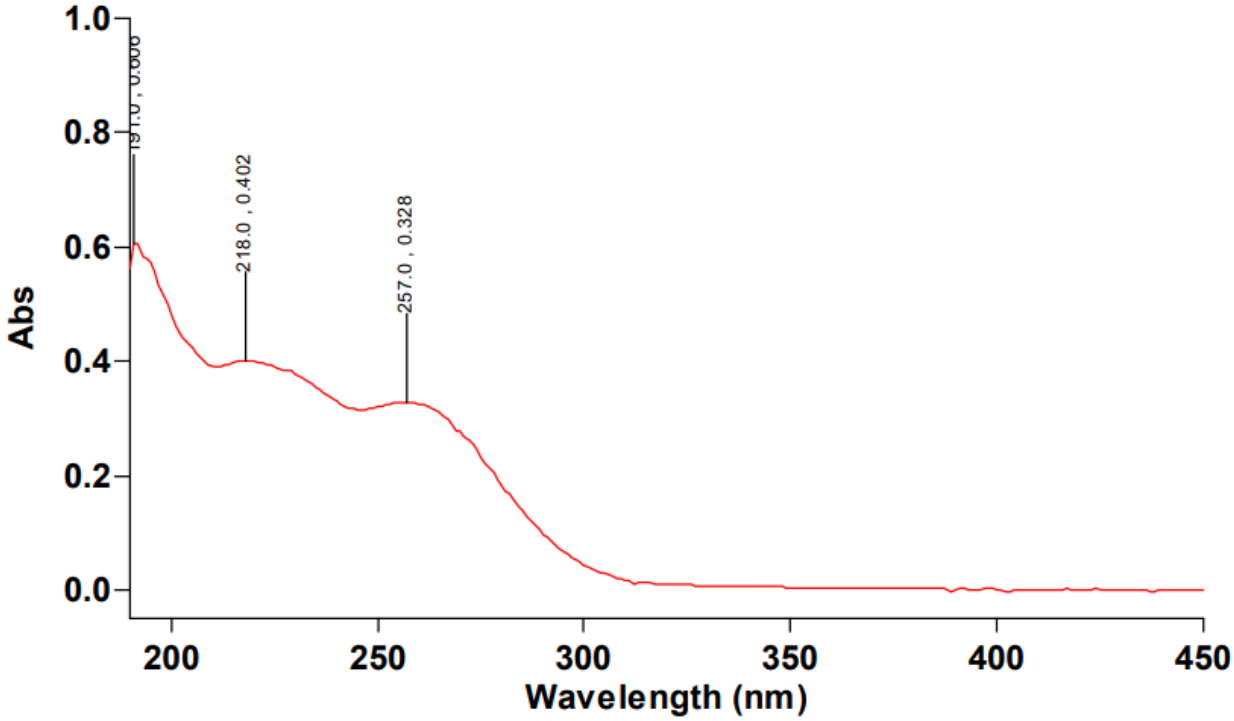

Figure 6: UV-Vis spectrum of **18**.

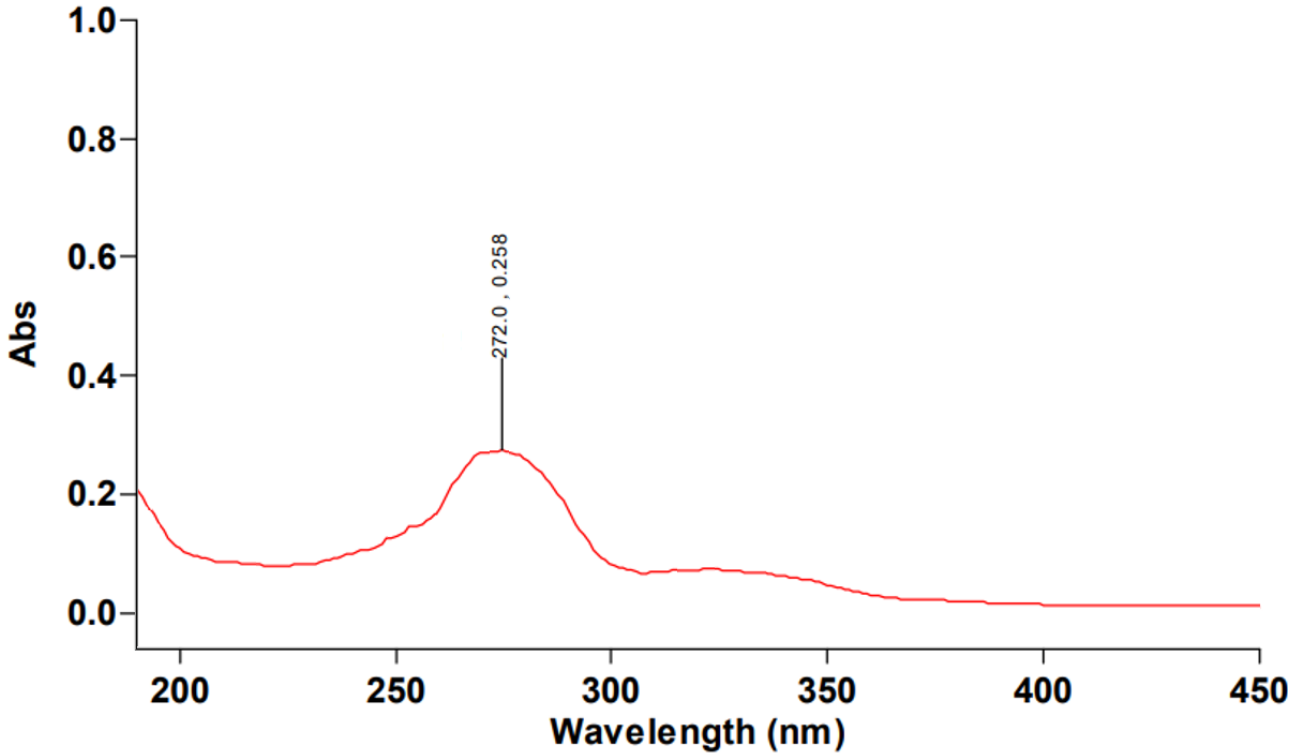

Figure 7: UV-vis spectrum of **19a**.

4.1.0.9 UV-visible analyses of reaction affording compounds 16a and 19a.

50 µL of the reaction mixtures affording compounds **16a** and **19a** were sampled at 0, 15 and 30 min into a quartz cuvette filled with 2950 µL of MeCN and immediately analyzed in the range from 190 nm to 450 nm. Following, original UV-visible spectra are reported.

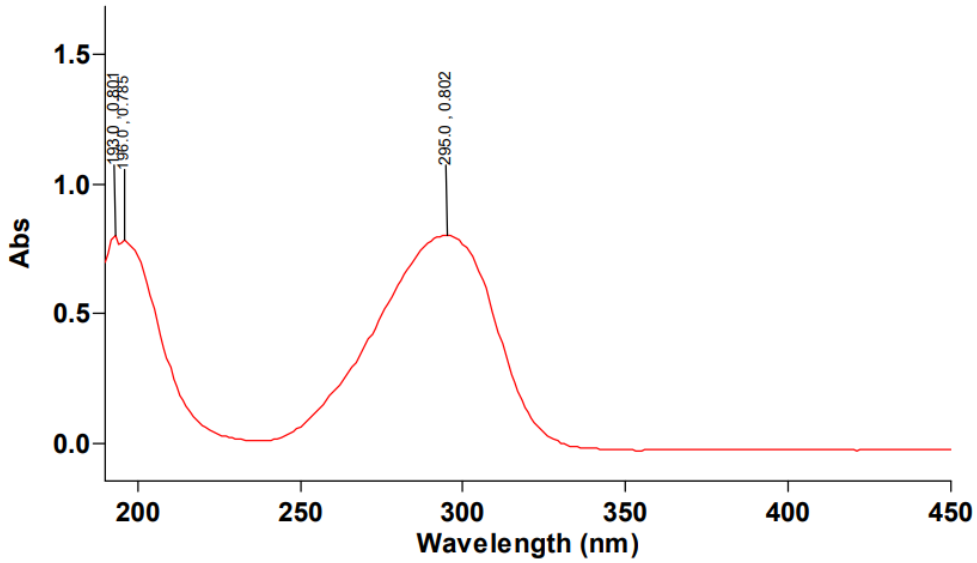

Figure 8: UV-Vis spectrum of reaction mixture for the synthesis of **16a**, at 0 min.

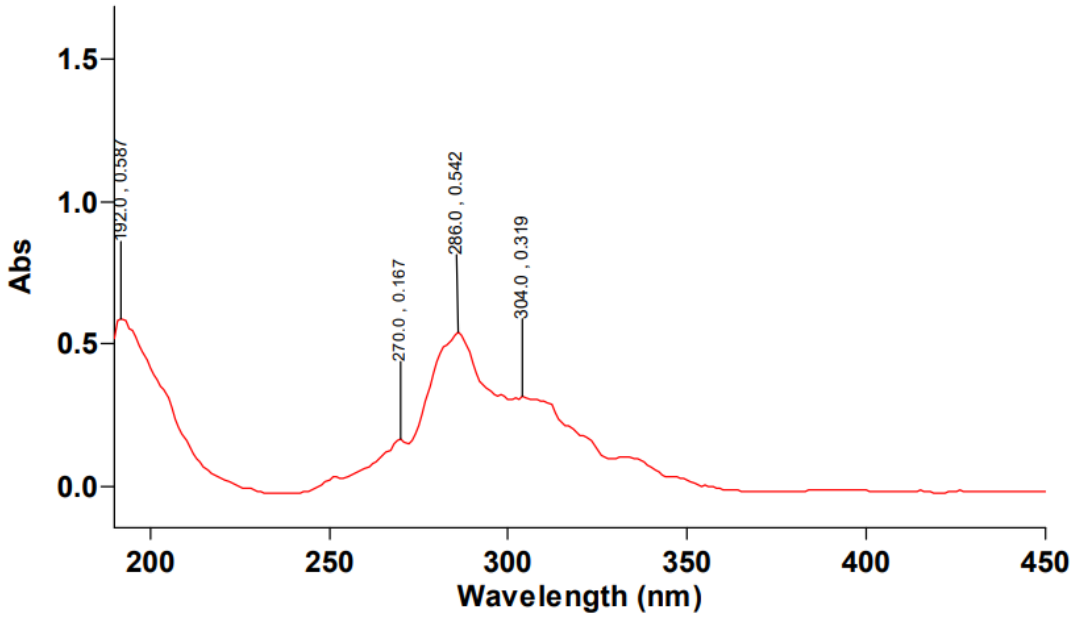

Figure 9: UV-Vis spectrum of reaction mixture for the synthesis of **16a**, after 15 minutes.

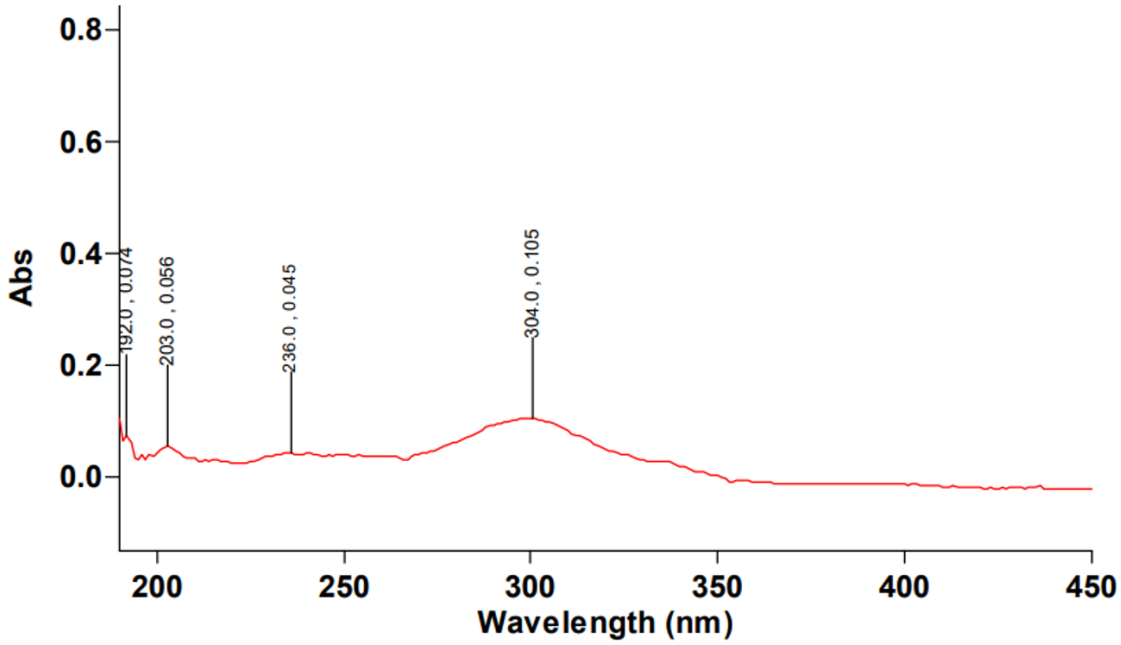

Figure 10: UV-Vis spectrum of reaction mixture for the synthesis of **16a**, after 30 minutes.

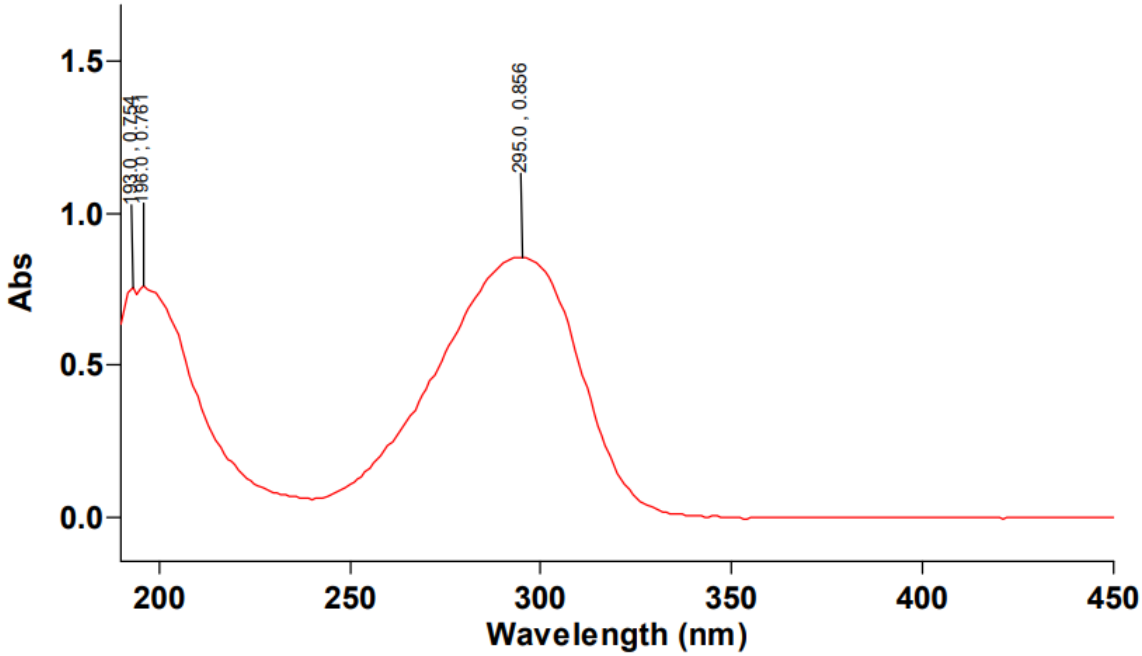

Figure 11: UV-Vis spectrum of reaction mixture for the synthesis of **19a**, at 0 min.

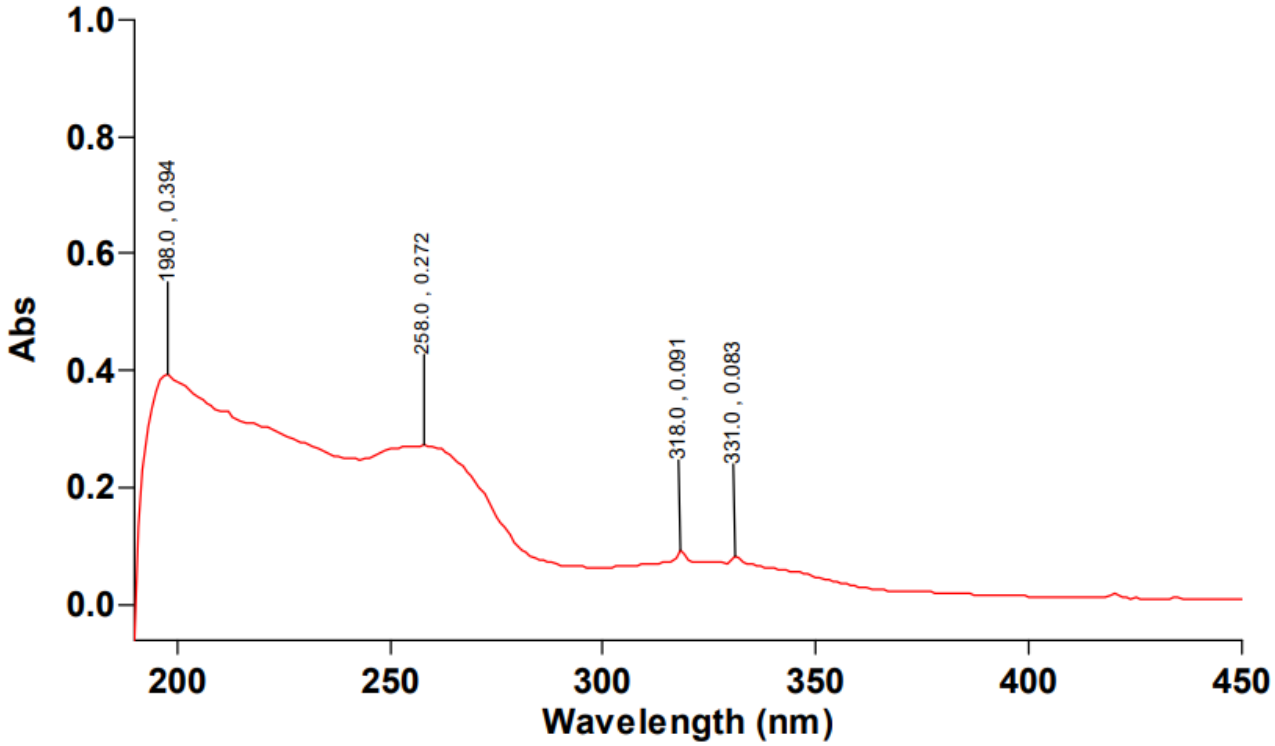

Figure 12: UV-Vis spectrum of reaction mixture for the synthesis of **19a**, after 15 minutes.

4.1.0.10 ATR FT-IR Analysis of compounds 13, 17 and of the reaction mixture affording compound 16a.

3 mg of compounds **13** and **17** were placed on the diamond attenuated total reflectance (ATR) crystal of the apparatus. The analyses were recorded in less than 30 seconds (64 scans at 4 cm^{-1} resolution). For reaction mixture**,** the crude analyzed in a similar way at 15 min from the beginning of the irradiation and after the complete evaporation of the solvent. Original ATR FT-IR spectra are reported below.

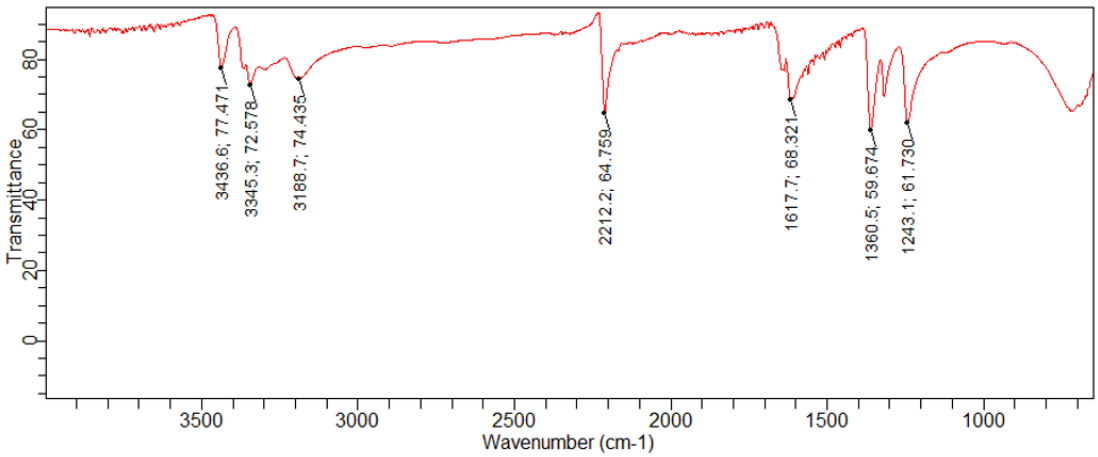

Figure 13: ATR-FTIR analyses of **DAMN 13**.

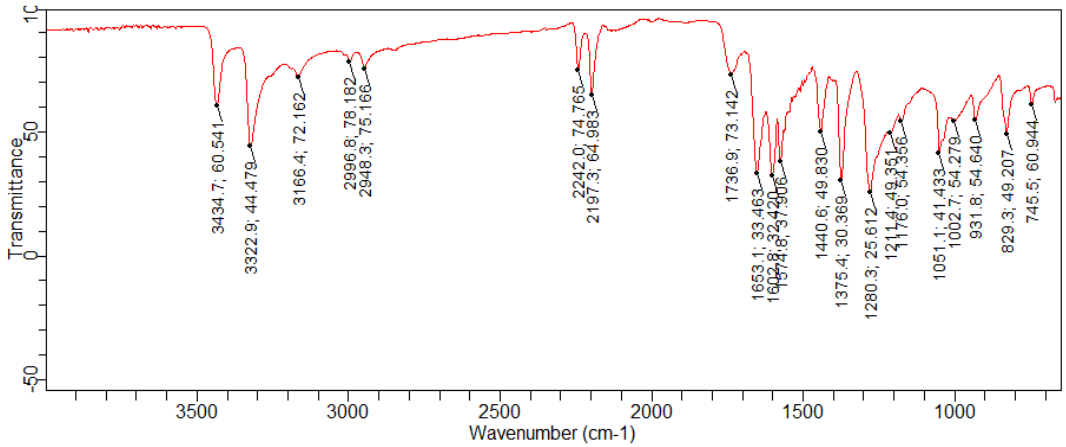

Figure 14: ATR-FTIR analyses of reaction mixture for the synthesis of **16a**.

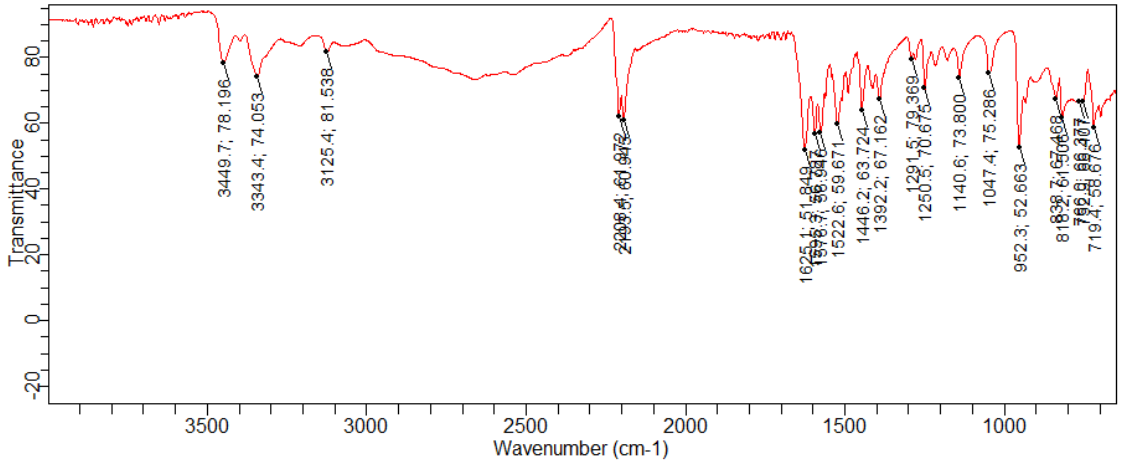

Figure 15: ATR-FTIR of **AICN 17**.

4.1.0.11 Cell Cultures

A 549 (human lung epithelial carcinoma) cell lines were grown in DMEM 1640 medium supplemented with 10% fetal calf serum (FCS); glutamine 0.3 mg/mL; penicillin 100 U/mL and streptomycin 100 mg/mL. Cell viability was estimated by trypan blue (0.02%) exclusion. All reagents were purchased from Invitrogen (Milan, Italy).

4.1.0.12 Cell toxicity assays

The cytotoxicity of the compounds was evaluated by the inhibition of MTT reduction into formazan and by the trypan blue staining assay. Briefly, in the MTT assay, A549 cells were seeded in 96-well plates at a density of $2x10^4$ cells/well in 100 µl of complete DMEM without phenol red for 24 h at 37 °C. Subsequently, cell monolayers were treated or not with increasing concentrations (range 5-80 µg/mL) of compounds for 24 h at 37 °C. After 24 h, 10 µl of MTT solution (5 mg/ml) were added to each well for 3-4 h at 37 °C. Each sample was then acidified by adding 0.1 N HCl in isopropanol (100 µl/well) for 30 min under mild agitation to ensure dissolution of all formazan crystals. Absorbance of samples was read at 570 nm, using an automatic plate reader (Multiskan EX, Ascent Software, Thermo Fisher Scientific). Untreated cells were used as control. The 50% cytotoxic concentration (CC50) was defined as the compound concentration required to reduce cell viability by 50% and calculated by regression analysis considering untreated cells as control (100%).

4.1.0.13 Virus Production and Infection

Influenza A/Puerto Rico/8/34 H1N1 (PR8) virus was grown in the allantoic cavities of 10-day-old embryonated chicken eggs. After 48 h at 37 °C, the allantoic fluid was harvested, centrifuged at 5000 rpm for 30 min to remove cellular debris, and stored at −80 °C. Virus titration was performed by Tissue Culture Infectious Dose 50% (TCID50%). Confluent monolayers of A549 epithelial cells were challenged for 1 h at 37 °C with PR8 at a multiplicity of infection (MOI) of 0.001 (TCID50%/cell) incubated for 1 h at 37 °C, washed with PBS, and then incubated with medium supplemented with 2% FCS. Mock infection was performed with the same dilution of allantoic fluid from uninfected eggs.[338]

4.1.0.14 In Cell Western (ICW) Assay

The ICW assay was performed using the Odyssey Imaging System (LI-COR, Lincoln, NE, USA) as previously described.[339] Briefly, A549 cells grown in 96-well plates ($2×10^4$ cells/well) infected with PR8, and treated or not with high concentrations (100, 150 and 200 µg/mL) of selected compounds

were fixed with 4% formaldehyde, washed, permeabilized with 0.1% Triton X-100 and incubated with Odyssey Blocking buffer for 1 h (LI-COR Biosciences, Lincoln, NE, USA). The cells were then stained at 4 °C overnight with mouse anti HA (Santa Cruz Biotechnology, Germany) diluted in Odyssey Blocking Buffer. Cells were then washed and stained with a fluorochrome-conjugated secondary antibody (fluorescence emission at 800 nm) (LI-COR Biosciences, Lincoln, NE, USA) properly diluted in Odyssey blocking buffer. Subsequently, three washes with PBS plus 0.1% Tween 20 were performed and plates were analyzed by the Odyssey infrared imaging system (LI-COR). The relative fluorescence unit (RFU) was expressed as a percentage compared to untreated infected cells (100%). The 50% infectious dose (IC50) was defined as the dose of compound required to reduce viral replication by 50%. The Selectivity Index (SI) of each compound was calculated as the ratio between CC50 and IC50 (SI = CC50/IC50).

References

1 P. T. Anastas and M. M. Kirchhoff, *Acc. Chem. Res.*, 2002, **35**, 686–694.

2 A. Ivanković, *Int. J. Sustain. Green Energy*, 2017, **6**, 39.

3 M. Jukic, S. Djaković, Ž. Filipović-Kovačević, V. Kovač and J. Furac, *Kem. u Ind. Chem. Chem. Eng.*, 2005, **54**, 255–272.

4 P. Anastas and N. Eghbali, *Chem. Soc. Rev.*, 2010, **39**, 301–312.

5 A. Valavanidis and T. Vlachogianni, *Sci. Adv.*, 2011, **1**, 1–12.

6 S. L. Y. Tang, R. L. Smith and M. Poliakoff, *Green Chem.*, 2005, **7**, 761–762.

7 R. A. Sheldon, *Catal. Today*, 2011, **167**, 3–13.

8 C.-J. Li and B. M. Trost, *Proc. Natl. Acad. Sci.*, 2008, **105**, 13197–13202.

9 P. G. Jessop, S. Trakhtenberg and J. Warner, in *Innovations in Industrial and Engineering Chemistry*, 2009, pp. 401–436.

10 T. Welton, *Proc. Math. Phys. Eng. Sci.*, 2015, **471**, 1-23.

11 P. T. Anastas, M. Kirchhoff and T. C. Williamson, *Appl. Catal. A-general*, 2001, **221**, 3–13.

12 H. W. Hill Jr. and D. G. Brady, *Polym. Eng. & Sci.*, 1976, **16**, 831–835.

13 C. Samorì, 2010.

14 L. H. Keith, L. U. Gron and J. L. Young, *Chem. Rev.*, 2007, **107**, 2695–2708.

15 J. M. Stellman and I. L. Office., *Encyclopaedia of occupational health and safety.*, International Labor Office, 1998.

16 S. Singh and P. Tandon, *J. Energy Chem. Eng.*, 2014, **2**, 106–115.

17 P. W. N. M. van Leeuwen, in *Reference Module in Chemistry, Molecular Sciences and Chemical Engineering*, Elsevier, 2016.

18 I. P. Beletskaya and L. M Kustov, *Russ. Chem. Rev.*, 2010, **79**, 441.

19 W. Grünert, *Zeitschrift für Phys. Chemie*, 1998, **205**, 130–131.

20 J. C. Védrine, *ChemSusChem*, 2019, **12**, 577–588.

21 B. M. Trost, *Science*, 1991, **254**, 1471–1477.

22 X. Creary, *J. Org. Chem.*, 1987, **52**, 5026–5030.

23 R. Epsztein and N. Le Goff, *Tetrahedron*, 1985, **41**, 5347–5352.

24 C. Wei and C.-J. Li, *Green Chem. - GREEN CHEM*, 2002, **4**, 39–41.

25 Z. Li and C.-J. Li, *Org. Lett.*, 2004, **6**, 4997–4999.

26 B. M. Trost, *Angew. Chemie Int. Ed. English*, 1995, **34**, 259–281.

27 D. Mijin, M. Stanković and P. D. Slobodan, *Hem. Ind.*, 2003, **57**, 199-214.

28 J. Warner, A. Cannon and K. Dye, *Environ. Impact Assess. Rev.*, 2004, **24**, 775–799.

29 R. A. Sheldon, *ACS Sustain. Chem. & Eng.*, 2018, **6**, 32–48.

30 R. C. Cioc, E. Ruijter and R. V. A. Orru, *Green Chem.*, 2014, **16**, 2958–2975.

31 M.-O. Simon and C.-J. Li, *Chem. Soc. Rev.*, 2012, **41**, 1415–1427.

32 S. Garbarino, D. Ravelli, S. Protti and A. Basso, *Angew. Chemie Int. Ed.*, 2016, **55**, 15476–15484.

33 A. Strecker, *Justus Liebigs Ann. Chem.*, 1850, **75**, 27–45.

34 A. Dömling, *Curr. Opin. Chem. Biol.*, 2000, **4**, 318–323.

35 I. Ugi, U. Fetzer, U. Eholzer, H. Knupfer and K. Offermann, *Angew. Chemie Int. Ed. English*, 1965, **4**, 472–484.

36 A. Hantzsch, *Berichte der Dtsch. Chem. Gesellschaft*, 1881, **14**, 1637–1638.

37 P. Biginelli, *Eur. J. Inorg. Chem.*, **24**, 1317–1319.

38 L. Weber, S. Wallbaum, C. Broger and K. Gubernator, *Angew. Chemie Int. Ed. English*, 1995, **34**, 2280–2282.

39 O. Lack and L. Weber, *Chimia (Aarau).*, 1996, **50**, 445–447.

40 K. Rossen, P. J. Pye, L. M. DiMichele, R. P. Volante and P. J. Reider, *Tetrahedron Lett.*, 1998, **39**, 6823–6826.

41 A. Roldão, A. C. Silva, M. C. M. Mellado, P. M. Alves and M. J. T. Carrondo, *Compr. Biotechnol.*, 2019, 633–656.

42 H. L. Van Epps, *J. Exp. Med.*, 2006, **203**, 803.

43 R. Saladino, M. Barontini, M. Crucianelli, L. Nencioni, R. Sgarbanti and A. T. Palamara, *Curr.*

Med. Chem. 2010, **17**, 2101–2140.

44 V. S. Hinshaw, R. G. Webster and R. J. Q. Rodríguez, *Arch. Virol.*, 2005, **62**, 281–290.

45 G. Neumann, T. Noda and Y. Kawaoka, *Nature*, 2009, **459**, 931–939.

46 M. I. Nelson and E. C. Holmes, *Nat. Rev. Genet.*, 2007, **8**, 196–205.

47 Y. Wu, Y. Wu, B. Tefsen, Y. Shi and G. F. Gao, *Trends Microbiol.*, 2014, **22**, 183–191.

48 B. G. Hale, R. E. Randall, J. Ortin and D. Jackson, *J. Gen. Virol.*, 2008, **89**, 2359–2376.

49 J. Beigel and M. Bray, *Antiviral Res.*, 2008, **78**, 91–102.

50 C. U. Kim, W. Lew, M. A. Williams, H. Liu, L. Zhang, S. Swaminathan, N. Bischofberger, M. S. Chen, D. B. Mendel, C. Y. Tai, W. G. Laver and R. C. Stevens, *J. Am. Chem. Soc.*, 1997, **119**, 681–690.

51 R. Saladino, C. Crestini, G. Costanzo and E. DiMauro, *Curr. Org. Chem.*, 2004, **8**, 1425–1443.

52 J. Pereto, *Int. Microbiol.*, 2005, **8**, 23–31.

53 C. Scharf, N. Virgo, H. J. Cleaves, M. Aono, N. Aubert-Kato, A. Aydinoglu, A. Barahona, L. M. Barge, S. A. Benner, M. Biehl, R. Brasser, C. J. Butch, K. Chandru, L. Cronin, S. Danielache, J. Fischer, J. Hernlund, P. Hut, T. Ikegami, J. Kimura, K. Kobayashi, C. Mariscal, S. McGlynn, B. Menard, N. Packard, R. Pascal, J. Pereto, S. Rajamani, L. Sinapayen, E. Smith, C. Switzer, K. Takai, F. Tian, Y. Ueno, M. Voytek, O. Witkowski and H. Yabuta, *Astrobiology*, 2015, **15**, 1031–1042.

54 D. Warmflash and B. Weiss, *Sci. Am.*, 2005, **293**, 64–71.

55 S. Sadanand, *Yale J. Biol. Med.*, 2011, **84**, 502.

56 E. A. Bell, P. Boehnke, T. M. Harrison and W. L. Mao, *Proc. Natl. Acad. Sci.*, 2015, **112**, 14518–14521.

57 S. D. Copley, E. Smith and H. J. Morowitz, *Bioorg. Chem.*, 2007, **35**, 430–443.

58 M. P. Robertson and G. F. Joyce, *Cold Spring Harb. Perspect. Biol.*, 2012, **4**, 1.

59 T. Cech, *Cold Spring Harb. Perspect. Biol.*, 2011, **4**, a006742.

60 M. A. Keller, A. V Turchyn and M. Ralser, *Mol. Syst. Biol.*, 2014, **10**, 725.

61 P. Ehrenfreund and J. Cami, *Cold Spring Harb. Perspect. Biol.*, 2010, **2**, a002097.

62 P. ~H. Rampelotto, in *Astrobiology Science Conference 2010: Evolution and Life: Surviving Catastrophes and Extremes on Earth and Beyond*, ed. LPI Editorial Board, 2010, vol. 1538, p. 5224.

63 A. Loeb, *Int. J. Astrobiol.*, 2014, **13**, 337–339.

64 C. Dreyfus, N. S. Laursen, T. Kwaks, et al. *Science*. 2012, **337**, 1343- 1348.

65 R. W. Graham, in NASA 1990.

66 G. Manhes, C. J. Allègre, B. Dupré and B. Hamelin, *Earth Planet. Sci. Lett.*, 1980, **47**, 370–382.

67 J. W. Schopf, A. B. Kudryavtsev, A. D. Czaja and A. B. Tripathi, *Precambrian Res.*, 2007, **158**, 141–155.

68 N. Noffke, D. Christian, D. Wacey and R. M. Hazen, *Astrobiology*, 2013, **13**, 1103–1124.

69 Y. Ohtomo, T. Kakegawa, A. Ishida, T. Nagase and M. Rosing, *Nat. Geosci.*, 2014, **7**, 25-28.

70 R. Saladino, C. Crestini, S. Pino, G. Costanzo and E. Di Mauro, *Phys. Life Rev.*, 2012, **9**, 84-104.

71 R. Stribling and S. L. Miller, *Icarus*, 1987, **72**, 48–52.

72 R. L. Hudson and M. H. Moore, *Icarus*, 1999, **140**, 451–461.

73 E. A. McKenna, A. Othoneos, N. Kiratzis and M. Stoukides, *Ind. & Eng. Chem. Res.*, 1993, **32**, 1904–1913.

74 Y. Takano, K. Marumo, T. Kaneko, K. Kobayashi, D. Hiroishi and H. Ikeda, *Earth, Planets Sp.*, 2004, **56**, 669–674.

75 D. E. Woon, *Int. J. Quantum Chem.*, 2002, **88**, 226–235.

76 T. Koike, T. Kaneko, K. Kobayashi, S. Miyakawa and Y. Takano, *Biol. Sci. Sp.*, 2003, **17**, 188–189.

77 P. A. Gerakines, M. H. Moore and R. L. Hudson, *Icarus*, 2004, **170**, 202–213.

78 S. Miyakawa, H. J. Cleaves, S. L. Miller, D. Rai, A. R. Felmy, S. C. Smith and J. L. Ryan, *Orig. Life Evol. Biosph.*, 1994, **32**, 195–208.

79 R. Stribling and S. L. Miller, *Orig. life Evol. Biosph.*, 1987, **17**, 261–273.

80 V. S. Nguyen, T. M. Orlando, J. Leszczynski and M. T. Nguyen, *J. Phys. Chem. A*, 2013, **117**, 2543–2555.

81 D. J. Drury, in *Kirk-Othmer Encyclopedia of Chemical Technology*, John Wiley & Sons, Ltd, 2000.

82 L. Čechová, P. Jansa, M. Šála, M. Dračínský, A. Holý and Z. Janeba, *Tetrahedron*, 2011, **67**, 866–871.

83 G. Costanzo, R. Saladino, C. Crestini, F. Ciciriello and E. Di Mauro, *BMC Evol. Biol.*, 2007, **7**, 1–8.

84 S. L. Miller, *Science*, 1953, **117**, 528-529.

85 J. P. Ferris and W. J. Hagan, *Tetrahedron*, 1984, **40**, 1093–1120.

86 P. M. Solomon, *Phys. Today*, 1973, **26**, 32–40.

87 M. Mumma, P. Weissman and S. Stern, Protostars and planets III, 1993, 1177-1252.

88 K. Magee-Sauer, M. J. Mumma, M. A. DiSanti, N. Dello Russo and T. W. Rettig, *Icarus*, 1999, **142**, 498–508.

89 W. M. Irvine, 1999, 203–204.

90 T. Hidayat, A. Marten, B. Bézard, D. Gautier, T. Owen, H. E. Matthews and G. Paubert, *Icarus*,

1997, **126**, 170–182.

91 T. B. McCord, R. W. Carlson, W. D. Smythe, G. B. Hansen, R. N. Clark, C. A. Hibbitts, F. P. Fanale, J. C. Granahan, M. Segura, D. L. Matson, T. V Johnson and P. D. Martin, *Science*, 1997, **278**, 271–275.

92 J. S. Hubbard, G. E. Voecks, G. L. Hobby, J. P. Ferris, E. A. Williams and D. E. Nicodem, *J. Mol. Evol.*, 1975, **5**, 223–241.

93 J. P. Ferris and L. E. Orgel, *J. Am. Chem. Soc.*, 1965, **87**, 4976–4977.

94 R. A. Sanchez, J. P. Ferbis and L. E. Orgel, *J. Mol. Biol.*, 1967, **30**, 223–253.

95 J. P. Ferris and L. E. Orgel, *J. Am. Chem. Soc.*, 1966, **88**, 3829–3831.

96 J. P. Ferris and L. E. Orgel, *J. Am. Chem. Soc.*, 1966, **88**, 1074.

97 A. Eschenmoser and E. Loewenthal, *Chem. Soc. Rev.*, 1992, **21**, 1-16.

98 R. A. Sanchez, J. P. Ferris and L. E. Orgel, *Science*, 1966, **154**, 784–785.

99 L. E. Orgel and R. Lohrmann, *Acc. Chem. Res.*, 1974, **7**, 368–377.

100 M. Ruiz-Bermejo, M.-P. Zorzano and S. Osuna-Esteban, *Life open access J.*, 2013, **3**, 421–448.

101 L. Moggio, A. Romanelli, R. Gambari, N. Bianchi, M. Borgatti, E. Fabbri, I. Mancini, B. di Blasio, C. Pedone and A. Messere, *Pept. Sci.*, 2007, **88**, 815–822.

102 P. E. Nielsen, M. Egholm, R. H. Berg and O. Buchardt, *Science*, 1991, **254**, 1497-1500.

103 D. R. Corey, *Trends Biotechnol.*, 1997, **15**, 224–229.

104 P. Nielsen and M. Egholm, *Curr. Issues Mol. Biol.*, 1999, **1**, 89–104.

105 M. Egholm, O. Buchardt, P. E. Nielsen and R. H. Berg, *J. Am. Chem. Soc.*, 1992, **114**, 1895–1897.

106 V. V Demidov, V. N. Potaman, M. D. Frank-Kamenetskil, M. Egholm, O. Buchard, S. H.

Sönnichsen and P. E. Nlelsen, *Biochem. Pharmacol.*, 1994, **48**, 1310–1313.

107 V. V. Demidov, *Drug Discov. Today*, 2002, **7**, 153–155.

108 P. E. Nielsen, *Curr. Opin. Struct. Biol.*, 1999, **9**, 353–357.

109 J. C. Hanvey, N. J. Peffer, J. E. Bisi, S. A. Thomson, R. Cadilla, J. A. Josey, D. J. Ricca, C. F. Hassman, M. A. Bonham, K. G. Au, S. G. Carter, D. A. Bruckenstein, A. L. Boyd, S. A. Noble and L. E. Babiss, *Science (80-.).*, 1992, **258**, 1481–1485.

110 T. Mayhood, N. Kaushik, P. K. Pandey, F. Kashanchi, L. Deng and V. N. Pandey, *Biochemistry*, 2000, **39**, 11532–11539.

111 R. Lee, N. Kaushik, M. J. Modak, R. Vinayak and V. N. Pandey, *Biochemistry*, 1998, **37**, 900–910.

112 J. Oro, T. Mills and A. Lazcano, *Orig. Life Evol. Biosph.*, 1992, **21**, 267–277.

113 D. M. Stone, *Nature*, 1996, **384**, 356–358.

114 R. Saladino, L. Botta and E. Di Mauro, *Life*, 2018, **8**, 6.

115 G. R. Adande, N. J. Woolf and L. M. Ziurys, *Astrobiology*, 2013, **13**, 476-482.

116 A. López-Sepulcre, A. Jaber, E. Mendoza, B. Lefloch, C. Ceccarelli, C. Vastel, R. Bachiller, J. Cernicharo, C. Codella, C. Kahane, M. Kama and M. Tafalla, *Mon. Not. R. Astron. Soc.*, 2015, **449**, 2438-2458.

117 R. Rubin, G. Swenson Jr, R. Benson, H. Tigelaar and W. Flygare, *Astrophys. J.*, 1971, **169**, L39-L44.

118 H. Slebocka-Tilk, F. Sauriol, M. Monette and R. S. Brown, *Can. J. Chem.*, 2002, **80**, 1343–1350.

119 E. Carota, G. Botta, L. Rotelli, E. Di Mauro and R. Saladino, *Curr. Org. Chem.*, 2015, **19**, 1.

120 R. Saladino, G. Botta, S. Pino, G. Costanzo and E. Di Mauro, *Chem. Soc. Rev.*, 2012, **41**, 5526-5565.

121 R. Saladino, C. E. Moyano-Cambero, L. Rotelli, E. Carota, E. Di Mauro, J. M. Trigo-Rodríguez and L. Botta, *Sci. Rep.*, 2016, **6**, 1–7.

122 L. Botta, R. Saladino, B. M. Bizzarri, B. Cobucci-Ponzano, R. Iacono, R. Avino, S. Caliro, A. Carandente, F. Lorenzini, A. Tortora, E. Di Mauro and M. Moracci, *Adv. Sp. Res.*, 2018, **62**, 2372-2379.

123 R. Saladino, G. Botta, M. Delfino and E. Di Mauro, *Chem. - A Eur. J.*, 2013, **19**, 16916-16922.

124 R. Saladino, E. Carota, G. Botta, M. Kapralov, G. N. Timoshenko, A. Y. Rozanov, E. Krasavin and E. Di Mauro, *Proc. Natl. Acad. Sci. U. S. A.*, 2015, **112**, E2746-E2755.

125 R. Saladino, E. Carota, G. Botta, M. Kapralov, G. N. Timoshenko, A. Rozanov, E. Krasavin and E. Di Mauro, *Orig. Life Evol. Biosph.*, 2016, **46**, 515-521.

126 R. Saladino, B. M. Bizzarri, L. Botta, J. Šponer, J. E. Šponer, T. Georgelin, M. Jaber, B. Rigaud, M. Kapralov, G. N. Timoshenko, A. Rozanov, E. Krasavin, A. M. Timperio and E. Di Mauro, *Sci. Rep.*, 2017, **7**, 14709.

127 M. Nuevo, Y.-J. Chen, W.-J. Hu, J.-M. Qiu, S.-R. Wu, H.-S. Fung, C. C. Chu, T.-S. Yih, W.-H. Ip and C.-Y. Wu, *Astrobiology*, 2014, **14**, 119-131.

128 J. Audouze, J. Lequeux and H. Reeves, *Astron. Astrophys.*, 1973, **28**, 85.

129 R. Saladino, C. Crestini, C. Cossetti, E. Di Mauro and D. Deamer, *Orig. Life Evol. Biosph.*, 2011, **41**, 437-451.

130 G. N. Timoshenko, E. Carota, E. Di Mauro, G. Botta, R. Saladino, E. Krasavin, A. Y. Rozanov and M. Kapralov, *Proc. Natl. Acad. Sci.*, 2015, **112**, E2746–E2755.

131 M. Chaussidon and F. Robert, *Nature*, 1995, **374**, 337–339.

132 F. E. Kühn, A. Scherbaum and W. A. Herrmann, *J. Organomet. Chem.*, 2004, **689**, 4149–4164.

133 G. S. Owens and M. M. Abu-Omar, *Chem. Commun.*, 2000, 1165–1166.

134 C. C. Romão, F. E. Kühn and W. A. Herrmann, *Chem. Rev.*, 1997, **97**, 3197–3246.

135 J. Arning, V. Korinth, U. Bottin-Weber, B. Jastorff, M. Cokoja, F. E. Kühn, H. T. T. Bui, C. Hartmann, A. Białk-Bielińska, S. Steudte, S. Stolte, V. Fetz, A. Hahlbrock, R. W. Fischer and R. Stauber, *Green Chem.*, 2014, **17**, 1136–1144.

136 I. R. Beattie and P. J. Jones, *Inorg. Chem.*, 1979, **18**, 2318–2319.

137 M. Crucianelli, R. Saladino and F. De Angelis, *ChemSusChem*, 2010, **3**, 524–540.

138 G. Bianchini, M. Crucianelli, C. Crestini and R. Saladino, *Top. Catal.*, 2006, **40**, 221–227.

139 R. Saladino, V. Neri, P. Checconi, I. Celestino, L. Nencioni, A. Palamara and M. Crucianelli, *Chemistry,- A. Europ. J.*, 2013, **19**, 2392-2404.

140 L. Botta, S. Filippi, B. M. Bizzarri, R. Meschini, M. Caputo, L. Proietti-De-Santis, C. Iside, A. Nebbioso, G. Gualandi and R. Saladino, *Bioorg. Med. Chem. Lett.*, 2019, **29**, 78–82.

141 A. Di Giuseppe, M. Crucianelli, F. De Angelis, C. Crestini and R. Saladino, *Appl. Catal. B Environ.*, 2009, **89**, 239–245.

142 R. Saladino, V. Neri, A. Farina, C. Crestini, L. Nencioni and A. T. Palamara, *Adv. Synth. \& Catal.*, 2008, **350**, 321–331.

143 R. Bernini, E. Mincione, M. Cortese, G. Aliotta, A. Oliva and R. Saladino, *Tetrahedron Lett.*, 2001, **42**, 5401–5404.

144 A. M. J. Rost, H. Schneider, J. P. Zoller, W. A. Herrmann and F. E. Kühn, *J. Organomet. Chem.*, 2005, **690**, 4712–4718.

145 R. Saladino, C. Crestini, M. Crucianelli, G. Soldaini, F. Cardona and A. Goti, *J. Mol. Catal. A Chem.*, 2008, **284**, 108–115.

146 R. Saladino, V. Neri, A. R. Pelliccia and E. Mincione, *Tetrahedron*, 2003, **59**, 7403–7408.

147 R. Saladino, M. C. Ginnasi, D. Collalto, R. Bernini and C. Crestini, *Adv. Synth. & Catal.*, 2010, **352**, 1284–1290.

148 R. Saladino, R. Bernini, V. Neri and C. Crestini, *Appl. Catal. A Gen.*, 2009, **360**, 171–176.

149 S. M. Nabavizadeh, *Inorg. Chem.*, 2003, **42**, 4204–4208.

150 P. Ferreira, W.-M. Xue, É. Bencze, E. Herdtweck and F. E. Kühn, *Inorg. Chem.*, 2001, **40**, 5834–5841.

151 F. E. Kühn, A. M. Santos and W. A. Herrmann, *Dalton Trans.*, 2005, 2483-2491.

152 W. Adam and C. M. Mitchell, *Angew. Chemie-international Ed.* 1996, **35**, 533–535.

153 A. Di Giuseppe, M. Crucianelli, M. Passacantando, S. Nisi and R. Saladino, *J. Catal.*, 2010, **276**, 412–422.

154 R. Saladino, V. Neri, A. Rita Pelliccia, R. Caminiti and C. Sadun, *J. Org. Chem.*, 2002, **67**, 1323–1332.

155 R. Saladino, V. Neri, E. Mincione and P. Filippone, *Tetrahedron*, 2002, **58**, 8493–8500.

156 R. Saladino, E. Mincione, O. A. Attanasi and P. Filippone, *Pure Appl. Chem.*, 2003, **75**, 265–272.

157 R. Saladino, A. Andreoni, V. Neri and C. Crestini, *Tetrahedron*, 2005, **61**, 1069–1075.

158 R. Buffon, A. Auroux, F. Lefebvre, M. Leconte, A. Choplin, J. Basset and W. A. Herrmann, *J. Mol. Catal.*, 1992, **76**, 287–295.

159 A. Sakthivel, G. Raudaschl-Sieber and F. E. Kühn, *Dalt. Trans.*, 2006, 468–472.

160 A. Gallo, A. Fong, K. C. Szeto, J. Rieb, L. Delevoye, R. M. Gauvin, M. Taoufik, B. Peters and S. L. Scott, *J. Am. Chem. Soc.*, 2016, **138**, 12935–12947.

161 D. Piccinino, I. Abdalghani, G. Botta, M. Crucianelli, M. Passacantando, M. L. Di Vacri and R. Saladino, *Appl. Catal. B Environ.*, 2017, **200**, 392–401.

162 S. M. Nabavizadeh and M. Rashidi, *J. Am. Chem. Soc.*, 2006, **128**, 351–357.

163 M.-D. Zhou, M.-J. Liu, L.-L. Huang, J. Zhang, J.-Y. Wang, X.-B. Li, F. E. Kühn and S.-L. Zang, *Green Chem.*, 2015, **17**, 1186–1193.

164 L. Botta, B. M. Bizzarri, M. Crucianelli and R. Saladino, *J. Mater. Chem. B*, 2017, **5**, 6490–6510.

165 G. Mittal, V. Dhand, K. Y. Rhee, S.-J. Park and W. R. Lee, *J. Ind. Eng. Chem.*, 2015, **21**, 11–25.

166 A. S. Attiyat, G. D. Christian, C. V. Cason and R. A. Bartsch, *Electroanalysis*, 1992, **4**, 51-56.

167 J. Camarena, H. Espinoza-Gomez, R. Somanathan, H. Tiznado, E. Vélez-López, R. Rivera, M. Martínez-López, M. Avalos-Borja, A. Bek, G. Alonso-Nuñez and E. Rogel-Hernández, *J. Nanosci. Nanotechnol.*, 2011, **11**, 5539–5545.

168 L.-J. Du, Y.-H. Hu, Q.-Y. Wang, Q.-D. Zhang, Y.-B. Chen, L.-Q. Peng, S.-L. Pan, Q. Li and J. Cao, *Food Chem.*, 2018, **262**, 118–128.

169 L. Danyang, N. Lanli, D. Yimin, Z. Jiaqi, C. Tianxiao and Z. Yi, *J. Mater. Sci. Mater. Electron.*, 2019, **30**, 1161–1174.

170 G. Kerric, E. J. Parra, G. A. Crespo, F. Xavier Rius and P. Blondeau, *J. Mater. Chem.*, 2012, **22**, 16611–16617.

171 M. A. Herrero, F. M. Toma, K. T. Al-Jamal, K. Kostarelos, A. Bianco, T. Da Ros, F. Bano, L. Casalis, G. Scoles and M. Prato, *J. Am. Chem. Soc.*, 2009, **131**, 9843–9848.

172 D. Astruc, D. Wang, C. Deraedt, L. Liang, R. Ciganda and J. Ruiz, *Synthesis*, 2015, **47**, 2017-2031.

173 Y.-P. Sun, W. Huang, Y. Lin, K. Fu, A. Kitaygorodskiy, L. A. Riddle, Y. J. Yu and D. L. Carroll, *Chem. Mater.*, 2001, **13**, 2864–2869.

174 M. Holzinger, J. Abraham, P. Whelan, R. Graupner, L. Ley, F. Hennrich, M. Kappes and A. Hirsch, *J. Am. Chem. Soc.*, 2003, **125**, 8566–8580.

175 S. Campidelli, C. Sooambar, E. Lozano Diz, C. Ehli, D. M. Guldi and M. Prato, *J. Am. Chem. Soc.*, 2006, **128**, 12544–12552.

176 A. Desmecht, T. Steenhaut, F. Pennetreau, S. Hermans and O. Riant, *Chem. - A Eur. J.*, 2018, **24**, 12992-13001.

177 L.-Y. Lin, K.-C. Ho, C.-Y. Liu, K.-F. Lin, R. Vittal, C.-G. Wu, K.-C. Huang, C.-Y. Chen and Y.-

H. Chang, *J. Mater. Chem.*, 2011, **21**, 18467.

178 L. Danyang, N. Lanli, D. Yimin, Z. Jiaqi, C. Tianxiao and Z. Yi, *J. Mater. Sci. Mater. Electron.*, 2019, **30**, 1161–1174.

179 M.-J. Li, C.-C. Ko, G.-P. Duan, N. Zhu and V. W.-W. Yam, *Organometallics*, 2007, **26**, 6091–6098.

180 B. M. Bizzarri, I. Abdalghani, L. Botta, A. R. Taddei, S. Nisi, M. Ferrante, M. Passacantando, M. Crucianelli and R. Saladino, *Nanomaterials*, 2018, **8**, 516.

181 E. J. Parra, P. Blondeau, G. A. Crespo and F. X. Rius, *Chem. Commun.*, 2011, **47**, 2438–2440.

182 D. Atzei, D. De Filippo, A. Rossi, R. Caminiti and C. Sadun, *Spectrochim. Acta Part A Mol. Biomol. Spectrosc.*, 1995, **51**, 11–20.

183 D. Atzei, D. De Filippo, A. Rossi, R. Caminiti and C. Sadun, *Inorganica Chim. Acta*, 1996, **248**, 203–208.

184 D. Atzei, C. Sadun and L. Pandolfi, *Spectrochim. Acta Part A Mol. Biomol. Spectrosc.*, 2000, **56**, 531–540.

185 R. Caminiti, M. Carbone, S. Panero and C. Sadun, *J. Phys. Chem. B*, 1999, **103**, 10348–10355.

186 D. Atzei, T. Ferri, C. Sadun, P. Sangiorgio and R. Caminiti, *J. Am. Chem. Soc.*, 2001, **123**, 2552–2558.

187 K. Jurkiewicz, M. Pawlyta and A. Burian, *C*, 2018, **4**, 68.

188 J. Takacs, P. Kiprof, J. Riede and W. A. Herrmann, *Organometallics*, 1990, **9**, 782–787.

189 R. M. Crooks, B. I. Lemon, L. Sun, L. K. Yeung and M. Zhao, in *Dendrimers III: Design, Dimension, Function*, ed. F. Vögtle, Springer Berlin Heidelberg, Berlin, Heidelberg, 2001, pp. 81–135.

190 A. S. Ertürk, M. Ulvi Gürbüz, M. Tülü and A. Bozdoğan, *Maced. J. Chem. Chem. Eng.*, 2016, **35**, 263-270.

191 L. Banci, A. Bencini, C. Benelli, D. Gatteschi and C. Zanchini, in *Structures versus Special Properties*, Springer Berlin Heidelberg, Berlin, Heidelberg, 1982, pp. 37–86.

192 V. Vasumathi, D. Pramanik, A. K. Sood and P. K. Maiti, *Soft Matter*, 2013, **9**, 1372–1380.

193 G. Zubay and T. Mui, in *Origins of Life and Evolution of the Biosphere*, 2001.

194 J. E. Šponer, J. Šponer and M. Fuentes-Cabrera, *Chem. - A Eur. J.*, 2011, **17**, 847-854.

195 J. E. Šponer, R. Szabla, R. W. Góra, A. M. Saitta, F. Pietrucci, F. Saija, E. Di Mauro, R. Saladino, M. Ferus, S. Civiš and J. Šponer, *Phys. Chem. Chem. Phys.*, 2016, 18, 20047-20066.

196 R. Saladino, J. E. Šponer, J. Šponer and E. Di Mauro, *ChemBioChem*, 2018, **19**, 22-25.

197 F. Micheel and H. Köchling, *Chem. Ber.*,1957, **90**, 1597-1598.

198 S. Konstas, I. Photaki and L. Zervas, *Chem. Ber.*, 1959, **92**, 1288-1293.

199 R. A. Sanchez and L. E. Orgel, *J. Mol. Biol.*, 1970, **47**, 531-543.

200 S. Becker, I. Thoma, A. Deutsch, T. Gehrke, P. Mayer, H. Zipse and T. Carell, *Science*, 2016, **352**, 833–836.

201 R. Saladino, E. Mincione, C. Crestini, R. Negri, E. Di Mauro and G. Costanzo, *J. Am. Chem. Soc.*, 1996, **118**, 5615-5619.

202 M. W. Powner and J. D. Sutherland, *Angew. Chemie - Int. Ed.*, 2010, **49**, 4641-4643.

203 M. W. Powner, B. Gerland and J. D. Sutherland, *Nature*, 2009, **459**, 239-242.

204 J. Xu, M. Tsanakopoulou, C. J. Magnani, R. Szabla, J. E. Šponer, J. Šponer, R. W. Góra and J. D. Sutherland, *Nat. Chem.*, 2017, **9**, 303-309.

205 W. D. Fuller, R. A. Sanchez and L. E. Orgel, *J. Mol. Biol.*, 1972, **67**, 25-33.

206 R. Saladino, G. Botta, S. Pino, G. Costanzo and E. Di Mauro, *Chem. Soc. Rev.*, 2012, **41**, 5526-5565.

207 J. E. Šponer, J. Šponer, O. Nováková, V. Brabec, O. Šedo, Z. Zdráhal, G. Costanzo, S. Pino, R. Saladino and E. Di Mauro, *Chem. - A Eur. J.*, 2016, **22**, 3572-3586.

208 R. Saladino, C. Crestini, G. Costanzo and E. Dimauro, *Top. Curr. Chem.*, 2005, **259**, 29–68.

209 B. Mattia Bizzarri, L. Botta, M. I. Pérez-Valverde, R. Saladino, E. Di Mauro and J. M. García-Ruiz, *Chem. - A Eur. J.*, 2018, **24**, 8126-8132.

210 Y. L. Jiang, C. J. Wiederholt, J. N. Patro, K. Haraguchi and M. M. Greenberg, *J. Org. Chem.*, 2005, **70**, 141–149.

211 L. Botta, B. Mattia Bizzarri, D. Piccinino, T. Fornaro, J. Robert Brucato and R. Saladino, *Eur. Phys. J. Plus*, 2017, **132**, 317.

212 M. Tomasz, R. Lipman, M. S. Lee, G. L. Verdine and K. Nakanishi, *Biochemistry*, 1987, **26**, 2010-2027.

213 M. Berger and J. Cadet, *Zeitschrift für Naturforsch. B.*, 2014, **40**, 1519-1531.

214 G. Costanzo, R. Saladino, G. Botta, A. Giorgi, A. Scipioni, S. Pino and E. Di Mauro, *ChemBioChem*, 2012, **13**, 999-1008.

215 B. M. Bizzarri, J. E. Šponer, J. Šponer, G. Cassone, M. Kapralov, G. N. Timoshenko, E. Krasavin, G. Fanelli, A. M. Timperio, E. Di Mauro and R. Saladino, *ChemSystemsChem*, 2019, **2**, e1900039.

216 N. E. Price, K. M. Johnson, J. Wang, M. I. Fekry, Y. Wang and K. S. Gates, *J. Am. Chem. Soc.*, 2014, **136**, 3483-3490.

217 N. E. Price, M. J. Catalano, S. Liu, Y. Wang and K. S. Gates, *Nucleic Acids Res.*, 2015, **43**, 3434-3441.

218 B. Shimizu and M. Miyaki, *Tetrahedron Lett.*, 1968, **9**, 855–859.

219 M. Miyaki and B. Shimizu, *Chem. Pharm. Bull.*, 1970, **18**, 1446-1456.

220 J. Boryski, *Nucleosides and Nucleotides*, 1996, **15**.

221 N. Kitadai and S. Maruyama, *Geosci. Front.*, 2018, **9**, 1117-1153.

222 M. J. McKay and H. M. Nguyen, *ACS Catal.*, 2012, **2**, 1563-1595.

223 V. S. Bogdanov, V. N. Nesterov, V. E. Shklover, Y. T. Struchkov and Z. O. Khim, 1989, 947–951.

224 Y. M. Ying, W. G. Shan, W. H. Liu and Z. J. Zhan, *Chem. Nat. Compd.*, 2013, **49**.

225 R. Huang, X. Zhou, Y. Peng, X. Yang, T. Xu and Y. Liu, *Chem. Nat. Compd.*, 2011, **46**, 1010-1011.

226 A. M. Downey, C. Richter, R. Pohl, R. Mahrwald and M. Hocek, *Org. Lett.*, 2015, **17**, 4604-4607.

227 A. Eschenmoser and E. Loewenthal, *Chem. Soc. Rev.*, 1992, **21**, 1–16.

228 G. T. Rogers, R. S. Shadbolt and T. L. V. Ulbricht, *J. Chem. Soc. C Org.*, 1969, 203-208.

229 H. Vorbrüggen and G. Höfle, *Chem. Ber.*, 1981, **114**, 1256-1268.

230 H. S. Bernhardt and L. Landweber, 2012, 1–10.

231 U. Kang, S. M. Ryu, D. Lee and E. K. Seo, *Chem. Nat. Compd.*, 2018, **54**, 1023-1026.

232 J. Ren, Y. G. Xie, Y. G. Guo, S. K. Yan and H. Z. Jin, *Chem. Nat. Compd.*, 2018, **55**, 552.

233 S. Becker, J. Feldmann, S. Wiedemann, H. Okamura, C. Schneider, K. Iwan, A. Crisp, M. Rossa, T. Amatov and T. Carell, *Science*, 2019, **366**, 76–82.

234 Y. Furukawa, H. J. Kim, D. Hutter and S. A. Benner, *Astrobiology*, 2015, **15**, 259-267.

235 G. Costanzo, R. Saladino, C. Crestini, F. Ciciriello and E. Di Mauro, *J. Biol. Chem.*, 2007, **282**, 16729-16735.

236 Y. Yamagata, H. Watanabe, M. Saitoh and T. Namba, *Nature*, 1991, **352**, 516–519.

237 L. E. Orgel, *Crit. Rev. Biochem. Mol. Biol.*, 2004.

238 L. Botta, R. Saladino, B. M. Bizzarri, B. Cobucci-ponzano, R. Iacono, R. Avino, S. Caliro, A. Carandente, F. Lorenzini, A. Tortora, E. Di and M. Moracci, *Adv. Sp. Res.*, 2018, **62**, 2372–2379.

239 S. Becker, I. Thoma, A. Deutsch, T. Gehrke, P. Mayer, Z. Hendrik and T. Carell, *Science*, 2016, **352**, 833-836.

240 A. Biscans, *Life*, 2018.

241 J. Criado-Reyes, B. M. Bizzarri, J. M. García-Ruiz, R. Saladino and E. Di Mauro, *Sci. Rep.*, 2021, **11**, 1–8.

242 B. M. Bizzarri, R. Saladino, I. Delfino, J. M. García-Ruiz and E. Di Mauro, *Int. J. Mol. Sci.*, 2021, **22**, 917.

243 R. C. Cioc, E. Ruijter and R. V. A. Orru, *Green Chem.*, 2014, **16**, 2958-2975.

244 B. Shirt-Ediss, S. Murillo-Sànchez and K. Ruiz-Mirazo, *Beilstein J. Org. Chem.*, 2017, **13**, 1388-1395.

245 K. Ruiz-Mirazo, C. Briones and A. de la Escosura, *Chem. Rev.*, 2014, **114**, 285-366.

246 R. F. Socha, A. H. Weiss and M. M. Sakharov, *J. Catal.*, 1981, **67**, 207-217.

247 J. Oró and A. P. Kimball, *Arch. Biochem. Biophys.*, 1961, **94**, 217-227.

248 L. Botta, B. Mattia Bizzarri, D. Piccinino, T. Fornaro, J. Robert Brucato and R. Saladino, *Eur. Phys. J. Plus*, 2017, **132**, 317.

249 B. Mattia Bizzarri, L. Botta, M. I. Pérez-Valverde, R. Saladino, E. Di Mauro and J. M. García-Ruiz, *Chem. - A Eur. J.*, 2018, **24**, 8126–8132.

250 R. Saladino, G. Botta, B. M. Bizzarri, E. Di Mauro and J. M. Garcia Ruiz, *Biochemistry*, 2016, **55**, 2806-2811.

251 R. Saladino, C. Crestini, F. Ciciriello, G. Costanzo and E. Di Mauro, *Chem. Biodivers.*, 2007, **4**, 694-670.

252 S. Freeman and J. M. Gardiner, *Appl. Biochem. Biotechnol. - Part B Mol. Biotechnol.*, 1996, **5**, 125-137.

253 B. Ndeboko, O. Hantz, G. J. Lemamy and L. Cova, *Biomolecules*, 2018, **8**, 55.

254 B. Friedland, *J. R. Soc. Health*, 1991, **111**, 170–171.

255 R. Saladino, J. E. Šponer, J. Šponer, G. Costanzo, S. Pino and E. Di Mauro, *Life*, 2018, **8**, 6.

256 P. E. Nielsen, *Chem. & Biodivers.*, 2007, **4**, 1996–2002.

257 C. Sharma and S. K. Awasthi, *Chem. Biol. & Drug Des.*, 2017, **89**, 16–37.

258 M. Frenkel-Pinter, M. Samanta, G. Ashkenasy and L. J. Leman, *Chem. Rev.*, 2020, **120**, 4707–4765.

259 A. W. Schwartz, *Curr. Biol.*, 1994, **4**, 758–760.

260 A. Gupta, A. Mishra and N. Puri, *J. Biotechnol.*, 2017, **259**, 148–159.

261 P. E. Nielsen, *Pure Appl. Chem.*, 1998, **70**, 105–110.

262 A. Ray and B. Nordén, *FASEB J.*, 2000, **14**, 1041–1060.

263 M. Egholm, O. Buchardt, L. Christensen, C. Behrens, S. M. Freier, D. A. Driver, R. H. Berg, S. K. Kim, B. Norden and P. E. Nielsen, *Nature*, 1993, **365**, 566–568.

264 D. W. Green, G. S. Watson, J. A. Watson, D. J. Lee, J. M. Lee and H. S. Jung, *Acta Biomater.*, 2016, **15**, 33-45.

265 P. S. Robertson and J. Vaughan, *J. Am. Chem. Soc.*, 1958, **80**, 2691–2693.

266 J. S. Hudson, J. F. Eberle, R. H. Vachhani, L. C. Rogers, J. H. Wade, R. Krishnamurthy and G. Springsteen, *Angew. Chemie - Int. Ed.*, 2012, **51**, 5134-5137.

267 R. Saladino, C. Crestini, G. Costanzo and E. DiMauro, in *Prebiotic Chemistry*, ed. P. Walde, Springer Berlin Heidelberg, Berlin, Heidelberg, 2005, pp. 29–68.

268 R. Saladino, G. Botta, S. Pino, G. Costanzo and E. Di Mauro, *Chem. Soc. Rev.*, 2012, **41**, 5526-5565.

269 J. P. Ferris, P. C. Joshi, E. H. Edelson and J. G. Lawless, *J. Mol. Evol.*, 1978, **11**, 293-311.

270 S. Nandi, D. Bhattacharyya and A. Anoop, *Chem. – A Eur. J.*, 2018, **24**, 4885–4894.

271 B. H. L., B. Ragan, G. A. Grieves, E. Di Mauro, N. V Hud and T. M. Orlando, *ChemBioChem*, 2010, **11**, 1240–1243.

272 N. Jazi, S. Fozooni and H. Hamidian, *J. Chem. Res.*, 2018, **42**, 80–85.

273 J. Dong, S. Chen, R. Li, W. Cui, H. Jiang, Y. Ling, Z. Yang and W. Hu, *Eur. J. Med. Chem.*, 2016, **108**, 605–615.

274 T. Eldebss, *Mini Rev. Med. Chem.*, 2016, **16**, 67-83.

275 M. Bollier, F. Klupsch, P. Six, L. Dubuquoy, N. Azaroual, R. Millet and N. Leleu-Chavain, *J. Org. Chem.*, 2018, **83**, 422–430.

276 A. Al-Azmi, A. Z. A. Elassar and B. L. Booth, *Tetrahedron*, 2003, **59**, 2749–2763.

277 M. Ferus, D. Nesvorný, J. Šponer, P. Kubelík, R. Michalčíková, V. Shestivská, J. E. Šponer and S. Civiš, *Proc. Natl. Acad. Sci.*, 2015, **112**, 657–662.

278 E. Boulanger, A. Anoop, D. Nachtigallova, W. Thiel and M. Barbatti, *Angew. Chemie Int. Ed.*, 2013, **52**, 8000–8003.

279 Y. A. Jeilani, P. N. Williams, S. Walton and M. T. Nguyen, *Phys. Chem. Chem. Phys.*, 2016, **18**, 20177–20188.

280 F. M. Kruse, J. S. Teichert and O. Trapp, *Chem. – A Eur. J.*, 2020, **26**, 14776–14790.

281 Z. Nazarian and M. Dabiri, *ChemistrySelect*, 2020, **5**, 4394–4412.

282 S. A. Scaringe, *Methods*, 2001, **23**, 206–217.

283 B. M. A. G. Piette and J. G. Heddle, *Trends Ecol. Evol.*, 2020, **35**, 397–406.

284 P. K. Martin, H. R. Matthews, H. Rapoport and G. Thyagarajan, *J. Org. Chem.*, 1968, **33**, 3758–3761.

285 A. A. Watson, *J. Org. Chem.*, 1977, **42**, 1610–1612.

286 E. Mohammadi, L. Petera, H. Saeidfirozeh, A. Knížek, P. Kubelík, R. Dudžák, M. Krůs, L. Juha, S. Civiš, R. Coulon, O. Malina, J. Ugolotti, V. Ranc, M. Otyepka, J. Šponer, M. Ferus and J. E. Šponer, *Chem. - A Eur. J.*, 2020, **26**, 12075-12080.

287 W.-Y. Lou, M.-H. Zong, Y.-Y. Liu and J.-F. Wang, *J. Biotechnol.*, 2006, **125**, 64–74.

288 E. I. Al-Afaleq and S. A. Abubshait, *Molecules*, 2001, **6**, 621–638.

289 A. A. Aly and S. A. Nassar, *Heteroat. Chem.*, 2004, **15**, 2–8.

290 E. Deau, Y. Loidreau, P. Marchand, M.-R. Nourrisson, N. Loaëc, L. Meijer, V. Levacher and T. Besson, *Bioorg. Med. Chem. Lett.*, 2013, **23**, 6784–6788.

291 R. Sgarbanti, D. Amatore, I. Celestino, M. E. Marcocci, A. Fraternale, M. Ciriolo, M. Magnani, R. Saladino, E. Garaci, A. Palamara and L. Nencioni, *Curr. Top. Med. Chem.*, 2014, **14**, 2529-2541.

292 S. Davidson, *Front. Immunol.*, 2018, **9**.

293 M. Kim, S.-Y. Kim, H. W. Lee, J. S. Shin, P. Kim, Y.-S. Jung, H.-S. Jeong, J.-K. Hyun and C.-K. Lee, *Antiviral Res.*, 2013, **100**, 460–472.

294 J. Leis, C.-H. Luan, J. E. Audia, S. F. Dunne, C. M. Heath and J. U. Jung, *J. Virol.*, 2021, **95**, e00190-21.

295 B. M. Bizzarri, A. Fanelli, L. Botta, M. De Angelis, A. T. Palamara, L. Nencioni and R. Saladino, *RSC Adv.*, 2021, **11**, 30020–30029.

296 R. Lohrmann, *J. Mol. Evol.*, 1972, **1**, 263–269.

297 J. P. Ferris, O. S. Zamek, A. M. Altbuch and H. Freiman, *J. Mol. Evol.*, 1974, **3**, 301–309.

298 M. P. Robertson and S. L. Miller, *Nature*, 1995, 375, 772–774.

299 S. W. Fox and K. Harada, *Science*, 1961, **133**, 1923–1924.

300 J. P. Ferris, R. A. Sanchez and L. E. Orgel, *J. Mol. Biol.*, 1968, **33**, 693–704.

301 K. Harada and S. Suzuki, *Tetrahedron Lett.*, 1976, **17**, 2321–2322.

302 G. J. F. Chittenden and A. W. Schwartz, *Nature*, 1976, **263**, 350–351.

303 A. W. Schwartz and G. J. F. Chittenden, *Biosystems*, 1977, **9**, 87–92.

304 R. Sarma and D. Prajapati, *Green Chem.*, 2011, **13**, 718–722.

305 S. Monticelli, L. Castoldi, I. Murgia, R. Senatore, E. Mazzeo, J. Wackerlig, E. Urban, T. Langer and V. Pace, *Monatshefte fur Chemie*, 2017, **148**, 37–48.

306 A. Ismael, A. Gevorgyan, T. Skrydstrup and A. Bayer, *Org. Process Res. \& Dev.*, 2020, **24**, 2665–2675.

307 C. Zippilli, B. M. Bizzarri, S. Gabellone, L. Botta and R. Saladino, *ChemCatChem*, 2021, **13**, 4151–4158.

308 G. W. Huber, S. Iborra and A. Corma, *Chem. Rev.*, 2006, **106**, 4044–4098.

309 H. Yue, Y. Zhao, X. Ma and J. Gong, *Chem. Soc. Rev.*, 2012, **41**, 4218–4244.

310 K. Sun, Y.-L. Zhang, X.-L. Chen, H.-F. Su, Q.-C. Peng, B. Yu, L.-B. Qu and K. Li, *ACS Appl. Bio Mater.*, 2020, **3**, 505–511.

311 F. Chemat and M. Poux, *Tetrahedron Lett.*, 2001, **42**, 3693–3695.

312 A. Banihashemi, H. Hazarkhani and A. Abdolmaleki, *J. Polym. Sci. Part A Polym. Chem.*, 2004, **42**, 2106–2111.

313 W. Zhang, H. Xu, S. Guan, C. Wang and G. Dong, *J. Med. Virol.*, 2022, **94**, 4406–4416.

314 T. Lampejo, *Eur. J. Clin. Microbiol.*, 2020, **39**, 1201–1208.

315 G. Devi, Z. Yuan, Y. Lu, Y. Zhao and G. Chen, *Nucleic Acids Res*., 2014, **42**, 4008–4018.

316 C. Annoni, T. Endoh, D. Hnedzko, E. Rozners and N. Sugimoto, *Chem. Commun.*, 2016, **52**, 7935–7938.

317 F. Wojciechowski and R. H. E. Hudson, *Org. Lett.*, 2009, **11**, 4878–4881.

318 J. T. Nguyen, J. D. Hoopes, M. H. Le, D. F. Smee, A. K. Patick, D. J. Faix, P. J. Blair, M. D. De Jong, M. N. Prichard and G. T. Went, *Plos One*, 2010, **5**, e9332.

319 D. F. Smee, B. L. Hurst, M.-H. Wong, E. B. Tarbet, Y. S. Babu, K. Klumpp and J. D. Morrey, *Antiviral Res.*, 2010, **88**, 38–44.

320 R. Sgarbanti, D. Amatore, I. Celestino, M. Marcocci, A. Fraternale, M. Ciriolo, M. Magnani, R. Saladino, E. Garaci, A. Palamara and L. Nencioni, *Curr. Top. Med. Chem.*, 2014, **14**, 2529-2541.

321 P. Checconi, M. De Angelis, M. E. Marcocci, A. Fraternale, M. Magnani, A. T. Palamara and L. Nencioni, *Int. J. Mol. Sci*., 2020, **21**, 4084.

322 M. Caffrey and A. Lavie, *Front Mol Biosci*., 2021, **8**, 1–6.

323 B. M. Bizzarri, A. Fanelli, S. Ciprini, A. Giorgi, M. De Angelis, R. Fioravanti, L. Nencioni and R. Saladino, *ACS Omega*, 2022, **7**, 45253–45264.

324 C. Grundke, C. Kong, C. J. Kampf, B. F. Gupton, D. T. McQuade and T. Opatz, *J. Org. Chem.*, 2021, **86**, 10320–10329.

325 M. Ruiz-Bermejo, J. L. de la Fuente, C. Pérez-Fernández and E. Mateo-Martí, *Processes*, 2021, **9**, 597.

326 M. Bollier, F. Klupsch, P. Six, L. Dubuquoy, N. Azaroual, R. Millet and N. Leleu-Chavain, *J. Org. Chem.*, 2018, **83**, 422-433.

327 F. Brotzel and H. Mayr, *Org. Biomol. Chem.*, 2007, **5**, 3814–3820.

328 Y. Yamada, N. Nagashima, Y. Iwashita, A. Nakamura and I. Kumashiro, *Tetrahedron Lett.*, 1968, **9**, 4529–4532.

329 R. S. Becker, J. Hole and W. Rothman, *J. Am. Chem. Soc.*, 1973, **95**, 1269–1273.

330 V. P. Gupta and P. Tandon, *Spectrochim. Acta Part A Mol. Biomol. Spectrosc.*, 2012, **89**, 55–66.

331 T. H. Koch and R. M. Rodehorst, *J. Am. Chem. Soc.*, 1974, **96**, 6707–6710.

332 N. J. Green, J. Xu and J. D. Sutherland, *J. Am. Chem. Soc.*, 2021, **143**, 7219–7236.

333 B. Jiang, T. Rajale, W. Wever, S.-J. Tu and G. Li, *Chem. – An Asian J.*, 2010, **5**, 2318–2335.

334 V. A. Chebanov, V. E. Saraev, S. M. Desenko, V. N. Chernenko, I. V Knyazeva, U. Groth, T. N. Glasnov and C. O. Kappe, *J. Org. Chem.*, 2008, **73**, 5110–5118.

335 E. Muravyova, S. Shishkina, V. Musatov, I. Knyazeva, O. Shishkin, S. Desenko and V. Chebanov, *Synthesis-stuttgart*, 2009, **2009**, 1375–1385.

336 B. Jiang, F. Shi and S.-J. Tu, *Curr. Org. Chem.*, 2010, **14**, 357–378.

337 T. L. March, M. R. Johnston, P. J. Duggan and J. Gardiner, *Chem. \& Biodivers.*, 2012, **9**, 2410–2441.

338 A. Di Sotto, S. Di Giacomo, D. Amatore, M. Locatelli, A. Vitalone, C. Toniolo, G. L. Rotino, R. Lo Scalzo, A. T. Palamara, M. E. Marcocci and L. Nencioni, *Molecules*, 2018, **23**, 2066.

339 C. Zippilli, L. Botta, B. M. Bizzarri, L. Nencioni, M. De Angelis, V. Protto, G. Giorgi, M. C. Baratto, R. Pogni and R. Saladino, *Int. J. Mol. Sci.*, 2021, **22**, 1337.

List of publications

1. Bizzarri, B.M., Fanelli, A., Botta, L., Sadun, C., Gontrani, L., Ferella, F., Crucianelli, M., Saladino, R. Dendrimer crown-ether tethered multi-wall carbon nanotubes support methyltrioxorhenium in the selective oxidation of olefins to epoxides; *RSC Adv*.**,** 2020,**10**, 17185-17194.
2. Bizzarri, B.M., Fanelli, A., Piccinino, D., De Angelis, M., Dolfa, C., Palamara, AT., Nencioni, L., Zippilli, C., Crucianelli, M., Saladino, R. Synthesis of Stilbene and Chalcone Inhibitors of Influenza A Virus by SBA-15 Supported Hoveyda-Grubbs Metathesis; *Catalysts* 2019, **9**(12), 983.
3. Bizzarri, B.M., Fanelli, A., Kapralov, M., Krasavin, E., Saladino, R. Meteorite-catalyzed intermoleculartrans-glycosylation produces nucleosides under proton beam irradiation. *RSC Adv.*, 2021, **11**(31), 19258–19264.
4. Bizzarri, B.M., Fanelli, A., Botta, L., Cesarini, S., Zippilli, C., Saladino, R. Dendrimeric structures in the synthesis of fine chemicals. *Materials*, 2021, **14**(18), 5318.
5. Botta, L., Cesarini, S., Zippilli, C., Bizzarri, B.M., Fanelli, A., Saladino, R. Multicomponent Reactions in the Synthesis of Antiviral Compounds. *Curr. Med. Chem*. 2022, **29**, 2013-2050.
6. Bizzarri, B.M., Fanelli, A., Botta, L., De Angelis, M., Palamara, AT., Nencioni, L., Saladino, R. Aminomalononitrile inspired prebiotic chemistry as a novel multicomponent tool for the synthesis of imidazole and purine derivatives with anti-influenza A virus activity. *RSC Adv.*, 2021, **11**, 30020-30029.
7. Bizzarri, B.M., Fanelli, A., Cesarini, S., Saladino, R. A Three-Way Regioselective Synthesis of Amino Acid Decorated Imidazole, Purine and Pyrimidine Derivatives by Multicomponent Chemistry Starting from Prebiotic Diaminomaleonitrile. *Eur. J. Org.Chem*. 2022, e202200598.
8. Bizzarri, B.M., Fanelli. A., Ciprini, S., Giorgi, A., De Angelis, M., Fioravanti, R., Nencioni, L., Saladino, R. Multicomponent synthesis of diaminopurine and guanine PNA's analogues active against influenza A virus from prebiotic compounds. *ACS Omega*, 2022, **7**, 45253–45264.